The function of *gametocyte specific factor 1* (*GTSF1*) in mammalian oocyte and ovarian follicle development

By

Georgios Liperis

Submitted in accordance with the requirements for the degree of

Doctor of Philosophy

The University of Leeds

School of Medicine

August, 2013

I confirm that the work submitted is my own and that appropriate credit has been given where reference has been made to the work of others

II

ACKNOWLEDGEMENTS

"Στους γονείς οφείλομεν το ζην, στους δε διδασκάλους το ευ ζην"
(To our parents we owe life, to our teachers a good life)
Alexander the Great

ABSTRACT

A detailed understanding of the genes and mechanisms that regulate oocyte growth and maturation underpins the development of improved methods of assisted conception. Gametocyte specific factor 1 (*GTSF1*)-a putative marker of gamete developmental competence, is highly conserved across species but in mammals demonstrates a sexual dimorphism in its function. In mice, male mutants for *Gtsf1* have an infertile phenotype, whereas female mutants appear to have normal ovarian function. It is hypothesised that *GTSF1* regulates oocyte development in monovular species such as the sheep.

Initial studies characterised the expression and cellular distribution of *GTSF1* across cDNA libraries spanning ovine oogenesis and embryogenesis and by using *in situ* hybridisation of fixed tissue. *GTSF1* expression was confined to gonadal and embryonic tissues with highest expression in the ooplasm of germinal vesicle (GV)-staged secondary oocytes. The gene sequence of *GTSF1* was obtained and the gene and predicted protein sequences revealed close homology across many species with two conserved CHHC zinc finger domains known to bind RNA.

Functional analysis of the role of *GTSF1* during sheep oocyte maturation was conducted using short interference RNA (siRNA injection) in conjunction with oocyte *in vitro* maturation (IVM) and oocytectomised cumulus shell co-culture. This system was validated using siRNA knockdown (kd) for a known oocyte-specific gene, Growth differentiation factor 9 (*GDF9*). The effect on *GTSF1* kd was evaluated following the microinjection of 770 GV oocytes with siRNA target against the sixth exon of ovine *GTSF1*. The effects of *GTSF1* kd were evaluated in 57 MII oocytes and cumulus shells. Targeted kd of *GTSF1* in GV oocytes followed by IVM and cumulus shell co-culture did not affect oocyte meiotic progression or cumulus expansion. Microarray analysis using the bovine GeneChip Affymetrix array revealed that 6 down-regulated genes (*TCOF1*, *RPS8*, *CACNA1D*, *SREK1IP1*, *TIMP1*, *MYL9*) following the *GTSF1* kd were associated with developmental competence, RNA storage, post-transcriptional modifications and translation. Immunofluorescent studies localized GTSF1 protein to the P-body in GV ovine oocytes.

Collectively these results suggest a possible role of GTSF1 in post-transcriptional control of RNA processing, translational regulation and RNA storage which may impact on oocyte developmental competence.

List of Contents

List of tables

List of figures

List of Abbreviations

A: Adenine
AA: Amino acids
ACTB: Beta actin
ACTR1: Activin type I receptor
ADP: Adenosine diphosphate
AGG: Arginine-Glycine-Glycine box
AGO2: Argonaute 2
ALK: Activin like receptor kinases
AMH: Anti-Müllerian hormone
AMP: Adenosine monophosphate
AMPK: AMP activated protein kinase
ANT1: Antagonism of C1 repression
APC/C: Anaphase promoting complex/cyclosome
APS: Ammonium Persulfate
ARB: Arbitrary
AREG: Amphiregulin
ARID2: AT rich interactive domain 2
ART: Assisted reproductive techniques
AS: Antisense
ATP: Adenosine triphosphate
AURK: Aurora kinase
bFGF: Basic fibroblast growth factor
BLAST: Basic local alignment search tool
BTC: Betacellulin
BMP: Bone morphogenetic protein
BP: Base pair
BSA: Bovine serum albumen
BUB: Budding uninhibited by benzimidazoles
C-MOS: Proto-oncogene serine/threonine-protein kinase Mos
CAK: CDK-activating kinase
CACNA1D: Calcium channel voltage-dependent L type alpha 1D subunit
cAMP: Cyclic adenosine monophosphate
CDC2: Cell division control protein 2 homolog
CDK: Cyclin-cyclin dependent kinase
cDNA: Complementary DNA
CFSE: Carboxyfluorescein succinimidyl ester
CG: Chorionic gonadotrophin
CGH: Comparative genomic hybridisation
cGMP: Cyclic guanosine monophosphate
CKAP: Cytoskeleton-associated protein
Co-SMADS: Common partner Smads
COC: Cumulus oocyte complex
COX17: Cytochrome c oxidase copper chaperone
CPEB: Cytoplasmic polyadenylation element-binding protein
cRNA: cDNA transcribed back to RNA
Ct: Cycle threshold
CYP11A1: Cholesterol side-chain cleavage enzyme
CYP17A1: 17α-hydroxylase/17,20- desmolase
CYP19: Aromatase cytochrome P450 19 enzyme
DAPI: Diamidino-2-phenylindole
DAVID: Database for annotation visualization and integrated discovery
ddRNAi: DNA-directed RNAi
DDX27: DEAD box polypeptide 27
DEAD: Asp-Glu-Ala-Asp
DEAE: Diethylaminoethyl cellulose
DEAH: Asp-Glu-Ala-His
DEPC: Diethylpyrocarbonate
DGCR8: Microprocessor complex subunit
DHX35: DEAH box polypeptide 35
DMSO: Dimethyl sulfoxide
DNA: Deoxyribonucleic acid
DNMT1o: DNA methyltransferase cytosine5,1
dNTP: Deoxyribonucleotide triphosphate
DPBS: Dulbecco's Calcium (Ca2+) and Magnesium (Mg2+)-free PBS
DPP3: Dipeptidyl-peptidase 3
DS: Double stranded
DTT: Diothiothreitol
EGA: Embryonic genome activation
EGF: Epidermal growth factor
eIF-4F: Eukaryotic initiating factor 4F
EREG: Epiregulin
ERK: Extracellular signal-regulated kinase
ESC: Embryonic stem cell
ETOH: Ethanol
EZH2: Enhancer of zeste homolog 2
EZR: Erzin
FAM112B: Family with sequence similarity 112 member B
FCS: Fetal calf serum
FGF: Fibroblast growth factor
FIGLA: Factor in the germline α
FIM: Follicle isolation medium
FISH: Fluorescent in situ hybridisation
FKBP4: FK506 binding protein 4
FOX: Forkhead box
FSH: Follicle stimulating hormone
GAPDH: Glyceraldehyde-3-phosphate dehydrogenase
GDF9: Growth differentiation factor 9
GH: Growth hormone
GJIC: Gap junctional intracellular communications
GnRH: Gonadotrophin releasing hormone surge
GPCR: G protein-coupled receptor
Gs: G protein

GTSF1: Gametocyte specific factor 1
GV: Germinal vesicle
GVBD: Germinal vesicle breakdown
H: Hour
H2A: Histone 2A
HAS2: Hyaluronan synthase 2
HSD3β: 3β-hydroxysteroid dehydrogenase
HSD17β: 17β-hydroxysteroid dehydrogenase
I-SMADS: Inhibitory Smads
IAP: Intracisternal A-particle
IGF: Insulin-like growth factor
IGFBP7: IGF binding protein 7
INCENP: Inner centromere protein
INHBA: Inhibin beta A
IQR: Inter-quartile range
ISH: *In situ* hybridisation, IVM: *In vitro* maturation
KD: Knockdown
KITL: Kit ligand
KOAc: Potassium acetate
LB: Luria broth
LH: Luteinising hormone
LHX8: Lim homeobox
LIF: Leukaemia inhibitory factor
LIMMA: Linear models for microarrays
LINE1: Long interspersed nuclear elements 1
LOESS: Locally weighted scatter-plot smoothing
LSM14A: Like-Sm 14A
MI: Metaphase I
MII: MetaphaseII
MAPK: Mitogen activated protein kinase
MCAK: mitotic centromere associated kinesin
MEM: Minimum essential medium
MET: Maternal to embryonic transition
MGC: Mammalian gene collection
MgOAc: Magnesium acetate
miRNA: Micro RNA
Min: Minutes
MIQE: Minimum information for publication of qRT-PCR experiments
mRNA: Messenger RNA
MM: Mismatch
MOS: Proto-oncogene serine/threonine-protein kinase
MPF: Maturation promoting factor
MSY2: Male specific region of the Y chromosome
MTOC: microtubule organising centres
mTOR: Mammalian target of rapamycin
MVH: Mouse VASA homolog
MW: Molecular weight
MYL: myosin regulatory light polypeptide
MYT1: myelin transcription factor 1
MZT: maternal to zygotic transition

NA: Not applicable
NALP5: Nacht leucine rich repeat-pyrin containing leucine rich repeat and pyrin domain containing 5
NC: Negative control
N.C. siRNA: Non-coding negative control siRNA
NCBI: National centre for biotechnology information
NF-κB: Nuclear factor kappa-light-chain-enhancer of activated B cells
NGF: Nerve growth factor
NOBOX: Newborn ovary homeobox
NPM2: Nucleophosmin 2
NR: Neutral red
NR5A2: Nuclear receptor subfamily 5 group A, member
NS: Not significant
NT: Nucleotide
OOX: oocytectomised complexes
OSBPL7: Oxysterol binding protein like 7
P: Phosphorylation
P-body: Processing bodies
PAGE: Polyacrylamide gel electrophoresis
PAL-1: Plasminogen activator inhibitor-1
PARP: poly ADP-ribose polymerase
PAZ: Piwi/Argonaute/Zwille
PBS: Phosphate buffer saline
PC: Positive control
PCBP1: Poly(rC) binding protein-1
PCR: Polymerase chain reaction
PDE3: Phosphodiesterase 3
PDK1: Phoshoinositide-dependent kinase
PELO: protein pelota homolog
PFA: Paraformaldehyde
PFKP: platelet phosphofructokinase
PGC: Primordial germ cell
piRNA: Piwi interacting RNA
PIWI: P-element-induced wimpy testis
PKA: Protein kinase A
PKB: Protein kinase B
PLM: Probe level models
PM: Perfect match
POS: Polycystic ovarian syndrome
PAP: Poly-(A) polymerase
Pri-miRNA: Primary micro RNA
PRE: Polyadenylation response element
Pre-miRNA: Precursor micro RNA
PTEN: Phosphatase and tensin homolog
PTGS2: Prostaglandin endoperoxide synthetase 2
PTM: Post-translational modifications
PVDF: Polyvinylidene fluoride
qRT-PCR: Quantitative real-time reverse transcriptase PCR

R: Receptor
R-SMADS: Receptor-regulated Smads
RACE: rapid amplification of cDNA ends
RBM17: RNA binding motif 17
RECE: Rapid amplification of cDNA ends
RBD: RNA binding domain
RBP: RNA binding protein
RINGO/SPY: Rapid inducer of G2/M progression in oocytes/speedy
RISC: RNA induced silencing complex
RMA: Robust multichip averaging
RNA: Ribonucleic acid
RNAi: RNA interference
RNase: Ribonuclease
RNP: Ribonucleoprotein
RPS8: Ribosomal protein S8
rRNA: Ribosomal RNA
RSK: Ribosomal S6 kinase
RT: Room temperature
RT-PCR: Reverse transcription PCR
SAC: Spindle assembly checkpoint
SDS: Sodium Dodecyl sulphate
SREK1IP1: Splicing regulatory glutamine/lysine rich protein 1 interacting protein 1
shRNA: Short hairpin RNA
siRNA: Short interference RNA
SMAD: small body size and mothers against decapentaplegic related protein
SOHLH: Spermatogenesis and oogenesis basic helix-loop-helix
SSC: Saline sodium citrate buffer

StAR: Steroidogenic acute regulatory protein
T: Thymine
TARDBP: TAR DNA-binding protein
TBE: Tris borate ethylenediaminetetraacetic acid
TCOF1: Treacher Collins-Franceschetti syndrome 1
TECR: trans-2,3-enoyl-CoA reductase
TGF: Transforming growth factor
TIMP1: tissue inhibitor of metalloproteinase 1
Tm: Melting temperature
TNFAIP6: Tnfα induced protein 6
TNRC6A: Trinucleotide repeat-containing gene 6A
TRM13: tRNA methyl-transferases
TS: Template switching
TSN: Translin
UCSC: University of California Santa Cruz
UPF: Uncharacterised protein family
UTP14A: U3 small nucleolar ribonucleoprotein homolog A
UTR: Untranslated region
V: Volts
YBX1: Nuclease-sensitive element binding protein 1
YBX2: Y box binding protein 2
YWHAZ: tyrosine 3-monooxygenase tryptophan 5-monooxygenase activation protein, zeta polypeptide
Zar1: Zygote arrest 1
ZNF: Zinc finger protein
ZP: Zona pellucida

Chapter 1: General introduction

1.1 INTRODUCTION

The basic functional unit of the ovary is the ovarian follicle which consists of an oocyte (female gamete) arrested at prophase I of meiosis I and surrounded by somatic cells. Follicles provide a specialised compartment for oocyte development, create signals and gather nutrients. The development of ovarian follicles and oocytes as well as the acquisition of fertilisation potential of the oocyte are dynamic processes controlled by endocrine as well as paracrine factors (Richards *et al.*, 1995; Gougeon, 1996). From birth, ovaries contain a certain number of immature follicles, the primordial follicles, although opposing views also exist (Johnson *et al.*, 2004). Cyclic gonadotrophin stimulation initiated at puberty, directs growth of the follicles and in monovular species such as humans, a single or small number of germ cells will resume meiosis during an ovarian cycle. This results in the release of a single oocyte by the dominant follicle following the preovulatory gonadotrophin surge, while most of the follicles undergo atresia (Mcgee and Hsueh, 2000). From around 400,000 primordial follicles present in human ovaries at puberty, only 300-400 oocytes will ovulate throughout the female reproductive life span (Gougeon, 1989; Gougeon, 1996; Starz-Gaiano and Lehmann, 2001). The fate of the great majority of ovarian follicles and the oocytes they contain is therefore degeneration.

An understanding of the factors that control follicle and oocyte growth and maturation is very important to human reproduction. In the post-genomic era, elucidation of gene functions can help in the development of gene based drug targets and therapies. In the field of assisted conception in commercially relevant species and humans, identification of vital genes and mechanisms can lead to improvement of success rates and to the development of new and improved technologies and culture environments such as the addition of improved supplements to the culture media used for the *in vitro* maturation (IVM) of oocytes. These technological advances can provide options for better treatments for patients at risk of ovarian hyper-stimulation syndrome following stimulation of the ovaries for the production of mature oocytes. It can also provide options for fertility preservation strategies in cancer patients where chemotherapy often results in the partial or complete depletion of the pool of primordial follicles (Demeestere *et al.*, 2012).

Advances in recombinant deoxyribonucleic acid (DNA) technology and *in silico* analysis have allowed identification and isolation of genes expressed during well defined periods of development during oogenesis and folliculogenesis. Although extensive research has been conducted on follicle and oocyte growth and development in rodents, more knowledge is required in the study of monovular species that provide a better model for the study of human reproductive function. A number of novel genes which are thought to regulate gamete quality have recently been identified. For example, gametocyte specific factor 1 (*GTSF1*)-a putative marker of gamete developmental competence, is highly conserved across species, but as shown in mice, it demonstrates a sexual dimorphism in its function (Yoshimura *et al.*, 2009). Male mutants for *Gtsf1* have an infertile phenotype, whereas female mutants appear normal (Yoshimura *et al.*, 2009). This review aims to provide an insight into the regulation of oocyte and follicle development as well as the background literature on *GTSF1* and the means of evaluating the function of this novel gene.

1.2 OOCYTE AND FOLLICLE DEVELOPMENT

1.2.1 Origin of germ cells

The mammalian ovary is responsible for the differentiation and maturation of the oocytes. In addition, the ovary is responsible for the production of steroids that allow the development of female secondary sexual characteristics and support pregnancy. It is estimated that human fetal ovary contains 4-7 million oocytes (Oktem and Urman, 2010), while sheep ovaries contain 2-3 million (Russe *et al.*, 1992). Dogma suggests that the oocyte population is established during fetal development and germ cells are not replenished after birth. Even though this is the basic doctrine of reproductive biology, studies in mice have shown that germ cells originating from the ovarian surface epithelium or bone marrow can be proliferative and sustain limited levels of oocyte and follicle production in the postnatal murine ovary (Johnson *et al.*, 2004; Tilly and Telfer, 2009). Additionally, embryonic stem cells (ESC) isolated from the ovarian surface epithelium of women with no naturally present follicles and oocytes, were shown to express specific markers of the germ line (Bukovsky *et al.*, 2005). None-the-less, the results obtained in the above studies could be explained differently. Specifically, DNA synthesis in the germ cells of the mouse ovary could be due to mitochondrial genome replication and DNA repair of oocytes that do not progress meiotically (Notarianni, 2011). False recognition of ovarian epithelium as oogonia from derived cultures of the

above studies or over-estimation of atresia could explain the obtained results. Similarly, there are arguments for the false identification of ovarian somatic cells as *de novo* oocytes (Notarianni, 2011). In general, the spontaneous generation of large number of *de novo* oocytes to sustain oogenesis in the adult ovary can be considered as an unrealistic assumption. Although *in vitro* cultured somatic cells may in some circumstances have the potential of developing into oocytes, or somatic cells may be transformed into oocytes, there is as yet little evidence to show that these oocytes are able to grow, be fertilised and develop into embryos (Notarianni, 2011). Only 1 study has shown the production of offspring when labelled mouse ESCs were injected into mouse embryos (Boland *et al.*, 2012). However even in that case it cannot be excluded that some primordial follicles were also collected along with the ESCs. The implications of such capability in humans could be immense for the preservation of fertility as well as for the prevention of health problems for women with premature ovarian failure due to aging or gonadotoxic chemotherapy and radiation (Oktem and Oktay, 2007).

Although the ovary is responsible for the differentiation and specialisation of the female gametes, their precursors arise from the somatic cells of the developing gonad, thus have to migrate across the embryo to reach their site of function (Raz, 2004). Female gametes arise from a group of uncommitted epiblast cells that during gastrulation move to the posterior part of the primitive streak to become primordial germ cells (PGC). The expression of bone morphogenetic proteins (BMP) 4 and 8b in extra-embryonic tissue has been shown to induce the formation of mouse PGCs in the proximal epiblast (Lawson *et al.*, 1999). Knowledge of PGC migration has emerged from model genetic organisms *Drosophila melanogaster*, *Danio rerio* and *Mus musculus* where live and fixed imaging approaches have identified PGC morphology, embryonic position and gene expression profile. These techniques in combination with genetic analysis have begun to indicate the mechanisms and behaviours that underlie PGC migration (Richardson and Lehmann, 2010). In the *Bos taurus*, PGCs which are originally recognised in the yolk sac at the fourth week of gestation, migrate through the hindgut into the genital ridge (Marion and Gier, 1971). In *Ovis aries*, migration into the gonad occurs around 23-35 days post fertilisation and by day 40, PGCs are situated in the cortex of the ovary (McNatty *et al.*, 2000). During migration, the PGCs actively proliferate; however a study in *D. melanogaster* suggests that not all PGCs migrate successfully to the gonads (Yamada *et al.*, 2008). Those PGCs that migrate incorrectly have been correlated with locations of germ cell tumours in humans (Schneider *et al.*,

2001). At the end of migration, when PGCs associate with the presumptive somatic cells of the gonad, they lose their motile properties. Evidence from *D. rerio* and *D. melanogaster* indicates that a simple model drives PGC's directional migration and this is due to localisation at the site of the highest attractant expression (Van Doren *et al.*, 1998; Reichman-Fried *et al.*, 2004). Also migration is assisted by the involution of development of other embryonic tissues which help the PGCs along their migrational path (Starz-Gaiano and Lehmann, 2001). Once the presumptive gonad is assembled containing somatic and germ cells, the PGCs termed oogonia, differentiate into primary oocytes when meiosis starts. In some mammals including *M. musculus*, *O. aries* and *Homo sapiens*, somatic cells from the rete ovary and/or the surface epithelium correlate with growing oocytes and form follicles (Buccione *et al.*, 1990a; Eppig, 1991), while in other species such as sea cucumber, junctions between somatic cells and oocyte surface are formed without forming follicles (Frick *et al.*, 1996). In mice, the PGC transition to meiosis has been shown to be regulated by signals from the somatic cells (Chuma and Nakatsuji, 2001). Oocytes do not complete meiosis, but rather they arrest at the diplotene stage of prophase I of the first meiotic division. In humans and sheep this occurs approximately 5 and 3 months into gestation, respectively (Peters, 1969; Sawyer *et al.*, 2002). The prophase I oocyte may remain at that stage of development for long periods of time until further meiotic progression occurs in the ovulatory follicle following puberty, when the cyclic stimulation of gonadotrophins initiates ovulatory reproductive cycles. In humans, primary oocytes can be arrested in the prophase I for up to 50 years (Mcgee and Hsueh, 2000).

1.2.2 Folliculogenesis

In all vertebrates, the number of germ cells is significantly diminished at birth in comparison with the number of cells present during fetal life (Aerts and Bols, 2010). In the bovine ovary for example, the number drops from several millions to approximately 130,000 (Aerts and Bols, 2010). The mechanism which regulates this process is believed to be apoptosis (Oktem and Urman, 2010). Loss of oocytes is continued through postnatal life. In mice, approximately 2/3 of oocytes are lost in the first 5 days of postnatal life (Pepling and Spradling, 1998). In sheep, these processes are not well described, however the majority of oocytes within ovarian follicles are lost prenatally (Juengel *et al.*, 2002). In humans the size of ovarian reserve decreases drastically with age (Figure 1.1), with follicles lost in a continuous stream (Gougeon, 2005). This rate of follicular depletion accelerates in women from the age of about 38 years onwards. By

the time women reach their 40th year of age, their fecundity is impaired and from the age of 45 onwards fecundity is progressively lost and the ovarian reserve is progressively depleted (Lass, 2001; Gougeon, 2005). Depletion of ovarian reserve leads to reproductive senescence and in humans this is termed menopause (Mcgee and Hsueh, 2000).
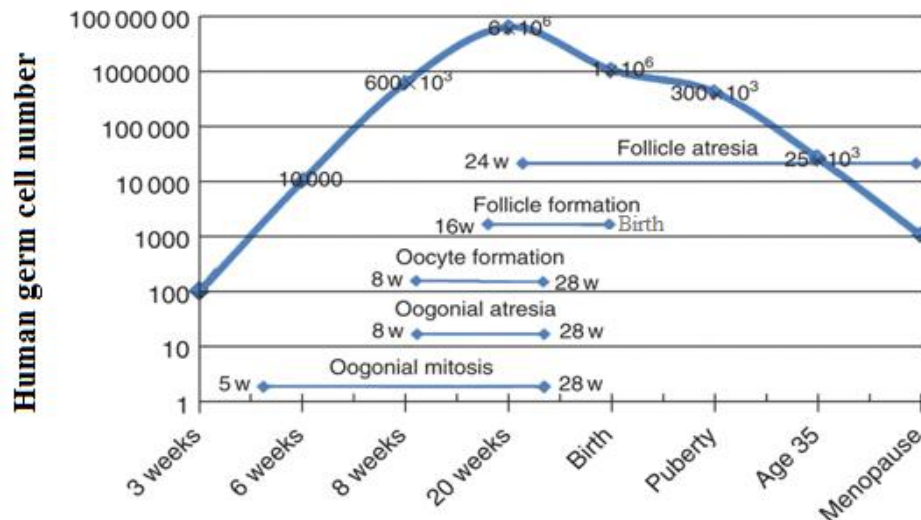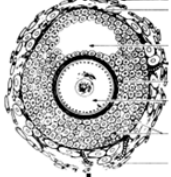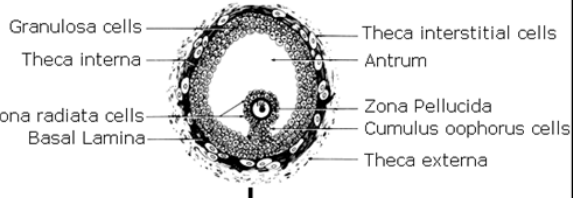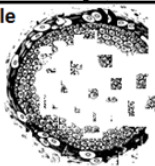
Figure1.1: Schematic representation of the life history of germ cells in humans. The cluster of 100 germ cells migrates, proliferates and colonizes the gonads from where their growth reaches around 600 X 10^3 at 8 weeks of gestation and to 7 million at 20 weeks of gestation. The number of the germ cells starts to decline after 20 weeks of gestation due to atresia and progressively declines, with only 300-400 oocytes (<1%) ovulating during the female reproductive life span. Image adapted from Oktem and Urman, (2010).

Follicular growth can be classified into 3 phases depending on developmental stage and gonadotrophin control. These are: (i) the gonadotrophin-independent phase, (ii) the gonadotrophin-responsive phase and (iii) the gonadotrophin-dependent phase. The first phase consists of growth from the primordial to primary and secondary stages of follicle development. During these stages, granulosa cells change from a single layer of flattened pre-granulosa cells in primordial follicles to a cuboidal morphology as cell division is initiated and progresses to form multi-layered granulosa cells in secondary follicles onwards. In the secondary stage follicles, ovarian cortical cells are actively transformed into theca cells by the presence of granulosa cells (Orisaka *et al.*, 2006). The theca cells are located on the outside of the basement membrane, separated from the granulosa cells. The second phase of follicle development involves growth from the secondary stage to the early antral stage at which point the follicles become gonadotrophin-responsive and the formation of the antral cavity occurs. In sheep, the end of the gonadotrophin-responsive phase is characterised by a peak in the mitotic index of granulosa cells at a follicle diameter of around 1.2 mm (Turnbull *et al.*, 1977).

Follicles at this phase are responsive to gonadotrophins as shown by studies where pre-pubertal animals respond to the external contribution of gonadotrophins and ovulate (Mcleod *et al.*, 1985; Sumbung *et al.*, 1987). With the onset of cyclic gonadotrophin stimulation initiated at puberty, follicles can enter the final gonadotrophin-dependent phase of their growth (Hirshfield, 1991; Gougeon, 1996). During this phase, follicle size in sheep increases from a diameter of 2-2.5 mm up to around 7-8 mm with the formation of the pre-ovulatory follicle also known as Graafian follicle. This change is accompanied by the loss of the majority of antral follicles by atresia in addition to increasing levels of steroidogenic enzymes and endocrine factors produced, as the somatic cells on the follicles differentiate (Mcnatty *et al.*, 1999). Very few follicles and in the majority of cases only 1 ovulatory follicle will be developed throughout each menstrual cycle (humans) and oestrous cycle (other placental animals including sheep). The gonadotrophin-dependent phase of follicular growth is characterised by increased follicular oestrogen production and the induction of the gonadotrophin surge during each reproductive cycle that will allow the Graafian follicle to ovulate and release the mature oocyte for fertilisation. Studies in sheep have shown that when gonadotrophin concentrations are maintained below threshold, follicle development is impaired with follicles being atretic and not progressing beyond the early antral stage (Picton *et al.*, 1990). Following ovulation, the granulosa and theca cells of the follicle are remodelled to form the corpus luteum at the luteal phase of the reproductive cycle that ends in either pregnancy or luteolysis (Gougeon, 1996). The stages of follicular development along with oocyte factors, somatic cell factors and endocrine signalling that affect each stage are shown in Figure 1.2. The individual stages of folliculogenesis and the factors involved are analysed in the sections that follow.

1.2.3 Primordial follicle development

The first stage of follicular development is the primordial follicle. Primordial follicles are formed when oocyte nests in the ovary breakdown resulting in segregation of individual germ cells (Pepling and Spradling, 2001). The individual germ cells recruit pre-granulosa germ cells with which they form a close association. Identification of oocyte factors as stimulators for the formation of follicles suggests that the ovary is the essential regulator of follicle assembly. Each stage of follicular development is characterised by follicle size and morphology. The size of the primordial follicle ranges from around 40 μm in humans and ruminants to 20 μm in the mouse (Gosden *et al.*, 1989; Picton *et al.*, 2003).

Folliculogenesis overview	Endocrine signal	Somatic factors	Oocyte factors
Primordial follicle — Basement lamina, Dictyate Oocyte, Granulosa cells	FSH	Activin A	mTOR, PTEN, FIGLA, NOBOX, LHX8, PDK1, SOHLH2, GDF9, NGF, BMP4, BMP7, BMP15
Primary follicle — Basement lamina, Granulosa cells, Fully grown oocyte, Zona Pellucida	FSH? AMH	Oestrogens KITL LIF bFGF	GDF9, bFGF, FOXL2, FOXO3a
Secondary follicle — Basement lamina, Granulosa cells, Zona Pellucida, Oocyte, Theca cells	FSH LH GH Insulin	TGFB, ALK3, ALK4, ALK6, IGF1, IGFII, AMH	BMP15
Early antral follicle — Theca externa, Basement lamina, Antrum, Zona Pellucida, Oocyte, Granulosa cells, Theca interna	FSH LH GH Insulin	IGF1	GDF9, BMP15, FGF8
Graafian follicle — Granulosa cells, Theca interna, Corona radiata cells, Basal Lamina, Theca interstitial cells, Antrum, Zona Pellucida, Cumulus oophorus cells, Theca externa	FSH LH GH Insulin	Oestrogens EGF	INHBA, GDF9, BMP15, FGF8
Peri-ovulatory follicle — Oocyte, Zona Pellucida, Cumulus oophorus cells	LH Insulin	AREG, EREG, BTC, Oestrogens, Progesterone, NR5A2	GDF9, BMP15

Figure 1.2: Schematic representation of folliculogenesis and signaling. The stages of follicular development from primordial follicle to ovulation along with the factors that affect each stage of development are shown. **Endocrine signals:** Follicle stimulating hormone (FSH), Anti-Müllerian hormone (AMH), Insulin, Growth Hormone (GH), Luteinising hormone (LH). **Somatic factors:** Activin A, Oestrogens, Kit ligand (KITL), Leukaemia inhibitory factor (LIF), Basic fibroblast growth factor (bFGF), Transforming growth factor β (TGFB), Activin-like receptor kinases 3, 4, 6 (ALK), Insulin-like growth factors 1, 2 (IGF), Epidermal growth factor (EGF), Amphiregulin (AREG), Epiregulin (EREG), Betacellulin (BTC), Progesterone, Nuclear receptor subfamily 5, group A, member 2 (NR5A2). **Oocyte factors:** Mammalian target of rapamycin (mTOR), Phosphatase and tensin homolog (PTEN), Factor in the germline α (FIGLA), Newborn ovary homeobox (NOBOX), Lim homeobox (LHX8), Phosphoinositide-dependent kinase 1 (PDK1), Spermatogenesis and oogenesis basic helix-loop-helix 2 (SOHLH2), Nerve growth factor (NGF), bFGF, Forkhead box L2 and O3a (FOX), Inhibin beta α (INHBA), Growth differentiation factor 9 (GDF9), BMPs 4, 7, 15, Fibroblast growth factor 8 (FGF8). Image adapted from Erickson, (1978).

It is believed that just after follicle formation, a small number of follicles are recruited (initial recruitment) to initiate growth while the rest remain quiescent (Wandji *et al.*, 1996). Initial recruitment of follicles in the mammalian ovary is an irreversible process and it is being driven by intra-ovarian and/or other unknown factors or alternatively by the release of an inhibitory stimuli that keeps follicles inactive (Hirshfield, 1991). Following activation, there is a gradual increase of oocyte diameter accompanied by proliferation of granulosa cells and change of their conformation from flattened to cuboidal. Initial recruitment is a continuous process and is not related to the cyclicity of gonadotrophic hormones (Mcgee and Hsueh, 2000).

Evidence suggests that several oocyte transcription factors have important roles in the regulation of oogenesis at this stage of follicle and oocyte development. Depletion of the oocyte-derived transcription factor in the germline α (*Figlα*) in mice was shown to prevent follicular assembly (Liang *et al.*, 1997). This gene is also responsible for the regulation and expression of other oocyte-specific genes (Eppig, 1991). Mouse Figlα protein has been shown to play a role in expression of zona pellucida (ZP) genes *Zp1*, *Zp2* and *Zp3* and in their coordinated expression (Liang *et al.*, 1997). In sheep, *FIGLA* was shown to be expressed mostly at primary and secondary follicle stages with limited expression at the primordial stage (Cotterill, 2008). Similarly in humans, *FIGLA* is detected at primordial, primary and secondary follicle stages as well as MII oocytes (Huntriss *et al.*, 2002). Thereafter, follicle growth is regulated by upstream transcription factors including newborn ovary homeobox (Nobox), lim homeobox (Lhx8) and spermatogenesis and oogenesis basic helix-loop-helix 2 (Sohlh2). From these factors, Nobox in particular is encoded by an oocyte-specific homeobox gene expressed in germ cell cysts and in primordial and growing oocytes (Suzumori *et al.*, 2002).

Knockout of the *Nobox* gene in mice was shown to accelerate the postnatal loss of oocytes and prevent further development of primordial follicles (Rajkovic *et al.* 2004). In addition, lack of *Nobox* was also shown to induce down-regulation of genes preferentially expressed in oocytes including growth differentiation factor 9 (*Gdf9*) and *Bmp15* (Rajkovic *et al.*, 2004; Krotz *et al.*, 2009). The transcription factor Sohlh2 was also shown to be critical for maintenance and differentiation of the oocyte during early mouse oogenesis (Choi *et al.*, 2008a). Following knockout of this gene in mice, the majority of follicles were lost prenatally while primordial follicles were unable to progress through development and exhibited abnormal expression of several germ-cell

and oocyte-specific genes (Choi *et al.*, 2008a). Another germ cell-specific gene, *Sohlh1,* encodes a basic helix-loop-helix protein (Pangas *et al.*, 2006). This particular gene has also been shown to be essential for oogenesis regulating the transcriptional stimulation of *Lhx8* and *Zp1* promoter activity, both of which are crucial for the primordial to primary follicle transition (Pangas *et al.*, 2006). The Lhx8 transcription factor in particular is critical for early follicle formation and oocyte differentiation as shown in murine studies and it acts by regulating the Nobox pathway (Choi *et al.*, 2008b). Both *Sohlh1* and *Sohlh2* were shown to have similar effects on the male gonad impairing spermatogonia progression and their mechanism of action was shown to be induced by stimulating transcription of the *Kit* gene (Barrios *et al.*, 2012). Oocyte-derived factors Bmp15 and Gdf9, both members of the transforming growth factor β (TGFB) superfamily, are also involved in follicle activation, however activation of follicles can initiate in their absence (Choi and Rajkovic, 2006). None-the-less, exogenous supplementation of *Bmp4* and *Bmp7* has been shown to enhance the primordial to primary transition (Drummond, 2005). Expression of mammalian target of rapamycin (mTOR) is also essential with inhibition of this protein in human *in vitro* cultures of ovarian cortical strips resulting in the destruction of the oocyte by the adjacent granulosa cells (Mclaughlin *et al.*, 2011). A tumour suppressor gene phosphatase and tensin homolog (*Pten*), is another gene that when lacking, the entire primordial follicle pool is activated, leading in the depletion of follicles and resulting in POF in mice (Adhikari *et al.*, 2010).

Somatic cell factors are also important for follicle development beyond the primordial stage. Deletion of the stem cell factor gene also known as Kit ligand (Kitl), expressed in granulosa cells was shown to impair mouse oocyte growth and follicle development (Moniruzzaman *et al.*, 2007). The Müllerian inhibiting substance also known as anti-müllerian hormone (AMH) is a granulosa cell factor that acts as an endogenous inhibitor of follicle growth (Durlinger *et al.*, 2002a). Even though early growth is independent of gonadotrophins, small growing follicles are responsive to follicle stimulating hormone (FSH). Different studies have shown that FSH receptor (FSHR) localizes exclusively on the granulosa cells of the rat, pig, sheep, cow and human with the expression starting from the primordial to primary follicle transition in some species and from secondary stage follicles in others (Sites *et al.*, 1994; Rannikki *et al.*, 1995; Yuan *et al.*, 1996; Oktay *et al.*, 1997). The reduction of the oestrogen levels in cattle has been shown to be tightly correlated with fetal follicular activation, indicating that

control of oestrogen production is essential for follicle activation (Yang and Fortune, 2008). Further to this, Forkhead box protein L2 transcription factor expression by granulosa cells in mice is essential for activation of follicles (Pisarska *et al.*, 2004).

1.2.4 Preantral follicle development

Granulosa cell numbers increase exponentially as the follicle develops (Channing *et al.*, 1980). During the primordial to primary transition, 2 layers of undifferentiated stromal cells are formed around the developing follicle (Orisaka *et al.*, 2006). When the follicle is recruited, these layers differentiate into the theca interna and the theca externa (Young and McNeilly, 2010). This stage is termed the secondary stage of follicle development and it is characterized by the development of a thecal blood supply in addition to the beginning of follicular fluid secretion from the granulosa cells which leads to follicle expansion (Young and McNeilly, 2010). The size of the follicles before cavity formation (pre-antral follicles) reaches 250 μm in humans and 200 μm in mice (Gosden *et al.*, 1989; Picton and Gosden, 2000). These early stages of development are characterized by the involvement of multiple paracrine factors in the communication between the oocyte and somatic cells with *Bmp15* and *Gdf9* in particular having significant roles. In null mice for *Gdf9* it has been shown that theca cells fail to organise around follicles and there is abnormal oocyte growth (Elvin *et al.*, 1999). In addition, granulosa cells fail to proliferate in primary follicles following *Gdf9* knockout (Dong *et al.*, 1996). This illustrates the importance of oocyte-granulosa cell interactions during the early stages of folliculogenesis. Regarding somatic cell factors, several factors including TGFB, follistatin, activin-like receptor kinases (ALK) 3, 5 and 6 and inhibin beta a (INHBA) have been found to be expressed in sheep preantral follicles (Mcnatty *et al.*, 2007). In particular, AMH has been shown to inhibit preantral follicle development, while insulin-like growth factors (IGF) 1 and 2 have been shown to stimulate development *in vitro* (Silva *et al.*, 2009). Growth hormone (GH) has also been related with survival of the preantral follicles (Slot *et al.*, 2006). During the transition from the preantral to early antral stage, follicle growth has been shown to be unaffected by the absence of gonadotrophins (Cattanach *et al.*, 1977; Halpin *et al.*, 1986), but FSH has been shown to stimulate growth (Mcgee and Hsueh, 2000; Fortune, 2003). Specifically, FSH is associated with bovine late preantral follicle diameter increase in addition to stimulation of growth and antral cavity formation (Hulshof *et al.*, 1995). Additionally, histological examinations of women with hypo-gonadotrophic hypo-gonadism have shown multi-layer follicle development in the ovaries (Goldenberg *et al.*, 1976). In

sheep, the effect of gonadotrophin supplementation in the culture media was tested on antrum formation of frozen-thawed granulosa oocyte complexes with the follicles grown in media lacking gonadotrophins resulting in reduced antrum formation (Newton *et al.*, 1999). None-the-less, the oocytes that survived the 30 days of culture were viable and had increased diameters (Newton *et al.*, 1999). In mice, luteinising hormone (LH) has been shown to be required for *in vitro* development of small preantral follicles (Wu *et al.*, 2000; Lefebvre *et al.*, 2002).

1.2.5 Antral follicle development

The next stage of development is the antral follicle with this stage marked by the formation of the antrum, a fluid filled cavity containing muco-polysaccharides and serum transudate (Pan *et al.*, 2005). This cavity is formed when fluid derived from the serum is attracted by an osmotic gradient between follicle and serum in the theca cell vasculature (Pan *et al.*, 2005). Antrum development is characterised by continuous granulosa and theca cell proliferation which is correlated with antrum volume increase. As the antrum forms, granulosa cells differentiate into a thin layer of cells that surround the oocyte, termed cumulus oophorus and to the mural granulosa cells that line the follicle wall. Healthy oocytes maintained at the GV stage of the oocyte form a heterologous gap junction syncytium-like structure with the surrounding layers of compact cumulus cells termed cumulus oocyte complex (COC) (Hunter *et al.*, 2004). Homologous gap junctions between granulosa cells as well as between theca cells are also important for follicle and oocyte development. In the mouse, the oocyte is attached to the mural layer and it acquires the capacity to resume meiosis at the same time as antrum formation (Eppig *et al.*, 1996).

Sex steroids have important roles in the growth and differentiation of the reproductive tissues. Cholesterol is the precursor to all steroid hormones including androgens, oestrogens and corticosteroids (Armstrong *et al.*, 1981). Different studies have formulated a hypothesis named the 2 cell, 2 gonadotrophin theory of ovarian steroidogenesis (Figure 1.3) (Baird *et al.*, 1974; Moon *et al.*, 1978; Armstrong *et al.*, 1981). The 2 cell, 2 gonadotrophin model suggests that LH stimulates androgen production by the theca cells. Thereafter, androgens defuse through the basal lamina and are converted to oestrogen by the aromatase enzyme in granulosa cells following FSH action upon them (Armstrong *et al.*, 1981). This model has been used to explain follicular oestrogen biosynthesis in several species including rat, pig, cow and rabbit

(Holder *et al.*, 1981; Mathews *et al.*, 1986; Murphy *et al.*, 1987). In accordance with this theory, a study in mice has shown that deletion of the *Lhr* gene resulted in the halting of follicle development at the antral stage even when exogenous gonadotrophins were supplied (Ahtiainen *et al.*, 2007).
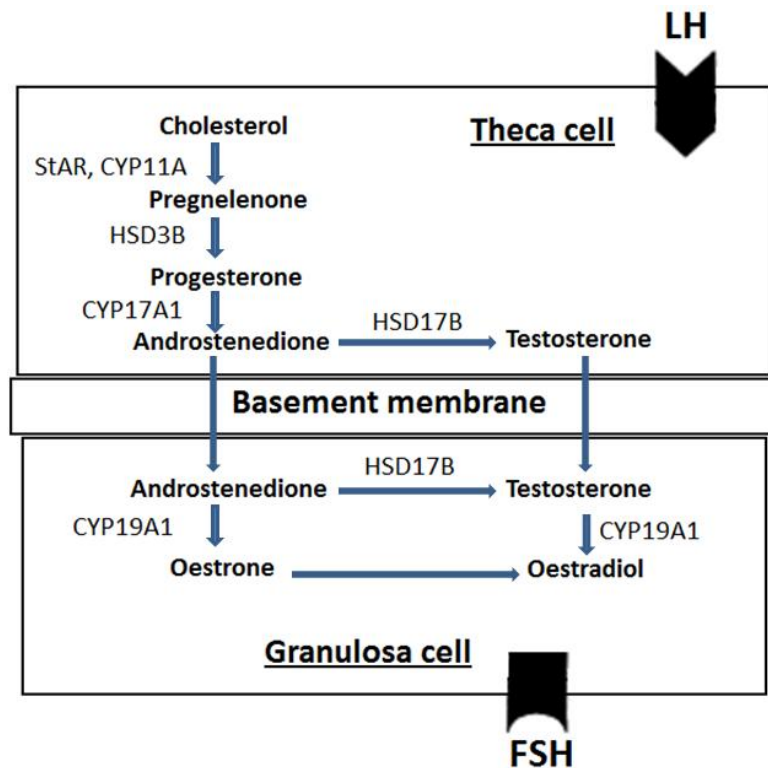
Figure 1.3: Schematic representation of the 2 cell, 2 gonadotrophin theory of ovarian steroidogenesis, according to which the ovarian steroids are synthesized from the co-operation of theca and granulosa cells. Originally in the theca cells, LH that binds to its receptor (LHR) stimulates the expression of steroidogenic enzymes that are essential for the production of androgens. Specifically, the steroidogenic acute regulatory protein (STAR) protein is responsible for the gathering of cholesterol inside the mitochondria where it is converted to pregnelenone by the cholesterol side-chain cleavage enzyme (CYP11A1). From there, pregnelenone is dispersed inside the endoplasmic reticulum and is metabolized by either the action of 17α-hydroxylase/17, 20-desmolase (CYP17A1) or hydroxysteroid dehydrogenase 3β (HSD3B) to produce dehydroepiandrosterone or progesterone respectively. The dehydroepiandrosterone is then either converted to androstenedione by HSD3B or to androstenediol by hydroxysteroid dehydrogenase 17β (HSD17B). Testosterone is synthesised from androstenedione by the action of HSD17B. Alternatively, androstenedione diffuses into the granulosa cell and by the actions of FSH can be used as a substrate for oestrone synthesis by the aromatase cytochrome P450 19 enzyme (CYP19) or testosterone synthesis by HSD17B. Oestrone and testosterone are converted to oestradiol-17β by HSD17B and CYP19A1 respectively. Image adapted from Payne and Hales, (2004).

The pituitary gonadotrophins FSH and LH are the major trophic hormones that drive follicular development. Both hormones bind to receptor proteins in the follicle (Simoni *et al.*, 1997). The gonadotrophin receptors belong to the family of G protein-coupled receptors (GPCRs) which are trans-membrane proteins characterised by hydrophobic helices inserted in plasma-lemma and by intracellular and extracellular domains

(Gudermann *et al.*, 1995). The biological effects of the gonadotrophins occur as a result of a cascade of events following the coupling of the intracellular part of the gonadotrophin receptor to a G protein (G) that results in receptor activation by the hormonal interaction with the extracellular domain (Simoni *et al.*, 1997). It is believed that at the stage of antral follicle development, increased sensitivity towards FSH builds up and the majority of follicles undergo atresia. The role of FSH is defined by the alteration of granulosa cell gene expression, increased proliferation of somatic cells and formation of the antrum for the separation of the COC from the mural layer of endocrine cells. This is caused by FSH action on granulosa cells which results in oestrogen production. In particular, FSH stimulates proliferation of granulosa cells by acting as a mitogen. In addition, FSH synergises with epidermal growth factor (Egf) for the initiation of proliferation and differentiation of granulosa cells as shown by a study in hamsters where Egf mediates the FSH effect by stimulation of the Egf receptor (Egfr) kinase that initiates DNA synthesis (Yang and Roy, 2006). Oestrogens that are produced following the action of FSH are potent mitogens themselves and can drive cell proliferation both *in vivo* and *in vitro* (Quirk *et al.*, 2004).

The moment at which FSH becomes required (gonadotrophin-dependant phase of follicle development), is as soon as granulosa cell proliferation and follicle growth reaches the stage at which cumulus cells are separated from mural granulosa cells. This separation suggests that control of mural granulosa cell function might be regulated by different factors and hormones than those originating from the COC (Richards, 2001a). In fact, there is growing evidence for the presence of survival factors for sustainability of folliculogenesis (Mcgee and Hsueh, 2000). A study in rodents has shown that culture of preantral follicles in serum-free conditions results in apoptosis even if the follicles are treated with gonadotrophins or cyclic adenosine monophosphate (cAMP) analogs (Mcgee *et al.*, 1997). None-the-less, the system in which follicles were cultured in the above study might have been suboptimal, thus resulting in the observations of the study. Even so, transition of small antral follicles to preovulatory follicles is not only dependent on gonadotrophins but on local organizational factors as well. The oocyte itself takes a part in antrum formation as shown when human cultured preantral and antral granulosa cells were unable to form antrum in the absence of an oocyte (Huang *et al.*, 2006). Oocytes from different species including mouse, rat and cow express fibroblast growth factor 8 (*FGF8*) at this stage, although oocyte-specific factor *Gdf9*, *Bmp15* and *Fgf8* transcripts are reduced during early antral formation in the mouse (Pan

et al., 2005; Sanchez *et al.*, 2009). Human oocytes were also shown to express *EGF* and *EGFR* after the preantral stage (Bennett *et al.*, 1996). It is hypothesised that within the antral follicle, mammalian oocytes continue to affect the surrounding granulosa cells with the production of oocyte secreted factors such as GDF9, BMP15 and BMP6 (Eppig, 2001). Studies in sheep have shown that BMP15 is necessary for development to the preovulatory stage (Juengel *et al.*, 2002). In addition, both Bmp15 and Bmp6 in rats were shown to suppress the expression of FSHR (Otsuka *et al.*, 2000). In a similar matter, Gdf9 has been shown to suppress both the FSH stimulated steroidogenesis and the FSH induced formation of the LHR (Vitt *et al.*, 2000). Progesterone secretion following gonadotrophin stimulation was shown to be inhibited by Bmp6, Bmp15 as well as Gdf9 (Otsuka *et al.*, 2001). In particular, Gdf9 has been shown to suppress the P450 aromatase activity (Vitt *et al.*, 2000). Studies in sheep and cow have shown that GDF9 and BMP15 alone and in combination can suppress the FSH-induced progesterone secretion (Mcnatty *et al.*, 2005).

Somatic cell factors are also regarded as essential for antrum formation. This is because in the female reproductive system, granulosa cells are the only cells expressing FSHR. In addition, insulin-like growth factors (IGF) 1 and 2 have been shown to induce antrum formation in serum-free cultures of bovine follicles (Itoh *et al.*, 2002). Further supporting evidence comes from *Igf1* knockout studies in mice, where the follicular antrum is not formed (Baker *et al.*, 1996). In bovine follicles, addition of *IGF1 in vitro*, drives antrum formation (Itoh *et al.*, 2002). The 2 TGFB superfamily members in particular, inhibins and activins, that are up-regulated by FSH action upon granulosa cells, are considered as key regulators of gonadotrophic stimulation. Both activins and inhibins act on the oocyte as well as the granulosa cells and have been shown to promote *in vitro* maturation of primate oocytes (Alak *et al.*, 1996). Inhibin A can suppress pituitary FSH by negative feedback on the anterior pituitary and increase LH induced androgen synthesis in human theca cells (Hillier *et al.*, 1991). Inhibin B on the other hand, has an important role in follicle development and regulation of FSH. Inhibin B is secreted by granulosa cells of preantral follicles while Inhibin A is secreted from small antral follicles (Fraser *et al.*, 1999; Welt and Schneyer, 2001). Both inhibins are made of 2 subunits with Inhibin A having the $\alpha\beta_A$ subunits and Inhibin B the $\alpha\beta_B$ which is the predominant form in the follicular fluid (Groome *et al.*, 1996). Binding of FSH to its receptor results in the increase of cyclic adenosine monophosphate (cAMP) levels with the cAMP response element binding protein up-regulating the inhibin gene by

binding to its promoter regions (Bernard *et al.*, 2001). Activins on the other hand stimulate FSH production and granulosa cell proliferation (Mclachlan *et al.*, 1989). In mammals including humans and rats, theca cell cultures in the presence of both LH and activin resulted in reduced levels of androgen production (Muttukrishna *et al.*, 2004).

Activins have different forms (A, B, AB) and function as homodimers like Activin A: βAβA and Activin B: βBβB or heterodimers like Activin AB: βAβB (De Kretser *et al.*, 2002). Other homodimers have also been identified including (C, D, E) that have not been shown to stimulate FSH production (Hotten *et al.*, 1995). The mechanism by which activins act is the serine/threonine kinase cell surface receptors found on granulosa cells, where activin binds initially to the activin type I receptor (ACTRI) which then recruits the type II receptor, ACTRII (Findlay *et al.*, 2002). Follistatin, also known as activin-binding protein, is another molecule secreted from the cells of the pituitary shown in rats which has been shown to have an inhibitory effect on FSH secretion which might be induced through neutralisation of pituitary Activin A (Ling *et al.*, 1986; Muttukrishna and Knight, 1991; Liu *et al.*, 1996).

Another factor that influences folliculogenesis at this stage of development is AMH which is expressed in the granulosa cells from the primary stage until the early antral stage in mice and from the primordial stage until the mid-antral stage in humans (Durlinger *et al.*, 2002a; Durlinger *et al.*, 2002b; Visser and Themmen, 2005). As discussed previously, AMH regulates the recruitment of primordial follicles (Durlinger *et al.*, 2001). It has been shown however that recombinant AMH inhibits late pre-antral murine follicles from entering the gonadotrophin-dependent phase, indicating a continuous functional involvement of AMH in folliculogenesis (Durlinger *et al.*, 2001). The actions of inhibins and activins as well as IGF1 suggests that there must be a feedback mechanism in follicles involving inhibins, activins, binding proteins, gonadotrophins and growth hormone (GH, Roche, 1996). The FSH and Igf pathways interact with each other and consequently activate specific kinase cascades like the serum and glucocorticoid-inducible kinase and protein kinase B (PkB) that activate transcription factors and survival pathways including expression and movement of glucose transporter type-4 to the plasma membrane (Gonzalez-Robayna *et al.*, 2000; Richards, 2001b). Overlapping hormonal cascades like this are responsible for the maintenance of follicle development to this stage.

1.2.6 Preovulatory follicle development

In monovular species, amongst the group of antral follicles, 1 is selected to continue to grow and to produce higher levels of oestrogens and inhibins (Zeleznik, 2004). This results in the suppression of the pituitary levels of FSH and the rest of growing follicles are subsequently deprived of FSH which is the ultimate survival factor and hence follicles cannot enter the gonadotrophin-dependent stage of development and they undergo atresia (Dizerega and Hodgen, 1981). During preovulatory development, biochemical remodelling of the follicle occurs. During differentiation of bovine preovulatory follicles, more than 7500 genes are activated in their somatic cells (Skinner *et al.*, 2008). Indeed, different stages of follicle development activate the transcription of different genes. Some of these genes are necessary for the progression of follicles to the preovulatory stage.

Specifically, the aromatase cytochrome P450 19 enzyme (*CYP19A1),* responsible for the production of the aromatase enzyme that regulates production of oestrogens, has maximal activity during preovulatory follicle development. In a similar manner, LHR is acquired in granulosa cells from the latter stages of antral development (Jeppesen *et al.*, 2012). The LH sensitivity and aromatase activity initiated by binding of LH to granulosa cell receptors results in the abundant secretion of oestrogens which are required for the terminal stages of ovulatory follicle development. The follicle that expresses both *CYP19A1* and *LHR* is 'selected' from the cohort of growing antral follicles to become the dominant follicle while growth of the rest of the follicles is inhibited. The rising levels of oestrogen produced by the dominant follicle that are secreted into the ovarian vein have a negative feedback on the secretion of pituitary FSH, thus impairing the ability of less advanced follicles to enter the gonadotrophin-dependent stage of development. Exogenous administration of FSH during the follicular phase therefore counteracts the natural follicular phase suppression of FSH and so stimulates the development of more than 1 preovulatory follicle (Edwards *et al.*, 1972).

Studies in sheep have shown that during the follicular phase of the oestrous cycle, the increased secretion of oestrogen from the preovulatory follicle is due to episodic pulses of LH which occur with increasing frequency (Baird, 1978). In the adult non-pregnant sheep, secretion of FSH results in the continuous growth and development of antral follicles to a size around 3-5 mm (gonadotrophin-responsive stage of development) with further development depending on adequate stimulation by LH (Baird and McNeilly,

1981). During both seasonal anoestrous and the luteal phase of the sheep oestrous cycle, LH pulses are not frequent enough to stimulate oestrogen production at the levels necessary to induce the preovulatory gonadotrophin surge (Baird and McNeilly, 1981). The frequency of LH pulses is controlled by the levels of another steroid hormone, progesterone. The elevated levels of progesterone which are found during the luteal phase of the oestrous cycle in combination with low levels of oestrogen result in low frequency LH pulses which cannot support growth of the dominant follicle if dominance is acquired at this stage of the cycle (Kasa-Vubu *et al.*, 1992). At the time of luteal regression in the sheep, the frequency of LH pulses increases due to the fall in progesterone secretion with a resultant increase in androgen synthesis by the theca cells (Baird, 1978). The increasing levels of oestrogen from the growing dominant follicle will eventually induce the gonadotrophin releasing hormone (GnRH) surge leading to a preovulatory surge of LH and FSH (Moenter *et al.*, 1990). When the dominant follicle regresses, the levels of oestrogen and inhibin production are reduced and the inhibition of FSH secretion from the pituitary is withdrawn. Thereafter a new rise in FSH will result in the recruitment of a new crop of small antral follicles that enter the gonadotrophin-dependent phase of terminal growth (Adams *et al.*, 1992). Dominance acquired at the follicular phase of the oestrous cycle, results in further development due to positive feedback of oestrogen on the hypothalamic-pituitary-ovarian axis and the resulting high frequency of LH pulses. In humans, the fall in progesterone and oestrogen during luteal regression is followed by the increase of the concentration of gonadotrophins with the LH pulse frequency increasing from <1 pulse per 6 hours during the mid-luteal phase, to around 4 pulses per 6 hours during the early follicular stages of the cycle (Backstrom *et al.*, 1982).

The LH surge itself initiates the expression of a number of genes, while somatic cells act in an autocrine and paracrine way in order to promote further development (Richards, 2001a). The follicular programme of gene expression in granulosa cells stops with the gonadotrophin surge and at the same time several genes such as cyclo-oxygenase 2, hyaluronan synthase 2 (*HAS2*) and tumour necrosis factor α stimulated gene 6, that control cumulus expansion are activated in the cumulus granulosa cells, while LH acts directly on somatic cells of the follicle and indirectly on the cumulus cells.

The action of the LH surge upon granulosa cells is also responsible for the expression of genes required for COC maturation and follicular luteinisation and ovulation (Richards *et al.*, 1998). Several signalling pathways are thought to be involved in this process including the protein kinase A (PKA) pathway, the cyclic guanosine monophosphate (cGMP) and the mitogen activated protein kinase (MAPK) cascades 1 and 3 (Duggavathi and Murphy, 2009; Fan *et al.*, 2009). Interestingly, studies in mice have shown that the follicular Egfr network mediates the LH-induced maturation of the COC (Conti *et al.*, 2006). Three members of the EGF family, amphiregulin (Areg), epiregulin (Ereg) and betacellulin (Btc) are induced by LH in mural granulosa to bind to the Egfr and induce COC maturation (Park *et al.*, 2004; Hsieh *et al.*, 2007). Their necessity for maturation of the cumulus cells *in vitro* has been indicated as these ligands have been shown to induce oocyte maturation in COC cultures but not in cultures of denuded oocytes (Park *et al.*, 2004). In addition, mutant mice for *Egfr* and *Areg* as well as double mutant animals were unable to undergo complete COC mucification and expansion, further exemplifying the necessity of the Egfr network in COC maturation *in vivo* in this species (Hsieh *et al.*, 2007). Recent data in sheep further support the hypothesis that AREG and EGFR are involved in gonadotrophin-induced cumulus expansion and oocyte maturation for oocytes matured *in vitro* (Cotterill *et al.*, 2012). The signalling of EGF is therefore a prerequisite for cumulus expansion and re-initiation of meiosis. Expression of *EREG* and *AREG* is induced by PKA following the LH surge and the downstream effectors of EGFR in cumulus cells are MAPK3/1 which are subsequently phosphorylated leading to COC maturation (Fan *et al.*, 2009). Another study in mice showed that *Egfr* knockout reduced the expression of *Gdf9* and *Bmp15* in the cumulus cells (Su *et al.*, 2010). Furthermore, removal of oocytes from COCs resulted in reduction of *Egfr* in cumulus cells with the levels restored after treatment with recombinant *Gdf9* or recombinant *Gdf9* with *Bmp15* (Su *et al.*, 2010). In addition, blocking phosphorylation of small body size (Sma-) and mothers against decapentaplegic (Mad-) related protein 2/3 (Smad2/3) *in vitro*, inhibits *Egfr* expression in COCs, with similar phenotype resulting *in vivo* by knocking out *Smad2* and *Smad3* (Su *et al.*, 2010).

A number of other factors have been shown to be critical for COC maturation and ovulation. Prostaglandins are examples of other somatic factors required for ovulation. Specifically, prostaglandin endoperoxide synthetase 2 (PTGS2) has been shown to be a downstream effector of the EGF response in granulosa cells (Park *et al.*, 2004).

Blocking this gene stops cumulus expansion and does not allow progression of growth and ovulation (Park *et al.*, 2004). Granulosa cell receptors are also required for ovulation. Progesterone receptor knockout in mice results in developmental halt prior to ovulation while oestrogen receptor α knockout prevents development to the preovulatory stage and oestrogen receptor *β* knockout results in sub-fertility (Conneely *et al.*, 2000; Hewitt *et al.*, 2005).

1.2.7 Peri-ovulatory follicle development and oocyte control of granulosa and cumulus cell function

Prior to ovulation, the follicle undergoes significant changes. The LH surge stimulates the COC expansion (Duggavathi and Murphy, 2009). The cumulus oophorus structure in mice is consisted of around 3000-5000 cumulus cells that are held together by a gap junction network and an extensive extracellular matrix before and after gonadotrophin surge respectively (Zhuo and Kimata, 2001). The cumulus oophorus matrix is rich in hyaluronic acid as shown by studies in mice (Salustri *et al.*, 1989). Cumulus cells secrete hyaluronic acid following gonadotrophin stimulation (Tirone *et al.*, 1997). Synthesis of hyaluronic acid in the cumulus oophorus is controlled by the messenger ribo-nucleic acid (mRNA) expression of *Has2* (Fulop *et al.*, 1997). The preovulatory deposition of the cumulus oophorus matrix results in the enlargement of COC and dissociation of the complex from the follicle wall which is thinned and broken down, followed by ovulation and transportation of the COC through the oviduct, while the oocyte resumes meiosis as characterised by germinal vesicle (GV) breakdown (GVBD) and extrusion of the first polar body by the oocyte (Zhuo and Kimata, 2001).

The LH surge-induced ovulation involves a continuous cross talk between the mural granulosa cells, the cumulus cells and the oocyte. Following the LH surge, different signalling pathways including the calcium-dependent pathway, phosphoinositol pathway, chloride ion influx and cAMP-dependent pathway are activated through the trans-membrane LHR in the granulosa and cumulus cells (Amsterdam *et al.*, 1999; Cooke, 1999; Mattioli and Barboni, 2000). In the cAMP dependent pathway in particular, the responses to the oocyte are transmitted through the gap junctions (Mattioli and Barboni, 2000). Following the LH surge, the ligand binding of LH to its cognitive receptors activates Gs which then stimulate adenylyl cyclase to increase the levels of intracellular cAMP (Cooke, 1999). The increased levels of cAMP activate the cyclo-oxygenase/Lipoxysenase pathway to produce prostaglandin and leukotriene

(Richards, 2001b). Another action of cAMP is to activate protein kinases to stimulate steroidogenesis (Downs and Hunzicker-Dunn, 1995).

Cumulus expansion is considered as 1 of the key steps for oocyte maturation, ovulation and fertilisation. One or more factors derived from the ovary and termed cumulus expansion enabling factors are considered to drive cumulus expansion (Buccione *et al.*, 1990b). One factor in particular, oocyte-derived Gdf9, which plays an essential role during early follicular development was proposed to be 1 of these factors when it was shown to induce cumulus expansion *in vitro* (Elvin *et al.*, 1999). Null mutation of *Gdf9* in mice resulted in the restraint of cumulus expansion *in vitro* supporting the involvement of this gene as a cumulus expansion enabling factor. In another study, a recombinant form of *Gdf9* was shown to promote cumulus expansion *in vitro* (Elvin *et al.*, 1999). In both of these studies however, folliculogenesis did not progress to the preovulatory stage at which point it is believed that the cumulus expansion enabling factors act (Vanderhyden, 1993). A number of other genes, including *Has2*, cyclo-oxygenase 2, the steroidogenic acute regulatory gene (*Star*) and the Bmp antagonist *Gremlin* have been shown to be induced following *Gdf9* expression in mice granulosa cells (Elvin *et al.*, 1999; Pangas *et al.*, 2004; Rajkovic *et al.*, 2004). In humans, increased expression of those genes has been correlated with better embryo quality (Mckenzie *et al.*, 2004). Another oocyte-derived factor believed to act in a paracrine way at the stage of the preovulatory follicle is BMP15 which is also considered as a potential cumulus expansion enabling factor (Hussein *et al.*, 2005). Addition of *Bmp6* or *Bmp15* to cumulus cells without the presence of oocytes *in vitro* was shown to result in the expression of anti-apoptotic genes such as B-cell lymphoma 2 (Hussein *et al.*, 2005). The role of BMP15 is well established in folliculogenesis. It has been reported to inhibit the induction of FSH-induced progesterone synthesis and it has also been implicated with the inhibition of luteinisation (Otsuka *et al.*, 2000; Shimasaki *et al.*, 2004).

Taken together, a number of other lines of evidence suggest that *BMP15* and *GDF9* are of great importance to mammalian oogenesis. Sheep homozygous for gene mutations that encode the BMP15 and GDF9 protein like the inverdale prolificacy gene (*FecXI*) have been shown to be anovulatory, whereas heterozygous animals for the mutations have higher ovulation rates (Galloway *et al.*, 2000). In addition, immunisation of ewes for either *GDF9* or *BMP15* identified them as crucial for normal follicular development

and for controlling ovulation rate (Mcnatty *et al.*, 2005). Studies *in vitro* have shown that both GDF9 and BMP15 are secreted into media as non-covalently linked homodimers or co-expressed as heterodimers (Liao *et al.*, 2003). In mammals, both GDF9 and BMP15 interact with their target cell(s) through 2 types of membrane serine/threonine kinases of which there are 7 type I receptors (ALK1-7) and 5 type II receptors (ACTRII, ACTRIIB, AMHRII, BMPRII and TGFBRII) (McNatty *et al.*, 2004). From these, GDF9 binds to a TGFB type I and BMPRII receptors and BMP15 binds to a BMPRI and BMPRII (Vitt *et al.*, 2002; Mazerbourg *et al.*, 2004). In sheep, ALK5, ALK6 and BMPRII are found in granulosa cells and oocytes of preantral follicles indicating the involvement of GDF9 and BMP15 in follicular development (Wilson *et al.*, 2001; Souza *et al.*, 2002). The downstream action of GDF9 and BMP15 involves activation of the SMAD proteins (Udagawa *et al.*, 2000; Kloos *et al.*, 2002; Miyazawa *et al.*, 2002). Smad proteins are major signalling molecules that act downstream of the serine/threonine kinase receptors (Heldin *et al.*, 1997). SMADs are divided into 3 classes being the receptor-regulated SMADS (R-SMADS), common partner Smads (Co-SMADS) and inhibitory Smads (I-SMADS). From the R-Smads, Smad2 and Smad3 are activated by activin, nodal and Alk receptors 4, 5 and 7. Other R-Smads including Smad1, Smad5 and Smad8, are activated by Bmp type I receptors Alk3 and Alk6. In mammals, only Smad4 acts as a Co-Smad, while Smad6 and 7 both function as I-Smads (Miyazawa *et al.*, 2002). Signalling of GDF9 has been shown to activate the SMAD2/3 pathway, while BMP15 activates the SMAD1/5/8 pathway (Kaivo-Oja *et al.*, 2003; Moore *et al.*, 2003). However, it is hypothesized that additional second messenger pathways other than the SMAD pathways might also be involved in signal transduction following GDF9 and BMP15 activation, as shown by the inhibition of human granulosa cell proliferation following BMP15 signalling and by the inhibition of the extracellular signal-regulated kinase (ERK)-MAPK pathway (Moore *et al.*, 2003). A recent study has indicated species specific differences in the cooperative actions of GDF9 and BMP15, where the SMAD2/3 but not the SMAD1/5/8 pathways were involved in both ovine and murine species, with the Nuclear factor kappa-light-chain-enhancer of activated B cells pathway and possibly the P38-MAPK pathway being important for mediating signalling following the synergistic action in the sheep, while the ERK-MAPK pathway was involved in signal transduction of murine subjects (Reader *et al.*, 2011).

As it is understood, the role of oocyte-secreted factors is very important for oocyte maturation. In a study conducted in cattle, it was shown that oocyte-secreted factors prevent cumulus cell apoptosis by creating a morphogenic gradient (Hussein *et al.*, 2005). Specifically it was shown that the anti-apoptotic actions of oocytes towards cumulus cells followed a gradient from the site of the oocytes with the layer of cumulus closest to the oocytes demonstrating lower levels of apoptosis while the levels of apoptosis increased with increased distance from the oocyte (Hussein *et al.*, 2005). None-the-less, the role of oocyte-secreted factors is not limited to the prevention of apoptosis or to cumulus cell expansion (Buccione *et al.*, 1990b; Vanderhyden *et al.*, 1992). Oocyte-derived factors perform a number of different functions from inhibition of luteinisation, to the regulation of energy metabolism and sterol biosynthesis (Vanderhyden, 1993; Sugiura *et al.*, 2005; Su *et al.*, 2008). On this basis it is considered that the oocyte drives the cumulus cells to perform a number of tasks which are crucial for the acquisition of oocyte developmental competence and which the gamete itself cannot perform, such as cumulus glycolysis (Sutton-Mcdowall *et al.*, 2010).

1.3 OOCYTE GROWTH AND MATURATION

Throughout folliculogenesis, the oocyte undergoes extensive growth and differentiation. Ovulation results in the release of the COC in most species with the oocyte arrested at the metaphase (MII) stage until fertilization occurs. The oocyte must undergo both nuclear and cytoplasmic maturation. Cytoplasmic maturation will prepare the gamete for fertilisation, activation and embryo development and is considered as the first step initiating the maturation process, while nuclear maturation and progression to the MII stage of meiosis I will result in the reduction of the chromosomes from a diploid to a haploid content (Eppig, 1996; Voronina and Wessel, 2003). The oocyte contains much more RNA and protein than an average somatic cell (Wassarman and Kinloch, 1992). Molecular reprogramming at this stage is important for the oocyte to acquire the expression of genes that are necessary for maturation as well as for the development of the zygote following fertilization until activation of the embryonic genome occurs.

Before the initiation of maturation, the oocyte has a large GV nucleus containing a large nucleolus. The chromosomes of the oocyte at this stage are decondensed and transcriptionally active (Wassarman and Kinloch, 1992). When maturation initiates, this transcription stops and the chromosomes start to condense and the nucleoli disperses (Masui and Clarke, 1979). At metaphase I (MI), the paired homologous chromosomes

are aligned in the middle of the forming meiotic spindle and separation of the paired homologous chromosomes is followed by cytokinesis as marked by extrusion of the first polar body (Voronina and Wessel, 2003). At this stage, the oocyte undergoes molecular reprogramming and the coordinated expression of essential genes result in replication of key organelles such as mitochondria, large numbers of Golgi, generate receptors; and in oviparous animals, gather nutritional reserves for embryonic development (Van Blerkom and Davis, 1995). Following extrusion of the first polar body, the MII oocyte enters a second meiotic block checkpoint which prevents completion of meiosis II. It takes approximately 14 hours (h) for the mouse oocyte to progress to the MII stage (Szollosi *et al.*, 1972), while in species such as sheep it takes up to 24 h (Moor and Crosby, 1985). Nuclear maturation of the oocyte resumes only upon fertilisation or parthenogenetic activation, at which point meiosis will be completed and extrusion of the second polar body occurs.

The gap junctions between the oocyte and somatic cells allow nutrient transfer to the developing oocyte and are the functional unit until the initiation of oocyte maturation (Eppig, 1996). In addition to cytoplasmic gap junctional communications, bidirectional cell to cell communications, as in follicle development, coordinate the development of the oocyte. These interactions are in the form of autocrine, paracrine and endocrine regulation. Gap junctions are not only important for oocyte growth but also for the maintenance of meiotic arrest in the oocyte, by allowing the passage of molecules that inhibit meiotic progression. When the cumulus cells expand and mucify, the gap junctions break and the contact between cumulus cells and the oocyte is lost, resulting in the removal of the inhibitory factors that prevent the resumption of meiosis (Isobe *et al.*, 1998). Studies in sheep have shown that connexin 43 which is 1 of the major gap junctional proteins expressed in the COC is still present between oocyte and cumulus cells suggesting that some sort of communication is still present (Valdimarsson *et al.*, 1993; Pant *et al.*, 2005).

As mentioned previously, the oocyte remains in meiotic arrest for extensive periods. One molecule in particular that has a role in the meiotic inhibition is cAMP, which maintains meiotic arrest (Dekel, 1988). Meiosis I has been shown to progress when cAMP concentrations were reduced *in vitro* (Downs, 1995). Also, oocytes have been shown to resume meiosis when removed from the follicular environment (Edwards, 1965). The oocyte has been shown to be able to produce cAMP without the presence of

cumulus cells (Mehlmann, 2005). However, following the LH surge, gap junctions break and it is generally suggested that this disruption of the communication decreases the concentration of cAMP in the oocyte so facilitating the progression of meiosis (Dekel, 1988). The actions of cAMP for maintenance of meiotic arrest are shown in Figure 1.4.
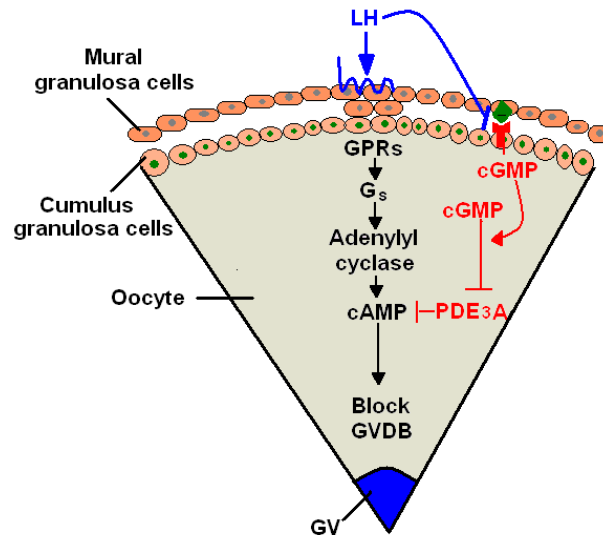
Figure 1.4: Schematic representation of the gap junctional communication in mammals where high levels of cAMP inhibit meiotic maturation. The oocyte produces cAMP by activating the GPCR3/G protein/adenylyl cyclase pathway. Cumulus cells produce cyclic guanosine monophosphate (cGMP) and through gap junctions cGMP is transferred into the oocyte and inhibits phosphodiesterase 3 (PDE3) that hydrolyses cAMP. The oocyte expresses natriuretic peptide receptor 2 which is a guanylyl cyclase in the cumulus cells (shown in red) Mural granulosa cells then secrete the NPR2 ligand, natriuretic peptide precursor type C (shown in green) that induces the generation of cGMP. The LH then binds to the GPCR (blue) and reverses the inhibition of maturation by decreasing cGMP synthesis in the somatic cells and the diffusion through gap junctions. Image adapted from Von Stetina and Orr-Weaver, (2011).

1.3.1 Nuclear maturation of oocytes

Resumption of meiosis is finely controlled by the endocrine actions of gonadotrophins along with intercellular kinases and phosphatases. A number of key proteins take part in the resumption of meiosis with the production of maturation promoting factor (MPF) being an essential component required for the nuclear maturation in oocytes (Abrieu *et al.*, 2001). The progesterone in *Xenopus laevis* and the LH surge in mammals are responsible for the inhibition of adenylyl cyclase that results in the decrease of cAMP levels and the subsequent reduction of PKA activity that results in the initiation of several intracellular signalling cascades. In *X. laevis*, the early events that regulate maturation begin with the induction of the G2/M progression in oocytes and the initiation of the rapid inducer of G2/M progression in oocytes/speedy (Ringo/Spy) that initiate mRNA translation resulting in activation of the cyclin-dependent kinase 2

24

(Cdk2) and aurora kinase A (AurkA) as well as other intracellular signalling pathways (Cheng *et al.*, 2005; Padmanabhan and Richter, 2006; Kim and Richter, 2007). Following the LH surge, disruption of gap junctions is triggered and results in a decrease of oocyte concentration of cAMP further activating MPF for continuation of meiosis (Rime *et al.*, 1992). The MPF is also believed to be involved in disassembly of the nucleus, chromosome condensation, cytoskeletal rearrangements and arrest of transcription (Moreno and Nurse, 1990). The MPF molecule is comprised of 2 different proteins, a regulatory subunit Cyclin B and a catalytic subunit Cdk1 also known as Cell division control protein 2 homolog (Cdc2) (Dunphy *et al.*, 1988). The MPF protein complex is controlled by phosphorylation and dephosphorylation of the 2 subunits. Specifically, MPF is maintained inactive by specific phosphorylation of the Cdc2 kinase while Cyclin B controls meiotic division (Murray and Kirschner, 1989). The molecular event that promotes meiotic maturation and release from the prophase arrest is activation of the Cdk1/Cyclin B (Sagata, 1996). The 2 protein kinases, Wee1 and Mik have been shown to be responsible for the inhibition of Cdc2 phosphorylation (Lundgren *et al.*, 1991). In mammals, regulation of the 2 subunits is achieved by the actions of Cdc25 that is activated following the reduction of cAMP concentration which subsequently removes the inhibition of Cdk1/Cyclin B (Karaiskou *et al.*, 2004). The downstream targets of Cdk1/Cyclin B results in GVBD, spindle assembly and chromosome condensation (Jones, 2004). The CDC25 molecule controls dephosphorylation and activation of MPF and is also a target of MPF and this catalytic loop that is formed might be necessary for the quick activation of MPF (Perry and Kornbluth, 2007). In mice, knockdown of 2 subunits of the constitutive photomorphogenic singnalosome resulted in disrupted activity of MPF accompanied by reduced degradation of the Anaphase promoting complex/Cyclosome (Apc/C) substrates; Cyclin B1 and Securin, demonstrating that constitutive photomorphogenic singnalosome subunits are involved in oocyte meiosis (Kim *et al.*, 2011). The LH surge also activates the MAPK which is another protein involved in cell cycle regulation as well as spindle formation (Liang *et al.*, 2007). The actions of MAPK also include phosphorylation of connexin 43 that results in a reduction of the permeability of the gap junctions (Norris *et al.*, 2008). Breakage of gap junctions results in reduced concentrations of cGMP and the release of phosphodiesterase 3 (PDE3A) which hydrolyses cAMP (Norris *et al.*, 2009). As mentioned previously, the gonadotrophin-induced signalling is transmitted by activation of the Egfr (Conti *et al.*, 2006). Binding of LH to the GPCR activates the G proteins and results in the production of cAMP that

in turn will promote PKA activation followed by synthesis and release of the Egfr ligands (Panigone *et al.*, 2008). The induction of Egfr in mice is necessary for the partial activation of MAPK which inhibits gap junctions (Panigone *et al.*, 2008). In addition, the LH surge induced Egfr activation results in the decrease of cGMP in murine granulosa cells (Vaccari *et al.*, 2009). A protein kinase named Proto-oncogene serine/threonine-protein kinase Mos (c-Mos) has been shown to up-regulate MPF activity in the oocytes from re-initiation of meiosis until fertilisation (Sagata *et al.*, 1989). Blockage of c-Mos activity in mouse oocytes has been shown to prevent meiosis and cause defects during meiosis II (Zhao *et al.*, 1990; Gebauer *et al.*, 1994). In *X. laevis* but not in mammals, c-Mos is required for complete activation of MPF forming a heterodimer with Cyclin B and Cdc2 (Brook *et al.*, 2009). In both mammals and *X. laevis,* c-Mos activates the cytostatic factor that maintains MPF activity causing meiosis MII metaphase arrest (Brook *et al.*, 2009).

It has also been suggested that adenosine monophosphate (AMP) produced following degradation of cAMP by PDE enzymes is involved in the control of nuclear maturation (Bilodeau-Goeseels, 2008). Activity of PDE within the oocyte could result in AMP generation followed by activation of AMP-activated protein kinase (AMPK); known to induce oocyte maturation in arrested mouse oocytes (Downs *et al.*, 2002). However, bovine and porcine oocyte meiotic resumption was inhibited when cultured in the presence of activators of AMPK (Mayes *et al.*, 2007; Bilodeau-Goeseels, 2008).

Other molecules have also been reported to be involved in the maturation process. Oocytes have been shown to overcome the inhibitory effects of cAMP when stimulated with maturation inducing substances (Grondahl *et al.*, 2003). In mammals, follicular fluid meiosis activating sterol is considered as a stimulatory factor for the meiotic resumption of the oocytes (Ruan *et al.*, 1998). This sterol was shown to induce maturation of cumulus denuded oocytes as well as in rat perfused ovaries *in vitro* (Ruan *et al.*, 1998; Hegele-Hartung *et al.*, 2001). Phoshoinositide 3 kinase is another proposed mediator of hormone induced maturation. Phoshoinositide 3 kinase binds to the PKB and this leads to PKB phosphorylation by pyruvate dehydrogenase kinase isozyme 1 (Okumura *et al.*, 2002). The activity of PKB can induce several cellular changes including cell polarisation, entry into the cell cycle, cell survival and oocyte maturation. A target of PKB is the myelin transcription factor 1 (Myt1) which is a kinase that phosphorylates and inhibits Cyclin B. When PKB is phosphorylated, Cyclin B

production results in re-initiation of meiosis (Okumura *et al.*, 2002). It has also been proposed that following increased Cyclin B synthesis and the appearance of active MPF complexes, Myt1 is inhibited upstream of the MPF/Cdc25 amplification loop (Gaffre *et al.*, 2011). An overview of the important signalling cascades and gene expression which occurs during oocyte maturation in vertebrates is shown in Figure 1.5.
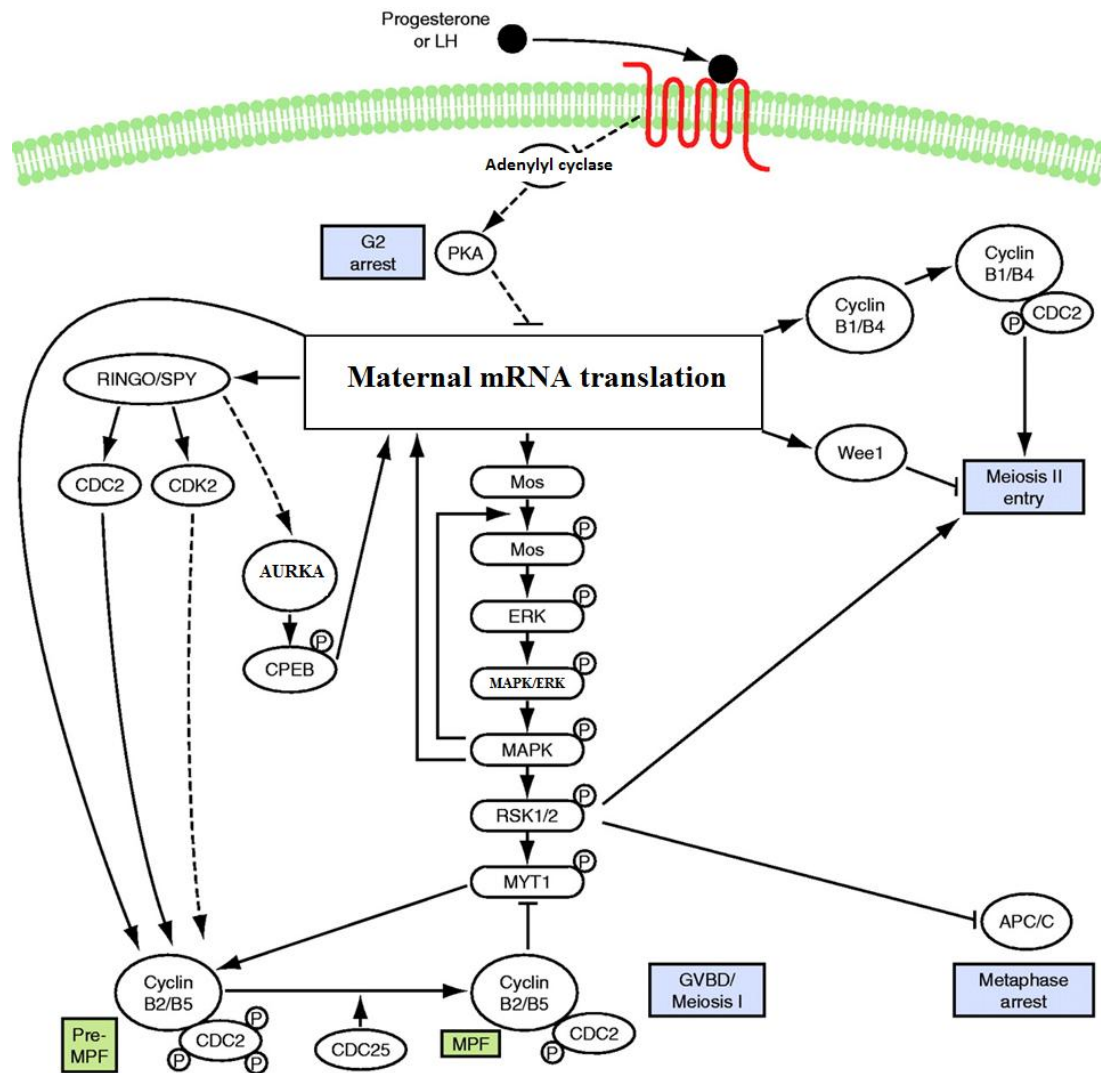
Figure 1.5: Schematic representation of important signaling and gene expression pathways during oocyte maturation in humans. Initially maturation is induced by hormones that activate cascades and translationally regulated mRNA. CPEB: Cytoplasmic polyadenylation binding protein, RSK: Ribosomal S6 kinase. Phosphorylation is shown by an encircled (P). Image adapted from Brook *et al.*, (2009).

1.3.2 Cytoplasmic maturation of oocytes

Other than the correct chromosome separation that consists nuclear maturation, the oocyte also undergoes cytoplasmic maturation which involves reorganisation of its intracellular machinery. Along with this, transcripts within the oocyte must be replicated and packaged in order to assist meiotic progression and early embryo

development. Cytoplasmic maturation therefore includes: (i) cytoskeletal dynamics, (ii) organelle redistribution and (iii) molecular maturation (Ferreira *et al.*, 2009). With regard to cytoskeletal dynamics, spindle formation is essential for the correct chromosome segregation and for the 2 asymmetric cell divisions that involve formation of polar bodies along with the polarised oocyte (Schatten and Sun, 2011). Following the gonadotrophin surge and GVBD, the first meiotic spindle is formed. In mice, around 4 h after meiotic resumption, the MI spindle migrates along its long axis (Verlhac *et al.*, 2000). This migration takes around 4 h to complete and at the end of it, anaphase occurs and the first polar body is extruded (Verlhac *et al.*, 2000). The second meiotic spindle forms following the first polar body extrusion. Following fertilisation and re-initiation of meiosis, the MII spindle rotates 90° before extrusion of the second polar body (Chaigne *et al.*, 2012). Positioning of the spindles is important for the asymmetric divisions and oocyte polarisation that follows (Chaigne *et al.*, 2012). Both oocyte divisions in meiosis for the production of the haploid gamete are very asymmetric and result in different sizes between polar bodies and the oocyte. In mammals, it is considered that the asymmetric divisions help the maintenance of maternal reserve of nutrients and organelles necessary for embryo support in early embryogenesis (Chaigne *et al.*, 2012). An alternative hypothesis is that the reason for the asymmetric divisions is a means to ensure that the sperm only fertilises the large oocyte and not the tiny first polar body (Brunet and Verlhac, 2011).

Microtubules are central to oocyte cytoplasmic maturation. They are cytoskeletal filaments involved in spindle formation which are constructed by asymmetric α/β-tubulin heterodimers which confers microtubule polarity and transport molecules and organelles (Desai and Mitchison, 1997). Microtubule polarity is responsible for the selective transport to one end of the polymer and is mediated by microtubule motor proteins that hydrolyse adenosine triphosphate (ATP). These proteins can be either Dyneins or members of the Kinesin superfamily (Kamal and Goldstein, 2002). Although in spermatogenesis there are centriole microtubule organising centres (MTOCs) that replicate during the S-phase as in mitosis, which results in the formation of the bipolar spindle with fusiform and astral poles, in oocytes, spindle formation is conducted in a different manner (Vogt *et al.*, 2008). In mammalian oocytes, the microtubules originate from the MTOCs but they lack centrioles (Szollosi *et al.*, 1972). The bipolar spindle is formed in the ooplasm as a result of the organisational capacity of the microtubules themselves along with motor proteins and microtubule associated

factors (Karsenti and Vernos, 2001; Eichenlaub-Ritter *et al.*, 2004; Brunet and Maro, 2005). AurkA has been shown to drive MTOC biogenesis in mouse oocytes matured *in vivo* (Solc *et al.*, 2012). Following GVDB the microtubules organise into a bipolar spindle (Albertini, 1992; Brunet *et al.*, 1998). Even though the microtubules have been shown to be able to form the bipolar spindle in the absence of chromosomes, the chromosomes as well as other factors including mitogen activated proteins and motor proteins have been shown to be involved in the regulation of the size of the spindle in correlation with the oocyte (Brunet *et al.*, 1998). In addition kinetochore structures located at the centromeres of both mitotic and meiotic chromosomes bind together with the forming microtubules (Vogt *et al.*, 2008).

Kinetochores are trilaminar structures located on the opposite sides of centromeric heterochromatin at the centromeres of each of the sister chromatids which are bound together by inner centromere proteins and cohesins (Vogt *et al.*, 2008). In mitosis, the kinetochores function to stabilise the microtubules by forming kinetochore fibers and along with the microtubules they result in the transportation of the chromosome to the equator of the spindle, once the 2 kinetochores of each chromosome connect to kinetochore fibers on the opposite spindle poles (Biggins and Walczak, 2003). In mouse oocytes where chromosomes are not able to connect with microtubules and form kinetochore fibers, the chromosomes are transferred to the equator of the spindle by microtubule motors of the kinesin like family (Vernos *et al.*, 1995; Funabiki and Murray, 2000). The chromosomes are then segregated during anaphase of meiosis. These processes are mediated by kinetochore motor proteins including cytoplasmic dynein, conserved centromere protein E and mitotic centromere associated kinesin (MCAK) (Schaar *et al.*, 1997; Maney *et al.*, 1998; Hunter *et al.*, 2003). From these proteins, cytoplasmic dynein is responsible for the direct movement of chromosomes, while conserved centromere protein E contributes to chromosome alignment (Wood *et al.*, 1997). The MCAK protein on the other hand is associated with disassembly of kinetochore fibres that allows movement of the chromosomes during anaphase (Hunter *et al.*, 2003). Aurora kinase B (AURKB) and MAP kinases have been shown to activate MCAK and other proteins associated with the kinetochore (Zhao and Chen, 2006; Ma *et al.*, 2010). AURKB in addition to other molecules like inner centromeric protein (Incenp) and Survivin that belong to the chromosomal passenger complex may be involved in cytokinesis due to the interaction of the chromosomal passenger complex with interpolar microtubules (Kelly *et al.*, 2007). It is considered therefore that both

29

MCAK and AURKB act upstream of the spindle assembly checkpoint that monitors microtubule attachment and tension on chromosomes in both meiosis and mitosis (Vogt *et al.*, 2008). Specifically, spindle assembly checkpoint (SAC) monitors the attachment of spindle fibres on the kinetochores of chromosomes as well as the tension by controlling the pulling forces from spindle fibres before entry into anaphase (Malmanche *et al.*, 2006). Studies in mice have confirmed the presence of SAC, when microtubule dynamics at both meiosis I and II were chemically impaired resulting in meiotic arrest (Eichenlaub-Ritter *et al.*, 2004; Tsurumi *et al.*, 2004).

Other than cytoskeletal dynamics, the second subcategory of cytoplasmic maturation is organelle redistribution. The transport of cytoplasmic organelles during maturation is controlled by cytoskeletal microfilaments and microtubules based on the necessities of the oocyte at different stages of development (Ferreira *et al.*, 2009). The mitochondria which constitute the energy providers of the oocyte by utilising ATP, associate more towards the perinuclear region as oocytes mature from MI to MII, thus changing from their original even homogenous distribution throughout the cytoplasm during growth of the GV oocytes in many species including human and bovine (Stojkovic *et al.*, 2001; Wilding *et al.*, 2001). Studies in mice have shown that the mitochondria rearrange around the MII spindle during meiotic maturation (Li and Fan, 1997). In addition, the number of mitochondria within the oocyte change through development and increase in readiness for maturation as shown in sheep (Cotterill *et al.*, 2013). In several species including human and mice it has also been shown that some polarised mitochondria localise in the sub-cortical/sub-plasmalemmal region of the cytoplasm and are involved in the acquisition of developmental competence (Van Blerkom *et al.*, 2002; Van Blerkom, 2008).

Protein synthesis itself is of imperative importance, not only for oocyte maturation but also for early embryo development. It is therefore essential that an adequate number of ribosomes exists during the maturation process (Ferreira *et al.*, 2009). Ribosomes are synthesised by the transcription of ribosomal RNA (rRNA) genes followed by processing of the transcripts and addition of ribosomal proteins to their subunits. During MI of meiosis, the protein synthesis in cattle oocytes is increased by 3 times in comparison to the GVBD stage, while at the MII, the oocytes exhibit basic levels of mRNA translation (Ferreira *et al.*, 2009).

Other cytoplasmic organelles are also subjected to change during maturation (Figure 1.6). One of these, the Golgi complex, present at the GV stage of bovine oocytes transforms into vesicles during GVBD (Payne and Schatten, 2003). Although the role of the Golgi membranes in maturation is still to be elucidated, there has been evidence to suggest that extracellular matrix proteins are phosphorylated and co-localised only with sites of endoplasmic reticulum in MII oocytes and not with the spindle as in mitosis (Payne and Schatten, 2003). Biochemical changes to the endoplasmic reticulum during maturation play an important role in intracellular calcium regulation (Ferreira *et al.*, 2009). In mammalian species such as the mouse, the endoplasmic reticulum is situated in small clusters of cortical regions throughout the oocyte cytoplasm and as maturation progresses to the MII stage, the endoplasmic reticulum becomes located around the meiotic apparatus (Kline, 2000). During fertilisation, a marked release of Ca^{2+} from the endoplasmic reticulum follows sperm binding. In mouse, Ca^{2+} oscillations depend upon inositol 1,4,5-triphosphate that come from the endoplasmic reticulum (Fitzharris *et al.*, 2007). The cortical granules are derived from the Golgi apparatus and are specific to oocytes (Hoodbhoy and Talbot, 1994). They are responsible for the prevention of polyspermic fertilisation at the ZP to prevent sperm adhesion, a process known as cortical reaction (Hoodbhoy and Talbot, 1994). In order for the cortical reaction to take place, granules migrate to the periphery of the oocyte and become associated with the Golgi apparatus at the MII stage (Fair *et al.*, 1997).
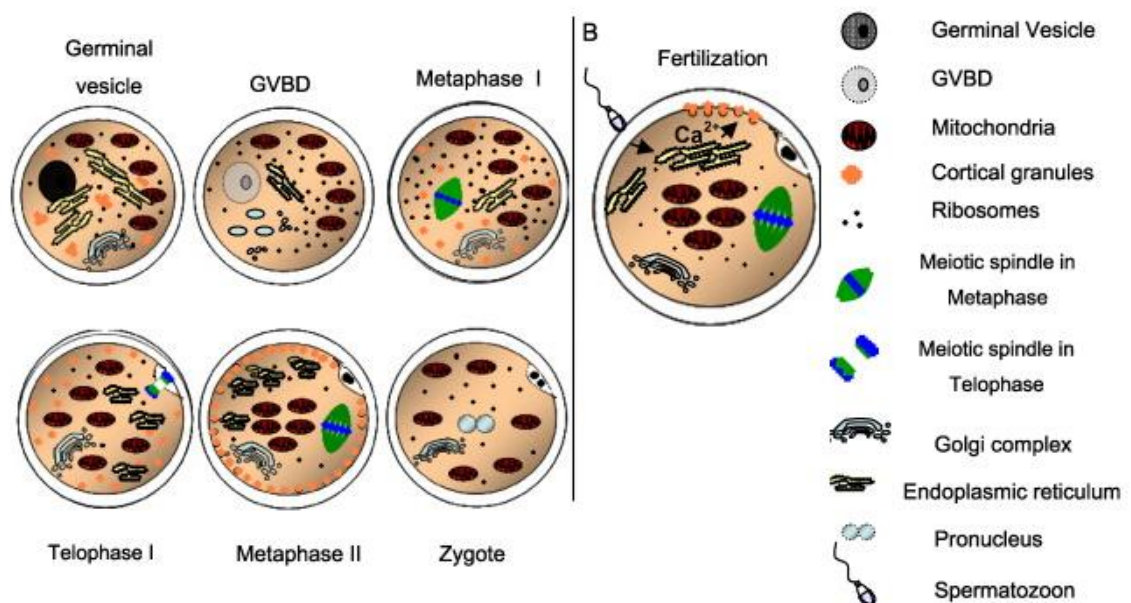
Figure 1.6: Schematic overview of bovine cytoplasmic organelle distribution during oocyte maturation, fertilization and zygote formation. **B:** The mechanism of cortical reaction following Ca^{2+} release when the spermatozoon enters the oocyte. Image adapted fromFerreira *et al.*, (2009).

The third subcategory of cytoplasmic maturation is molecular maturation and this involves the transcription, storage and processing of mRNA that is necessary for oocyte maturation and for the subsequent development, including fertilisation and early embryo development (Figure 1.7).
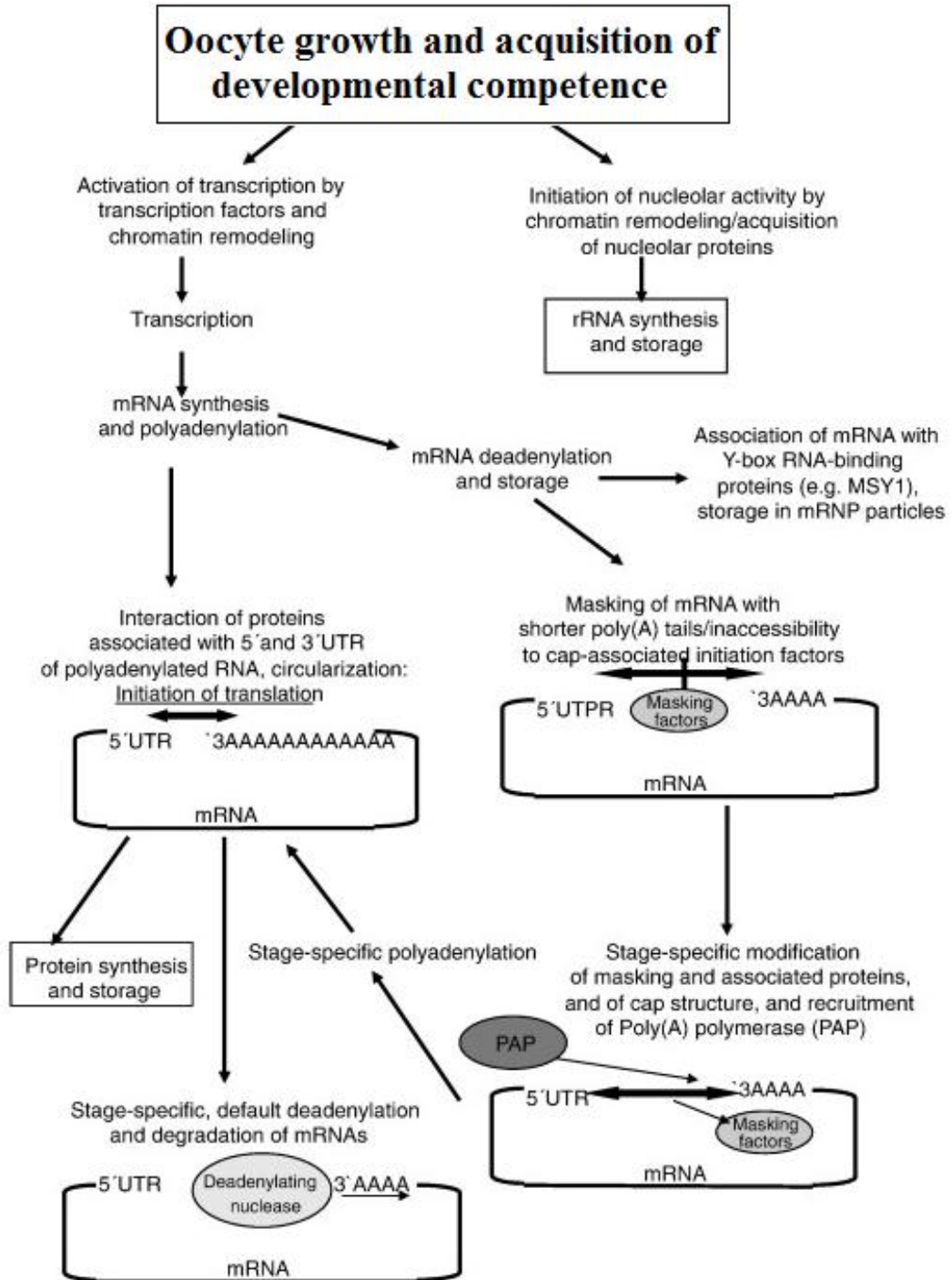
Figure 1.7: Schematic overview of the general events involved in the regulation of expression in the oocyte during growth and maturation. The fate of the mRNAs varies and following transcription, mRNAs can either be translated after polyadenylation or they can undergo deadenylation and be stored to be translated when needed. Gathering of the oocyte transcripts and proteins is necessary for both meiotic and cytoplasmic development. UTR: Untranslated region, PAP: Poly-(A) polymerase, MSY1: Male specific region of the Y chromosome 1. Image adapted from Sanchez and Smitz, (2012).

Since there is no gene expression, the mRNA transcribed during that maturation stage is gathered into an inactive state following the resumption of meiosis (Sirard, 2001). The proteins necessary for fertilisation and early embryo development are therefore stored until they are required (Sirard, 2001). The mRNA in its packed form is protected from nucleolytic degradation (Fulka *et al.*, 1998). There are many mechanisms that take place in order to activate these inactive mRNAs and these include phosphorylation of factors that initiate translation, phosphorylation of ribosomal associated molecules and de-phosphorylation of poly-adenine (A) polymerase (Thach, 1992; Colgan *et al.*, 1996; Gavin and Schorderetslatkine, 1997). The addition of 250 to 300 A residues to the mRNA (polyadenylation) for the formation of the poly-(A) tail, stimulates the release of repressor molecules and initiates translation (Meric *et al.*, 1996). The mRNA is transported to the cytoplasm by splicing the poly-(A) tail whereas shortening the poly-(A) tail inhibits effective translation, while deletion of the poly-(A) tail results in degradation of the molecule (Tomek *et al.*, 2002). Therefore, addition of the poly-(A) tail activates translation and the deadenylation that follows results in the degradation of that mRNA. In the bovine species it was observed that abnormal levels of polyadenylation in some maternal mRNAs of the oocyte were associated with lower developmental competence to the embryo stage (Brevini *et al.*, 2002). The main transcripts produced during molecular maturation of the bovine COC encode molecules like MPF, Cyclin B, CDC2, c-MOS, MAPK, ATP molecules and numerous other important molecules required for maturation (Stojkovic *et al.*, 2001; Calder *et al.*, 2003).

1.4 THE ROLE OF *GTSF1* IN THE REGULATION OF GAMETOGENESIS

As it is understood, there is a complexity of signals regulating follicle and oocyte growth and maturation. Prior to oocyte maturation there are several developmental checkpoints that oocytes and follicles have to progress through and which require the coordination of endocrine, autocrine and paracrine control mechanisms. The oocyte and the somatic cells of the follicle play inter-dependent roles in all stages of development. There are still however many unanswered questions regarding the control of oocyte and follicle development. Therefore, the identification of genes, pathways and mechanisms that drive growth and regulate maturation of both cellular compartments is of importance to advance understanding of these processes. Many genes that are involved in gametogenesis are preferentially expressed in germ cells. There are a lot of expressed

sequence tags available in databases that have allowed the analysis of gene expression profiles *in silico*. One expressed sequence tag which exhibits high expression in the unfertilised oocyte, high expression in the germ cells of the testis or ovary and lacks expression in somatic cells, is *GTSF1*. In addition, germ cell specific-patterns of gene expression during maturation have allowed identification of novel genes from analysis of microarray data (Li *et al.*, 2013). A number of potential genes involved in maturation have been identified with these methods. Global gene analysis from early stages of human folliculogenesis showed high expression of genes including the anti-proliferative trans-membrane protein with an epidermal growth factor-like and 2 follistatin-like domains, the Rho-GTPase-activating protein oligophrenin 1 and the mitochondrial-encoded ATPase6 (Markholt *et al.*, 2012).

Preparations of cDNA libraries from *X. laevis* oocyte mRNA have been used for the isolation of maternal RNAs that are solely expressed in oogenesis and early embryogenesis and are possibly coding for proteins important in oocyte maturation (Dworkin *et al.*, 1985). Using this approach a cDNA clone called *D7.0* (originally *D7*) (Dworkin *et al.*, 1985), derived from *X. laevis* maternal mRNA (*D7* mRNA), was shown to be present throughout oogenesis but decreased after 2 days of embryo development (Smith *et al.*, 1988). Antibodies to the T7 protein that were obtained from immunised rabbits against the T7 polypeptide fused with β–galactosidase recognised a single 36 kDa protein expressed in a developmentally restricted pattern from oocytes until the early stage embryo (Smith *et al.*, 1988). The level of D7 protein was highest in embryos during the first day of development and then was decreased. The first study of the function for D7 protein was attempted by constructing phenocopies of null mutants for D7 by eliminating *D7* mRNA from the *X. laevis* oocyte. This was performed by injecting 20-mer oligonucleotides into oocytes (Smith *et al.*, 1988). The loss of *D7* was shown to affect the progesterone induced maturation process by significantly delaying the time of GVBD. However, it was shown that injections of *D7* RNA into full grown oocytes followed by translation to D7 protein did not induce oocyte maturation or affect the kinetics of hormone-induced maturation (Smith *et al.*, 1991). Unfertilised *X. laevis* oocytes lacking D7 protein could be activated and fertilised and embryos developed normally to the tailbud stage. It was therefore proposed that D7 is not essential for oocyte maturation, activation, fertilisation or early embryonic development in *X. laevis* (Smith *et al.*, 1991). In a later study, in order to examine whether D7 synthesis was associated with the induction of oocyte maturation, agents other than progesterone were

34

tested for their ability to induce D7 synthesis (Smith *et al.*, 1992). The hormones insulin and testosterone were shown to induce D7 protein synthesis and also injections of *X. laevis* Cyclin B1 and c-Mos had a similar effect to progesterone treatment. All of these agents acted through activation of Mpf and crude preparations of Mpf were also shown to induce D7 protein synthesis (Smith *et al.*, 1992). Although Mpf as a protein kinase is believed to induce protein phosphorylation during *X. laevis* oocyte maturation, phosphatases were unable to affect the modification and D7 was not labelled by [^{32}P]-ATP, therefore protein modification of D7 was not shown to be performed through phosphorylation (Smith *et al.*, 1992).

Another study of expression profile analysis *in silico* that used real-time polymerase chain reaction (PCR) also known as quantitative reverse transcription PCR (qRT-PCR) to identify mouse embryonic sequence tags, showed that *Cue110* (a previous name for *GTSF1*) was exclusively expressed at moderate levels in unfertilised oocytes and ovaries and was abundant in the testis of the adult mouse (Yoshimura *et al.*, 2007). The full sequence of the gene was acquired by performing rapid amplification of cDNA ends (RACE)-PCR and as shown in Figure 1.8, the gene is comprised of nine exons with the protein being encoded by 7 exons (Yoshimura *et al.*, 2007).

Using a conserved domain database, it was shown that the gene belongs to the uncharacterised protein family 0224 (UPF0224) similar to the D7 protein identified in *X. laevis* (Yoshimura *et al.*, 2007). Several genes of the UPF0224 exist in many species including invertebrates, showing the evolutionary preservation of this family (Yoshimura *et al.*, 2007). Specifically, there is a 28-48% shared amino acid sequence in the N-terminal region. In addition, a hypothetical protein encoded by the human ortholog-family with sequence similarity 112 member B (FAM112B) was shown to have a 91% identity to the murine *GTSF1*. Using *in situ* hybridisation (ISH), the *GTSF1* gene was shown to be specifically expressed in the differentiating germ cells in both the testis and the ovary of mice (Yoshimura *et al.*, 2007). Specifically, *GTSF1* was expressed from the pre-leptotene spermatocytes to the elongating spermatic in the testis, while in the ovary it was shown to be expressed in the primary oocytes (Yoshimura *et al.*, 2007).. Immunostaining showed that GTSF1 protein was present in the cytoplasm of pachytene spermatocytes and round spermatids while it was not detected in oocytes. Similar results were also supported by real-time PCR and Western blotting (Yoshimura *et al.*, 2007).

Figure 1.8: The murine sequence and structure of the *Gtsf1* gene is shown. (a): cDNA, derived from exons 1–9, is 796 nucleotides long and encodes a 167-amino acid protein. Exon 1.1 is single underlined. (b): Schematic representation of the *Gtsf1* locus. * and @ indicate the positions of the start and stop codons, respectively. Image adapted from Yoshimura *et al.*, (2007).

Initial functional studies of the role of *Gtsf1* during mammalian gametogenesis involved the generation of *Gtsf1* knockout mice (Yoshimura *et al.*, 2009). Although the mice grew normally and appeared healthy in the absence of *Gtsf1*, the males were sterile due to apoptotic death of their germ cells after postnatal day 14, while the null female mice were fertile. In null males, meiocytes were specifically shown to cease meiotic progression before the zygotene stage, thereby indicating the significance of this factor in meiotic progression beyond the early stages (Yoshimura *et al.*, 2009). The same study showed that loss of *Gtsf1* increased the transcription of Long interspersed nuclear elements 1 (*Line1*) and Intracisternal A-particle (*Iap*) retrotransposons and demethylations of their promoter regions, thus leading to a retrotransposon activation (Yoshimura *et al.*, 2009). Recently, it was shown that expression of *Line1* and Iap in the male gonad is regulated by a transcriptional silencing mechanism involving DNA methylation (Aravin and Bourc'his, 2008). This silencing mechanism requires *Mili* and *Miwi2* which are P-element-induced wimpy testis (Piwi) family members that act by recognising specific methylation targets. The silencing mechanism controls the

expression of retrotransposons in the germline, over-expression of which can be deleterious for the offsprings (Aravin *et al.*, 2007a). Although, the effects of *Gtsf1* knockdown did not result in loss of female fertility in mice, it could be that the gene still affects female fertility indirectly. The reason for the sexual dimorphism of the mutants has not been clarified. However, the cellular mechanisms that regulate prophase I events during mammalian meiosis appear to be more sensitive in males than females and this might be the reason for the fertility preservation of female *Gtsf1* knockouts (Hunt and Hassold, 2002). During oogenesis there are 2 meiotic checkpoints, 1 that responds to synaptic failure and 1 that responds to DNA damage, in marked contrast to spermatogenesis where such checkpoints do not exist (Odorisio *et al.*, 1998; Di Giacomo *et al.*, 2005). This is of particular interest considering the high degree of localisation of *Gtsf1* to the cytoplasm of primary follicles and to less extend to primordial follicles in murine ovaries as identified by ISH (Krotz *et al.*, 2009). In addition, expression analysis of *GTSF1* in human ovarian tissue by real-time PCR has revealed expression in primordial, primary, secondary, GV, MII oocytes as well as in pronuclear zygotes and late stage preimplantation embryos (JD Huntriss and HM Picton, unpublished data). Similar data have also been replicated in bovine tissue (Lu *et al.*, 2012).

1.4.1 The function of *GTSF1*

A previously uncharacterised CHHC Zn-finger domain was identified in the *GTSF1* sequence of many species including humans and mice, in addition to U11-48K proteins and tRNA methyl-transferases (TRM13) (Andreeva and Tidow, 2008). Homologs of U11-48K are found in vertebrates, plants and insects and their presence goes hand in hand with the suggested early evolutionary stages of the minor spliceosome (Russell *et al.*, 2006). In contrast, the TRM13 family is found in protozoa, plants and metazoan and in yeast the enzyme catalyses ribose methylation, a modification that is conserved in many species including humans. Both the U11-48K and TRM13 domains are characterised by the presence of 4 invariant Cystein and Histidine residues. The Cystein and Histidine residues are usually involved in metal ion coordination (Morcock *et al.*, 2000; Shi *et al.*, 2005). The size of the identified fragments in addition to their repetitive nature and conservation suggests that this independent domain is folded around a central zinc ion such that it is referred as the CHHC Zn-finger domain (Michalek *et al.*, 2011). There are 2 copies of this motif found in *GTSF1* homologs of different species separated by a short linker (Andreeva and Tidow, 2008). This could be due to a gene

duplication event taking place in the early stages of eukaryotic evolution (Andreeva and Tidow, 2008). This domain does not have any similarity to other characterised Zn-finger domains. Multiple alignment of all previously identified Zn-finger domains showed the presence of several conserved residues that may be a prerequisite for a specific backbone conformation (Andreeva and Tidow, 2008). Also, the positively charged residues might have a functional role. In addition, CHHC Zn-fingers can exist as an independent folding unit (Andreeva and Tidow, 2008). A possible biological function for this motif arises from the fact that the domain is present in 2 protein forms that are known to bind RNA (U11-48K and TRM13) (Turunen *et al.*, 2008). Additionally, the motif contains sequence determinants that can mediate functions like RNA-binding.

Drawn together, the gamete-specific expression patterns of the *GTSF1* gene alongside its conserved domain containing 2 tandem copies of CHHC Zn-finger suggests that the gene may play a role in RNA-binding which makes this gene a very promising candidate for functional investigation in relation to mammalian oocyte development. The importance of RNA-binding is described in detail in the section that follows.

1.4.2 RNA-binding

While the oocyte progresses through maturation, it is necessary to perform transcription, storage and processing of the mRNA that is expressed from the chromosomes which will be later translated by the ribosomes (Ferreira *et al.*, 2009). In eukaryotes, transcription and translation takes place in the nucleus and the cytoplasm respectively and post-transcriptional modification of precursor mRNA (pre-mRNA) enables further gene regulation (Glisovic *et al.*, 2008). Pre-mRNA processing involves splicing, editing and polyadenylation and these are all mechanisms that initiate when pre-mRNA is transcribed. Post-transcriptional modification of mRNA and storage is crucial for translation of important proteins for maturation, fertilisation and early embryo development (Ferreira *et al.*, 2009). It is therefore necessary for some of these proteins to be stored until the stage that are to be employed (Sirard, 2001).

In mouse oocytes, an mRNA storage region has been identified recently called the subcortical ribonucleoprotein (RNP) particle domain (Flemr *et al.*, 2010). In somatic cells, RNPs like processing bodies (P-bodies) as well as stress granules, regulate mRNA metabolism (Balagopal and Parker, 2009). In particular, P-bodies regulate repression of

translation and mRNA decay (Sheth and Parker, 2003). In the germ cells of many species, RNAs are localised to germ cell granules that regulate the maternal RNAs (Anderson and Kedersha, 2006). The germ cell granules contain both stress granule components as well as orthologs of the P-body demonstrating a conserved role of these proteins (Anderson and Kedersha, 2006). Although there are no specific germ cell granules identified in mice, Balbiani bodies which are clusters of organelles in young oocytes have been identified (Kloc *et al.*, 2004; Li *et al.*, 2008). Packaging of mRNA protects it from nucleolytic degradation and the mRNA will remain stored until the appropriate signals are generated for either maturation, zygote formation or early embryo development (Fulka *et al.*, 1998).

Along with RNPs, regulation of pre-mRNA processing is controlled by RNA-binding proteins (RBP) (Burd and Dreyfuss, 1994). The capacity for RBP to bind to RNAs is based upon different specificities and affinities of their sequence (Lunde *et al.*, 2007). The most characterised RNA-binding molecule is the RNA-recognition motif, also known as the RNA-binding domain (RBD) (Lunde *et al.*, 2007). The RBDs are composed of 80-90 amino acids that form a 4 stranded anti-parallel β-sheet with 2 helices packed against it (Oubridge *et al.*, 1994). Thousands of RBDs have been identified so far and most of them function in post-transcriptional modifications (Finn *et al.*, 2006). There are some well characterised RBDs and these domains include the K-homology domain, the Arginine-Glycine-Glycine box, the Sm domain, the Asp-Glu-Ala-Asp (DEAD)/Asp-Glu-Ala-His (DEAH) box, the Zn-finger, the double stranded (ds)RBD, the cold-shock domain Pumilio/Fem 3 binding factor domain and the Piwi/Argonaute/Zwille (PAZ) domain (Baugh *et al.*, 2005; Shalom-Paz *et al.*, 2010). In humans, 0.5-1% of all genes contain RBDs and often in multiple copies within 1 polypeptide (Finn *et al.*, 2006). In other species like *Caenorhabditis elegans* and *D. melanogaster*, studies have shown that around 2% of the genome corresponds to RBDs (Lasko, 2000). This percentage could be even higher due to the number of RNA-binding proteins which have not yet been discovered. One possible explanation for the abundance of RBPs might be evolutionary development of the post-transcription processes by eukaryotes to regulate gene expression (Anantharaman *et al.*, 2002).

The RBPs have various functions and are involved in different cellular processes. Following mRNA translation, post-transcriptional control of gene expression is initiated. This process is largely regulated by RBPs (Finn *et al.*, 2006). The RBPs

associate with mRNA and a lot of different RBPs interact with different small non-coding RNAs (Anantharaman *et al.*, 2002). The resulting RNP complexes that form are implicated in multiple aspects of cell metabolism, like DNA-replication, expression of histone genes, regulation of transcription and translational control (Anantharaman *et al.*, 2002; Glisovic *et al.*, 2008). In addition, RBPs cover every aspect of RNA biology from transcription, pre-mRNA splicing and polyadenylation of mRNA, as well as modification, transport, localisation and mRNA turnover (Hilleren *et al.*, 2001). The role of RBPs extends the regulation of these processes into providing a cross-link between them (Hilleren *et al.*, 2001; Millevoi *et al.*, 2006).

Alternative splicing entails utilisation of RBPs and through this mechanism, the majority of human genes express multiple mRNAs (Johnson *et al.*, 2003). Modification of RNA changes the sequence from the 1 encoded by the genome, thus resulting in an increase of gene products and diversity (Valente and Nishikura, 2005). Although most RNA editing takes place in non-coding regions, some genes have been identified that appear to be edited in their coding regions (Nishikura, 2006). The most common RNA modification is the deamination of adenosine-inosine, which occurs by conversion of an adenosine to an inosine (Valente and Nishikura, 2005).

Polyadenylation, is regulated by RBPs (Jackson and Standart, 1990). Polyadenylation is the addition of adenine of the 3´ terminal portion of the cytoplasmic mRNA, that stimulates the release of repressor molecules that are linked at the 5´ end and in that way initiates translation (Jackson and Standart, 1990). The process of adding a 3´ poly-(A) tail of around 200 nucleotides has a significant effect on the nuclear transport, translation and stability of mRNA (Tomek *et al.*, 2002). All eukaryotic mRNAs undergo polyadenylation except for replication dependent histone mRNAs (Glisovic *et al.*, 2008). Following pre-mRNA processing, mRNA is exported from the nucleus to the cytoplasm where translation takes place. In order for the mRNA to be exported, it must be fully processed. In other words, transcription, splicing and polyadenylation of the mRNA must be completed (Glisovic *et al.*, 2008). Export of mRNA is a complicated procedure in which RBDs have an active role and it involves the generation of a carrier complex inside the nucleus followed by translocation of the complex through the nuclear pore and the subsequent release of the mRNA in the cytoplasm. The carrier complex is then recycled (Gruter *et al.*, 1998). The export of RNA is an energy

dependent process and that different pathways are involved with different RNA species (Gerace, 1995).

Different RNA-binding proteins are involved in mRNA localisation, a process critical for gene expression and regulated protein production. In *Sacharomyces cerevisiae* for example, the absent-small or homeotic mRNA localises to the bud of the daughter cell when it associates with the binding proteins Myosin 4 and Actin (Bobola *et al.*, 1996). In a different example, Beta actin localises to the lamella region in different asymmetric cell types by the help of the Zipcode binding protein 1 (Ross *et al.*, 1997). Regulation of translation can control gene expression and there are many regulatory proteins that control the initiation step of this mechanism in a range of cellular processes like metabolism, cell growth and differentiation (Mootz *et al.*, 2004). Translational silencing during different stages of development is used by many species as a method of translational regulation and offers gene control (Mootz *et al.*, 2004). In transcriptionally active cells, regulation of translation offers accurate spatial and temporal expression of proteins (Berleth *et al.*, 1988). A characteristic example comes from *D. Melanogaster* where it was shown that the *Bicoid* mRNA is localised to the anterior pole of the oocyte only to be translated following fertilisation to create an anterior to posterior protein gradient (Driever and Nusslein-Volhard, 1988). In contrast, although the *Caudal* mRNA is localised in a uniform pattern, its protein is expressed in a posterior to anterior gradient following translational repression of the gene (Rivera-Pomar *et al.*, 1996).

The diversity of RBD functions extends into the regulation of meiotic procedures. The early development of metazoans is regulated by translation and localisation of maternal mRNA in the embryo. This process is achieved by RBDs (Colegrove-Otero *et al.*, 2005). Hermes is 1 of those RBDs found in oocytes of several species from *X. laevis* to *H. sapiens* and it was shown to targets RNA encoding proteins that are involved in meiotic maturation, early cleavage and germline development (Song *et al.*, 2007). Several other RBDs have been identified as mediators of meiotic maturation. The Translin protein, functions as a post-transcriptional regulator of a group of genes in post meiotic male germ cells. Knockout of *Translin* in male mice results in a reduced sperm count as a consequence of apoptosis, which indicates a possible role for *Translin* during meiosis (Cho *et al.*, 2005).

An additional role for RBDs is the regulation of mRNA storage in the oocyte. It is well established that the differentiation of an oocyte into a 2 cell embryo is controlled by regulated translation of maternal mRNAs (Pepling, 2010). In order for this to be achieved, these mRNAs must be stored in the oocyte and activated at the specific time of development (Colegrove-Otero *et al.*, 2005). Other than the subcortical RNP particle domain, several other RBDs have been identified to be involved in the storage of both paternal and maternal mRNAs (Flemr *et al.*, 2010). In *X. laevis*, the Y-box proteins mRNP3 and Frgy2/mRNP4 are major RNA-binding components of maternal storage mRNPs in oocytes (Matsumoto *et al.*, 2003). In mouse male germ cells, the DNA-RNA binding protein Msy2 has been shown to mark specific transcripts for cytoplasmic storage in mouse male germ cells (Yang *et al.*, 2005).

1.5 EVALUATION OF NOVEL GENE FUNCITON

Even though the genomes of a number of species including *C. elegans* (Consortium., 1998) *D. melanogaster* (Adams *et al.*, 2000) and *H. sapiens* (Gregory *et al.*, 2006) have been completely sequenced, the function of the majority of genes remains undetermined. In the post-genomic era, elucidation of gene functions can help in the development of gene based drug targets and therapies. The complexity however of acquiring all protein encoding genes in addition to events such as RNA-splicing and post-transcriptional modification make this a challenging task. In order to overcome it, the whole of non-coding RNAs and their functions must be identified (Appasani, 2004).

Until recently, knockout experiments in mice were the primary method used to determine the function of an unknown gene (Larue *et al.*, 1994; Roy and Matzuk, 2006). This technology however has the disadvantage of being very laborious with the effects taking a long time to become evident. The method of homologous recombination can be difficult and expensive, especially in species in which embryonic stem cells have not been isolated (Gerhard *et al.*, 2004). In addition, the conventional knockout experiments require a lot of time and cannot keep pace with the new sequence information generated by different genome projects, further to the fact that knockout of many genes can be embryo lethal (Brusselmans *et al.*, 2005; Schellander *et al.*, 2007). For this reason selective degradation of transcripts by post-transcriptional gene silencing using dsRNA or RNA interference (RNAi) technologies, has emerged for the study of unknown gene functions in many organisms (Fire, 1999; Brusselmans *et al.*, 2005; Schellander *et al.*, 2007). Initial studies using dsRNA injection into *C. elegans* resulted in degradation of

the targeted mRNA. Since then, RNAi has been successfully applied to several mammals, including human, mouse and pig (Brusselmans *et al.*, 2005; Schellander *et al.*, 2007). The process of RNAi is highly conserved and assumed to originate as an ancient self defence mechanism of cells against RNA viruses that acts either by suppressing transcription or by degrading the RNA (Lau, 2005). The technology is based on the functions of small RNA pathways that can negatively regulate gene expression by binding to complementary sequences in the 3´ UTRs of target mRNA transcripts leading to gene silencing (Fire, 1999).

1.5.1 The role of small RNA pathways in reproduction

Small RNA pathways have been identified as having important roles in both male and female reproduction (Fire, 1999). Small RNAs in general can be divided into different categories based on nucleotide length: (i) the more than 24 nucleotides P-element-induced wimpy testis (PIWI) interacting RNA (piRNA), (ii) the less than 24 nucleotides micro RNA (miRNA) and (iii) the siRNA (Hawkins *et al.*, 2011). The piRNA were first identified by their interaction with Piwi family members of *D. melanogaster* and their functions have been shown to mostly affect gametogenesis and to be necessary for mammal spermatogenesis and maintenance of the germline (Khurana and Theurkauf, 2010). The piRNA loci are transcribed by the same strand as long primary transcripts. Individual piRNAs do not however have conserved sequences; instead, these precursor (pre)-RNAs are cleaved by Argonaute RNA endonucleases; which are PIWI subfamily members, in order to generate their 5´ ends (Hawkins *et al.*, 2011). Germ cell formation in *D. melanogaster* has been shown to be controlled by Piwi and embryos lacking maternal Piwi were shown to have decreased germ cell formation (Megosh *et al.*, 2006). This molecule has also been shown to co-localise with polar granule markers like Vasa which is an RNA helicase necessary for germ cell formation, therefore indicating that Piwi is a polar granule component (Hay *et al.*, 1988). The Piwi molecule also associates with Dicer which is interrelated with miRNA generation and function (Bernstein *et al.*, 2001). In addition to this, the association of PIWI with a number of miRNAs and piRNAs suggests that the PIWI might act through the miRNA mechanism (Yin and Lin, 2007).

In mice, the 3 Piwi family members *Miwi2*, *Mili* and *Miwi* are expressed in different stages of the male germline cycle (Deng and Lin, 2002; Aravin *et al.*, 2007b; Carmell *et al.*, 2007). From these members, *Mili* and *Miwi2* cause spermatogenic stem cell arrest

when their expression is disrupted (Carmell *et al.*, 2007; Unhavaithaya *et al.*, 2009). The above phenotype is most predominant in the *Mili* knockouts and the few stem cells that do not arrest can generate spermatocytes that arrest at the pachytene stage of prophase I (Kuramochi-Miyagawa *et al.*, 2004). In *Miwi2* knockouts, spermatogenesis is blocked at the leptotene stage of prophase I (Carmell *et al.*, 2007).

There is also some evidence from *D. melanogaster* and *D. rerio* for the function of Piwi molecules in oogenesis. In *D. melanogaster*, *Piwi* knockouts abolish germline stem cell division (Lin and Spradling, 1997). In addition, screens for mutations in abnormal *D. melanogaster* oocytes have indicated mutations of the *Aubergine* locus which is a *Piwi* homolog (Schupbach and Wieschaus, 1991). Furthermore, embryos generated following the knockout also demonstrated abnormalities in the EGFR pathway (Schupbach and Wieschaus, 1991).

The second category of small RNAs consisting of less than 24 nucleotides includes the miRNAs and siRNAs. The miRNAs are the best characterised endogenous small RNAs in eukaryotes and are mostly engaged in development and differentiation (Watanabe *et al.*, 2008). These RNAs are processed from the pre-miRNA and regulate gene expression by repressing translation or by cleaving mRNA (Ambros, 2004). In contrast, siRNAs are generated from long dsRNAs and share similar functions with miRNAs (Shi *et al.*, 2004).

The pathway for miRNA synthesis in mammals involves the actions of the microprocessor complex DROSHA, the microprocessor complex subunit (DGCR8) and DICER, while only DICER is required for the synthesis of siRNAs (Figure 1.9). Mice lacking *Dicer* are unable to survive due to faults in the development of ESCs (Bernstein *et al.*, 2003). In addition, argonaute 2 (*Ago2*) has also been shown to be necessary for early development; as mice lacking the molecule do not survive beyond embryonic day 9.5 (Liu *et al.*, 2004). Mice lacking *Dicer* also demonstrate an infertile phenotype with spindle defects, chromosome alignment and meiosis arrest at MI (Bernstein *et al.*, 2003; Tang *et al.*, 2007). Similarly, *Ago2* knockout mice also demonstrate meiotic arrest along with chromosome and spindle flaws (Kaneda *et al.*, 2009). Because Dicer is necessary for the biosynthesis of both siRNA and miRNA, absence of either or both of them could be responsible for the observed oocyte defects in the above studies. Transcript analysis conducted in the same studies showed that the transcripts affected were involved in

meiosis regulation and spindle formation demonstrating similarities with the defects associated with the deletion of piRNA in males (Liu *et al.*, 2010).
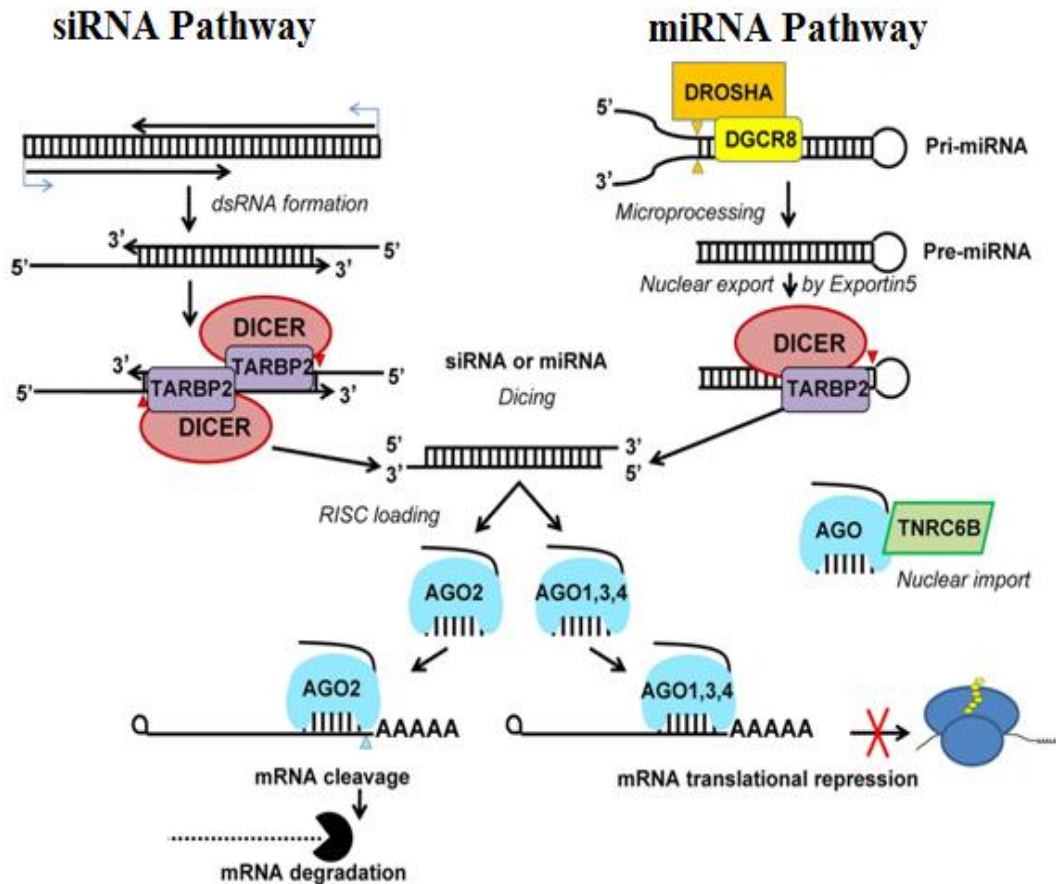
Figure 1.9: Biogenesis of siRNA and miRNA in animals. The siRNA is firstly transcribed with the transcripts forming a region of dsRNA. The miRNA are transcribed from RNA-polymerase II and fold into a hairpin structure containing a region of dsRNA called primary-miRNA (pri-miRNA). These pri-miRNAs are then processed by the microprocessor complex which is composed of a nuclear type III endonuclease named RNASES/DROSHA and its cofactor DGCR8. The pri-miRNAs are cleaved and the pre-miRNA is excised and then exported from the nucleus by Exportin 5. When in the cytoplasm, a second RNase III endonuclease, DICER along with its cofactor TAR binding protein 2 (TARBP2) cleaves the 5´ overhangs of the siRNA precursor or the loop of the pre-miRNA as shown in the red triangles. The mature siRNA or miRNA produced are then loaded onto the AGO containing effector complex named RNA-induced silencing complex (RISC). In mammals there are 4 AGO molecules (AGO1-4) with the endonucleolytic activity for cleavage of mRNA contained in AGO2. Following the mRNA endonucleolytic cleavage, mRNA is decapped and exonuclease proceeds with the digestion. The other AGO molecules may also have alternative roles in the repression of translation. Adapted from Hawkins *et al.*, (2011).

In general, miRNAs and siRNAs negatively regulate gene expression by binding to complementary sequences in the 3´ UTR regions of target mRNA-transcripts leading to gene silencing (Fire, 1999). The importance of the small-RNA mechanisms to mammalian oocyte development were further clarified when Watanabe *et al*, (2008) found that the siRNAs produced in oocytes are depleted following *Dicer* knockout in

addition to mRNA up-regulation of siRNA targets. The above result demonstrates that siRNAs regulate endogenous targets in mammals (Watanabe *et al.*, 2008). In a recent study, knockout of *Dgcr8* in mouse oocytes resulted in reduced repression of translation (Ma *et al.*, 2010). In another study where *Dgcr8* was deleted, oocytes matured normally and had healthy offsprings with the mRNA profiles of *Dgcr8* knockout oocytes being at similar levels with wild types, confirming that it is the siRNAs and not the miRNAs that cause the *Dicer* knockout phenotype in oocytes (Suh *et al.*, 2010). The above studies demonstrate the necessity of siRNA production by Dicer for normal oocyte maturation with miRNAs not having such a significant role (Hawkins *et al.*, 2011). Additionally, introduction of artificial 3´ UTRs with multiple target sites into mouse oocytes in addition to introduction of an excess of miRNAs did not result in increased suppression of mRNA stability translation (Ma *et al.*, 2010). It can therefore be assumed that miRNA function is suppressed in fully grown oocytes even though miRNA biogenesis is not affected. One hypothesis is that suppression of miRNA function could be associated with the P-bodies which are lost in maturing oocytes; however it is unknown whether the loss of P-bodies is a primary or secondary consequence of the loss of the miRNA function (Flemr *et al.*, 2010). An overview of the small RNA characteristics and tissue of function in mammalian reproduction is shown in Table 1.1.

Table 1.1: Small RNA characteristics and tissue of function in mammalian reproduction. Adapted from Hawkins *et al.*, (2011).

/	piRNA	siRNA	miRNA
Approximate size	25-30 nucleotides	18-24 nucleotides	18-24 mucleotides
Major cell type	Male germ cells	Oocyte	Multiple
DICER-dependent	No	Yes	Yes
Drosha-dependent	No	No	Yes
DGCR8-dependent	No	No	Yes
Major function	Suppression of transposon synthesis	Cleavage of transposon mRNAs	mRNA cleavage, translation repression
Estimated number	>10,000	>10,000	600-1000
Types of RNAi delivery	Transfection, Electroporation, Viral vector, Microinjection, Cell culture incubation, Feeding, Use of reagents,		
Examples of phenotypes in oocyte following RNAi	*c-MOS* dsRNA (mouse): Spontaneous activation of oocytes *Cyclin B1* dsRNA (mouse and bovine): Reduced activity of Mpf *Msy2* dsRNA (mouse): Impaired resumption of meiosis II *GDF9* dsRNA (mouse and ovine): Reduced cumulus expansion BMP15 dsRNA (mouse and ovine): Reduced cumulus expansion Has2 shRNA (mouse): Reduced cumulus expansion		

1.5.2 RNAi as means to moderate oocyte gene function

Synthetic methods have also been developed to silence endogenous genes. The most common methods employ synthetic RNAi effectors (mimics of siRNA, short hairpin

RNA (shRNA) and pri-miRNA) that emulate different precursors of the endogenous pathway (Sibley *et al.*, 2010). Also, second generation approaches involving asymmetric RNAi, small internally segmented interfering RNAs and RNA-DNA chimeras have been employed in order to reduce some of the off-target effects of RNAi effectors. These RNAs can limit sense strand activity and off-target effects of antisense strands (Sibley *et al.*, 2010). In addition, alternative mechanisms of shRNA introduction by using alternative delivery mechanisms of shRNA to the cytosol can avoid some of the toxicity caused by Exportin 5, for which shRNA compete with endogenous miRNAs and is believed to cause fatality in mice (Grimm *et al.*, 2006). The RNA effectors can also be used for transcriptional gene silencing that can induce epigenetic changes. Another advantage is that tandem siRNAs, tandem shRNAs and miRNA clusters can be used to target multiple sites (Sibley *et al.*, 2010).

The discovery of RNAi resulted in the generation of numerous studies *in vivo* and *in vitro* that evaluated the function of genes or encoded proteins. When it comes to the reproductive system, there are many unanswered questions concerning the complexity and changes that oocytes undergo during the final stages of growth and the acquisition of developmental competence. During the process of oogenesis, oocytes acquire the majority of transcripts correlated with maturation and early embryo development (Bachvarova, 1992). RNAi can therefore be used as a tool to study both the molecular and cellular events during oocyte development and maturation, by silencing the expression of single or multiple genes (Schellander *et al.*, 2007). The procedure of RNAi involves the introduction of long dsRNA, siRNA or shRNA to serve as siRNA substrates (Roignant *et al.*, 2003; Amanai *et al.*, 2006; Sarnova *et al.*, 2010). It is estimated that 10% of possible siRNAs will have significant off target effects in the genomes of *H. sapiens, C. elegans,* and *Schizosaccharomyces pombe* (Qiu *et al.*, 2005). In most mammalian cells, siRNAs are preferred instead of dsRNAs because of the interferon response caused by long dsRNAs (Reynolds *et al.*, 2006). Interferon response is a form of innate immunity to any foreign genetic material. Mouse oocytes have been shown to lack the non-specific effects of RNAi triggered by the introduction of long dsRNA and consequently murine oocytes have been used as a model system for studying the effects of gene knockdown in mammals (Stein *et al.*, 2005).

The success of RNAi experiments is largely dependent on the design of the siRNA species used and the efficiency of their delivery into the cells of interest. Several

different techniques including microinjection, electroporation and transfection have been developed for introducing the RNAi mediators. The efficacy of the delivery strategies varies depending on the target cell or organism. Some organisms in particular are susceptible to several ways of siRNA introduction for example *C. elegans* that may be injected or fed (Tabara *et al.*, 1998; Fire, 1999; Fraser *et al.*, 2000); whereas in *D. melanogaster,* embryos can be microinjected, while cell culture incubation with siRNA has also proved effective in *D. melanogaster* (Kennerdell and Carthew, 1998; Clemens *et al.*, 2000). Stable transfection with a plasmid encoding the sequence transcribing siRNA is another method being used for avoiding direct introduction of siRNA (Brummelkamp *et al.*, 2002), while lentiviral vector systems allow an inducible control of transcription activation or deactivation, known as conditional RNAi (Tiscornia *et al.*, 2004). The effect of RNAi can also be achieved by RNA produced enzymatically from DNA-transcription. The method termed DNA-Directed RNAi (ddRNAi) allows use of standard transfection reagents and methods. Gene delivery can also be performed by using different reagents and methods including cationic lipids, calcium phosphate, polybrene-dimethyl sulfoxide (DMSO), diethylaminoethyl cellulose (DEAE)-dextran or electroporation (Caplen *et al.*, 2001; Elbashir *et al.*, 2001). From the above methods, electroporation is most frequently used and it functions by increasing electrical conductivity and by applying an electrical field to introduce into cells large highly charged molecules that would not passively diffuse across the cell membrane (Neumann *et al.*, 1982). Morpholinos are also used as vehicles for the introduction of RNA species into cells by microinjection or electroporation. These are molecules that bind to complementary sequences of RNA and modify gene expression by preventing cells from making a targeted protein and also by modifying the splicing of pre-mRNA (Summerton, 1999; Draper *et al.*, 2001).

Microinjection has been shown to be an effective means of introducing RNA species into oocytes and embryos from a variety of species (Svoboda *et al.*, 2000; Wianny and Zernicka-Goetz, 2000; Paradis *et al.*, 2005). In comparison with electroporation and transfection, microinjection is easier to apply at the oocyte level and the volume injected can be regulated and thus allows a better control of the amount of dsRNA or siRNA that is introduced into the oocyte (Paradis *et al.*, 2005). This is very important because the efficiency of targeted suppression of gene transcripts is believed to be dependent on the phenotype it produces. Developmental phenotypes have been related to the concentration of dsRNA introduced when different concentrations of dsRNA *c-Mos*

resulted in significant differences in the spontaneous activation of oocytes (Wianny and Zernicka-Goetz, 2000). None-the-less, microinjection frequently results in physical injury or stress to the oocytes being manipulated (Favetta *et al.*, 2007). The original studies on RNAi in oocytes, involved injection of dsRNA in mouse oocytes that resulted in altered expression of targeted genes. Specifically, Wianny and Zernicka-Goetz, (2000) showed that epithelial-*Cadherin* and *c-Mos* dsRNA injections into oocytes resulted in an 80% reduction of the target transcript and so produced phenotypes similar to those of null mice. Similar results were shown for injections of *c-Mos* and tissue plasminogen activator dsRNAs (Svoboda *et al.*, 2000). Since then, a number of studies have used RNAi in oocytes and embryos of different species targeting different genes and resulting in different levels of suppression. Specifically, *c-Mos* introduction in bovine oocytes by microinjection was shown to reduce the target transcript by 70% (Nganvongpanit *et al.*, 2006). In a different study conducted in mice, maternal mRNAs of different genes were suppressed by 90% (Xu *et al.*, 2003). Lazar *et al.*, (2004) showed that exposure of rat oocytes to *Cyclin B1* dsRNA resulted in the complete degradation of this molecule. This result is important as the 2 subunits of Cyclin B1 (regulatory and catalytic) form Mpf (Nurse, 1990). Down-regulation of *Cyclin B1* caused the down-regulation of its protein product and the resultant reduced activity of Mpf. The reduced Mpf activity resulted in suppression of the addition of poly-(A) tail to the *c-Mos* mRNA which impeded its translation. Translation of *c-Mos* is a critical step in oocyte maturation and specifically the control of meiotic progression. Knockout mice for *c-Mos* have been shown to have a reduced fertility in comparison to the controls due to the failure of mature oocytes to arrest during meiosis (Colledge *et al.*, 1994). Specifically, *c-Mos* knockouts were shown to undergo GVBD and extrusion of the 2 polar bodies with some progressing through cleavage. These results highlighted the role of *c-Mos* in preventing spontaneous parthenogenetic activation of unfertilised oocytes. Conversely, treatment of mice with *c-Mos* dsRNA resulted in spontaneous activation of around 50% of the oocytes (Wianny and Zernicka-Goetz, 2000). Further elucidation of the role of *c-Mos* was conducted by examining MII arrest of mouse oocytes in conjunction with the c-Mos/Mapk pathway (Lefebvre *et al.*, 2002). Specifically Mapk was shown to have an important role in maintaining spindle integrity at the oocyte arrest stage when dsRNA specific transcripts were injected. In addition, Mapk interacting and spindle stabilising protein was shown to be the substrate for the c-Mos/Mapk pathway. By using RNAi, other important genes playing an important role in oocyte maturation were identified like the *Msy2*, which was shown to regulate maternal

mRNA translation during oogenesis and was essential for completion of meiosis II in mouse oocytes. Knockdown of this protein resulted in impaired resumption of the second meiotic division (Yu *et al.*, 2004). However, a similar study in bovine revealed an alternative outcome. Introduction of *C-MOS* dsRNA into bovine oocytes resulted in only a 2.5% spontaneous activation of oocytes, although *C-MOS* transcription and translation were significantly lessened (Nganvongpanit *et al.*, 2006). Overall, the above results show that phenotypical appearances following suppression of transcripts are different between species. Similarly, null mutation studies and suppression of other specific transcripts contributing to oocyte maturation such as *Gdf9* and *Bmp15* supported these species specific differences in oocyte behaviour (Schellander *et al.*, 2007).

The role of the oocyte-derived factors *Gdf9* and *Bmp15* in oocyte maturation has also been evaluated by RNAi. In order to study the relation between these oocyte-specific transcripts and cumulus expansion in mice, a long dsRNAi approach was used (Gui and Joyce, 2005). Evaluation of *Has2* and *Ptgs2* mRNA levels were used as markers of cumulus expansion and showed lower levels when *Gdf9* was knocked-down in the oocyte in comparison to *Bmp15* knockdown and controls. The above results in addition to the lower degree of expansion of mouse cumulus cells when cultured with oocytes injected with dsRNA for *Gdf9*, supports the concept that Gdf9 is a key mediator of oocyte enabled cumulus expansion in mice as has been previously suggested by the studies of Sugiura *et al*., in 2005 (Gui and Joyce, 2005).

Following the successful application and potential of RNAi in determining functional characteristics of genes in mice, the technology has been applied to study other oocyte-specific transcripts in other species including *B. taurus*, *O. aries* and *Macaca mulata* (Paradis *et al.*, 2005; Wu, 2009; Tang *et al.*, 2012). An RNAi approach to study gene function has been developed for bovine oocytes and *Cyclin B1* dsRNA microinjection in GV oocytes successfully resulted in the decrease in *Cyclin B1* mRNA and protein while *Cyclin B2* mRNA levels were not affected (Paradis *et al.*, 2005). In ovine oocyte maturation, injection of siRNA duplexes for *GDF9* and *BMP15* in denuded GV oocytes resulted in a lower degree of cumulus cell expansion when the knockdown oocytes were matured *in vitro* with compacted oocytectomised cumulus complexes (Cotterill, 2008). In addition, *GDF9* or *BMP15* dsRNA injections resulted to reduced mRNA levels for *HAS2*, while *GDF9* dsRNA injections resulted to reduced *GREMLIN1* mRNA levels

(Cotteril, 2008). In another study, targeted suppression of *Has2* mRNA in mouse COC's was accomplished by adenovirus mediated shRNA expression (Sugiura *et al.*, 2009). In addition to the reduced expansion of cumulus cells, levels of *Areg* and *Ereg* mRNAs were decreased in *Has2* mRNA targeted intact COCs, while *Btc* mRNA levels were not affected (Sugiura *et al.*, 2009). Even though *Has2* expression levels were reduced by more than 70%, expression levels of other genes required for cumulus expansion including *Ptgs2*, pentaxin related protein 3 and tumour necrosis α induced protein 6 were not affected (Sugiura *et al.*, 2009). It is worth mentioning, however, that the levels of these genes in the adenovirus infected COC's were lower compared to controls and *Egf* treatment recovered their levels; suggesting that expression of these genes was stimulated by *Egf* (Sugiura *et al.*, 2009). Although the enzyme hyaluronan synthase is critical for cumulus expansion, the role of *Has2* isoform in the process remains unclarified. Several other isoforms for the enzyme are shown to be expressed in bovine and porcine oocytes (Kimura *et al.*, 2002; Schoenfelder and Einspanier, 2003). Since the co-culture of denuded gene knockdown oocytes with intact oocytectomised cumulus shells regenerates the 2 compartments of COCs, further research using this approach will allow better understanding of the mechanisms behind COC development, maturation and signalling to and from each of the cellular compartments.

While the application of RNAi as an effective tool for studying gene function in oocytes is emerging; the efficiency of this technology remains an important issue. One factor that has been shown to have an impact on the efficiency of RNAi is the siRNA sequence used. Indeed nucleotide mismatches within the siRNA can alter the specificity of target recognition (Holen *et al.*, 2002). In particular, properties of the targeted mRNA such as the secondary structure, RNA-associated proteins and sub-cellular localisation of the mRNA can all affect the efficiency of gene knockdown (Holen *et al.*, 2002). In addition, the culture conditions affect the target degradation by RNAi. In another study, sequence specific dsRNA efficiency of knockdown was shown to be directly related to the culture environment and it affected availability of transcripts during oocyte and embryo development (Tesfaye *et al.*, 2007). Despite these criticisms, the application of RNAi technology and evaluation of the expression of siRNA at specific stages of oocyte and embryo development has great potential as a tool for basic research aiming at understanding the function of genes during gamete development.

1.6 AIMS AND OBJECTIVES

A detailed understanding of the genes and mechanisms that regulate oocyte growth and maturation is essential for the development of improved methods of assisted conception. On the basis of the evidence reviewed here is clear that folliculogenesis in addition to oocyte development and maturation requires the coordinated interaction between multiple cell types and the timely expression of specific genes and transcription factors. A lot of research has been conducted on the factors that influence folliculogenesis and oocyte maturation in rodents, however less is known about follicle growth and development in monovular species such as human and sheep. From the literature it is now understood that the oocyte itself plays a crucial role in regulating most stages of folliculogenesis and this is highlighted by the actions of oocyte-derived factors which are facilitated by the cross talk between the oocyte and the somatic compartments of the follicle through growth and maturation. One of these oocyte-specific factors is *GTSF1*. *GTSF1* is a putative marker of gamete developmental competence that is highly conserved across species but which demonstrates a sexual dimorphism in its function. The cellular distribution of function of *GTSF1* in the regulation of gametogenesis of monovular species as the sheep has not yet been investigated. On the basis of the published literature it is hypothesized that the gamete specific expression of *GTSF1* along with its conserved domain containing 2 tandem copies of a CHHC Zn-finger, suggests that *GTSF1* plays a role in gamete production in monovular species and that the function of the gene may relate to RNA-binding during oocyte development. The objectives of the research presented in this thesis were:

1. To clone and sequence ovine *GTSF1* and characterise the cellular distribution and expression patterns of the gene across all stages of ovine follicle, oocyte and early embryo development using molecular screening methods and ISH.

2. To validate the efficiency of the microinjection of siRNA as a vehicle for gene knockdown on a known oocyte-derived factor; *GDF9*.

3. To evaluate the function of *GTSF1* during sheep oocyte maturation *in vitro* by studying the impact of *GTSF1* knockdown on parameters such as: (i) meiotic maturation of ovine oocytes, (ii) cumulus mucification and expansion and (iii) gene expression pathways.

4. To determine if GTSF1 was confined to the P-body of ovine oocytes and so provide preliminary insights into the role in RNA processing in this species.

Chapter 2: Materials and Methods

The reagents used in the experiments of the thesis were purchased from Sigma-Aldrich (Dorset, UK) unless otherwise stated. Sterile culture plastics were purchased from Nunc (Nunclon, Roskilde, Denmark) unless otherwise stated. All addresses of suppliers are shown in Appendix I. All glassware used in the experiments was originally soaked overnight in a mixture of Trigene (Medichem International, Sevenoaks, Kent) and sterile-distilled H_2O in a dilution of 1 in 50. Glassware was then rinsed twice with tap water and twice more with Milli-Q water (MQ-H_2O, Millipore, Billerica, USA). Following washing, glassware was left to dry for 2 days in an oven at 30° C (Philip Harris Ltd, Shenstone, England). When dried, glassware was wrapped in foil and sterilised by heating in an autoclave at 180° C. New glassware was treated in a 5% (v/v) HCl before following the same procedure as detailed above.

2.1 OVINE TISSUE COLLECTION AND IVM

Sheep reproductive tracts were collected from the abattoir (J.C. Penny and sons, Rawdon, Leeds, UK) and placed in an insulated carrier at room temperature (RT) before being transported to the laboratory where the tissue was cleaned and prepared for analysis. The methods for ovine tissue collection and IVM of ovine oocytes have been described previously (Danfour, 2007; Cotterill, 2008, Cotterill *et al.*, 2012).

2.1.1 Tissue preparation

Following arrival of the ovine tracts, the ovaries were cut from the tracts and washed 3 times in an autoclaved glass beaker (Scientific Laboratory Supplies (SLS), Yorkshire, UK) containing 150 ml of ovary washing medium The ovary washing medium was prepared by adding 1 tablet of phosphate buffer saline (PBS, Invitrogen Ltd, Paisley, UK) to 500 ml of sterile-distilled H_2O and 5 ml of antibiotic-antimycotic solution containing penicillin G (100 IU/ml), streptomycin sulphate (100 μg/ml) and amphotericin B (250 ng/ml). The values shown for each solution represent the final working concentration. Ovary washing medium was pre-warmed in a non-gassed incubator overnight at 39° C (Stuart hybridisation oven, SLS). Following cutting of all the ovaries and 2 additional 150 ml rinses with the washing medium, ovaries were placed in a 170 ml sterile plastic container (SLS) containing follicle isolation medium (FIM) at 39° C in the non-gassed incubator until processing. The composition of the

FIM medium is shown in Table 2.1. The solution was sterilised with a 0.2 μm cellulose acetate rapid vacuum filtration system (Techno Plastic Products, TPP, Trasadingen, Switzerland) and left to equilibrate overnight in the non-gassed incubator at 39° C prior to use. All culture media and additives were made-up as appropriate in sterile tissue culture grade embryo tested H_2O. The composition of all stock solutions is shown in Appendix II.

Table 2.1: Composition of follicle isolation medium (FIM)

Component	Stock	Vol. (ml)	Final Concentration
MEM 10X stock	-	50	-
Buffer 10X stock	-	50	-
*BSA	2.0% (w/v)	25	1 mg/ml
Penicillin	6 mg/ml	2.5	0.06 mg/ml
Streptomycin	5 mg/ml	2.5	0.05 mg/ml
Heparin	5000 U/ml	2	20 U/ml
Sodium Pyruvate stock	47 mM	0.5	0.047 mM
Make up to 500 ml with embryo tested sterile-distilled H_2O			

Media was kept overnight at 39°C in a non-gassed incubator before use. Extra media was stored at 4°C for up to 2 weeks. MEM: Minimum essential medium, *BSA: Bovine serum albumen, fraction V cell culture grade.

2.1.2 Aspiration of cumulus oocyte complexes

The COCs were aspirated from antral follicles of approximately 2-5 mm diameter using a 20 ml sterile syringe (BD Plastipak^{TM}, Drogheda, Ireland) attached to a size 19 gauge needle (Terumo UK Ltd, Surrey, UK) which was pre-loaded with 1 ml of pre-warmed Hepes buffered medium 199 (H199$^+$). The composition of H199$^+$ is shown in Table 2.2. The solution was sterilised with a 0.2 μm cellulose acetate rapid vacuum filtration system before use and was left to equilibrate overnight at 39°C in a non-gassed incubator. When 6 ovaries had been aspirated, the loaded COCs were dispensed into a sterile 90 mm plastic Petri dish containing H199$^+$ and evaluated using a stereo microscope (Olympus Ltd, Southhall, Middlesex, UK) fitted with a heated stage set at 39°C (MTG Medical Technology Verrtriebs GmbH, Altdorf, Germany). Before oocyte aspiration, parallel lines were drawn on the bottom of the 90 mm Petri dish using a marker pen in order to assist with COC searching. Multiple aspirates were pooled into a dish and the COCs with an intact oocyte cytoplasm and at least 3 layers of cumulus cells surrounding the oocyte were selected for culture and multiple COCs were pipetted into a sterile 35 mm nunc dish containing 2 ml of pre-warmed H199$^+$. The dish containing the selected COCs was thereafter placed in the non-gassed incubator at 39°C and the same procedure was followed for all the remaining ovaries.

Table 2.2: H199$^+$ oocyte holding media composition

Component	Stock	Vol.	Final Concentration
M199 stock 10X (Gibco, UK)	-	25 ml	-
Bicarbonate stock	250 mM	4 ml	4 mM
Hepes Stock	250 mM	21 ml	21 mM
Heparin	180U/mg	5 mg	0.02 mg/ml
*BSA	-	1g	-
Penicillin	6 mg/ml	2.5 ml	1.2 mg/ml
Streptomycin	5 mg/ml		0.1 mg/ml
Make up to 500 ml with embryo tested sterile-distilled H$_2$O			

Media was kept overnight at 39°C in a non-gassed incubator before use. Extra media was stored at 4°C for up to 2 weeks. Osmolarity was in the range of 283±5. The pH was adjusted to 7.2-7.4 using 1 M HCl or NaOH. *BSA: Fraction V cell culture grade.

2.1.3 *In vitro* maturation of COCs

The COCs contained in the 35 mm nunc dishes were transferred to new sterile 35 mm nunc dishes containing 40 µl micro-drops of serum-free IVM media prepared as shown in Table 2.3 and overlaid with 2 ml of mineral oil. The serum-free IVM solution was sterilised with a 0.2 µm cellulose acetate syringe filter (Acrodisc, Pall Corporation, Portsmouth, UK) and left to equilibrate overnight in a humidified gassed incubator at 5% CO$_2$ in air at 39°C (New Branswick-Eppendorf, Stevenage, UK). Prior to use, the oil was also equilibrated overnight in the gassed incubator at 39°C. Groups of 10 COCs were washed twice in separate 40 µl serum-free IVM media drops before being transferred in a new culture drop. The plates containing the COCs were then placed in the humidified gassed incubator at 39°C for a 24 hour (h) culture. The methodology for the IVM of sheep oocytes has previously been extensively validated by Danfour, (2007) and Cotterill *et al.*, 2012).

Table 2.3: Serum-free IVM media composition

Component	Stock	Vol.	Final Conc.
αMEM base		9.768 ml	µg/ml
Transferin	5 mg/ml	10 µl	5
Sodium Pyruvate	47 mM	100 µl	0.47 mM
Sodium Selinite	50 µg/ml	1 µl	5 ng/ml
L-Glutamine (Gibco)	200 mM	100 µl	3 mM
Bovine insulin*	10 mg/ml	10 µl	10 ng/ml
Long-R3 IGF-1	100 µg/ml	1 µl	10 ng/ml
Ovine FSH (0.91 U/ml)	200 µg/ml	5 µl	100 ng/ml
Ovine LH (0.55 U/ml)	200 µg/ml	5 µl	100 ng/ml

Media was made up to a total volume of 10 ml. Extra media was stored at 4° C for 1 week. *Bovine insulin stock was diluted 1:1000 in αMEM basic media immediately prior to use.

2.1.4 Isolation of ovine follicles

Follicles from the primordial to the early antral stages were isolated from ovine ovarian cortex using a collagenase and DNase digestion. The collagenase solution was

comprised of 90 ml of Leibovitz L-15 medium, 10 ml of fetal calf serum (FCS, 10% v/v) and 100 mg of collagenase (740 U/mg). The solution was then aliquoted in sterile universal tubes (BD Plastipak™) each containing 10 ml of collagenase solution and stored at -20°C. The DNase was prepared by adding 1 ml of sterile PBS (pH 7.4) into a vial of DNase (0.5 mg) and creating aliquots of 42 μl (0.5 mg/ml) in sterile 0.5 microcentrifuge tubes stored at -20°C. For the isolation experiments, 40 μl of DNase was added to the universal containing 10 ml of collagenase solution that was pre-warmed at 37°C before use in a non-gassed incubator. The protocol for follicle isolation has been previously validated (Newton *et al.*, 1999; Huntriss *et al.*, 2002). Ovaries contained in the FIM media (Section 2.1.1) were transferred into a sterile glass Petri dish (SLS) where they were dissected. All the instruments used for the ovary dissection including scalpel blades and forceps were wet sterilised in 70% (v/v) ethanol in sterile-distilled H_2O for a minimum of 15 minutes (min) prior to use. The ovaries were originally halved using a scalpel blade and holding the ovary with forceps and the inner cortex was then removed so that the outer cortex retained. The same process was repeated for 6-8 ovaries and the retained cortex was minced into pieces of around 1-3 mm in size. The pieces were then added to the 10 ml digestion solution containing the collagenase with DNase and the universal was left to agitate gently in a non-gassed incubator for 1 h at 39°C. The digestion solution was then removed and the tissue was washed twice in 'stop' medium containing 9 ml of Leibovitz L-15 media plus 10% v/v FCS (1 ml) at 4°C that has been filter sterilised with a 0.2 μm syringe filter and stored at -20°C until use. Follicles were isolated under the stereo microscope using 2 size 26 gauge needles (SLS) attached to 2 ml syringes (SLS). Once isolated, follicles were transferred to a clean 35 mm nunc dishes containing 1 ml of cold FIM media (kept at 4°C) and their diameter was measured using an occular graticule attached to the eye-piece of an inverted microscope (Olympus Ltd). Follicles were classified according to their size and morphology (Huntriss *et al.*, 2002) as follows: Primordial (20-30 μm), early primary (30-45 μm), primary (60-90 μm), secondary (100-150 μm), preantral (180-200 μm) and early antral (>250 μm). Classified follicles were grouped and transferred into separate wells of 4-well nunc dishes containing 500 ml of cold FIM. From there, different staged follicles were pooled into groups and transferred in 0.5 sterile microcentrifuge tubes (Starlab, Milton Keynes, UK) containing lysis buffer (Section 2.2.1) and snap-frozen in liquid nitrogen before storage at -80°C, until use for molecular analysis as detailed in Chapter 3.

2.2 GENERAL MOLECULAR METHODS

2.2.1 Library construction

For the molecular work all pipette tips and microcentrifuge tubes were purchased from Starlab (Starlab, Milton Keynes, UK). All other reagents used in the experiments were purchased from Sigma-Aldrich unless otherwise stated. Libraries were constructed for all stages of ovine folliculogenesis (Section 2.1.4) as well as denuded GV and MII oocytes, somatic cell types of the ovary and early developmental stages, detailed in Chapter 3. In addition, archived ovine cDNA libraries were also obtained from Cotterill, (2008). For cDNA library construction, the selected tissue was originally washed twice in sterile Dulbecco's Calcium (Ca^{2+}) and Magnesium (Mg^{2+})-free PBS (DPBS, Invitrogen Ltd) solution and then placed in sterile 0.5 ml microcentrifuge tubes containing 10μl of Lysis buffer (Table 2.4). Samples were subsequently snap-frozen in liquid nitrogen and stored at -80°C for subsequent molecular analysis.

Table 2.4: Lysis buffer

Component	Volume
Dynal lysis buffer (Dynal biotech)*	910 μl
RNA later (Ambion)*	50 μl
20% (w/v) Sodium Dodecyl sulphate (SDS)	20 μl
Ipegal (0.08 mM)	20 μl

Lysis buffer was made up to a total volume of 1 ml. *Dynal lysis buffer and RNA later were purchased from (Invitrogen Ltd).

2.2.2 Isolation of mRNA

Samples stored in lysis buffer were used for creating cDNA libraries based on methodology previously described by Huntriss *et al.*, (2002). Samples were thawed and placed on a hot block set at 80°C for 10 min to make sure that lysis of the cells was complete. In order to isolate mRNA, the Dynabead mRNA extraction kit (Invitrogen Ltd) was used. The dynabeads were washed before use. To do this, 25 μl of Dynabeads and 25 μl of lysis buffer were mixed in a sterile 1.5 ml microcentrifuge tube and then placed on a magnetic holding apparatus as supplied by Invitrogen Ltd, allowing the beads to be attracted towards a magnet that pulls them to the periphery of the tube at the side of the magnetic apparatus that allows removal of the excess buffer using a Gilson pipette (Gilson Inc, Middleton, USA). A further 25 μl of lysis buffer was then added to the tube. All procedures were performed at RT. After removing the samples from the hot block and allowing them to cool for 2 min, the mixture of dynabeads in lysis buffer (50 μl) was added to the 0.5 microcentrifuge tube containing the tissue sample. The tube was then placed on a rotator (Labinco B.V, Bredo, Netherlands) for 30 min. During the

30 min incubation, the oligo d-Thymine of the Dynabeads paired with the poly-(A) tail of the mRNA. The mRNA was then separated from the cellular components by placing the tube in the magnetic apparatus so that the excess liquid could be removed. Samples were then washed twice in 40 μl of buffer A and twice in 40 μl of buffer B (Invitrogen Ltd) in consecutive steps according to the manufacturer's recommendations, with the excess liquid being removed in each wash on the magnetic apparatus as described above. At each buffer step, the beads were thoroughly mixed with the buffers through vigorous pipetting avoiding the creation of any bubbles. Finally, following removal of the excess buffer the samples were re-suspended in 3 μl of sterile distilled water and stored at -80°C until use.

2.2.3 Synthesis of cDNA

The total mRNA gathered from the samples as detailed above was used for complementary DNA (cDNA) synthesis using primers described previously (Eberwine *et al.*, 1992) as shown in Table 2.5 (Invitrogen Ltd). For cDNA synthesis the SMART system (Switching mechanisms at the 5´ end of RNA transcript) was used (Takara Bio, Saint-Germain-en-Lave, France). This technology can produce high-quality full-length cDNA libraries from nanograms of total RNA (50 ng). The primers were diluted to a concentration of 50 μg/ml. A mastermix was then created containing 1μl of oligo (dT)$_{24}$, 1 μl of template switching (TS) primer, 2 μl of 5 X first strand reaction buffer (Invitrogen Ltd), 1 μl Deoxyribnonucleotide triphosphate (dNTP) mix (10mM, Bioline Ltd, London, UK), 1 μl diothiothreitol (DTT, 0.1M, Invitrogen Ltd) and 1 μl Superscript reverse transcriptase RNase-H (200 U/μl, Invitrogen Ltd) for each sample. A 7 μl aliquot of the mastermix was then added to each mRNA sample, producing a final volume of 10 μl. The sample was then incubated for 2 h at 42°C.

Table 2.5: cDNA primer sequences

Primer	Sequence
Oligo (dT)24 primer	5´ AAACGACGGCCAGTGAATTGTAATACGACTCACT ATAGGGCGCTTTTTTTTTTTTTTTTTTTTTTTTT 3´
TS primer	5´ AAGCAGTGGTATCAACGCAGAGTACGCGGG 3´

2.2.4 Long distance PCR of total cDNA

The 10 μl of cDNA obtained as detailed in Section 2.2.3 was used to create an amplified library. In order to perform the reaction, a mastermix was created containing 5 μl of 10 X Advantage 2 PCR buffer (Takara Bio, Saint-Germain-en-Lave, France), 1 μl of oligo (dT)$_{24}$ primer, 1 μl of TS primer, 1 μl of 50x dNTP mix (10mM), 31 μl of sterile

distilled H$_2$O and 1 μl of 50x Advantage 2 Taq Polymerase Mix (Takara Bio) for each sample. From the mastermix, 40 μl were added to each of the 10 μl of cDNA and the PCR reaction was conducted by the Veriti 96 Well Thermal Cycler (Applied Biosystems, Foster City, USA). The program was set as follows:

- 1 cycle: 95°C for 1 min
- 35 cycles: 95°C for 30 sec followed by 65°C for 6 min
- 1 cycle: 72°C for 5 min

Hold at 4°C

2.2.5 Verification PCR

The successful construction of each cDNA library was verified using specific housekeeping primers with the protocol previously validated by (Huntriss *et al.*, 2002). In order to design primers, the sequences of ovine genes of interest were obtained from the National Centre for Biotechnology Information (NCBI) website (http://www.ncbi.nlm.nih.gov/.). When the sequence of the gene of interest was not available for the sheep, sequences were obtained from species with close homology such as bovine and human. The obtained sequences were then inserted into the primer 3 program (http://frodo.wi.mit.edu/primer3/) to produce the different sets of primers. Widely expressed housekeeping genes with proven stable expression levels in both somatic and gametic cells at the relevant stages of follicle/oocyte development were used for the experiments detailed in the thesis. These included glyceraldehyde-3-phosphate dehydrogenase (*GAPDH*), a gene involved in almost all cellular procedures with both a glyceraldehyde-3-phosphate dehydrogenase activity associated with glycolysis and a nitrosylate activity involved with nuclear functions (Ercolani *et al.*, 1988; Barber *et al.*, 2005; Jeong *et al.*, 2006). Another housekeeper gene used in the experiments was histone 2A (*H2A*), which encodes a conserved nuclear protein that together with other histones forms the eukaryotic nucleosome core and has high expression in oocytes regulating chromatin formation (Kleinschmidt *et al.*, 1985; Thatcher and Gorovsky, 1994). The beta actin (*ACTB*) gene that encodes 1 of the highly conserved actin proteins involved in cell motility, structure and integrity and also cytoskeleton formation and which is expressed in all eukaryotic cells was also used where appropriate as housekeeper, but this gene is known to have less stability during the early stages of development (Mamo *et al.*, 2007; Perrin and Ervasti, 2010). Tyrosine 3-monooxygenase tryptophan 5-monooxygenase activation protein zeta polypeptide (*YWHAZ*) gene was also used. This is a highly conserved gene across many species encoding a protein

involved in signal transduction that binds to phosphoserine containing proteins and the gene has a stable expression across folliculogenesis and early embryo development (Tommerup and Leffers, 1996a; Mamo *et al.*, 2008). Finally, the *ZP2* gene which is specifically expressed in oocytes was used as a quality control for the oocyte and embryo cDNA libraries to confirm consistent library formation from low cell numbers of cells. The *ZP2* human primers have been used in previous experiments and their expression in ovine samples has been confirmed (Huntriss *et al.*, 2002). All primers were diluted to 25 pmol/µl before use. The primer sequences of the housekeeper and library verification genes are shown in Table 2.6

Table 2.6: Primer sequences of housekeeper genes used for PCR verification of cDNA library generation (F: forward primer, R: reverse primer)

Gene	Primer Sequence	Temp (°C)	Reference
GAPDH ovine	F: 5´ GAACCACGAGAAGTATAAACA 3´ R: 5´ AGGAAATGAGCTTGACAAAG 3´	60	AF030943
H2A ovine	F: 5´ AGGTATGTCAGGCCGTGGTA 3´ R: 5´ AGCACAGCCTGGATGTTAGG 3´	60	AY074805
ACTB ovine	F: 5´ GGGCCAGAAAGACAGCTATG 3´ R: 5´ GTGACACCATCCCCTGAATC 3´	60	NM001009784
YWHAZ ovine	F: 5´ AGACGGAAGGTGCTGAGAAA 3´ R: 5´ CCGATGTCCACAATGTCAAG 3´	60	NM001267887
ZP2 human	F: 5´ AACGTTGTCGTGGATGGCTGT 3´ R: 5´ GGAGTCATCTGACAACAGGAG 3´	60	(Huntriss *et al.*, 2002)

The controls set-up alongside the test samples included 0.5 µl of sterile-distilled H_2O as a negative control (NC) and 0.5 µl of a previously verified MII cDNA library containing 10 oocytes as a positive control (PC). In order to perform the PCR reaction, the BIOTAQ polymerase Kit was used (Bioline Ltd). The mastermix contained 1.25 µl of PCR buffer, 2 µl of dNTP (1.25 mM), 0.75 µl Mg^{2+} (50mM), 1 µl forwards specific housekeeper PCR primer (25 µM), 1 µl reverse specific housekeeper PCR primer (25 µM), 5.9 µl H_2O for each sample. A 12 µl aliquot of the mastermix was added to each of the microcentrifuge tubes containing 0.5 µl of cDNA and the RT-PCR reaction was conducted using the Veriti 96 Well Thermal Cycler (Applied Biosystems, Foster City, USA). The program was set as follows:

- 1 cycle : 95°C for 5 min
- 35 cycles: 94°C for 30 sec, followed by 60°C for 30 sec, followed by 72°C for 30 sec
- 1 cycle : 72°C for 5 min

Hold at 4°C

2.2.6 Agarose gel electrophoresis

Agarose gel electrophoresis was performed immediately after the verification PCRs. The agarose gel was prepared by adding 100 ml of 1 X tris-borate ethylenediaminetetraacetic acid (TBE) buffer (Appendix II) to 1.5 g molecular grade agarose powder (Bioline Ltd) in a glass beaker, resulting in a final concentration of 1.5% (w/v). The beaker was then heated for 2 min in a 750 V microwave oven until the agarose was dissolved and after cooling, 2.5 μl of ethidium bromide (10 mg/ml) was added. The gel was then poured into a gel clamp (Bio-Rad laboratories Ltd, Hertfordshire, UK) containing a 10, 15 or 20 well comb to allow regular spacing for the addition of each test sample when set and the gel was then allowed to settle for 40 min at RT. Loading buffer (Appendix II) was added to the samples (in a 1:3 ratio of loading buffer to sample) and samples vortexed. When the gel was set, it was placed in a Sub Cell GT Tank with Powerpac 300 (Bio-Rad), covered with 1 X TBE and then the comb was removed, resulting in spaced wells. The samples were then loaded. For all gels, 8 μl of a 100 bp molecular weight (MW) marker (Invitrogen Ltd) was pipetted into the first well of the gel. The subsequent samples were loaded separately into consecutive wells followed by the positive and negative controls as described in Section 2.2.5. The TBE electrophoresis was performed at 100 V for 60 mins at RT. Using a ultraviolet transilluminator (Bio-Rad), PCR products were visualised by their molecular weight size in the form of bands. Gel images were captured by the Grabber Version 2.0 software (Nonlinear Dynamics, Newcastle, UK).

2.3 CLONING AND SEQUENCING

2.3.1 Gel extraction

In order to obtain the nucleotide sequence of a gene of interest following agarose gel electrophoresis for a specific gene, the DNA fragment representing the gene of interest as determined by the ultraviolet transilluminator (Bio-Rad), was excised from the gel by a scalpel blade. The excised fragment was placed in a sterile 1.5 ml weighed microcentrifuge tube and the tube with the fragment was weighed again on a micro-balance (Melter Toledo Ltd, Leicester, UK) to determine the weight of the gel fragment. For the gel extraction procedure, the QIAquick gel extraction kit (Qiagen Ltd, West Sussex, UK) was used according to the manufacturer's recommendations. Accordingly, 3 gel volumes of QC buffer were added and the sample was incubated at 50°C for 10 min on a hot block, while flicking the tube with the finger during incubations to allow

proper mixing of the buffer with the sample. Thereafter, 1 gel volume of isopropanol was added and the sample was pipetted into a QIAquick spin column inserted into a sterile 2 ml collection tube as supplied in the kit. The sample was then centrifuged at 13,000 rpm for 1 min at RT in a Micro centaur centrifuge (MSE/Sanyo, London, UK) and the column flow through was then discarded. Thereafter, 0.75 ml of PE buffer (provided) was added and the spin column was centrifuged again at 13,000 rpm for 1 min at RT and the flow through was once again discarded. Another 1 min of centrifugation under the same conditions was used to ensure any residual PE buffer was removed and the column was then placed into a sterile 1.5 ml microcentrifuge tube. In order to elute the DNA, 20 μl of sterile-distilled H_2O was added to the centre of the QIAquick spin column membrane and; after allowing the sample to stand for 1 min, the column was centrifuged at 13,000 rpm for 1 min at RT to elute the DNA in the flow through.

2.3.2 Addition of poly-(A) tail

Polyadenylation of the purified DNA from the gel extraction was undertaken immediately after the gel extraction step (Section 2.3.1). Polyadenylation is the addition of a poly-(A) tail consisting of multiple AMPs that will assist with the further ligation step. In order to add the poly-(A) tail, a mastermix was created containing 1 μl of 10 X reaction buffer (Bioline Ltd), 0.4 μl of Mg^{2+} (50 mM), 1 μl of adenosine triphosphate (dATP, 2 mM), 0.1 μl Taq polymerase (5 U/ml, Bioline Ltd) and 0.5 μl of sterile-distilled H_2O for each sample. From the mastermix, 3 μl was added to 7 μl of the purified DNA contained in a sterile 0.5 ml microcentrifuge tube and the reaction tube was incubated for 20 min at 72°C on a hot block. Cloning was then performed immediately after the addition of the poly-(A) tail.

2.3.3 Cloning into pGEM-Teasy

The purified DNA with the poly-(A) tail was cloned into a pGEM-Teasy plasmid as shown in Figure 2.1 (Promega Ltd, Hampshire, UK). In order to perform this, the Promega pGEM-Teasy vector kit was used according to the manufacturer's recommendations. For each sample, 1 μl of pGEM-Teasy vector (50 ng) was added to 1 μl of T4 ligase (3 U/μl, Invitrogen Ltd), 6 μl of reaction buffer (Invitrogen Ltd) and to 1 μl of dATP (2 μl). To this reaction, 5 μl of DNA from Section 2.3.2 was added and the total 14 μl contained in the microcentrifuge reaction tube was allowed to ligate on the bench top overnight at RT.
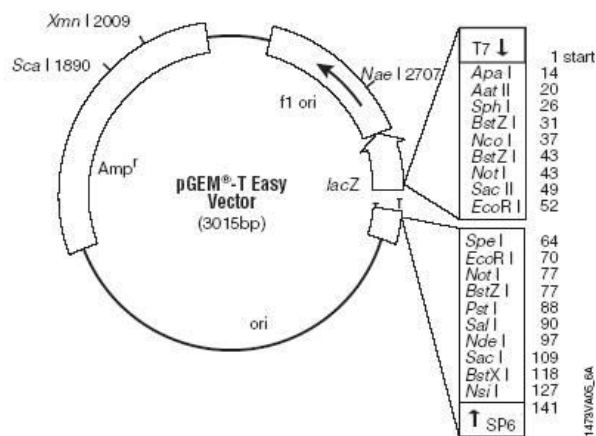
Figure 2.1: Map of the pGEM-T Easy vector system (Promega, pGEM-T Easy Vector System technical manual: http://www.promega.com).

2.3.4 Transformation into *Escherichia coli*

Transformation is the genetic alteration of cells resulting from incorporation and expression of exogenous genetic material. This process occurs commonly in bacteria and the cells that are capable of transformation are called competent cells (Hanahan, 1983; Inoue *et al.*, 1990). For this process, *Escherichia coli* competent cells were used (TOP10, Invitrogen Ltd). Competent cells were thawed from -80°C and 5 μl of the ligated product was added to 50 μl of TOP10 cells in a sterile 0.5 ml microcentrifuge tube. The reaction was then placed on ice for 1 h followed by a heat shock at 42°C for 45 sec on a heat block. The sample was then placed on ice and 450 μl of autoclaved Luria broth (LB) media was added comprising: 10 g Tryptone, 5 g Yeast extract and 10g NaCl in 1L of sterile-distilled H_2O which was heated to boiling to dissolve the agar, followed by incubation at 37°C for 1.5 h on an orbital shaker. Agar plates were prepared in advance by spreading high gel strength 1.5% (w/v) agar (Melford, Suffolk, UK) in sterile-distilled H_2O containing 100 μg/ml of ampicillin, 40 μg/ml of 5-bromo-4-chloro-3-indolyl-beta-D-galactopyranoside and 0.1 mM of isopropyl thiogalactoside into 9.5 cm Petri dishes (SLS). Plates were allowed to set before use. A 100 μl aliquot of the cloned product was spread across the agar plate using a sterile polypropylene cell spreader (VWR, Lutterworth, UK) and the plate was placed in a non-gassed incubator set at 37°C overnight. On the next day, white colonies were removed from the plate using a sterile polystyrene loop (VWR) and they were placed in 0.5 ml sterile microcentrifuge tubes each containing 15 μl of sterile-distilled H_2O. The samples were mixed by flicking the tube gently followed by repeat pipetting. From the 15 μl solution, 12 μl was pipetted into a 10 ml falcon tube that contained 3 ml of LB broth with 3 μl of ampicillin (50 μg/ml). The above steps were performed next to a flaming Bunsen burner

to avoid contamination. The falcon tube was incubated overnight at 37°C in the humidified gassed incubator. The remaining 3 µl of product was used to perform verification PCR (Section 2.2.5) followed by agarose gel electrophoresis (Section 2.2.6) to confirm the presence of the gene of interest.

2.3.5 Plasmid purification

The Qiagen miniprep plasmid purification kit (Qiagen Ltd) was used to purify the plasmid DNA. Initially 1.5 ml sample of transformed plasmid was pipetted into a 1.5 ml sterile microcentrifuge tube and the sample was centrifuged for 5 min at 13.000 rpm in a bench top centrifuge at RT. The supernatant was removed by pipetting and another 1.5 ml of the sample was added into the same tube followed by further centrifuging for 5 min at 13.000 rpm at RT. At the end of centrifuging, the supernatant was once again removed and the pellet was resuspended in 250 µl of P1 buffer according to the manufacturer's recommendations. Next, 250 µl of P2 buffer was added and mixed thoroughly by vortexing and immediately after, 350 µl of N3 buffer was added and immediately mixed. The sample was then centrifuged for 10 min at 13.000 rpm at RT on a bench top centrifuge. The supernatant was then added to a Qiagen spin column inserted in a 1.5 ml sterile microcentrifuge tube and centrifuged for 1 min at 13.000 rpm at RT. The supernatant was removed and 0.75 ml of PB buffer was added to the column followed by centrifugation for an additional 1 min. The flow through was removed and an additional 1 min centrifugation was performed to remove any residual ethanol contained in the buffer. The spin column was then placed into a 0.5 ml sterile microcentrifuge tube and in order to elute the DNA, 50 µl of sterile-distilled H_2O was added to the centre of the spin column membrane. The sample was allowed to stand for 1 min before centrifugation at 13.000 rpm for 1 min at RT to elute the DNA in the flow through. The cDNA sample was stored at -20°C until further analysis.

2.3.6 Sequence analysis

The concentration of the sample as provided from the previous step was measured and recorded using a Nanodrop ND 1000 spectrophotometer (Thermo-Scientific, Wilmington, USA). The sample was diluted to 50 ng/ml in sterile-distilled H_2O and 10 µl was used for sequence analysis. If the concentration of the sample was less than 50 ng/ml, an additional PCR reaction was performed to increase the concentration. This PCR was based on amplification with M13 primers because of the pGEM-Teasy Vector's M13 binding sites (pGEM-Teasy Vector Map and Sequence Reference Points,

Promega). The PCR program followed was the same as the verification PCR (Section 2.2.5) with the annealing temperature set at 48°C. Following PCR, the sample was diluted to a concentration of 50 ng/ml. Sequencing was performed using the ABI prism sequencer (DNA sequencing services, Dundee, UK).

2.4 REAL-TIME PCR ANALYSIS

Real-time PCR (qRT-PCR) can result in a simultaneous quantitative gene expression for a few genes in many different samples and can be performed on samples containing only few cells (Heid *et al.*, 1996). This method has dramatically improved studies requiring quantitative gene expression because of its speed, ease of use, high sensitivity, reproducibility and lack of radioactive materials (Radonic *et al.*, 2004). The results of real-time PCR depend on the successful application of mRNA isolation, cDNA synthesis and the use of appropriate controls is necessary for the final analysis (Gal *et al.*, 2006). Real-time analysis in this thesis was performed on the basis of relative quantification of the amount of mRNA in each sample. To facilitate comparisons across different tissue types and between treatments it was necessary to normalise the transcript levels against the transcript levels measured for the relevant housekeeper genes. The use of valid reference genes for normalisation is important in order to both interpret the real-time PCR results accurately and to understand the biological dynamics of events of oocyte and embryo development (Mamo *et al.*, 2007). Different studies have compared a wide range of the most commonly used housekeeping genes in order to determine which housekeepers are more stable for normalisation of gene expression data in the early developmental stages (Gal *et al.*, 2006; Jeong *et al.*, 2006; Mamo *et al.*, 2007). Out of the different commonly used housekeeping genes, *H2A* has been shown to be 1 of the most stable gene tested in mouse oocytes and preimplantation staged embryos produced both *in vivo* and *in vitro* (Jeong *et al.*, 2005). Recently a set of guidelines that propose a minimum standard for real-time PCR experiments has been established (Bustin, 2010). According to the minimum information for publication of qRT-PCR experiments (MIQE) guidelines, the utility of the housekeeper used for normalisation must be validated experimentally for particular tissues or cell and unless fully validated, normalisation should be performed against multiple reference genes, chosen from a sufficient number of candidates (Bustin *et al.*, 2010). In the experimental series of this thesis, normalisation of gene expression was performed against 2 housekeepers, *H2A* which has been validated in the oocyte (Mamo *et al.*, 2007) as well as *GAPDH* which has also been validated and previously used for normalisation of gene

expression in ovine oocytes (Cotterill *et al.*, 2012). For the experiments, SYBR green technology (Applied biosystems) was used to quantify the total amount of each transcript. Different primers were designed using the primer 3 programme as described previously (Section 2.2.5) and the parameters of the primer design product size of ~100bp, avoidance of the guanine-cytosine clamp at the 3´ (not more than 2 guanine or cytosine residues in the last 5 bases) and avoidance of base repeats. Primer specificity for each of the genes of interest used in the thesis was tested by verification PCR (Appendix III) and by generating dissociation curves following real-time PCR analysis on groups of ten oocytes for oocyte expressed genes or groups of 2 cultured cumulus shells for cumulus expressed genes. The primer information and sequences of housekeepers used for real-time PCR are shown in Table 2.7.

Table 2.7: Primer sequences of housekeeper genes used for real-time PCR

Gene	Primer Sequence	Size (bp)	Reference
GAPDH ovine	F: 5´ TGATTCCACCCATGGCAAGT 3´	93	AF030943
	R: 5´ CGCTCCTGGAAGATGGTGAT 3´		
H2A ovine	F: 5´ GAGTAGGCGGCTGGTTCTC 3´	109	AY074805
	R: 5´ GGAGTCCTTCCCAGCCTTAC 3´		

Forward and reverse primers were mixed with sterile-distilled H_2O to a concentration of 10 μM. The mastermix for the reaction was then set-up in a 1.5 ml sterile microcentrifuge tube with the addition of 12.5 μl of SYBR green master mix (Applied Biosystems), 1.25 μl specific primer set (500 pM) and 10.25 μl of sterile-distilled H_2O. Different mastermixes were created for different genes and housekeepers. Out of the mastermix, 24 μl were added to 1 μl of each test sample. Test samples were evaluated in triplicates to minimise pipetting errors and increase stability of the results. In addition, 3 negative controls were also set-up for each real-time PCR reaction to make sure that there was no contamination in the reaction reagents. In order to avoid non-specific amplification, dissociation curves were run with each real-time PCR experiment. This was achieved by progressively heating and cooling the real-time PCR products and by this way SYBR green was released as shown in Figure 2.2 (Ririe *et al.*, 1997). The release of SYBR green resulted in the creation of either single peaks which resembled high specificity for the target gene, or multiple peaks that represented low specificity. Using this approach, only primers with a high specificity for the target gene were selected.

In order to obtain accurate relative quantification of an mRNA target, the expression levels of 2 endogenous control housekeepers were also obtain in at least 3 repeats along with the expression levels of the mRNA target in triplicates. The measurements from different repeats were averaged for both the gene of interest and the 2 housekeepers and the average concentration of the sample's gene of interest was divided by the endogenous control concentration in order to normalise the data. The endogenous control concentration was defined as the average of the 2 housekeeper concentrations as defined by the number of repeats. The endogenous controls were therefore used as active reference in order to quantify target differences in the amount of total nucleic acid in each reaction. In this way, the differences in the expression levels of multiple genes between the different experimental samples and control samples were calculated.
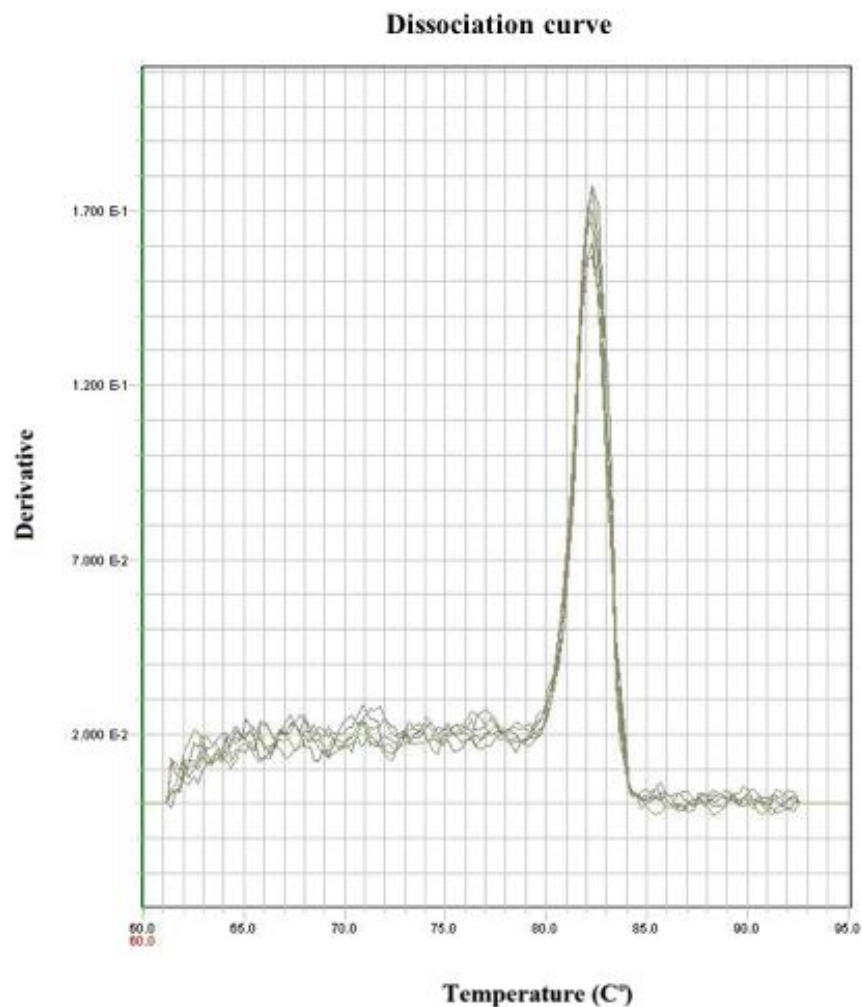
Figure 2.2: Image of a representative dissociation curve following real-time PCR. The dissociation curve was generated in triplicates using a cDNA library of 10 oocytes and *GAPDH* primers indicating high specificity for the target gene following real-time PCR. Each of the lines represents the absorbance value at a given temperature.

2.5 WESTERN BLOTTING

Western blotting is an analytical technique employed to study the protein expression of samples of tissue that are either extracted or homogenised (Towbin *et al.*, 1979). The technique is based on the electrophoretic separation of denatured proteins with the degree of separation being determined by the protein size. The separated proteins are then transferred onto a nitrocellulose membrane where a target protein can be stained with an antibody specific to that protein (Renart *et al.*, 1979; Towbin *et al.*, 1979).

2.5.1 Tissue preparation

For the series of experiments described in Chapter 3, gametes, gonadal tissue and somatic tissue was used for Western blotting analysis. Sample pieces of ovine ovary and bovine testis tissue were collected under sterile conditions into 1.5 ml sterile microcentrifuge tubes and snap-frozen in liquid nitrogen and then stored at -80°C until use. Similarly, ovine kidney and lung pieces were also stored. For Western analysis, tissue was processed and lysed in lysis buffer made up in a final volume of 50 ml in sterile-distilled H_2O. The lysis buffer was made up with 100 mM of potassium acetate (KOAc, 1 ml), 0.1% (v/v) Triton X-100 (50μl), 1 M Hepes (pH 7.4, 2.5 ml), 2 mM magnesium acetate (MgOAc, 0.5 ml), 10% (v/v) Glycerol and 1 tablet of Proteinase inhibitor (Roche, Sussex, UK). Originally 1 small piece of tissue of approximately 0.2 cm^3 was transferred into a porcelain pestle and mortar (SLS) that has been previously cleaned with 70% (v/v) ethanol in Milli-Q H_2O (Millipore Ltd, Watford, UK) followed by a wash with Milli-Q H_2O. The sample was then added to the clean pestle and mortar and submerged in liquid nitrogen. The sample was then ground to a fine powder until the liquid nitrogen evaporated. In case the tissue had not been completely processed, more liquid nitrogen was added. The pestle was then allowed to cool a little before 1 ml of lysis buffer was added. The powdered tissue was at that point mixed with the 1 ml of lysis buffer allowing the ground tissue to lyse and the lysate was collected up into a 1.5 ml sterile microcentrifuge tube. All the samples were prepared in a similar way and kept on ice. The samples were then centrifuged at 13,000 rpm for 20 min at 4°C and the supernatant was retained and filtered with a 0.2 μm cellulose acetate syringe filter into a new 0.5 ml sterile microcentrifuge tube. Protein concentration was determined using the Nanodrop ND 1000 spectrophotometer. Samples were kept at -20°C until use.

Oocyte samples were prepared in a different way. Specifically, following collection of intact COCs, GV denuded oocytes were harvested (Section 2.1.2). Following IVM

(Section 2.1.3), denuded MII oocytes were also collected. Both GV and MII oocytes were removed from the COC environment by denudation. This process involved using a flexi-pet (Cook Medical, Brisbane, Australia) attached to a 170 μm pipette tip (Cook Medical) followed by gentle repeat pipetting in order to separate the oocytes from the majority of the surrounding cumulus cells. In order to remove all the cumulus cells, the pipette tip of the flexi-pet was changed to 140 μm diameter pipette tip followed by further gentle repeat pipetting. Denudation was performed in 4 well nunc dishes with 10 oocytes/well contained in 400 μl of oocyte holding media H199$^+$ (Section 2.2.1). Oocytes were denuded before being transferred and washed twice in fresh wells containing 400 μl of DPBS (Invitrogen Ltd). From there, each group of oocytes was transferred in the minimum volume into a 0.5 ml sterile microcentrifuge tubes containing 10 μl of lysis buffer (Section 2.2.1) and the samples were immediately snap-frozen by submerging the tube in liquid nitrogen. When all the samples were collected, protein concentration was determined using the Nanodrop ND 1000 spectrophotometer and samples were transferred to a -80°C freezer until further analysis.

2.5.2 Sodium Dodecyl Sulfate-Polyacrylamide gel electrophoresis

The method of Sodium Dodecyl Sulfate-Polyacrylamide Gel Electrophoresis (SDS-PAGE) is a widely used biochemical method and proteins can be successfully fractioned using this method (Laemmli, 1970). The SDS itself is an anionic detergent that linearises proteins and conveys them a negative charge and with electrophoresis proteins are fractioned according to their approximate size (Shapiro *et al.*, 1967; Laemmli, 1970). For the SDS-PAGE, the Mini-Protean Tetra Electrophoresis System (Bio-Rad Ltd) was used that contained combs, plates and casting accessories for 10-well, 0.75 and 1 mm thick gels. Before setting up the gel, all glass casting plates were washed twice with 70% (v/v) ethanol in Milli-Q H$_2$O and then dried with a soft tissue. The casting plates were then washed with Milli-Q H$_2$O and dried with a soft tissue before being assembled into the gel clamp. Clamps were pressed together slowly and simultaneously to ensure even pressure was applied in order to prevent leaks. The clamps were then secured in the rack. A 10% (w/v) lower resolving gel was then prepared by adding 2.5 ml of sterile-distilled H$_2$O, 1.25 ml stacking gel buffer (18.15 g Tris buffer in 100 ml of sterile-distilled H$_2$O at a pH of 8.8), 0.52 ml 40% (w/v) acrylamide mix in sterile-distilled H$_2$O, 25 μl 20% w/v SDS in sterile-distilled H$_2$O, 100 μl ammonium persulfate stock (APS, 0.1g APS in 1 ml of sterile-distilled H$_2$O) and 10 μl TEMED (Appendix II). Both APS and TEMED were added quickly and around 3.5

ml of the 10% resolving gel were quickly dispensed into the casting cassette. Immediately after dispensing the resolving gel, Milli-Q H_2O was layered on top of the gel up to the top of the cassette to ensure that the gel set evenly. Water was dispensed slowly to avoid disturbing the gel. The gel was then left to set for at least 15 min. Thereafter, the water was removed by placing tissue paper in the top corner and tipping the casting tray up until all of the water has been drawn up by the tissue paper. A 4% (w/v) stacking gel was then made up by adding 3.2 ml of sterile-distilled H_2O, 1.25 ml stacking gel buffer (6.05 g Tris buffer in 100 ml of sterile-distilled H_2O at a pH of 6.8), 0.52 ml 40% (w/v) acrylamide mix in sterile-distilled H_2O, 25 μl 20% (w/v) SDS in sterile-distilled H_2O, 100 μl APS and 10μl TEMED. Again APS and TEMED were added quickly and around 2 ml of the stacking gel were dispensed quickly on top of the resolving gel until the gel reached near the top of the glass plate. The comb was then carefully inserted and the gel was left to set for at least 30 min.

At this point, the samples (Section 2.5.1) were prepared. Sample pieces of ovine cortex, bovine testis as well as non gonadal somatic tissue were diluted in a ratio of 1:1 with 2 X SDS buffer and 40 μg of crude samples was used for loading. Oocyte samples were also diluted in a ratio of 1:1 with 2 X SDS buffer and the total 20 μl of each oocyte sample was used for loading. The 2 X SDS buffer was prepared by adding 5 ml of Stacking Gel buffer, 2 ml of 10% (w/v) SDS in sterile-distilled H_2O, 1 ml of 0.1% (v/v) bromophenol blue in sterile-distilled H_2O, 5 ml of 60% (v/v) glycerol in sterile distilled H_2O, 1 ml β-mercaptoethanol and 6 ml of sterile-distilled H_2O (Appendix II). If samples required further dilutions based on the intensity of the signal the antibodies produced, 1:5 dilutions were created by adding 6 μl of sample to 9 μl of sterile-distilled H_2O and 15 μl of 2 X SDS buffer. Further dilutions where then made by diluting this stock. The samples were denatured by warming a glass beaker to boiling point and placing the samples in a foam rack so that the sample itself was in direct contact with the boiling water and the samples were boiled for 7 min.

For the electrophoresis, 4 X running buffer was prepared by adding 57.6 g of glycine to 12 g of Tris and 10 ml of 20% (w/v) SDS in Milli-Q H_2O in 1 L of Milli-Q H_2O at a pH of 8.3. From this stock, a 1 X running buffer was made fresh each time by mixing 250 ml of running buffer with 750 ml of Milli-Q H_2O. The SDS-PAGE gel that was prepared as described above was placed into a clamp and the clamp was inserted into the tank. The inner tank containing the clamp and the gel was filled with 1 X running

buffer and was left for 2 min to confirm that there were no leaks. If leaks were detected, the gel was re-clamped and the same process was repeated. The comb was then removed allowing the 1 X running buffer to insert into the wells and any excess acrylamide within the wells was removed using a long thin pipette tip by gentle pipetting the 1 X running buffer within the wells. The outer tank was also filled with the remaining 1 X running buffer. The samples were then loaded into the wells. In the first well, 5 μl of precision plus protein standards (Bio-Rad) was used as a marker. The rest of the test samples were then loaded (20 μl) into the subsequent wells. Electrophoresis was conducted with a PowerPac basic power supply (Bio-Rad) set on 160 V for 70 min at RT or until the coloured dye in the sample loading buffer began to elute from the bottom of the gel.

At this stage, to test the efficiency of the electrophoresis on the samples, the separated protein bands in the polyacrylamide gel were visualised using an EZ blue Gel staining reagent (Diezel *et al.*, 1972). In order to perform this, a probe fixation buffer was prepared by adding 50% (v/v) Methanol (50 ml) and 10% (v/v) Acetic acid (10 ml) in Milli-Q H_2O (40 ml). Following electrophoresis, the gel was placed in a plastic tray with fixation buffer and left to agitate for 15 min at RT followed by 3 washes in Milli-Q H_2O. The ready to use EZ blue Gel staining reagent (Sigma-Aldrich) was then added to the plastic tray (10 ml) and left to agitate for 1 h at RT. The staining reagent was then poured off and following 2 washes with Milli-Q H_2O the separated proteins were stained blue and could be visualised on the gel.

2.5.3 Protein transfer
Transfer was conducted immediately after electrophoresis. This step is required to make the separated proteins accessible to antibody selection and it incorporates moving them from within the gel onto a membrane that can be either nitrocellulose or a polyvinylidene fluoride (PVDF) (Matsudaira, 1987). For this step the mini trans-blot cell was used (Bio-Rad). A 4 X transfer buffer was prepared by adding 12 g of Tris and 57.6 g glycine making it up to 1 L with Milli-Q H_2O. From this stock, the 1 X transfer buffer was made by adding 250 ml of 4 X transfer buffer to 200 ml of methanol and making it up to 1 L with Milli-Q H_2O. Following electrophoresis the gel was removed from the clamp and the gel situated in between the spacer glass plate and the shorter plate was placed into a plastic tray containing Milli-Q H_2O. The gel was then carefully removed from the glass plates and washed once with Milli-Q H_2O. The gel was then

equilibrated through 2 10 min washes of 10 ml in 1 X transfer buffer on a shaking platform. For all experiments in this thesis the Immobilon PVDF membrane was used (Sigma-Aldrich). Originally, a piece of membrane covering the surface of the gel itself was wetted in 100% methanol for 30 sec followed by a rinse with Milli-Q H_2O and equilibration with 2 X transfer buffer for 10 min on a shaker with agitation. Following the washes, the transfer clamp was opened and the black mesh was placed on each side of the clamp. Whatman filter papers were cut to the size of the gel and 3 of those papers were wetted with 1 X transfer buffer and placed on each side on top of the mesh. The gel was then placed on top of the Whatman paper on the black side of the transfer clamp making sure that no air bubbles were trapped beneath the gel. The gel was thereafter covered with the membrane and the transfer clamp was closed securing the gel with the membrane in between the Whatman papers. The transfer clamp was then placed inside the transfer tank. An icepack was then added into the tank and the tank was filled with 1 X transfer buffer. Transfer took place for 60 min at 4°C set at 400 A on a PowerPac basic power supply.

2.5.4 Blocking and Detection

To avoid non-specific binding between the membrane and the antibody, the membrane was blocked in blocking buffer solution containing 1.5 g of non-fat dry milk powder and 50 μl of Tween-20 in 50 ml of 1% (v/v) PBS in Milli-Q H_2O. Before this step took place, originally the membrane was removed from the transfer clamp and rinsed 3 times in a plastic tray containing 15 ml of 1% (v/v) PBS in Milli-Q H_2O with 0.1% (v/v) Tween-20. Thereafter, 15 ml of the blocking buffer were added in the plastic tray and placed on a shaker for 1 h to block at RT. The membrane was then ready to be probed for the protein of interest using an appropriate primary antibody linked to a reporter enzyme that produces a colour when the enzyme is exposed to an appropriate substrate. This was performed with a 2-step process that was comprised of incubation with a primary and a secondary antibody. Initially, the blocking buffer was poured off and replaced with 15 ml of non-fat dry milk powder dissolved in 1% (v/v) PBS in Milli-Q H_2O containing the appropriate primary antibody diluted to the manufacturer's recommended concentration. The blot was then left to agitate in the solution overnight in a cold room at 4°C. The following day, the primary antibody was poured off the plastic tray and 3 subsequent washes of 15 ml in 1% (v/v) PBS in Milli-Q H_2O with 0.1% (v/v) Tween-20 in order to remove any unbound primary antibody were performed. This was followed by incubation with a secondary antibody that was

directed at a species specific region of the primary antibody and is usually linked to a reporter enzyme. The secondary antibody was reconstituted according to the manufacturer's recommended concentration in 15 ml of non-fat dry milk powder dissolved in 1% (v/v) PBS in Milli-Q H_2O. Following the washes, the reconstituted secondary antibody was added in the tray and placed on a shaker for 1 h at RT. Detection was performed with the Lumingen TMA6 kit (Amersham Biosciences, Little Chalfont, UK) according to the manufacturer's recommendations. The Kit provides a substrate for chemiluminescent detection of peroxidise conjugates on the transfer membranes. For the reaction, 1.5 ml of Solution A was added to 1.5 ml of Solution B and the mixture was added directly on top of the blot and left to agitate for 5 min at RT in day light. The blot was then removed from the detection solution and wrapped in cling film. Detection was then performed by a charged coupled device camera on a LAS-3000 imaging system attached to the Image Reader LAS-3000 computer software (Fujifilm UK Limited, Bedford, UK). Following detection the blot was wrapped in cling film to retain hydration and kept at 4°C for re-probing if required.

2.6 GENERAL HISTOLOGY METHODS

2.6.1 Fluorescence *in situ* hybridisation

The fluorescence *in* situ hybridisation (FISH) technology uses a labelled complementary DNA or RNA strand (probe) in order to localise a specific DNA or RNA sequence in the tissue (Femino *et al.*, 1998; Levsky and Singer, 2003). In order to perform this method successfully, ribonucleases (RNases) that catalyse the degradation of RNA must not come in contact with the tissue at any point (Nicholson, 1996). This was achieved by using sterile technique in conjunction with washing of all tissue and equipment with diethylpyrocarbonate (DEPC) treated H_2O that inactivates the RNase enzymes in H_2O and all other utensils. To prepare this product, 0.1% (v/v) DEPC was added to Milli-Q H_2O followed by autoclaving (in order to hydrolyse it) before tissue collection. Using the same approach, PBS was made up by adding 2 tablets of PBS (Invitrogen Ltd) in 1 L of 0.1% (v/v) DEPC treated H_2O followed by autoclaving. Before usage, all instruments were washed in 0.1 N NaOH (4g of NaOH in 1 L of 0.1% (v/v) DEPC treated H_2O) for 2 h before being rinsed with 1% (v/v) DEPC treated H_2O.

2.6.2 Tissue collection and processing

Ovine tissue was collected as described previously (Section 2.1). Individual ovine ovaries were removed from FIM and transferred to an autoclaved 90 mm glass Petri dish (SLS) that was previously washed in 0.1 N NaOH for 2 h and rinsed with 0.1% (v/v) DEPC treated H_2O. The ovaries were then cut into half using sterile scalpel blades. With the help of the scalpel blade, the stroma of the ovary was removed and the cortex was placed in 4% (w/v) paraformaldehyde (PFA) was added in 0.1% (v/v) DEPC treated PBS (2 g of paraformaldehyde powder in 50 ml of PBS in 0.1% (v/v) DEPC treated H_2O). The PFA was prepared fresh on the day of use and was filter sterilised before use with a 0.2 μm syringe filter. Following 2 consecutive washes in different 100 ml sterile glass beakers containing 50 ml of 4% (w/v) PFA in each, ovaries were transferred in a new 100 ml sterile glass beaker containing 50 ml of 4% (w/v) PFA and left overnight on the bench at RT. Approximately 6-8 ovary pieces were fixed each time. The volume of the fixative was always set to be at least 12 times that of the tissue volume and was adjusted accordingly if more tissue was used. The day after, PFA was replaced with 70% (v/v) ethanol in 0.1% (v/v) DEPC treated H_2O and incubated for 2 h at RT. Finally, the tissue was washed twice with fresh 70% (v/v) ethanol in 0.1% DEPC treated H_2O and stored at RT for no more than 3 months until embedding in wax.

2.6.3 Tissue embedding

After the tissue was fixed it was embedded according to the method previously described by Chambers *et al.*, (2010). The tissue was manually embedded in paraffin wax (VWR). Pieces of tissue were placed in Histosette® II embedding cassettes (Simport, Beloeil, Canada) and the cassettes were placed in a 250 ml glass beaker containing 150 ml of 90% ethanol in 0.1% (v/v) DEPC treated H_2O. If more cassettes were used, the volume of ethanol added was increased accordingly in order for the cassettes with tissue to be fully covered with ethanol. The beaker containing the cassettes was placed in a shaking hybridisation oven/shaker (Hybaid, SLS) at RT and left to agitate gently for 1 h. The 90% ethanol in 0.1% (v/v) DEPC treated H_2O was then replaced with 100% ethanol and incubated at RT with agitation for a further 1 h. The ethanol was replaced with fresh 100% ethanol for a further hour under the same conditions. The ethanol was then replaced with 100% Histological clearing agent (Histo-clear, National diagnostics, North Humberside, UK) and the tissue was left to agitate for 1 h at RT. The histo-clear was then replaced with fresh reagent and the temperature of the hybridisation oven/shaker was set to 60°C with the samples agitating

for 30 min. At the same time a sterile glass beaker was filled with pellets of paraffin wax and the wax was left to melt on a hot plate (VWR) set at 100°C. When the wax was completely melted, the beaker was transferred to the shaking hybridisation oven/shaker at 60°C. To avoid damaging the tissue, a thermometer was used throughout all the steps that followed, to make sure that temperature of the wax did not exceed 60°C. After the cassettes had been washed for 30 min with histo-clear, wax was added to the histo-clear to an approximate ratio of 75% histo-clear to 25% wax, and the samples were left to agitate in the hybridisation oven/shaker at 60°C for 1 h. More molten wax was then added to the beaker with the cassettes resulting in a volume of 50% histo-clear to 50% wax and the samples were left to agitate at 60°C for an additional hour. At the end of the incubation time, more wax was added resulting in a volume of 75% wax to 25% histo-clear and the cassettes with the tissue were incubated with agitation at 60°C for another hour. Finally, all the wax and histo-clear was removed and replaced with fresh molten wax. The samples were then left agitating at 60°C overnight. The next day, the molten wax was replaced and left for 2 h under the same conditions. The ovary pieces were then transferred out of the cassettes with the help of forceps washed in 0.1% (v/v) DEPC treated H_2O and each piece was transferred in stainless steel base molds (VWR) and blocked in wax. Blocks were left to solidify at RT and were then kept at -20°C until sectioning. Blocks were cut into 5 μm thin sections with a microtome (Thermo Fisher Scientific, Hempstead, UK). The cut sections were transferred on a mounting bath (Keison, Essex, UK) set at 37°C containing 0.1% (v/v) DEPC treated H_2O and from there they were placed on Superfrost plus glass slides (Thermo Fisher Scientific) until analysis.

2.6.4 Template preparation

The DNA template required for the FISH experiments was obtained following the cloning procedure as described in Section 2.3. Specifically, a PCR was run using primers for the gene of interest on an ovine MII cDNA library, the DNA fragment representing the length of the gene of interest was excised from the Agarose gel and the cloning processes were then applied. Sequencing that followed verified the specificity for the gene of interest. For FISH analysis, the FISH Tag RNA green Kit (Invitrogen Ltd) was used. This system is based on traditional *in vitro* transcription using a 2-step labelling approach in order to provide improved dye incorporation (Cox and Singer, 2004). The first step employs incorporation of an amine-modified nucleotide into the probe template, whilst in the second step, incubation with the amine-reactive dyes

results in dye labelling of the purified amine-modified RNA-incorporation (Cox and Singer, 2004). For the experiment, initially *in vitro* transcription was performed to a final volume of 20 μl according to the manufacturer's recommendations and 2 reactions were set up using different RNA polymerases T7 and SP6 that have opposite orientations. The RNA can be selectively synthesized from either strand of the DNA with the different polymerases (Figure 2.3). The use of the 2 different RNA polymerases for the synthesis of the amine-modified RNA in separate reactions, results in the generation of an anti-sense RNA probe and a sense RNA probe. The anti-sense RNA probe with complementary sequence to the target hybridises *in situ* to the specimen, while the sense RNA probe with identical sequence to the target does not hybridise and therefore serves as a negative control.
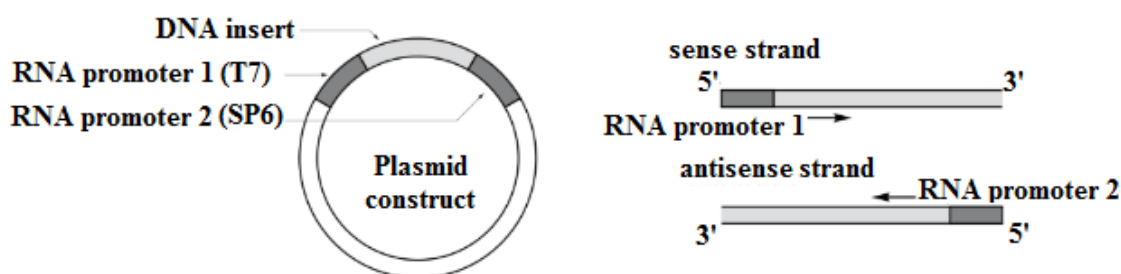
Figure 2.3: Schematic representation of the plasmid construct for *in vitro* transcription using the FISH Tag kit. The DNA insert for the gene of interest is contained between different RNA promoter sequences (T7 and SP6) on opposite strands and ends of the vector. Based on the orientation of the DNA insert, T7 and SP6 polymerases create an antisense RNA probe complementary to the target that results in hybridisation and a sense RNA that does not result in hybridisation. One example is shown. Image from: www.invitrogen.com.

2.6.5 Synthesis and labelling of amine-modified RNA

The procedures were conducted accordingly to the manufacturer's recommendations for the FISH Tag RNA green Kit (Invitrogen Ltd). The first step employed incorporation of an amine-modified nucleotide into the probe template, whilst in the second step, incubation with the amine-reactive dyes resulted in dye labelling of the purified amine-modified RNA incorporation (Cox and Singer, 2004). For the experiment, *in vitro* transcription was performed to a final volume of 20 μl according to the manufacturer's recommendations and 2 reactions were set up using different RNA polymerases T7 and SP6. The reactions were set up in sterile 0.5 ml microcentrifuge tubes as follows: 4 μl of 5 X transcription buffer (either T7 or SP6), 2 μl of 10 X RNA nucleotide mix, 1 μg of DNA template (Section 2.6.4), 1 μl of RNase-OUT inhibitor and 1 μl of RNA polymerase (T7 or SP6). 1 μl of 0.1 M DTT was added for the reaction using T7 RNA

polymerase, while 2 μl of 0.01 M DTT was added for the reaction using SP6 RNA polymerase. The nuclease-free H_2O provided in the kit was added to a final volume of 20 μl. The transcription reaction was then mixed gently by pipetting the mixture and it was incubated at 37°C for 1 h on a hot block. Thereafter, 1 μl of DNase I was added and mixed gently by pipetting and the reaction was incubated at 37°C for 15 min. Next, 79 μl nuclease-free H_2O provided in the kit was added to the sample and the reaction was vortexed for 10 sec in order to inactivate the DNAse I.

After *in vitro* transcription, the amine-modified RNA was purified. For this, 400 μl of binding buffer with isopropanol provided in the kit was added to the reaction microcentrifuge tube and mixed. The entire volume contained in the reaction tube was then pipetted into a spin column contained inside a sterile 2 ml collection tube. The column was centrifuged at 13,000 rpm for 1 min with the RNA binding to the column. The flow-through was then discarded and the column was washed with 650 μl wash buffer containing ethanol as recommended by the manufacturer's recommendations. The column was then centrifuged at 13,000 rpm for 1 min and the flow through was discarded. An additional centrifugation was then performed under the same conditions to remove any residual wash buffer. A sterile 1.5 ml microcentrifuge collection tube was added to the spin column and 55 μl of nuclease-free H_2O was supplied in the kit was applied to the centre of the column. The column was allowed to stand at RT for 1 min followed by centrifugation at 13,000 rpm for 1 min. The purified amine-modified RNA contained in the collection tube was then precipitated. This was performed by adding 10 μl of 3M sodium acetate (pH 5.2), 1 μl glycogen and 39 μl nuclease-free H_2O as supplied in the kit. From there, 300 μl of 100% ethanol was added and the sample was stored at -80°C for 30 min. The sample was subsequently centrifuged at 13,000 rpm for 10 min and the supernatant was removed without disturbing the pellet. The pellet was rinsed with 400 μl of 70% (v/v) ethanol in 0.1% (v/v) DEPC treated H_2O, followed by removal of the supernatant with a second repetition of this rinse step. Using a pipette the residual ethanol was removed without disturbing the pellet and the sample was allowed to air-dry. Then 5 μl of nuclease-free H_2O was added to the pellet and the sample was incubated at 37°C for 5 min. The sample was then vortexed to fully resuspend the RNA. The template was then ready to proceed immediately to the fluorescent dye labelling step.

To add a fluorescent label to the amine-modified RNA it was denatured by incubation at 65°C for 5 min. The sample was then placed on ice for 3 min and centrifuged at 13,000 rpm for 3 min. Next, 3 μl of sodium bicarbonate sodium as supplied in the kit was added to the sample. The reactive dye provided in a 1.5 ml microcentrifuge tube was resuspended in 2 μl DMSO and vortexing was performed to fully resuspend the dye. The 2 μl of the reactive dye in DMSO was then added to the RNA sample at RT and vortexed at maximum speed for 15 sec. The labelling reaction was then wrapped in foil and incubated in the dark for 1 h at RT. Thereafter, 90 μl of nuclease-free H_2O was added to the sample and the fluorescent dye-labelled RNA was purified and precipitated as described in the above paragraph. Following air-drying of the pellet, 40 μl of nuclease-free H_2O was added to the pellet followed by incubation at 37°C for 5 min. The sample was then vortexed to fully resuspend the dye-labelled RNA and it was stored at -80°C by wrapping in foil to protect it from light. The labelled amine-modified RNA with fluorescent dye was used within 2 weeks of preparation.

2.6.7 FISH protocol

For FISH, the selected slides were placed in a stainless steel slide rack (Thermo Fisher Scientific) and were de-waxed and re-hydrated by immersing the slide rack in 300 ml of reagents in different glass staining dishes (Thermo Fisher Scientific) at RT as follows:

- 10 min in Xylene
- 10 min in fresh Xylene
- 5 min in 100% ethanol
- 5 min in 70% ethanol in 0.1% (v/v) DEPC treated H_2O
- 5 min in 50% ethanol in 0.1% (v/v) DEPC treated H_2O
- 10 min in 0.1% (v/v) DEPC treated PBS
- 10 min in fresh 0.1% (v/v) DEPC treated PBS

The slides were then treated with 4% PFA (w/v) in 0.1% (v/v) DEPC treated PBS by placing the slides in a coplin-jar (Thermo Fisher Scientific) filled with 4% (w/v) PFA (100 ml). Following treatment with 4% (w/v) PFA, the slides were transferred back to the slide rack and were washed twice as previously for 10 min in 0.1% (v/v) DEPC treated PBS. The slides were then treated with 0.2 N HCl in 0.1% (v/v) DEPC treated PBS for 10 min again in a staining dish followed by another 2, 10 min washes in PBS. Subsequently, the slides were treated with 1 mg/ml Proteinase K in phosphate buffer

Tween buffer (0.1% (v/v) DEPC treated PBS containing 0.1% Tween 20) for 10 min. For this step the slides were removed from the slide rack and after carefully wiping off the excess PBS on the glass slides with soft clinical tissues (Lotus Professional, Sheffield, UK), 200 μl of 1mg/ml Proteinase K in phosphate buffer Tween buffer were pipetted directly onto the tissue section and then covered by a piece of Parafilm (VWR) to assure that the tissue sections didn't dry out. The slides were then once again transferred back into the slide rack and were washed twice for 10 min in 0.1% (v/v) DEPC treated PBS. The next step of hybridisation was the pre-hybridisation step, where the slides were incubated with pre-hybridisation solution at 53°C for 3 h. The pre-hybridisation solution consisted of 50% (v/v) formamide in 0.1% (v/v) DEPC treated H_2O, 4 X 3 M sodium chloride with 300 mM trisodium citrate (SSC) in 0.1% (v/v) DEPC treated H_2O, 100 μg/ml denatured salmon sperm DNA, 50 μg/ml heparin, 0.1% (v/v) Tween 20 in 0.1% (v/v) DEPC treated H_2O and 5% (w/v) dextran sulphate in 0.1% (v/v) DEPC treated H_2O.

For the pre-hybridisation step, slides were initially placed in a metallic slide container (VWR) so that the tissue sections on each slide were facing upwards. After removing the excess PBS on the glass slides with soft clinical tissues, 200 μl of the pre-hybridisation solution pre-warmed for an hour at 53°C was pipetted directly onto the tissue section and then covered by a piece of parafilm. The metallic container with the slides was then incubated for 3 h at 53°C in a non-gassed incubator. At the end of 3 h, the hybridisation step followed in which 1 μg/ml of dye-labelled RNA (Section 2.6.6) was added to new pre-warmed pre-hybridisation solution to form the hybridisation solution. This step was followed for both the T7 and the SP6 originating dye-labelled RNAs. Half of the slides were hybridised with the T7 dye-labelled RNA and half of the slides were hybridised with the SP6 dye-labelled RNA. The hybridisation solution was added to the slides (200 μl per slide) following the same procedure as the pre-hybridisation solution. The metallic slide container was then closed to avoid light exposure and placed in the non-gassed incubator set at 53°C overnight.

The following day, the slides were placed in a coplin-jar filled with pre-warmed washing solution (100 ml) at 53°C and the jar was incubated in the non-gassed incubator at 53°C for 10 min. The washing solution was consisted of 50% (v/v) formamide in 0.1% (v/v) DEPC treated H_2O, 2 X Saline-sodium citrate buffer (SSC) in 0.1% (v/v) DEPC treated H_2O and 0.1% (v/v) Tween 20 in 0.1% (v/v) DEPC treated

H$_2$O. The 2 X SSC was made up from the 20 X SSC stock of 3M NaCl and 300 mM of Sodium Citrate in sterile-distilled H$_2$O, pH adjusted at 7.0 and sterilised by autoclaving (Appendix II). Washing was repeated for an additional 10 min with new pre-warmed washing solution. Following the 2 washes, the excess washing solution was removed with soft clinical tissues and a drop of antifade solution (supplied in the FISH Tag green kit) was added on the slides before being covered with a 24 X 50 mm cover slip (VWR). The slides were then wrapped in aluminium foil to avoid light exposure and were viewed under a fluorescent microscope (Zeiss Axioplan2, Carl Zeiss Ltd, Cambridge UK) fitted with a filter with an excitation wavelength range between 495 and 520 nm to capture green fluorescence. Images were captured using the Cytovision 4.5 computer software (Leica Microsystems Ltd, Milton Keynes, UK).

2.7 STATISTICAL ANALYSIS

Data generated in the thesis were processed using Microsoft Excel and PowerPoint. All statistical analyses were performed by Minitab 15.0 software. The Anderson-Darling test was used to test data for normality. Culture data were analysed using the Student's t-test or chi-square for normally distributed data. Mann Whitney U tests were performed on data that were not normally distributed. In all analyses P values of <0.05 were considered to be statistically significant.

Chapter 3: Characterisation of ovine *GTSF1*

3.1 INTRODUCTION

Identifying the best oocyte for fertilisation in assisted reproduction is a daunting task. The methods that have already been established include morphological evaluations of oocytes as well as polar body analysis with FISH and comparative genomic hybridisation (CGH) in order to provide insights to oocyte genetics (Patrizio *et al.*, 2007). Assays both at the molecular and cellular level have allowed identification of many potential predictors of oocyte quality associated with the oocyte and the surrounding somatic cells (Wang and Sun, 2007). In addition, the cyclic growth of follicles and the atresia that occurs is likely to affect oocyte quality and be associated with changes in the follicular fluid composition (Hunter *et al.*, 2005). The importance of identifying markers of gamete developmental competence and in particular oocyte quality cannot be emphasized enough, since identification of the functional significance of oocyte markers can provide improved fertility treatment options for patients with limited oocyte supply as detailed in Chapter 1, Section 1.1.

Genes involved in gametogenesis are usually preferentially expressed in germ cells. There is a large number of ESTs available in databases that have allowed the analysis of gene expression profiles *in silico*. Gene expression profiling has revealed an abundance of genes vital for oogenesis and early embryo development (Zheng and Dean, 2007). The functional significance of these genes can be indicated by the generation of murine transgenic mutants that do not express the gene of interest and the subsequent examination of the resulting phenotype. Some of these germ cell specific genes have been shown to have important roles in folliculogenesis and oocyte maturation including the deleted in azoospermia like, *Figla*, *Nobox*, *Sohlh1*, Y box binding protein 2 (*Ybx2*), cAMP response element binding protein 1 and *Gdf9*. Other genes are important for fertilisation like *Zp1*, *Zp2* and *Zp3*; and others for early embryo development including nucleophosmin (*Npm2*), zygote arrest 1 (*Zar1*), nacht leucine rich repeat-pyrin containing leucine rich repeat and pyrin domain containing 5 (*Nalp5*) and dipeptidyl-peptidase 3 (*Dpp3*) (Zheng and Dean, 2007). In addition, although oocyte growth is controlled exogenously, the resumption of meiotic progression is controlled by genes that regulate chromatin and spindle like *Cdk,* histone *H1oo*, formin 2 and budding uninhibited by benzimidazoles 3 (*Bub3*) (Acevedo and Smith, 2005). Another putative

marker of gamete developmental competence is *GTSF1*. This gene belongs to the UPF0224 family that is highly conserved amongst different species. *In silico* analysis of gene expression profiles based on EST's allowed the identification of several members of UPF0224 family, 1 of them being *GTSF1* also known as *Cue110*. The predicted amino acid sequences that are encoded by non-mammalian genes were shown to have a 28-48% identity with *GTSF1* at the N-terminal and the protein shares 91% with FAM112B which is the protein encoded by the human orthologue (Yoshimura *et al.*, 2007).

Characterisation studies in mice have shown that this gene is specifically expressed in differentiating germ cells of both the testis and the ovary (Yoshimura *et al.*, 2007; Krotz *et al.*, 2009). Specifically, ISH on adult murine ovarian tissue showed high degree of localisation of *Gtsf1* to the cytoplasm of primary follicles and less to primordial follicles (Krotz *et al.*, 2009). Anti-*Gtsf1* staining in newborn mouse ovary was localised primarily in the cytoplasm of oocytes within germ cell cysts and primordial follicles. Staining of primordial and primary follicles was also noted in 8 week old ovaries. The above results indicate that *Gtsf1* is expressed throughout the early stages of folliculogenesis (Krotz *et al.*, 2009). With regard to the male, the same study indicated that on postnatal day 10 in the murine testis *Gtsf1* was found in spermatogonia but not in spermatocytes (Krotz *et al.*, 2009). Similar results were also shown by Yoshimura *et al.,* (2007). Specifically, weak *in situ* hybridisation signals demonstrating *Gtsf1* were observed in mouse primary oocytes of primordial, primary and secondary follicles but the protein was not detected by immunocytochemistry. In the testis, a faint signal was observed in the spermatocytes, mostly at the pre-leptotene stage and more clear in early elongating spermatids (Yoshimura *et al.*, 2007).

The interest for this gene as a putative marker of gamete development arises from the fact that male mice mutants for *Gtsf1* have an infertile phenotype, while female mutants appear normal (Yoshimura *et al.*, 2009). Although female mutants do not demonstrate an infertile phenotype, the gene could still have functional role in gamete developmental competence as the mechanisms of mammalian meiosis are more robust in females than males (Yoshimura *et al.*, 2009). In addition, although it has been demonstrated that *Gtsf1* expression can be successfully detected, the study did not detect Gtsf1 protein using immunostaining in oocytes of wild type animals although the protein was detected in male gametes and specifically pachytene spermatocytes and round spermatids

(Yoshimura *et al.*, 2007). A further indication of the potential functional significance of *GTSF1* as a molecular marker of oocyte development is enhanced by the 2 copies of a conserved CHHC Zn-finger domain found in *GTSF1* homologs that can serve as an RNA-binding domain. The significance of RNA-binding in several cellular procedures including meiosis is detailed in Chapter 1, Section 1.4.2. In monovular species such as the cow and humans, research conducted in Leeds indicates that *GTSF1* is present in gametes and undifferentiated cells of early development (Lu *et al.*, 2012). In the bovine and human ovaries, analysis of *GTSF1* by real-time PCR revealed expression at primordial, primary, and secondary follicles, GV and MII oocytes, zygotes and late stage preimplantation embryos with expression being highest in GV oocytes. The functional significance of *GTSF1* in gamete development in monovular species has yet to be fully established

3.1.1 Aims

The aim of this study was therefore to characterise the expression and cellular distribution of *GTSF1* in sheep. This study represents the first step towards investigating the function of this gene in a physiologically relevant monovulatory animal model to human. The sheep is generally considered as a good model for evaluation of human reproductive endocrinology and ovarian biology (Campbell *et al.*, 2003). The developmental sequence of oogenesis and folliculogenesis and the size of the ovulatory oocyte is comparable between sheep and human ovaries (Campbell *et al.*, 2003). Similarly, the mechanisms regulating follicle development and ovulation are similar between sheep and humans (Campbell *et al.*, 2003).

The primary aim of the current experiments was to sequence and map the expression pattern of *GTSF1* in ovine follicles and oocytes and during early embryo development by interrogating verified cDNA libraries from all of these stages of development by PCR. Given the discrepancy in the published literature between gene expression and protein distribution across oogenesis, the work also aimed to further characterise the cellular distribution of *GTSF1* by FISH analysis of ovarian sections and to detect GTSF1 protein. Cellular distribution of *GTSF1* and protein analysis was also characterised in the testis.

3.2 MATERIALS AND METHODS

3.2.1 Follicle, oocyte, embryo and ovarian somatic cell isolations

The methods used for isolations of follicle stages, oocytes and granulosa cells for cDNA library generation have been previously used and validated by Cotterill, (2008). Sets of 3 independent libraries were created for primordial, early primary, primary, secondary, preantral and antral follicles, GV and MII oocytes as well as cumulus and mural granulosa cells and ovarian cortex. Additionally, analysis was conducted on archived cDNA libraries of *in vitro* derived preimplantation sheep embryos prepared by Cotterill, (2008). These included 2 cell staged embryos (groups of 3 embryos), 4 cell staged embryos (groups of 3 embryos) and blastocyst staged embryos (groups of 3 embryos) and 3 independent cDNA libraries were created for each developmental stage. For these preparations-in brief, ovarian follicles were isolated from abattoir-derived sheep ovaries as described in Chapter 2, Sections 2.1.2-2.1.4, and GV oocytes were obtained following aspiration of COC's from 2-5 mm follicles. Groups of 10 GV oocytes were denuded in oocyte holding media (H199$^+$) from the surrounding cumulus cells using a flexipet (Cook Medical) attached consecutively to a 170 μm and a 140 μm pipette tip as described previously (Chapter 2, Section 2.5.1). For generation of MII oocytes, collected COC's were subjected to IVM for 24 hours in serum-free IVM medium as detailed in Chapter 2, Section 2.1.3, according to the protocol of Cotterill *et al.*, (2012), followed by denudation of groups of 10 COC's (Chapter 2, Section 2.5.1). After denudation, oocyte meiotic status was confirmed by detection of the presence of the first polar body using an inverted microscope. Verified MII oocytes were pooled in groups of 10 and snap-frozen in lysis buffer (Chapter 2, Section 2.1.1). For follicle isolations, groups of 50 primordial follicles, 40 early primary, 10 primary, 10 secondary, 10 preantral and 6 antral follicles were generated according to the methodology described by Huntriss *et al.,* 2002 as described in Chapter 2, Section 2.1.4. For isolation of mural granulosa cells, groups of dissected antral follicles were ruptured with a scalpel blade and their cellular contents were scraped into 100 μl of H199$^+$ medium. Follicle-free ovarian cortex samples containing no visible follicles were prepared by cutting the ovary with a scalpel blade as described previously (Chambers *et al.*, 2010). Each section was transferred to a 4 well dish containing 500 ml of ovary holding medium (FIM) with 50 mg/ml of neutral red (NR) dye. The NR dye stains lysosomes of living cells red and is commonly used as a viability stain (Samaj *et al.*, 2005). Following incubation, the presence of follicles was easy to determine under an inverted microscope. Only cortex tissue pieces that did not contain follicles were

selected for analysis. Cumulus granulosa cells were obtained following denudation of groups of 3 GV oocytes. All tissue was washed twice in a 4 well dish containing 500 ml of DPBS before being transferred into a 0.5 ml microcentrifuge tube containing 10 μl of lysis buffer (Chapter 2, Section 2.2.14). The tube containing the tissue was then snap-frozen in liquid nitrogen and stored at -80°C. Sets of 3 cDNA libraries were created for each follicle/oocyte stage and cell type following mRNA isolation as described in Chapter 2, Sections 2.2.2-2.2.4.

3.2.2 Somatic tissue cell isolations

Further cDNA libraries were created from samples of sheep heart, liver, kidney, lung and adrenal cortex with the tissue obtained from the abattoir. In order to obtain the RNA from the tissue, the RNeasy plus kit (Qiagen Ltd) was used in accordance with the manufacturer's recommendations. Small tissue pieces were collected from the animals and placed into a sterile 1.5 ml microcentrifuge tube and stored at -80°C until usage. Tissue was placed in a weighed 1.5 ml microcentrifuge tube and not more than 30 mg of tissue was added. The tissue was then disaggregated and homogenised within each tube using customized 1 ml pipette tips (Figure 3.1).
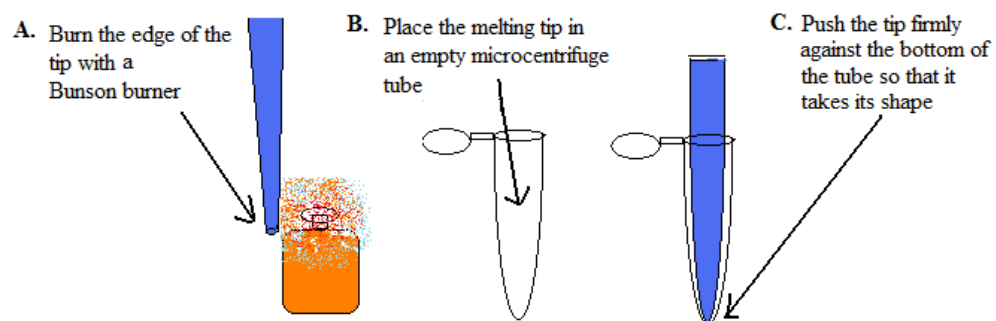
Figure 3.1: Schematic representation of creation of modified tip by applying heat on the pipette tip edge with a Bunsen burner before placing it in an empty sterile tube.

For tissue weights of 20-30 mg, 600 μl of RNeasy lysis buffer RLT plus (provided in the kit) was added to the tube for the lysis of the cells and inactivation of RNases to ensure isolation of intact RNA. The lysate was then centrifuged in a microcentrifuge for 3 min at maximum speed. The supernatant was removed by pipetting and transferred to a gDNA eliminator spin column. Further centrifugation for 30 sec at 10,000 rpm was applied and flow through was kept. An equivalent volume of 70% (v/v) ethanol in sterile-distilled H_2O was then added to the flow-through and mixed by pipetting. The sample was then placed in an RNeasy spin-column and centrifuged for 15 sec at 10,000

rpm. Flow-through was discarded and 700 µl of wash buffer RW1 (provided in the kit) were added to the column followed by centrifuging at the same conditions. Once again the flow-through was discarded and 500 µl of wash buffer RPE were added to the column followed by centrifuging for 2 min at 10,000 rpm. The column was then placed in a 1.5 ml sterile microcentrifuge tube and centrifuged at full speed for 1 min. The column was then placed in a new sterile microcentrifuge tube and 30 µl of RNase free H_2O were added. The sample was then centrifuged for 1 min at 10,000 rpm and the RNA was eluted. Libraries of cDNA were then created for each stage and cell type as described in Sections 2.2.3-2.2.4 of Chapter 2.

3.2.3 Molecular evaluation of the ovine developmental series

The primers used for interrogation of the cDNA libraries across all stages of sheep oocyte, follicle and embryo development and as non-ovarian somatic tissue were designed as detailed in Section 2.2.5 of Chapter 2. The *GAPDH*, *H2A*, *ACTB*, and *YWHAZ* housekeeper primers along with the oocyte-specific *ZP2* primer (Chapter 2, Section 2.2.5) were used to verify the consistency of the cDNA libraries. The libraries were then interrogated against *GTSF1* with the primer sequences shown in Table 3.1

Table 3.1: Primer sequences of GTSF1 for RT-PCR

Gene	Primer Sequence	Temp (°C)	Reference
GTSF1 bovine	F: 5´ TCAAGTGCAGAAAGAATCATCC 3´ R: 5´ TGCATTTCCATTGTTTTTCC 3´	52	E3353A11

Three cDNA samples for each stage of follicle, oocyte and early embryo development were analyzed by PCR as described in Section 2.2.5 of Chapter 2, with the temperature of the amplification step changing accordingly to the primer's melting temperature (Tm). Following the PCR analysis, 10 µl of each sample was run on a 1% agarose gel at 90 V for 60 min as described in Chapter 2, Section 2.2.6. Positive and negative controls were also run in each analysis to show PCR efficiency and lack of contamination. Sterile-distilled H_2O was used as a negative control, while a previously established sheep MII library was used as a positive control.

3.2.4 Cloning and sequencing ovine GTSF1

3.2.4.1 Nested PCR

In order to obtain a portion of the expressed ovine *GTSF1* sequence, primers for *GTSF1* were designed from the bovine sequence retrieved from NCBI using the primer 3 program as described previously (Chapter 2, Section 2.2.5), followed by verification

PCR with *GTSF1* primers on ovine MII cDNA libraries. The cloning procedures were then performed as detailed in Chapter 2, Section 2.3. The first approach used to obtain the full sequence of ovine *GTSF1*, involved a nested PCR reaction and analysis. This strategy has previously been used by Huntriss *et al.,* (2002) and the technology was based on designing 3 different sets of primers used in 3 successive runs of PCR, with the second set intended to amplify a secondary target within the product of the first PCR and with the third PCR reaction further amplifying a different target within the product of the second PCR reaction. For this purpose, 3 different sets of primers were designed, from the partially cloned ovine *GTSF1* sequence obtained from Section 3.2.4. The 3 primer sets are shown in Table 3.2.

Table 3.2: Nested GTSF1 primer sequences

Gene	Primer Sequence	Temp (°C)
Nested *GTSF1*-(a)	F: 5´ GCGGGATTAGCATTTCCAT 3´	65
	R: 5´ TCCTGATGTCGCAAACAAAC 3´	
Nested *GTSF1*-(b)	F: 5´ AGCATTTCCATTGTTTTTCCA 3´	64
	R: 5´ GCAGGATGTTGTCAACCAAA 3´	
Nested *GTSF1*-(c)	F: 5´ ATGTTGCTTGCAGGGCTATT 3´	66
	R: 5´ GGATGTTGTCAACCAAACCA 3´	

For this series of experiments, the pGEM-Teasy vector system (3000 bp, Promega Ltd) was used according to the manufacturer's recommendations. This vector system includes M13 primer binding sites as well as T7 RNA polymerase transcription initiation site and T7 RNA polymerase promoter SP6 (Figure 3.2).
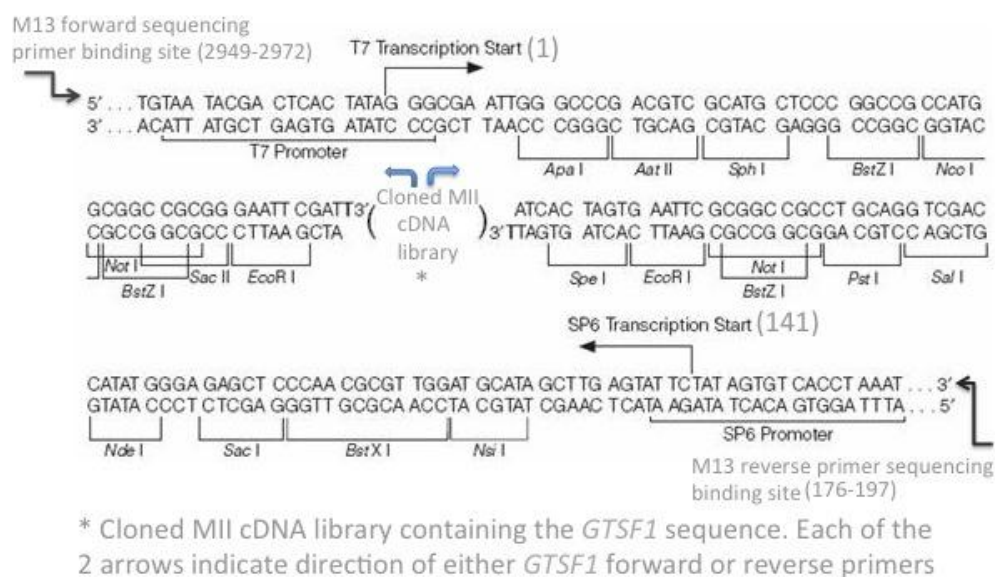
Figure 3.2: Schematic representation of the pGEM-Teasy Vector sequence reference points including the T7 and SP6 transcription start points and the M13 forward and reverse primer sequencing binding sites. Adjusted from pGEM-Teasy technical manual, http://www.promega.com).

The template for the first PCR reaction was created by generating an ovine MII cDNA library (Chapter 2, Sections 2.2.1-2.2.4) followed by verification PCR to confirm the presence of the *GTSF1* gene (Chapter 2, Section 2.2.5). The beads were then removed from the library using the magnetic apparatus and the cDNA library was pipetted into a new sterile 1.5 microcentrifuge tube. The library was then purified using the QIAquick PCR purification Kit according to the manufacturer's recommendations. Specifically, 5 volumes of buffer PB were added to 1 volume of the PCR reaction and mixed and the mixture was then transferred into QIAquick column inside a 2 ml collection tube. The tube was then centrifuged for 1 min at 13,000 rpm in a microcentrifuge at RT and the flow-through was discarded. Then 750 µl of buffer PE were added to the column and the tube containing the column was once again centrifuged for 1 min at 13,000 rpm at RT. Flow-through was discarded and the column was centrifuged for an additional minute under the same conditions. Flow-through was once again discarded and the column was placed in a clean sterile 1.5 ml microcentrifuge tube. Then 30 µl of sterile distilled H_2O were added to the centre of the QIAquick membrane and was left to stand for 1min. The purified product was then eluted inside the 1.5 ml tube by 1 min centrifugation at maximum speed at RT. Following purification, the poly-(A) tail was added and the product was cloned into the pGEM-Teasy vector as described previously (Chapter 2, Sections 2.3.2-2.3.3).

For each of the 3 consecutive PCRs, 4 reactions were set using different primers, in a final volume of 20 µl. Each of the reaction mixes was composed by 2 µl of 10 X buffer, 4 µl of dNTPs (1.25 mM), 1.5 µl $MgCl_2$, 2 µl of forward primer, 2 µl of reverse primer, 0.2 µl of Taq polymerase, 7.3 µl sterile distilled H_2O and 1 µl of cDNA sample. For the first PCR, 4 µl of template were used for each of the 4 reactions reducing the amount of sterile distilled H_2O accordingly. The primers used in the first PCR were as follows:

- A: M13 F primer and GTSF1 1F primer
- B: M13 R primer and GTSF1 1F primer
- C: M13 F primer and GTSF1 1R primer
- D: M13 R primer and GTSF1 1R primer

For the second PCR, 1 µl from each of the 4 products of the first PCR was used as template and 4 additional reactions were set up with primers based as follows:

- A: M13 F primer and GTSF1 2F primer
- B: M13 R primer and GTSF1 2F primer
- C: M13 F primer and GTSF1 2R primer
- D: M13 R prime and GTSF1 2R primer

For the third PCR, 1 µl of the 4 reactions of the second PCR was used as template with the primers for the 4 reactions being as follows:

- A: M13 F primer and GTSF1 3F primer
- B: M13 R primer and GTSF1 3F primer
- C: M13 F primer and GTSF1 3R primer
- D: M13 R primer and GTSF1 3R primer

Because of the presence of T7 and SP6 transcription sites on the vector system, 4 more reactions were set up for the third PCR, once again using 1µl of the product of the second PCR as template with the primer sets being the following for each reaction:

- A: T7 F primer and GTSF1 3F primer
- B: SP6 R primer and GTSF1 3F primer
- C: T7 F primer and GTSF1 3R primer
- D: SP 6 R primer and GTSF1 3R primer

The program for the PCRs was set for 1 cycle step of 3 min at 95°C, followed by 5 cycle steps of 95°C for 30 sec, 65°C (changed to 64°C for the second PCR and to 66°C for the third PCR) for 30 sec and 72°C for 30 sec (first amplification step), 30 cycle steps of 95°C for 30 sec, 58°C for 30 sec and 72°C for 30 sec and 1 cycle step of 72°C for 5 min before holding at 4°C.

3.2.4.2 Degenerate primer PCR

An alternative approach used to obtain the full ovine *GTSF1* sequence was the design and use of degenerate *GTSF1* primers. This method is based on the amplification of unknown DNA sequences related to a known DNA sequence and is useful for identification of orthologous genes from different organisms (Lang and Orgogozo, 2011). For this purpose the basic local alignment search tool (BLAST) was used on the NCBI website to compare the full sequence of *GTSF1* in different species. (Altschul *et al.*, 1990). Degenerate primers were designed from 4 species: *Bos taurus* (Zimin *et al.*, 2009), *Pan troglodytes* (NCBI reference sequence: XM_509113.2), *Canis familiaris* (NCBI reference sequence: XM_534784.2) and *Sus scrofa* (NCBI reference sequence: XM_001927807.1). The primers were designed by identifying the differences in nucleotide bases at the 5´ and 3´ end of the transcripts between them. All different nucleotide bases located were then introduced into degenerate primers. This was based on the IUPAC code. For example if in 3 out of 4 species the first base was A and in the fourth the equivalent base was T, the degenerate primer sequence included both A+T (IUPAC code: W). In the same way A+C+G is represented by V, A+T+G by D, T+C+G

89

by B, A+T+C by H, A+T by W, C+G by S, T+G by K, A+C by M, C+T by Y, A+G by R and A+G+C+T by N. The degenerate primers used are shown in Table 3.3.

Table 3.3: Degenerate GTSF1 primer sequences

Gene	Primer Sequence	Temp (°C)
Degenerate *GTSF1*	F: 5´ GCWYCTTMRTTYCCAACATGGAA 3´	68
	R: 5´ TCTTDYYATTTRASAGACACTGAA 3´	

3.2.5 Characterisation of the cellular localisation of *GTSF1* expression across ovine gametogenesis

FISH technology was employed to localise the presence of *GTSF1* sequence in the ovine ovary and testis. The processes followed are described in detail in Chapter 2, Section 2.6. The cloned *GTSF1* sequence generated using the methods described above (Section 3.2.4) was used as a template for the generation of the sense and antisense probes. After FISH, the presence or absence of *GTSF1* was determined for all stages of follicle development and spermatogenesis. The different stages of folliculogenesis were classified according to the size and the morphological characteristics of the follicles at each stage as shown in Figure 3.3 (Lundy *et al.*, 1999; Ireland *et al.*, 2008).
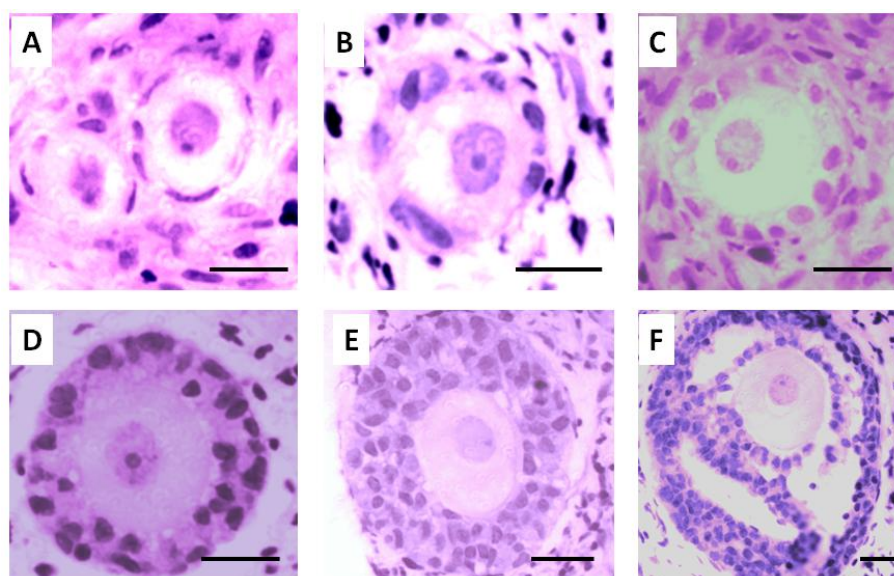
Figure 3.3: Histological classification of ovine follicles stained with hematoxylin and eosin (Stained ovarian slides were a courtesy of J Ping and L Blackwell). **A:** Follicles with a compact oocyte surrounded by a single layer of flattened granulosa cells classified as primordial follicles. **B:** Follicle containing an oocyte surrounded by a single layer of mixed flattened and cuboidal granulosa cells classified as early primary follicle. **C:** Follicle with the oocyte surrounded by 1 layer of cuboidal granulosa cells classified as primary follicle. **D:** Follicle with the oocyte surrounded by 2 layers of cuboidal granulosa cells classified as early secondary follicle **E:** Follicle with the oocyte surrounded by multiple layers of cuboidal granulosa cells and no antrum classified as secondary follicle. **F:** Follicle with multiple layers of cuboidal granulosa cells with a fully formed theca interna and a forming antral cavity classified as early antral follicle. Bars= 20 μm.

Ovine testis from sheep prepubertal animals was supplied in collaboration with Professor Bruce Campbell (Faculty of medicine and health sciences, University of Nottingham) and Professor Alan McNeilly (University of Edinburgh).

3.2.6 Western blotting

To further characterise *GTSF1*, Western blotting was conducted to detect protein levels of the gene in ovarian tissue containing viable follicles as determined by neutral red, bovine testis, GV oocytes and somatic tissue of ovine kidney and lung. The methodology followed for tissue preparation and Western blotting is detailed in Chapter 2, Section 2.5. A total of 3 repeat analyses were run for each different sample. For the series of experiments, a commercially made monoclonal antibody for *GTSF1* was used (SC-240545, Santa Cruz Biotechnology, Midlesex, UK) in a concentration of 1:1000 in 15 ml of non-fat dry milk powder dissolved in 1% (v/v) PBS in Milli-Q H_2O. The secondary antibody was the Zymax HRP-Rabbit Anti-Goat IgG (H+L) conjugate (Invitrogen, Ltd), used in a concentration of 1:100,000 diluted in the same conditions as the primary antibody. An additional blot was performed for all the tissue analysed with the presence of a blocking peptide as a negative control (SC-240545p, Santa Cruz Biotechnology). The blocking peptide is used to neutralise the GTSF1 antibody; thus to determine any non-specific binding of the antibody to proteins other than the antigen. For the experiment, the GTSF1 antibody was neutralised by incubating it with an excess of peptide (5 X the concentration of primary antibody, 1:200 dilution) that corresponds to the epitope recognised by the antibody. This resulted in the binding of the antibody to the blocking peptide with the antibody no longer being able to bind to the epitope present in the protein on the Western blot. The blot containing the neutralised antibody was then compared with the blot containing only the antibody and any bands absent from the blot containing the neutralised antibody represented specific binding of the antibody.

3.3 RESULTS

3.3.1 Verification of cDNA libraries

All cDNA libraries that were created were verified using *GAPDH* and *ZP2* primers. Somatic cell libraries that failed to demonstrate expression of the *GAPDH* housekeeper gene and oocyte libraries that failed to demonstrate expression of both *GAPDH* and *ZP2* were discarded. The cDNA synthesis resulted in the generation of full-length clones

originating from the mRNA sequences for all stages of follicle and embryo development as well as for ovine somatic tissue.

3.3.2 Expression analysis of *GTSF1* across ovine oocyte and embryo development

The profile of *GTSF1* expression was analysed throughout development of the oocyte, follicle and early embryo using the created cDNA libraries. The analysis of oocyte-specific gene *ZP2* was also conducted along with the expression profile of different housekeeper genes (Figure 3.4).
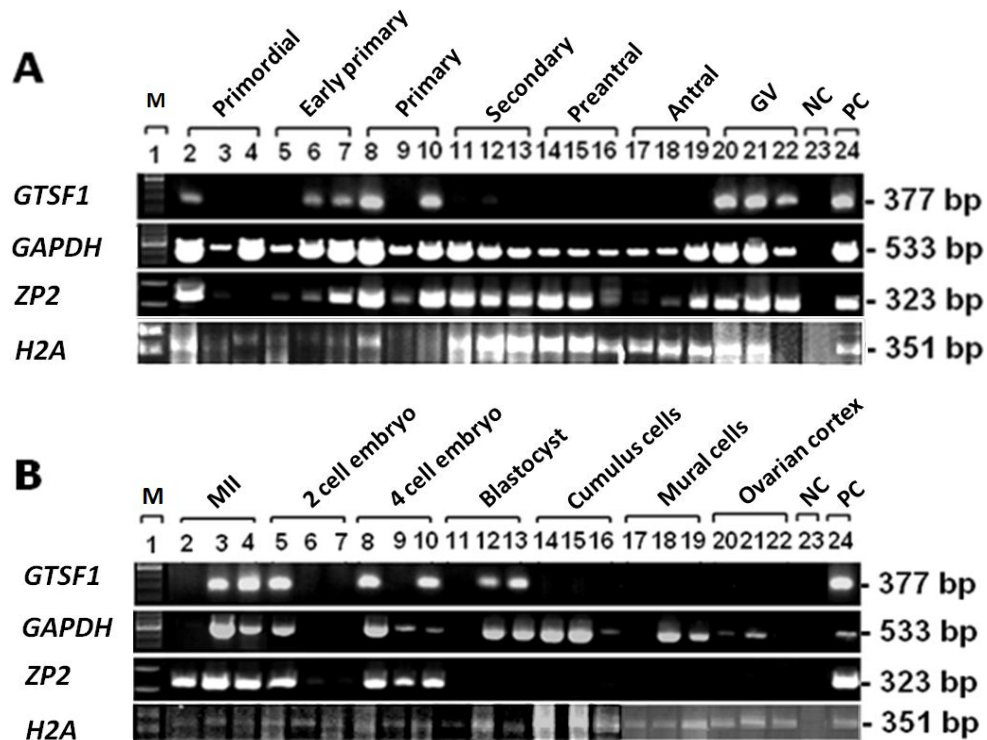
Figure 3.4: Montage showing expression profiles obtained by RT-PCR of different genes throughout ovine oogenesis and embryo development. Each developmental stage is represented by a triplicate of independent cDNA libraries. Lanes 1 contain 1 kb MW marker. Lanes 23 contain sterile-distilled H_2O and no cDNA library (NC), while lanes 24 contain a previously verified cDNA library of a cohort of 10 denuded GV ovine oocytes (PC). **A:** Lanes 2-22 contain cDNA libraries from pools of: Lanes 2-4: 50 primordial follicles; Lanes 5-7: 40 early primary follicles; Lanes 8-10: 10 primary follicles; Lanes 11-13: 10 secondary follicles; Lanes 14-16: 10 preantral follicles; Lanes 17-19: 6 antral follicles; Lanes 20-22: 10 denuded GV oocytes. **B:** cDNA libraries from pools of: Lanes 2-4: 10 denuded MII oocytes; Lanes 5-7: 3, 2-cell embryos; Lanes 8-10: 3, 4 cell embryos; Lanes 11-13: 3, blastocysts; Lanes 14-16: Compact cumulus cells from 3 denuded GV oocytes; Lanes 17-19: Mural granulosa cells from 10 antral follicles; Lanes 20-22: Ovarian cortex containing no follicles.

The data showed that *GTSF1* was expressed from primordial to primary stages of follicle development as well as GV and MII oocytes and in the early stages of embryogenesis until the blastocyst stage. In contrast, the gene had either low expression or was not expressed at all in secondary, preantral and antral follicle stages, suggesting that even though the gene is gamete and early embryo specific, it is not expressed at all

92

stages of folliculogenesis. In addition, there was no expression of *GTSF1* in mural granulosa cells of late follicular stages and in ovarian cDNA cortex samples that did not contain primordial follicles. These consistencies verify that expression of the gene is limited to the gamete and early embryo. The expression levels of *GTSF1* appeared to be higher at the GV and MII stage. Not all cDNA libraries confirmed the expression of the gene at the early stages of development. Specifically, *GTSF1* expression was only confirmed in 1 out of 3 primordial cDNA libraries and 2 out of 3 primary cDNA libraries. This could be attributed to the limited expression of the gene at these stages of development in comparison with the housekeeper genes and the variability of each of the cDNA libraries from the same devlopmental stage.

The profile of *ZP2* expession, showed that the gene is expressed in all stages of follicle, oocyte and embryo development until the 4 cell embryo stage while it was not expressed in other somatic tissue of the ovary confirming its oocyte and embryo specific pattern of expression and the validity of the cDNA libraries. Housekeeper expression levels of *GAPDH* and *H2A* also confirmed the validity of all cDNA libraries throughout the developmental series. The results also showed incosistencies in the expression levels of each gene between libraries originating from the same developmental stage as well as between libraries of different developmental stages as indicated by the width and brightness of the bands. In addition, some libraries appeared to lack expression of certain genes. For this purpose, all developmnetal stages were intorrogated in triplicates of cDNA libraries and 2 different housekeepers, *GAPDH* and *H2A* were utilised. The levels of housekeepers *GAPDH* and *H2A* were also variable amongst the different cDNA libraries. The observed differences could be attributed to grouping of samples with varied cell numbers in addition to the library construction methodology that can result in different levels of cDNA between samples. In addition to the above, the presence of more than 1 cell type for most developmnetal stages as well as the expression levels for each gene at different developmnetal stages could exlain the observed discrepancies.

3.3.3 Expression of *GTSF1* in somatic tissue

The profile of *GTSF1* expression was analysed in a series of 5 different non-ovarian somatic tissue. Specifically, *GTSF1* expression was analysed for adrenal, lung, kidney, heart and liver tissue. The expression profile of housekeeper genes as well oocyte-specific gene *ZP2* was also conducted for each triplicate of cDNA libraries (Figure 3.5).
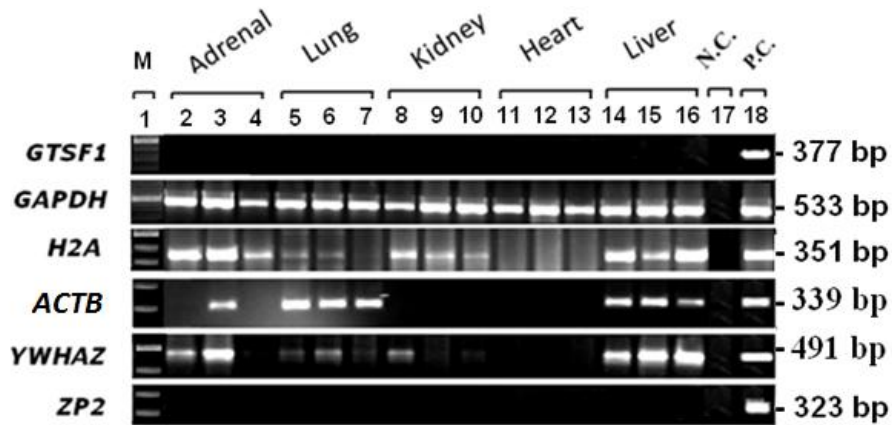
Figure 3.5: Montage showing expression profiles obtained by RT-PCR of different genes in non-ovarian tissue. Each somatic tissue of ovine adrenal, lung, kidney, heart and liver is represented by a triplicate of independent cDNA libraries. Lane 1 contains 1 kb MW marker. Lanes 2-4: Adrenal tissue; Lanes 5-7: Lung tissue; Lanes 8-10: Kidney tissue; Lanes 11-13: Heart tissue; Lanes 14-16: Liver tissue. Lane 17 contains sterile-distilled H_2O with no cDNA library (NC). Lane 18 contains a previously verified cDNA library of a cohort of 10 denuded GV ovine oocytes (PC).

The results showed that *GTSF1* was consistenly not expressed in any of the somatic tissues tested confirming its specificity as a gamete and early development specific gene. The data also indicated the variability in housekeeper gene expression across different somatic cell types. For example *ACTB* expression was not detected in kidney or heart samples; whereas the same samples showed detectable expression of *H2A* in kidney samples and both *GAPDH* and *H2A* in heart samples. The *YWHAZ* gene was the most variable of housekeepers tested. As expected, no *ZP2* expression was detected in any of the somatic tissue confirming the value of this gene as an oocyte/ovary specific.

3.3.4 Cellular localisation of *GTSF1* expression in the ovine ovary and testis

Three replicate FISH analyses were conducted. For each experiment, 3 slides of ovarian tissue containing follicles from all follicular stages and 3 slides of testicular tissue were used to hybridise with each of the 2 probes. An overview of the localisation of *GTSF1* in the ovine ovary and testis is shown in Figure 3.6. Following hybridisation, a total of 30 primordial, 30 primary, 15 secondary, 10 antral and 6 preovulatory follicles were analysed for each of the positive and negative control probes. In the ovary, FISH analysis showed cell-specific localisation of *GTSF1*. Specifically, gene expression was detected in primordial follicles (25/30), primary follicles (28/30) and transitional follicles (27/30 follicles), while it was not detected in secondary (0/15), antral (0/10) or preovulatory staged follicles (0/6). At the stages of follicular development that *GTSF1* was detected (Figure 3.6, B-D), it was localised uniformly in the cytoplasm of the

oocyte, while it was not localised in any of the somatic cells (granulosa or theca cells). In the ovine testis seminiferous tubules, *GTSF1* was detected in the cytoplasm of spermatogonia (29/30), primary spermatocytes (30/30), secondary spermatocytes (30/30) as well as round spermatids (27/30) (Figure 3.6, H-I).
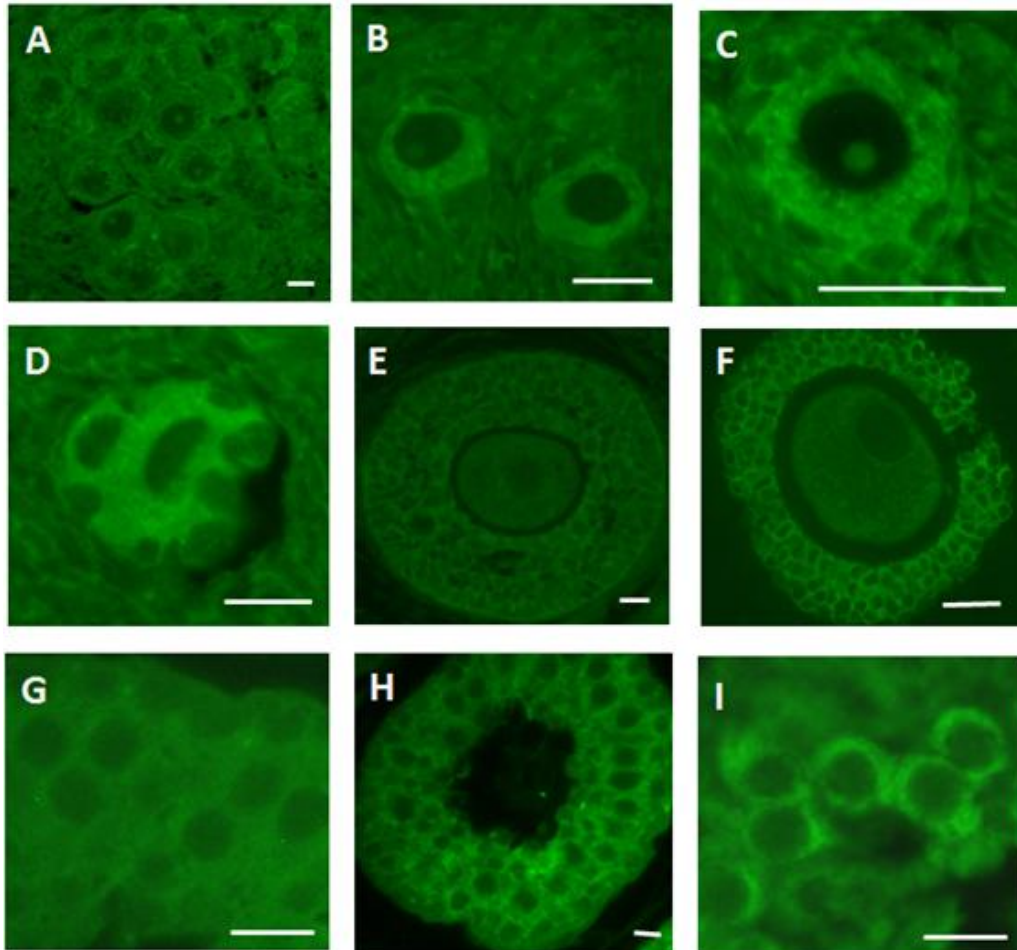
Figure 3.6: Representative images of the characterisation of *GTSF1* gene expression in the ovine ovary and testis following FISH analysis **A:** Ovarian tissue overview of the noise from negative control probed by sense *GTSF1* **B-D:** Hybridised anti-sense *GTSF1* in ovary. **B:** Primordial follicles. **C:** Early primary follicle. **D:** Primary follicle. **E-F:** Non-hybridised follicles by anti sense *GTSF1*. **E:** Pre-antral follicle. **F:** COC complex from an antral follicle. **G:** Testicular tissue overview of the noise from negative control probed by sense *GTSF1* (spermatogonia and primary spermatocytes). **H-I:** Hybridised anti-sense *GTSF1* in testis. **H:** Overview of seminiferous tubules showing *GTSF1* signal in the spermatogenic cells. **I:** Primary spermatocytes. Scale bar: 20 μm.

3.3.5 Analysis of the *GTSF1* ovine sequence

A partial sequence for *GTSF1* was obtained by designing primers for *GTSF1* based on the region of high homology with the *GTSF1* sequence for the bovine species. Cloning using MII libraries as described in detail in Chapter 2, Section 2.2.2 and sequencing,

revealed a 377 nucleotide ovine sequence. This sequence showed a very close homology with the *Bos taurus GTSF1* sequence (Figure 3.7).

```
O. aries    1   CCATGGGAGAACATATGGCAGAGACTTGGGAACACGCATGCCTGAAGCCAGGTTACTCTT   60
                ||||||  |||||||||||  ||||||||||||||||||||||||||||||||||||||||
B. taurus  513   CCATGGCAGAACATATGGAAGAGACTTGGGAACACGCATGCCTGAAGCCAGGTTACTCTT   454

O. aries   61   ATGTTCCATAACTATGTTGCTTGCAGGGCTATTGTTGCCACAGTAGTTGGCTGTGCCCCA   120
                ||||||||||||||||||||||||||||||||||||||||||||||||||||||||||||
B. taurus  453   ATGTTCCATAACTATGTTGCTTGCAGGGCTATTGTTGCCACAGTAGTTGGCTGTGCCCCA   394

O. aries  121   GACAAATGGGGTGCTGGTCTGTTCCCACAAATCTTTGTCCCAGTCTTCATCGCAAGGAGG   180
                ||||||||||||||||||||||||||||||||||||||||||||||||||||||||||||
B. taurus  393   GACAAATGGGGTGCTGGTCTGTTCCCACAAATCTTTGTCCCAGTCTTCATCGCAAGGAGG   334

O. aries  181   GCACCGCCATGTGCTCTCAGCCAGAGTCTCTTGTCCAAGGCTCCTGGTTTGGTTGACAAC   240
                ||||||||||  ||||||||||||  |||||||||||||||||||||||||||||||  ||
B. taurus  333   GCACCGCCACGTGCTCTCAGCCATAGTCTCTTGTCCAAGGCTCCTGGTTTGGTTGACTAC   274

O. aries  241   ATCCTGCTCAATACAGCTTTTGTCATCACAGCTTGAGATATGATGACTGATTTCAGCCCG   300
                ||||||||||||||||||||||||||||||||||||||||||||||||||||||||||||
B. taurus  273   ATCCTGCTCAATACAGCTTTTGTCATCACAGCTTGAGATATGATGACTGATTTCAGCCCG   214

O. aries  301   AGGAACCTGATGGCGAGCATTGAAGGGACAAGTCGCCAGTTTGTTTGCGACATCAGGATG   360
                |||||||||||||||||||||||||||||||||||| |||||||||||||||||||||||
B. taurus  213   AGGAACCTGATGGCGAGCATTGAAGGGACAAGTTGCCAGTTTGTTTGCGACATCAGGATG   154

O. aries  361   ATTCTTTCTGCACTTGA   377
                |||||||||||||||||
B. taurus  153   ATTCTTTCTGCACTTGA   137
```

Figure 3.7: Sequence alignment of the ovine partially cloned *GTSF1* sequence with the known *Bos taurus GTSF1* sequence. The 2 species share a 98% nucleotide homology for the sequence with 371 out of the 377 being identical (http://blast.ncbi.nlm.nih.gov/).

In particular, 371 out of 377 nucleotides were shown to be identical between the 2 species, indicating a 98% homology with 0% gaps. The partial ovine sequence was shown to be 93% homologus with *Macaca mullata*, 92% homologus with *Mus musculus and* 91% homologus with *Homo sapiens*, *Rattus norvegicus* and *Pan troglodytes,* as determined by blast search (http://blast.ncbi.nlm.nih.gov/).

Nested PCR was performed to try to obtain the full sequence of the ovine gene. This method reduced the contamination of PCR products caused by amplification of unexpected primer sites. The series of reactions based on combination of primers from the partially cloned *GTSF1* sequence with opposite end primers located on the vector system should theoretically result in amplification of the ovine gene containing the unknown parts of the sequence of the gene. However, this approach did not result in specific amplification of the gene of interest and non-specific amplification was observed throughout the 3 steps of the reaction. A second approach using degenerate primer PCR was therefore tested in order to obtain the full sequence of the gene. The degenerate primers were used to amplify an ovine MII oocyte cDNA library with the agarose gel electrophoresis that followed shown in Figure 3.8.
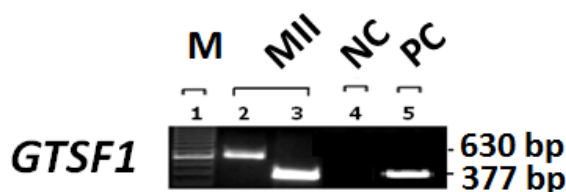
Figure 3.8: Montage showing expression profiles of *GTSF1* obtained by degenerate primer RT-PCR. Lane 1 contains a 1 kb MW marker. Lane 2 contains an ovine MII oocyte cDNA library amplified with degenerate *GTSF1* primers corresponding to the full length of the sequence. Lane 3 contains an ovine MII oocyte cDNA library amplified with bovine *GTSF1* primers (Section 3.2.3) corresponding to a partial sequence of *GTSF1*. Lane 4 contains sterile-distilled H$_2$0 with no cDNA library (NC). Lane 5 contains a previously verified cDNA library of a cohort of 10 denuded GV ovine oocytes amplified with bovine *GTSF1* primers (PC).

The corresponding molecular weight of the cloned product with the degenerate primers (Lane 2) was 630 bp in comparison with the 377 bp that was amplified using the bovine *GTSF1* primers. The size of 630 bp, based on other species, corresponds to the expected full sequence of ovine *GTSF1*. The resulting PCR product was cloned into the pGEM-Teasy vector system following the cloning procedure as described in Chapter 2, Section 2.3. The nucleotide sequence of ovine *GTSF1* retrieved following sequencing is shown in Table 3.4.

Table 3.4: Full sequence of ovine *GTSF1* obtained using degenerate primer PCR on an ovine MII cDNA library and cloning into the pGEM-Teasy vector system

GTSF1 sequence
5´ CCTTAGTTCCCAACATGGAAGAAACTTACATCGATACTCTGGACCCTGAAAAGCT GTTACAATGCCCCTATGATAAAAACCACCAGATCAGGGCCTGCAGGTTTCCTTATCA TCTAATCAAGTGCAGAAAGAATCATCCTGATGTCGCAAACAAACTGGCGACTTGTCC CTTCAATGCTCGCCATCAGGTTCCTCGGGCTGAAATCAGCCATCATATCTCAAGCTG TGATGACAAAAGCTGTATTGAGCAGGATGTTGTCAACCAAACCAGGAGCCTTGGAC AAGAGACTCTGGCTGAGAGCACATGGCGGTGCCCTCCTTGCGATGAAGACTGGGAC AAAGATTTGTGGGAACAGACCAGCACCCCATTTGTCTGGGGCACAGCCAACTACTG TGGCAACAATAGCCCTGCAAACAACATAGTTATGGAACATAAGAGTAACCTGGCTT CAGGCATGCGTGTTCCCAAGTCTCTGCCATATGTTCTCCCATGGAAAAACAATGGAA ATGCACAGTAACTGAATATTTCATCAAATGCCAGACCCTGGAAGACTCTTCTTCCTG CTACAGTGGGTTCTTCATTTTTTTTTCTCCTAATCTAATTATAGAAAGATAAACTGTC TGTGACTT 3´

Following BLAST searching of the ovine *GTSF1* sequence from the NCBI database (http://www.ncbi.nlm.nih.gov/), the ovine *GTSF1* sequence indicated a total of 38 blast hits. Specifically the ovine sequence showed a 98% homology with the sequence for *Bos taurus* (Zimin *et al.,* 2009), while there was a 91% homology with the published sequence for *Mus musculus* (Diez-Roux *et al.,* 2011) and *Rattus norvegicus* (Strausberg *et al.*, 2002) and 90% with *Homo sapiens* (Gerhard *et al.*, 2004) as shown in Figure 3.9. The sequence was also aligned with the predicted sequence from several species like *Sus scrofa* (93%), *Canis familiaris* (93%), *Pan troglodytes* (90%) and several more.

97
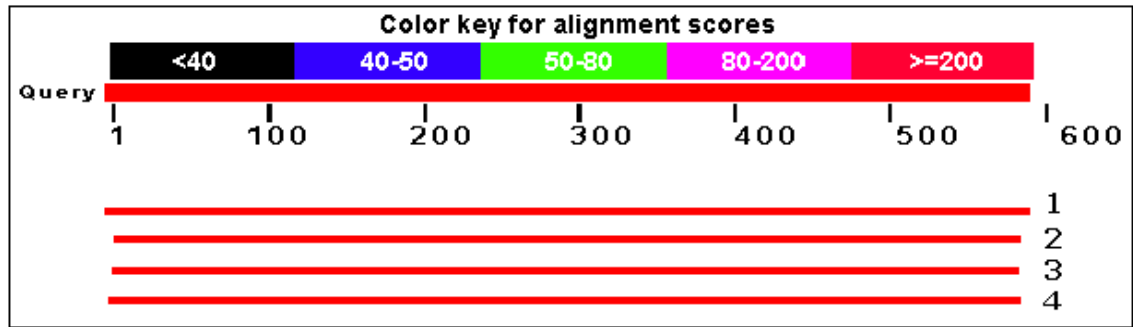
Figure 3.9: Distribution of blast hits on the ovine nucleotide sequence for *GTSF1*. The score of each alignment is indicated by 1 of 5 different colours that show the range of scores in 5 groups (in bps). Alignment of ovine *GTSF1* with: **1:** *Bos taurus GTSF1.* **2:** Alignment with *Mus musculus GTSF1.* **3:** Alignment with *Rattus norvegicus GTSF1.* **4:** Alignment with *Homo sapiens GTSF1.* The ovine *GTSF1* sequence has an alignment of over 600 bp in comparison with the *GTSF1* sequence of the other species. Image from: http://www.ncbi.nlm.nih.gov/.

Further evaluation revealed that *GTSF1* encodes a 167-amino acid protein of 19.11 kilodaltons molecular weight. Multiple sequence alignment of the GTSF1 protein from different species by BLAST-P (http://www.ncbi.nlm.nih.gov/) indicated the high conservation of the protein. Specifically, the predicted ovine GTSF1 protein appeared to have 99% homology with that for *Bos taurus,* a 96% similarity with the protein sequence of GTSF1 for *Homo sapiens* and *Sus scrofa*, 92% with *Pan troglodytes,* 76% with *Rattus norvegicus* and *Mus musculus* and *61%* with *Xenopus laevis* (Figure 3.10). This suggests a high degree of conservation of the GTSF1 protein across species.
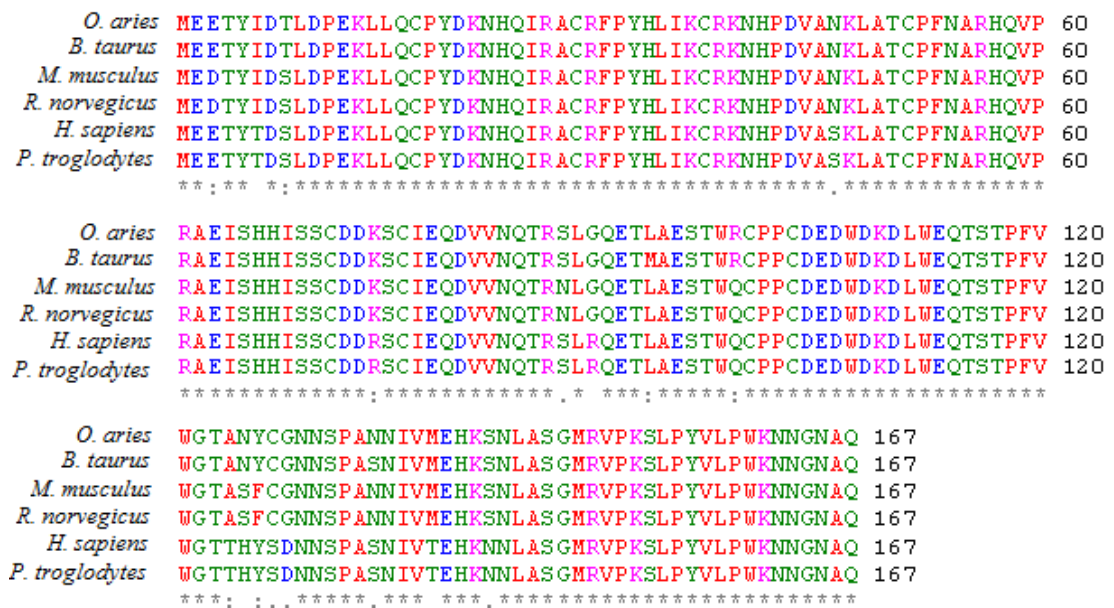
Figure 3.10: Multiple sequence alignment of the predicted ovine GTSF1 protein from various species by BLAST-P (http:/www.ncbi.nlm.nih.gov) shows the high conservation of GTSF1. Identities for *Ovis aries* against: *Bos Taurus* (99%), *Mus musculus* (76%), *Rattus norvegicus* (76%), *Homo sapiens* (96%), *Pan troglodytes* (92%).

In addition, blast searches of the ovine predicted protein sequence against known protein superfamilies confirmed the presence of 2 CHHC-type Zn-finger domains in the ovine protein which were located at amino acids 17-37 and 51-71 as shown in the figure below (Figure 3.11). These Zn-finger domains were previously identified in spliceosomal U11-48K proteins, tRNA methyl-transferases TRM13 and gametocyte specific factors (Andreeva and Tidow, 2008).
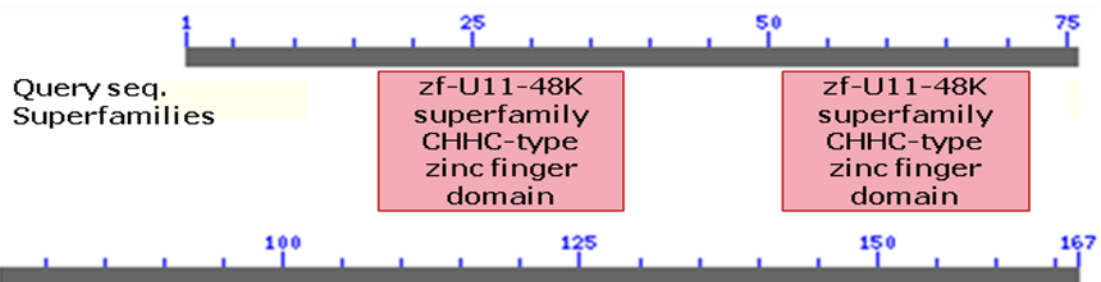
Figure 3.11: Schematic representation of the putative conserved domains detected by BLAST-P with the predicted ovine GTSF1 protein of 167 amino acids (aa). Scale bar represents the length of the ovine predicted GTSF1 protein of 167 aa. The 2 conserved CHHC Zn-finger domains were located at amino acids 17-37 and 51-71.

The predicted ovine GTSF1 protein was then compared to the *X. laevis* D7 protein which is the only other member of the UPF0224 family that has been characterised. BLAST searches revealed that the predicted ovine GTSF1 protein was aligned with the D7 protein and shared a 47% homology accross these 2 species as shown in Figure 3.12.

Figure 3.12: Protein sequence alignment following protein BLAST of the predicted ovine GTSF1 protein with the D7 protein in *X. laevis*. Identities 47/99 (47%), Positives 69/99 (70%), Gaps 4/99 (4%).

The confirmed sequence of ovine *GTSF1* isolated from ovine MII oocytes containing all its coding sequence and the predicted protein sequence along with the location of the 2 CHHC Zn-finger domains are shown in Figure 3.13.

Primer F →

CCTTAGTTCCCAAC ATGGAAGAAACTTACATCGATACTCTGGACCCTGAAAAGCTGTTAC
　　　　　　　　 M　E　E　T　Y　I　D　T　L　D　P　E　K　L　L

AATGCCCCTATGATAAAAACCACCAGATCAGGGCCTGCAGGTTTCCTTATCATCTAATCA
Q　C　P　Y　D　K　N　H　Q　I　R　A　C　R　F　P　Y　H　L　I

AGTGCAGAAAGAATCATCCTGATGTCGCAAACAAACTGGCGACTTGTCCCTTCAATGCTC
K　C　R　K　N　H　P　D　V　A　N　K　L　A　T　C　P　F　N　A

GCCATCAGGTTCCTCGGGCTGAAATCAGCCATCATATCTCAAGCTGTGATGACAAAAGCT
R　H　Q　V　P　R　A　E　I　S　H　H　I　S　S　C　D　D　K　S

GTATTGAGCAGGATGTTGTCAACCAAACCAGGAGCCTTGGACAAGAGACTCTGGCTGAG
C　I　E　Q　D　V　V　N　Q　T　R　S　L　G　Q　E　T　L　A　E

AGCACATGGCGGTGCCCTCCTTGCGATGAAGACTGGGACAAAGATTTGTGGGAACAGAC
S　T　W　R　C　P　P　C　D　E　D　W　D　K　D　L　W　E　Q　T

CAGCACCCCATTTGTCTGGGGCACAGCCAACTACTGTGGCAACAATAGCCCTGCAAACA
S　T　P　F　V　W　G　T　A　N　Y　C　G　N　N　S　P　A　N

ACATAGTTATGGAACATAAGAGTAACCTGGCTTCAGGCATGCGTGTTCCCAAGTCTCTGC
N　I　V　M　E　H　K　S　N　L　A　S　G　M　R　V　P　K　S　L

CATATGTTCTCCCATGGAAAAACAATGGAAATGCACAG TAACTGAATATTTCATCAAATG
P　Y　V　L　P　W　K　N　G　N　A　Q

CCAGACCCTGGAAGACTCTTCTTCCTGCTACAGTGGGTTCTTCATTTTTTTTTCTCCTAATC

Primer R ←

TAATTATAGAAAGATAAACTGTCTGTGACTT

Figure 3.13: Confirmed sequence of the ovine *GTSF1* gene isolated from ovine MII oocytes. The isolated PCR fragment includes the whole coding sequence (primers F to R) and the amino acids corresponding to the nucleotide sequence are shown. The 2 CHHC Zn-finger motifs possibly involved in RNA-recognition and binding are double underlined. The coding sequence is shown in red with letters indicating the translated amino acid.

3.3.6 Expression of GTSF1 protein in the ovine ovary

To further characterise the expression of the ovine *GTSF1* gene, Western blotting was performed to confirm whether GTSF1 protein was expressed in the ovine ovary. Three replicate Western analysis were conducted. All 3 replicates showed the same result that the gene encodes a 20 kDa protein in the ovine ovary (Figure 3.14).
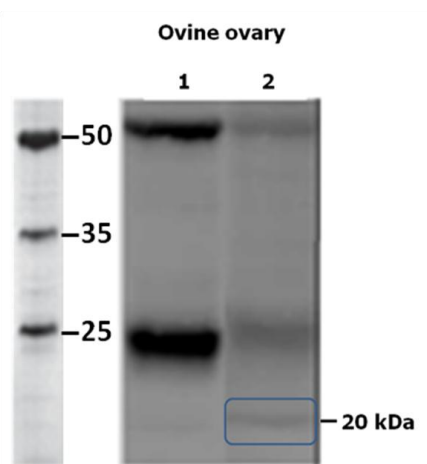
Figure 3.14: Montage showing expression of GTSF1 protein in the ovine ovary obtained by Western blotting. Molecular weight marker represents weight in kDa. Lane 1 contains GTSF1 antibody with GTSF1 blocking peptide. Lane 2 contains the GTSF1 antibody alone.

100

Since the data in this study as well as other studies have shown that the *GTSF1* gene is expressed solely in the gametes, the protein expressed in the ovine ovary should be derived from the oocytes. To confirm this, a second series of 3 replicate Western blotts were performed and the expression of the GTSF1 protein was examined in a pool of GV oocytes as well as somatic tissues of ovine kidney and lung as shown in Figure 3.15. Due to the unavailability of ovine testis samples, the expression of ovine GTSF1 protein was compared with protein in the bovine testis and ovary. The results of the Western blotting showed that the ovine and bovine ovary both express a 20 kDa protein for GTSF1. Similarly the pool of GV oocytes expressed the GTSF1 protein of 20 kDa, further confirming the presence of the protein in the female ovine gamete. The protein was not expressed in the ovine somatic tissue of kidney and lung, while in the bovine testis, the protein was present in 2 forms, 1 of 20 kDa and 1 of 23 kDa. All 3 replicates were consistent in these results.
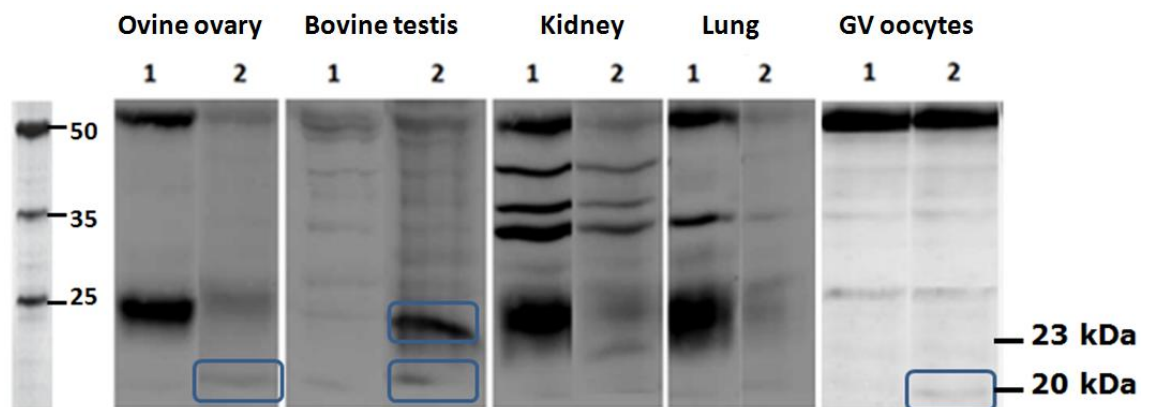
Figure 3.15: Montage showing Western blotting of GTSF1 protein in ovine ovary tissue, bovine testis, ovine somatic tissues of kidney and lung and a pool of GV oocytes. Molecular weight marker represents weight in kDa. For each pair of samples, lane 1 contains GTSF1 antibody with GTSF1 blocking peptide and lane 2 contains the GTSF1 antibody alone. The pool of GV oocytes was created from 60 oocytes.

3.4 DISCUSSION

This study has demonstrated the successful construction of ovine cDNA libraries across all stages of folliculogenesis, oocyte development and preimplantation embryo development and has used the libraries to map the expression pattern of ovine *GTSF1* as well as the housekeeper genes *GAPDH* and *H2A* and the oocyte-specific gene *ZP2* by PCR. Specifically, *GTSF1* was expressed from primordial to secondary staged follicles and in GV and MII oocytes as well as the early cleavage and blastocyst staged embryos, while it was not expressed at the secondary and antral stages of follicle development or in the ovarian cortex. Furthermore, interrogation of non-ovarian somatic tissue confirmed its specificity as a gamete specific gene. These results were confirmed by

FISH which showed the cytoplasmic localisation of the gene in the oocytes of early stage follicles and its absence from the cytoplasm of oocytes from pre-antral and antral follicles. Similarly in the testis, *GTSF1* was detected in the cytoplasm of spermatogonia, primary and secondary spermatocytes as well as round spermatids. These data demonstrate that expression of *GTSF1* is gamete specific in the ovine species. The full sequence of ovine *GTSF1* gene was identified and showed high homology with *Bos taurus*, *Mus musculus*, *Rattus norvegicus* and *Homo sapiens*. Alignment of the predicted ovine GTSF1 protein sequence with different species showed a high evolutionary conservation of this gene suggesting that it might serve important functions regarding developmental processes in the ovine gonad.

The expression analysis of *GTSF1* across ovine folliculogenesis and embryogenesis reported here is in agreement with other studies performed in different species. Specifically, expression of *GTSF1* showed similar oocyte-specific patterns in humans (JD Huntriss and HM Picton, unpublished data), in bovine (Lu *et al.*, 2012) and mouse (Krotz *et al.*, 2009; Yoshimura *et al.*, 2009). The expression of *GTSF1* from the early follicular stages suggests either that the gene might have a functional role from the early stages of development and the activation of early growth of the oocyte and/or that the gene might be stored and processed at a later stage of oocyte development. The absence of this gene's expression at secondary and early antral stages might have been observed due to the dilution of the genetic material caused by the greater abundance of the somatic cells at those follicle stages compared to primordial to primary follicles. However, successive FISH analysis confirmed that the gene was not expressed by oocytes in secondary and antral follicles further confirming the accuracy of the PCR-based expression data. The results also showed that the gene was expressed throughout the early stages of embryogenesis and following embryonic genome activation that occurs after the 8 cell stage in the sheep (Crosby *et al.*, 1988). Even though expression of the gene at the earlier embryonic stages could represent residual carryover of maternal transcripts, expression at the blastocyst stage suggests that the embryo itself transcribes the gene (Crosby *et al.*, 1988). Similarly, studies in humans, sheep, cow and mice have shown that the embryo itself expresses oocyte genes following maternal to zygotic transition (MZT) even though the timing of embryonic gene activation is species-specific (Braude *et al.*, 1988; Crosby *et al.*, 1988; Schultz, 1993; Viuff *et al.*, 1998). In mouse, MZT occurs at the 2 cell stage, in the bovine species at the 4 cell stage while in humans at the 8-16 cell stage (Braude *et al.*, 1988; Schultz, 1993; Viuff *et al.*,

1998). In marked contrast to the evidence presented for *GTSF1,* the majority of oocyte-specific transcription factors such as *NOBOX* and *FIGLA* are known to be expressed in the oocyte but not in the subsequent stages of early embryo development (Huntriss *et al.,* 2002; Huntriss *et al.,* 2006). Interestingly, *Gtsf1* has been shown to be down-regulated in *Nobox* deficient mouse ovaries and this might suggest an important role of the gene in activation of follicle growth since *Nobox* in mammalian species is related to primordial follicle activation (Rajkovic *et al.*, 2004)*.* However, expression of *GTSF1* after MZT as shown by the results of this Chapter suggests that the gene might be up-regulated by other transcription factors during preimplantation development. This is because the transcripts of *NOBOX* only exist as residual maternal transcript at the preimplantation stage of development and are depleted by the blastocyst stage as shown in humans (Huntriss *et al.*, 2006).

Despite some inconsistencies, the gene expression data in Figure 3.4, showed higher expression of *GTSF1* at the primary follicle and GV and MII secondary oocyte stages, which might indicate different functions of the gene at the different stages of oocyte development. Similarly, the housekeepers that were selected also demonstrated variability in their expression from library to library. For this purpose, 2 widely expressed housekeeper genes *GAPDH* and *H2A* with relevantly stable expression levels in both somatic and gametic cells were included for analysis of their expression to verify the successful construction of each library (Jeong *et al.*, 2006; Mamo *et al.*, 2008). Both of these housekeepers were characterised across oocyte, follicle and embryo development and the libraries were verified if at least 1 of the 2 housekeeper genes was expressed. Expression of the oocyte-specific zona pellucida gene *ZP2* that encodes a part of the glycoprotein membrane that surrounds the plasma membrane of the oocyte was then examined (Conner *et al.*, 2005). The oocyte-specific gene *ZP2* was expressed at all stages of follicle and oocyte development while it was not present in the analysed somatic cells of the ovary, confirming its specificity as an oocyte expressed gene and further validating the successful creation of cDNA libraries. Furthermore, the demonstration of *ZP2* expression in cDNA libraries from secondary and antral stages of follicle development for which *GTSF1* was not present, indicated that the oocytes contained in these pooled follicle samples were capable of generating a detectable gene expression profile, thus confirming the authenticity of the *GTSF1* results. *ZP2* was also shown to be expressed throughout the early stages of embryogenesis, similarly to *GTSF1*, and following the MZT. The above observation is in agreement with other

studies in humans where *ZP2* was shown to be expressed until the blastocyst stage of preimplantation embryo development (Huntriss *et al.*, 2002).

Somatic tissue cDNA libraries from ovine adrenal, lung, kidney, heart and liver tissue were examined in triplicate to evaluate the specificity of expression of *GTSF1*. The results showed that *GTSF1* was not expressed in any of these somatic libraries confirming further its specificity as a germ cell expressed gene in the sheep. The housekeeper genes characterised across this series of somatic tissue included *ACTB* and *YWHAZ* (Chapter 2, Section 2.2.5). Out of the 4 housekeeper genes, *GAPDH* and *H2A* demonstrated the most stable expression pattern. Additional confirmation of the quality of the somatic cDNA libraries was derived from the lack of expression of *ZP2* in any of the somatic tissue. On the basis of these observations, *GAPDH*, *H2A* and *ZP2* were used as the housekeeper genes and oocyte-specific genes in all subsequent molecular analyses reported in this thesis.

Previous studies in mice have shown that *GTSF1* has higher expression levels in the male germline in comparison to the female (Yoshimura *et al.*, 2009), a result also reproduced in the bovine (Lu *et al*., 2012). This observation could be due to the relatively small number of germ cells in the ovary in relation to the somatic cells in this tissue type, relative to the testis. To evaluate the expression of ovine *GTSF1* in the male germline and to further confirm the results observed by RT-PCR in the female germline were correct, FISH analysis was conducted on both ovine ovary and testis samples. In the ovine ovary, the results showed that *GTSF1* was localised in the cytoplasm of oocytes from primordial to transitional follicles while in the testis, expression was detected in spermatogonia, spermatocytes as well as spermatids. Similar results were observed in a study in mouse where ISH confirmed the expression of the gene in the oocytes of early stage follicles of the adult mouse (Krotz *et al.*, 2009). The results obtained from the FISH analysis of the ovine ovary as reported here confirm the results of the PCR-expression mapping study reported earlier.

To further characterise ovine *GTSF1*, experiments were undertaken to obtain the sequence of the ovine gene and protein. The data reported here represent the first report of the full coding sequence of the ovine *GTSF1* gene. Ovine *GTSF1* encodes a 167 amino acid protein that belongs to the UPF0224 family (Yoshimura *et al.*, 2007). Several genes of the UPF0224 protein family are found in several species, including

invertebrates, suggesting that the UPF0224 family is of evolutionary significance (Yoshimura *et al.*, 2007). From this family, the *X. laevis* D7 protein has been reported and identified using a specific antibody (Smith *et al.*, 1991; Smith *et al.*, 1992). Ovine GTSF1 protein as reported here shares a 47% homology to the *X. laevis* D7 protein and is also homologous to other members of the UPF0224 protein family that have been previously studied (Yoshimura *et al.*, 2007; Krotz *et al.*, 2009). Like *GTSF1*, the *X. laevis D7* appears to have the same oocyte-specific expression profile in oocytes and early embryos (Smith *et al.*, 1988). Unlike mammalian *GTSF1*, *D7* mRNA appears to be translationally repressed during oogenesis and is only expressed during oocyte maturation (Smith *et al.*, 1988). Although it was shown that when *D7* mRNA is depleted from the oocyte by oligodeoxynucleotide injections the oocyte delays its maturation, the effects of *D7* in a subsequent study appeared to be non-specific (Smith *et al.*, 1988; Smith *et al.*, 1990). Indeed oocyte maturation was confirmed to be normal following depletion of the gene's mRNA (Smith *et al.*, 1990). Protein D7 synthesis is induced by maturation promoting factors including c-Mos, Cyclin B and crude Mpf preparations and the D7 protein can be post-translationally modified (Smith *et al.*, 1992). The precise reproductive function of D7 protein and other proteins that belong to the UPF0224 remains to be elucidated.

The deduced products of the UPF0224 family are characterised by 2 tandem copies of CHHC Zn-fingers that may be responsible for RNA-binding (Andreeva and Tidow, 2008). In the Zn-finger motif, there are 2 Cystein and Histidine amino acids that associate with the core ion, thus allowing the other amino acids to form a loop structure. The α-helix of each loop can bind to specific sites on DNA or RNA (Brown, 2005). Both the U11-48K and TRM13 proteins that contain a copy of the CHHC Zn-finger motif interact with RNAs (Wilkinson *et al.*, 2007; Turunen *et al.*, 2008). These motifs may be involved with RNA-binding; however, at the time of writing, there are no reports that show a direct functional interaction between the proteins encoded by the UPF0224 family genes and RNAs. Therefore, it is not yet clear whether GTSF1 functions as an RNA-binding protein during gametogenesis; but this suggestion merits further investigation.

Members of the UPF0224 family that appear to be preferrentially expreessed in the female and male germline may play important roles during gametogenesis. This was shown by Yoshimura *et al.*, (2009) who showed that *Gtsf1* is involved in

spermatogenesis and retrotransposon suppression in murine testis. Specifically, it was shown that male mice deficient of *Gtsf1* were infertile and that their spermatogenesis was disturbed in the early meiotic prophase I. This sterility was male specific and not shown in the *Gtsf1* null female mice. Moreover the male *Gtsf1* null mice had increased expression of *Line1* and *Iap* retrotransposons, suggesting a possible role for *Gtsf1* in their suppression. *Mael, Mili* and *Miwi2* are other important genes that have been decribed to be important for suppression of retrotransposon activity in the testis (Carmell *et al.*, 2007; Aravin and Bourc'his, 2008; Soper *et al.*, 2008). Male mice that do not have these genes show an arrest of spermatogenesis at the early meiotic stages (Carmell *et al.*, 2007), while female mice defficient in these genes do not appear to have any phenotypic defects. The reason for this sexual dimorphism between male and female mice mutants has not been determined, but it might be that the cellular mechanisms that regulate meiosis I during mammalian meiosis are more stringent in males than females (Hunt and Hassold, 2002).

The Western blotting conducted in this thesis has confirmed the presence of the GTSF1 protein in the ovine ovary and specifically in the GV oocytes which again supports the notion that GTSF1 may play a functional role during oocyte maturation. Specifically, *GTSF1* encodes a 20 kDa protein present in ovine GV oocytes and the protein was not detected in the ovine kidney or lung tissues. Furthermore, in the bovine testis, GTSF1 protein was shown to be present in 2 forms, 1 of a 20 kDa and 1 of 23 kDa. The presence of 2 forms of the protein might be suggesting a post-translational modification (PTM) of the protein in the male gonad. The PTM of proteins is considered essential in elucidation of complex cellular processes including cell division, growth and differentiation (Larsen *et al.*, 2006). The modification of proteins involves changes in the polypeptide chain that can be the result of adding or removing specific chemical moieties to amino acids, proteolytic processing of protein termini or addition of covalent crosslinks between domains of the proteins (Larsen *et al.*, 2006). Although there might be species-specific differences between bovine and ovine animals, the presence of a modified GTSF1 protein in the bovine testis that is absent from the female gonad might account for the sexual dimorphism observed between the sexes following *Gtsf1* knockout. Other studies have also detected the presence of the GTSF1 protein in the gametes. Immunohistochemistry has shown the presence of GTSF1 protein in the cytoplasm of germ cell clusters and primordial follicles of newborn mice ovaries and in oocytes of secondary and antral follicles of 8-week adult ovaries (Krotz *et al.*, 2009).

The above result suggests that species specific differences exist between animals and further signifies the importance of determining the role of GTSF1 in the regulation of oocyte development in monovular species.

Initial experiments of characterisation of *GTSF1* in monovular species conducted in the bovine species, showed that *GTSF1* mRNA was found in round spermatids and matured sperm indicating that the gene acts during post-meiotic spermatogenesis in addition to its characterised functions during the early stages of spermatogenesis (Lu *et al.*, 2012). In addition, GTSF1 protein was localised within the bovine chromatoid bodies in spermatocytes, suggesting that the protein is collaborating with piRNA and associated proteins in the regulation of retrotransposon suppression in the male germline, while in the bovine female germline, *GTSF1* was localised in the P-body (Lu *et al.*, 2012). The localisation of GTSF1 with chromatoid bodies and P-bodies in the cytoplasm of both male and female gametes adds further weight to the possibility that GTSF1 functions as a cargo shuttle to transport RNA and/or proteins between these sub-cellular organelles. In further support of this idea, knockout of *GTSF1* in male mice demonstrated similar phenotypes to *Mili* and *Miwi2* knockouts which are known to moderate meiotic arrest and retrotransposon activation (Aravin *et al.*, 2007b; Carmell *et al.*, 2007; Yoshimura *et al.*, 2009). Collectively, these data indicate that *GTSF1* could be associated with the piRNA related pathway for silencing retrotransposon activation during male meiotic division in spermatogenesis, while it could also interact with the siRNA pathway in the regulation of gene translation in both male and female.

3.4.1 Conclusion

This work has mapped the expression pattern and confirmed the cellular localisation and gamete specificity of *GTSF1* in ovine gametogenesis. The high degree of homology of the ovine *GTSF1* gene and protein sequence with other species together with the presence of 2 CHHC-Zn fingers and the cytoplasmic localisation of *GTSF1* in the ovine oocyte along with GTSF1 protein expression in the oocyte, suggests that this gene may be functionally important in the regulation of oocyte development and maturation in this species. While the importance of *GTSF1* in spermatogenesis and male fertility has been established in rodents, the functional significance of *GTSF1* to the acquisition of oocyte developmental competence in species such as the sheep has yet to be established.

Chapter 4: Validation of targeted gene knockdown during the IVM of ovine oocytes by the microinjection of siRNA species

4.1 INTRODUCTION

The acquisition of fertile competence by oocytes and their abilities to support subsequent embryonic development encompasses a number of critical biological events (Chapter 1, Sections 1.2-1.3). Oocytes must go through cytoplasmic maturation that involves preparation for fertilisation, activation and early embryo development as well as nuclear maturation so that the chromosomes are reduced to a haploid state (Eppig, 1996; Picton *et al.*, 1998). When it comes to IVM of oocytes, the culture system must fulfil the biological requirements observed *in vivo* and so support both the cytoplasmic and nuclear maturation of fully grown secondary oocytes arrested in prophase I of meiosis I (Trounson *et al.*, 2001). In a clinical setting, IVM has been proposed as a safe treatment for patients undergoing assisted conception in that it avoids or reduces ovarian stimulation with gonadotrophins and possible risks, such as ovarian hyperstimulation syndrome (Jaroudi *et al.*, 1997). In humans, this technique was originally implemented for the treatment of patients with polycystic ovarian syndrome, but the indications are widening to include patients with poor quality embryos in repeated cycles of IVF and poor responders to stimulation (Trounson *et al.*, 1994). This method is also being used for oocyte donors and fertility preservation in cancer patients undergoing gonadotoxic therapy with a number of pregnancies and live births being reported (Shalom-Paz *et al.*, 2010). Both *in vivo-* and *in vitro*-derived fully grown immature oocytes are suitable for IVM. However, despite encouraging results, the pregnancy rates following IVM of human oocytes are frequently lower than conventional assisted conception treatment and there are many parameters that can affect maturation and developmental competence, such as culture media, cumulus granulosa cell associations and differentiation, follicle size and atresia at oocyte harvest and the inclusion or exclusion of serum in the IVM medium (Junk and Yeap, 2012). In a research setting, IVM can be used to study oocyte maturation and the biology of key genes involved in oocyte fertility, oocyte quality and early embryo developmental potential *in vitro*. In the long-term, identification of such genes and factors that affect maturation can help improve IVM culture media and the success of assisted reproduction.

In order for IVM to be successful, the conditions and changes that occur during oocyte maturation *in vivo* must be replicated *in vitro*, including the autocrine and paracrine signalling between the cellular compartments of the follicle and the presumptive gamete as described in Chapter 1, Sections 1.2-1.3, that are important to promote oocyte meiotic progression (Gilchrist *et al.*, 2006; Cecconi *et al.*, 2008). These interactions between cell types in the COC are necessary to drive the preovulatory surged-induced changes that promote cytoplasmic and nuclear maturation in addition to a progesterone based environment established by granulosa cell steroid synthesis and also hyaluronic acid synthesis (Fulka *et al.*, 1998). Hyaluronic acid production by the cumulus cells promotes mucification and expansion of the cumulus as well as the loss of gap junctional communication with the oocyte (Tirone *et al.*, 1997).

Many approaches have been developed for IVM in different species including sheep (Szollosi *et al.*, 1988; O'brien *et al.*, 1996) and human (Trounson *et al.*, 1994). Maturation of oocytes can occur spontaneously *in vitro* as a result of removal of the oocytes from their surrounding cumulus cells (Pincus and Enzmann, 1935) or from their follicular environment in mice (Hartshorne *et al.*, 1994; Leonardsen *et al.*, 2000). In most studies, *in vitro* cytoplasmic and nuclear maturation is induced following the harvest of COCs and placing them in culture, although the time frame of the cultures for optimal maturation varies from 24-48 h between species (Trounson *et al.*, 2001). The follicle size from which COCs are harvested also affects the developmental competence of IVM oocytes. Oocytes from more advanced human follicles as indicated by follicle diameter of >10 mm diameter and granulosa production of oestrogen and inhibin A have shown greater developmental competence, as indicated by higher maturation rates, as well as better fertilisation and embryo development rates when compared with oocytes harvested from small antral follicles (<10mm diameter) (Mikkelsen *et al.*, 2000).

Many studies have shown that the composition and conditions of the IVM culture system have a significant effect on oocyte maturation capacity and embryo developmental potential (Chauchan *et* al., 1997; Wang and Day, 2002; Shabankareh et al, 2011). Addition of human or bovine serum to the culture media can be effective, but studies in several species including cow and sheep have shown that it can lead to epigenetic modifications that can result to the large offspring syndrome (Van Wagtendonk-De Leeuw *et al.*, 2000; Young *et al.*, 2001). Serum-free medium is

considered as a safer option to avoid these epigenetic errors and it is able to support the development of oocytes in many species (Keskintepe *et al.*, 1995; Wynn *et al.*, 1998). Even so, it has been shown that serum-free media in mouse cultures can lead to premature cortical granule release and subsequent hardening of the ZP (Schroeder *et al.*, 1990). Never-the-less, serum-free medium is considered a far safer option for oocyte maturation and embryo culture, while the effects of premature cortical granule release are not seen in species other than mice (Wynn *et al.*, 1998; Gandhi *et al.*, 2000). Culture of COCs and embryos in groups have been shown to be more beneficial for oocyte or embryo developmental competence than single COC and embryo cultures (O'Doherty *et al.,* 1997; Brum *et* al., 2005; Otoi *et al.*, 2002). It has also been shown that the blastocyst formation rates of single cultured embryos were significantly increased when conditioned medium derived from multiple embryo culture was added to the culture medium (Fujita *et al.*, 2006). However the variety of experimental conditions in each of the studies does not allow for any joint comparisons.

In an early study (Buccione *et al.*, 1990b), the role of cumulus cells during oocyte maturation *in vitro* and the dialogue between oocytes and cumulus used intact bovine COCs collected by puncturing antral follicles from which the oocyte was microsurgically removed in order to produce oocytectomised complexes These complexes can be cultured with or without bovine oocytes (Ralph *et al.*, 1995). Results of studies of this nature showed that the oocytectomised complexes only expanded in the presence of the denuded oocytes showing that cumulus expansion enabling factors were released from the oocytes into the surrounding media (Ralph *et al.*, 1995). Further studies have also verified the importance of oocytes in granulosa cell proliferation (Cecconi and Rossi, 2001; Eppig *et al.*, 2002).

A candidate oocyte-derived gene which contributes to these effects is considered to be *GDF9* as detailed in Chapter 1, Section 1.2.7. The presence of receptors for *GDF9* on the oocyte, binding to both TGFB type-1 receptors, ALK5 and BMPRII suggests an important role for *GDF9* in cell to cell signalling during oocyte growth and maturation (Vitt *et al.*, 2000; Mazerbourg *et al.*, 2004). This gene has been shown to have several regulatory roles including: cumulus cell progesterone synthesis, suppression of LH receptor expression, regulation of granulosa cell growth and cumulus expansion (McGrath *et al.*, 1995; Elvin *et al.*, 1999; Elvin *et al.*, 2000; Yan *et al.*, 2001; Dragovic *et al.*, 2005).

Several methods have been used to study the effect of candidate oocyte genes on follicle development. These include the generation of gene knockouts in mice (Koller *et al.*, 1989; Roy and Matzuk, 2006). Other techniques include the use of antibodies (Nepom *et al.*, 1981), antagonists (Nakajima *et al.*, 1995), Morpholino oligos (Heasman, 2002), ribozymes (Bertrand *et al.*, 1994) and antisense transcripts of genes (Korneev *et al.*, 1999; Huppi *et al.*, 2005). The use of RNAi is an alternative method which exploits the naturally occurring post-transcriptional gene silencing mechanism, triggered by miRNAs. RNAi can be used as a tool to study both the molecular and cellular events during oocyte development and maturation. This can be achieved by silencing expression of single or multiple genes at different levels (Schellander *et al.*, 2007). Knockdown of specific genes within individual cells has the advantage over traditional knockout experiments in that this technique can be directly applied to specific stages of oocyte development rather than eliminating expression of the gene throughout all stages of oogenesis. Other synthetic methods besides the endogenous method of RNAi-induced gene silencing, have also been developed, with second generation approaches involving the use of asymmetric siRNAs that reduce some of the off-target effects of RNAi effectors (Sibley *et al.*, 2010). When it comes to studies of the oocyte and embryo, microinjection is the preferred delivery system for the introduction of siRNAs (Svoboda *et al.*, 2000). In comparison with other techniques such as electroporation and transfection, microinjection is easy to apply to oocytes. With this method it is relatively easy to control the volume of siRNA introduced into the oocyte which is very important for it to produce the desired phenotype (Paradis *et al.*, 2005). Microinjection and specifically intracytoplasmic sperm injection is routinely used in assisted conception treatment (Palermo *et al.*, 1992).

Within the last 2 decades, a small number of studies have used RNAi to target different genes in order to elucidate gene function in oocytes and embryos as detailed in Chapter 1, Section 1.5.2. In order to investigate the effect of gene knockdown in GV oocytes on oocyte maturation, it is necessary to microinject siRNA species into denuded GV oocytes. As stated above, removal of the oocyte from the COC environment can trigger the spontaneous resumption of meiosis (Pincus and Enzmann, 1935). Therefore, in order to allow the injected siRNA species time to take effect, the oocyte meiotic maturation resumption has to be temporarily prevented. This can be achieved using inhibitory molecules that prevent meiotic maturation by antagonising the effects of a specific PDE as detailed in Chapter 1, Section 1.3. From the 5 PDEs that have been

identified to date, inhibitors of PDE3 can inhibit both second messengers cAMP and cGMP by hydrolysing the PDE bond (Conti, 2000). In this way MPF and MAPK are upregulated allowing the cell cycle to progress. The successful inhibition of meiotic maturation using PDE3 inhibitors has been shown in both sheep and mice (Cotterill, 2008; Gui and Joyce, 2005).

A candidate oocyte-specific gene whose role in oocyte maturation has been tested by RNAi is *GDF9*. Specifically, *Gdf9* long dsRNAi injections into murine oocytes resulted in decreased cumulus expansion accompanied by a decreased mRNA level of *Has2* and *Ptgs2*-both are markers of cumulus expansion (Gui and Joyce, 2005). Similarly, during ovine oocyte maturation, injection of dsRNA for *GDF9* into denuded GV oocytes resulted in reduced cumulus cell expansion when oocytectomised cumulus shells were co-cultured with the injected oocytes (Cotterill, 2008). This effect was accompanied by lower mRNA expression levels of *HAS2* and *GREMLIN* in the oocytectomised cumulus shells (Cotterill, 2008). In the above study the PDE3 inhibitors milrinone or cilostamide were used to inhibit meiotic progression of murine (Gui and Joyce, 2005) and ovine (Cotterill, 2008) oocytes respectively. Validation studies of the inhibitory efficacy of cilostamide for dsRNAi in sheep oocytes indicated that 20 mg/ml of cilostamide retained a higher percentage of oocytes at the GV stage compared to other cilostamide doses and to all concentrations of milrinone tested (Cotterill, 2008). Following siRNA uptake by the oocyte and the inhibition of meiosis, oocytes must then be removed from the inhibitory environment and the bi-directional communication between the oocyte and cumulus cells must be re-established to allow for maturation to progress. This can be achieved by oocytectomy of COCs as described by Buccione *et al*., (1990b) followed by co-culture with the dsRNA injected oocytes (Gui and Joyce, 2005; Cotterill, 2008). Further studies are needed to validate the use of IVM in conjunction with siRNA as a vehicle to study the function of novel genes during ovine oocyte maturation and cumulus expansion.

4.1.1 Aims
The aims of this chapter were therefore to use *GDF9* as a candidate gene to establish siRNA as a means to knockdown genes in ovine oocytes and to study their effects on:
1. Oocyte meiotic progression
2. Cumulus mucification and expansion

The end points of gene knockdown evaluations will be based on morphological evaluations of the oocyte and cumulus cells as well as molecular evaluation of oocyte and cumulus gene expression following 24 h of co-culture with oocytectomised cumulus shells using a serum-free IVM system.

4.2 MATERIALS AND METHODS

This experimental series used the physiological, serum-free IVM system which had been previously been developed for sheep oocytes by Cotterill *et al.*, (2012). The cultures were conducted during the sheep breeding season (Ortavant *et al*., 1988), between October 2008 and February 2009 as well as between October and November 2009. Tissue was collected from the abattoir twice a week on consecutive days during this period. The procedures detailed in Chapter 2, Section 2.1 were used to harvest COCs. All culture media compositions and conditions were as described in Chapter 2. All oocyte recovery procedures and manipulations were conducted on a microscope fitted with heated stage at 39°C. All media were prepared the day before use and all culture dishes, media and oil were prepared a minimum of 3 h before use and allowed to equilibrate at 39°C under appropriate incubation conditions.

4.2.1 Experiment 1: Pilot evaluations of microinjection methodology

Before proceeding with the IVM of oocytes, a pilot experimental series was conducted to test the efficiency of the injection methodology developed by Cotterill (2008). The first experimental series consisted of 3 replicate cultures in which GV oocytes were injected either with a fluorescent dye or buffer and then visualised under a fluorescent microscope to confirm that (i) microinjection had taken place and (ii) that the oocytes survived the injection procedure. For each culture, following their collection, COCs with an intact cytoplasm and more than 3 layers of cumulus cells surrounding the oocytes were selected and the COCs were transferred to a 35 mm sterile nunc dish containing 2 ml of pre-warmed H199[+]. The COCs were then divided equally into 2 groups. The oocytes from different groups were transferred into separate 35 mm nunc dishes that were prepared prior to the culture and kept in the non-gassed incubator at 39°C. For this experiment, 2 sets of 5 oocytes were transferred into individual 20 μl drops of H199[+] contained in each of the injection plates. One dish was used for treatment, the other contained control oocytes. Each of the 2 dishes was comprised of 4,

20 µl drops and 2 central drops containing 10 µl of H199$^+$, overlaid with mineral oil as shown in Figure 4.1.
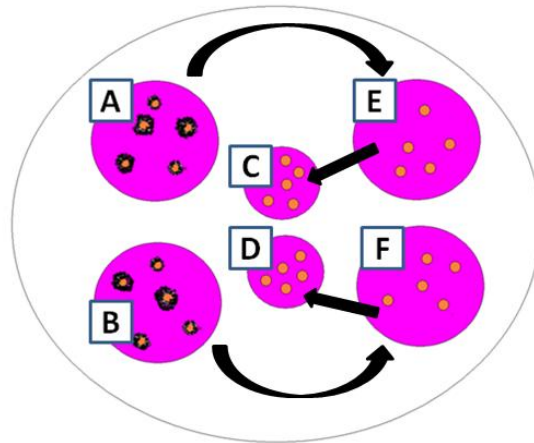
Figure 4.1: Schematic representation of the constitution of the denudation and microinjection 35 mm nunc dish. **A, B, E, F:** 20 µl drops containing H199$^+$. **C-D:** 10 µl injection drops containing H199$^+$. **A-B:** 5 oocytes are placed in each collection drop for denudation. **E-F:** Denuded oocytes are transferred in the wash drops before each group of 5 oocytes are transferred in drops **C-D:** where injections took place. The arrows indicate oocyte movements between drops.

After transferring the COCs into the collection drops, both dishes were placed back in the non-gassed incubator. One dish at a time was taken out of the incubator and placed on the stereo microscope; COCs were denuded by gentle repeat pipetting using a flexi-pet attached to a 170 µm pipette tip. Pipetting was performed for less than 1 min for each of the 5 oocytes. Denudation was then completed by additional repeat pipetting using a 140 µm pipette tip until all of the oocytes were completely denuded. The 2 sets of 5 denuded oocytes were transferred through the wash drop and placed into the adjacent 10 µl drops of H199$^+$ located in the centre of each dish. The dish was placed on the stage of the micromanipulation system which consisted of an Olympus IX70 inverted microscope fitted with Hoffman modulation contrast optics and heated stage at 39°C (Olympus Ltd), Integra Ti micromanipulators (Research Instruments Ltd, Cornwall, UK) and a Sony ex-wave HAD digital camera (Sony, Pencoed, UK). For this pilot experiment, 1 holding and 2 injection pipettes (bore of 5-6 µm) were adjusted on an angle of 35° (MIC-50-30, Humagen, Charlottesville, USA). The first injection pipette was preloaded with 0.557 mg/ml (w/v) carboxyfluorescein succinimidyl ester (CFSE, Invitrogen Ltd) in Ca^{2+} and Mg^{2+}-free DPBS solution (Invitrogen Ltd). Loading was performed by applying negative pressure using an SAS air syringe (Research Instruments Ltd) with the injection pipette held on a Leica DM IL microscope (Leica Microsystems Ltd) inserted in a 10 µl drop of injection medium in a 35 mm nunc plate under oil. The loaded injection pipette containing CFSE and the holding pipette were

inserted into the Integra Ti micromanipulation system and were aligned to the same plane with 35° angle to the injection plate. Following adjustment of the tips so the pipettes were at the same level as the injection plate, the pipettes were lowered into the first drop that contained 5 denuded oocytes. The magnification of the microscope was then increased from low power (40X) to high power magnification (400X) to obtain better visualisation of the oocyte, alignment of the pipettes to the same plane and optimal control of the injection process. Each oocyte in the drop was consecutively held with the holding pipette by applying negative pressure by mouth pipetting and the injection pipette was used to puncture the ZP and oolemma and enter the cytoplasm of the oocyte. The injection pipette outflow was based on a constant outflow microinjection system (Femtojet, Eppendorf Ltd, Stevenage, UK). The appropriate flow rate for the microinjection system which provided the best survival rates was previously optimised at 40 hPa (Cotterill, 2008).

Each oocyte was injected with approximately 10 pl of CFSE, before the injection pipette was removed. The injected oocyte was then released from the holding pipette and the rest of the oocytes in the drop were injected following the same procedure, ensuring that the injected oocytes were kept in different areas of the drop from the uninjected cells. After injecting all 5 oocytes in the drop, the magnification power was lowered, pipettes were lifted and the same process was repeated for the second drop containing the other 5 oocytes. After injection of all 10 oocytes with CFSE, the dish was placed back in the non-gassed incubator and held at 39°C. The same process was then followed for the dish containing the control group of COCs. Following denudation, the oocytes of this dish were injected with a different injection pipette loaded with DPBS solution, using the same process as described above.

The CFSE injected oocytes were compared against the DPBS injected oocytes under a fluorescence microscope. In order to compare the 2 groups, oocytes were washed in a 4 well dish containing 500 ml of DPBS to remove any excess CFSE and 10 μl of DPBS containing the oocytes were then transferred onto Superfrost Plus microscope slides (Thermo Fisher Scientific) and overlaid with a number 1 thickness coverslip (0.13-0.16 mm) onto vaseline pillars. The oocytes from the 2 different groups were then visualised using an epi-fluorescence Zeiss Axiovert microscope (Carl Zeiss Ltd) attached to a digital smart capture image system (Applied Imaging International, Newcastle upon Tyne, UK) using spectrum green filter (495/520 nm).

4.2.2 Experiment 2: Optimisation of *GDF9* knockdown using siRNA and IVM of ovine oocytes

Following validation of the microinjection system, the physiological, serum-free, IVM system for ovine oocytes was used in conjunction with microinjection to assess the efficacy of 4 different *GDF9* siRNAs in creating a gene specific knockdown. The previous studies of Gui and Joyce, (2005) and Cotterill, (2008) had both used dsRNA for oocyte gene knockdown. The siRNA oligos used for *GDF9* knockdown here were synthesized by Invitrogen Ltd based on the sequence of ovine *GDF9* and the oligo sequences used are shown in Table 4.1. Four siRNA oligos were generated and each oligo was assessed by the company to decrease homology with other genes in order to guarantee that at least 2 of the siRNAs would result in a gene specific knockdown.

Table 4.1: *GDF9* siRNA oligo sequences

Primer	Sequence
GDF9 siRNA-1	Sense : r(CAG UGG AUG UGC UGU UUA UUA A)dTdT Antisense : r(UUA AAC AGC AGA UCC ACU G)dAdT
GDF9 siRNA-2	Sense : r(CGU UUA UAA AGA AUA UGA A)dTdT Antisense : r(UUC AUA UUC UUU AUA AGC G)dAdT
GDF9 siRNA-3	Sense : r(GAA CAU CAU CCA UGA GAA A)dTdT Antisense : r(UUU CUC AUG GAU GAU GUU C)dTdG
GDF9 siRNA-4	Sense : r(AGA GCU CCA UAC UCA UUU A)dTdT Antisense : r(UAA AUG AGU AUG GAG CUC U)dAdG

The efficacy of these oligos in providing a *GDF9* knockdown was assessed in a series of 4 replicate cultures each conducted using 1 of the 4 *GDF9* siRNA sets of oligos. In each culture, oocytes were divided into 2 groups and injected either with 1 of the 4 *GDF9* siRNA species or Ca^{2+} and Mg^{2+}-free DPBS buffer (controls). The RNAi system utilised here was based on a 3 day culture system which had been extensively validated by Cotterill, (2008). This approach maintains the meiotic arrest of ovine denuded GV oocytes by 24 h incubation in 20 mg/ml of the PDE3 inhibitor cilostamide (Tsafriri *et al.*, 2005). The following protocol was used:

Day 1: siRNA microinjection and culture of oocytes

Ovaries and COCs were collected as detailed in Chapter 2, Sections 2.2.1-2. After assuring that only good quality COCs had been selected, the oocytes were divided equally into 2 groups, the *GDF9* siRNA injection group and the buffer injection control

group. For the microinjections, 2 injection pipettes were used in consecutive order, with the first injection pipette loaded with 1 of the 4 *GDF9* siRNA species and the second loaded with DPBS for control oocytes. Three denudation and injection dishes were prepared for each group (a total of 6 dishes) similar to the dish as shown in Figure 4.1, with the difference that the central drops of 10 µl of H199$^+$ were also supplemented with 20 mg/ml cilostamide to prevent the GV oocytes from resuming meiosis. Up to 30 oocytes were transferred to the denudation and injection dishes for each group per culture, based on the availability of good quality COCs. After denudation, wash and transfer of the oocytes into the central injection drop containing cilostamide, 1 microinjection dish was processed for microinjection at a time.

After injecting all 10 oocytes in the dish as detailed in Section 4.2.1, the oocytes were transferred to a fresh 35 mm nunc dish and washed in an 18 µl central drop containing serum-free media supplemented with 20 mg/ml cilostamide and basal levels of gonadotrophins (0.5 ng/ml of FSH, 0.1 ng/ml of LH), overlaid with mineral oil. These gonadotrophin concentrations represent the basal gonadotrophin levels required to support the growth of small antral follicles < 2 mm *in vivo* (Picton *et al.*, 1990; Picton and McNeilly, 1991) and *in vitro* (Newton, 1998); this gonadotrophin concentration does not trigger preovulatory maturation. The culture dish was made up of 4 microdrops each containing 18 µl of serum-free culture media with 20 mg/ml cilostamide. A total of 6 identical culture dishes were prepared for each group of 10 oocytes (3 dishes per treatment), to avoid exposuring the oocytes to adverse temperature and pH fluctuations. The microdrop volume used for serum-free media has previously been optimised as 2 µl per denuded oocyte (Danfour, 2001). Using a pipette, all 10 oocytes were transferred in a volume of 2 µl from the centre drop to an adjacent drop to wash and then they were transferred again into a volume of 2 µl to another drop to give a final culture drop volume of 20 µl (containing 10 oocytes). The dish was then placed in the gassed incubator at 5% CO_2, 6% O_2 and 89% N_2 atmosphere and kept at 39°C for a 24 h culture. The time at which each dish was placed into culture was noted. The same process was then followed for the remaining 2 dishes containing denuded oocytes injected with the same *GDF9* siRNA species. The process of denudation-injection and placing into culture was followed to completion for 10 oocytes at a time. After placing all 3 dishes of the same injection group into culture, the injection pipette was replaced. The new injection pipette was loaded with DPBS for injection of control oocytes and

the process was repeated for the remaining 3 dishes as detailed previously. The procedure used is summarised in Figure 4.2.
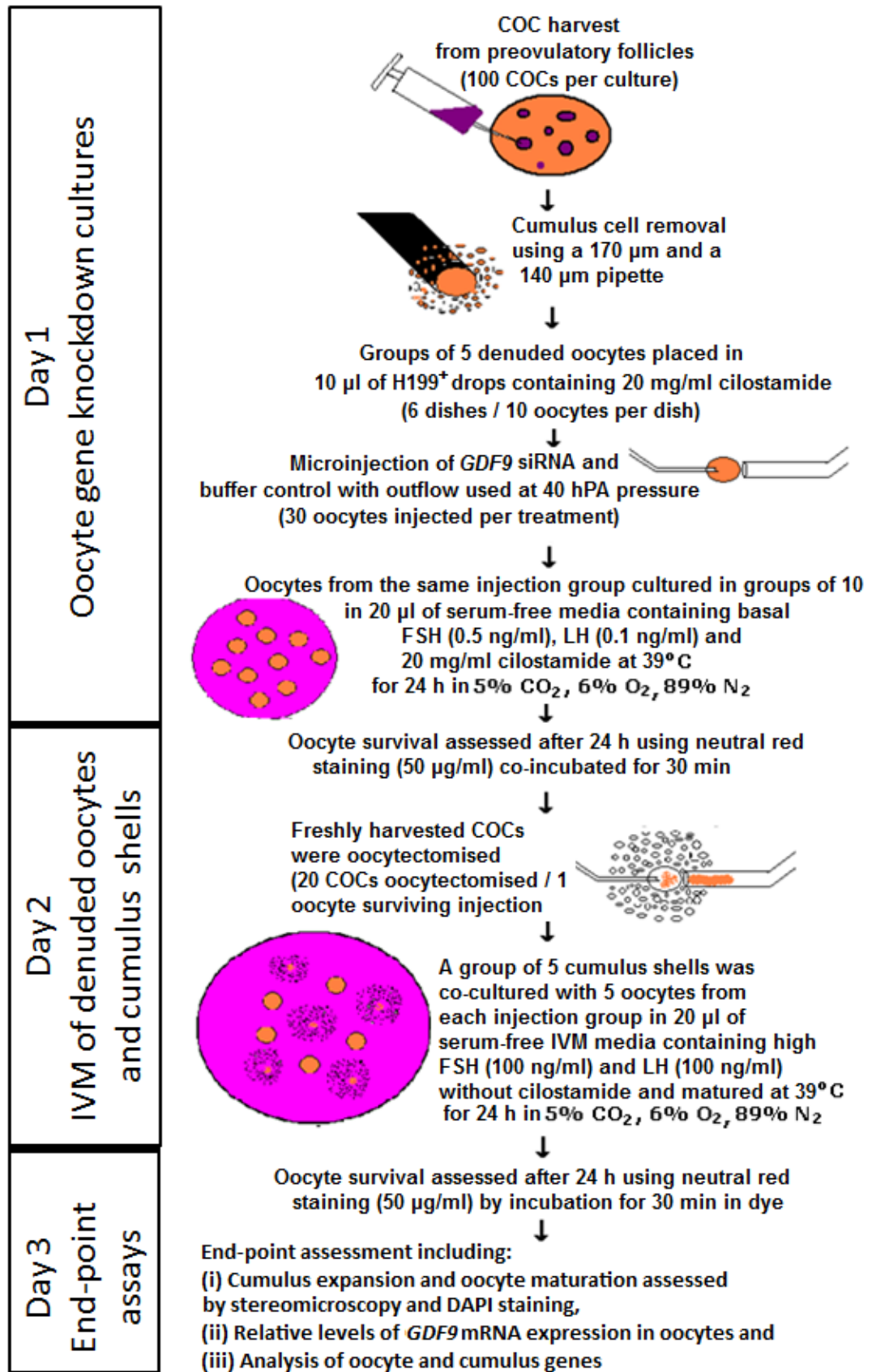
Figure 4.2: Schematic representation of the siRNA procedure and culture system.

Day 2: **Oocytectomy of COCs and IVM co-culture with gene knockdown oocytes**

Only the oocytes that survived the microinjections were selected for progression to the maturation stage of the experiment. The survival of oocytes was assessed after 24 h of culture using NR dye. This dye stains lysosomes red and is used as a vital stain because it can be applied to living cells without killing them (Winckler, 1974). This staining method has previously been validated for use on ovarian tissue by Chambers *et al*., (2010) and granulosa cells (Campbell *et al.*, 1996). Furthermore, NR has been used to confirm the viability of ovine oocytes following microinjections (Cotterill, 2008). After 24 h incubation (as noted by the time each dish was placed into culture), each group of 10 injected oocytes was collected into a volume of 2 μl and added to a central drop of a 35 mm nunc dish that contained 4, 18 μl micro-drops each comprised of serum-free media with cilostamide (as above) and further supplemented with 50 μg/ml NR solution. Once again a total of 6 dishes were prepared and allowed to calibrate at 39°C in the gassed incubator; oocytes were incubated in NR solution for 30 min. The viable oocytes stained red were selected for co-culture with cumulus shells on day 2, in order to assess the impact of *GDF9* knockdown on meiotic progression and cumulus expansion and mucification. Oocytes which did not stain red were considered to be un-viable and were discarded.

In parallel, fresh COCs were collected from a second set of ovine ovaries. Freshly harvested oocytectomised COCs generated as described previously by Buccione *et al*., (1990b) and Cotterill, (2008), were cultured with viable, siRNA-injected oocytes to target the impact of gene knockdown on the 2 way communication between the oocyte and cumulus compartment. Approximately 30 COCs were oocytectomised for each day 2 co-culture for which 3 injection dishes were prepared. Following, 2 groups of 5 COCs were placed in the 2, 10 μl drops of H199[+] contained in each of the 35 mm nunc dishes and overlaid with mineral oil and placed back in the non-gassed incubator at 39°C. The Olympus microinjection system was setup as detailed for day 1, with the difference that the injection pipette was not loaded and a manually made holding pipette was used. The holding pipette was manually made using a microforge by pulling glass pipettes (0.78x1.00x80mm, Science Products, Hofheim, Germany) so that the diameter of the opening of the holding pipette was wider than the tip of the injection pipette but did not exceed the diameter of a GV oocyte (<120 μm). The pipettes were then aligned to the same plane at a 35° angle to the injection dish. One dish was then placed on the heated stage of the micromanipulation system and the pipettes were lowered and aligned with

the COCs. The magnification was then increased as in day 1 and each COC was held by the holding pipette operated by mouth suction while the injection pipette was manually guided to penetrate right-through both sides of the zona and oolemma of the oocyte and into the holding pipette. Slow movements of the injection pipette were applied in order to create an opening in the zona from where the cytoplasm and nucleus of the oocyte could be removed. By applying negative pressure on the holding pipette using mouth suction, the cytoplasm and nucleus of the oocyte was aspirated from the COC leaving an intact cumulus shell surrounding an empty oocyte. Cumulus shells were then graded for their degree of cumulus coverage ranging from 0-2 according to the system previously used (Wynn *et al.*, 1998).

> Coverage classification 0: 0-3 layers of cumulus cells surrounding the oocyte.
> Coverage classification 1: 3-10 layers of cumulus cells.
> Coverage classification 2: More than 10 layers of cumulus cells.

The graded cumulus shells were then allocated equally into 2 groups based on their classification. The higher grade shells from each group were selected for co-culture with the denuded *GDF9* siRNA- and buffer-injected control oocytes. Separate equilibrated IVM dishes were prepared for the co-cultures for each oocyte treatment. Each of the 6 dishes contained 4, 18 μl drops of serum-free IVM media (Chapter 2, Table 2.3) with maturation-inducing levels of FSH (100 ng/ml, bioactivity 0.91 U/ml) and LH (100 ng/ml, bioactivity 0.55 U/ml) overlaid with mineral oil and kept in a gassed incubator at 39°C. The levels of FSH and LH used were equivalent to the preovulatory gonadotrophin surge measured in the peripheral circulation of sheep *in vivo* (Baird and McNeilly, 1981) and have previously been shown to drive high levels of sheep oocyte maturation *in vitro* (Cotterill *et al.*, 2012). It was vitally important to use the appropriate volume of medium for the IVM and co-cultures with cumulus cells, as it is essential to maintain the paracrine interaction between the oocyte and the cumulus cells in co-culture. The volume of medium used for IVM and co-culture here has previously been optimised at 4 μl for single oocyte and single cumulus shell pairs (Cotterill, 2008). After 24 h of microinjection and knockdown culture in cilostamide and basal levels of FSH and LH, viable oocytes as indicated by NR positive staining were transferred into the central drop of each IVM dish. For each oocyte that survived the first 24 h of culture, 1 oocytectomised cumulus shell was also transferred into the central drop. A group of 5 injected, denuded oocytes along with 5 cumulus shells were then transferred to an adjacent drop in a pipette volume of 2 μl; the final IVM culture volume was 20 μl for each group of 5 oocytes and 5 cumulus shells. The volume of the culture drop was

adjusted to maintain the correct ratio of oocyte and cumulus shell/4 µl of medium when fewer or more oocytes from each plate had survived the first 24 h of culture. The dish was then placed in culture at 39°C for 24 h at 5% CO_2, 6% O_2 and 89% N_2 atmosphere. The process was repeated for all culture dishes and the IVM start time was recorded for each culture dish.

Day 3: Developmental assessments

At the end of the 24 h IVM and co-culture period, oocyte survival was assessed by NR red as detailed above. Oocytes from each dish that survived the complete 48 h culture were separated from the cumulus shells and transferred to a 4 well dish containing 500 µl of pre-warmed H199⁺. Oocyte maturation was then assessed by examining the MII progression of oocytes as determined by the presence of a polar body visualised under the stereo microscope. To confirm the meiotic progression of oocytes following injection with either *GDF9* siRNA or DPBS buffer, additional staining with 4´-6 Diamidino-2-phenylindole (DAPI) was applied. Half of the oocytes that progressed to the MII stage from each of the 2 injection groups were used for staining while the rest of the oocytes were used for molecular evaluation of gene knockdown. The DAPI reagent passes through intact cell membranes and it can stain both live and fixed cells by producing a blue fluorescence with excitation at 360 nm and emission at 460 nm (Kapuscinski, 1995). Oocytes were stained with 5 µg/ml DAPI in 500 ml of DPBS for 15 min at RT. After this time, 10 µl of DPBS containing the oocytes were pipetted onto a glass slide and the oocytes were overlaid by a coverslip onto vaseline pillars and viewed using a fluorescence microscope. The oocytes that were not used for staining with DAPI were washed in 500 µl of DPBS in a 4 well dish and groups of 1-2 MII oocytes were transferred to a sterile 1.5 ml microcentrifuge tube containing 10 µl of lysis buffer (Chapter 2, Table 2.4). Samples were snap-frozen in liquid nitrogen and stored in -80°C for subsequent molecular analysis. The cumulus shells from the co-cultures of the 2 injections groups were also assessed for their developmental competence. The degree of cumulus expansion was recorded according to the 3 classifications as used previously (Wynn *et al.*, 1998).

      Expansion classification 0: Exhibited very poor or no expansion characterised by compact cumulus bundle.
      Expansion classification 1: Demonstrated a degree of partial expansion, where the cumulus mass was partially loosened.
      Expansion classification 2: Showed full expansion, where the cumulus mass was fully mucified.

Cumulus shells were transferred into a well of a 4 well dish that contained 500 ml of DPBS where they were washed. From there, a set of 2 representative cumulus shells from each culture drop based on cumulus expansion assessment were transferred into a sterile 1.5 ml microcentrifuge tube that contained 10 μl of lysis buffer. Samples were then immediately snap-frozen in liquid nitrogen and stored in -80°C until subsequent molecular analysis.

4.2.2.1 Molecular evaluation of *GDF9* knockdown

The stored pools of 1-2 knockdown MII oocytes for each of the *GDF9* siRNA species along with their respective injection controls containing equal numbers of oocytes were thawed and the mRNA isolation procedure was followed as described in Chapter 2, Section 2.2.2. In the final step of the isolation and extraction procedure, samples were re-suspended in 3 μl of Tris-HCl (Dynal, Invitrogen Ltd) and placed on a hot block set at 90°C for 2 min, before the mRNA was separated from the Dynal magnetic bead apparatus. The cDNA synthesis by reverse transcription was then performed as described in Chapter 2, Section 2.2.3. Real-time PCR was used to quantify the transcript level of ovine *GDF9* relative to the expression of housekeeper genes *GAPDH* and *H2A* for the 2 treatment groups (Chapter 2, Table 2.7). The primer sequence information used for ovine *GDF9* is shown in Table 4.2. Real-time PCRs were run in triplicate per sample. The siRNA species that provided the highest levels of *GDF9* knockdown in comparison with their respective controls were selected from each culture for subsequent molecular analysis.

Table 4.2: Primer sequences of ovine *GDF9* used for real-time PCR

Gene	Primer Sequence	Size (bp)	Reference
GDF9	F: 5´ AGTAAGCTGGAACCGGAATCG 3´	95	AF078545
ovine	R: 5´ GGTGGCCGACAAGAGAAGTCT 3´		(ovine)

4.2.3 Experiment 3: Assessment of the impact of *GDF9* knockdown on ovine oocyte maturation and cumulus expansion *in vitro*

Following evaluation of the efficacy of the siRNA species in creating a *GDF9* knockdown in GV oocytes, a series of 10 cultures were conducted using the most efficient siRNA species in creating a *GDF9* knockdown. The methodology followed was the same as described above. An average of 100 COCs were collected per culture, from which around 60 oocytes were microinjected. For the 10 cultures, a total of 302 oocytes were injected with *GDF9* siRNA, while 301 oocytes were injected with buffer,

averaging around 30 oocytes per injection group per culture. The effects of *GDF9* knockdown on oocyte meiotic progression, cumulus expansion and gene expression were assessed. Morphological assessments of the knockdown included oocyte survival as assessed by NR at 24 and 48 h of culture as well as developmental assessments based on cumulus expansion after co-culture and morphological evaluation of oocyte nuclear status (presence/absence of the first polar body) in comparison with the buffer-injected, control oocytes. All the oocytes that progressed to the MII stage were used for molecular evaluations following the methodology described above (Section 4.2.2.2). Initial molecular evaluations were performed for each culture to determine the degree of *GDF9* knockdown in cDNA libraries generated from pools of 1-2 MII siRNA-injected oocytes in comparison with their respective control cDNA libraries containing an equal number of MII buffer-injected oocytes. The mRNA levels of *GDF9* were quantified relative to the expression of *H2A* and *GAPDH*, both of which have been shown to be stable for the normalisation of gene expression data in the oocyte and early embryo stages (Gal *et al.*, 2006; Jeong *et al.*, 2006; Mamo *et al.*, 2007). Oocyte expression of *BMP15* was also quantified relative to the 2 housekeeper genes to evaluate any off-target effects of the *GDF9* siRNA species. This method of evaluating the specificity of *Gdf9* knockdown by interrogation of *Bmp15* expression levels following RNAi has been used previously in murine studies (Gui and Joyce, 2005).

The impact of oocyte *GDF9* knockdown on the relative mRNA expression of a range of candidate genes in the cumulus shells generated following co-culture with siRNA-injected oocytes and buffer-injected control oocytes was also assessed. Cumulus cell target analysis was conducted on the sets of 2 cumulus shells originating from the co-culture drops with oocytes that progressed to the MII stage and demonstrated significant levels of *GDF9* knockdown. These were compared to the sets of 2 cumulus shells originating from the co-culture drops with oocytes that were used as controls for the verification of *GDF9* knockdown. The same process as described in Section 4.2.2.1 was followed for the generation of cDNA libraries from stored cumulus shell samples. The list of genes analysed included potential targets of *GDF9* that are associated with cumulus mucification and expansion such as *HAS2* (Usui *et al.*, 1999) and *GREMLIN1* (Gui and Joyce, 2005), genes considered to be regulated by paracrine factors from the oocyte including *AMH* (Kitahara *et al.*, 2012) and *LDH1* (Moore *et al*., 2007), as well as members of the EGF family and signalling molecules including *AREG* (Cotterill *et al.*, 2012), *EREG* (Zimin *et al.*, 2009) and *BTC* (Cotterill *et al.*, 2012), which are induced by

LH in mural granulosa to bind to the *EGFR* and promote COC maturation (Salmon *et al.*, 2004; Hussein *et al.*, 2005; Hsieh *et al.*, 2007; Sugiura *et al.*, 2009). The relative levels of the receptors in the cumulus cells were also analysed for *EGFR* (Elsik *et al.*, 2009), *FSHR* (Chu *et al.*, 2012a) and *LHR* (Bacich *et al.*, 1994). The primers for the genes used for real-time PCR for the evaluation of the role of *GDF9* knockdown are shown in Table 4.3. The cumulus samples for the real-time PCR analysis were run in triplicates and the mRNA levels of the target genes were quantified relative to the expression of *GAPDH* and *H2A*.

Table 4.3: Primer sequences of targets genes following *GDF9* knockdown used for real-time PCR

Gene	Primer Sequence	Size (bp)	Reference
BMP15	F: 5´ GGCAAAAGCTCTGGAATCACA 3´	102	AF236079 (bovine)
	F: 5´ TGCCATGCCACCAGAACTC 3´		
HAS2	F: 5´ GCCACGGTAATCCAGCTCTTC 3´	107	NM174079 (bovine)
	R: 5´ AGGCAGCTGGCAAAAGATGA 3´		
GREMLIN1	F: 5´ GAAGCGAGACTGGTGCAAAAC 3´	93	AY942576 (ovine)
	R: 5´ CCGTAGCAGAAGCGGTTGA 3´		
AMH	F: 5´ TGGTGCTGCTGCTAAAGATG 3´	99	NM173890 (bovine)
	R: 5´ GACAGGCTGATGAGGAGCTT 3´		
LDH1	F: 5´ ATCTCCAACATGGCAGCCTTT 3´	103	BC146210 (bovine)
	R: 5´ GCCCCAGCTGTGATAATAACCA 3´		
AREG	F: 5´ AAAAGGGAGGCAAAAATGGA 3´	170	(Cotterill *et al.*, 2012)
	R: 5´ CTTTTCCCCACATCGTTCAC 3´		
EREG	F: 5´ AGTCCACAGCTGGCTAGGAA 3´	140	XM2688367 (predicted bovine)
	R: 5´ CGGGTTTTGTGGAAGACAAT 3´		
BTC	F: 5´ GACCGAGGCACTGGTACATT 3´	178	(Cotterill et al., 2012
	R: 5´ GTCGGACAAAGCTGTTTGCT 3´		
FSHR	F: 5´ CAGGACAGCAAGGTGACAGA 3´	188	NM1009289 (ovine)
	R: 5´ GGCAGGTTGGAGAACACATT 3´		
LHR	F: 5´ CACGGTACCAGGAAATGCTT 3´	145	L36329 (ovine)
	R: 5´ CAGGTGTGCATTCTCCTTCA 3´		
EGFR	F: 5´ GAGGTGGTCCTTGGGAATTT 3´	137	XM592211 (predicted bovine)
	R: 5´ AGGTTTTCCAGCGGAATCTT 3´		

4.2.4 Experiment 4: Assessment of the effect of gonadotrophins on maturation and cumulus expansion following *GDF9* knockdown in ovine oocytes

Due to the poor survival rates recorded in the early pilot studies, the effect of gonadotrophins on the survival and IVM potential of oocytes injected with *GDF9* siRNA and buffer was assessed. This was conducted by altering the concentration of gonadotrophins during the cumulus and IVM co-cultures established on day 2. The effect of high maturation-inducing levels of FSH (100 ng/ml) and LH (100 ng/ml) associated with the preovulatory surge (Baird and McNeilly, 1981; Cotterill *et al.*, 2012) were compared to the basal concentration of gonadotrophins used to maintain follicle

growth *in vivo* and *in vitro* (0.5 ng/ml FSH, 0.1 ng/ml LH) (Picton *et al.*, 1990; Picton and McNeilly, 1991; Newton, 1998). The effects of LH and FSH on oocyte nuclear progression and cumulus behaviour were assessed following 24 h of cumulus IVM co-culture as described in Section 4.2.2. A series of 8 cultures were conducted as described in Section 4.2.2.1 with maintenance of the FSH and LH levels at basal concentrations during the IVM and cumulus co-cultures. Data from the high gonadotrophin IVM cultures reported in Experiment 3 were compared with the basal gonadotrophin culture series.

4.2.5 Statistical analysis

Chi-square tests were used to analyse the results of oocyte survival, meiotic progression, cumulus coverage and cumulus expansion according to proportional analysis of the total cohort of oocytes and cumulus within each treatment. All data were checked for normality using the Anderson-Darling test and Student's t-test was used for normally distributed data including *GDF9* and *BMP15* mRNA levels in oocytes and *HAS2*, *GREMLIN1*, *AMH*, *LDH1*, *AREG*, *EREG*, *BTC*, *EGFR*, *FSHR* and *LHR* in cumulus cells. Values presented for real time data are the arithmetic means ±SEM for the number of observations shown. The presentation format used for both the culture data and real time data has previously been used by Cotterill *et al.*, (2012). Results for IVM and gene knockdown were evaluated for the total numbers of oocytes treated across all cultures.

4.3 RESULTS

Overall, 1058 oocytes were microinjected over 4 experimental series; of these 538 oocytes were microinjected with *GDF9* siRNA and 520 control oocytes were microinjected with DPBS buffer in a total of 18 cultures.

4.3.1 Experiment 1: Pilot evaluations of microinjection methodology

A total of 30 denuded oocytes were injected with CFSE, while 30 oocytes were injected with DPBS buffer over 3 repeat cultures (10 oocytes per group per culture). The injection methodology is shown in Figure 4.3.
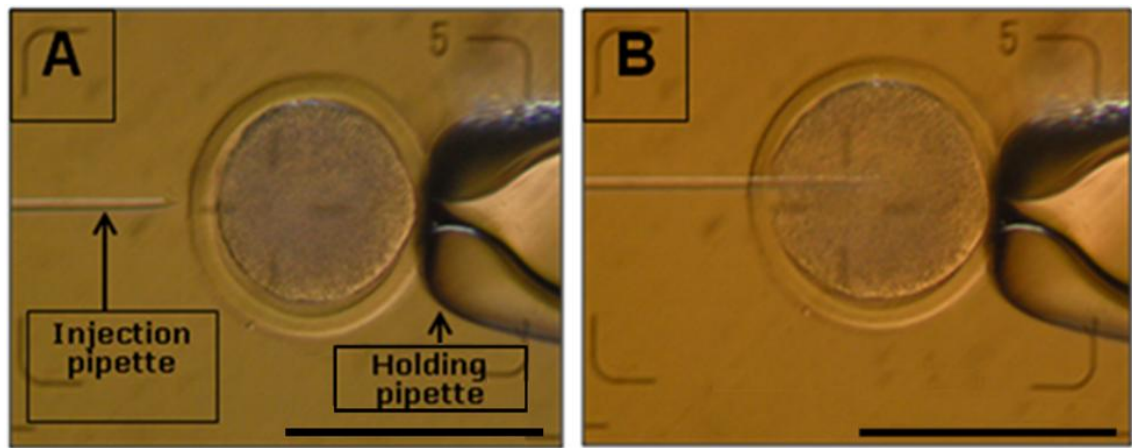
Figure 4.3: Microinjection of CFSE into an immature GV oocyte. **A:** The oocyte was stabilized by the holding pipette while the loaded injection pipette was positioned in the same plane as the denuded oocyte. **B:** The injection pipette was inserted into the oocyte until approximately 10 pl of solution based on a constant outflow system was injected into the oocyte. Scale bar: 120 μm.

In the 3 repeat cultures, 22/30 (73.3%) CFSE injected oocytes showed cytoplasmic fluorescence, while buffer-injected oocytes were invisible when viewed under the fluorescent microscope (0/30, 0.0%, Figure 4.4). The cytoplasmic localisation of CFSE was clearly visible and confirmed the injection methodology as a mean to deliver 10 pl of a known substance within the oocyte.
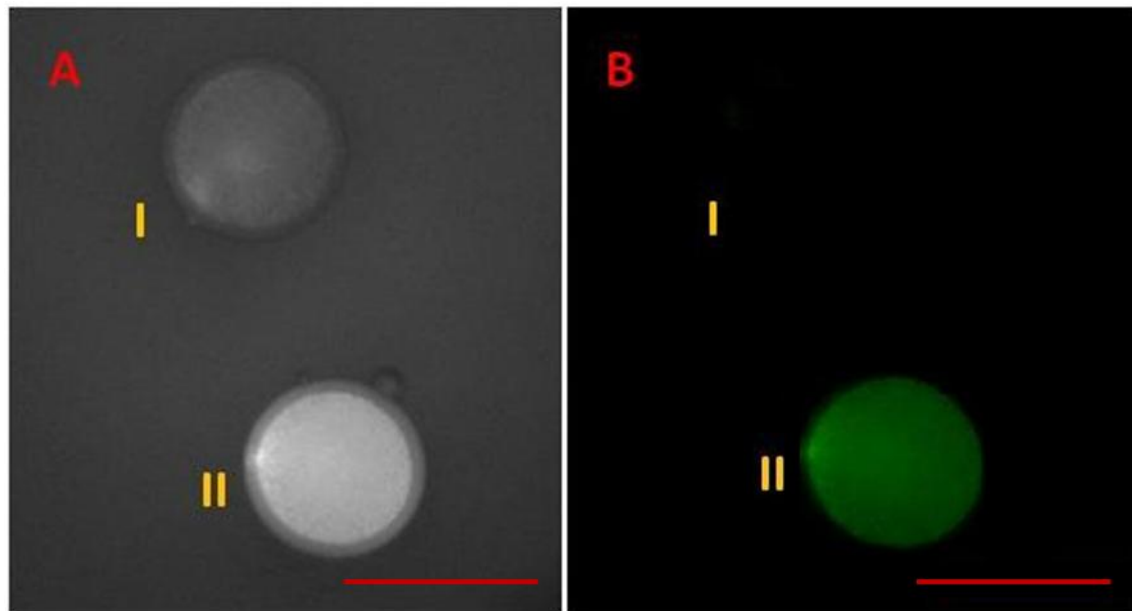
Figure 4.4: Oocytes injected with (i) DPBS buffer or (ii) CFSE. **A:** Brightfield image. **B:** Fluorescence image. Cytoplasmic localisation of CFSE is clearly visible. Scale bar: 120 μm.

4.3.2 Experiment 2: Optimisation of *GDF9* knockdown using siRNA and IVM of ovine oocytes

Following validation of the injection methodology, 4 cultures were carried out to quantify the efficiency of gene knockdown using the 4 siRNA species. In each culture, 30 oocytes were injected with 1 of the 4 different *GDF9* siRNAs (a different *GDF9* siRNA was used in each culture). An equal number of oocytes were injected with control buffer (n=30). The purpose of these preliminary cultures was to select the best siRNA species for *GDF9* knockdown in comparison to controls. Due to the low number of oocytes surviving microinjection in this pilot experiment, no statistical analysis was performed on data collected after 48 h of culture. This experimental series also served as a pilot study to assess the efficacy of the IVM system when used in conjunction with the microinjection system and oocytectomised cumulus shell co-culture to study the effect of candidate gene knockdown on oocyte meiotic progression and cumulus function. Representative images of COCs prior and following oocytectomy are shown in Figure 4.5.
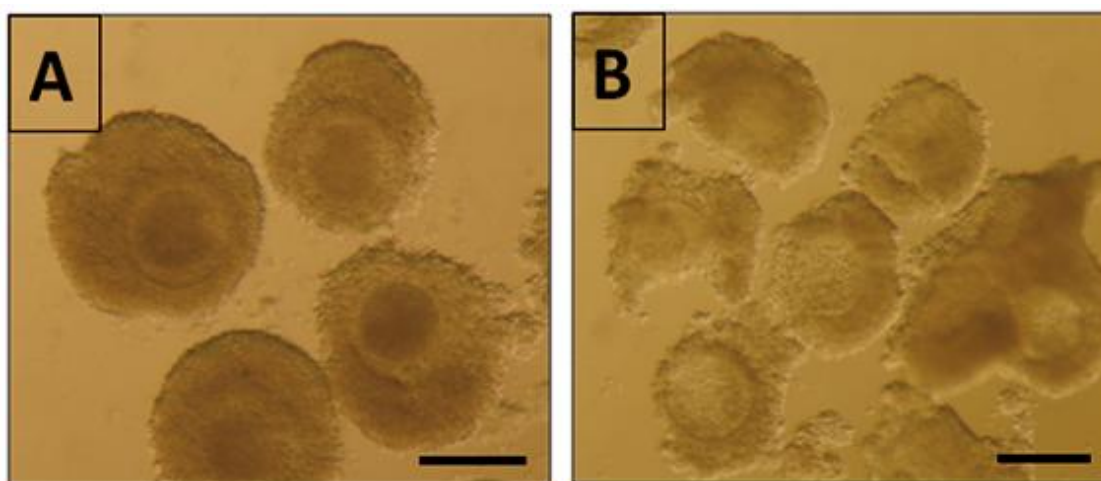
Figure 4.5: Oocytectomy of COCs. **A:** Intact COCs retrieved from ovine ovaries. **B:** COCs following oocytectomy by micromanipulation. Scale bar: 120 μm.

Oocyte survival was monitored at 24 and 48 h of each culture period by NR staining as shown in Figure 4.6 and Table 4.4. None of the 4 *GDF9* siRNAs were lethal to the oocytes relative to the controls, with the proportions of the total number of oocytes surviving at 24 and 48 h for all siRNAs not significantly different to the proportions of the total number of controls (P>0.05). The majority of oocytes for both siRNA and controls were not viable after the first 24 h of culture following denudation, microinjection and culture in a serum-free media containing cilostamide. Almost all

oocytes surviving the first 24 h of culture remained viable after IVM co-culture for both the siRNA and control groups (Table 4.4).

Table 4.4: Oocyte survival as quantified by NR staining

Oocyte survival	Culture 1		Culture 2		Culture 3		Culture 4		Significance P<0.05
	GDF9 siRNA-1 (n=30)	Buffer (n=30)	*GDF9* siRNA-2 (n=30)	Buffer (n=30)	*GDF9* siRNA-3 (n=30)	Buffer (n=30)	*GDF9* siRNA-4 (n=30)	Buffer (n=30)	
24 h No.	5/30	8/30	8/30	8/30	6/30	8/30	12/30	10/30	NS
24 h %	16.7	26.7	26.7	26.7	20.0	26.7	40.0	33.3	
48 h No.	5/30	7/30	8/30	7/30	6/30	8/30	12/30	10/30	NS
48 h %	16.7	23.3	26.7	23.3	20.0	26.7	40.0	33.3	
24 h Vs 48 h	5/5	7/8	8/8	7/8	6/6	8/8	12/12	10/10	NA
	100%	87.5%	100%	87.5%	100%	100%	100%	100%	

NS = Not significant, NA = Not applicable
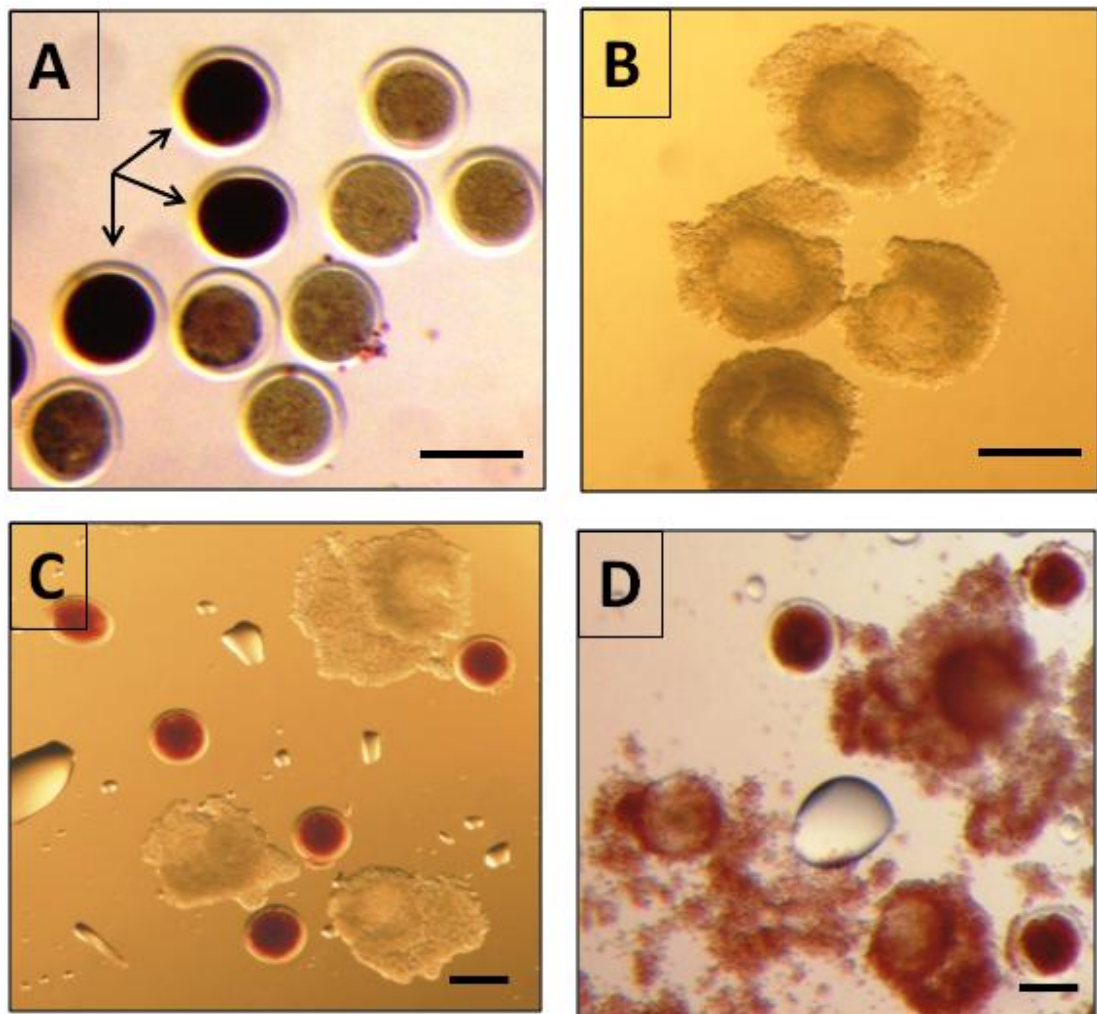
Figure 4.6: Brightfield images showing: **A:** Denuded oocytes on day 1, 24 h after injection with *GDF9* siRNA-2 and culture in serum-free media with 20 mg/ml cilostamide. Surviving oocytes were stained red (arrows). **B:** Oocytectomised cumulus shells before culture. **C:** Surviving oocytes (A), were placed into culture with equal numbers of compact cumulus shells (B) (only 3 of 5 cumulus shells are shown). **D:** Co-cultured oocytes with cumulus shells stained with NR at the end of day 2, after 24 h of IVM co-culture. Surviving oocytes and expanded cumulus shells are stained red. Scale bar: 120 μm.

The meiotic maturation of gene knockdown oocytes was quantified relative to buffer-injected controls by assessment of MII progression rates after placing the oocytes that survived the first 24 h of culture into IVM co-culture with cumulus shells. In all 4 cultures, oocytes from both treatment and control injection groups progressed to the MII stage after 48 h as assessed by the presence of the first polar body (Table 4.5). For all treatment groups, the numbers of MII oocytes were very low and meaningful statistical analysis was therefore not possible. The developmental competence of selected oocytes was assessed by DAPI staining. The GV nucleus was present in oocytes that remained at the GV stage whereas, condensed chromatin and discrete chromosomes were detected in MII oocytes as well as the first polar body (Figure 4.7)

Table 4.5: Oocyte meiotic progression after knockdown of *GDF9* at 48 h of culture

MII progression	Culture 1		Culture 2		Culture 3		Culture 4	
	GDF9 siRNA-1	Buffer	*GDF9* siRNA-2	Buffer	*GDF9* siRNA-3	Buffer	*GDF9* siRNA-4	Buffer
No.	2/5	2/8	1/8	2/8	1/6	1/8	2/12	2/10
%	40.0	25.0	12.5	25.0	16.7	12.5	16.7	20.0
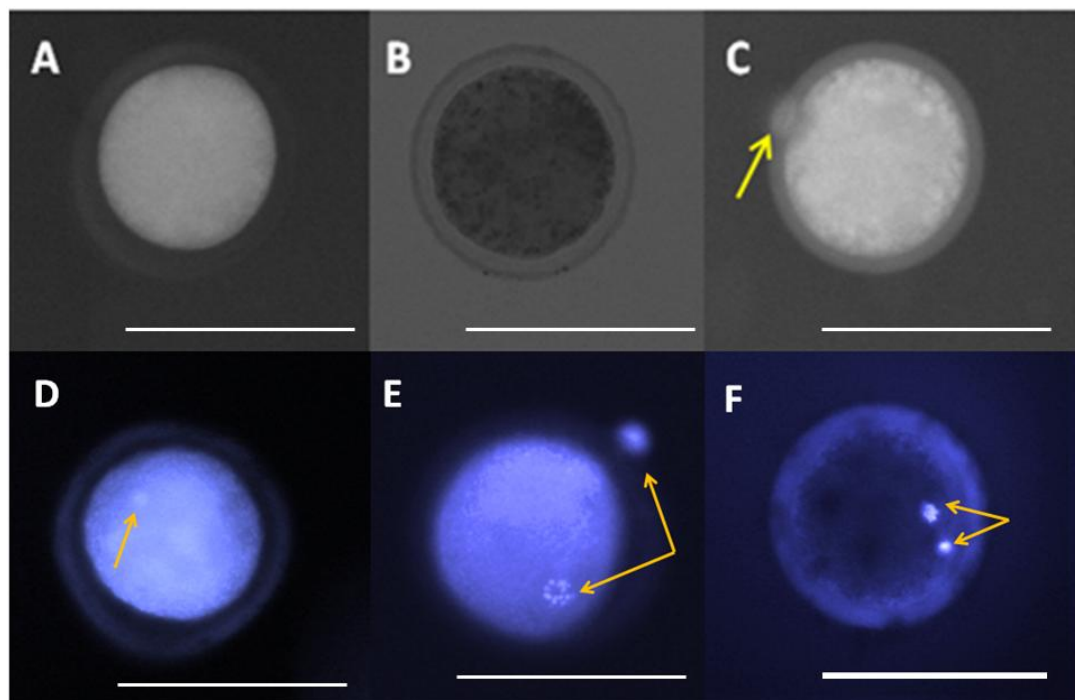
Figure 4.7: Day 2 verification of oocyte maturation following microinjection with siRNA or buffer and IVM, as determined by DAPI staining. **A,B,C:** Brightfield images of: **A:** Denuded GV oocyte before culture, **B:** Dead oocyte after 24 h of culture **C:** MII oocyte following IVM. **D,E,F:** Fluorescent images of DAPI staining following 48 h of culture: **D:** GV oocyte, **E:** MII control oocyte that had been subjected to buffer injection and co-cultured with cumulus shells. **F:** MII oocyte that has been subjected to *GDF9* siRNA-1 injection and co-cultured with cumulus shells. Arrows indicate positions of polar body (C, E, F), GV nucleus (D) and oocyte chromosomes (E) as shown by DAPI staining. Scale bar: 120 μm.

Evaluation of the impact of gene knockdown and IVM on cumulus expansion following the co-cultures of denuded oocytes with oocytectomised cumulus shells are shown in Figure 4.8. The co-cultures of injected oocytes from the 2 injection groups with oocytectomised cumulus shells resulted in fully expanded cumulus cells as shown in Table 4.6.
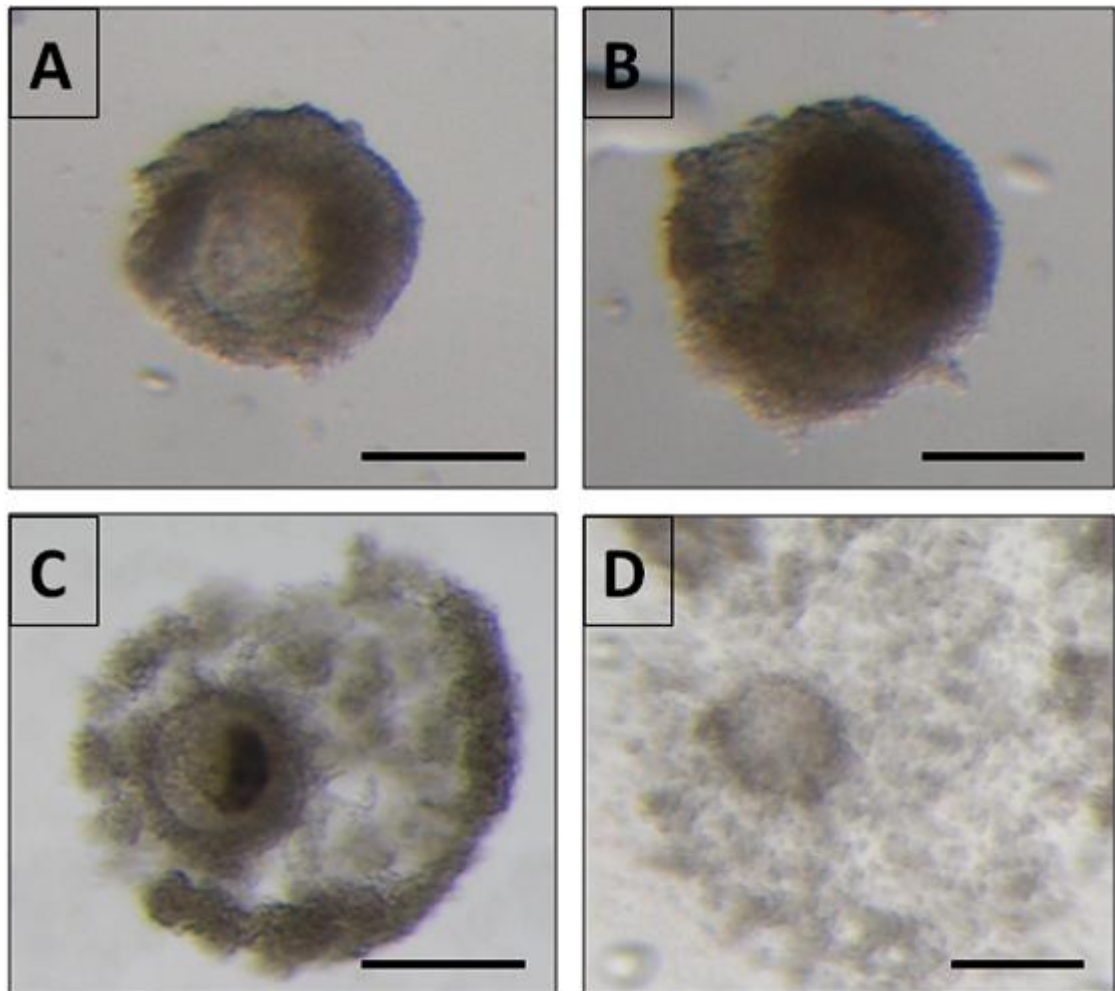
Figure 4.8: Cumulus shell morphology before and after IVM co-culture. **A:** Oocytectomised cumulus shell prior to culture. **B-D:** Oocytectomised cumulus shell expansion scores following 24 h of IVM co-culture with control oocytes microinjected with DPBS buffer. Cumulus shell expansion scores are based on images **B:** Unexpanded (grade 0), **C:** Partially expanded (Grade 1), and **D:** Fully expanded (Grade 2). Scale bar: 120 μm.

Although the data is very preliminary in nature and the number of oocytes and cumulus complexes were too low per siRNA species for meaningful statistical analysis, the data demonstrated overall that the IVM co-culture of oocytectomised cumulus shells and denuded oocytes in serum-free IVM medium containing surge levels of FSH and LH supports cumulus expansion *in vitro*.

Table 4.6: Evaluation of cumulus expansion following *GDF9* knockdown and IVM co-culture

Culture No.	Treatment	Cumulus expansion classification at 48 h		
		Grade 0	Grade 1	Grade 2
Culture 1	*GDF9* siRNA-1	2/5 (40.0%)	2/5 (40.0%)	1/5 (20.0%)
	Buffer	2/8 (25.0%)	3/8 (37.5%)	3/8 (37.5%)
Culture 2	*GDF9* siRNA-2	2/8 (25.0%)	4/8 (50.0%)	2/8 (25.0%)
	Buffer	2/8 (25%)	3/8 (37.5%)	3/8 (37.5%)
Culture 3	*GDF9* siRNA-3	2/6 (33.3%)	3/6 (50.0%)	1/6 (16.7%)
	Buffer	3/8 (37.5%)	2/8 (25.0%)	3/8 (37.5%)
Culture 4	*GDF9* siRNA-4	7/12 (66.7%)	3/12 (16.7%)	2/12 (16.7%)
	Buffer	3/10 (37.5%)	4/10 (25.0%)	3/10 (37.5%)

At the end of each culture, MII oocytes from each injection group were analysed for their *GDF9* expression levels. For each treatment group, 1 MII oocyte was used for analysis. Because of the low numbers of oocytes that progressed to the MII stage from each of the 4 *GDF9* siRNAs and their respective controls (up to 2 MII oocytes produced in each treatment), no repeat samples were generated. All samples were run in triplicates for each real-time PCR and 3 replicate real-time PCRs were conducted. The results showed that *GDF9* transcript levels were reduced for 3 out of 4 siRNAs used, when *GDF9* siRNA-injected oocytes were compared with their buffer-injected control oocytes using *GAPDH* and *H2A* expression to normalise data from real-time PCR. Specifically, the expression level of *GDF9* was reduced when using *GDF9* siRNA-1 with relative expression value of 2.15 arbitrary (arb.) units, in comparison with the control (relative expression value of 5.3 arb. units). The expression of *GDF9* was reduced much more when using *GDF9* siRNA-2 (0.8 arb. units) in comparison with the control (6.6 arb. units) and when using *GDF9* siRNA-3 (0.6 arb. units) in comparison with the control (4.7 arb. units). For *GDF9* siRNA-4, interrogation of *GDF9* transcript levels showed a small reduction in the *GDF9* transcript following the knockdown (3.7 arb. units) relative to the buffer-injected control (3.8 arb. units). These data are very preliminary. Analysis of the oocytes that were retained at the GV stage at the end of each of the 4 cultures following injections with the different *GTSF1* siRNAs and control buffer injections verified the efficiency of the siRNA-2 and siRNA-3 in generating a *GDF9* knockdown (data not shown). Based on these preliminary results, a mixture of *GDF9* siRNA-2 and *GDF9* siRNA-3 of equal proportions was used to study the effect of *GDF9* knockdown on oocyte maturation and cumulus function in Experiment 3. The *GDF9* mRNA is 1605 bp long and has 3 exons. The *GDF9* siRNA-2 relates to a sequence located on the second exon of the ovine *GDF9* (base pairs 1309-1329), while *GDF9* siRNA-3 relates to a sequence located on the first and second exon of the gene (base pairs 1204-1224).

4.3.3 Experiment 3: Assessment of the impact of *GDF9* knockdown on ovine oocyte maturation and cumulus expansion *in vitro*

A series of 10 cultures were conducted to study the effect of *GDF9* knockdown on oocyte maturation and cumulus function. In these cultures a total of 302 oocytes were injected with the selected mixture of *GDF9* siRNA-2 and siRNA-3 now referred to as *GDF9* siRNA and 301 control oocytes were injected with DPBS buffer.

4.3.3.1 Oocyte survival after microinjection

Oocyte survival was assessed at 24 h and 48 h of culture. From all the cultures, a total of 61 oocytes (61/302, 20.7%) survived the first 24 h as assessed by NR staining when injected with *GDF9* siRNA, while 73 control oocytes (73/301, 24.3%) survived the buffer injections. At 48 h, a total of 60 *GDF9* siRNA-injected oocytes (60/61, 98.4%) remained viable, while 62 buffer oocytes remained viable (62/73, 85.0%). No significant differences were observed between the buffer and the siRNA-injected oocytes at the 2 time points as shown in Figure 4.9. These data indicate that the denudation and/or micromanipulation and culture with 20 mg/ml of cilostamide compromised oocyte viability, rather than extended culture in serum-free medium or the use of siRNA.
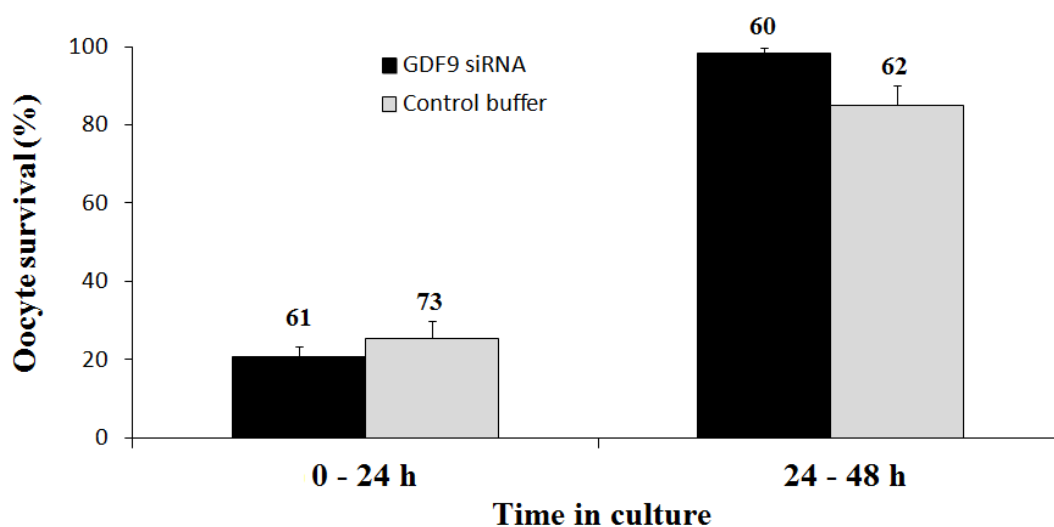
Figure 4.9: Influence of *GDF9* siRNA injection and buffer injection on oocyte survival at 24 and 48 h of culture. Oocytes were microinjected with either *GDF9* siRNA or buffer and cultured in serum-free basal gonadotrophin media with cilostamide (20 mg/ml) for 24 h. Surviving oocytes were then co-cultured with oocytectomised cumulus shells in serum-free IVM media and maturation inducing levels of gonadotrophins for an additional 24 h (total of 48 h). Values represent proportions of the total cohort of injected oocytes over 10 repeat cultures. Individual bars show the mean ±SEM for 10 independent cultures. The numbers of oocytes falling into each category are shown. No significant differences were observed between siRNA- injected oocytes and their controls at each time point (P>0.05).

132

4.3.3.2 The impact of oocyte *GDF9* knockdown on meiotic progression *in vitro*

The developmental competence of oocytes following *GDF9* knockdown and IVM co-culture with cumulus shells was assessed by confirming the MII progression of oocytes. The proportion of MII oocytes produced out of the oocytes that survived the first 24 h of culture following *GDF9* siRNA injections were 13.1% (8/61 oocytes progressed to MII) that was significantly different (P<0.05) to the proportion of MII oocytes from the buffer injected treatment (26.0%, 19/73 oocytes) as shown in Figure 4.10.
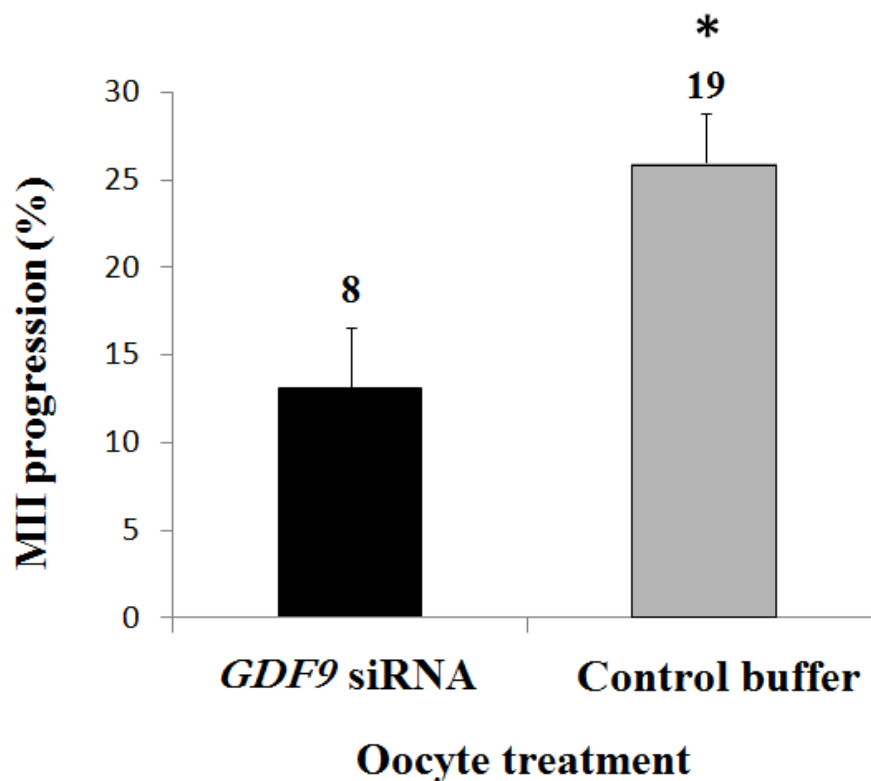
Figure 4.10: Impact of *GDF9* knockdown on meiotic progression during IVM co-culture. Values represent proportions of the meiotic progression of viable *GDF9* siRNA and buffer-injected oocytes as determined at 24 h of culture that were subjected to an additional 24 h of IVM co-culture with cumulus shells. Individual bars show the mean ±SEM for 10 independent cultures. The numbers of oocytes falling into each category are shown. *GDF9* siRNA-injected oocytes exhibited a significant reduced capacity to progress to MII (*=P<0.05) when compared to the buffer-injected control group.

4.3.3.3 The effect of oocyte *GDF9* knockdown on cumulus mass and expansion *in vitro*

Cumulus shell mass and expansion were assessed prior to the start of the second phase of oocyte culture at 24 h and at the end of the 24 h IVM co-culture giving a total of 48 h *in vitro*. Equal numbers of cumulus shells and viable oocytes were co-cultured during IVM for each treatment. In total, 61 cumulus shells were oocytectomised and cultured with viable *GDF9* siRNA-injected oocytes, while 73 cumulus shells were co-cultured with viable buffer-injected oocytes. Cumulus shells were divided equally for the 2

133

groups of oocytes based on their coverage scores at the start of culture and at the end of the culture, with the coverage scores of the cumulus reamained unchanged during the period of the co-culture for both treatments. Comparison of the cumulus coverage for the 2 groups did not show any significant differences as shown by the proportion of cumulus coverage for the 2 treatment groups at the end of the cultures (Figure 4.11).
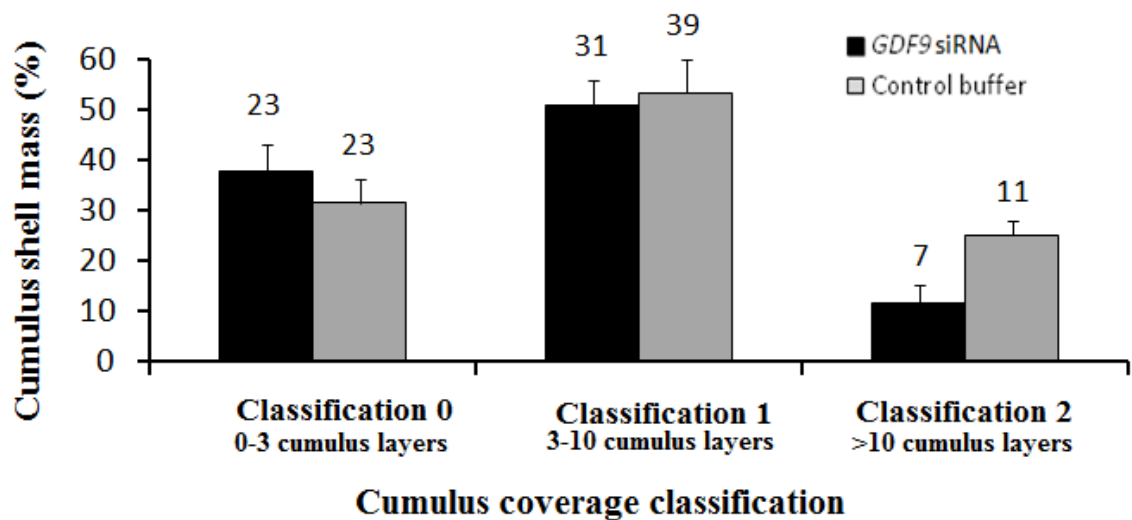
Figure 4.11: Effect of oocyte *GDF9* knockdown on cumulus shell mass classification after 24 h of serum-free IVM co-culture with *GDF9* siRNA or buffer-injected oocytes. Values represent proportions of the total numbers of cumulus shell mass classifications over 10 repeat cultures. Individual bars show the mean ±SEM for 10 independent cultures. The numbers of cumulus shells falling into each category are shown. No significant differences were observed between the 2 treatment groups (P>0.05).

Analysis of cumulus expansion following IVM co-culture with microinjected oocytes showed that *GDF9* knockdown in oocytes generated by siRNA injection significantly inhibited the capacity of cumulus shells to undergo full expansion during IVM co-culture, as evidenced by the presence of a significantly reduced number of fully expanded cumulus shells (P<0.05) when compared to the buffer-injected control oocyte co-culture group. Cumulus expansion comparisons showed that there were more partially expanded cumulus shells following co-culture with *GDF9* knockdown in comparison to controls but no significant differences were noted (P>0.05). This suggests that *GDF9* knockdown impairs cumulus shell full expansion rather than partial expansion. Representative images for the 2 treatments following 24 h of co-culture are shown in Figure 4.12. Figure 4.13 illustrates the mean proportion of cumulus expansion for the 2 treatment groups. Since there was no significant effect of treatment on cumulus coverage, the morphological differences in cumulus expansion were not due to gross changes in cumulus coverage.
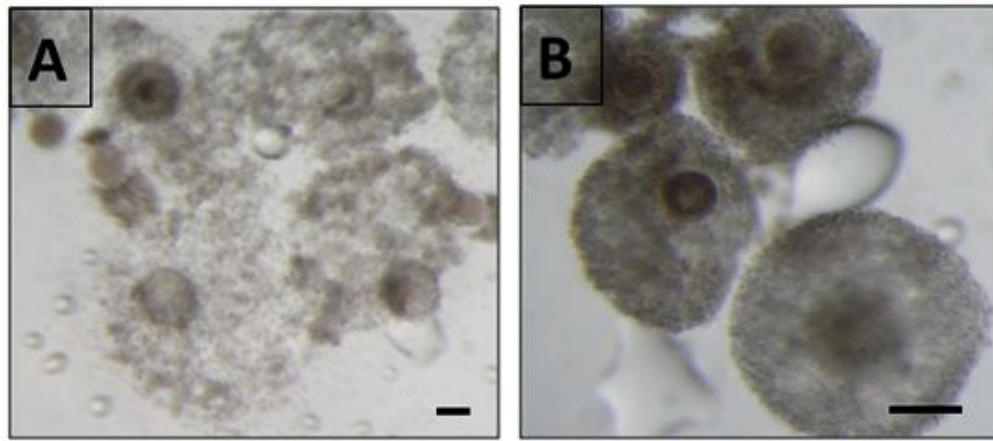
Figure 4.12: Impact of *GDF9* knockdown on cumulus expansion following IVM co-culture. **A:** Representative images for full cumulus expansion in buffer-injected control oocyte following co-culture with cumulus shells. **B:** Representative image for partial cumulus expansion following oocyte *GDF9* siRNA treatment and co-culture with cumulus shells. Scale bar: 120 μm.
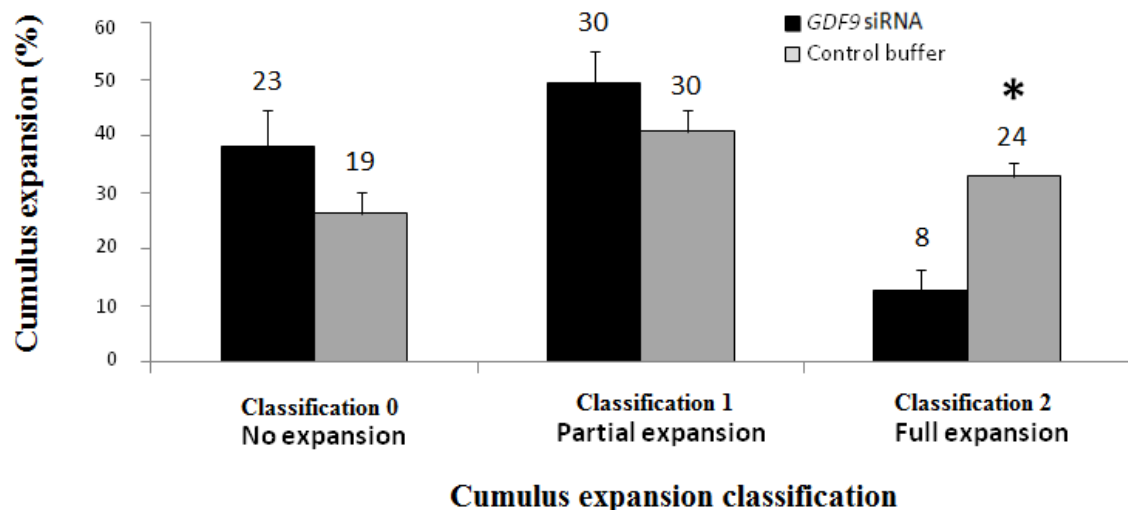
Figure 4.13: Effect of oocyte *GDF9* knockdown on cumulus expansion following 24 h of serum-free IVM co-culture. Values represent proportions of the total numbers of cumulus shell expansion classifications over 10 repeat cultures. Individual bars show the mean ±SEM for 10 independent cultures. The numbers of cumulus shells falling into each category are shown. Cumulus shells that were co-cultured with oocytes microinjected with *GDF9* siRNA exhibited a significantly reduced capacity to undergo complete expansion *in vitro* (*=P<0.05), when compared to buffer-injected control oocytes.

4.3.3.4 Molecular analysis of gene expression following *GDF9* siRNA microinjection

A total of 6 cDNA libraries for each treatment were successfully generated from pools of 1-2 MII oocytes (4 cDNA libraries containing 1 MII oocyte and 2 cDNA libraries containing 2 MII oocytes for each treatment), originating from separate IVM culture microdrops within each culture. The number of cDNA libraries created was very limited because of the low number of oocytes surviving and progressing to the MII stage from

each treatment group. Oocytes from each of the 2 treatment groups were analysed for their *GDF9* and *BMP15* expression levels based on absolute mRNA levels of *GDF9* and *BMP15* normalised against both *H2A* and *GAPDH* as determined by real-time PCR (Figure 4.14). All individual MII cDNA libraries showed a reduction of >50% in their *GDF9* transcript levels in comparison with their respective controls. Specifically, *GDF9* transcript levels were significantly reduced ($P<0.05$) in *GDF9* siRNA-injected oocytes (0.7 ± 0.2 arb. units, n=6) in comparison with controls (6.7 ± 3.2 arb. units, n=6) following the targeted knockdown. The specificity of the targeted knockdown of *GDF9* was evaluated by assessing the transcript levels of *BMP15*, another oocyte-derived gene which is also a member of the TGFB superfamily, on the same MII cDNA libraries. The data showed a small reduction in the expression levels of *BMP15* following *GDF9* siRNA injections (1.4 ± 0.3 arb. units, n=6) but this reduction was not significant ($P>0.05$) when compared to the *BMP15* mRNA levels measured in control oocytes (1.7 ± 0.3 arb. units, n=6), suggesting no/low off target effects that confirmed the specificity of *GDF9* knockdown using siRNA (Figure 4.14).
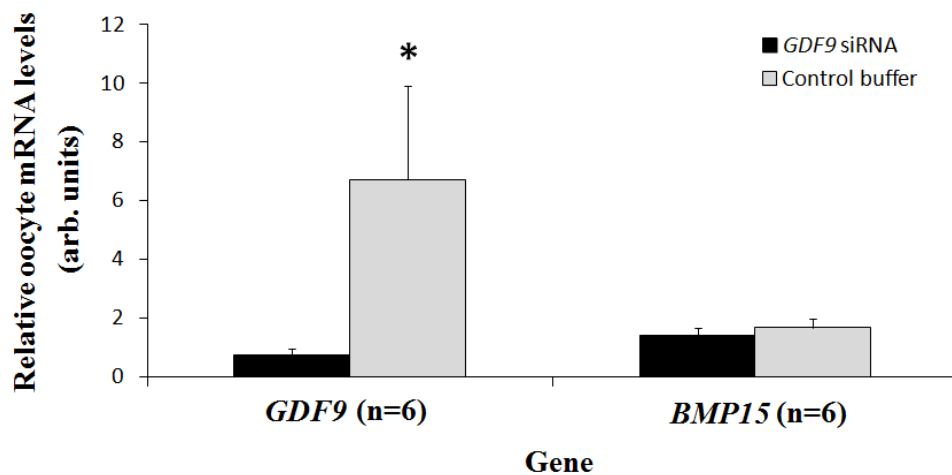
Figure 4.14: Real time quantification of the effect of *GDF9* knockdown by siRNA injection on oocyte *GDF9* and *BMP15* mRNA levels, compared to buffer-injected control oocytes. The data was standardised against the oocyte *GAPDH* and *H2A* mRNA levels. Individual bars show the mean ±SEM for 6 independent cDNA libraries (each library analysed in triplicate). Each cDNA library contained 1-2 oocytes. *GDF9* siRNA-injected oocytes exhibited a significant reduction of the *GDF9* mRNA levels (*=$P<0.05$) when compared against the buffer-injected control group which contained a similar number of oocytes/sample, while no statistical difference was detected between the 2 treatments for the *BMP15* mRNA levels ($P>0.05$).

Analysis of the mRNA expression levels in cumulus shells for the 2 treatments was conducted following confirmation of *GDF9* knockdown in the oocytes. Pools of 2 representative cumulus shells from separate IVM culture microdrops within each culture were used to generate cDNA libraries. Only cumulus shells originating from co-cultures

with IVM oocytes that progressed to the MII stage and were confirmed as having significant reduction in their *GDF9* transcript levels along with their respective controls were analysed. Out of the 6 sets of samples, 1 was discarded because the cDNA library failed to be generated, while another 3 libraries were discarded at different stages of analysis because of contamination. Cumulus levels of *GREMLIN1, HAS2, AMH, LDH1, AREG, EREG, BTC, EGFR, FSHR* and *LHR* were analysed (Figure 4.15).
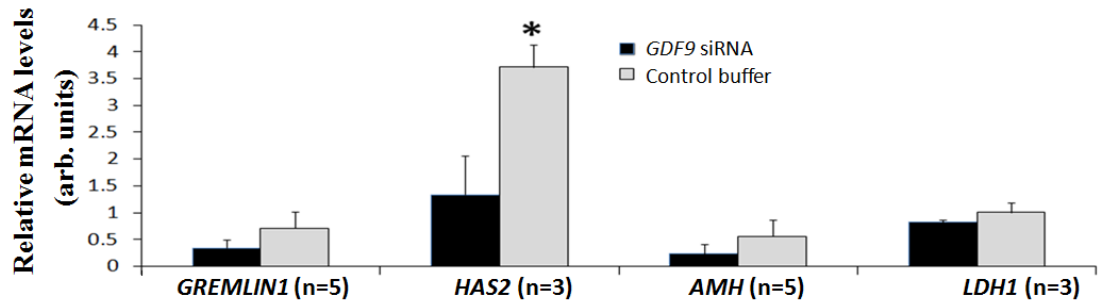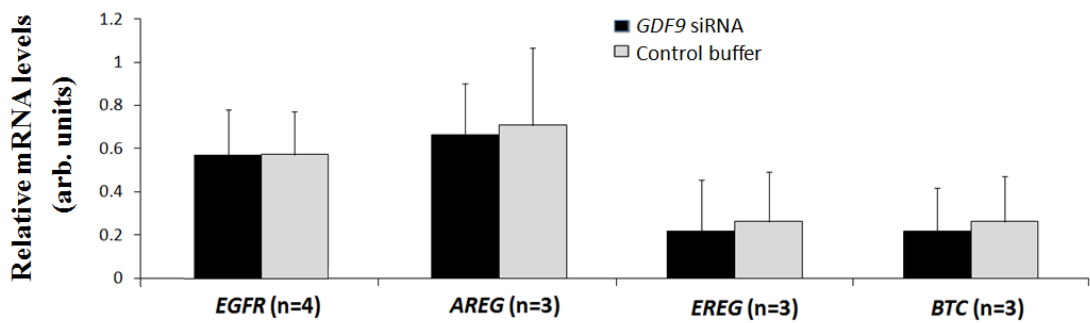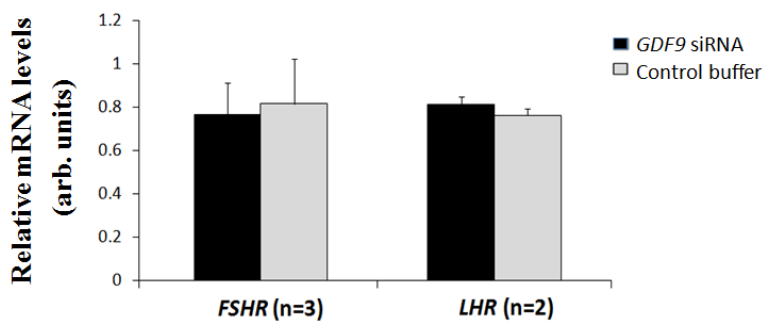
Figure 4.15: Effect of *GDF9* knockdown on cumulus cell's mRNA levels of **(a):** Somatic marker and oocyte quality including genes *GREMLIN1, HAS2, AMH* and *LDH1*. **(b):** Regulin genes *AREG, EREG, BTC* and *EGFR*. **(c):** Cumulus cell receptors *FSHR* and *LHR*. Data for all 3 graphs were normalised against the cumulus *GAPDH* and *H2A* mRNA levels. Individual bars show the mean ±SEM for the number (n) of repeat cDNA libraries (each library analysed in triplicate). Each cDNA library contained pools of 2 cumulus shells. Expression levels of *HAS2* in cumulus shells co-cultured with *GTSF1* knockdown oocytes showed significant differences (*=P<0.05) when compared against cumulus cells co-cultured with buffer-injected controls.

Levels of *HAS2* were significantly reduced (P<0.05) following *GDF9* knockdown (1.3±0.7 arb. units, n=3) compared to cumulus shells co-cultured with buffer-injected control oocytes (3.7±0.4 arb. units, n=3). Although, cumulus *GREMLIN1* expression was also reduced to (0.3±0.2 arb. units, n=5) following *GDF9* knockdown compared to controls (0.7±0.3 arb. units, n=5), no statistical differences were noted (P>0.05). Interrogation of cumulus *LDH1* mRNA levels indicated a reduction between the 2 groups from 0.8±0.05 arb. units (n=3) following the knockdown to 1±0.2 arb. units (n=3) in the controls which was not significant (P>0.05), while cumulus levels of *AMH* were reduced to (0.2±0.1 arb. units, n=5) following *GDF9* knockdown compared to controls (0.6±0.3 arb. units, n=5), but were also not significantly different (P>0.05) (Figure 4.15.a). Cumulus transcript levels of *AREG, EREG* and *BTC* were similar between cumulus shells co-cultured with *GDF9* siRNA-injected oocytes (0.5±0.4 arb. units, n=3; 0.7±0.3 arb. units, n=3; 0.2±0.3 arb. units, n=3) respectively, compared to cumulus shells co-cultured with buffer-injected control oocytes (0.7±0.6 arb. units, n=3; 0.7±0.3 arb. units, n=3; 0.3±0.4 arb. units, n=3) and were not statistically different (P>0.05) (Figure 4.15.b). In addition cumulus levels of *EGFR* were the same between the *GDF9* knockdown (0.6±0.4 arb. units, n=4) and the controls (0.6±0.4 arb. units, n=4). Finally, interrogation of a range of receptors on cumulus cells did not show any significant differences between cells co-cultured with the *GDF9* knockdown oocytes and buffer-injected control gametes, as no changes in the transcript levels were detected between groups (P>0.05). Cumulus *FSHR* and LHR transcript levels were 0.8±0.3 arb. units (n=3) and 0.8±0.1 arb. units (n=2), respectively, following oocyte *GDF9* knockdown in comparison with controls (0.8±0.4 arb. units, n=3; 0.8±0.1 arb. units, n=2) (Figure 4.15.c).

4.3.4 Experiment 4: Assessment of the effect of gonadotrophins on maturation and cumulus expansion of *GDF9* knockdown on ovine oocytes

The effect of gonadotrophin concentration on oocyte meiotic progression and cumulus expansion following *GDF9* knockdown was studied by reducing the concentrations of FSH and LH in the culture media during the IVM co-culture from preovulatory surge levels of day 2 (10 cultures, Experiment 3), to basal levels (8 repeat cultures, Experiment 4). In the first instance, oocyte survival, maturation and cumulus expansion were compared between the 2 oocyte treatment groups (*GDF9* knockdown and controls) following reduction of the gonadotrophin concentrations. Survival rates in the treatment and control groups were not significantly different (P>0.05) following culture with

basal levels of gonadotrophins. From the total of 236 *GDF9* siRNA-injected oocytes and 219 buffer-injected oocytes, 63 (26.7%) oocytes injected with *GDF9* siRNA survived the first 24 h of the culture, while 67 (30.6.%) oocytes survived the buffer injections. At 48 h, a total of 59 *GDF9* siRNA-injected oocytes (59/63, 93.7%) remained viable, while 62 buffer oocytes remained viable (62/67, 92.5%). The proportions of MII oocytes produced out of the viable oocytes from the first 24 h of culture following *GDF9* siRNA knockdown were 12.7% (8/63 oocytes) which was not statistically different (P>0.05) to the proportion of 11.9% for the buffer-injected control oocytes (8/67 oocytes). In the absense of the high levels of gonadotrophins, the cumulus shells from neither of the oocyte treatment groups (*GDF9* knockdown or controls) were able to expand fully after 24 h of co-culture (Figure 4.16). In addition, although there were fewer cumulus shells partially-expanded following *GDF9* siRNA, no significant differences (P>0.05) were noted in comparison with the controls suggesting that the gonadotrophins are the main drivers of cumulus expansion.
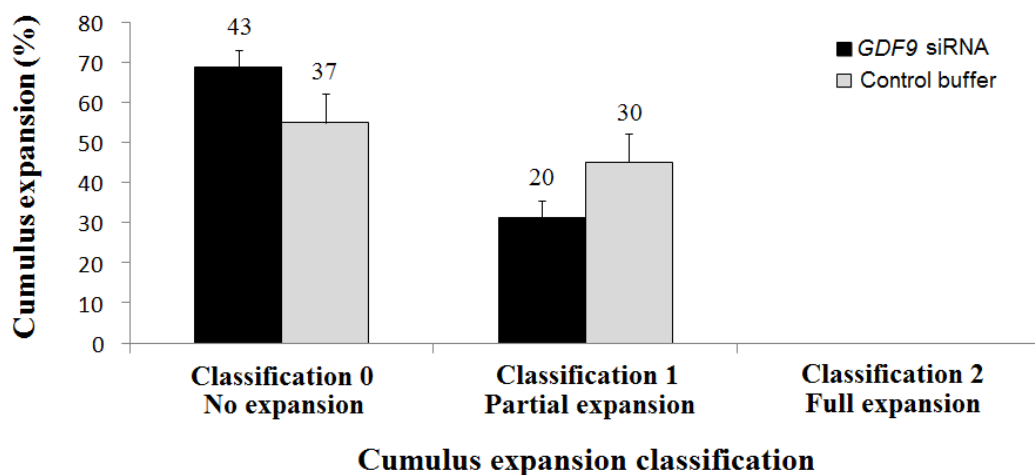
Figure 4.16: Cumulus expansion following 24 h of co-culture with *GDF9* gene knockdown oocytes compared to buffer-injected control oocytes in a basal gonadotrophin culture system. Values represent proportions of the total numbers of cumulus shell expansion classifications over 8 repeat cultures. Individual bars show the mean ±SEM for 10 independent cultures. The numbers of cumulus shells falling into each category are shown. No statistical differences were noted between the 2 treatments.

The effects of surge level gonadotrophins vs. basal level gonadotrophins were then compared for the 2 treatment groups. The proportions of oocyte survival in the culture system with basal levels of gonadotrophins were similar to the proportions when preovulatory surge levels of gonadotrophins were used and no significant differences (P>0.05) were noted between the 2 different culture systems (Table 4.7). These data indicate that for both gonadotrophin cultures, the denudation, micromanipulation and

culture with 20 mg/ml of cilostamide compromise oocyte viability, rather than the use of siRNA or the extended culture in serum-free medium. Comparison between the preovulatory surge gonadotrophin IVM system and the basal level gonadotrophin system showed significant differences in the proportions of oocytes progressing to MII from viable oocytes at 24 h following control buffer injection (P<0.05). No differences (P>0.05) were observed for the MII progression proportions of viable oocytes at 24 h following injection with *GDF9* siRNA, in the 2 different gonadotrophin levels (Table 4.7). Analysis of cumulus expansion for the 2 gonadotrophin levels, confrirmed that the high levels of FSH and LH are significanly important to support full cumulus expansion *in vitro* following *GDF9* injections (P<0.01) and buffer control injections (P<0.005), as shown in Table 4.7. These results indicate that the concentration of gonadotrophins affects cumulus expansion and oocyte meiotic progression with *GDF9* being important only when surge gonadotrophin concentrations are used.

Table 4.7: Comparison of the effect of cumulus co-culture basal or surge gonadotrophin supplementation following oocyte *GDF9* knockdown

Treatment	Basal gonadotrophin levels	Surge gonadotrophin levels	Significance
Oocyte survival at 24 h			
GDF9 siRNA	63/236 (26.7%)	61/302 (20.7%)	NS
Control buffer	67/219 (30.6%)	73/301 (25.4%)	NS
Oocyte survival at 48 h (based on viable oocytes at 24 h)			
GDF9 siRNA	59/63 (93.7%)	60/61 (98.4%)	NS
Control buffer	62/67 (92.5%)	62/73 (85.0%)	NS
Oocyte maturation of viable oocytes			
GDF9 siRNA	8/63 (12.7%)	8/61 (13.1%)	NS
Control buffer	8/67 (11.9%)	19/73 (26.0%)	P<0.05
Cumulus expansion			
Classification 0			
GDF9 siRNA	43/63 (68.3%)	23/61 (37.7%)	P<0.05
Control buffer	37/67 (55.2%)	19/73 (26.0%)	P<0.05
Classification 1			
GDF9 siRNA	20/63 (31.7%)	30/61 (49.2%)	NS
Control buffer	30/67 (44.8%)	30/73 (41.1%)	NS
Classification 2			
GDF9 siRNA	0/63 (0.0%)	8/61 (13.1%)	P<0.01
Control buffer	0/67 (0.0%)	24/73 (32.9%)	P<0.005

4.4 DISCUSSION

The results showed that it was possible to create a targeted and functional knockdown of *GDF9* in sheep oocytes over 24 h without compromising the potential for oocyte meiotic progression during IVM co-cultures with oocytectomised cumulus shells,

following removal of a specific PDE inhibitor. Gene knockdown by siRNA was specific to *GDF9*. Furthermore, the data from Experiment 3 showed a significant functional effect of oocyte *GDF9* knockdown on the capacity of oocytes to complete meiosis as indicated by: (i) the significant decrease in MII progression of gene knockdown oocytes ($P<0.05$) and (ii) the significant reduction in full expansion of cumulus cells following the co-cultures of somatic cells with *GDF9* depleted oocytes when compared to controls ($P<0.01$). In addition, the knockdown of oocyte *GDF9* resulted in a significant decrease in the expression levels of *HAS2* in the cumulus cells compared to controls ($P<0.05$). The results showed that ovine oocyte meiotic progression was significantly reduced when siRNA targeted against the first and second exons of ovine *GDF9* gene were injected into the oocytes in comparison to the buffer-injected control gametes.

These results provide proof of principle of the efficiency of the micromanipulation and IVM co-culture system for studying the function of novel oocyte-derived genes by the means of siRNA. Oocytes were able to survive through the 48 h culture and mature both meiotically and cytoplasmically as shown by MII progression and the ability of the oocytes to re-establish cell to cell communication after gene knockdown *in vitro*, through paracrine secretions. This study has confirmed extended previous observations of the potential of dsRNAi as a means of knocking down *GDF9* and studying its function in the mouse (Gui and Joyce, 2005) and sheep (Cotterill, 2008). Similarly, the study has confirmed that the oocyte maturation and cumulus expansion observed were induced by preovulatory levels of LH and FSH exposure, rather than a spontaneous maturation and expansion as a result of *in vitro* conditions such as denudation and oocytectomy.

4.4.1 The impact of *GDF9* knockdown on oocyte meiotic progression and cumulus cell expansion *in vitro*

One of the genes vital to the production of a fertile oocyte is *Gdf9*, as this oocyte-specific factor orchestrates cumulus expansion during oocyte meiotic maturation (Buccione *et al.*, 1990b). Other factors include Bmp15 (Su *et al.*, 2004; Gui and Joyce, 2005), LH (Elvin *et al.*, 1999), Egf (Diaz *et al.*, 2006), and the LH-induced Egf ligands Areg, Ereg and Btc (Park *et al.*, 2004; Hsieh *et al.*, 2007). From the above factors, the role of *Gdf9* has been extensively detailed in the introductory Chapter 1. So far, the majority of research has been conducted in rodents and not much is known about the function of specific oocyte-secreted factors such as *GDF9* in monovular species

including the cow and the sheep. An original approach for the study of oocyte secreted genes in monovular species has been recently applied by *GDF9* and *BMP15* targeted knockdown approach in sheep oocytes that resulted in a functional effect in both gene knockdowns (Cotterill, 2008). Specifically, injection of dsRNA for *GDF9* and *BMP15* resulted in targeted gene knockdown associated with reduced oocyte maturation and cumulus expansion for both genes in comparison with controls. Knockdown of *GDF9* was also shown to directly regulate gene function within the COC microenvironment by moderation of *HAS2* expression following *GDF9* and *BMP15* knockdown and by regulation of *GREMLIN1* following *GDF9* knockdown (Cotterill, 2008). Similarly, in this thesis there was an effect of *GDF9* on oocyte maturation, cumulus expansion and on *HAS2* expression levels, following oocyte *GDF9* knockdown by siRNA.

Understanding the effects of gonadotrophin stimulation on intracellular communications is very important in order to understand the mechanisms that regulate oocyte maturation. After the LH surge, soluble factors activate meiosis-inducing signalling molecules in the cumulus cells that are transmitted to the oocytes through gap junctions (Su *et al.*, 2009). For example, evidence from mouse cumulus cells indicate that LH promotes Areg-induced progesterone induction in granulosa cells through Neuregulin1 (Noma *et al.*, 2010). In sheep granulosa and cumulus cells, recent evidence suggests that surge levels of LH rapidly induce a peak in *AREG* expression *in vitro* relative to the other regulin genes, suggesting that *AREG* is key to sheep IVM (Cotterill *et al.*, 2012). The promotion of maturation may involve modulation of PDE3A activity (Sasseville *et al.*, 2009). Indeed, relatively higher levels of *AREG* were detected in cumulus cells in the present study compared to *EREG* and *BTC* and although no direct effects of *GDF9* knockdown on *AREG* were recorded here, *GDF9* has been suggested to act through differential gradients in bovine follicles (Hussein *et al.*, 2005). Other studies suggest that the cumulus expansion is a result of the cumulative action of oocyte-secreted factors (Dragovic *et al.*, 2005; Su *et al.*, 2010). In fact, studies in cows have shown that *BMP15* has an important role as an oocyte survival factor and mutant mice for *Bmp15* have been shown to have reduced cumulus expansion and *Has2* synthesis (Su *et al.*, 2004; Hussein *et al.*, 2005). Other murine studies have shown that together *Gdf9* and *Bmp15* can promote expression of the *Egfr* thus allowing cumulus cells to respond to the LH-induced Egf-like factors Areg, Ereg and Btc (Su *et al.*, 2010). Other studies investigating the functional significance of both *GDF9* and *BMP15* in sheep have shown that mutations of these genes as well as the ALK6 receptor for *BMP15* can

change the ovulation quota (Wilson *et al.*, 2001; Hanrahan *et al.*, 2004). Mutations have also been found in humans for both genes that have been associated with premature ovarian failure (Laissue *et al.*, 2006). However, species specific differences have been identified for the actions of *BMP15* in driving ovulation rate. Specifically, although mutations in the *BMP15* gene in sheep results in an increased ovulation rate, knockout mice for *Bmp15* have reduced fertility (Galloway *et al.*, 2000; Yan *et al.*, 2001). These differences could be species specific or they could be due to the different and/or synergistic roles that *GDF9* and *BMP15* have in the sheep (Moore *et al.*, 2003). In fact an even higher ovulation rate is observed in heterozygous sheep for both *GDF9* and *BMP15* than in heterozygous sheep for only 1 of the 2 genes (Galloway *et al.*, 2000; Hanrahan *et al.*, 2004). From the above studies it can be suggested that *BMP15* may have a role in cumulus expansion or that the nature of action of oocyte-derived factors may be species specific. Furthermore in relation to this thesis, the cumulative actions of *GDF9* and *BMP15* could explain why although there was a significant decrease in cumulus expansion following *GDF9* knockdown by siRNA injection, some cumulus shells retained the capacity to undergo full expansion in the presence of surge levels of LH and FSH and/or that the high gonadotrophin levels are overriding some changes in paracrine regulation effects by *GDF9* knockdown. Alternatively, *GDF9* acts in concert with other LH-driven signalling molecules such as AREG in stimulating cumulus expansion.

4.4.2 The impact of *GDF9* on gene expression

Although the selection of the most suitable siRNA species for generating the *GDF9* knockdown was based on results from 1 oocyte, the analysis of the oocytes that were retained at the GV stage following injections with the different *GTSF1* siRNAs and control buffer injections verified the efficiency of the siRNA-2 and siRNA-3 in generating a *GDF9* knockdown. The targeted functional knockdown of *GDF9* by the selected mixture of siRNA injection in the present studies was verified by molecular evaluation with real-time PCR that showed a significant reduction ($P<0.05$) in the oocyte expression levels of *GDF9* (0.72 ± 0.2 arb. units, n=6) following *GDF9* siRNA injection in comparison with buffer-injected control oocytes (6.7 ± 3.17 arb. units, n=6) producing a high level knockdown for all oocytes analysed. The specificity of the knockdown for the target gene was then confirmed by assessing the transcript levels of another oocyte-secreted member of the TGFB super family namely-*BMP15*, which was not significantly different ($P>0.05$) relative to controls. This observation replicates the

work of Gui and Joyce, (2005) in mice as well as Cotterill, (2008) in sheep using dsRNA species.

Following evaluation of the *GDF9* and *BMP15* transcript levels, the effect of the knockdown was assessed by examination of transcript levels of cumulus cell markers. Mouse knockout studies have identified certain genes as potential targets of *Gdf9*. One of such genes is the *Has2* gene encoding the Has2 enzyme which is responsible for conversion of UDP-N-acetyl glucosamine to hyaluronic acid (HA). This enzyme holds together cumulus cells after expansion and mucification (Scott *et al.*, 1991). Knockdown of *Has2* in cumulus cells through adenovirus transfections was shown to reduce cumulus expansion (Sugiura *et al.*, 2009). In addition, reduction of the levels of *Has2*, resulted in a reduction of *Areg* and *Ereg* mRNA (Sugiura *et al.*, 2009). Lower levels of *HAS2* in human cumulus cells are associated with poor embryo quality (Cillo *et al.*, 2007). In this thesis the results showed that *GDF9* knockdown by siRNA injection in oocytes resulted in a significant reduction ($P<0.05$) of *HAS2* mRNA expression in the cumulus cells in comparison with the controls which was marked by the reduced levels of cumulus expansion in the same cells. Similar findings were noted when the same system was used to inject dsRNA in order to induce a *GDF9* knockdown (Cotterill, 2008). Previous studies in the mouse have also produced similar results (Elvin *et al.*, 1999; Dragovic *et al.*, 2005). In fact, genes involved in cumulus expansion including *Has2* are thought to be stimulated by gonadotrophins and/or oocyte-derived factors (Dragovic *et al.*, 2005; Dragovic *et al.*, 2007).

Another cumulus specific gene shown to moderate cross talk between Gdf9 and Bmp15 via a regulatory loop is *Gremlin1* (Pangas *et al.*, 2004). Studies in mice have shown that this gene is up-regulated through paracrine actions from the oocyte and *Gdf9* (Pangas *et al.*, 2004). Gremlin is also considered an antagonist of BMP signalling (Canalis *et al.*, 2003) and is involved in the intra-follicular BMP signalling pathways as part of the negative feedback of thecal androgen production (Glister *et al.*, 2005). In particular up-regulation of *GREMLIN1* induced by GDF9 antagonises BMP15 for receptor binding and promotes bovine oocyte-induced cumulus expansion (Hussein *et al.*, 2005). This is because of the different receptors that GDF9 and BMP15 bind to, with GDF9 binding to both ALK5 and BMPRII receptors, while BMP15 recruits ALK6 and BMPRII (Vitt *et al.*, 2002; Moore *et al.*, 2003; Mazerbourg *et al.*, 2004). The different receptor binding results in alternate-intracellular responses for GDF9, which signals through the SMAD

2/3 intracellular pathway, while BMP15 signals through SMAD 1/5/8. As an outcome, up-regulation of *Gremlin1* antagonises BMP signalling induced from mural and theca cells, thereby allowing oocyte-derived factors like *GDF9* to promote cumulus cell expansion and prevent apoptosis (Hussein *et al.*, 2005*)*. Because of this involvement in the COC regulatory loop, *Gremlin* has been identified as a marker for oocyte quality along with *Has2* and *Ptx3 (Mckenzie et al., 2004)*. The role played by *Gremlin* in relation to oocyte quality is not very clear. In this study there was a trend for reduction of *GREMLIN1* mRNA levels following *GDF9* knockdown (0.3±0.2 arb. units, n=5) compared to controls (0.7±0.3 arb. units, n=5), however due to the low number os samples and variability of the data, no statistical differences were noted (P>0.05). Injections of dsRNA for *GDF9* in sheep oocytes have previously shown that cumulus *GREMLIN1* expression was significantly reduced relative to controls (Cotterill, 2008). The reduction in the transcript level of *GREMLIN1* mRNA following *GDF9* knockdown in comparison with controls observed in this thesis might prove to be significant with further experimentation.

The expression of *AMH* was compared in cumulus cells following *GDF9* knockdown in ovine oocytes. This gene is considered to have important roles in folliculogenesis. At the primordial follicle stage, *Amh* was shown to inhibit primordial follicle recruitment in the mouse (Durlinger *et al.*, 2002a). At the preantral stage, *Amh* has been shown to inhibit follicle recruitment of growing follicles to the preovulatory stage (Salmon *et al.*, 2004). In addition, *Amh* expression by follicular granulosa and cumulus cells is also considered to be regulated by paracrine factors from the oocyte because of the close proximity of *Amh* expression with other factors regulated by the oocyte such as *Lhr*, *Kl* and *Ptgs* (Salmon *et al.*, 2004). In this study, a reduction of *AMH* transcript levels was observed when *GDF9* was knocked down (0.2±0.1 arb. units, n=5) compared to controls (0.6±0.3 arb. units, n=5), but due to the low number of samples analysed and the variability of the data, this difference was not significant (P>0.05). Similar data were observed following injection of dsRNA in sheep oocytes (Cotterill, 2008), while *Amh* levels have been significantly reduced following *Gdf9* knockdown at the preantral stage of follicle development in mice (L Gui and HM Picton, unpublished data). Extension of the number of culture replicates in the present experimental series is required to confirm the significance of this observation. Furthermore, the relatively low levels of *AMH* and *GREMLIN1* mRNA transcripts in cumulus cells compared to the

high levels of *HAS2* mRNA expressions in cumulus cells may be linked to the significantly lowered levels of *HAS2* expression observed following *GDF9* knockdown.

The effect of oocyte *GDF9* knockdown on the expression of *LDH1* in the cumulus cells was evaluated. This gene encodes a product of glycolysis and it is expressed by the cumulus cells (Sugiura *et al.*, 2007). Glycolysis in cumulus cells is regulated by paracrine factors by the oocyte (Sugiura *et al.*, 2005). Cumulus cells express higher levels of mRNA encoding glycolytic enzymes such as platelet phosphofructokinase (*Pfkp*) and *Ldhα* and when oocytes are removed from COCs the levels of these transcripts are reduced with the effect being reversed following co-culture with cumulus cells (Sugiura *et al.*, 2005). The levels of *LDH1* gene transcript were therefore investigated in this study to indicate whether *GDF9* affects the metabolic pathways of the oocyte. No significant differences (P>0.05) were noted for the transcript in cumulus cells following oocyte *GDF9* knockdown (0.8±0.05 arb. units, n=3) compared to controls (1±0.2 arb. units, n=3). Similar findings were demonstrated following dsRNA injection and *GDF9* knockdown in sheep oocytes (Cotterill 2008). This observation agrees with a previous study conducted in the mice which showed that the paracrine factors that regulate glycolysis are Bmp15 along with Fgf8 (Sugiura *et al.*, 2007).

The expression of the 3 key members of the EGF family, *AREG*, *EREG* and *BTC* along with the *EGFR* were compared in cumulus cells following *GDF9* knockdown in oocytes. The regulin genes are induced by LH in mural granulosa cells and bind to the Egfr and have been shown to induce COC maturation (Park *et al.*, 2004; Hsieh *et al.*, 2007). These ligands are necessary for IVM as shown by their ability to induce oocyte maturation in COC cultures but not in cultures of denuded oocytes (Park *et al.*, 2004). In addition, mutant mice for *Egfr* and *Areg* as well as double mutant animals are unable to promote COC maturation, further demonstrating that the Egfr network is vital in COC maturation *in vivo (Hsieh et al., 2007).* Knockout of *Egfr* was shown to reduce the expression of *Gdf9* and *Bmp15* in murine cumulus cells (Su *et al.*, 2010) and removal of oocytes from COCs resulted in the reduction of cumulus *Egfr* with the levels restored after treatment with recombinant *Gdf9* or mixture of recombinant *Gdf9* and *Bmp15* (Su *et al.*, 2010). Recent work by Cotterill *et al.*, 2012 has demonstrated the presence of *AREG*, *EREG* and *BTC* in ovine mural and granulosa cells. In particular, *AREG* appeared to be most important for LH signalling events in sheep cumulus and mural granulosa cells but not in oocytes (Cotterill *et al.*, 2012). Analysis of transcript levels of

the EGF family members *AREG, EREG* and *BTC* in the present study did not indicate any significant differences (P>0.05) in cumulus cell expression following *GDF9* gene knockdown in oocytes after 24 h of IVM culture (0.5±0.4 arb. units, n=3; 0.7±0.3 arb. units, n=3; 0.2±0.3 arb. units, n=3) compared to cumulus shells co-cultured with buffer-injected control oocytes (0.7±0.6 arb. units, n=3; 0.7±0.3 arb. units, n=3; 0.3±0.4 arb. units, n=3) respectively. None-the-less, the results were quite variable and thus the experiment needs repetition. An alternative explanation for the observations in this experimental series is that induction of *AREG* expression occurs very rapidly and peaks after LH exposure (Cotterill *et al.*, 2012). Therefore, the levels of *AREG* could have been dropped back down again during the 24 h exposure window of IVM in the present study. Investigation of the expression levels of the *EGFR* following the knockdown did not demonstrate a significant difference (P>0.05) between treatment groups. This receptor is the EGF-like ligand considered to facilitate communication with the secreted members of the EGF family through cumulus cells, resulting in a target cell response through the MAPK signalling cascade (Conti *et al.*, 2006). In fact, the MAPK pathway has an established role in cumulus expansion and oocyte maturation (Panigone *et al.*, 2008). The kinases that act in this pathway are the Mapk1/3 and Erk1/2 and their phosphorylation has been shown to be sustained by the actions of Egfr in rat preovulatory follicles. Studies have shown that inhibition of EGFR results in reduced cumulus expansion and oocyte maturation in rats and primates (Nyholt De Prada *et al.*, 2009; Reizel *et al.*, 2010). In sheep, the MAPK pathway is active in COCs during oocyte maturation and cumulus expansion (Cecconi *et al.*, 2008). In addition, *EGFR* expression in sheep was detected in cumulus cells before and after gonadotrophin exposure *in vitro,* but *EGFR* expression did not reach to the same extent as *AREG* after LH surge in IVM, suggesting species specific differences and that *AREG* is the most important regulin and LH driven signalling molecule during the maturation of sheep oocytes *in vivo* and *in vitro* (Cotterill *et al.*, 2012).

Transcript levels of *LHR* and *FSHR* were also investigated in the cumulus cells to evaluate the physiological responses to gonadotrophins in the cumulus cells. Both gonadotrophin receptors need to be expressed in the somatic cells of the follicle for the gonadotrophins to be effective at stimulating growth, steroidogenesis and ovulation (Tisdall *et al.*, 1995; Logan *et al.*, 2002). The transcript levels of the *FSHR* and *LHR* were not statistically different (P>0.05) in cumulus cells after oocyte *GDF9* knockdown (0.8±0.3 arb. units, n=3 and 0.8±0.1 arb. units, n=2) respectively relative to controls

(0.8±0.4 arb. units, n=3 for *FSHR* and 0.8±0.1 arb. units, n=2 for *LHR*), suggesting that oocyte-derived *GDF9* plays no role in the regulation of cumulus cell *FSHR* and *LHR* levels. However, due to the low number of samples, this experiment requires further replication.

4.4.3 The effect of gonadotrophins on maturation and cumulus expansion of *GDF9* knockdown on ovine oocytes

The importance of gonadotrophins in the development of a physiological relevant IVM system was further enhanced by the results in this study following reduction of the surge level of gonadotrophins in the IVM system to a much lower concentration. The cultures conducted with lower concentrations of gonadotrophins significantly reduced oocyte maturation rates (P<0.05) in the buffer injection group in comparison with the IVM cultures conducted with surge levels of gonadotrophins. The reduction of the gonadotrophin levels also resulted in reduced expansion of the cumulus cells in comparison with the IVM system containing surge levels of gonadotrophins, with no cumulus reaching full expansion in either of the 2 injection groups. Although there were fewer partially expanded cumulus shells, in the *GDF9* siRNA-injected group compared to the controls, no significant differences were noted (P>0.05). The IVM system used in this study is a gonadotrophin driven maturation system for sheep COCs and it has been shown that gonadotrophin exposure during IVM improved oocyte quality and blastocyst potential (Cotterill *et al*., 2012). Previous studies have also revealed the effects of gonadotrophin stimulation on the developmental capacity of oocytes matured *in vitro*. In the bovine species, inclusion of surge levels of both gonadotrophins in the culture media resulted in significantly more cumulus expansion and oocyte maturation compared with treatments containing either of the 2 gonadotrophins individually (Pandey *et al.*, 2010). Similarly, in sheep, culture of COCs in serum-free IVM media without gonadotrophins has been shown to result in impaired cumulus expansion (Cecconi *et al.*, 2008). The addition of gonadotrophins *in vitro* has been shown to increase oocyte progression to MII (Galli and Moor, 1991). Studies in humans have shown that nuclear maturation of the oocytes is possible in *vitro* and the concentration of gonadotrophins and the sequence of the FSH and FSH-LH exposure may impact on oocyte meiotic progression (Trounson *et al.*, 2001). Finally, the gonadotrophins together with oocytes and oocyte-derived factors stimulate some important genes that are prerequisite for cumulus expansion (Dragovic *et al.*, 2005; Dragovic *et al.*, 2007). Addition of FSH to the media is known to affect oocyte maturation and this is mediated

through the cumulus cells as shown by studies where removal of the cumulus cells does not result in developmental progression (Gilchrist *et al.*, 2008). In fact, the preovulatory levels of gonadotrophins induce the secretion of hyaluronic acid from the cumulus cells that results in their expansion and mucification (Schoenfelder and Einspanier, 2003). Together FSH and EGF signalling contribute to mouse oocyte maturation through the exchange of factors necessary for oocyte and early embryo development (Yeo *et al.*, 2009). The *EGFR* and LH driven *AREG* in sheep have also been shown to contribute to oocyte maturation (Cotterill *et al.*, 2012). All the above published studies are therefore in agreement with the observations in the present study that gonadotrophins are the main regulators of cumulus expansion and that they override the effects of oocyte-derived cumulus expansion factors like *GDF9*.

The molecular basis of oocyte signalling is still being elucidated in an attempt to find to mechanisms that control oocyte growth and maturation. Recent studies have highlighted the potential association of oocyte-secreted factors with miRNAs. As stated in Chapter 1, Section 1.5.1, small RNAs have important regulatory roles in many different cellular processes including cell proliferation, differentiation and apoptosis and may play important roles during development as shown by their tissue specific expression pattern and evolutionary conservation (Lewis *et al.*, 2003). Dicer, an RNase III-containing enzyme, is considered the critical enzyme in small RNA-regulated cell development, required to process miRNA precursors or dsRNA into RNAi molecules for miRNA and siRNA pathways respectively (Carmell and Hannon, 2004; Jin and Xie, 2007). In a recent study, conditional knockout of *Dicer1* in mouse ovarian tissue resulted in significant differences in the expression of follicle development-related genes including *Gdf9*, *Bmp15*, *Amh*, *Inhba* and *Cyp17α1* (Lei *et al.*, 2010). A similar phenotype to the *Dicer1* knockouts including poor oocyte maturation associated with abnormal spindles and chromosomes that did not cluster properly was reported following *Ago2* deletion in growing mouse follicles (Kaneda *et al.*, 2009). The Argonaute family proteins including Ago2 are responsible for binding miRNA to mRNA within RISC that leads to repression of the target gene expression by either reducing the length of the poly-(A) tail of mRNA or by inhibiting translation (O'carroll *et al.*, 2007). The above studies illustrate that the genes involved in RNAi can affect oocyte development through global regulation of miRNA stability that affects gene expression in developing oocytes. The association of the *GDF9* gene with pathways such as the RNAi pathway through investigation of potential oocyte candidate genes following the gene specific

knockdown for *GDF9* requires further investigation. Unfortunately, the oocyte cDNA libraries generated in this study for both treatment groups degenerated within a short time of creation and did not allow further investigation of genes and pathways associated with the knockdown. This is because each library was generated using reverse transcription of isolated mRNA from 1-2 oocytes. Thus there was a limited amount of nucleic acid in each oocyte library making the samples susceptible to degradation. A reduction of the target nucleic acid was also noted for the cumulus shell samples and this was proportional to the time taken for analysis by real-time PCR, however the relatively large number of cells contained in each sample allowed the completion of analysis for all cumulus cell markers. In future experiments, it will be important to use methods that better preserve oocyte cDNA within each sample, such as the generation of double-stranded DNA that is more robust than single stranded DNA.

4.4.4 Optimisation of microinjection and IVM system

A major limitation of the siRNA approach used in the present study was the low survival rates of the microinjected, denuded, oocytes. The survival of oocytes was 20.7% and 25.4% after the first 24 h of culture for the *GDF9* siRNA and buffer-injected oocytes respectively. While these results indicate that introduction of siRNAs *per se* into the oocyte did not compromise survival, further damage to the oolemma induced by microinjection was a significant cause of oocyte loss. Microinjection of both control buffer or siRNAs resulted in expansion of oocyte volume with resultant membrane damage even though the constant flow injection system was operated on the lowest possible flow rate of 40 hPa. In addition, the majority of oocytes were lost within the first 24 h of culture following cumulus removal. The process of denudation itself therefore appears to have a major and negative impact on oocyte survival. Furthermore, mechanical stresses like the injection procedures are known to induce apoptosis in the oocyte (Paradis *et al.*, 2005). The poor survival rates might be due to the osmotic stress inflicted to the oocyte and oocyte cell membrane.

Another possible explanation for the low survival rates observed was the use of cilostamide to delay meiotic progression. For the culture system used in the present studies, inhibition of the meiotic progress during the first 24 h of culture is necessary to enable the knockdown of the target gene to occur before oocyte maturation progresses. Cilostamide, prevents binding of the phosphodiesterases to both cAMP and cGMP and stops hydrolysation of the 3´ phosphoester bond (Conti, 2000). In the bovine species it

has been shown that the higher levels of cAMP produced by the action of the PDE3 inhibitor are able to maintain meiotic arrest in the oocytes (Mayes and Sirard, 2002). Previous dose response experiments have shown that culture with cilostamide at a concentration of 20 mg/ml resulted in GV retention of 38.2% of denuded oocytes with 49% of ovine oocytes not surviving the process of denudation and subsequent culture (Cotterill, 2008). This concentration of cilostamide retained a higher percentage of oocytes at the GV stage when compared to the other cilostamide doses tested as well as a range of different concentrations of milrinone, another meiotic inhibitor (Cotterill, 2008).

Other components of the microinjection system which may affect experimental outcomes are temperature and pH. The temperature for the current cultures was set at 39°C as this is the sheep body temperature and has previously been used in the validation of RNAi and IVM for sheep oocytes (Cotterill *et al.*, 2012). All oocytes were overlaid with oil in order to minimise temperature and pH fluctuations but even so, temperature variations are possible because of the time necessary to handle the oocytes and monitor their developmental progress. The meiotic spindle is highly temperature sensitive (Inoue, 1981). Cooling of sheep oocytes at selected stages during maturation has also been shown to affect their nuclear morphology, their ability to synthesize protein as well as their *in vivo* developmental potential (Moor and Crosby, 1985). For this reason, incubator temperature was checked on a daily basis. Also incubator doors were not opened for long periods to sustain temperature of the cultures. All microscopes used were fitted with heated stages to minimise this problem.

The culture environment has a profound influence on the success of IVM systems. One of the most important parameters is the culture media. The composition of serum-free media is based on components of the follicular environment to which oocytes would be exposed during maturation *in vitro* (Picton, 2002). Importantly, this media supports high-levels of gonadotrophin-driven oocyte maturation and cumulus expansion whilst the cumulus cells remain sensitive to other culture additives, as the media has been carefully optimised to reflect the physiological needs of the somatic granulosa cells and oocytes across a range of species (Campbell *et al.*, 1996; Picton *et al.*, 1998; Cotterill *et al.*, 2012). Another important parameter for optimisation is the culture media volume and the number of oocytes and cumulus shells or embryos cultured per microdrop of media. Culture drop volume is considered very important for the IVM culture not only

for the autocrine and paracrine signalling between the oocytes but also for the re-establishment of cell-cell communication and signalling during the co-culture with the oocytectomised cumulus shells. Removal of the cumulus cells before IVM has been shown to be detrimental for oocyte maturation in many species such as mice, rats, cattle and pigs (Schroeder and Eppig, 1984; Vanderhyden and Armstrong, 1989; Chian *et al.*, 1994; Wongsrikeao *et al.*, 2005). In contrast, the co-culture of COCs or oocytes with cumulus cells has been shown to partially restore the developmental competence of denuded oocytes in cows and mice (Zhang *et al.*, 1995; Cecconi *et al.*, 1996; Hashimoto *et al.*, 1998). It is understood that cumulus cells play an important role in oocyte maturation in terms of regulating the meiotic progression and the support of cytoplasmic maturation (Tanghe *et al.*, 2002). Cumulus cells promote oocyte maturation by the alteration of timing of nuclear maturation and redistribution of cortical granules, disturbance of spindle assembly, redistribution of mitochondria and increased MPF activity as shown in a mouse study, with the excessive increase of MPF activity being relieved following co-culture with cumulus cells (Ge *et al.*, 2008). In the present study, the ratio of oocytes and cumulus shell number in each culture drop to medium volume was always kept the same to 2 μl per oocyte and 2 μl per cumulus shell or 4 μl per COC as previously optimised by Danfour, (2001).

4.4.5 Conclusions

In conclusion, these experiments have provided insight into the efficiency of siRNA and microinjection as vehicles to generate gene knockdowns in ovine oocytes and therefore to study the effect of novel genes in oocytes. The known oocyte-specific gene *GDF9* was used to test the validity of this approach as *GDF9* has a proven role in oocyte maturation and cumulus behaviour established in a number of species. The present experimental series using siRNA microinjection, IVM and cumulus co-culture demonstrated the importance of *GDF9* in oocyte meiotic progression by functional analysis of cumulus expansion as well as alteration of cumulus gene, *HAS2* expression. On this basis, siRNA microinjection, IVM and cumulus co-culture will be used to test the role of *GTSF1*, during ovine oocyte maturation.

Chapter 5: Functional evaluation of the role of *GTSF1* during the during the maturation of ovine oocytes *in vitro*

5.1 INTRODUCTION

The experimental results presented in Chapter 3 have shown that *GTSF1* is localised in the cytoplasm of ovine oocytes and that *GTSF1* is also expressed during spermatogenesis in the testis and during early preimplantation embryo development in this species. Furthermore, the gene and protein sequence appear to be being highly conserved across species. Although the importance of *Gtsf1* in spermatogenesis and male fertility have been established in rodents (Yoshimura *et al.*, 2009), the significance of this gene in acquisition of developmental competence of oocytes has not been established in monovular species such as the sheep. In polyovular mice, *Gtsf1* knockout animals grew normally and appeared healthy, but the males were sterile due to apoptotic death of their germ cells after postnatal day 14 while the null female mice were fertile (Yoshimura *et al.*, 2009). The null male meiocytes were shown to cease meiotic progression before the zygotene stage, thereby indicating the significance of this factor in meiotic progression beyond the early stages (Yoshimura *et al.*, 2009). Although the effects of *Gtsf1* knockdown did not result in infertility in female mice, it could be that the effects of the gene are more subtle in female mice. In particular, female *Gtsf1* knockout mice were fertile when examined over a period of 6 months and histological analyses did not show any abnormalities following the knockout in the ovaries. Mating of male *Gtsf1* knockout mice with normal female C57BL/6 mice resulted in fertilisation as confirmed by the formation of vaginal plugs, but no pups were born since the male mice were infertile (Yoshimura *et al.*, 2009). The lack of a major effect of *Gtsf1* knockout on oocyte growth and function is very surprising, considering the high degree of localisation of *Gtsf1* to the cytoplasm of primary follicles and to lesser extend to primordial follicles following ISH in mice, as represented by Krotz *et al.*, (2009). This is supported by expression analysis of *GTSF1* in human ovarian tissue by real-time PCR that shows expression at primordial, primary, secondary, GV, MII, zygotes and late stage preimplantation embryos (JD Huntriss and HM Picton, unpublished data). The results of this thesis as shown in Chapter 3 are in agreement with the human data. The specific expression of the gene along with its conserved domain containing 2 tandem copies of CHHC Zn-finger that may be responsible for RNA-binding (Andreeva and

Tidow, 2008), makes *GTSF1* as a very promising marker of oocyte quality in monovular species.

As stated in the introductory Section 1.4.2, of Chapter 1, RNA-binding is involved in several cellular processes including regulation of meiotic procedures, post-transcriptional and translational control of gene expression (Mootz *et al.*, 2004; Song *et al.*, 2007; Glisovic *et al.*, 2008). More interestingly, cellular localisation of GTSF1 in bovine round spermatids and mature sperm indicates that the GTSF1 protein functions during post-meiotic spermatogenesis in addition to its already established role during the early primary spermatocyte development (Lu *et al*., 2012). It is possible therefore that *GTSF1* is involved in RNA processing.

piRNA and its interacting proteins have been shown to be involved in retrotransposon silencing in order to preserve the germ cell genome (Kuramochi-Miyagawa *et al.*, 2004). In addition to this, the association of Piwi with a number of miRNAs and piRNAs in *D. melanogaster* suggests that the Piwi might act through the miRNA mechanism (Yin and Lin, 2007). The increased transcription of *Line1* and *Iap* retrotransposons and demethylations of their promoter regions following Gtsf1 knockout in mice, suggests therefore a possible implication of *Gtsf1* with the RNAi mechanism (Yoshimura *et al.*, 2009). It is apparent that if *GTSF1* is involved in RNA processing, this might involve germinal granules including the chromatoid bodies in the sperm and P-bodies in the oocyte that contain RNA and RNA-binding proteins with known roles in differentiation of germ cells and early embryo development including RNA-storage and processing (Kotaja *et al.*, 2006; Kotaja and Sassone-Corsi, 2007).

The experimental results of Chapter 4 have validated the efficiency of siRNA microinjection as a vehicle for gene knockdown in ovine oocytes. In addition, the data have demonstrated that oocyte siRNA microinjection in conjunction with IVM and co-culture with oocytectomised cumulus cells can be used to test the function of novel genes during ovine oocyte maturation. The cloning, sequencing and characterisation of ovine *GTSF1* in Chapter 3 has enabled us to design ovine *GTSF1* siRNA oligos and to use these with the microinjection and IVM system detailed in Chapter 4 to directly study the effects of *GTSF1* on ovine oocyte maturation *in vitro*.

5.1.1 Aims

The aims of this chapter were therefore to knockdown *GTSF1* in ovine GV oocytes and study the effects of the knockdown on functional parameter of oocyte maturation *in vitro* including:

1. Oocyte meiotic progression
2. Cumulus mucification and expansion
3. Analysis of candidate oocyte and cumulus genes which are markers of oocyte and cumulus maturation

This experimental series used the validated IVM microinjection system detailed in Chapter 4 to produce the targeted knockdown of *GTSF1*. The functional end-points measured were based on morphological evaluations of oocyte meiotic progression as well as gene expression analysis of *GTSF1* and other candidate genes by real-time PCR. Pilot studies of the effect of *GTSF1* knockdown on oocyte meiotic spindle formation were also conducted by immunofluorescent detection of α-Tubulin staining in whole oocyte mounts.

5.2 MATERIALS AND METHODS

This experimental series utilised the physiological serum-free IVM and microinjection system which had been previously developed for sheep oocytes by Cotterill *et al.*, 2012 as described in Chapter 4. Following the experimental assessment of the efficacy of gene knockdown using 4 different *GTSF1* siRNAs the experiment was conducted during the sheep breeding season between November 2010 and February 2011.

5.2.1 Assessment of gene knockdown using 4 different *GTSF1* siRNAs

Tissue was collected from the abattoir on 2 consecutive days every week. All the procedures media used were as detailed in Chapter 2. The validity of 4 different *GTSF1* siRNAs in creating a gene specific knockdown was evaluated using the methodology described in Chapter 4, Section 4.2.2. The oligos were synthesized by Invitrogen Ltd based on the full ovine sequence of *GTSF1* obtained in Chapter 3 (Table 3.4). The oligo sequences are shown in Table 5.1. The efficacy of these oligos in providing a *GTSF1* knockdown was assessed over a series of 4 replicate cultures each using 1 set of the 4 siRNA oligos. In each culture, oocytes were divided into 2 groups and injected either with 1 of the 4 *GTSF1* siRNA oligos or DPBS buffer. In brief, *GTSF1* siRNA was microinjected into denuded GV oocytes and groups of 10 oocytes were incubated in 20 μl of culture medium supplemented with basal gonadotrophin levels (FSH: 0.5 ng/ml,

LH: 0.1 ng/ml) containing 20 mg/ml cilostamide. After 24 h of culture, groups of 5 viable oocytes as observed by NR staining from each treatment were co-cultured with groups of 5 oocytectomised cumulus shells in 20 μl of IVM medium supplemented with the high levels of gonadotrophins (FSH: 100 ng/ml, LH: 100 ng/ml).

Table 5.1: *GTSF1* oligo sequences used to generate 4 species of *GTSF1* siRNAs

Primer	Sequence
GTSF1 siRNA-1	Sense : r(GGC UGA AAU CAG CCA UCA UTT)dTdT Antisense : r(AUG AUG GCU GAU UUC AGC CCG)dAdT
GTSF1 siRNA-2	Sense : r(CUC AAG CUG UGA UGA CAA ATT)dTdT Antisense : r(UUU GUC AUC ACA GCU UGA GAT)dAdT
GTSF1 siRNA-3	Sense : r(AUA UGU UCU CCC AUG GAA ATT)dTdT Antisense : r(UUU CCA UGG GAG AAC AUA UGG)dTdG
GTSF1 siRNA-4	Sense : r(ACU GAA UAU UUC AUC AAA UTT)dTdT Antisense : r(AUU UGA UGA AAU AUU CAG UTA)dAdG

At the end of the cultures, the oocytes that survived 48 h of culture and progressed to the MII stage from each culture microdrop were pooled into lysis buffer and snap-frozen. These pools were used for mRNA isolation and real-time PCR to determine the level of knockdown as described in Chapter 4, Section 4.2.2-4.2.2.1. The primer sequence of ovine *GTSF1* used for real-time PCR was obtained from the cloned ovine sequence (Chapter 3) and is shown in Table 5.2. The mRNA levels of ovine *GTSF1* were quantified relative to the expression of the housekeeper genes *GAPDH* and *H2A* (Chapter 2, Section 2.4).

Table 5.2: Primer sequence of ovine *GTSF1* used for real-time PCR

Gene	Primer Sequence	Size (bp)	Reference
GTSF1 ovine	F: 5´ CTC TGG ACC CTG AAA AGC TG 3´ R: 5´ GTT TGT TTG CGA CAT CAG GA 3´	120	Chapter 3, Table 3.5

5.2.2 Experimental assessment of the impact of *GTSF1* knockdown during maturation of ovine oocytes *in vitro*

Following the experimental assessment of the 4 different siRNA species in creating a *GTSF1* knockdown in GV oocytes, a total of 11 cultures were conducted using the siRNA that was most efficient in generating a *GTSF1* specific knockdown. The methodology followed was similar to the methodology described in Chapter 4, Section 4.2.3., with a few differences in the experimental procedure. One difference was the injection pipette outflow applied for the injection of the oocytes of the different groups.

The constant outflow of the injection pipette was set at 40 hPa for the injections of both the *GSF9* siRNA and control buffer during the validation experiments of Chapter 4. Although this method resulted in substantial levels of gene knockdown, it was hypothesised that the survival rates of oocytes could be improved by reducing the amount of siRNA or buffer injected into the oocytes. During the validation experiments of Chapter 4, the process of penetrating the oolemma and removing the injection pipette had to be extremely rapid in order to allow an equal amount of siRNA or buffer to be injected inside the cytoplasm of each oocyte and this could have inflicted damage to the oocytes reflected by the poor survival rates of the first 24 h of cultures for both treatments. In this experimental series therefore, the Femtojet microinjection system was used without a constant outflow. Instead, the oocytes were held with the holding pipette and after the injection pipette was inserted into the cytoplasm of the oocyte, the pressure of 40 hPa was applied using a start-stop button for approximately 0.5 sec. After stopping the outflow, the injection pipette was carefully removed from the oocyte avoiding further damage. The same process was applied to all oocytes from the different injection groups. All other experimental conditions were kept the same for day 2 and day 3 of the culture and all developmental assessments were recorded as described previously (Chapter 4, Section 4.2.2).

For the last 3 cultures of this experiment, an additional group was created and used for injections. In addition to *GTSF1* siRNA and control buffer-injected oocytes, a third group of oocytes were injected with non-coding, negative control siRNA (N.C. siRNA, Qiagen Ltd). This additional group was introduced into the experimental design, as the siRNA has no homology to any known mammalian gene that had previously been validated with Affymetrix GeneChip arrays and many cell based assays (Technical specifications, Qiagen Ltd). As recommended by the manufacturer, the N.C. siRNA enters RISC and ensures that the comparison of the gene specific siRNA to the N.C. siRNA reflects a genuine picture of the effects of the target gene knockdown on gene expression and phenotype, therefore offering a much more reliable control than buffer injection. All culture conditions and experimental protocols were kept the same throughout the experimental series. For the last 3 cultures, the oocytes were divided equally into 3 groups during day 1 of the cultures and oocytes from each group were inserted into pre-made injection dishes (2 dishes for each group) as described previously in Chapter 4, Section 4.2.2. Injections for the different groups took place using 3 different injection pipettes with pipette loading and microinjections performed as stated

previously (Chapter 4, Section 4.2.2). At the end of the culture period, assessment of oocyte survival and maturation as well as cumulus expansion and coverage took place as previously described (Chapter 4, Section 4.2.2). All the steps followed are shown in the diagram below (Figure 5.1).
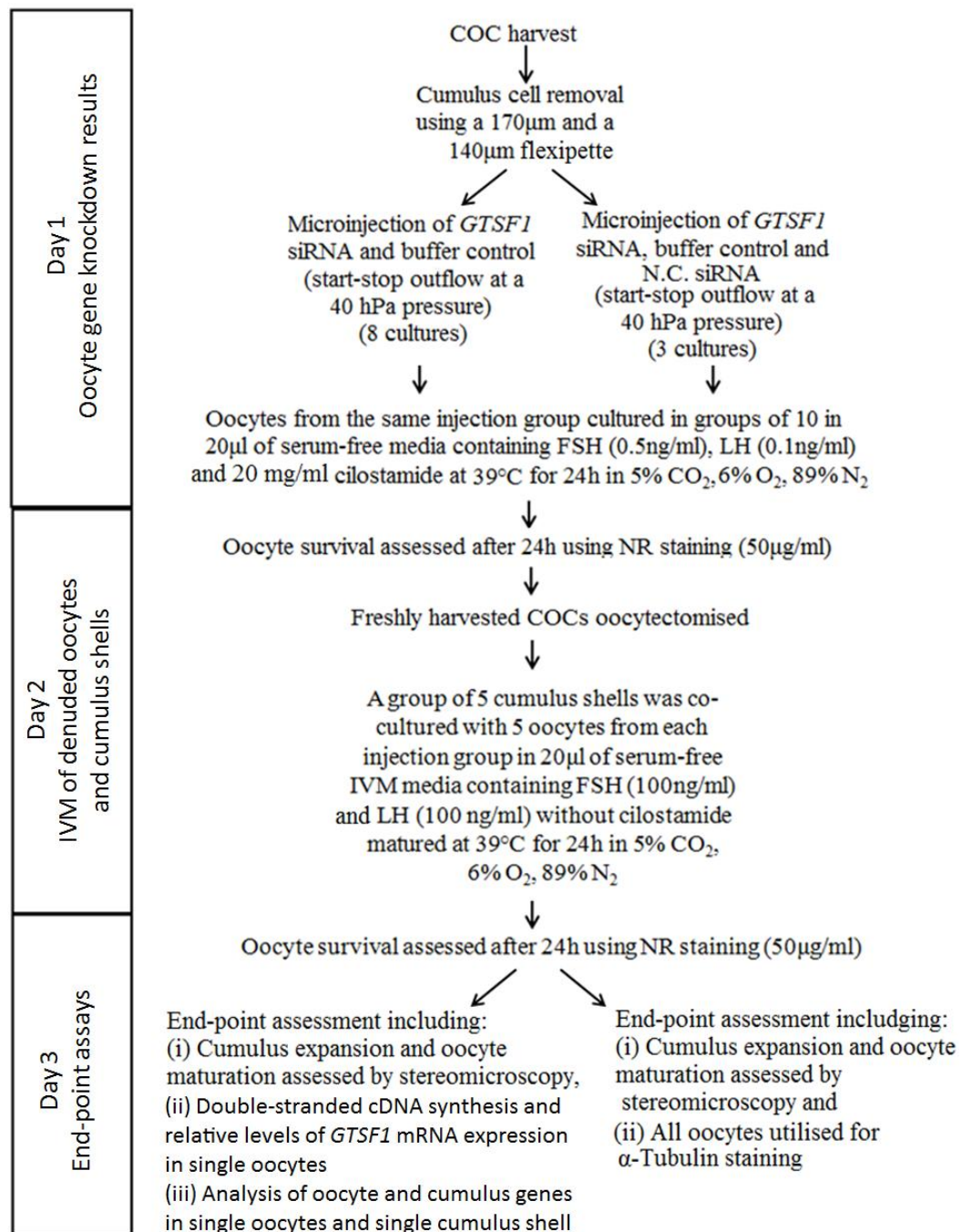
Figure 5.1: Schematic representation of the *GTSF1* siRNA procedure followed and the end-points following generation of *GTSF1* knockdown.

5.2.2.1 Molecular evaluation of *GTSF1* knockdown

At the end of the first 8 cultures, all oocytes that survived the 48 h of culture were transferred individually to labelled 1.5 ml microcentrifuge tubes containing 10 µl of

lysis buffer and all samples were snap-frozen in liquid nitrogen and stored in -80°C for subsequent analysis. Similarly, individual cumulus shells from each drop were also placed in lysis buffer and snap-frozen until molecular analysis. The stored samples of single oocytes or cumulus shells originating from 8 co-cultures of injected oocytes for the different groups and oocytectomised cumulus shells were thawed and used for mRNA isolation as described in Chapter 2, Section 2.2.2 and then they were re-suspended in 3 µl of Tris-HCl (Invitrogen Ltd, Dynal) followed by incubation on a hot block at 90° for 2 min. The mRNA was separated from the Dynal magnetic bead apparatus and the cDNA synthesis by reverse transcription was performed as described in Chapter 2, Section 2.2.3. At this point, a second-strand synthesis protocol was followed to synthesize second-strand cDNA from the 10 µl first strand reactions. This step was followed to increase stability of the cDNA libraries originating from single oocytes based on the results from the validation experiments for the microinjections (Chapter 4). Specifically, the previous cDNA libraries derived from samples containing groups of 1-2 injected oocytes as generated in Chapter 4, showed signs of DNA degeneration following a few cycles of freeze-thawing and did not allow further pathway analysis and investigations following the *GDF9* knockdown.

In the current experimental series where cDNA libraries were created for individual oocytes and individual cumulus shells, a Superscript Double-Stranded cDNA Synthesis Kit (Invitrogen Ltd) was used following the first-strand synthesis. To each of the 10 µl cDNA libraries, the following reagents from the kit were added: 18.2 µl of DEPC-treated H20, 6 µl of 5 X second-strand reaction buffer, 0.6 µl of 10 mM dNTP mix, 0.2 µl of *E. coli* DNA Ligase (10 U/µl), 0.8 µl of *E. coli* DNA Polymerase I (10 U/µl) and 0.2 µl of *E. coli* RNase H (2 U/µl), resulting to a final volume of 36 µl. The tube was then vortexed gently and incubated for 2 h at 16° C. Following the 2 h incubation, 2 µl (10 units) of T4 DNA Polymerase (Kit) were added and the samples were incubated for an additional 5 min at 16° C. The samples were then subjected to heat-deactivation at 95° C for an additional 5 min. At the end of the incubation the level of knockdown for each of the *GTSF1* siRNA-injected oocyte in comparison with the oocyte injected with controls was determined by real-time PCR as described in Section 5.2.1

5.2.2.2 Impact of *GTSF1* knockdown on gene expression

All single MII oocytes that produced a substantial level of *GTSF1* specific knockdown following *GTSF1* siRNA injection (>50% reduction in the *GTSF1* transcript level)

along with their respective controls were selected for further molecular analysis. The cumulus shells originating from the same co-culture drops were also selected for analysis. Candidate gene mRNA expression was evaluated in both the cumulus shells and oocytes. The list of the genes analysed in oocytes included known oocyte-specific factors such as *GDF9* and *BMP15* as well as genes thought to be associated with *GTSF1* expression such as *NOBOX2* situated upstream of *GTSF1* (Krotz *et al.*, 2009). Other oocyte targets included the *CDC20* gene, the trinucleotide repeat-containing gene 6A (*TNRC6A*) gene, the like-Sm 14A (*LSM14A*) gene and the *INCENP* gene. The primers for the genes used in the real-time PCRs for the evaluation of the effect of the *GTSF1* knockdown on oocyte gene expression are shown in Table 5.3. In addition to oocyte gene analysis, candidate gene expression was also assessed in the cumulus shells originating from the co-cultures with the *GTSF1* siRNA-injected oocytes in comparison with buffer-injected controls and N.C. siRNA-injected oocytes. The genes analysed were relevant to cumulus expansion and signalling and included *HAS2*, *GREMLIN1*, *AMH*, *LDH1*, *AREG*, *EREG*, *BTC*, *EGFR*, *FSHR* and *LHR*.

Table 5.3: Primer sequences of oocyte targets genes following *GTSF1* knockdown used for real-time PCR

Gene	Primer Sequence	Size (bp)	Reference
NOBOX2	F: 5´ GTGCCTATTTCCTGCACCAT 3´	119	HQ589330 (predicted bovine)
	R: 5´ CTCCTGTCTTCGTGGAGAGC 3´		
CDC20	F: 5´ CCCAGAGGGTTACCAGAACA 3´	86	XM004023553 (predicted ovine)
	R: 5´ GAATGTAGCGGCAGGTCTTC 3´		
TNRC6A	F : 5´ CAGACCAGCAAGCACAGGTA 3´	168	XM614640 (predicted ovine)
	R : 5´ GCCCACTGTCTACGGGTTTA 3´		
LSM14A	F: 5´ GTGTGGTTGGTTCTGCCTTT 3´	129	NM001034654 (bovine)
	R: 5´ AGGCGGTCTGTACTGCTTGT 3´		
INCENP	F: 5´ TGCTCAGATCGACGAGAAGA 3´	156	XM584352 (predicted bovine)
	R: 5´ TCCTCCTGCTGTAGCCACTT 3´		

5.2.2.3 Pilot assessment of the impact of *GTSF1* knockdown on oocyte spindle integrity

To determine the effect of *GTSF1* on the structure of the oocyte meiotic spindle and the distribution of microtubules, α-Tubulin immunofluorescent staining was applied using a technique previously described (Li *et al.*, 2006). Tubulin is a member of the globular proteins with the α-Tubulin and β-Tubulin family members of tubulins making up the microtubules (Weisenberg, 1972). For the last 3 cultures out of the 11 conducted, after the completion of culture, mature MII oocytes from each treatment group (*GTSF1* siRNA-injected, buffer-injected and N.C. siRNA-injected) were used for α-Tubulin

staining. Oocytes from the different groups were placed in separate drops of a 4 well dish and fixed in 500 μl of 4% PFA (w/v) in PBS overnight at 4ºC. The PBS solution was made by dissolving 1 PBS tablet (Invitrogen Ltd) in 500 ml of Milli-Q H_2O followed by filter sterilization with a 0.2 μm cellulose acetate Acrodisc syringe filter. The oocytes were then washed in a separate well of 500 μl of PBS at RT for 5 min and were then transferred into clean wells pre-filled with 500 μl of 1% (v/v) Triton X-100 and 0.3% (w/v) BSA (lyophilized powder, ≥96%) in PBS at 37°C and incubated for 1 h at 37ºC. The oocytes were washed twice in 500 μl of 0.01% (v/v) Triton X-100 in PBS at RT for 5 min per wash and were then incubated in 500 μl of 150 mM Glycine and 1% (v/v) Triton X-100 in PBS for 1 h at 37ºC to block any residual fixative. Oocytes were then washed thoroughly in 500 μl of PBS at RT for 5 min. At this stage, all oocytes from each of the 3 treatments were transferred into separate wells of a 4 well dish, in which a small glass coverslip was placed onto the bottom of each well containing 25 μl drops of mouse monoclonal anti α-Tubulin antibody (1:400 working stock in 0.01% v/v sodium azide in PBS) overlaid with 400 μl of mineral oil. The oocytes were incubated for 1 h at 37ºC. Oocytes were then washed thoroughly in PBS and oocytes from each treatment then transferred into separate wells of a 4 well dish with an inserted small glass coverslip on the bottom of the well containing 25 μl of polyclonal FITC-conjugated rabbit anti-mouse antibody (1:100 working stock in 0.01% v/v sodium azide in PBS) overlaid with 400 μl of mineral oil. Both the primary and secondary antibodies were purchased from Sigma-Aldrich. The oocytes were once again incubated for 1 h at 37ºC. The oocytes were then washed in 500 μl of PBS for 5 min at RT before being incubated in 25 μl drop of DAPI (10 μg/ml in PBS) in 4 well dishes with a glass coverslip at the bottom and overlaid with 400 μl of mineral oil. The incubation period lasted for 15 min at RT in the dark. Oocytes were then washed once again in 500 μl of PBS at RT for 5 min before they were mounted on slides with 20 μl drop of Vectashield mountant (Vector Laboratories Ltd, Peterborough, UK). The Vectashield was placed onto the centre of a pre-cleaned Superfrost Plus glass microscope slide (Thermo Fisher Scientific) and 2-3 oocytes from each treatment were placed into the drop and were allowed a few minutes to sink to the bottom of the drop. A coverslip was then placed onto the drop and lowered slowly to avoid introduction of drops under the coverslip or squashing of the oocytes. Oocytes were kept at 4ºC in the dark and visualized under a fluorescent microscope (Zeiss Axioplan2, Carl Zeiss Ltd) using the Cytovision 4.5 computer software (Leica Microsystems Ltd). Additionally, oocytes were also visualized under a confocal microscope (Zeiss LSM 510, Carl Zeiss Ltd) using the

confocal microscopy software 3.2 (Carl Zeiss Ltd). Both microscopes were fitted with a filter with an excitation wavelength range between 495 and 520 nm to capture green fluorescence and a filter with an excitation wavelength between 420 and 495 nm to capture blue fluorescence.

5.2.4 Statistical analysis

Chi-square tests were used to analyse the results of oocyte survival, meiotic progression, cumulus coverage and cumulus expansion according to proportional analysis of the cohort of oocytes and cumulus within each treatment. All data were checked for normality using the Anderson-Darling test. Normally distributed data for mRNA levels of *GTSF1*, *GDF9*, *BMP15*, *NOBOX2*, *CDC20*, *TNRC6A*, *LSM14A* and *INCENP* mRNA levels within oocytes and *HAS2*, *GREMLIN1*, *AMH*, *LDH1*, *AREG*, *EREG*, *BTC*, *EGFR*, *FSHR* and *LHR* within cumulus cells were compared using Student's t-test. Values for real time data presented are the arithmetic means ±SEM for the number of observations shown.

5.3 RESULTS

Overall 1038 oocytes were microinjected over 2 experimental series; of these 465 denuded oocytes were injected with *GTSF1* siRNA, while 463 denuded oocytes were injected with buffer and 110 denuded oocytes were injected with N.C. siRNA in a total of 15 cultures.

5.3.1 Assessment of the 4 different *GTSF1* siRNA species in generation of knockdown following microinjection and IVM of GV oocytes

A total of 4 cultures were conducted using the 4 commercially made *GTSF1* siRNAs for the generation of knockdowns (30 oocytes injected per culture) with buffer-injected oocytes as controls (30 oocytes injected per culture). The observations through the cultures showed that none of the 4 *GTSF1* siRNAs was lethal to the oocytes and no significant differences were observed between the 4 siRNAs and the controls at 24 and 48 h (P>0.05, Table 5.1). The majority of oocyte losses occurred in the first 24 h of culture in both siRNA-injected and buffer-injected controls in response to denudation and/or membrane damage due to injection (Table 5.1). Additionally, assessment of oocyte developmental competence showed that oocytes from both injection groups for all 4 cultures progressed to the MII stage at the end of the 48 h of incubation as assessed by the presence of the first polar body as shown in Table 5.4. The numbers of MII

oocytes however were very low (1-2 per siRNA and control) and meaningful statistical analysis was therefore not possible. Cumulus expansion monitoring in cumulus cells co-cultured with viable *GTSF1* siRNA-injected oocytes and buffer-injected control oocytes showed that cumulus shells from the co-cultures of both the *GTSF1* siRNA-injected oocytes and buffer-injected oocytes were able to fully expand following the 4 co-cultures (Table 5.1). Although the data is very preliminary and the numbers of cumulus complexes were too low for meaningful statistical analysis, the data demonstrate that cumulus expansion is supported through the IVM co-culture of oocytectomised cumulus shells and denuded oocytes (Table 5.1).

Table 5.4: Comparison of the 4 different siRNAs following *GTSF1* knockdown

Treatment	*GTSF1* siRNA	Control buffer	Significance
Oocyte survival at 24 h			
GTSF1 siRNA-1	2/30 (6.7%)	3/30 (10.0%)	
GTSF1 siRNA-2	7/30 (23.3%)	8/30 (26.7%)	NS
GTSF1 siRNA-3	2/30 (6.7%)	3/30 (10.0%)	
GTSF1 siRNA-4	5/30 (16.7%)	4/30 (13.3%)	
Oocyte survival at 48 h (based on viable oocytes at 24 h)			
GTSF1 siRNA-1	2/2 (100%)	3/3 (100%)	
GTSF1 siRNA-2	7/7 (100%)	8/8 (100%)	NS
GTSF1 siRNA-3	2/2 (100%)	3/3 (100%)	
GTSF1 siRNA-4	5/5 (100%)	4/4 (100%)	
Oocyte maturation of viable oocytes at 24 h			
GTSF1 siRNA-1	1/2 (50.0%)	1/3 (33.3%)	
GTSF1 siRNA-2	2/7 (28.6%)	2/8 (25.0%)	NA
GTSF1 siRNA-3	1/2 (50.0%)	1/3 (33.3%)	
GTSF1 siRNA-4	1/5 (20.0%)	1/4 (25.0%)	
Cumulus expansion			
Classification 0			
GTSF1 siRNA-1	0/2 (0.0%)	0/3 (0.0%)	
GTSF1 siRNA-2	0/7 (0.0%)	0/8 (0.0%)	NA
GTSF1 siRNA-3	0/2 (0.0%)	0/3 (0.0%)	
GTSF1 siRNA-4	0/5 (0.0%)	0/4 (0.0%)	
Classification 1			
GTSF1 siRNA-1	0/2 (0.0%)	1/3 (33.3%)	
GTSF1 siRNA-2	5/7 (71.4%)	4/8 (50.0%)	NA
GTSF1 siRNA-3	1/2 (50.0%)	2/3 (66.7%)	
GTSF1 siRNA-4	3/5 (60.0%)	2/4 (50.0%)	
Classification 2			
GTSF1 siRNA-1	2/2 (100%)	2/3 (66.7%)	
GTSF1 siRNA-2	2/7 (28.6%)	4/8 (50.0%)	NA
GTSF1 siRNA-3	1/2 (50.0%)	1/3 (33.3%	
GTSF1 siRNA-4	2/5 (40.0%)	2/4 (50.0%)	

Molecular analysis of *GTSF1* transcript levels in oocytes showed a reduction for 3 out of 4 siRNAs when *GTSF1* siRNA-injected MII oocytes were compared with buffer-

injected MII oocytes using *GAPDH* and *H2A* as reference standards. The expression levels of *GTSF1* were reduced when siRNA-1 was injected (19.1 arb. units) in comparison with the buffer-injected control oocyte (32.3 arb. units). When siRNA-2 was injected there was a higher reduction in the transcript levels of *GTSF1* following the knockdown (14.9±3.3 arb. units, n=2) in comparison to the control oocyte (43.7±10.9 arb. units, n=2). The highest reduction in *GTSF1* levels was noted when siRNA-3 was injected (8.8 arb. units) in comparison to the control (49.1 arb. units), while there was a small reduction in the *GTSF1* transcript levels when siRNA-4 was injected (22.5 arb. units) in comparison to its respective control (26.3 arb. units). Because of the low numbers of oocytes progressing to the MII stage (1-2 single MII oocytes available for analysis), further analysis of the oocytes retained at the GV stage at the end of the cultures verified the findings for the efficiency of *GTSF1* siRNA-3 in generating a substantial level of knockdown (data not shown). On the basis of these preliminary results, the *GTSF1* siRNA-3 was considered more suitable for generation of oocyte *GTSF1* knockdowns. The *GTSF1* siRNA-3 relates to a sequence located on the sixth exon (www.ensembl.org) of the *GTSF1* sequence (base pairs 476-497) and was thereafter used in the subsequent experiments (referred to as *GTSF1* siRNA) in order to study the effect of *GTSF1* in oocyte development and cumulus function.

5.3.2 Experimental assessment of the impact of *GTSF1* knockdown during maturation of ovine oocytes *in vitro*

In a total of 11 cultures, 345 denuded oocytes were injected with the selected *GTSF1* siRNA (*GSF1* siRNA-3), while 343 denuded oocytes were injected with buffer and 110 denuded oocytes were injected with N.C. siRNA.

5.3.2.1 Oocyte survival after microinjection

Oocyte survival was assessed at 24 h and 48 h of culture. From all the cultures, a total of 45/345 oocytes (13%) survived the first 24 h as assessed by NR staining when injected with *GTSF1* siRNA, 56/343 oocytes (16.3%) survived the buffer injections and 15/110 oocytes survived the N.C. siRNA injections (13.6%). At 48 h all IVM oocytes remained viable with 45/45 *GTSF1* siRNA-injected oocytes surviving (100%), 56/56 buffer-injected oocytes surviving (100%) and 15/15 N.C. siRNA-injected oocytes surviving (15/15%) as shown in Figure 5.2. No significant differences (P>0.05) in oocyte survival were observed between the 3 injection groups at the 2 time points

showing that neither the *GTSF1* siRNA nor the N.C.siRNA *per se* were toxic to the oocytes.
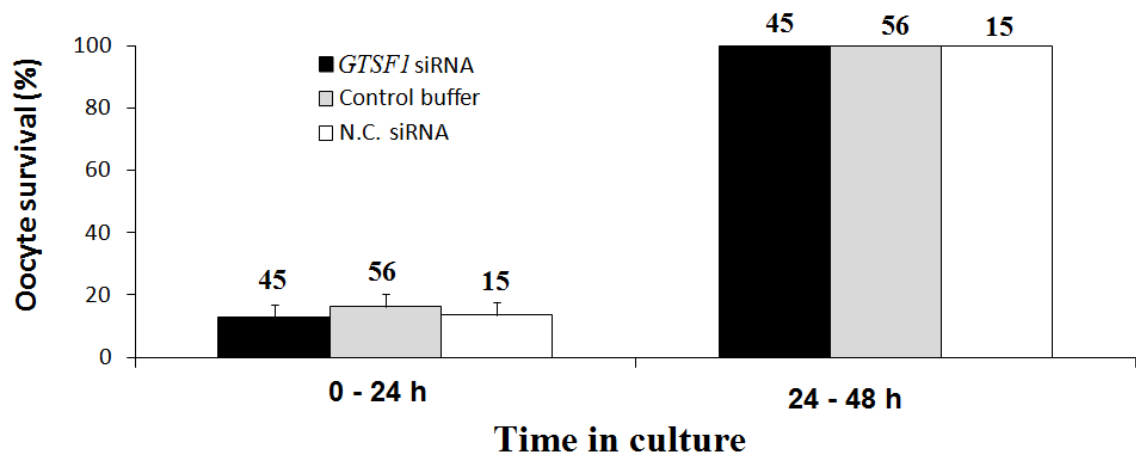
Figure 5.2: Influence of oocyte *GTSF1* siRNA injection, buffer injection and N.C.siRNA injection on oocyte survival as assessed by NR uptake at 24 h and 48 h of *in vitro* culture. Before the first time point, oocytes were denuded, microinjected with either *GTSF1* siRNA, control buffer or N.C. siRNA and cultured in serum-free media with cilostamide (20 mg/ml) and basal levels of gonadotrophins for 24 h. Surviving oocytes were then co-cultured with oocytectomised cumulus shells in serum-free IVM media and maturation inducing levels of gonadotrophins for an additional 24 h (total of 48h). Values represent the cohort of injected oocytes over 11 repeat cultures for *GTSF1* siRNA and control buffer and 3 repeat cultures for N.C. siRNA. Individual bars show the mean ±SEM for independent cultures with the numbers of oocytes falling into each category shown. No significant differences were observed (P>0.05).

5.3.2.2 The impact of *GTSF1* on meiotic progression

Developmental competence of oocytes following microinjection and IVM was assessed by confirming the MII progression rates of viable oocytes at 24 h after 48 h of culture (Figure 5.3).
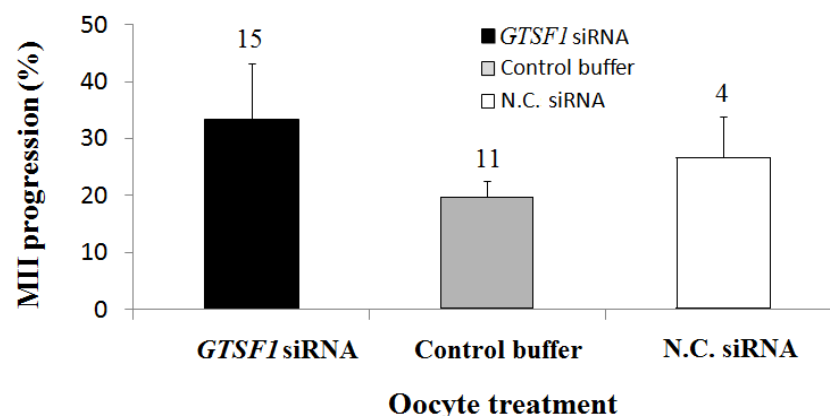
Figure 5.3: Impact of *GTSF1* knockdown on meiotic progression of viable *GTSF1* siRNA, buffer and N.C. siRNA-injected oocytes as determined at 24 h of culture that were subjected to an additional 24 h of IVM co-culture with cumulus shells. The 3 groups did not demonstrate any significant differences (P>0.05). Values represent proportions of surviving oocytes over 11 repeat cultures for *GTSF1* siRNA and control buffer and 3 repeat cultures for N.C. siRNA. Individual bars show the mean ±SEM for independent cultures with the numbers of oocytes falling into each category shown. No statistical differences were observed (P>0.05).

165

The proportion of viable oocytes following the first 24 h of cultures progressing to the MII stage was not significantly different between the 3 groups (P>0.05) with 33.3% of viable oocytes following *GTSF1* knockdown progressing to MII (15/45 oocytes) in comparison to 19.6% of buffer-injected oocytes (11/56 oocytes) and 26.7% of N.C. siRNA-injected control oocytes (4/15 oocytes) (Figure 5.3).

5.3.2.3 The effect of oocyte *GTSF1* knockdown on cumulus expansion

Cumulus shell mass and expansion were assessed prior to the start of the second phase of oocyte culture at 24 h and at the end of the IVM co-culture at 48 h. Equal numbers of cumulus shells and viable oocytes from the first phase were co-cultured per treatment. A total of 45 cumulus shells were oocytectomised and cultured with viable *GTSF1* siRNA-injected oocytes, while 56 and 15 cumulus shells were co-cultured with viable buffer-injected oocytes and viable N.C. siRNA-injected oocytes respectively. Cumulus shells were divided equally between the 3 groups of oocytes based on their coverage scores and at the end of the culture, with the coverage scores of the cumulus remaining unchanged during the period of the co-culture for all 3 treatments. There were no significant differences (P>0.05) between the 3 groups as shown by the mean proportion of cumulus coverage at the end of the cultures (Figure 5.4).
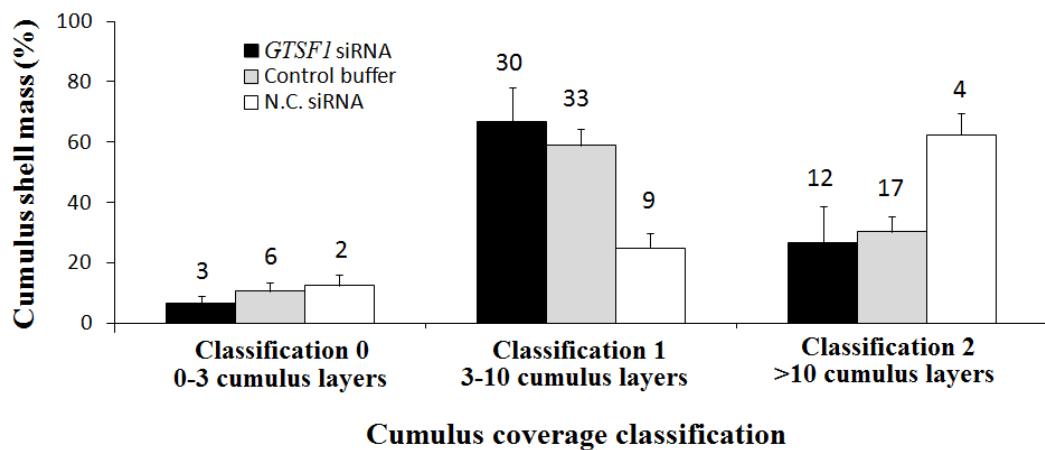
Figure 5.4: Effect of oocyte *GTSF1* knockdown on cumulus shell mass classification after 24 h of co-culture with *GTSF1* siRNA, buffer or N.C. siRNA-injected oocytes. Values represent proportions of cumulus shell mass classifications over 11 repeat cultures for *GTSF1* siRNA and control buffer and 3 repeat cultures for N.C. siRNA. Individual bars show the mean ±SEM for independent cultures with the numbers of cumulus shells falling into each category shown. No significant differences were observed (P>0.05).

Analysis of cumulus expansion showed that cumulus shells underwent expansion over the 24 h of IVM culture as indicated by the progression of cumuls expnasion score 0 to expansion score 2 for all treatment groups. However, knockdown of *GTSF1* in oocytes

generated by siRNA injection did not have a significant effect on the capacity for cumulus expansion (P<0.05) when compared with the control buffer and the N.C. siRNA-injected oocyte treatment groups. Figure 5.5 shows the mean proportion of cumulus expansion for the 3 treatment groups. This result indicates that *GTSF1* does not affect cumulus-oocyte-cumulus interactions and the signalling required to drive cumulus expansion during 24 h of IVM.
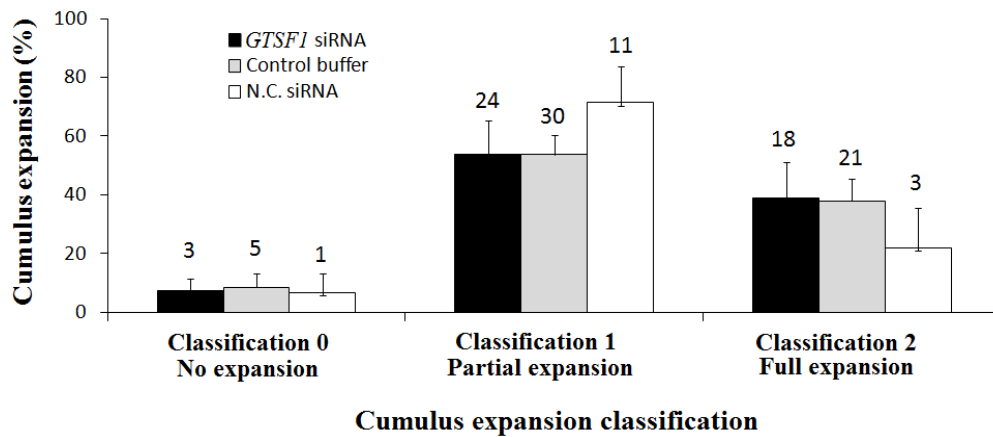
Figure 5.5: Effect of oocyte *GTSF1* knockdown on cumulus expansion following 24 h of IVM co-culture. Values represent proportions of cumulus shell expansion classifications over 11 cultures for *GTSF1* siRNA and control buffer and 3 repeat cultures for N.C. siRNA. Individual bars show the mean ±SEM for independent cultures with the numbers of cumulus shells falling into each category shown. No statistically significant differences were noted between the 3 groups (P>0.05).

5.3.2.4 Molecular analysis of gene expression following *GTSF1* knockdown

The function of *GTSF1* was further investigated by analysis of the expression of potential target genes associated with the knockdown in the oocyte and cross-talk with cumulus cells. Individual oocytes that progressed to the MII stage from the first 8 cultures following *GTSF1* siRNA and control buffer injections were used for molecular evaluations. A total of 15 MII oocytes from the *GTSF1* siRNA injection group along with their respective controls from each individual culture (15 control oocytes) were analysed. Real time analysis showed that *GTSF1* expression was reduced following *GTSF1* siRNA injection (35.2±8.4 arb. units, n=15) in comparison with the control injected oocytes (78.0±20.3 arb. units, n=15), but this reduction was not significant (P>0.05) (Figure 5.6.a). This was based on absolute oocyte mRNA levels of *GTSF1* normalised against both *H2A* and *GAPDH*. The observed variability in the levels of *GTSF1* knockdown between different samples in comparison with the controls could be the result of altering the injection methodology. The MII oocytes that showed a reduction in their *GTSF1* expression level of >50% based on their relative expression

levels with the controls were selected from the cohort. The total of 4 individual oocytes were verified by real-time to have a significant reduction (P<0.05) in the *GTSF1* transcript levels following *GTSF1* siRNA injection (10.7±3.2 arb. units, n=4) in comparison with controls (111.2±58.6 arb. units, n=4) (Figure 5.6.b). These oocytes along with their respective controls and single cumulus shells from their respective co-cultures were selected for subsequent analysis.
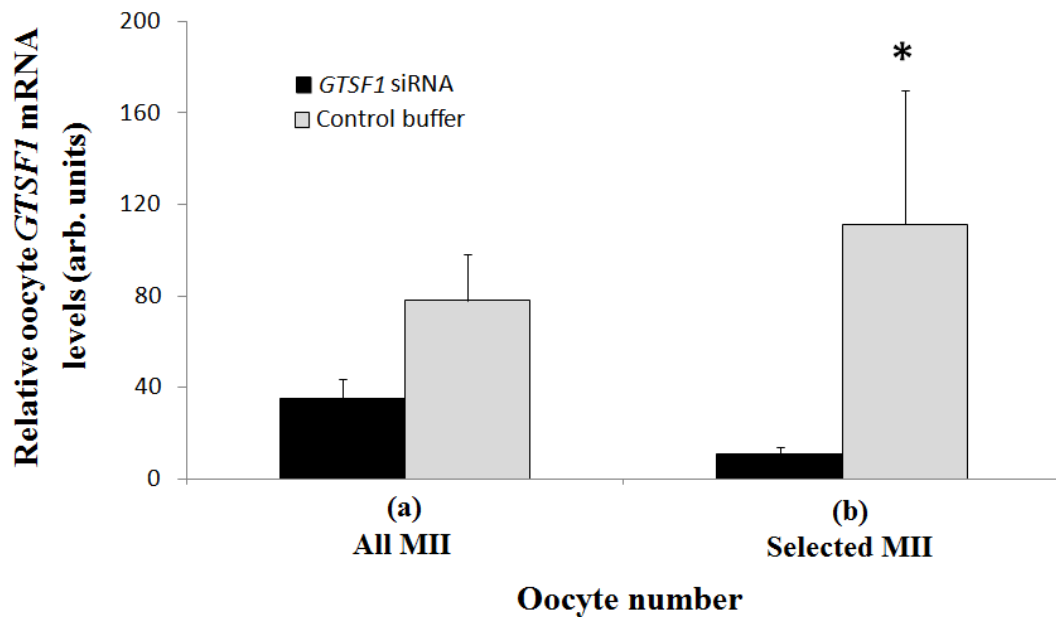
Figure 5.6: Real-time PCR quantification of the effect of *GTSF1* siRNA injection on the *GTSF1* expression levels of (**a**): All MII oocytes (n=15) injected with *GTSF1* siRNA and their respective controls, (**b**): Selected MII oocytes (n=4), that showed a relative reduction in the *GTSF1* expression level of over 50% in comparison with the controls. The data were standardised against the oocyte *GAPDH* and *H2A* mRNA levels. Individual bars show the mean ±SEM for (a) 15 repeat cDNA libraries and (b) 4 repeat cDNA libraries (each cDNA library analysed in triplicate). Each cDNA library contained a single oocyte. The selected *GTSF1* siRNA-injected oocytes (b) exhibited a statistically significant difference for the *GTSF1* mRNA levels (*=P<0.05) when compared against the buffer-injected control samples.

The specificity of the knockdown for the target gene was thereafter further examined by assessing the transcript levels of oocyte-derived genes *GDF9* and *BMP15* as well as *NOBOX2* (Figure 5.7.a). Expression levels of *GDF9* were reduced to 0.2±0.1 arb. units (n=4) following *GTSF1* knockdown in comparison with controls (0.4±0.1 arb. units, n=4) and *BMP15* mRNA levels were reduced to 617.6±365.0 arb. units (n=4) following *GTSF1* knockdown in comparison with controls (1189.8±433.6 arb. units, n=4), but neither of these reductions were significant (P>0.05). The mRNA levels of *NOBOX2* were increased in the *GTSF1* siRNA-injected oocytes (0.4±0.3 arb. units, n=4) when compared to the controls (0.3±0.1 arb. u, n=4). These differences were not significant (P>0.05).

168
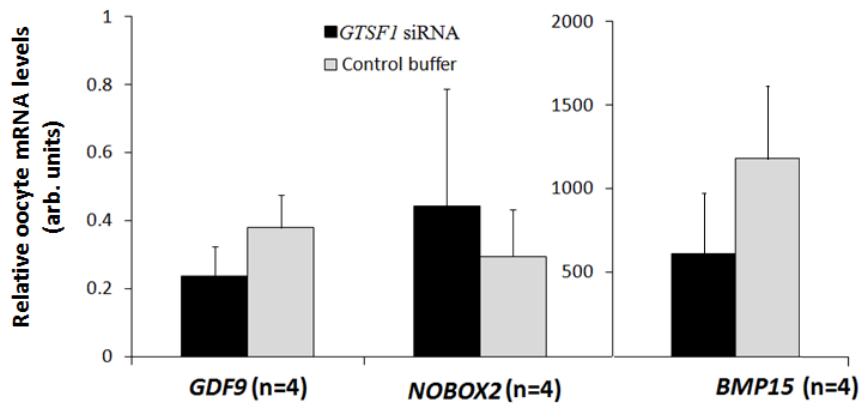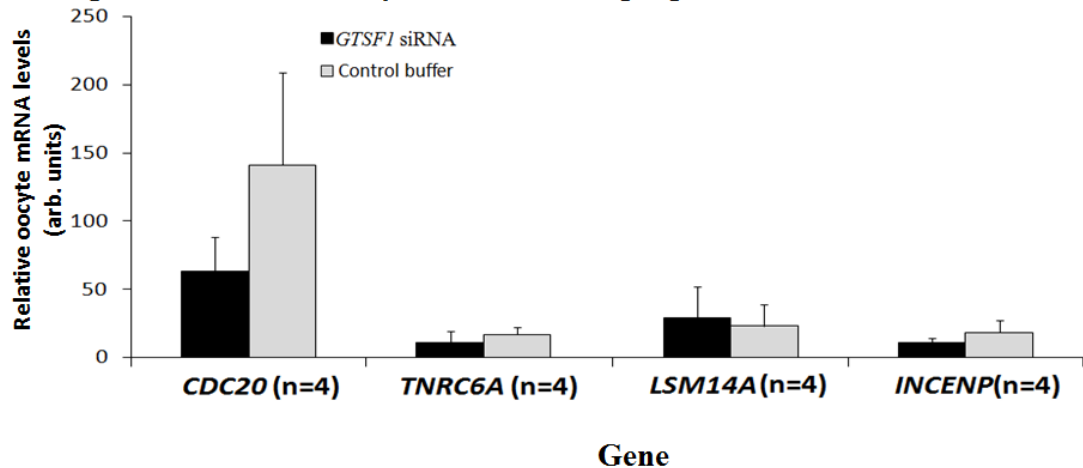
Figure 5.7: Real-time PCR quantification of the effect of *GTSF1* siRNA injection on oocyte mRNA levels of: **(a):** Oocyte expressed genes: *GDF9*, *NOBOX2* and *BMP15*. **(b):** Other candidate target genes for *GTSF1* knockdown: *CDC20*, *TNRC6A*, *LSM14A* and *INCENP*. Data for both graphs were normalised against the cumulus *GAPDH* and *H2A* mRNA levels. Individual bars show the mean ±SEM for the number (n) of repeat cDNA libraries respectively (each library analysed in triplicate). Each cDNA library contained a single oocyte. No significant differences were observed for the 2 treatments (P>0.05).

Other target gene transcripts were also evaluated following oocyte *GTSF1* knockdown as shown in Figure 5.7.b. Specifically, the mRNA transcripts of *CDC20* were reduced in *GTSF1* siRNA-injected oocytes (63.6±25.1 arb. units, n=4) in comparison with the control samples (141.0±68.2 arb. units, n=4), while the mRNA levels of *TNRC6A* were reduced (11.3±8.1 arb. units, n=4) in the *GTSF1* siRNA-injected oocytes in comparison with controls (16.8±5.6 arb. units, n=4). The mRNA levels of *LSM14A* were increased (29.2±23.1 arb. units, n=4) following *GTSF1* siRNA injection in comparison with the controls (23.1±15.9 arb. units, n=4) and the transcripts of *INCENP* were decreased in *GTSF1* siRNA-injected oocytes (10.9±3.6 arb. units, n=4) in comparison with the buffer-injected control oocytes (18.3±9.0 arb. units, n=4). None of the 4 target genes analysed showed a significant reduction in the transcript levels for the 2 treatment

groups (P>0.05). Although the transcripts levels were considerably different for some target genes and in particular for *CDC20*, the data were too variable for any of the transcript differences to be confirmed as a result of a *GTSF1* knockdown effect on subsequent gene expression in MII oocytes. For all gene transcripts analysed, all 4 *GTSF1* knockdown samples containing individual MII oocytes as well as their respective buffer-injected controls containing individual MII oocytes were used.

The transcript levels of somatic genes in the cumulus shells were analysed in order to examine whether the *GTSF1* knockdown in oocytes had an effect on the gene expression levels of cumulus shells. In particular, individual cumulus shells originating from co-cultures with MII oocytes for the 2 injection groups that were used for the molecular analysis above were selected for analysis of target genes in the cumulus. For all gene transcripts analysed, all 4 cDNA libraries from each treatment (each cDNA containing a single cumulus shell) were used and 1 sample was excluded during analysis due to contamination. Levels of *HAS2* were reduced in the *GTSF1* knockdown treatment group (10.7±2.0 arb. units, n=4) in comparison with the controls (55.0±35.8 arb. units, n=4); while levels of *AMH* and *LDH1* were increased in *GTSF1* siRNA-injected oocytes (0.1±0.1 arb. units, n=3; 0.5±0.2 arb. units, n=3) respectively, in relation with the controls (0.1±0.1 arb. units, n=3; 0.3±0.1 arb. units, n=3) (P>0.05) (Figure 5.8.a). The relative expression levels of *GREMLIN1* and *EREG* were very low for accurate detection and were therefore not included (data not shown). Transcript levels of *AREG* were reduced in the *GTSF1* knockdown treatment group (0.8±0.6 arb. units, n=4) in comparison with the control group (0.9±0.8 arb. units, n=4), while the levels of *BTC* were increased following *GTSF1* siRNA injection (0.2±0.1 arb. units, n=4) respectively in comparison with the controls (0.1±0.1 arb. units, n=4) (P>0.05) (Figure 5.8.b). The expression of the receptors *EGFR*, *FSHR* and *LHR* was (*EGFR* 0.3±0.1 arb. units, n=4; *FSHR* 1.5±0.9 arb. units, n=4; *LHR* 0.4±0.3 arb. units, n=4) respectively for the knockdown group in comparison with the controls (*EGFR* 0.3±0.2 arb. units, n=4; *FSHR* 0.9±0.5 arb. units, n=4; *LHR* 0.3±0.3 arb. units, n=4) (P>0.05) (Figure 5.8.c). Even though there were high differences in the expression levels of several genes as shown for the 2 different treatment groups, variability of the data did not allow any connections to be made to a possible effect of the knockdown on gene expression in cumulus shells. Therefore for future experiments, a greater number of sample needs to be analysed and/or alternative strategies considered.
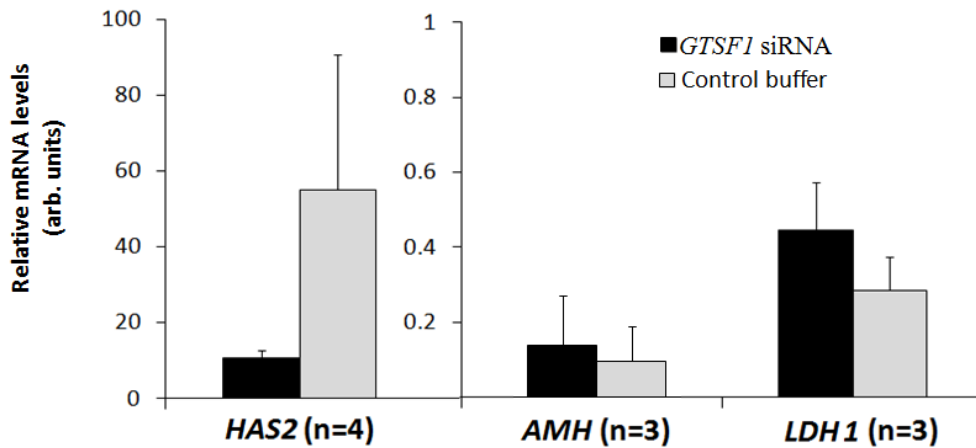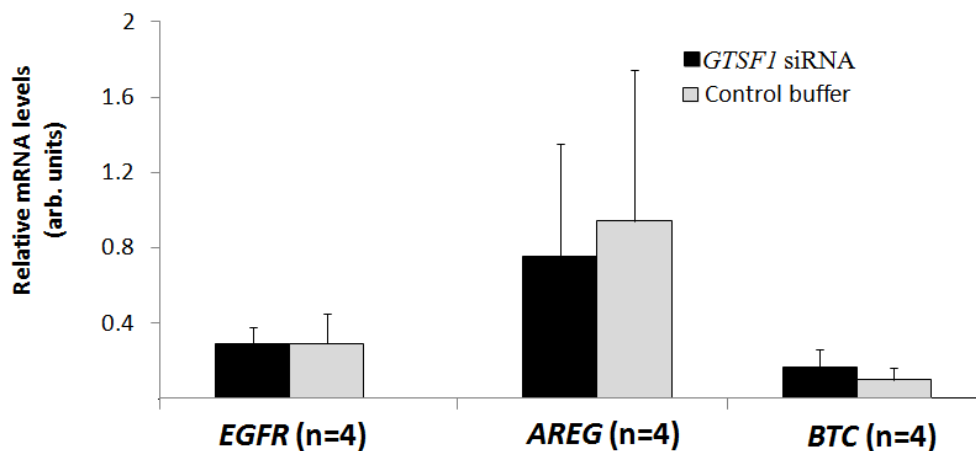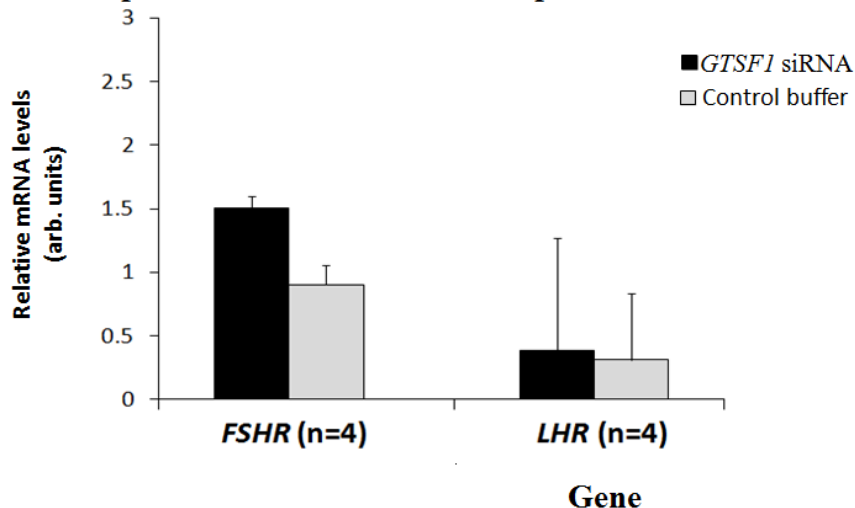
Figure 5.8: Effect of *GTSF1* knockdown on cumulus shell gene expression as determined by real-time PCR. **(a):** Somatic marker genes: *HAS2, AMH* and *LDH1*. **(b):** Regulin genes *AREG, BTC* and *EGFR*. **(c):** Cumulus cell receptors *FSHR* and *LHR*. Data for all 3 graphs were normalised against the cumulus *GAPDH* and *H2A* mRNA levels. Individual bars show the mean ±SEM for the number (n) of repeat cDNA libraries respectively (each library analysed in triplicate). Each sample contained individual cumulus shells that were co-cultured with injected oocytes for each treatment group. No significant differences were observed for the 2 treatments ($P > 0.05$).

5.3.2.5 The impact of *GTSF1* knockdown on oocyte spindle formation

The functional association of *GTSF1* was further investigated by immunostaining whole MII oocyte mounts for α-Tubulin. In this pilot study, oocytes produced from the last 3 cultures were used to assess the impact of gene knockdown on meiotic spindle formation. A total of 11 MII oocytes were used for immunofluorescent staining for α-Tubulin of which 3 were produced from *GTSF1* siRNA injections, 4 from control buffer and 4 from N.C. siRNA injections (Figure 5.9).
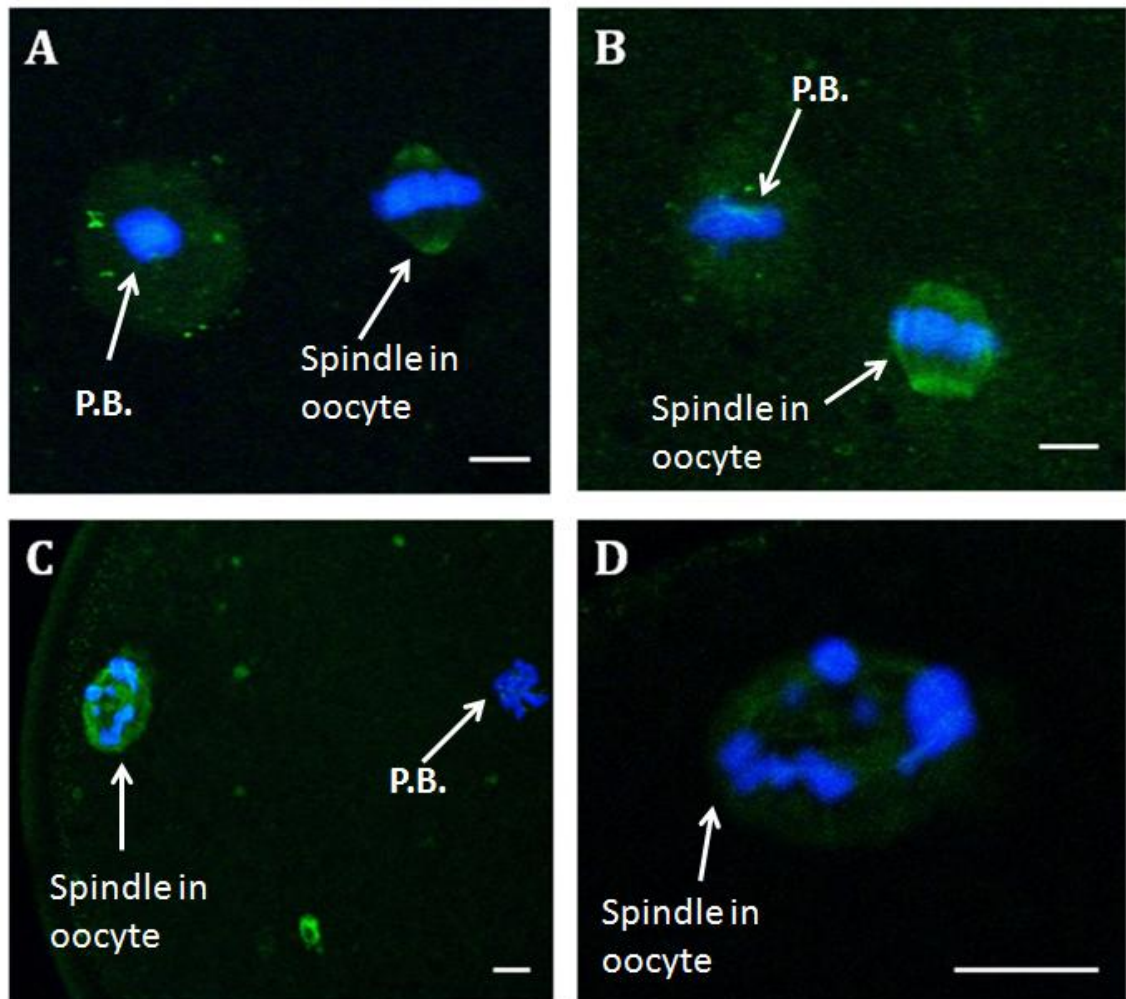
Figure 5.9: Immunofluorescent staining of α-Tubulin (green) and DAPI counter-staining of chromosomes (blue) following microinjections. **A-B:** Metaphase chromosomes of MII oocytes after spindle formation. **A:** Buffer control injected MII oocyte. **B:** N.C. siRNA-injected MII oocyte. **C-D:** Pro-metaphase II stage oocytes following *GTSF1* siRNA injections (**D:** High power magnification). Scale bar: 5 μm.

The results showed that all 4 MII oocytes from both the control buffer and N.C. siRNA treatment groups formed meiotic spindles which were of the expected shape as shown by the representative images of Figure 5.9 (A and B). A similar observation was made for 1 of the *GTSF1* siRNA-injected oocytes while the other 2 oocytes injected with

GTSF1 siRNA also formed microtubules but these gametes demonstrated retardation of spindle polymerisation and appeared to be at the pro-metaphase II stage (Figure 5.9.C and D). A possible explanation is that the gene knockdown affects spindle formation at the MII stage. Further replicates are clearly needed to confirm these preliminary observations. However, it was decided to focus future efforts on generating sufficient MII oocytes for molecular evaluations which would incorporate a broader screen of the effects of *GTSF1* knockdown on genes relating to spindle formation and chromosome segregation, so this pilot staining study was not repeated.

5.4 DISCUSSION

In this study it was shown that it was possible to generate a targeted knockdown of *GTSF1* in sheep oocytes without compromising oocyte survival and oocyte meiotic progression following removal of a specific PDE inhibitor and co-culture with oocytectomised cumulus shells. Oocyte maturation and cumulus expansion data did not appear to be significantly affected based on oocyte MII progression or cumulus expansion levels following co-cultures of *GTSF1* siRNA-injected oocytes with cumulus shells in comparison with the buffer-injected control oocytes and the N.C. siRNA controls. In addition, pilot data on α-Tubulin staining showed that there might be a relationship between gene knockdown and oocyte developmental competence but further experimentation is required. Analysis of mRNA expression levels for potential oocyte and cumulus cell gene targets following the knockdown did not indicate any significant differences between knockdown and control group due to the high levels of variability between samples.

5.4.1 The impact of *GTSF1* on meiotic progression and cumulus cell expansion

The results of the experiments reported in this Chapter did not show any significant effect of *GTSF1* knockdown on MII progression as illustrated by the extrusion of the polar body. The proportions of MII progression were slightly higher for the viable oocytes 24 h after injection with *GTSF1* siRNA that were co-cultured with maturation inducing gonadotrophins (33.3%) in comparison with the viable buffer-injected oocytes (19.6%) and the viable N.C. siRNA-injected oocytes (26.7%), but no significant differences were noted (P>0.05). This suggests that *GTSF1* is not essential for either meiotic progression or for cumulus expansion, as results between the treatment groups for cumulus expansion and mucification showed no significant differences (P>0.05). Specifically, 38.8% of cumulus shells from the *GTSF1* siRNA treatment group were

shown to fully expand, compared to 38% and 22% of control buffer and N.C. siRNA group cumulus shells respectively (P>0.05). Cumulus expansion reflects oocyte developmental competence and factors derived from the ovary and termed cumulus expansion enabling factors are responsible for driving cumulus expansion (Buccione *et al.*, 1990b). From the results it can be suggested that knockdown of *GTSF1* does not affect the expression of the factors responsible for cumulus expansion. However, since not all MII oocytes were confirmed to have a significant reduction in their *GTSF1* expression levels following the knockdown in comparison with the controls, the *GTSF1* effect on maturation requires further experimentation. The group culture of oocytes that were subjected to different levels of *GTSF1* knockdown did not allow evaluation of cumulus expansion based on each oocyte's level of knockdown. For future experiments different strategies must be considered.

The lack of impact of *GTSF1* knockdown in GV oocytes during meiotic progression *in vitro* and the lack of effect on cumulus cell expansion does not exclude the potential function of *GTSF1* as a factor of oocyte quality. It is well established that at MI, the paired homologous chromosomes are aligned in the middle of the meiotic spindle and separation of the paired homologous chromosomes is followed by the formation of the first polar body. At this stage the oocyte undergoes molecular reprogramming for the coordinated expression of essential genes and will construct mitochondria, large numbers of Golgi, generate receptors and gather nutritional reserves for embryonic development (Van Blerkom and Davis, 1995). With the role of *GTSF1* likely to be connected to RNA-binding and storage it could be that the gene affects oocyte growth initiation and development prior to the formation of the secondary oocytes, and/or fertility and early embryo development. The mouse *Gtsf1* knockout showed that female mice were found to be fertile (Yoshimura *et al.*, 2009). However, even though *GTSF1* knockout female mice ovulated, it is still possible that the gene affects oocyte developmental competence and/or early embryo development. Furthermore there may be differences in gene function between polyovular and monovular species and therefore investigating fertility potential and early embryo development in the sheep would be important. Further studies containing more oocytes for gene knockdown are required to investigate the effect of oocyte *GTSF1* knockdown on oocyte fertility and embryo development are required.

5.4.2 The impact of *GTSF1* on gene expression

Quantification of the levels of *GTSF1* expression of all MII oocytes following *GTSF1* knockdown by real-time PCR did not show a significant difference in comparison with controls. The MII oocytes that showed a reduction of more than 50% *GTSF1* expression were selected and verified by real-time PCR to have a significant reduction ($P<0.05$) in the levels of *GTSF1* following the siRNA injection (10.7 ± 3.2 arb. units, n=4) in comparison with their respective control buffer-injected oocytes (111.2 ± 58.6 arb. units, n=4). The transcript levels of target genes in the oocyte and the cumulus shells were assessed for these oocytes. Oocyte-derived genes *GDF9* and *BMP15* did not show significant differences in their expression levels relative to control samples ($P<0.05$) following *GTSF1* knockdown. The expression of *NOBOX2* was also evaluated in the oocytes because of its relationship to *GTSF1*. In particular, *GTSF1* functions downstream of *NOBOX* and *NOBOX is* a homeobox gene that is preferentially expressed in the oocytes and has been shown to be essential for folliculogenesis with an oocyte-specific gene expression in mice and humans (Huntriss *et al.*, 2006; Krotz *et al.*, 2009). The *GTSF1* knockdown did not show significant differences in the transcripts of *NOBOX2* in comparison with the controls ($P>0.05$). Generation of double stranded cDNA libraries in this experiment allowed for analysis of a total of 10 genes per sample by real-time PCR. Therefore, other than the 2 housekeeper genes and the 4 genes listed above, the expression of 4 additional candidate genes relevant to *GTSF1* predicted functions were examined. Genes associated with the miRNA-mediated gene silencing such as the trinucleotide repeat-containing gene 6A (*TNRC6A*) was analysed (Nishi *et al.*, 2013). The *TNRC6A* gene was selected in order to study the association of oocyte *GTSF1* knockdown with the RNAi pathway. This gene navigates the AGO protein into the nucleus to lead to miRNA-mediated gene silencing (Nishi *et al.*, 2013). Argonaute family proteins are responsible for binding of the miRNA to mRNA within the RISC that leads to repression of the target gene expression by either reducing the length of the poly-(A) tail of mRNA or by inhibiting translation (O'Carroll *et al.*, 2007). Knockout of *Ago2* in murine growing follicles was shown to result in oocyte maturation impairment which was accompanied by abnormal spindles and incorrect chromosome clustering (Kaneda *et al.*, 2009). Expression of the *LSM14A* gene was evaluated because of its relationship to RNA-processing in P-bodies (Gache *et al.*, 2010; Li *et al.*, 2012). As stated in the introduction of this Chapter, Piwi is a polar granule component that associates with Dicer and piRNAs along with their interacting proteins and is involved in retrotransposon silencing (Kuramochi-Miyagawa *et al.*, 2004). The association of

Gtsf1 knockout with retrotransposon activation as shown by (Yoshimura *et al.*, 2009), suggests that examination of targets involved with RNA-processing and storage following the *GTSF1* knockdown is worth investigating. The next 2 genes, *INCENP1* and *CDC20* were examined because of the possible functional role of *GTSF1* during meiosis, as indicated by its RNA-binding potential as well as the initial immunostaining experiments that indicated a possible association with cytokinesis of the chromosomes. Incenp is a regulatory protein in the chromosome passenger complex involved in the catalytic regulation of AURKB (Earnshaw and Cooke, 1991). In mouse oocytes it has been shown that the depletion of either *Incenp* or the combined inhibition of *AurkB* and *AurkC* activates the Apc/C before chromosome synapsis in meiosis I and prevents cytokinesis and inhibits the extrusion of the first polar body (Sharif *et al.*, 2010). The *CDC20* gene is the activator of APC/C. The Apc/C has been shown to have a role in the ubiquitination of Cyclin B and Securin and to induce their degradation along with its involvement in the physiological M-phase progression and the meiotic maturation of oocytes in many species (King *et al.*, 1995). Degradation of both Cyclin B and Securin during the first meiosis in mouse oocytes was reported to be mediated by Apc/C (Cdc20) activity, with Cdc20 initiating sister-chromatid separation (Reis *et al.*, 2007). The results showed no significant differences (P>0.05) in the expression levels between the *GTSF1* siRNA and the buffer control group for all genes investigated. The variability of the data throughout the interrogated cDNA double-stranded pooled oocyte samples was a restricting factor for interpretation of any trends in the data. Therefore increased numbers of samples and/or an alternative strategy should be devised for future experiments. Cumulus cell gene targets were also analysed for the cumulus shells that originated from co-cultures with the oocytes that were confirmed to have a significant level of *GTSF1* knockdown. The cumulus cell targets did not show any significant differences between the 2 treatment groups for any of the genes analysed (P>0.05). This latter observation suggests that *GTSF1* function is confined to the oocyte and that oocyte-derived *GTSF1* does not affect cumulus cell expansion or gene expression in the cumulus cells, although further experimentation is needed.

5.4.3 The impact of *GTSF1* on microtubule formation

A pilot study investigated the effect of *GTSF1* knockdown on meiotic spindle formation as illustrated by immunostaining of α-Tubulin. As stated in Chapter 1, microtubules are cytoskeletal filaments involved in spindle formation which are constructed by asymmetric α/β-tubulin heterodimers which confers microtubule polarity and serves to

transport molecules and organelles (Desai and Mitchison, 1997). Microtubule polarity controls transport to/from the end of the polymer and is mediated by microtubule motor proteins like Dyneins or members of the Kinesin superfamily (Kamal and Goldstein, 2002). The meiotic spindle is formed in the ooplasm following GVBD by organisation of the microtubules and motor proteins as well as microtubule associated factors (Karsenti and Vernos, 2001; Eichenlaub-Ritter *et al.*, 2004; Brunet and Maro, 2005). The results of this pilot study suggest that polymerisation of α-Tubulin on some degree of spindle formation had occurred in all 3 treatment groups (*GTSF1* siRNA-injected oocytes, buffer-injected and N.C. siRNA-injected oocytes) as oocytes from each group had matured *in vitro* to the MII stage. However, unlike the control oocytes, 2 of the 3 oocytes examined following *GTSF1* knockdown failed to show chromosome alignment at the equator of the spindle during meiosis II but rather the oocytes were shown to be at the pre-metaphase stage of the second meiotic division. The kinetochore structures found at the centromeres of some species bind to the forming microtubules (Vogt *et al.*, 2008). This process is regulated by kinetochore motor proteins including cytoplasmic dynein, Cenp-E and Mcak (Schaar *et al.*, 1997; Maney *et al.*, 1998; Hunter *et al.*, 2003). Cytoplasmic dynein is responsible for the direct movement of chromosomes, while Cenp-E contributes to chromosome alignment (Wood *et al.*, 1997) and Mcak protein is associated with disassembly of kinetochore fibres that allows movement of the chromosomes during anaphase (Hunter *et al.*, 2003). Kinases including the AurkB kinase and Map kinases have been shown to activate Mcak and other proteins associated with the kinetochore (Zhao and Chen, 2006; Ma *et al.*, 2010). AurkB in addition to other molecules like Incenp and Survivin that belong to the chromosomal passenger complex might be involved in cytokinesis due to the interaction of the chromosomal passenger complex with interpolar microtubules (Kelly *et al.*, 2007). It is considered therefore that both Mcak and AurkB act upstream of the spindle assembly checkpoint that monitors microtubule attachment and tension on chromosomes in both meiosis and mitosis (Vogt *et al.*, 2008). Although the number of oocytes examined in this study was very low, it is possible that *GTSF1* knockdown affects cytokinesis of the chromosomes in a direct or indirect manner. More detailed investigation is required to substantiate this hypothesis. Unfortunately the difficulties in obtaining enough MII oocytes after gene knockdown prevented further experimentation to confirm the above observations. In addition, immunostaining was not compatible with molecular evaluations on the same cell which is needed to confirm the level of knockdown and establish a direct connection between spindle defects and the knockdown itself. Alternative molecular

methods for the examination of the effects of *GTSF1* knockdown on oocyte maturation which include assessment of key genes involved in spindle formation and chromosome segregation therefore represents a more favourable alternative means of confirming and extending these preliminary observations on α-Tubulin and meiotic spindles.

5.4.4 Optimisation of microinjection and IVM co-culture systems

Generation of double-stranded DNA libraries successfully resolved the issue of DNA degeneration encountered in the validation experiments detailed in Chapter 4. In this series of experiments however, there was an observed variability in the *GTSF1* expression levels following the knockdown in comparison with the controls. This variability in the levels of knockdown could be attributed to the change of the outflow system during the microinjections, from a constant outflow of 40 hPa to a controlled start-stop outflow of 40 hPa. Based on the results presented here it is assumed that the latter method resulted in variable injection volume even though the pressure of 40 hPa was kept constant for about 0.5 sec. It is possible that the release of the flow (initiated by the start button) increased the 'release' pressure and therefore small variations in the time of injection could have resulted in differences of injection volume. Less volume injected into the oocytes could be responsible for the reduced levels of *GTSF1* knockdown. Furthermore, increased injection volume could be detrimental for the oocytes and this could be the reason for the reduced survival rates in comparison with the validation experiments of Chapter 4. For this reason, only the oocytes that showed a reduction of the *GTSF1* transcript of more than >50% following the knockdown in comparison with the controls were selected. For future experiments, the constant outflow system should be reinstated. Another possible explanation for the observed differences in the levels of *GTSF1* expression following *GTSF1* knockdown was that the selected siRNA species was not optimal for generation of a gene specific *GTSF1* knockdown. Perhaps pooling *GTSF1* siRNA-2 and siRNA-3 species would have been better since both siRNAs showed a significant reduction in the *GTSF1* expression. None-the-less, analysis of the oocytes that were retained at the GV stage at the end of each of the 4 cultures following injections with the different *GTSF1* siRNAs and control buffer injections verified the efficiency of the siRNA-2 in generating a high-level *GTSF1* knockdown.

Molecular analysis of target genes in the oocytes and the cumulus cells for the oocytes verified to have a significant reduction in their *GTSF1* expression levels along with

cumulus shells from the same culture drop also showed discrepancies in the data. The group cultures could be responsible for the observed variability in the expression levels of target genes. Although the developmental advantages of oocyte group cultures have been established in the validation experiments for the applied microinjection system (Cotterill, 2008), the autocrine and paracrine signalling between the maturing oocytes and their surrounding cumulus shells could affect gene expression. Since oocytes in the same culture drop might have had different levels of *GTSF1* knockdown, gene expression could be affected. Not all oocytes in the culture drop may have been competent to reach the MII stage. As a result, the different numbers of maturing oocytes present in each culture drop may have been present in each culture drop could have been responsible in part for the observed differences in gene expression from cells recovered from different drops. In addition, the effect of the morphogenic paracrine gradients as determined by the numbers and position of oocytes and cumulus shells within each culture drop may be a contributing factor in oocyte maturation (Hussein *et al.*, 2005). All of the above culture conditions could have a cumulative effect on the observed variability of gene expression in the individual MII oocytes analysed for both treatment groups. Therefore, for future experiments, the culture method should be changed to single oocyte co-cultures with a single oocytectomised cumulus shell per drop.

5.4.5 Conclusions

In conclusion, these experiments generated *GTSF1* knockdown in ovine oocytes by microinjection of gene specific siRNAs and have conducted pilot studies of the function of *GTSF1* on oocyte maturation in this species. The gene appears not to affect the maturation potential of sheep oocytes *in vitro*. However there are indications that *GTSF1* might have a functional role during oocyte maturation. Further investigations of the function of the gene in oocyte maturation and development are needed.

Chapter 6: Transcriptome analysis following *GTSF1* knockdown during ovine oocyte maturation *in vitro*

6.1 INTRODUCTION

Messenger RNA expression profiling has been developed in the recent years as a useful tool in order to identify factors that affect development in oocytes and early embryos (Chu *et al.*, 2012b). There have been a number of studies that have indicated the relationship between oocyte maturation and quality through measurement of mRNA abundance in various groups of genes (Robert *et al.*, 2000; Mourot *et al.*, 2006; Dorji *et al.*, 2012). The assessment of oocyte quality for these studies has been based on parameters such as (i) morphological evaluations (Fair *et al.*, 1995), (ii) timing of embryo development (Lechniak *et al.*, 2008), (iii) stage of follicular development and diameter of follicles during isolation of oocytes (Pfeffer *et al.*, 2007), (iv) *in vitro* or *in vivo* development (Lonergan *et al.*, 2003) and many more.

The acquisition of comprehensive mRNA expression profiles from biological samples has been enhanced significantly by the advent of microarray technology. Microarrays were first developed in 1995 by printing DNA microarrays onto glass microscope (Schena *et al.*, 1995). Since then, the development of microarrays into hybridisation-based assays which facilitate the comparison of gene expression levels has revolutionised the field of gene expression analysis (Gautier *et al.*, 2004). The goal of microarray analysis is to characterise genes and clusters of genes that coordinate gene expression during different biological states. In order to generate meaningful data, all components of the microarray mRNA expression measurements must be thoroughly evaluated. There can be numerous technical errors, hidden biological variances that are not relevant to the experimental processes as well as linear and non-linear systematic biases (Aimone and Gage, 2004). Technical variance can come from different sources including the array itself, different efficiencies of fluorescent dye labelling and hybridisation, location of array spots on the chip, gene-dye interactions and there can be technical variances in the RNA preparation method in addition to variations in the measurement method (Goryachev *et al.*, 2001). It is therefore necessary for the microarray data to be normalised and correctly analysed in order to remove technical variation and to accurately reflect gene expression levels in cells of different biological states (Irizarry *et al.*, 2003). The type of normalisation used depends on the type of

microarray platform used with the 2 main types being the 1 channel technology including Clontech membranes and Affymetric GeneChips that are hybridised with cDNA from 1 sample and the second being the 2 channel array that is hybridised with cDNA which is prepared from the 2 samples to be compared on 1 array (Shalon *et al.*, 1996).

The Affymetrix oligonucleotide chips are now considered to be a standard in microarray-based analyses (Lockhart *et al.*, 1996). These arrays have a high density of content and can be used not only for expression profiling but also for high-throughput mutation detection, chromosomal abnormalities detection and single nucleotide polymorphism genotyping. Their clinical applications include genetics, cytogenetics, oncology, pathogen recognition and pharmacogenetics (Ragoussis and Elvidge, 2006). The Affymetrix microarray system is based on photolithographic synthesis of oligonucleotides on microarrays, where a set of 11-20 oligonucleotide probes is used, each of which are 25 bases long to represent a gene. These GeneChips in particular represent a transcript, also called a probe-set, which contains 11 pairs of 2 nucleotides, 1 being a perfect match (PM) oligo to the mRNA reference sequence and another corresponding mismatch (MM) oligo that has an identical sequence to the PM oligo but with 1 central mismatch in the 25 bases as shown in Figure 6.1 (Irizarry *et al.*, 2003).
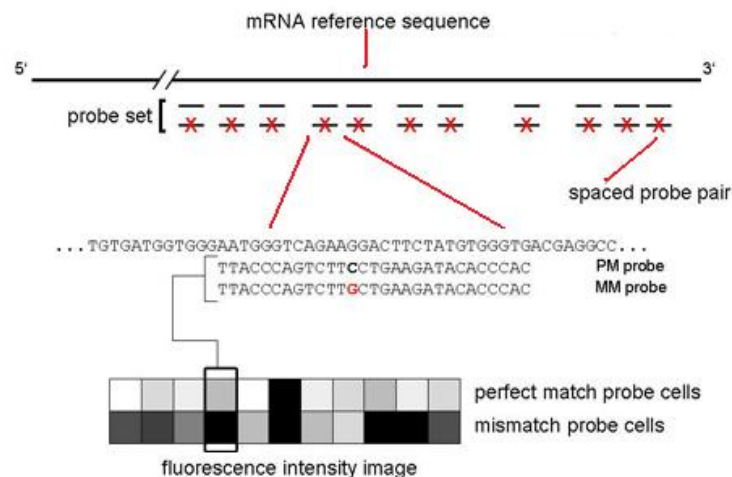
Figure 6.1: GeneChip expression array design. Image from: http://www.affymetrix.com.

The presence of mRNA is detected by the series of probe pairs that differ in 1 nucleotide. The use of the probe pair system allows the signals caused by non-specific cross hybridisation to be subtracted. The difference in signals between the probe pair is the indicator of specific target abundance. Gene expression is quantified by laser

scanning of the chip surface and the expression level for a gene represents the summary of the data from the whole probe set (Irizarry *et al.*, 2003). As it is shown in Figure 6.2, GeneChips are packed in cartridges that protect the chip and it is where the hybridisation takes place; hybridisation of fluorescent mRNA to each probe on the chip is indicated by the intensity of the feature on the array.
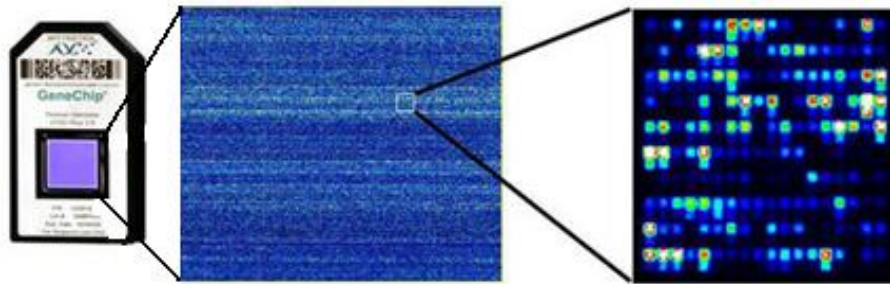
Figure 6.2: GeneChip in cartridge and fluorescent intensity image. **A:** GeneChip and Cartridge. **B:** Full expression array after scanning including all features **C:** Magnified view of a section of the array showing fluorescent intensity scan of 324 features. A wide range of intensities is observed. Black features represent no hybridisation to the probe (no intensity), while the intensity levels from highest to lowest by colour is: White, Red, Orange, Yellow, Green, Light Blue, Blue, Dark blue. Image from: http://www.affymetrix.com.

All microarray mRNA expression measurements components must be thoroughly evaluated in order to accurately characterise the gene expression patterns that are truly attributable to biological differences between samples. Other than the normalisation of the data for the removal of technical variance, the experimental design also has a vital role for the success of the microarray experiment. If it is not carefully planned it can significantly add to the technical variance of the data (Churchill, 2002). The elements that have to be considered when designing a microarray experiment are primarily the nature of the experiment and the number of experimental factors involved (Churchill, 2002). Other important points for consideration are the statistical power that is required in order to detect significantly differentially expressed genes between samples with a ratio greater or equal to a specific value. Consideration must also be given to the level of false discovery rate allowed, and the number of replicates required to provide more power for multiple significance testing (Hochberg and Benjamini, 1990). The presence of replicate spots of each cDNA oligonucleotide on the microarray slide provides technical precision for each hybridisation (Churchill, 2002).

The categorisation of genes on the basis of their shared functions otherwise known as functional grouping is considered to be a very powerful component of microarray analysis (Smith and Rosa, 2007). It enables the effect of a treatment to be evaluated

across an entire functional group of genes. Functional grouping is based on the assumption that if several genes belonging to 1 functional category and demonstrate similar patterns of change under a specific treatment, then each of the genes borrows significance from the neighbouring gene; thus the significance characterises the whole group. Several studies have used functional grouping for data analysis following the use of microarrays in oocytes, cumulus cells and embryos (Dorji *et al.*, 2012; O'shea *et al.*, 2012). Microarray studies can also be integrated from multiple studies of data that has already been normalised or by comparison of gene lists (Cahan *et al.*, 2007). This kind of meta-analysis increases the statistical power and can detect important effects that did not appear in individual analyses (Choi *et al.*, 2003). Using different datasets can therefore be an important tool to indicate candidate markers and biological pathways (Hong and Breitling, 2008). Meta-analysis on previously published microarray data on models of oocyte and embryo quality has been applied in a recent study that has identified candidate genes and networks of developmental competence in oocytes and cumulus cells (O'shea *et al.*, 2012). From this study, many potential biomarkers associated with increased and decreased competence in the oocyte and surrounding cumulus cells were identified. These included the negative regulation of *Wnt* signalling in several animal models of oocyte competence; the alpha thalassemia/mental retardation syndrome X-linked expression which was associated with decreased competence in the oocyte and the cumulus cells as well as the up-regulation of methionyl aminopeptidase 2 linked to mRNA and protein synthesis in competent oocytes (O'shea *et al.*, 2012).

From the above it can be understood that careful execution of microarray analysis is required, in order to competently characterise the gene expression profiles that are associated with developmental and reproductive processes. Previous studies have shown that microarray analysis can reveal the differentially expressed genes between various stages representative of follicular and oocyte development. For example, comparison of GV and MII stage oocytes produced from IVM experiments of adult and prepubertal Japanese black cattle has identified a number of differentially expressed genes of which subsequent gene ontological classification has revealed genes that are up-regulated in adult oocytes are associated with signal transduction, transcriptional control and transport (Dorji *et al.*, 2012). In a different study, the global analysis of gene expression in oocytes isolated from the early stages of human folliculogenesis has revealed a high expression of novel reproductive genes that are associated with functional categories

including RNA-binding, initiation of translation and structural molecule activity (Markholt *et al.*, 2012). In another study, human GV and IVM-produced MII oocytes were analysed by miRNA microarray that showed dynamic changes of specific miRNAs during meiosis (Xu *et al.*, 2011). The effects of the different ART protocols upon the *in vitro* production of cattle embryos at different laboratories have also been examined by microarrays and such analyses have proved useful for the confirmation of transferability of embryo production protocols (Plourde *et al.*, 2012). Microarray studies of gene expression have also been conducted to assess whether there were specific mRNA transcript profiles of granulosa cells that were associated with the oocytes that did or did not reach the blastocyst stage of embryo development (Gilbert *et al.*, 2012).

In summary therefore, a number of different approaches have used microarrays to study mRNA expression and to identify gene pathways during mammalian oocyte development and under specific experimental conditions. The applications of microarray technology will also allow examination of the function effects of novel genes during oocyte development and maturation, such as *GTSF1*. This can be achieved by comparison of oocyte mRNA transcripts following targeted gene knockdown in comparison with the control oocyte samples. The results of the last 3 cultures of Chapter 5 in which both buffer control and N.C. siRNA-injected oocytes were used as controls showed that there were no significant differences (P>0.05) in oocyte maturation levels or the degree of cumulus expansion for the 2 control treatment groups. Taking into consideration the advantages offered by the N.C. siRNA control in that it mimics the effect of the gene specific siRNA injection by entering RISC but ensuring minimal non-specific effects on gene expression and phenotype, N.C. siRNA will be used as the preferred control in all subsequent gene knockdown studies. Therefore generation of *GTSF1* knockdown oocytes and N.C siRNA control oocytes can be used for transcriptome analysis by microarray. The unique challenges faced in this thesis relative to other studies was (i) the creation of oocytes in which *GTSF1* has been proven to be knocked down; (ii) the generation of verified quality libraries from single oocytes and (iii) the necessity to carry out the arrays on such small number of samples that limits the amount of RNA available for array experiments. To overcome the first problem, *GTSF1* knockdown must first be proven in each oocyte to be analysed by array. In order to overcome the last difficulty it is necessary to amplify the cDNA libraries as described previously (Chapter 2, Section 2.2.4), something that added to the complexity of the project.

6.1.1 Aims

The aims of this chapter were therefore to generate *GTSF1* knockdown oocytes and assess their ability to progress to the MII stage as well as cumulus expansion following co-culture with cumulus shells in comparison with N.C. siRNA controls. The levels of *GTSF1* knockdown were then determined and a comprehensive microarray analysis using Affymetrix GeneChip microarrays was used to identify gene expression differences between the siRNA *GTSF1* injected oocytes and N.C. siRNA-injected control oocytes. Bioinformatic analysis was used to further characterise the differentially expressed genes in these treatment groups by performing gene ontology analysis and functional annotation of the candidate genes. Finally, differentially expressed genes identified by the arrays were verified by real-time PCR.

6.2 MATERIALS AND METHODS

6.2.1 Generation of *GTSF1* knockdown

This series of cultures for the generation of the *GTSF1* knockdown oocytes took place between October 2011 and February 2012 and a total of 17 cultures were conducted. The methodology followed was slightly different to the methodology described in Chapter 5. For this experimental series, only 2 injection groups were used: *GTSF1* siRNA and N.C. siRNA. Furthermore, the constant outflow system set at 40 hPa was reinstated as described in Chapter 4, Section 4.2.1 to try to compensate for the inconsistencies in the levels of *GTSF1* knockdown and the poor oocyte survival observed in the Chapter 5 results. Additionally, the co-culture conditions of microinjected oocytes and oocytectomised cumulus cells were adjusted. Specifically, on the second day of the cultures, the co-cultures were established by culturing single oocytes with single oocytectomised cumulus shells instead of group co-cultures of 5 oocytes with 5 cumulus shells. This alteration was implemented to increase the quality of the microinjection data such that results would originate from single oocytes with clear developmental checkpoints monitored and level of the knockdown established. The IVM dishes contained an additional 6 peripheral IVM drops; each containing 2μl of IVM media. The drops were overlaid with mineral oil. A total of 6 dishes were prepared prior to the culture and allowed to equilibrate at 39°C for 24 h at 5% CO_2, 6% O_2 and 89% N_2 atmosphere. The steps followed are shown in Figure 6.3.
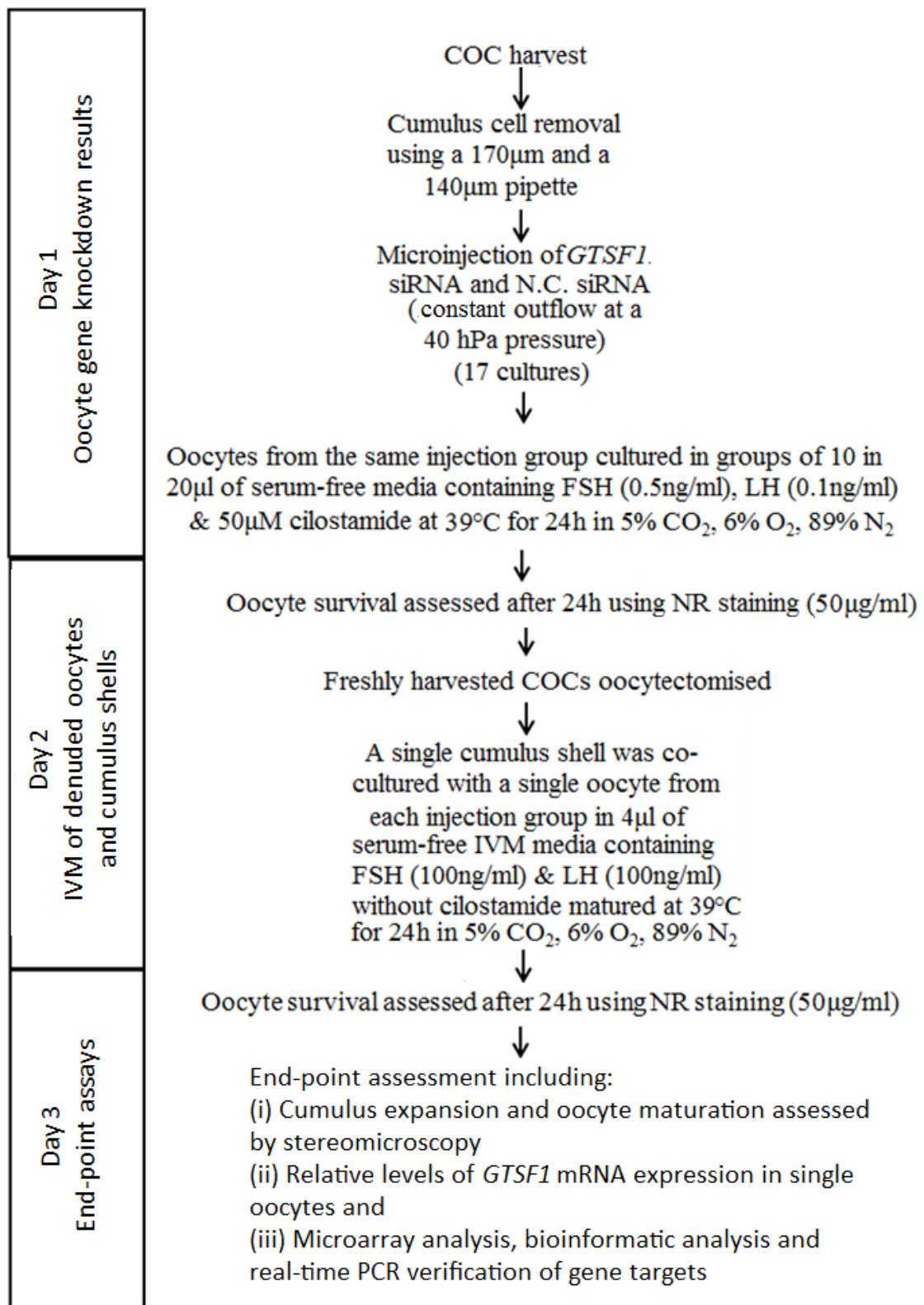
Figure 6.3: Schematic representation of the *GTSF1* siRNA procedure followed and the end-points following generation of *GTSF1* knockdown.

The experimental process for the co-cultures of single oocytes with single cumulus shells was as follows: Viable oocytes were selected at 24 h of culture from both injection groups *GTSF1* siRNA and N.C. siRNA. Equal number of COCs were oocytectomised and groups of 6 oocytes from each experimental group that survived the

injection process as indicated by the NR stain, were transferred in the central drop of previously prepared 35 mm IVM dish containing 20μl of IVM media (Chapter 2, Table 2.3). For each oocyte that survived the first 24 h of culture, 1 oocytectomised cumulus shell was also transferred into the central drop. Single oocytes along with 1 cumulus shell were then transferred to 1 of the peripheral drops in a pipette volume of 2 μl to give a final culture volume of 4 μl per oocyte/cumulus co-culture. Cumulus coverage and expansion was scored at the start of IVM as described previously (Chapter 4, Section 4.2.2). The same process was followed for all dishes of the 2 treatments and the time at which each of the plates was placed into culture was noted. This alteration of culture conditions from group oocyte co-culture to single oocyte co-culture with a single oocytectomised cumulus shell was applied to help reduce interactions between oocytes with different levels of gene knockdown (as established at the end of the cultures) and oocytectomised cumulus shells contained within the same drop. All developmental assessments took place at the end of the 24 h period of IVM co-culture. These included oocyte survival, oocyte maturation, cumulus cell coverage and expansion. Single oocytes were then transferred in labelled 1.5 ml microcentrifuge tube containing 10 μl of lysis buffer (Chapter 2, Table 2.4). Single cumulus shell samples were also stored individually in lysis buffer. All samples were stored in -80°C until subsequent analysis.

6.2.2. Molecular analysis

This experimental series utilised the Affymetrix GeneChip bovine genome arrays (Affymetrix, High Wycombe, UK) to study the expression of over 23,000 gene transcripts. At the time that the analysis took place, no equivalent ovine genome arrays were available from Affymetrix, therefore the bovine genome arrays were selected because of the close relation of the genomes between the 2 species (Dalrymple *et al.*, 2007). In the recent years there has been a substantial amount of research conducted in cattle with several ESTs being available in public databases. The bovine genome has also been assembled (Womack, 2005). The sheep genome has not yet been fully sequenced (Dalrymple *et al.*, 2007). The individual knockdown oocytes produced by the microinjection of *GTSF1* siRNA and N.C. siRNA were compared to assess the function of *GTSF1* during ovine oocyte maturation and the libraries from the 2 groups were then used for comparison of mRNA expression levels based on the analysis of the Affymetrix GeneChip bovine arrays. Next, the cDNA libraries from the 2 groups were hybridised to the Affymetrix GeneChip bovine arrays in order to ascertain whether

GTSF1 depletion affected global mRNA expression in ovine oocytes and to identify a series of gene targets that could clarify the function of *GTSF1* in the mammalian oocyte.

6.2.2.1 Experimental setup and sample preparation for microarrays

The first step before proceeding with the microarray analysis was to assess the level of *GTSF1* knockdown in the siRNA-injected oocytes. Microinjected oocytes for the 2 injection groups were thawed and then subjected to the mRNA isolation as described in Chapter 2, Section 2.2.2. The samples were re-suspended in 3 µl of Tris-HCl followed by incubation on a hot block at 90° for 2 min. The mRNA was then separated from the Dynal magnetic bead apparatus and the cDNA was synthesised by reverse transcription as described in Chapter 2, Section 2.2.3. After cDNA synthesis, long distance PCR of total cDNA was performed for all individual oocyte libraries as detailed in Chapter 2, Section 2.2.4. The level of knockdown for each of the *GTSF1* siRNA-injected oocytes in comparison with the control oocytes injected with N.C. siRNA from the same culture repeat was determined by real-time PCR as described in Chapter 2, Section 2.4. After analysing all individual oocyte MII samples, a total of 14 *GTSF1* injected oocyte cDNA libraries were identified which demonstrated a significant reduction (P<0.005) in the *GTSF1* knockdown level of >50% in comparison with the N.C. siRNA-injected control oocytes. The 14 *GTSF1* siRNA-injected oocytes were divided based on their levels of *GTSF1* knockdown, 5 showed a high-level knockdown, 5 showed a medium-level knockdown and 4 showed a low-level knockdown when compared with the N.C. siRNA controls. A total of 6 arrays were performed, 3 arrays to analyse the pools of oocyte cDNA from the *GTSF1* siRNA-injected group (high-level knockdown, medium-level knockdown, low-level knockdown) and 3 arrays to analyse the pools of oocytes from their respective controls injected with N.C. siRNA. The microarrays were conducted on the basis of the levels of knockdown as follows:

      Microarray set A: (based on high-level knockdown of *GTSF1*)

            Sample A1: 5 pooled *GTSF1* siRNA-injected oocytes

            Sample A2: 5 pooled N.C. siRNA-injected oocytes

      Microarray set B: (based on medium-level knockdown of *GTSF1*)

            Sample B1: 5 pooled *GTSF1* siRNA-injected oocytes

            Sample B2: 5 pooled N.C. siRNA-injected oocytes

      Microarray set C: (based on low-level knockdown of *GTSF1*)

            Sample C1: 4 pooled *GTSF1* siRNA-injected oocytes

            Sample C2: 4 pooled N.C. siRNA-injected oocytes

All individual oocyte cDNA libraries were then purified from the residual PCR reactions components (primers, nucleotides, polymerases and salts) using the QIAquick PCR purification kit protocol and a microcentrifuge (Qiagen). Specifically, from each cDNA library, 15 μl were placed in a new sterile microcentrifuge tube and 5 volumes of buffer PB (75 μl) were added to 1 volume of the PCR sample and mixed by pipetting. The mixture was then added into a QIAquick spin column and the column was placed into a 2 ml collection tube (provided in the kit). To bind DNA, the tube was then centrifuged for 1 min at maximum speed. The flow-through was discarded and the QIAquick column was placed back into the same tube. For the next step, 750 μl of buffer PE were added to the QIAquick column and centrifuged for 1 min at maximum speed in order to wash the samples. The flow-through was once again discarded and the column was placed back in the same tube followed by an additional centrifugation for 1 min at maximum speed to remove residual wash buffer. The QIAquick column was then placed in a clean 1.5 ml microcentrifuge tube and 20 μl of sterile-distilled H_2O were added to the centre of the column. The column was then left to stand for 1 min at RT followed by centrifugation for 1 min at maximum speed in order to elute the DNA. The concentration of each of the purified cDNA samples was measured and recorded using a NanoDrop ND 1000 spectrophotometer (Thermo-Scientific). Subsequently, an aliquot of the cDNA from each of the individual oocytes was pooled together in order to create the pooled sample pairs (A1:A2, B1:B2, C1:C2) that were then used for array analysis. For each microarray, 2 μg of cDNA were required (total concentration per array) and therefore equal amount of cDNA were pooled into sterile 1.5 ml microcentrifuge tube to create a volume that was determined by the cDNA concentration of each of the individual samples. All 6 pooled samples were then vacuum-dried in a centrifuge (Savant Speed Vac, Thermo-Scientific) set at 35° C for 30 min at 5000 rpm before being sent for analysis.

6.2.2.2 Microarray analysis

Following mRNA extraction and cDNA synthesis (as described above), all pooled samples and arrays (total of 6 pooled samples and 6 arrays) were sent to for analysis (Figure 6.4). The microarray analysis was conducted by the University of Glasgow's Affymetrix service (Glasgow Polyomics, http://www.gla.ac.uk/colleges/mvls/research institutes/gpf/microarrays/facilities-theaffymetrixservice/). For the microarray analysis, samples were labelled with Biotin by using uracil bases tagged with Biotin when cDNA was *in vitro* transcribed back to RNA (cRNA). Subsequently, the labelled cRNA was

randomly fragmented in pieces ranging from 30 to 400 base pairs length using an RNA fragmentation buffer and the fragmented Biotin-labelled cRNA was then hybridised to the array. Next, the arrays were washed in order to remove unbound RNA and then stained with Cy5 conjugated to streptavidin that binds to Biotin. Finally the whole array was scanned with a laser and to generate the gene expression data.
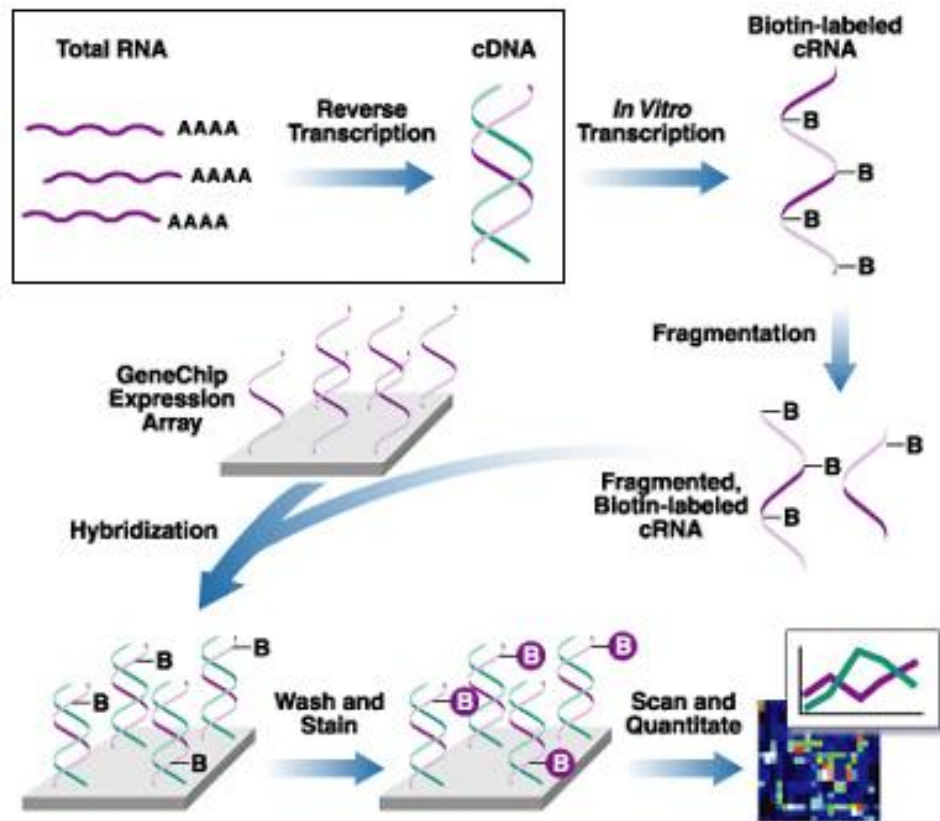
Figure 6.4: Schematic overview of the different steps involved in an Affymetrix GeneChip experiment. Steps in box represent the steps that took place prior to sending the samples for analysis to the Affymetrix service (Downloaded from: http://www.affymetrix.com).

6.2.2.3 Bioinformatic analysis

The bioinformatic analysis that followed generation of the mRNA expression levels for the 2 treatment groups in each of the 3 array sets (A, B and C) for treatments and controls was performed in co-operation with Lee Hazelwood and Praveen Baskaran (Bioinformatics Technology Group, Biomedical and Health Research Centre, Faculty of Biological Sciences and Leeds Institute of Molecular Medicine, University of Leeds). As there were no replicates in each array, the arrays were grouped into AB (A1+B1 vs. A2+B2), BC (B1+C1 vs. B2+C2) and ABC (A1+B1+C1 vs. A2+B2+C2) for comparison assuming A and B microarray sets were replicated in AB (Section 6.2.2.1). Similarly for the ABC, A, B and C microarray sets were considered replicates. The AB

sample group was assumed as high-level knockdown, while the BC sample group was considered a low-level knockdown. The raw Affymetrix files were originally analysed using AFFY and affyPLM (Probe Level Models) packages and normalised using the Robust Multichip Averaging (RMA) method (Bolstad *et al.*, 2004; Gautier *et al.*, 2004; Alvord *et al.*, 2007). AFFY is a package of functions for the storage, management and analysis of Affymetrix probe level data written in the statistical scripting language R (Gautier *et al.*, 2004). This package includes analytic routines including some of the most widely used algorithms and the number of statistical routines included into R makes it operator friendly for customisation of existing functions (Gautier *et al.*, 2004). The affyPLM package, extends and improves the functionality of the base AFFY package by implementing methods for fitting probe-level models and tools using models of compiled code for heavily used routines and includes several PLM based quality assessment tools (Alvord *et al.*, 2007). The PLMs are used for high-density oligonucleotide microarrays with multiple probes per gene like the ones used in this study in order to obtain quality measures (Ritchie *et al.*, 2006). In addition, the image plots of robust weights or residuals produced from robust PLMs can indicate artefacts on the array surface to assist quality assessment at the array level (Ritchie *et al.*, 2006). The RMA procedure was used for normalisation of the arrays as this procedure is generally used for background correction, normalisation and summarisation of probe-level data in order to obtain expression level data and find which genes are differentially expressed (Alvord *et al.*, 2007). Following normalisation, the differentially expressed genes were identified using linear models for microarray data (LIMMA) R package using fold change=1.0 and P<0.05 as cut off value for gene selection (Ritchie *et al.*, 2006). Linear models provide a suitable tool for measuring and testing differential expression in microarray experiments by combining many different RNA sources (Kerr, 2003; Smyth, 2004). This approach allows combination of a wide variety of microarray experiments including common reference experiments without complicating the analysis when compared with simple replicated experiments (Ritchie *et al.*, 2006). Multiple testing corrections were then applied using the Benjamini-Hochberg method, however the adjusted P-values were greater than P>0.0.5 and the values were therefore used without corrections. Finally, the differentially expressed genes were annotated using the bovine.db package from bioconductor (Affymetrix bovine annotation data, chip bovine, http://www.bioconductor.org/packages/2.12/data/annotation/html/bovine. db.html). The differentially expressed genes under each condition were separated into up and down-regulated gene lists. Gene ontology analysis was performed using Bingo

in Cytoscape software (Cline *et al.*, 2007). By using this software, the measurements of expression profiles were filtered and used to map cellular processes and their dynamics. This was conducted by combination of expression profiles with cellular network information including protein-protein interactions as well as DNA-protein interactions to reveal the mechanisms behind biological processes as well as genes and mechanisms affected by the different treatment groups from the arrays (Cline *et al.*, 2007). For the analysis of this data set, over-represented ontologies were reported using the Hyper-geometrix test with Benjamini-Hochberg False Directory Rate Correction. The cut off value was set at P<0.05. Functional annotation of the differentially expressed genes was then carried out using DAVID web tools (Huang *et al.*, 2009). These enrichment tools play an important role and have been shown to contribute to the gene functional analysis of large gene lists for many different high-throughput biological studies such as microarrays (Huang *et al.*, 2009).

6.2.2.4 Real-time PCR verification of target genes

The bioinformatic analysis revealed lists of potential gene targets that were either up-regulated or down-regulated following *GTSF1* specific knockdown in oocytes. Real-time PCR was used to validate the expression profile of selected transcripts to confirm the differences in the expression levels of transcripts between the *GTSF1* siRNA-injected oocytes and the control N.C. siRNA-injected oocytes. The differential expression of candidate transcripts for the 2 different treatment groups was examined in individual oocyte cDNA libraries by real-time PCR as detailed in Chapter 2, Section 2.4, relative to the expression of housekeeper genes *GAPDH* and *H2A* as detailed in Chapter 2, Section 2.4, with minor modifications. Only the oocyte cDNA libraries from the high knockdown group A and their respective N.C. siRNA controls were used for the real-time PCR analysis. Since the oocyte cDNA libraries used for the analysis were amplified by long distance PCR and were also PCR purified as described in Section 6.2.2.1, 5 µl of each sample in a 1:100 dilution in sterile-distilled H_2O were used for each individual oocyte analysis. This dilution was determined by serial dilution and real-time PCR analysis of 3 control cDNA libraries of single uncultured denuded oocytes that were created using the same methodology as the treated samples. Each individual oocyte cDNA library was analysed with 4 repeats for each test gene and 4 repeats for the housekeeper gene. For each reaction the volume of sterile-distilled H_2O was reduced to 6.25 µl (Chapter 2, Section 2.4). The primer information and sequences used are shown in Table 6.1.

Table 6.1: Real-time PCR primer sequences of targets genes following *GTSF1* knockdown and microarray primary bioinformatic analysis

Gene	Primer Sequence	Size (bp)	Reference
MYL9	F: 5´ TCATCCATGAGGACCACCTT 3´	134	(Harhay *et al.*, 2005) (bovine)
	R: 5´ GCGGGTGAACTCCACATAGT 3´		
MYL12A	F: 5´ CATCCCTCCAAATCTGTGCT 3´	127	(Harhay *et al.*, 2005) (bovine)
	R: 5´ ATAGAACCTTCGGGGGCTAA 3´		
CKAP2	F: 5´ GGGCTGTGAAACTGATGCTT 3´	137	(Zimin *et al.*, 2009) (bovine)
	R: 5´ CAGCCAACCACTCTTGGAAT 3´		
AURKA	F: 5´ TTGGATCAGCTGGAGAGCTT 3´	154	(Uzbekova *et al.*, 2008) (bovine)
	R: 5´ AGGCTCCAGAGGTCCACTTT 3´		
CDK2	F: 5´ GCTCACTGGCATTCCTCTTC 3´	134	(Zimin *et al.*, 2009) (bovine)
	R: 5´ ACCCATCTGCGTTGATAAGC 3´		
COX17	F: 5´ ATTGAAGCCCACAAGGAGTG 3´	124	XM002684734 (predicted bovine)
	R: 5´ TCAGCAAGGAACTCCCAAAG 3´		
PCBP1	F: 5´ CGGAATTGACTCCAGCTCTC 3´	153	(Zimin *et al.*, 2009) (bovine)
	R: 5´ GACATCTGGCGGATCTCATT 3´		
FKBP4	F: 5´ TTGCTGTAGCGACCATGAAG 3´	153	(Zimin *et al.*, 2009) (bovine)
	R: 5´ TCAGGTCCTCACCCTTGAAC 3´		
ZNF706	F: 5´ CGTGGACAGCAGAAGATTCA 3´	149	(Strausberg *et al.*, 2002) (bovine)
	R: 5´ TTAGGGTCTGGCATTTGTGTC 3´		
TECR	F: 5´ GCGTGGATGGCCTATTACAT 3´	125	(Zimin *et al.*, 2009) (bovine)
	R: 5´ GCCATGTGGATGGAGAAGTT 3´		
TIMP1	F: 5´ CCCAGACATCCGATTCATCT 3´	140	(Galloway *et al.*, 2000) (ovine)
	R: 5´ CAAAACTGCAGGTGGTGATG 3´		

MYL: Myosin regulatory light polypeptide *CKAP2*: Cytoskeleton associated protein 2, *COX17*: Cytochrome c oxidase copper chaperone, *PCBP1*: Poly-(rC) binding protein-1, *FKBP4*: FK506 binding protein 4, *ZNF706*: Zinc finger protein 706, *TECR*: Trans-2,3-enoyl-co-enzyme A reductase, *TIMP1*: Tissue inhibitor of metalloproteinase 1.

6.2.2.5 Secondary bioinformatic analysis

A secondary bioinformatic analysis was needed as the primary bioinformatic analysis in combination with the real-time PCR verification of target genes revealed discrepancies in the data. These differences could be attributed to the fact that the GeneChip arrays used in the study were based on bovine genome, while the samples were of ovine origin. This meant that although the 2 species share a close homology in their genome, there could still be a significant amount of incorrect hybridisation between the arrays and the samples. Therefore, a different approach bioinformatic analysis (secondary bioinformatic analysis) took place in which only the bovine probe sequences that aligned to the sheep genome sequence were selected. The secondary analysis was led by Dr. David Iles from the Faculty of Biological Sciences of the University of Leeds. For this analysis the latest release of the sheep genome (Oar3.1) was used to forge a Biostrings package BSgenome.Oaries. ISGC.Oarv3.1 for probe mapping. This latest release has been passed onto the University of California Santa Cruz (UCSC) and the NCBI by the sheep genome sequencing consortium for annotation and genome browser

track assembly, and also included a significant amount of unmapped scaffolds. These were written into the new package as well to maximise coverage of the sheep genome. All the individual bovine probe sequences were thereafter aligned to the mapped and unmapped sheep genome sequence. Only probes with perfect matches to the sheep genome were taken forward. The individual (raw, unprocessed) probe intensities were then extracted from the arrays and those that did not match the list of mapped probes were discarded. For quality control purposes, both PM and MM data were included. A novel algorithm (SCAN.UPC, http://www.bioconductor.org/packages/2.12/bioc/html/SCAN.UPC.html) was then used for processing and normalising the bovine arrays. This code has been specifically written for difficult arrays such as those hybridised to RNAs extracted from fixed and embedded tumour samples, and allows therefore more flexibility than standard methods. In particular, rather than processing microarray samples as groups that can have biases and be more complicated, it normalises each sample individually by removing probe and array background noise using data from within each array. A LIMMA analysis was thereafter ran on the SCAN-normalised data. In the analysis the designated arrays A1, B1 and C1 were considered as factors in the matrix design along with A2+B2+C2 as control input (C) and A1 vs. C, B1 vs. C and C1 vs. C were contrasted using the 'topTable' function within Bioconductor to identify a gene list containing the transcripts with the most significant changes in expression from start to end of the experiment. The probes generated from topTable were annotated using the bovine probe Generic Feature Format 3 (GFF3, http://www.sequenceontology.org/gff3.shtml) from AFFY (Gautier *et al.*, 2004). These probes were then attached to the individual probe intensities for each topTable transcript. From there some bovine probe sequences were found to hit multiple sites in the sheep genome, but others appeared to hit unique loci in the sheep genome, and the latter were shown to be well represented in the final results.

6.2.2.6 Real-time PCR verification of target genes from the secondary bioinformatic mapped sequences

The transcripts that were identified from the secondary bioinformatic analysis were analysed with real-time PCR to verify the microarray results. All transcripts analysed corresponded to bovine array probes that had been successfully matched to the ovine genome. A total of 9 candidate gene transcripts were analysed by real-time PCR. Real-time analysis was performed as described in Chapter 2 with modifications as described in Section 6.2.2.4. Once again, only the individual oocyte cDNA libraries from the high

knockdown group A1 and the N.C. siRNA controls from A2 were used for the analysis. The primer information and sequences used are shown in Table 6.2.

Table 6.2: Real-time PCR primer sequences of targets genes following *GTSF1* knockdown and secondary microarray bioinformatic analysis

Gene	Primer Sequence	Size (bp)	Reference
TCOF1	F: 5´ TTGTGACACCCCAAGTCAAA 3´	165	XM004023527 (ovine)
	R: 5´ TGGCAGGACTAGGAGCAACT 3´		
PARP12	F: 5´ GGCTTGGACCACCTCAACTA 3´	105	(Zimin *et al.*, 2009) (bovine)
	R: 5´ CGGTCCATCTCCTTTGTTGT 3´		
RPS8	F: 5´ ACCGACAGTGGTACGAGTCC 3´	155	(Harhay *et al.*, 2005) (bovine)
	R: 5´ ACTGCTGATTTTCGCGTTCT 3´		
SREK1IP1	F: 5´ TGTGCTTACCAGGTGCAGAC 3´	126	XM004016940 (predicted ovine)
	R: 5´ TTTTAAAGGCGGCTACTGGA 3´		
CACNA1D	F: 5´ TGTCCAAAGGCCTTCAATTC 3´	125	(Zimin *et al.*, 2009) (bovine)
	R: 5´ TTGAGCTGGGAACTTGCTTT 3´		
TARDBP	F: 5´ CCGGAATCCAGTGTCTCAGT 3´	176	(Zimin *et al.*, 2009) (bovine)
	R: 5´ TCTGGACCGCTCTTTTCACT 3´		
DHX35	F: 5´ GGGTCAGACTGGGATGAAGA 3´	190	XM004014573 (predicted ovine)
	R: 5´ CTTCACGAAGCCACAGTCAA 3´		
PELO	F: 5´ CCGGCCTAGAATTTCTTTCC 3´	111	XM004014573 (predicted ovine)
	R: 5´ TCCTTCCTCACGAGCTTCAT 3´		
IGFBP7	F: 5´ ATTTGAGCTGCGAGGTCATC 3´		NM001145181 (ovine)
	R: 5´ CACCCAGCCAGTAGCTTCAT 3´		

TCOF1: Treacher Collins-Franceschetti syndrome 1, *PARP12*: Poly adenosine diphosphate (ADP)-ribose polymerase 12, *RPS8:* Ribosomal protein S8, *SREK1IP1:* Splicing regulatory glutamine/lysine rich protein 1 interacting protein 1, *CACNA1D:* Calcium channel, voltage-dependent, L type alpha 1D subunit, *DHX35*: DEAH box polypeptide 35, *PELO*: Protein pelota homolog, *IGFBP7*: Insulin-like growth factor binding protein 7.

6.2.3 Statistical analysis

Chi-square tests were used to analyse the results of oocyte survival, meiotic progression, cumulus coverage and cumulus expansion according to proportional analysis of the cohort of oocytes and cumulus within each treatment. Normally distributed data for oocyte mRNA levels of *GTSF1* as determined by Anderson-Darling, were compared using Student's t-test. For the primary bioinformatic analysis, the raw Affymetrix files were analyzed using AFFY and AFFYPLM R packages and the data were normalized using the RMA method. The differential expressed genes were identified using LIMMA R package using fold change=1.0 and P<0.05 as cut off for gene selection. The Benjamini-Hochberg method was used for multiple testing correction, but the adjusted P-values were greater than 0.05. The P-values were therefore used without corrections. For gene ontology analysis using Bingo in Cytoscape, over-represented ontologies were reported using Hypergeometric test with Benjamini-Hochberg false discovery rate correction and cut off value P<0.05.

Secondary bioinformatic analysis used a novel algorithm (SCAN.UPC) to process and normalise the raw probe intensities extracted from the arrays that were aligned to the sheep genome. The differentially expressed genes were identified using the LIMMA R package using fold change=1.0 and P<0.05 as cut off for gene selection. For real-time PCR that followed primary and secondary bioinformatic analysis, normally distributed data for mRNA levels of *MYL9*, *MYL12A*, *CKAP2*, *AURKA*, *CDK2*, *COX17*, *PCBP1*, *FKBP4*, *ZNF706*, *TECR* and *TIMP1* from the primary bioinformatic analysis and *TCOF1*, *PARP12*, *RPS8*, *SREK1IP1*, *CACNA1D*, *TARDBP*, *DHX35*, *PELO* and *IGFBP7* from the secondary bioinformatic analysis were compared using Student's t-test. Values for real-time data presented are the arithmetic means ±SEM for the number of observations shown. The experimental plan followed for the Microarrays and the bioinformatics analysis is shown in Figure 6.4.

Assessment of the level of *GTSF1* k/d in the siRNA oocytes
⇓
Selection of the oocytes with the higher levels of *GTSF1* k/d along with their respective controls and grouping them into a total of 6 arrays for Microarray analysis
⇓
Microarray analysis

Bioinformatic analysis	Secondary bioinformatic analysis
⇓	⇓
Quality assessment of the data	Bovine probe sequences aligned to the sheep
⇓	⇓
Normalisation using the RMA method	Normalisation (SCAN.UPC algorithm)
⇓	⇓
Identification of differentially expressed genes using LIMMA	Identification of differentially expressed genes (LIMMA)
⇓	⇓
Annotation of genes (Bioconductor)	Annotation of genes (Bioconductor)
⇓	⇓
Gene ontology (Cytoscape)	Gene ontology (Cytoscape)
⇓	⇓
Functional annottation (DAVID)	Functional annottation (DAVID)
⇓	⇓
Real-time PCR verification of target genes	Real-time PCR verification of target genes

Figure 6.5: Schematic representation of the experimental plan followed for the microarray analysis after *GTSF1* knockdown.

196

6.3 RESULTS

6.3.1 Generation of *GTSF1* knockdown oocytes

In a total of 17 cultures, 425 oocytes were injected with the *GTSF1* siRNA, while 415 were injected with N.C. siRNA.

6.3.1.2 Oocyte survival after microinjection

Oocyte survival was assessed at 24 h and 48 h of culture. A total of 77/425 oocytes (18.1%) survived the first 24 h of culture when injected with *GTSF1* siRNA and 102/415 oocytes (24.6%) survived the N.C. siRNA injections (Figure 6.6). At 48 h the survival rates remained largely unaffected with a total of 74/77 *GTSF1* siRNA-injected oocytes surviving (96.1%) and 100/102 N.C. siRNA-injected oocytes surviving (98%). No significant differences (P>0.05) in survival were observed between the 2 injection groups at the 2 time points demonstrating that knockdown of *GTSF1* or injection of N.C. siRNA *per se* does not affect oocyte viability.
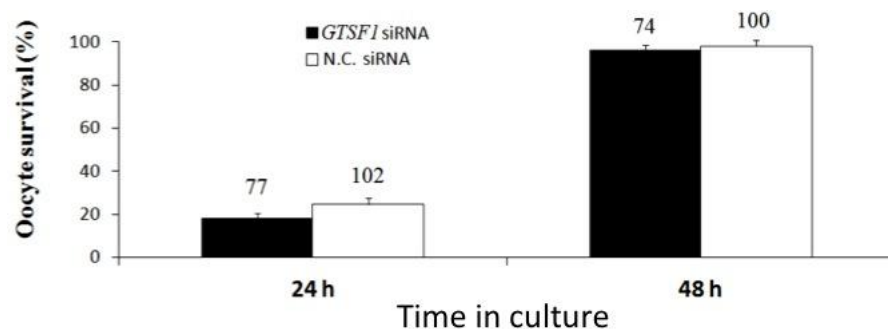
Figure 6.6: Influence of *GTSF1* siRNA injection and N.C. siRNA injection on oocyte survival at 24 and 48 h of culture. Before the first time point, oocytes were denuded, microinjected with either *GTSF1* siRNA or N.C. siRNA and cultured in serum-free media with cilostamide (20 mg/ml) and basal levels of gonadotrophins for 24 h. Surviving oocytes were then co-cultured individually with oocytectomised cumulus shells in serum-free IVM media and maturation inducing levels of gonadotrophins for an additional 24 h. Values represent proportions of the total cohort of injected oocytes over 17 repeat cultures. Individual bars show the mean ±SEM for independent cultures with the numbers of oocytes falling into each category shown. No significant differences were observed (P>0.05).

6.3.1.3 Impact of *GTSF1* on meiotic progression

The developmental competence of oocytes following microinjection and IVM was assessed by evaluating MII progression of oocytes after 48 h of culture. There were no significant differences (P>0.05) between the proportions of viable GV oocytes injected with *GTSF1* siRNA at 24 h of culture, which progressed to MII (42/77 oocytes, 54.5%) in comparison to 47.1% of N.C. siRNA-injected control oocytes (48/102 oocytes) as shown in Figure 6.7.

197
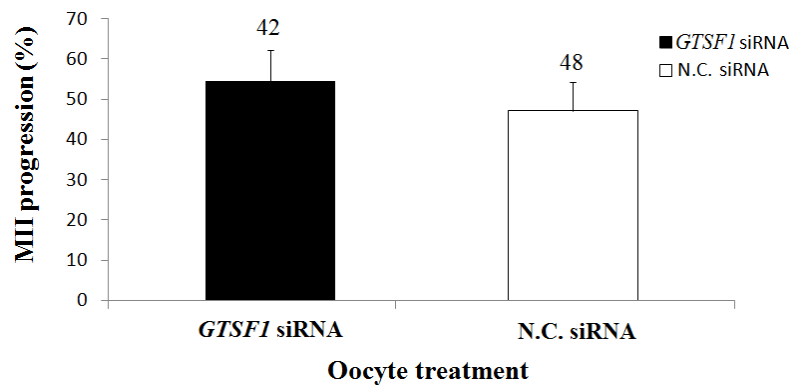
Figure 6.7: Impact of *GTSF1* knockdown on meiotic progression of viable *GTSF1* siRNA and N.C. siRNA-injected oocytes as determined at 24 h of culture that were subjected to an additional 24 h of IVM co-culture with cumulus shells. Values represent proportions of surviving oocytes over 17 repeat cultures. Individual bars show the mean ±SEM for independent cultures with the numbers of oocytes falling into each category shown. The 2 groups did not demonstrate any significant differences (P>0.05).

6.3.1.4 Effect of oocyte *GTSF1* knockdown on cumulus expansion

The cumulus shell mass and expansion were assessed at the start of oocyte and cumulus cell co-culture and at the end of the 24 h IVM co-cultures. Equall numbers of cumulus shells and viable oocytes were co-cultured individually (single oocyte with single cumulus shell) for each treatment. For this experimental series, a total of 77 cumulus shells were oocytectomised and co-cultured with viable *GTSF1* siRNA-injected oocytes, while 102 cumulus shells were co-cultured with viable N.C. siRNA-injected oocytes. Cumulus shell mass classification remained unchanged during the period of the co-culture for both treatments and comparison of the cumulus coverage for the 2 groups at the end of the culutre showed no significnat differences (P>0.05) (Figure 6.8).
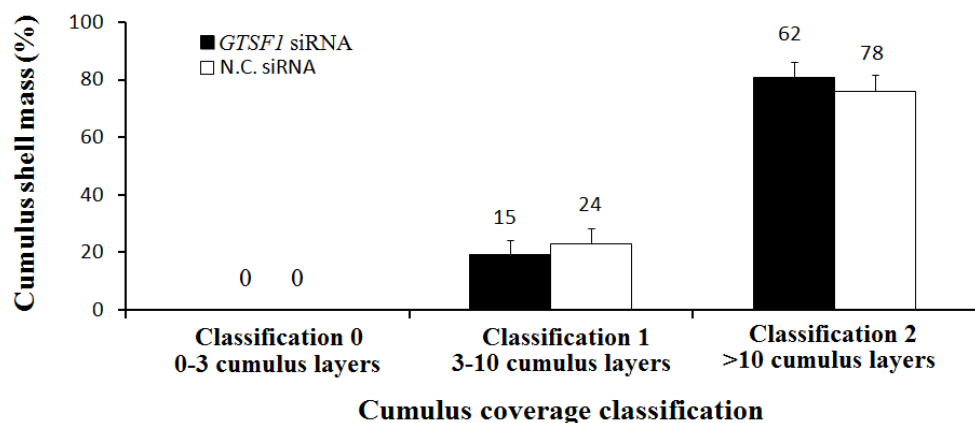
Figure 6.8: Effect of *GTSF1* knockdown on cumulus shell mass classifications after 24 h of individual cumulus shell co-culture with individual *GTSF1* siRNA or N.C. siRNA-injected oocytes. Individual bars show the proportions of cumulus shells from 17 different cultures. The numbers of cumulus shells falling into each category are shown. Individual bars show the mean ±SEM for independent cultures with the numbers of cumulus shells falling into each category shown. No significant differences were observed (P>0.05).

Analysis of cumulus expansion showed that knockdown of *GTSF1* in oocytes did not have a significant effect (P>0.05) on the expansion of cumulus shells compared to the N.C. siRNA-injected control group (Figure 6.9).
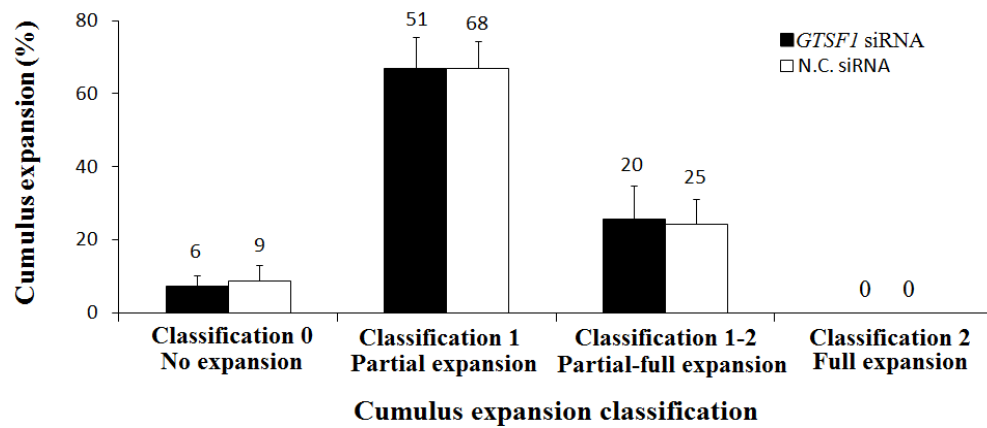
Figure 6.9: Effect of oocyte *GTSF1* knockdown on cumulus expansion following 24 h of individual cumulus shell co-culture with individual *GTSF1* gene knockdown oocytes compared to co-cultures of individual cumulus shells with individual N.C. siRNA-injected oocytes. Individual bars show the proportions of cumulus shells from 17 repeated cultures. The numbers of cumulus shells falling into each category are shown. Individual bars show the mean ±SEM for independent cultures with the numbers of cumulus shells falling into each category shown. No statistically significant differences were noted (P>0.05).

Cumulus shells from the *GTSF1* siRNA injection group were not able to expand fully but rather expand up to an intermediate stage between partially and fully expanded. Similar observations were made for the N.C. siRNA group. This suggests that group culture of oocytes and cumulus shells as used in Chapters 4 and 5 is better able to support cumulus expansion than the single oocyte/cumulus shell cultures used in the current experimental series.

6.3.1.5 Molecular analysis of *GTSF1* gene expression following *GTSF1* knockdown

All single MII oocytes were analysed for their expression of *GTSF1* by real-time PCR. A total of 42 MII oocytes from the *GTSF1* siRNA injection group along with their respective control N.C. siRNA MII oocytes (42 control oocytes) were analysed. Real time analysis showed that *GTSF1* expression was significantly reduced (P<0.005) in all oocytes following *GTSF1* siRNA injection (1.5±0.1 arb. units, n=42) in comparison with the N.C. siRNA controls (2.8±0.2 arb. units, n=42) (Figure 6.10.a). From the cohort of MII oocytes, a total of 14 MII oocytes had levels of *GTSF1* transcript reduced by >50% in comparison with the control oocytes, indicative of a successful outcome of the siRNA experiments in these oocytes. Furthermore, these 14 oocytes were confirmed

by real-time PCR to have a significant reduction (P<0.005) in the *GTSF1* transcript levels following *GTSF1* siRNA injection (0.8±0.1 arb. units, n=14) in comparison with the N.C. siRNA controls (2.7±0.3 arb. units, n=14) (Figure 6.10.b). These oocytes were selected for transcriptome analysis using microarrays.
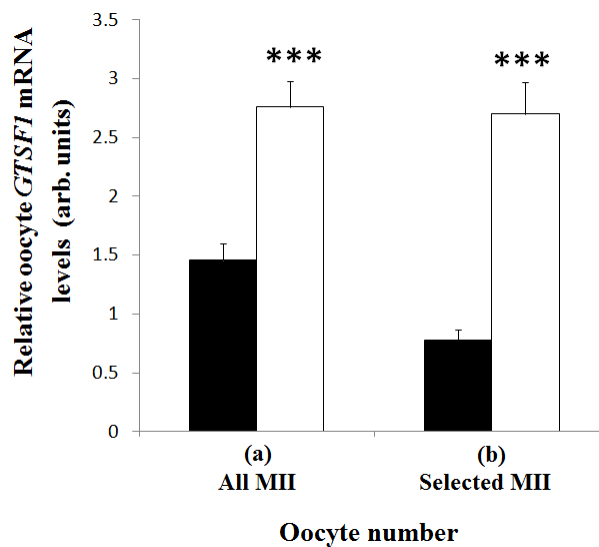
Figure 6.10: Real-time PCR quantification of the effect of *GTSF1* siRNA injection on the *GTSF1* expression levels of **(a)**: All MII oocytes (n=42) injected with *GTSF1* siRNA and their respective N.C. siRNA controls, **(b)**: Selected MII oocytes (n=14), that showed a relative reduction in the *GTSF1* expression level of over 50% in comparison with the N.C.siRNA controls. The data were standardised against the oocyte *GAPDH* and *H2A* mRNA levels. Individual bars show the mean ±SEM for (a) 42 repeat cDNA libraries and (b) 14 repeat cDNA libraries (each cDNA library analysed in triplicate). Each cDNA library contained a single oocyte. The *GTSF1* siRNA-injected oocytes exhibited a statistically significant difference for the *GTSF1* mRNA levels (***=P<0.005) when compared against the buffer-injected control samples for both oocyte populations.

Oocytes were further grouped on the basis of their *GTSF1* transcript levels in comparison with the controls (Figure 6.11). The 5 oocytes producing the higher level of *GTSF1* knockdown (0.5±0.1 arb. units, n=5) in comparison with the controls (2.9±0.4 arb. units, n=5) were pooled together. Similarly, the 5 control oocytes injected with N.C. siRNA were pooled and both arrays consisted the microarray group A (A1 being the *GTSF1* injected oocytes and A2 the N.C. siRNA-injected control oocytes). The next 5 MII oocytes producing a medium-level of *GTSF1* knockdown (0.9±0.1 arb. units, n=5) in comparison with the controls (2.5±0.2 arb. units, n=5) were also pooled together and the corresponding N.C. siRNA-injected control oocytes were also pooled to create the microarray group B (B1 and B2 respectively). The last 4 oocytes producing a low-level knockdown of *GTSF1* transcript (1.1±0.1 arb. units, n=4 following *GTSF1* siRNA injection in comparison with controls (2.8±0.8 arb. units, n=4) and their associated controls comprised the microarray group C (C1 and C2 respectively).
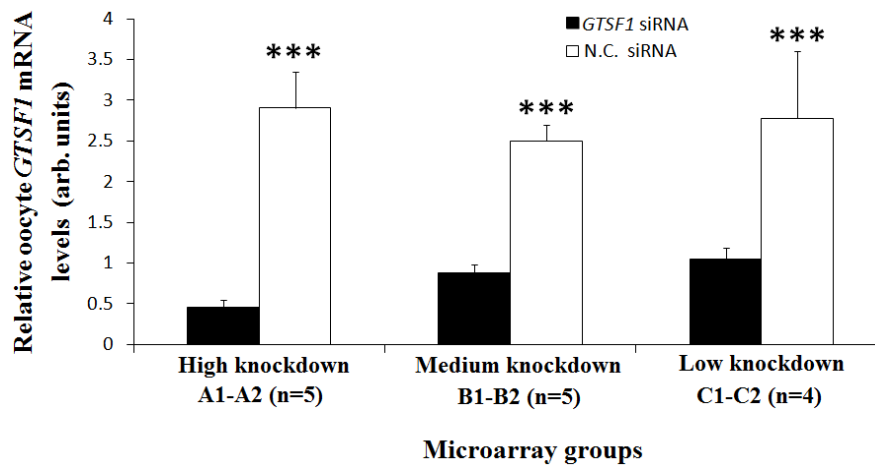
Figure 6.11: Real-time PCR quantification of the effect of *GTSF1* siRNA injection on oocyte *GTSF1* mRNA levels for oocytes comprising each microarray group (treatment and control). The data was standardised against the oocyte *GAPDH* and *H2A* mRNA levels. Individual bars show the mean ±SEM for 5 individual oocytes (A, B) and 4 cDNA libraries containing individual oocytes (C) (each library analysed in quadruplicate). *GTSF1* siRNA-injected oocytes exhibited a statistically significant difference for the *GTSF1* mRNA levels (***=P<0.005) when compared against their respective N.C. siRNA-injected oocytes.

6.3.2 Primary bioinformatic analysis

Following microarray analysis, the first step for the bioinformatic analysis was the quality assessment of the data. In order to do that, an exploratory data analysis took place in which the image plots of the (PM and MM) probe-level data were observed for anomalies including spatial artefacts or other non-homogenous patterns. The image plots for the 6 conducted arrays appeared similar to each other with no obvious anomalies (not shown). The next step involved plotting box-plots and density plots of the probe-level data to determine whether any arrays were potentially defective.
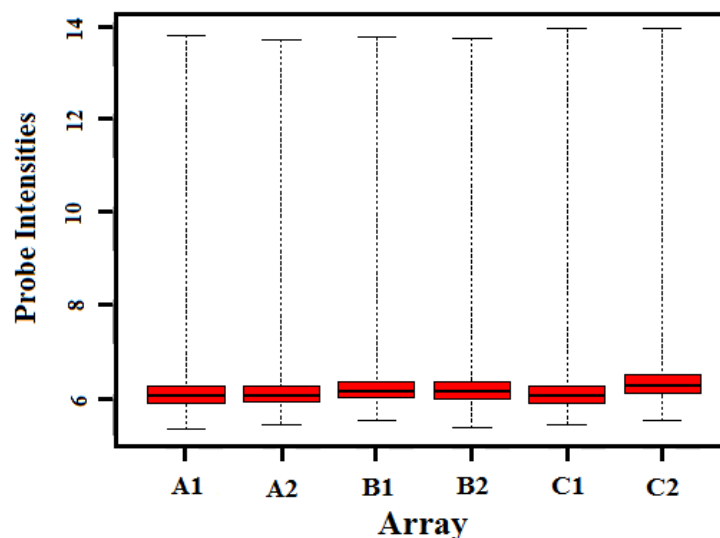
Figure 6.12: Box-plots of ovine probe intensities from 6 arrays. Probe level data A1, B1 and C1, corresponding to *GTSF1* siRNA-injected oocytes and A2, B2 and C2, corresponding to N.C. siRNA-injected oocytes.

201

By plotting box-plots of the arrays, marginally different ranges or displaced boxes from the box-plots inter-quartile ranges (IQR) indicate defective arrays (Heber and Sick, 2006). Similarly, by observing the density plots, defective arrays could be noticed when there were densities that were not in the other arrays, or when arrays have different shapes, bimodalities and other abnormalities (Heber and Sick, 2006). The box-plots as shown in Figure 6.12 showed a similar distribution on the log scale for the first 5 arrays (A1, A2, B1, B2 and C1) with their inter-quartile ranges overlapping to each other, while there was a different distribution of the probe intensities observed in the C2 array. From the density plots shown in Figure 6.13 there were no bimodalities or other abnormalities between the first 5 arrays (A1, A2, B1, B2, C1), whilst bimodalities were observed for the C2 array. Together the density plots and box-plots conducted for the 6 arrays suggest good quality in 5/6 microarrays.
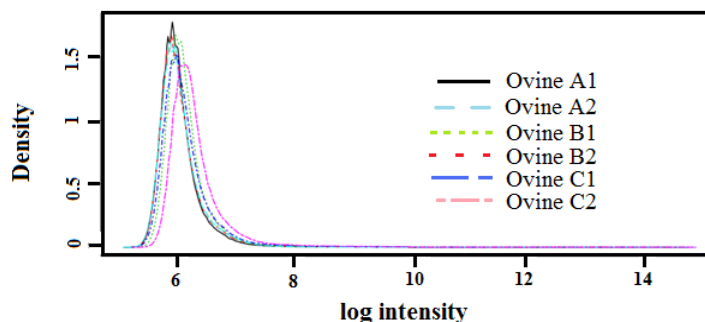
Figure 6.13: Density plots of ovine probe densities from 6 arrays. Probe level data A1, B1 and C1, corresponding to *GTSF1* siRNA-injected oocytes and A2, B2 and C2, corresponding to N.C. siRNA-injected oocytes.

Exploratory plots were then created as an additional quality assessment of the microarrays. These plots are generally used when different arrays are to be compared (Alvord *et al.*, 2007). For comparing more than 2 arrays, a synthetic approach is created by using the probe-wise medians across all arrays (Bolstad *et al.*, 2004). Figure 6.14 shows the MA plots for all 6 arrays with the median synthetic array centred at zero. The MA-plot is a plot of the distribution of the log of the red/green intensity ratio ('M') plotted by the log of average intensity ('A'). A locally weighted scatter-plot smoothing (LOESS) regression line (indicated by red colour) is also illustrated in each of the MA plots. The MA plot provides an overview of the distribution of the data. Since most of the genes in the array would not show changes in their expression levels, they would be located at 0 on the y-axis (M) since Log(1) is 0. The straight red LOESS regression lines for all 6 arrays passing close to 0 suggests that the arrays did not have quality issues.
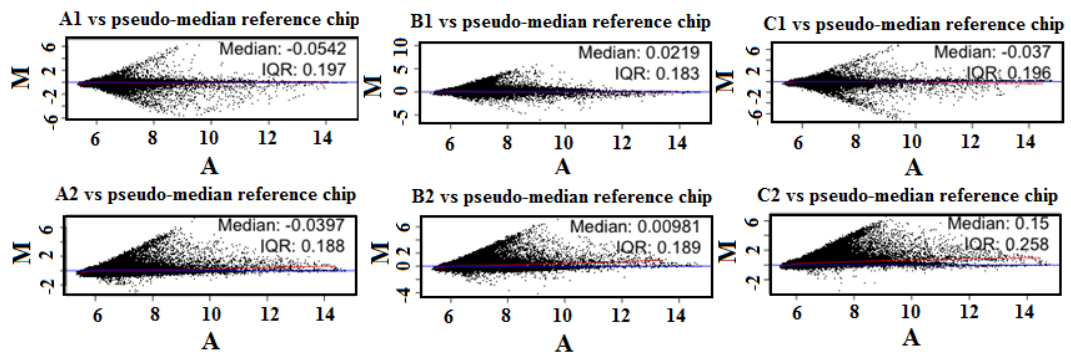
Figure 6.14: MA plots of 6 arrays of probe level data versus the synthetic (median) array, centred at zero. A LOESS regression line was added to each of the plots.

Using the Bioconductor package, RNA degradation was detected (Alvord *et al.*, 2007). For all microarrays, individual probes were sequentially numbered from the 5´ end of the targeted transcript and if severe degradation of RNA occurs, the PM intensities were found to be elevated at the 3´ of the probe set in comparison with those at the 5´ end. The average of all probe's RNA degradation within each array are shown in Figure 6.15. No severe RNA degradation was noticed for the first 5 arrays (A2, A2, B1, B2 and C1), while some RNA degradation was apparent for the C2 array.
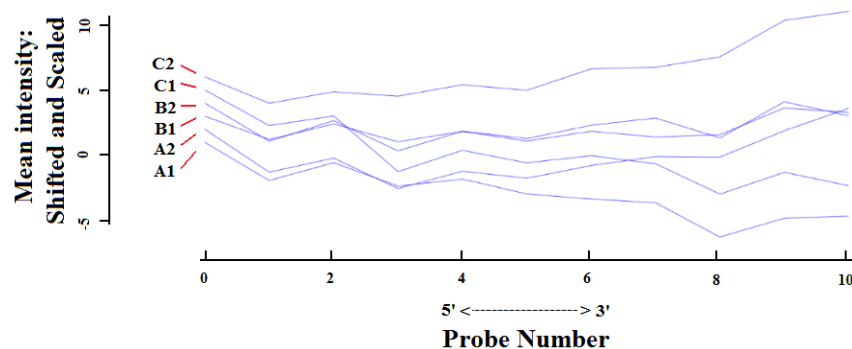
Figure 6.15: RNA degradation plot for 6 microarrays.

Following pre-processing of the data, it was necessary to transform results into a final expression value for each gene. For Affymetrix data sets, this usually involved 3 steps which are background adjustment, normalisation and summarisation (Huber and Gentleman, 2004). Background adjustment was necessary and observed intensities needed adjustment to avoid taking into account non-specific hybridisation caused by noise in the optical detection system. Normalisation was necessary to compare measurements between different array hybridisations that have much variability caused by several reasons including transcription efficiency, labelling, hybridisation and more. Finally, summarisation was necessary because the transcripts were represented by multiple probes and therefore for each gene, both adjusted background and normalised

probe intensities needed to be represented into 1 final value. The RMA method was used for this procedure and the probe-level data were transformed into expression level data with a single expression level value for each gene. The box-plot following RMA background adjustment, normalisation and summarisation is shown in Figure 6.16. The alignment of the expression level values following RMA transformation indicated the success of the normalisation and summarisation procedure and not the quality of the probe level data.
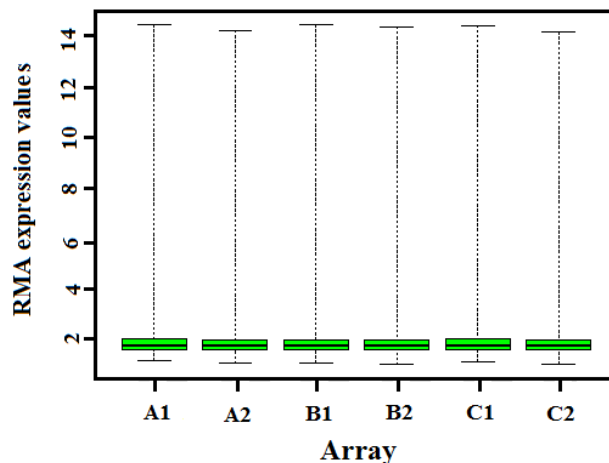
Figure 6.16: Box-plots of ovine expression level data of the 6 arrays following RMA background adjustment, normalisation and summarisation.

Following transformation of the data, the differentially expressed genes between the 2 treatments were identified. Because there were no replicates for each array conducted, the arrays were grouped into AB, BC and ABC for comparison assuming A and B were replicates in AB grouping. Similarly for the ABC group, A, B and C were considered replicates, while B and C were considered replicates for the BC group. The 3 groups were compared and differentially expressed genes were identified using fold change=1.0 and a P<0.05 as the cut off for gene selection, but multiple testing correction did not reveal any statistical significance. Therefore the P-values were used without being corrected. The differentially expressed genes annotated using the bovine.db R package, were separated to down-regulated and up-regulated for each condition. The genes with altered expression levels for each group are shown in the Venn diagrams (Figure 6.17). From the diagrams, it can be observed, that there were a number of genes whose expression was altered for each group of arrays (AB, BC and ABC) in comparison with controls. There were only a few transcripts that were common in all groups. Some transcripts were identified to be differentially expressed in 2 groups in comparison to controls, but most genes were either up-regulated or down-regulated within individual groups. Out of these groups of arrays, the AB assumed as a

higher-level knockdown, was considered as the most important to follow-up. The list of down-regulated and up-regulated genes from the AB group as determined from the Venn diagrams are shown in Appendix IV.
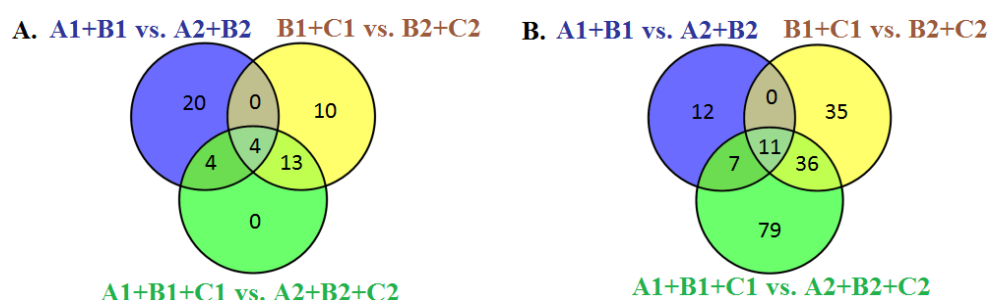
Figure 6.17: A: Venn diagrams showing number of differentially expressed genes that were **A:** down-regulated and **B:** Up-regulated, as determined by primary bioinformatics analysis of *GTSF1* knockdown oocytes vs. control oocytes. Grouped arrays were compared to find common differentially expressed transcripts using a 1 fold change and no significance cut offs.

Table 6.3: Ontology analysis of *GTSF1* knockdown following primary bioinformatic analysis

Biological Processes
Down-regulated genes: The affected biological processes included oocyte development, oogenesis, oocyte differentiation, oocyte morphogenesis, oocyte growth, as well as RNA processing, actin cytoskeleton organisation, actin filament spindle assembly, maintenance of cell polarity, maintenance of apical/basal cell polarity.
Up-regulated genes: Annotation of up-regulated genes revealed genes involved with spindle assembly checkpoint, cell cycle checkpoint, regulation of chromosome segregation, post-transcriptional regulation of gene expression, negative regulation of ossification and bone mineralisation, regulation of protein stability, steroid metabolic process, cellular component organisation, cell division and organelle organisation.
Cellular components
Down-regulated genes: Gene ontology analysis of down-regulated cellular components included intracellular organelle parts, non-membrane bounded organelles, microtubule organising centre, cytoskeletal part, microtubule basal body, ribonucleoprotein complex, macromolecular complex, protein complex as well as mitochondrial components.
Up-regulated genes: The list of cellular components based on annotation of up-regulated genes included spindle, microtubule organising centre, condensed chromosome kinetochore, chromosomal part, protein complex, intracellular organelle part, endoplasmic reticulum part, intracellular membrane-bounded organelle, cytoplasm, endoplasmic reticulum membrane and nuclear membrane-endoplasmic reticulum network
Molecular functions
Down-regulated genes: Molecular functions affected following *GTSF1* knockdown were nucleotide binding, DNA-binding, cell adhesion molecule binding, calcium ion binding, ATP dependent helicase activity, helicase activity, motor activity, pyro-phosphatase activity, hydrolase activity acting on acid anhydrides, hydrogen ion trans-membrane transporter activity, cytochrome c oxidase activity and oxido-reductase activity
Up-regulated genes: These included structure-specific DNA binding, polyubiquitin binding, enzyme binding, protein kinase binding, metallo-chaperone activity, oxido-reductase activity, histone-kinase activity, serine/threonine kinase activity, cyclin-dependent kinase activity.

Gene ontology analysis of the genes from the AB group was then carried out to define representing gene product properties. The ontology analysis covered 3 domains being

(i) the cellular component that includes cellular and extracellular environment; (ii) molecular function defined by the activity of the gene at a molecular level; and (iii) biological processes that portray the function of the cells. The ontology analysis generated for down-regulated and up-regulated genes from the AB microarray group following *GTSF1* knockdown is shown in Table 6.3. The product properties from the gene ontology analysis incorporated several different properties, covering maturation, spindle formation, and RNA processing. Most of these processes are in agreement with the background information concerning the inferred function of *GTSF1* and reveal the importance of this gene during the maturation stages of the oocyte.

6.3.3 Real-time PCR verification of transcripts from the primary bioinformatic analysis

Real-time PCR was used to verify the gene-targets originating from the primary bioinformatic analysis. The gene targets originated from the list of down-regulated and up-regulated genes that were identified to have different expression in the AB knockdown group (Appendix IV). The targets included *AURKA*, *CDK2*, *COX17*, *ZNF706*, *TECR*, *PCBP1*, *FKBP4* and *TIMP1* from the down-regulated gene list and *MYL9, MYL12A* and *CKAP2* from the up-regulated gene list. Differential expression of the transcripts for the 2 different treatment groups was examined from the individual oocyte cDNA libraries of the high knockdown group (5 oocytes of A1) and the N.C. siRNA controls (5 oocytes of A2). One cDNA library from the treated samples was disregarded due to contamination; therefore a total of 4 individual cDNA libraries were interrogated for their expression levels of each of the target primers. Only a small number of oocytes were analysed in this experimental series and few of the data attained statistical significance. Never-the-less the results presented in Figure 6.17 show striking trends of the impact of *GTSF1* knockdown on the expression of key genes which are known to have important functional roles in cell division. Further replicates are required to substantiate the current observations. Individual transcript levels of *COX17*, *PCBP1*, *TECR* and *ZNF706* were very variable between the *GTSF1* knockdown cDNA libraries and were therefore disregarded prior to the analysis (data not shown). As shown in Figure 6.18.a., transcript analysis of the down-regulated genes showed that expression levels of *AURKA* were reduced in the *GTSF1* knockdown group (0.3 ± 0.1 arb. units, n=4) in comparison with the controls (1.1 ± 0.4 arb. units, n=4), but this reduction was not significant (P>0.05) due to the relatively small number of samples analysed. Similarly, *FKBP4* and *CDK2* transcript levels were reduced in the knockdown group

(0.4±0.1 arb. units, n=4; 0.3±0.1 arb. units, n=4) respectively in comparison with the controls (5.2±2.9 arb. units, n=4; 2.9±1.3 arb. units, n=4), but these reductions were not significant (P>0.05). For all 3 target genes, although there was a high rate of reduction in the expression levels between knockdown and controls, the control data were still quite variable between individual libraries and produced large error bars. Transcript levels of *TIMP1* showed a significant reduction (P<0.05) between the knockdown and controls transcript levels (0.5±0.1 arb. units, n=4) in comparison with the controls (5.0±1.5 arb. units, n=4). Real-time PCR did not verify the results from the primary bioinformatic analysis for the up-regulated genes (Figure 6.18.b).
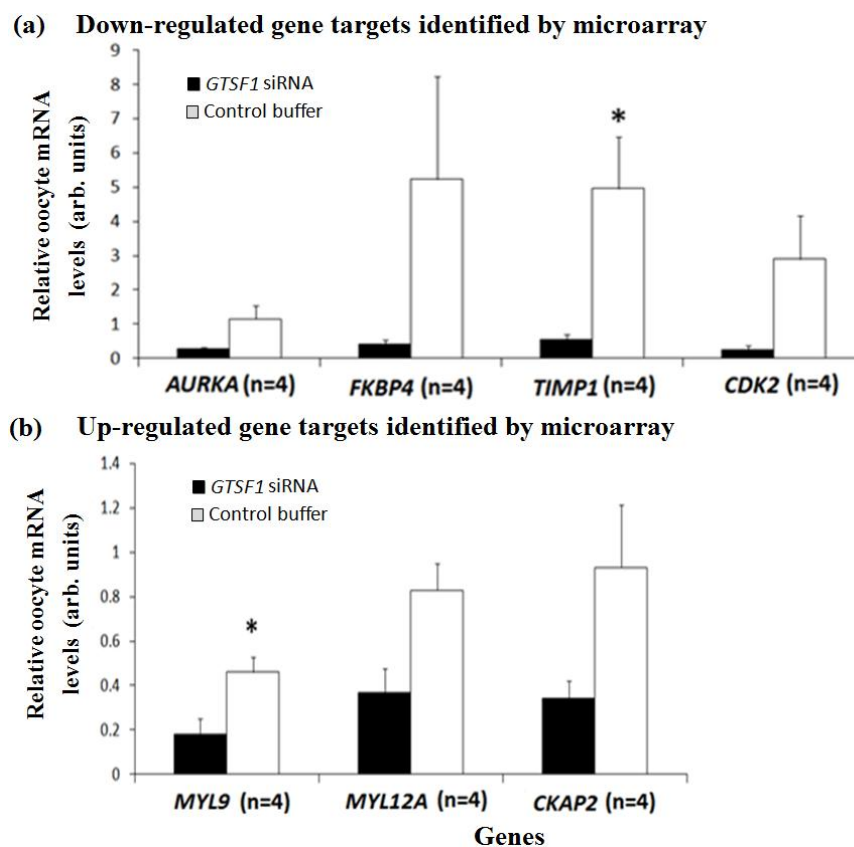
Figure 6.18: Real-time PCR quantification of the effect of *GTSF1* knockdown on target gene expression cDNA derived from high-level *GTSF1* knockdown oocytes (n=4) that were analysed individually by real-time PCR shown together with the data for N.C. siRNA oocytes (n=4) based on **(a):** Down-regulated genes and **(b):** Up-regulated genes identified by primary bioinformatic analysis. The data was standardised against the oocyte *GAPDH* and *H2A* mRNA levels. Individual bars show the mean ±SEM for 4 individual oocyte cDNA libraries (each library analysed in quadruplicate). *GTSF1* knockdown oocytes exhibited a statistically significant difference for the *TIMP1* and *MYL9* mRNA levels (*=P<0.05) when compared against the N.C. siRNA oocytes, while no other significant differences were observed (P>0.05) due to the variability of the control data.

Gene transcript levels of *MYL9* were significantly reduced (P<0.05) in the *GTSF1* knockdown oocytes (0.2±0.1 arb. units, n=4) in comparison with the controls (0.5±0.1 arb. units, n=4). Transcript levels of *MYL12A* were also reduced (0.4±0.1 arb. units,

n=4) following *GTSF1* knockdown in comparison with the controls (0.8±0.1 arb. units, n=4), while *CKAP2* transcript levels were reduced (0.3±0.1 arb. units, n=4) compared with the controls (0.9±0.3 arb. units, n=4), but no significant differences were shown (P>0.05).

6.3.4 Secondary bioinformatic analysis

The variability of the data from the primary bioinformatic analysis and the lack of concordance between the array data and the real-time PCR verification data of target genes meant that there could have been a large number of incorrect hybridisations between the bovine arrays and the ovine samples. A different analytical approach was therefore necessary, in which the bovine probe sequences from the arrays were aligned to the sheep genome sequence and these were used to annotate genes and provide targets for real-time PCR verification. Only 2 bovine probes were matched to the sheep *GTSF1* sequence. The microarray A1 containing the high-level knockdown oocytes, the microarray B1 containing medium-level knockdown oocytes and the microarray C1 containing low level knockdown oocytes were all contrasted to controls (A2+B2+C2). After the secondary bioinformatic analysis, the list of candidate transcripts that were confirmed to be up-regulated in *GTSF1* depleted oocytes was entirely different to those identified during the primary analysis. The number of genes with altered expression levels for each group is shown in the Venn diagrams in Figure 6.19.
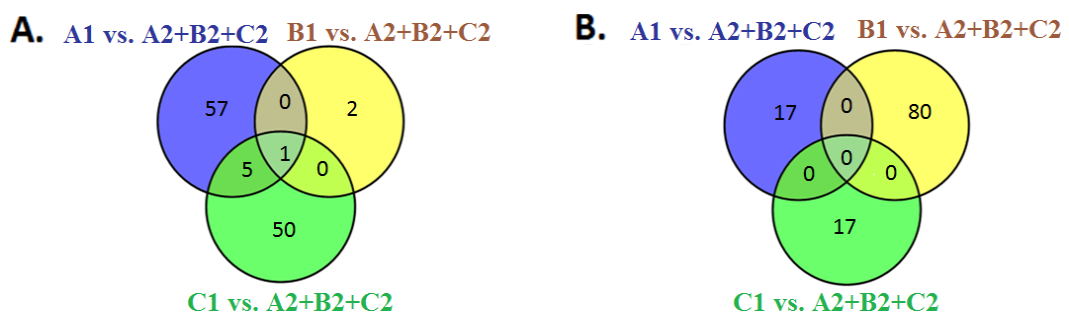
Figure 6.19: A: Venn diagrams showing number of differentially expressed genes that were **A:** down-regulated and **B:** Up-regulated, as determined by bioinformatic analysis of *GTSF1* knockdown oocytes Vs control oocytes. Microarrays A (high-level knockdown) and C (low-level knockdown) were compared to find common differentially expressed transcripts using a 1 fold change and no statistical significance cut-offs.

Only 1 gene showed common transcript variation for all groups and that was the down-regulated gene *PARP12*. A further 5 other genes showed common transcript reduction in the 2 groups. These genes were *TCOF1, RPS8, SREK1IP1, CACNA1D* and *TARDBP*. All these genes were selected as targets for real-time verification. Additionally, *DHX35*

from the high-knockdown microarray group (A1) against controls was selected to be followed by real-time PCR. The targets also included 2 genes from the up-regulated gene list from the high-knockdown microarray group (A1) against controls, *PELO* and *IGFBP7*. The list of down-regulated and up-regulated genes from the high-knockdown group (A1 against controls) is shown in Table 6.4.

Table 6.4: Secondary bioinformatic analysis list of down-regulated and up-regulated genes from high knockdown microarray A1 against control microarrays (A2, B2, C2)

Down-regulated genes
A only (57 genes)
DHX35, PARP12, UBE2O, PAPD7, SLC15A4, TOB2, SLC25A4, EZH2, C27H8orf40, MPHOSPH8, DERL1, BOLA2B, ALMS1, LOC787094, TTC4, CKAP2, MTMR2, SYS1, COX7C, ZBTB49, CIAPIN1, OSBPL7, RPL28, THAP7, RPL26, TSG118, ZMYND8, GADD45GIP1, DEPDC7, RPL26L1, ARHGAP32, MGC134282, PARD3B, SLC7A6OS, LOC785691, RPS25, LAMC1, EXOSC2, UTP14A, TMEM117, UBFD1, SUPV3L1, ARFIP1, LOC281370, CETN4, ATP5I, COX7B, RAB5A, RSL1D1, CNGB1, MRVI1, YBX1, PSMA7, LOC100295338, UPS7, ARPC2, DLG5, SUGT1
Common to A-C (5 genes)
TCOF1, RPS8, SREK1IP1, CACNA1D, TARDBP
Common to A-B-C (1 gene)
PARP12
Up-regulated genes
A only (17 genes)
PELO, IGFBP7, MGC128036, PCBP2, MIR147, GUSB, GDPD1, DMBT1, TRAPPC6B, DUSP10, SPTLC2, LOC514296, SDC2, PTPN11, CDK2, PHOSPHO2, PABPC1

Gene ontology analysis of the genes from the microarray A against controls was then carried out to define representing gene product properties as shown in Table 6.5. The analysis indicated that following *GTSF1* knockdown, ribosome function and RNA-binding were negatively affected. In particular, the biological processes of most of the genes that were down-regulated following the knockdown were associated with RNA processing and translation, while there were also genes associated with microtubule cytoskeleton organisation. In addition, the affected cellular components following the knockdown as indicated by the down-regulated genes were the RNPs and MTOCs, while the majority of the down-regulated gene's molecular functions involved RNA-binding. All these negatively affected biological processes, molecular functions and cellular components are in agreement and closely correlated with the proposed function of *GTSF1* (Yoshimura *et al.*, 2009; Lu *et al.*, 2012). Functional annotation showed that the knockdown of *GTSF1* affected the ribosome. Five genes in particular appeared to be down-regulated following *GTSF1* knockdown as indicated from the high-knockdown array (Figure 6.20).

Table 6.5: Ontology analysis of *GTSF1* knockdown following secondary bioinformatic analysis

Biological Processes
Down-regulated genes: The affected biological processes of down-regulated genes following the knockdown, were mostly associated with translation, rRNA processing, RNA processing, rRNA metabolic process, ribonucleoprotein complex biogenesis, ribosome biogenesis, ribosome assembly, regulation of transcription, protein transport and localisation, response to unfolded protein, tRNA metabolic processes, DNA modification, transcription, cell cycle, microtubule cytoskeleton organisation, chromatin organisation, actin polymerisation oxidative phosphorylation, intracellular signalling cascade and ion transport.
Up-regulated genes: Affected biological processes from the up-regulated gene list were associated with cell cycle, cell cycle checkpoint, DNA damage checkpoint, activation of MAPK activity, translation, cell cycle, cell proliferation, protein amino-acid phosphorylation.
Cellular components
Down-regulated genes: Annotation of down-regulated genes revealed cellular components associated with ribosome, ribonucleoprotein complex, microtubule organising centre, cytoskeleton, mitochondrion, chromatin, proteasome complex, endoplasmatic reticulum and Golgi apparatus.
Up-regulated genes: Cellular components from the up-regulated list included lysosome, lytic vacuole, spliceosome, cytosol, ribonucleoprotein complex, mitochondrion and extracellular region.
Molecular functions
Down-regulated genes: Annotation of down-regulated genes revealed molecular functions affected RNA binding, structural constituent of ribosome, rRNA binding, Zinc ion binding, ribonucleotide binding, DNA binding, chromatin binding, actin binding, cytoskeletal protein binding, ion channel activity and cytochrome c oxidase activity.
Up-regulated genes: Finally molecular functions affected by up-regulated genes following the knockdown included scavenger receptor activity, ion binding, phosphatase activity, RNA binding and cytoskeletal protein binding.
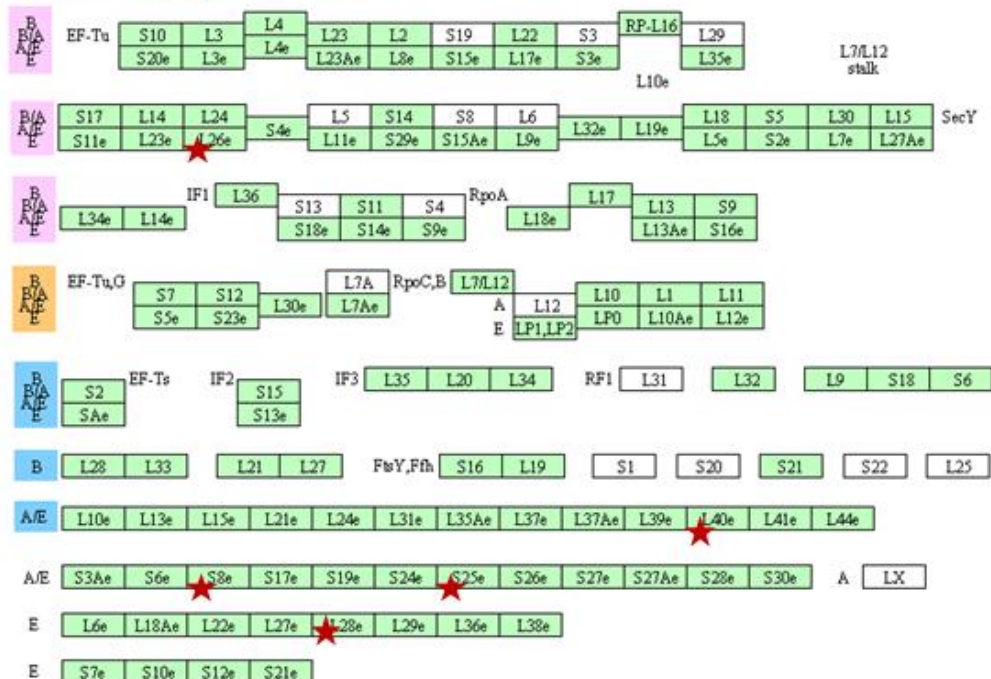
Figure 6.20: A functional analysis diagram showing the effect of the knockdown on ribosomal proteins following secondary bioinformatic analysis as determined using DAVID tools. Stars indicate proteins affected by down-regulated genes.

These genes were the ribosomal proteins (RP): *RPL26*, *RPL28*, *RPS8* and *RPS25* as well as the ubiquitin A-52 residue ribosomal protein fusion product 1 (*RPS40*). These genes encode proteins in both the large subunit (*RPL26, RPL28*, *RPS40*) and the small subunit of the ribosome (*RPS8*, *RPS25*). Functional analysis of these 5 genes showed very high relationship with ribosome, RNP complex, translation and structural constituent of ribosome (Kappa>0.75) and a high relationship with ribosomal subunits, structural molecule activity and the cytosolic ribosome (Kappa>0.5). The KEGG pathway, that is a collection of pathway maps and represents the existing knowledge on the molecular interactions and reaction networks, was used to examine the effect of *GTSF1* knockdown on the ribosomes.

6.3.5 Real-time PCR verification of transcripts from the secondary bioinformatic analysis

The expression of the 7 down-regulated genes (*TCOF1*, *PARP12*, *RPS8*, *CACNA1D*, *SREK1IP1*, *TARDBP*, *DHX35*) and 2 up-regulated genes (*PELO*, *IGFBP7*) that were selected following secondary bioinformatic analysis, were analysed by real-time PCR to verify the bioinformatic analysis. The transcripts that were identified from the secondary bioinformatic analysis were assayed with real-time PCR to verify the microarray results. All transcripts analysed here therefore corresponded to bovine array probes that had been successfully mapped to the ovine genome.

Target gene transcript levels were reduced in 7 out of 9 genes following *GTSF1* knockdown oocytes in comparison with the controls in agreement with the secondary bioinformatic analysis, with 4 gene transcripts having significant differences between the treatments (Figure 6.21). In particular, expression levels of *TCOF1* were significantly reduced (P<0.05) following *GTSF1* knockdown (2.0±1.0 arb. units, n=4) in comparison with controls (7.8±1.7 arb. units, n=4) oocytes, while transcript levels of *RPS8* and *CACNA1D* were significantly reduced (P<0.01) following *GTSF1* knockdown (2.7±0.9 arb. units, n=4; 5.1±1.4 arb. units, n=4) respectively in comparison with controls (12.9±2.2 arb. units, n=4; 19.3±1.5 arb. units, n=4). The levels of *SREK1IP1* had the most significant reduction (P<0.005) in the expression levels following the knockdown (3.0±0.7 arb. units, n=4) in comparison with the controls (16.4±0.7 arb. units, n=4). Transcript levels of *PARP12*, *TARDBP* and *DHX35* were reduced following the knockdown (2.6±1.1 arb. units, n=4; 2.4±0.5 arb. units, n=4; 1.7±1.1 arb. units, n=4) respectively, in comparison with controls (11.2±4.0 arb. units,

n=4; 6.8±1.2 arb. units, n=4; 4.3±1.8 arb. units, n=4), but significant differences were not noted (P>0.05). Finally the transcript levels of the 2 up-regulated genes *PELO* and *IGFBP7* as identified by the secondary bioinformatic analysis were increased following the gene specific knockdown (5.9±3.9 arb. units, n=4; 8.5±4.2 arb. units, n=4) respectively in comparison with controls (5.3±2.2 arb. units, n=4; 3.2±1.1 arb. units, n=4), in agreement with the bioinformatic analysis, but significant differences were not noted (P>0.05). Therefore in summary, the real-time PCR verification experiment for the targets identified by the secondary bioinformatic analysis were closely aligned with the expected patterns of up or down-regulation as indicated by the microarray. This provides a high-degree of confidence that the alignment of the bovine probes to the ovine genome was a necessary step that improved the validity of the microarray data.
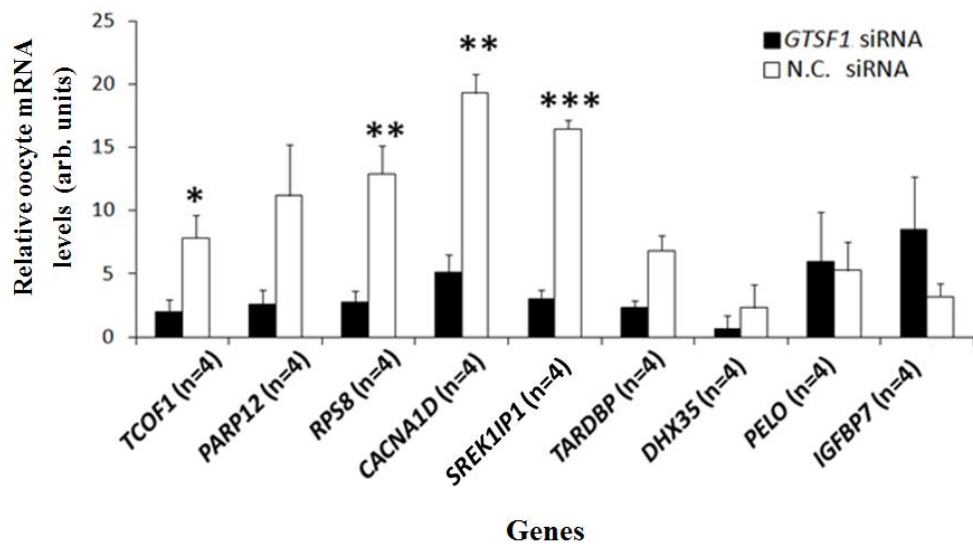
Figure 6.21: Real-time PCR quantification of the effect of *GTSF1* knockdown on target gene expression using cDNA derived from high-level *GTSF1* knockdown oocytes that were each analysed individually are shown together with the data for N.C. siRNA oocytes based on secondary bioinformatic analysis. The data was standardised against the oocyte *GAPDH* and *H2A* mRNA levels. Individual bars show the mean ±SEM for 4 individual oocyte cDNA libraries (each library analysed in quadruplicate). *GTSF1* knockdown oocytes exhibited a statistically significant difference for the *TCOF1* mRNA levels (*=P<0.05), *RPS8* and *CACNA1D* mRNA levels (**=P<0.01) as well as *SREK1IP1* (***=P<0.005), when compared against the N.C.siRNA oocytes, while no other significant differences were observed (P>0.05).

6.4 DISCUSSION

Overall the results showed that it was possible to create and validate individual *GTSF1* knockdown oocytes. The targeted knockdown of *GTSF1* in sheep oocytes did not affect oocyte meiotic progression or cumulus expansion. The microarray experiments performed on groups of *GTSF1* knockdown *in vitro* matured MII oocytes and N.C. siRNA *in vitro* matured MII oocytes showed that a number of genes were differentially

expressed between the 2 treatment groups. The results of this study show the value of microarrays for studying the function of *GTSF1* during maturation, however caution must be exercised when using heterologous arrays, where incorrect gene annotation and hybridisation can be a significant problem. Bioinformatic analysis showed that *GTSF1* knockdown is associated in a direct or indirect manner with several cellular processes and biological functions including translation, RNA-binding, oocyte development and meiosis, microtubule formation, cytoskeletal organisation, post-transcriptional regulation of gene expression and many more, further signifying the importance in identifying the function of the gene. Real-time PCR confirmation of the significant differences in the mRNA transcript levels of 6 candidate target genes from the separate primary (2 genes) and secondary (4 genes) bioinformatic analysis that are affected by *GTSF1* depletion, suggests that *GTSF1* knockdown is associated with production of ribosomal RNA, regulation of cytoskeletal microfilaments, post-transcriptional modification and gene transcriptional control.

6.4.1 The impact of *GTSF1* on meiotic progression and cumulus expansion

The culture results showed that it was possible to generate a targeted knockdown of *GTSF1* in sheep oocytes without compromising oocyte survival in agreement with the results of Chapter 5. The survival rates of the oocytes in this experimental series were not different for the 2 treatment groups at 24 h of culture indicating that neither the *GTSF1* siRNA nor the N.C. siRNA were toxic to the oocyte. Prior to this series of experiments it was hypothesised that the volume of injection was an important parameter to improve in order to increase survival of the oocytes. Since the change from a constant outflow (Chapter 4) to a controlled injection (Chapter 5) under the minimum pressure of 40 hPa resulted in reduced survival of oocytes as shown by Chapter 5 results, the constant outflow was reinstated as in Chapter 4. The survival proportions in this experimental series were much higher compared to Chapter 5 survival proportions and were slightly higher to the survival proportions obtained in Chapter 4 for the first 24 h of culture, where the same system of constant outflow was used for the microinjections. The increased survival rates could be attributed to the change of the microinjection pressure system and the reduced volume of injection resulting to reduced osmotic stress in the ooplasm.

The individual culture of oocytes meant that the morphological evaluations of the oocytes and cumulus shells along with the level of *GTSF1* knockdown could be

monitored individually for each oocyte. Oocyte meiotic progression was not significantly different between the 2 treatment groups (54.5% for viable *GTSF1* siRNA injected oocytes and 47.1% for viable N.C. siRNA controls). Furthermore, the maturation proportions of viable oocytes at 24 h that were matured with individual cumulus shells for both treatments were much higher than maturation proportions obtained from Chapter 4 and Chapter 5 results. The improved levels of maturation in this series of experiments could be explained because of the improvements to the culture system and microinjection technique as well as the tighter control of the timing of tissue processing. Cumulus shell expansion and mucification did not show differences between the 2 treatments groups. Although cumulus shells did not have the potential of fully expanding in this series of experiments, 25.7% of cumulus shells from the *GTSF1* siRNA group and 24.3% of cumulus shells from the N.C. siRNA group were partially-fully expanded, demonstrating that *GTSF1* does not affect expansion of the cumulus cells. The lack of fully expanded cumulus shells could be attributed to the change of group co-cultures to single oocyte and single cumulus shell co-culture. None-the-less, even though the cumulus shells did not expand fully as in Chapter 4 and Chapter 5, oocyte maturation was not impaired as demonstrated from the maturation proportions for both injection groups.

Furthermore, all 42 oocytes that progressed to the MII stage following injection with *GTSF1* siRNA showed significant differences in their levels of *GTSF1* knockdown in comparison with the N.C. siRNA controls (P<0.005), indicating that the single oocyte culture strategy used in the current experiments produced far more consistent gene knockdown data than the group oocyte culture approach used in Chapter 5. The effects of high levels of oocyte *GTSF1* knockdown on oocyte meiotic progression and cumulus expansion in the present experiments were consistent with the results recorded for gene knockdown oocytes in Chapter 5.

6.4.2 Microarray analysis following *GTSF1* knockdown

In order to identify the underlying molecular mechanisms and functions of *GTSF1* during the maturation stages, the effects of the depletion of the gene on the transcriptome of the oocyte needed to be acquired. It is well established that the causes of poor developmental competence of oocytes are complex and depend on several changes in the mRNA transcript levels of numerous genes (Donnison and Pfeffer, 2004). A number of studies have shown that changes in the gene expression like *GDF9*

or *BMP15* in oocytes or *HAS2* in cumulus cells can be monitored in order to select oocytes for fertilisation as well as embryos for implantation (Elvin *et al.*, 1999; Yan *et al.*, 2001; Cillo *et al.*, 2007). Gene expression studies can therefore identify factors involved in oocyte maturation as well as provide molecular markers for abnormal gene expression that can affect developmental competence (Gasca *et al.*, 2007). Oocytes from such studies may have differences at the molecular level in the synthesis, degradation and modification of mRNAs and proteins which can be reflected in the differences of gene expression between the different conditions. It is apparent therefore that if *GTSF1* functions during maturation of the oocyte, this will be reflected by the mRNA transcript level. There have been studies where real-time PCR has been used to determine mRNA expression patterns in bovine oocytes and embryos (Oropeza *et al.*, 2004; Zaraza *et al.*, 2010). In this thesis, speculative real-time PCR of candidate genes, following knockdown of *GTSF1* as conducted in Chapter 5 did not reveal any specific differences on their expression levels. Application of the microarray technology that contains tens of thousands of gene probes was considered therefore very useful for the identification of targets following the gene specific knockdown.

In a recent study conducted in mice, microarrays were used to identify germ cell-specific genes in mammalian meiotic prophase (Li *et al.*, 2013). Similarly, genes from MII oocytes that correlated with the oocyte's ability to develop to the blastocyst stage have been identified in another murine study (Biase *et al.*, 2012). Microarrays have also been used for expression analysis of specific sets of genes or specific miRNAs during oocyte maturation and early embryo development (Xu *et al.*, 2011; Mondou *et al.*, 2012). Molecular and hormonal characterisation of follicular fluid, cumulus cells and oocytes has been used to determine developmental competence (Jose De Los Santos *et al.*, 2012). The *in vitro* culture of oocytes has been shown to affect gene expression and signalling pathways in bovine cumulus cells (Salhab *et al.*, 2013). In fact microarrays have been used to study the transcriptome of cumulus and granulosa cells as non-invasive predictors of oocyte maturation, embryo competence or live birth (Anderson *et al.*, 2009; Feuerstein *et al.*, 2012; Wathlet *et al.*, 2012; Uyar *et al.*, 2013).

Microarrays have been used to study genes and mechanisms that affect oocyte development. Transcriptome analysis during the oocyte maturation stages of the oocyte can reveal a lot of information. In the past few years, a number of studies have argued on the subject of the timing of transcription initiation following the resumption of

meiosis in oocytes (Xu *et al.*, 2011). A number of transcripts have been shown to be up-regulated during oocyte maturation in cattle and humans between GV and MII oocytes (Assou *et al.*, 2006; Mamo *et al.*, 2011). In the bovine oocytes, a total of 1528 transcripts were found to be significantly lower and 589 were significantly higher in IVM MII oocytes in comparison with GV oocytes (Mamo *et al.*, 2011). In human oocytes, 803 genes were down-regulated and 444 genes were up-regulated in the MII oocytes compared to the GV (Assou *et al.*, 2006). The genes that were found to be overexpressed might represent expression patterns that are related to the completion of meiosis (Xu *et al.*, 2011). The approach of inflicting a gene specific knockdown by the means of microinjecting siRNA in GV oocytes followed by IVM and transcriptome analysis by microarrays in order to study the function of a novel gene has been successfully applied in a recent study, where *Pcbp1* has been knocked down in mouse oocytes (Xia *et al.*, 2012). In this study, knockdown of *Pcbp1* resulted in remarkable changes in the transcriptional state of the oocytes with around 4000 transcripts up-regulated following the knockdown; suggesting that knocking down the gene disrupted the quiescent status of transcription in MII oocytes and the regulation of global transcription silencing (Xia *et al.*, 2012). A similar approach was followed in this thesis for the study of the function of *GTSF1* during the maturation of ovine oocytes by injecting siRNA for *GTSF1*.

The experimental procedure for the successful application of microarrays consists of multiple stages covering from RNA extraction, reverse transcription, amplification to labelling and hybridisation; each of which adds a possible systematic or random variation in the resulting data. This in addition to the selection of the appropriate statistical methods, as well as the large gene ontology databases, make the microarray experiments very complex and require a thoroughly evaluated experimental design (Uyar *et al.*, 2013). In this thesis there was a finite number of *GTSF1* knockdown oocytes, thus careful planning was needed. It is well established that oocytes able to mature to the MII stage do not necessarily have the same competency in developing to the blastocyst stage (Leoni *et al.*, 2007). There can be severe differences at the molecular level in the synthesis, degradation and modification of mRNAs and proteins between oocytes, especially during the GV to MII transition where the transcriptome abundance is reduced (Leoni *et al.*, 2007). The 14 oocytes that demonstrated >50% of *GTSF1* knockdown ($P<0.005$) along with their respective N.C. siRNA oocytes were selected for microarray analysis. The oocytes compiling each microarray set used here

were separated based on their levels of *GTSF1* knockdown into A1, B1 and C1 along with their respective controls A2, B2 and C2.

6.4.3 Primary bioinformatic analysis

Following normalisation of the arrays, *GTSF1* knockdown arrays were grouped together (A1+B1, B1+C1, A1+B1+C1) and then compared against their respective control groups. Target genes were identified and gene ontology analysis that followed primary bioinformatic normalisation and grouping of the microarrays revealed that knockdown of *GTSF1* down-regulated several biological processes such as oocyte development, actin cytoskeleton organisation, spindle assembly and cell polarity (*AURKA*, *CDK2*, p59, *FKBP4*) in addition to RNA processing (RNA binding motif 17 (*RBM17*), *PCBP1*). Similarly, down-regulated genes were mostly associated with cellular components associated with microtubule cytoskeleton, the myosin complex as well as mitochondrial components and membrane transporters (COX17, mammalian gene collection 80625 (*MGC80625*), AURKA) in addition to RNP components (*RBM17*, *PCBP1*), while down-regulated genes affected molecular functions including nucleotide binding, ATP dependent helicase activity, calcium ion and cell adhesion binding, motor activity, cytochrome c oxidase activity and ion trans-membrane transporter activity (*FKBP4*, *MGC80050*, *MGC85413*, *RBM17*, *AURKA*, *COX17*, *ZNF706*). Down-regulated biological processes of oocyte development, oogenesis, oocyte growth and differentiation, developmental cell growth as well as the actin filament based processes and spindle assembly put forward the idea that *GTSF1* affects the developmental competence of the oocyte. Down-regulated cell cycle and cell division processes indicate that *GTSF1* might be important for development of the oocyte as well as the early embryo. Although in this thesis no developmental differences were observed between the IVM potential of ovine oocytes following *GTSF1* knockdown (Chapter 5 results and Chapter 6 culture results), the developmental competence of these oocytes could still be impaired as a result of defective spindle assembly and/or alterations in transcriptional and translational control which compromise oocyte quality. The ability of oocytes to resume meiosis, to be fertilised, to develop into blastocyst and to produce healthy offspring are all individual events and success in the first events does not guarantee subsequent success in the following events (Sirard *et al.*, 2006). However, the molecular cascades that the oocytes acquire during maturation are necessary for subsequent embryonic genome activation and development to the blastocyst stage, thus

the molecular maturation of each oocyte defines its inherent capacity to continue its development (Sirard *et al.*, 2006).

Although nuclear maturation and cytoplasmic maturation are different processes, they are interlinked and occur at the same time, even if molecular programming initiates at earlier stages of oocyte growth (Sirard *et al.*, 2006). Redistribution of cytoplasmic organelles is a necessity for successful cytoplasmic maturation and repositioning of the organelles occurs through the actions of cytoskeletal microfilaments and microtubules (Ferreira *et al.*, 2009). Microtubules are directly involved in movement of organelles and they adhere to motor proteins such as Dynein and Kinesin that promotes their movement (Sun and Schatten, 2006). Microfilaments are associated with microtubules since the polarised movement of chromosomes is mediated by actin filaments (Sun and Schatten, 2006). In murine and bovine oocytes it has been shown that cytoskeleton associated processes during maturation are regulated by different molecules including AURKA that localises with chromosomes and so regulates chromosome segregation, maintenance of the MII state and formation of the polar body (Yao *et al.*, 2004; Uzbekova *et al.*, 2008). In addition, cytoskeleton associated molecules, ATP binding and calcium ion binding, all transcripts that were down-regulated following gene ontology analysis in the present study, are usually found in abundance in dominant follicles in comparison to growing follicles; suggesting that competent gametes are enriched with these transcripts (Sirard *et al.*, 2006; Ghanem *et al.*, 2007). Furthermore, calcium signalling has been shown to be associated with successful implantation of blastocyst mouse embryos (Wang *et al.*, 2002).

Other than the microtubules and cytoskeleton, certain metabolic pathways involved in protein synthesis and phosphorylation, need to be activated in order for cytoplasmic maturation to progress. Mitochondria are crucial components of the metabolic machinery and supply the necessary energy that is consumed during the maturation stage (Stojkovic *et al.*, 2001). These organelles in oocyte have vital roles in several physiological events including the first stages following fertilisation (Van Blerkom, 2004). Mitochondrial components were also shown to be down-regulated following the *GTSF1* knockdown. Additionally, cytochrome c oxidase activity which was also shown to be down-regulated, is the terminal enzyme of the mitochondrial respiratory chain and reductions of mRNA and protein expression of this oxidase have been shown to significantly increase apoptosis in mouse embryos (Cui *et al.*, 2006). Studies have

shown that the mitochondria synthesize ATP during the maturation stage which is necessary for protein synthesis and subsequent embryo development (Krisher and Bavister, 1998; Stojkovic *et al.*, 2001). In addition, the number of mitochondria is important, since reduced numbers have been shown to be responsible for abnormal distribution of the organelle during the early stages of embryogenesis (Shoubridge and Wai, 2007).

Gene ontology analysis revealed that some genes were up-regulated following the targeted knockdown of *GTSF1*. These included cell cycle and spindle checkpoint genes, while genes associated with lipid and steroid biosynthesis and protein stability were also up-regulated (*CKAP2*, *MAPK6*, AT rich interactive domain 2 (*ARID2*), erzin (*EZR*) and oxysterol binding protein like 7 (*OSBPL7*). In addition, DNA-binding gene transcripts were up-regulated along (*ARID2*, DEAD box polypeptide 27 (*DDX27*), antagonism of C1 repression (*ANT1*). It is possible therefore that the knockdown of *GTSF1* uncouples key components of oocyte maturation such that it down-regulates some molecules that are associated with maturation and may induce other transcripts to be up-regulated to compensate and thus assist with the progression of oocyte maturation. It is well established that during meiotic progression, oocytes are error-prone and that the spindle assembly checkpoints act to ensure the successful attachment of kinetochores to homologous chromosomes during MI as this has been shown in mouse oocytes (Wassmann *et al.*, 2003; McGulnness *et al.*, 2009). In particular it has been shown that the Apc/C spindle assembly checkpoint molecule is activated 5 h earlier in oocytes that lack *Bub1*, with depletion of *Bub1* responsible for chromosome missegregation at meiosis I and loss of cohesion between sister centromeres (Mcgulnness *et al.*, 2009).

The primary bioinformatic analysis provided several targets for real-time PCR analysis including *MYL9* and *MYL12A* that are non-muscle regulatory light chains of Myosin II, an actin-binding protein and normal levels of non-muscle regulatory light chains are vital for the maintenance of the integrity of myosin II and essential for cell structure and dynamics (Park *et al.*, 2011). Another gene that appeared to be up-regulated following the primary bioinformatic analysis was the *CKAP2* gene that was previously found to be co-localised with MTOC and microtubules in human cell lines illustrating that it might be associated with microtubule networks (Bae *et al.*, 2003). Targets included the *AURKA* gene that transcribes an important mitotic kinase which plays important roles in the G2/M transition, centrosome maturation and separation and spindle formation in

somatic cells (Hannak *et al.*, 2001). More importantly a recent study has shown that the gene regulates MTOC number and spindle length in mouse oocytes as well as gamma-tubulin recruitment to MTOCs (Solc *et al.*, 2012). Another gene shown to be down-regulated was *CDK2* which transcribes an enzyme that it is part of the CDK complex that regulates the G1/S transition, although cells lacking *CDK2* have been shown to be viable and progress with the cell cycle (Berthet *et al.*, 2003). A further target analysed was the cytochrome c oxidase copper chaperone (*COX17*) that is a terminal component of the mictochondrial respiratory chain and catalyses the transfer from reduced cytochrome c to oxygen (Amaravadi *et al.*, 1997). The *PCBP1* gene was also selected for analysis from the down-regulated gene list following *GTSF1* knockdown. This gene contains 3, K-homologous domains that may be involved in RNA-binding and amongst others the protein that it encodes plays a role in the co-activation of poliovirus RNA and is also suggested to play a part in the formation of the alpha-globin mRNP complex associated with alpha-globin mRNA stability (Tommerup and Leffers, 1996b). Another gene analysed was the *FKBP4* gene that encodes a protein that can act as a regulator of microtubule dynamics by inhibiting TAU protein that promotes microtubule assembly (Chambraud *et al.*, 2010). The *ZNF706* gene expression was also examined. Zinc fingers are small DNA and RNA-binding peptide motifs that are considered to be the building blocks for the construction of larger protein domains that bind to specific sequences (Klug, 1999). The TECR protein encoded by the *TECR* gene found in the endoplasmic reticulum catalyses the reduction of trans-2,3-enoyl-CoA to saturated acyl-CoA as part of the elongation of microsomal chain fatty acids (Caliskan *et al.*, 2011). Finally the *TIMP1* gene transcript was analysed for the 2 treatment groups. The glycoprotein encoded by this gene has an inhibitory role against matrix metalloproteinases that control the degradation of the extracellular matrix and has also been shown to have an anti-apoptotic function acting to increase cell proliferation in several cell types in addition to a decreased collagenase activity (Reichenstein *et al.*, 2004). Real-time PCR analysis showed significant reductions in the transcript levels of only 2 genes, *MYL9A* and *TIMP1*. These genes are both involved in the cell cycle regulation. Specifically, functional annotation of *MYL9A* showed that this gene was involved in signal transduction mechanisms, cytoskeleton, cell division and chromosome partitioning in agreement with the gene ontology analysis, while *TIMP1* is involved in cell cycle progression. Other than the 2 genes with significant reduction, the knockdown of *GTSF1* showed a trend for reduced levels of *AURKA* and *CDK2*, both of which have known roles in microtubule formation and oocyte maturation (Solc *et al.*,

2012). None-the-less, failure to verify the majority of gene targets from the primary bioinformatic analysis led to a different analysis approach.

6.4.4 Secondary bioinformatic analysis

Gene ontology based on the secondary bioinformatic analysis that used the matched ovine sequences to the bovine probe, revealed that knockdown of *GTSF1* down-regulated mostly ribosomal genes and RNPs (*RPL26, RPL28*, *RPS8*, *RPS25*, *RPS40*, U3 small nucleolar ribonucleoprotein homolog A (*UTP14A*), in addition to RNA processing functions (*DDX35*, nuclease-sensitive element binding protein 1 (*YBX1*), *TARDBP*, *TECR1*). Ribosomes are important during maturation of the oocyte and are synthesized by the transcription of ribosomal RNA as well as the addition of several ribosomal proteins to their subunits. During MI of meiosis, the protein synthesis has been shown to be 3 times higher than the equivalent at GVBD (Ferreira *et al.*, 2009). A previous study has shown that ribosomes produced at the GV stage together with the ribosome production for mRNA translation that follows means that more of these organelles are stored in the oocytes during the MI stage (Van Blerkom *et al.*, 2000). At the MII stage however, the number or ribosomes are reduced which could be because of the high usage of these organelles during oocyte maturation (Tomek *et al.*, 2002). Overall, these organelles are necessary for protein synthesis during important periods of development and the results of this thesis with several ribosomal genes down-regulated, suggests that the *GTSF1* knockdown possibly affects translation. In addition, the RNPs are very important. It is well established that RNPs like P-bodies as well as stress granules, regulate mRNA metabolism (Balagopal and Parker, 2009). In particular, P-bodies regulate repression of translation and mRNA decay (Sheth and Parker, 2003). In addition, down-regulation of genes which are involved in maintaining the transcriptional repressive state of genes including the enhancer of zeste homolog 2 (*EZH2*) further supports the postulation that *GTSF1* is associated with gene transcriptional control and the RNAi pathway.

Secondary bioinformatic analysis provided several targets for real-time PCR analysis. The *TCOF1* gene encodes the treacle protein associated with the production of ribosomal RNA that drives the assembly of amino acids into proteins (Hayano *et al.*, 2003). The treacle molecule might be involved in nucleolar-cytoplasmic transport and might also have an important role in early embryonic development and the craniofacial complex development (Hayano *et al.*, 2003). Next target was the *PARP12* gene (Katoh,

2003). Members of the PARP family catalyse post-translational modification of proteins by the addition of several ADP riboses to the proteins (Virag, 2005). The *RPS8* gene (Davies and Fried, 1993) encodes a ribosomal protein that is a component of the 40S subunit and is co-transcribed with several other small nucleolar RNA genes (Poguegeile *et al.*, 1991). Another gene on the list was *SREK1IP1* gene (Barnard and Patton 2000). This encodes a member of the serine/arginine rich splicing proteins that contains RNA recognition motif domains and the encoded protein interacts with other serine/arginine rich proteins in order to alter the splice site (Zhang *et al.*, 2002). Another gene analysed was *CACNA1D* (Bock *et al.*, 2011). Voltage-dependent calcium channels have been shown to control the entry of calcium ions into cells that can be stimulated to create a tiny electrical current (excitable cells) have also been shown to be involved in other calcium-dependent functions such as muscle contraction, hormone release and gene expression as indicated by functional analysis. The *TARDBP* gene was also analysed (Ou *et al.*, 1995). This gene has been shown to be involved in both DNA and RNA-binding and to have several functions in transcriptional repression, pre-mRNA splicing, mRNA stability and transport as well as translational regulation (Strong *et al.*, 2007; Kuo *et al.*, 2009). Another target provided from the secondary bioinformatic analysis was the *DHX35* gene. Members of the DEAH box including *DHX35* are considered to be RNA helicases involved in several cellular processes including splicing, ribosome and spliceosome assembly and also possibly involved in embryogenesis, spermatogenesis and cellular division (Matsumoto *et al.*, 2005; Buratti and Baralle, 2010). The *PELO* gene that was shown to be up-regulated following secondary bioinformatic analysis was also analysed. This gene encodes the protein Pelota homolog (Shamsadin *et al.*, 2000). The protein that this gene encodes has a conserved nuclear localisation signal and has been proposed to have roles in spermatogenesis, cell cycle control and meiotic cell division. In particular, *PELO* is associated with actin microfilaments of mammalian cells and has been shown to increase cell growth, cytoskeleton organisation and cell spreading (Burnicka-Turek *et al.*, 2010). Lastly the *IGFBP7* gene from the up-regulated gene list was analysed (Oh *et al.*, 1996). The function of this protein has been established as being required for modulating the regulation of the availability of insulin-like growth factors in tissue as well as the control of IGF binding to its receptors (Oh *et al.*, 1996).

The results of the real-time PCR analysis verified significant reductions in the transcript levels of *TCOF1, RPS8, CACNA1D* and *SREK1IP1*. These genes are mostly associated

with post-transcriptional modification. In particular, the association of *TCOF1* with the production of rRNA and its implication in the transport of molecules between the nucleus and cytoplasm suggests that this gene supports different functions necessary for development, such as protein synthesis which was negatively regulated following the *GTSF1* knockdown. In addition, the gene associates with upstream binding factor to regulate rRNA transcription, however the precise mechanisms of the gene are still unknown (Lin and Yeh, 2009). This could be associated with the significantly lower transcript levels of a ribosomal gene, *RPS8*, upon *GTSF1* depletion. The negatively expressed *SREK1IP1* gene following *GTSF1* knockdown encodes a protein that contains an RNA-recognition motif and is involved in post-transcriptional modification further enhancing the hypothesis that *GTSF1* has an important role during maturation. The *CACNA1D* gene of which the transcripts were significantly reduced might also be important. Calcium channels are not only important for calcium-dependent processes like muscle contraction and hormone release but they are also involved in gene expression. Even though knockout of *Gtsf1* in mice showed that fertility was not impaired, it is possible that knockdown of *GTSF1* might affect fertility and/or early development in the sheep because of the pivotal role that calcium has in fertilisation and early development (Whitaker, 2006).

The associated function of the genes affected by *GTSF1* knockdown strongly supports the hypothesis that *GTSF1* directly or indirectly affects RNA-packaging, transcriptional modification of RNA and translation in addition to spindle assembly, all of which are linked to the demonstration of oocyte developmental competence rather than maturation potential *per se*. The results of this Chapter do match the inferred function of *GTSF1* as deduced by structural analysis (Krotz *et al.*, 2009). In particular, the conserved domain of *GTSF1* with 2 CHHC Zn-fingers that may function as an RNA-recognition and binding molecule is in agreement with the down-regulated transcripts that were shown to affect RNA storage and post-transcriptional modifications such as *TCOF1*, *RPS8*, *SREK1IP1* and *CACNA1D*. Furthermore, the results of this study correlate with the *Gtsf1* knockout study, where there was an increase in the *Line1* and *Iap* retrotransposons and their promoter region leading to a retrotransposon activation in male mice following the knockout, while no effects were observed in female mice (Yoshimura *et al.*, 2009). Although the results of this thesis did not show a direct relation of *GTSF1* with the miRNA silencing mechanism, the association of the knockdown with transcripts related with RNPs, suggests that *GTSF1* might have similar

effects in the female. Ongoing analysis of other target genes originating from the secondary bioinformatic analysis might reveal a possible involvement of *GTSF1* with the RNAi silencing mechanism.

6.4.5 The potential pitfalls of microarrays

The complex data analysis that are required for the processing of the data from the microarray experiments poses significant challenges because of the many experimental procedures involved, the need for simultaneous multiple hypothesis testing and the size of the gene ontology databases that are used for identification of the differentially expressed genes (Uyar *et al.*, 2013). The experimental design therefore has to be based on these factors in addition to the reliability, comparability and reproducibility of the microarray experiments (Uyar *et al.*, 2013). It has been shown that data from different sites and platforms can produce diverse results (Chen *et al.*, 2007). Comparison of the reproducibility of 18 microarray results from published articles showed that only 2 were reproduced with 6 being partially reproducible (Ioannidis *et al.*, 2009). Therefore the correct analysis of the microarrays is of imperative importance for obtaining valid experimental results. In this experimental series, the limited number of oocytes available for analysis has increased the complexity analysis and has raised questions regarding the accuracy of data analysis. The use of heterologous bovine microarrays for the analysis of ovine samples added to the complexity. Unfortunately at the time of the analysis there were no GeneChip ovine arrays available. These are now commercially available (www.affymetrix.com). None-the-less, heterologous arrays have been used before to study gene expression profiles in sheep tissues (Graham *et al.*, 2011). In this study, the Human GeneChip Affymetrix array was used and more than 20,000 transcripts were detected in triplicate ovine skeletal muscle and liver samples (Graham *et al.*, 2011).

Even though the 2 species have many similar homologies in their genome, there were still many inconsistencies that resulted in incorrect hybridisations for some genes on the array, with the result that it was not possible to verify all array data. This problem was revealed when real-time PCR verification following primary bioinformatic analysis did not confirm the findings. The probe design for the microarrays is related to the genomic constitution of the species and this restriction limited the detection of unmapped genes and alternative splicing patterns (Uyar *et al.*, 2013). The problem was partially resolved by a different approach secondary bioinformatic analysis in which the bovine probe

sequences were aligned to the sheep genome sequence. A total of 2 bovine probes were matched to the sheep *GTSF1* sequence. Only matching probes were used to annotate genes and provide targets for real-time PCR verification. The data from the real-time PCR were in agreement with the secondary bioinformatic analysis and the expression of 4 genes was shown to be significantly reduced following the knockdown.

The experimental design could have been improved if the GeneChip ovine array now available was used. Conducting more arrays using the GeneChip ovine arrays with the necessary number of repeat arrays for each of the treatment (3 for each) are necessary in future experiments to avoid the inconsistencies presented in this study. In addition, microarrays cannot detect the compressed fold change in the expression levels of highly expressed genes (Uyar *et al.*, 2013). An alternative approach that would avoid these pitfalls would be the use of RNA sequencing that provides a more precise characterisation of all RNA species (Mortazavi *et al.*, 2008; Wang *et al.*, 2009). The use of this technology has been shown to be quite reproducible with the data between Affymetrix arrays and RNA sequencing having 81% similarity in the number of differentially expressed genes (Marioni *et al.*, 2008). The involvement of *GTSF1* in RNA storage and processing during oocyte development can be also examined by immunofluorescent studies.

6.4.6 Conclusion

The creation and validation of individual *GTSF1* knockdown oocytes proved invaluable in progressing knowledge of the functional role of *GTSF1*. The validation of some selected transcripts with real-time PCR suggests important implications of *GTSF1* in key biological processes during oocyte maturation. From these observations it can be proposed that *GTSF1* affects the expression of genes that could be involved in RNA storage and processing such as *TCOF1*, *RPS8*, *SREK1IP1* and *CACNA1D* as well genes that could influence spindle assembly and cellular cytoskeleton and oocyte developmental competence, such as *MYL9A* and TIMP1. However, it appears that the molecular effects following knockdown of *GTSF1* are quite complex and accordingly, may have a profound effect on oocyte quality and subsequent development. Analysis of additional *GTSF1* knockdown oocytes is required to determine if the trends observed in the real-time PCR results have functional significance in relation to oocyte meiosis. Further studies are also needed to confirm the role played by *GTSF1* in post-transcriptional modification of RNA in oocytes.

Chapter 7: Localisation of GTSF1 protein during ovine oogenesis

7.1 INTRODUCTION

Both male and female gametes have post-transcriptional modifications in place that control mRNA stability and translation (Watanabe *et al.*, 2008). Translation initiation and repression is mainly controlled by a 3´ UTR regulating element called the cytoplasmic polyadenylation element (CPE) as well as its binding partner along with the polyadenylation response element (PRE) and its binding partners (Charlesworth *et al.*, 2004). The chromatoid bodies in mammals that contain RNA and RNA-binding proteins have established roles in differentiation of germ cells and early embryo development (Kotaja *et al.*, 2006; Kotaja and Sassone-Corsi, 2007). In this context *Vasa* is an evolutionary conserved germ cell specific Dead-box RNA-helicase essential for germ cell development and oogenesis which acts by regulating target mRNAs (Saga, 2008; Siomi and Kuramochi-Miyagawa, 2009). The mouse *Vasa* homolog (*Mvh*) is also germ cell specific as is its *Vasa* homolog (Toyooka *et al.*, 2000) as knockout of *Mvh* has been shown to block spermatogenesis at the first meiotic cell division, while PGC development was not affected (Tanaka *et al.*, 2000). The Mvh protein has been shown to be localised in the chromatoid bodies of round spermatids of adult male mice (Kotaja and Sassone-Corsi, 2007). Localisation of Mvh protein in the chromatoid body, suggests that Mvh is likely to have important roles in RNA processing in male germ cells (Kuramochi-Miyagawa *et al.*, 2010). The Mvh protein along with the mouse Piwi family members Mili and Miwi2 are indispensable for piRNA processing with *Mili* and *Miwi2* knockouts resulting in elevated retrotransposon expression (Tanaka *et al.*, 2000; Kuramochi-Miyagawa *et al.*, 2004; Carmell *et al.*, 2007). The Mvh protein is also involved in piRNA processing and gene silencing of retrotransposons (Kuramochi-Miyagawa *et al.*, 2010).

The cellular localisation of GTSF1 in bovine round spermatids and mature sperm suggests that the GTSF1 protein functions during post-meiotic spermatogenesis in addition to its already established role during the early primary spermatocyte development (Lu *et al.*, 2012). Chromatoid bodies have similarities with the somatic P-bodies that are highly evolutionary conserved in many organisms and found in somatic cells and the oocytes (Kotaja *et al.*, 2006). Dicer and components of miRISC including

members of the Argonaute family and several miRNA species are found in the chromatoid body which further supports the functional analogy with the P-bodies including RNA-storage and processing (Kedersha *et al.*, 2005; Kotaja *et al.*, 2006). The microarray results of Chapter 6 suggest that *GTSF1* may play a role in post-transcriptional modification in the oocyte. In order to extend these findings on the functional role of *GTSF1*, further studies are needed to investigate how *GTSF1* functions during post-transcriptional modification of RNA in gametes.

7.1.1 Aims

The aim of this study was to evaluate the relationship between GTSF1 and the P-body in ovine oocytes by immunofluorescent microscopy MVH to locate P-bodies in histological preparations across sheep oogenesis.

7.2 MATERIALS AND METHODS

This study utilised immunofluorescence microscopy to pinpoint GTSF1 expression during ovine gametogenesis. For this experimental series, immunofluorensense was used on histological preparations of the ovine ovary and on isolated ovine GV and MII oocytes. Preparations of the ovine testis were used as positive and negative scoring control tissues. Ovine testis and ovary were fixed overnight in 4% (w/v) PFA in 0.1% (v/v) DEPC treated PBS and sequentially washed in 70% (v/v) ethanol in 0.1% (v/v) DEPC treated H_2O and embedded in paraffin as described in Chapter 2, Sections 2.6.2-3. The ovary and testis embedded tissue were then cut into 4 μm sections and mounted on Superfrost Plus slides (VWR). The slides were de-waxed, rehydrated, and post-fixed in 4% (w/v) PFA in 0.1% (v/v) DEPC treated PBS for 10 min as described previously (Chapter 2, Section 2.6.7). The cellular localisation of MVH was examined by immunofluorescence along with GTSF1 to examine whether there was co-localisation between these 2 proteins in ovine gametes. Anti-MVH (Ab 13840, Abcam, Cambridge UK) and Alexa Flour 488 (A21441, Life Technologies, Paisley, UK) were used to detect MVH, while Anti-GTSF1 antibodies (SC-240545, Santa Cruz Biotechnology, Wembley, UK) and Alexa Flour 594 (A11058, Life Technologies) were used to detect the cellular localisation of GTSF1. The blocking peptide SC-240545p (Santa Cruz Biotechnology) was used to neutralise the GTSF1 antibody and was used as negative control. For this purpose, a 5 times excess concentration of the blocking peptide (10 μg/ml) was incubated with GTSF1 antibody (2 μg/ml) for 1 h in a 1.5 ml sterile

microcentrifuge tube on a shaking incubator at RT, before this combined solution was applied as the primary antibody for the negative control slides. Statistical analysis for the co-localisation of GTSF1 and MVH at the different stages of development was conducted by chi-square analysis of the numbers at each stage that demonstrated co-localisation out of the cohort analysed compared with the numbers at the same stage where co-localisation of the 2 proteins was found out of the cohort when using the blocking peptide (negative controls)

7.2.1 Immunofluorescence of ovarian and testicular tissue

Three replicate experiments were conducted. In each individual experiment, 3 slides containing sections of ovine ovarian tissue and 3 slides containing sections of testicular tissue positive control were initially permeabilised in freshly made 0.5% (v/v) Triton X-100 PBS with 2% (w/v) BSA (lyophilized powder, ≥96%) by adding 200 μl of the solution to each slide for 15 min at RT. The PBS solution was made by dissolving 1 PBS tablet (Gibco) in 500 ml sterile-distilled H_2O followed by 0.2 μm cellulose acetate filter sterilization. The slides were then blocked in blocking buffer containing 2% (w/v) BSA in PBS with 0.05% (v/v) Tween-20. Specifically, 200 μl of the blocking solution was added to each slide and covered with a piece of parafilm to prevent drying out. The slides were blocked for 1 h at RT. The ovarian and testicular slides were then divided equally into 2 groups (3 ovarian and testicular slides per group), 1 being the experimental group and 1 the negative control group. The slides of the experimental group were incubated with 2 μg/ml primary antibodies (anti-GTSF1 and anti-MVH) in blocking buffer overnight at 4°C in the dark, while the slides of the negative control were also incubated in a similar manner with 2 μg/ml of primary antibodies but with GTSF1 antibody being incubated in advance with blocking peptide (10 μg/ml) as described above. A volume of 200 μl was applied to each slide and the slides were covered with a piece of parafilm prior to incubation. All slides were sequentially washed 3 times in PBS for 15 min at RT in the dark in a coplin-jar. The secondary antibodies were then applied (1:200 dilution) in blocking buffer. A volume of 200 μl was applied to each slide and the slides were covered with a piece of parafilm and incubated for 1 h at RT. The slides were then inserted in a coplin-jar containing PBS. The slides were counterstained with 1 μg/ml DAPI in 2 X SSC (Appendix II) by applying 20 μl of the solution on each slide and covering them with a coverslip. The slides were wrapped in aluminum foil and kept at 4°C until visualization (Section 7.2.2).

7.2.2 Immunofluorescence of oocytes

Three replicate experiments were conducted. The denuded GV oocytes were obtained from ovine COCs as described previously (Chapter 3, Section 3.2.1), while denuded MII oocytes were obtained following IVM of COCs as described previously (Chapter 2, Section 2.1.3). A similar approach was used for the immunofluorescent analysis of the GV and MII ovine oocytes. In each of the 3 replicate experiments, the isolated GV and MII oocytes (approximately 30 for each stage) were placed in separate wells of a 4 well dish and fixed in 500 μl of 4% PFA (w/v) in PBS overnight at 4ºC. The oocytes were then washed in 500 μl of PBS at RT for 5 min in clean wells and were then pre-treated in clean wells of a 4 well dish containing 500 ml of freshly made 0.5% (v/v) Triton X-100 (Sigma-Aldrich) in PBS with 2% (w/v) BSA (lyophilized powder, ≥96%) in PBS for 15 min at RT. Both GV and MII oocytes were then divided into 2 equal groups, 1 being the experimental group and 1 the negative control group and they were placed in separate wells of a clean 4 well dish each containing 500 μl of blocking buffer followed by incubation for 1 h at RT. The oocytes were then transferred in a clean 4 well dish and 1 set of GV and MII oocytes were incubated in a 40 μl drop containing 2 μg/ml of primary antibodies (anti-GTSF1 and anti-MVH) in blocking buffer overnight at 4°C in the dark, while the other set of GV and MII oocytes were incubated with 2 μg/ml of anti-GTSF1 antibody incubated with pre-incubated blocking peptide along with 2 μg/ml of anti-MVH antibody. Prior to incubation, the 4 well dishes were wrapped in parafilm to avoid evaporation of the solution in each of the wells. The oocytes were then transferred into separate wells of clean 4 well dishes and sequentially washed 3 times in 500 ml of PBS for 15 min at RT in the dark followed by 2 h incubation in clean wells of 4 well dishes containing a 40 μl drop of secondary antibody (1:200 dilution in blocking buffer) at RT. Once again the 4 well dishes were wrapped in parafilm to avoid evaporation. Oocytes were then washed in clean wells containing 500 ml of PBS (similar to Section 7.2.1). Oocytes from each drop (3-4 oocytes each time) were pipetted onto clean Super-frost Plus slides containing a 20 μl drop of 1 μg/ml DAPI in 2 X SSC and were covered with a coverslip using vaseline pillars. Slides were wrapped in aluminum foil and kept at 4ºC. All slides used for immunofluorescent analysis of oocytes and ovarian and testicular sections were visualized with a Zeiss Axioplan2 microscope fitted with different wave length filters to capture blue, green and red fluorescences (420-495 nm; 495-520 nm; 590-650 nm; respectively).

7.3 RESULTS

By using immunofluorescence, signals of GTSF1 and MVH were detected in both the male and female germline with the overall results for the immunofluorescent analysis of GTSF1 and MVH in the ovary and testis shown in Table 7.1. In the figures that follow, representative images of GTSF1 and MVH localisation along with the merged images of the 2 proteins are shown at the different stages of development (Figure 7.1, Figure 7.2). The GTSF1 protein was located in the cytoplasm of primary spermatocytes in the male germline (Figure 7.1 B). The protein was also located in spermatogonia and secondary spermatocytes (images not shown). In the ovine ovary, immunofluorescence analysis showed a strong and even cytoplasmic staining pattern of GTSF1 in the oocytes at the primordial (Figure 7.1 C), primary (Figure 7.1 C), and transitional stages of follicle development (image not shown), in agreement with the detection of mRNA transcripts at these stages of development (Chapter 3). The negative control lacked GTSF1 expression as shown in the control image of testicular tissue (Figure 7.1 A), further confirming the findings. Simultaneous immunofluorescent staining for GTSF1 and MVH showed that MVH was expressed in abundance in the cytoplasm of the oocytes and also showed that granular aggregates of GTSF1 were associated with chromatoid bodies in the sperm and P-bodies in the oocyte (Figure 7.1 B-D).

Table 7.1: Immunofluorescent analysis of GTSF1 and MVH protein co-localisation

Stage of follicle and oocyte development						
Ovary	Primordial follicle	Primary follicle	Transitional follicle	Secondary follicle	GV oocyte	MII oocyte
Cellular localisation	Ooplasm	Ooplasm	Ooplasm	Ooplasm	Ooplasm	Ooplasm
No. of stage analysed	30	30	26	12	33	28
GTSF1 and MVH co-localisation	29/30 follicles (96.7%)	28/30 follicles (93.3%)	22/26 follicles (73.3%)	0/12 follicles (0.0%)	31/33 oocytes (93.9%)	27/28 oocytes (96.4%)
Statistical significance	$P<0.005$	$P<0.005$	$P<0.005$	NS	$P<0.005$	$P<0.005$
Stage of spermatogenesis						
Testis	Spermatogonia		Primary spermatocytes		Secondary spermatocytes	
Cellular localisation	Cytoplasm		Cytoplasm		Cytoplasm	
No. Of stage analysed	23		30		29	
GTSF1 and MVH co-localisation	23/23 spermatogonia (100%)		28/30 spermatocytes (93.3%)		27/29 spermatocytes (93.1%)	
Statistical significance	$P<0.005$		$P<0.005$		$P<0.005$	
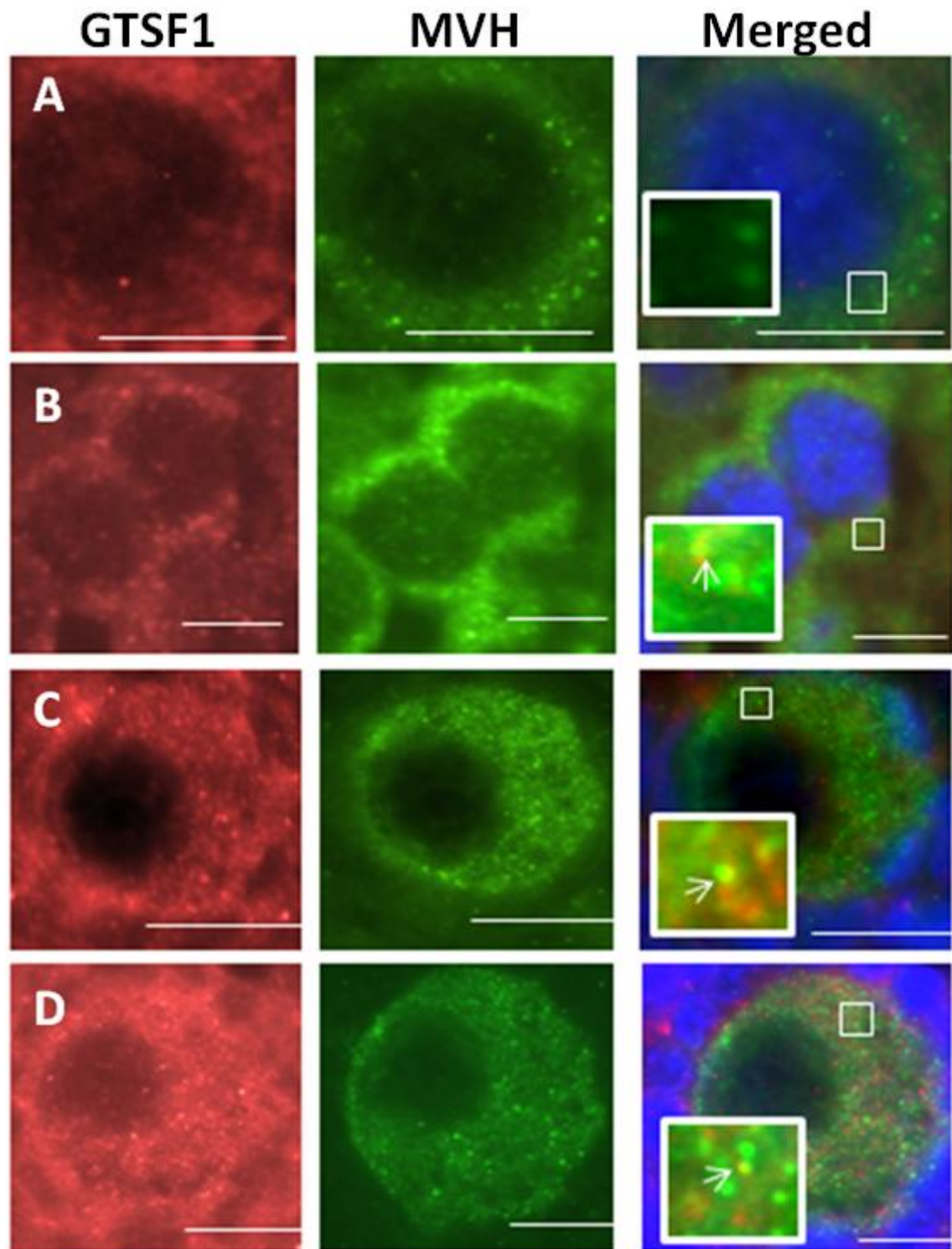
Figure 7.1: Characterisation of GTSF1 and MVH localisation by immunofluorescence during ovine follicular development and in the ovine testis. **A:** Negative control in primary spermatocyte in which anti-GTSF1 was neutralised in 5 X excess of its specific blocking peptide before immunofluorescence. **B-D:** GTSF1 (Red) and MVH (Green) localisation in the cytoplasm of: **B:** Ovine primary spermatocytes (positive control). **C:** Primordial follicle, **D:** Primary follicle. The first of the 3 columns represents GTSF1 staining, the second represents MVH staining and the third represents the merged images of GTSF1 and MVH counterstained with DAPI. Arrows in magnified images for each stage indicate co-localisation of GTSF1 and MVH granules (Yellow). Scale bar: 10µm.
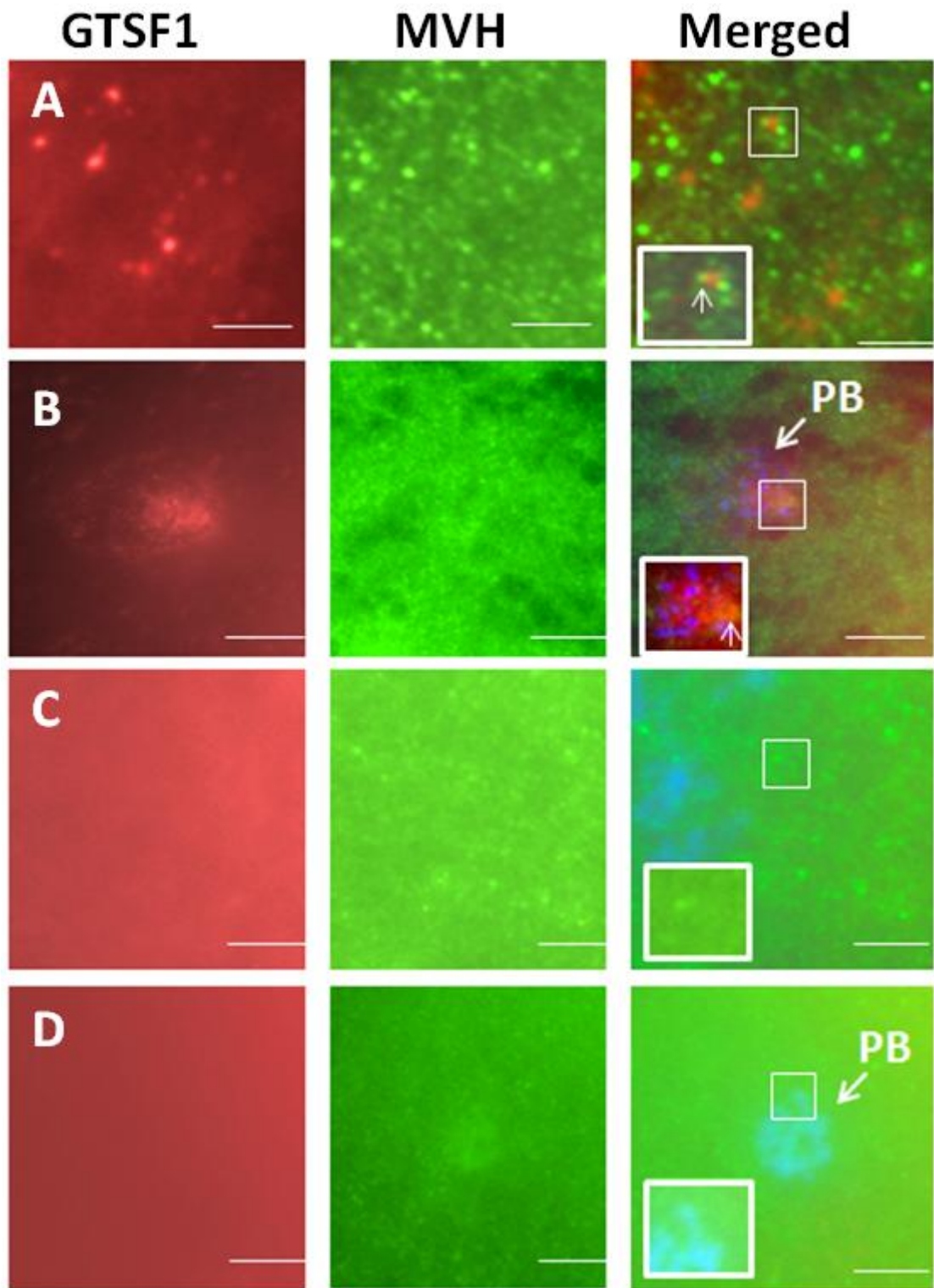
Figure 7.2: Characterisation of GTSF1 and MVH localisation by immunofluorescence in GV and MII oocytes. **A:** GTSF1 (Red) located in GV oocytes associated with P-bodies (anti-MVH, Green) as indicated by arrows in the magnified merged image (Yellow). **B:** GTSF1 (Red) located in the polar body of an MII oocyte associated with P-body (anti-MVH, Green) as indicated by arrows in the magnified merged image (Yellow). **C-D:** Negative control of **C:** GV and **D:** MII oocytes in which anti-GTSF1 was neutralised with 5 X excess of its specific blocking peptide before immunofluorescence. Co-localisations of GTSF1 and MVH are highlighted by arrows in the merged images of A and B. The first of the 3 columns represents GTSF1 staining, the second represents MVH staining and the third represents the merged images of GTSF1 and MVH counterstained with DAPI. Scale bar: 1μm. (PB: Polar body).

232

Immunofluorescent staining for GTSF1 in the isolated GV and MII oocytes also showed localisation of the GTSF1 protein in the ooplasm of GV and MII oocytes (Figure 7.2 A-B). In GV oocytes, GTSF1 immunofluorescence showed a number of small granules distributed throughout the oocyte cytoplasm. In the same oocytes, numerous MVH granules were found. Further analysis showed that a few of the GTSF1 granules were co-localised with the MVH located P-bodies in most of the oocytes analysed (Figure 7.2 A merged image). In MII oocytes, GTSF1 staining was concentrated mostly within and around the polar body as shown in the figure below (Figure 7.2 B). In MII oocytes, the MVH protein was still observed to be in granular form, however there were much fewer granules present compared to the GV stage oocyte. The few MVH granules were dispersed throughout the cytoplasm including the polar body where the GTSF1 protein was located (Figure 7.2 B). The above observations were confirmed by the negative control staining in which GTSF1 protein was completely blocked in both the GV and MII oocyte, while the MVH protein was not affected, with numerous granules located in the GV oocytes and fewer granules in the MII oocyte (Figure 7.2 C-D).

7.4 DISCUSSION

The results show that GTSF1 is expressed during ovine gametogenesis and confirms the previous findings for the characterisation of *GTSF1* in this study (Chapter 3) in the sheep and by others in mice (Yoshimura *et al.*, 2007; Krotz *et al.*, 2009). The results also show that GTSF1 is localised to the P-body in the GV and MII ovine oocyte which suggests that GTSF1 may be involved in small RNA post-transcriptional regulation as has been reported for the P-body in other species (Kedersha *et al.*, 2005; Kotaja *et al.*, 2006). These findings agree with a recent study conducted in the bovine, in which the GTSF1 protein was shown to be localised to the chromatoid body in male and the P-body in female gametogenesis (Lu *et al*., 2012). Localisation of GTSF1 to the P-body in GV oocytes suggests that there are similarities between meiotic progression in the male and female (Aravin *et al.*, 2007b; Carmell *et al.*, 2007). In previous studies conducted in mice, expression of GTSF1 in gametogenesis was only detected in the cytoplasm of sperm and not in the oocytes (Yoshimura *et al.*, 2007). Expression of the GTSF1 protein in ovine oocytes in this study but not in the mouse study could be attributed to species differences between monovular species such is the sheep in contrast to the polyovular mice, or to different sensitivities of the assays applied.

Localisation of GTSF1 within the P-body in GV oocytes shows that GTSF1 may be involved in post-transcriptional gene expression during meiotic maturation from the GV to the MII stage. The gene could also be involved in retrotransposon repression similar to the findings of the mouse study following the *Gtsf1* knockout of male mice (Yoshimura *et al.*, 2009). Moreover, a potential 3´ UTR PRE domain has been identified in the sequence of *GTSF1* of several species including bovine, human and mouse, with this domain being vital for the translational activation of several genes following progesterone stimulation, including *D7*, proto-oncogene serine/threonine-protein kinase *MOS*, *FGFR1*, *AURKA*, *B4* and *G10* (Lu *et al.*, 2012). Comparison of the ovine *GTSF1* sequence as acquired in this study also showed sequence alignment for the potential 3' UTR PRE domain as in the other species. This suggests that *GTSF1* may be important during the meiotic progression from the GV to the MII stage. The *AURKA* gene has been shown to be involved in resumption of meiosis, spindle formation and oocyte progression as an MTOC (Saskova *et al.*, 2008). Furthermore the microarray analysis following *GTSF1* knockdown showed a trend in the reduction of the transcripts of this gene in comparison with the controls following the knockdown (Chapter 6). Moreover, *MOS* is also involved in microtubule organisation and polar formation during oocyte maturation (Choi *et al.*, 1996). Identification of this putative PRE domain within the 3´ UTR signifies the finding of this study in that the *GTSF1* appears to be translated during the maturation stages and functions during this stage by affecting RNA processing and translation. The expression of GTSF1 protein in MII oocytes in this study was restricted to the first polar body and the area surrounding it, while the few MVH granules were localised in both the first polar body and the ooplasm of the oocyte. The expression of these MVH granules suggests that P-bodies might be present in MII oocytes. This is in agreement with the findings in the bovine species, where MVH staining was also observed in the MII oocyte (Lu *et al.*, 2012). Previous studies in mice have shown that P-bodies are not present in MII oocytes but rather they disappear during *in vitro* meiotic maturation and that they are completely absent in MII-arrested secondary oocytes (Swetloff *et al.*, 2009). The differences observed in the murine species could be due to species differences or to the different antibodies used. Furthermore, localisation of GTSF1 in the polar body and not in the cytoplasm of the MII oocyte suggests that the protein is not active in the oocyte following polar body extrusion. A possible explanation for the gathering of the GTSF1 protein within the polar body at the MII stage as observed in this study could be that GTSF1 carries its binding RNAs to the first polar body for them to be excluded from further function

during the fertilisation and early development of the zygote. The presence of the *GTSF1* transcript during the early embryo stages until the blastocyst stage as observed here in Chapter 3 as well as in human and bovine tissue (Lu *et al*., 2012) suggests that *GTSF1* may function during early development through association with other RNAs. In order to confirm this initial observation, further experimentation is required. Generation of ovine embryos and culture to the blastocyst stage following *GTSF1* knockdown in GV oocytes would confirm the impact of *GTSF1* knockdown on oocyte developmental competence.

7.4.1 Conclusion

In summary, the co-localisation of GTSF1 within the P-body during development of the ovine oocyte from the GV to the MII stage suggests that GTSF1 may be involved in RNA binding and be associated with the RNAi pathway.

Chapter 8: General Discussion

The results presented in this thesis have extended our understanding of the biology of *GTSF1* during sheep oocyte maturation. The data presented has mapped the expression of *GTSF1* transcript and its translated protein across gametogenesis. Furthermore, experiments using siRNA have provided preliminary insights into the roles played by *GTSF1* during the GV to MII transition in oocytes *in vitro*. Overall, the data suggest that *GTSF1* is involved in post-transcriptional control of RNA processing, translational regulation and RNA storage which may impact on oocyte developmental competence.

8.1 Characterisation of ovine *GTSF1*

Identification of markers of gamete developmental competence (quality) is of importance for providing improved treatment options for patients undergoing assisted conception. Gene expression profiling has revealed a number of novel genes expressed in germ cells with *GTSF1* being 1 of these putative markers of oocyte development. This gene is highly conserved across species and has previously been shown to have a sexual dimorphism in its function in mice, where male mutants for *Gtsf1* had an infertile phenotype, whereas female mutants demonstrate normal ovarian function. The cellular distribution of function of *GTSF1* in the regulation of gametogenesis of a monovular species such as the sheep which is a physiological relevant model to the human has not been investigated. In order to study the role of this novel gene in the regulation of follicle development and oocyte maturation in sheep, it was necessary to sequence the ovine gene and to characterise the expression pattern of *GTSF1* across all stages of ovine follicle, oocyte and embryo development to the blastocyst stage by interrogating staged cDNA libraries. To further interpret the expression of this gene in gametogenesis, the cellular distribution of *GTSF1* mRNA was characterised by FISH and the presence of protein was confirmed by Western blotting.

The results indicated the gamete specific expression of *GTSF1* throughout ovine gametogenesis. *GTSF1* was expressed in the male germline and in the female primordial to the secondary stage follicles, GV and MII oocytes as well as the early embryo. Conversely, *GTSF1* was not expressed in oocytes from secondary and antral stage follicles and was absent from all somatic cells of the ovary. Furthermore, *GTSF1* was not expressed in non-ovarian somatic tissue, further confirming its specificity as a

gamete specific gene. The data from Chapter 3 also illustrated that *GTSF1* was localised in the cytoplasm of the oocyte of early staged follicles and not in the oocytes from pre-antral and antral follicles, while in the testis, the expression of the gene was detected in spermatogonia, spermatocytes and spermatids.

Comparison of the ovine *GTSF1* sequence showed high homology with several other species. The alignment of the predicted ovine GTSF1 protein sequence confirmed the high conservation of this gene in evolution. Moreover the existence of 2 tandem copies of CHHC Zn-fingers in the conserved sequence of *GTSF1* capable of binding RNA, suggests that *GTSF1* might be important for functions regarding the developmental processes of the gonad (Andreeva and Tidow, 2008). Other studies were consistent with our observations and also showed that *GTSF1* transcripts were expressed in the oocytes and preimplantation embryos in mice (Yoshimura *et al.*, 2009), humans (JD Huntriss and HM Picton, unpublished data) and bovine (Lu *et al*., 2012) with highest expression being observed in secondary oocytes at the GV stage of development. The results of the characterisation of ovine *GTSF1* during gametogenesis reported in Chapter 3 provided the basis for the investigation of the function of the gene during the IVM of oocytes from this species.

8.2 Validation of targeted gene knockdown during IVM of ovine oocytes by microinjection of siRNA species

It was hoped that targeted gene knockdown during IVM of ovine oocytes by microinjection of siRNA species would support investigation of the function of novel genes such as *GTSF1*. In order to achieve this, the IVM system ought to be able to stimulate and support the resumption of meiosis and the cytoplasmic maturation in fully grown meiotically competent prophase I oocytes (Picton, 2002). The autocrine and paracrine signalling between the oocyte and the somatic cells of the follicle have been shown to be necessary in order to lead to the induction of the preovulatory surge that promotes cytoplasmic and nuclear maturation in addition to a progesterone environment established by granulosa cell steroid synthesis and to hyaluronic acid synthesis (Fulka *et al.*, 1998). Creation therefore of a targeted knockdown in sheep oocytes *in vitro* should not compromise oocyte survival or oocyte meiotic progression. A 2 day culture system involving microinjection of oocytes with siRNA and culture with a specific PDE meiosis inhibitor (cilostamide), followed by removal of the inhibitor and co-culture with oocytectomised cumulus shells in order to re-establish the paracrine interaction

necessary for oocyte maturation was therefore utilised as described previously (Cotterill, 2008). The known oocyte-derived gene *Gdf9* (Dong *et al.*, 1996) was used to validate the microinjection system and to establish the validity of microinjection of siRNAs as a means to knockdown genes in ovine oocytes and to study their effect on oocyte maturation. The previous study of Cotterill, (2008) used dsRNA as the vehicle to effect gene knockdown in sheep oocytes. In this thesis, introduction of siRNA species was validated and reported in Chapter 4. As stated in the introductory Section 1.5.1 of Chapter 1, introduction or expression of dsRNA triggers the RNAi pathway. The Dicer cleaves the dsRNA into 21-23 bp siRNAs that then unwind and assemble into RISC with the antisense siRNA strand guiding RISC to complementary RNA molecules to cleave the mRNA resulting to gene silencing (Hawkins *et al.*, 2011). However, since most mammalian cells build-up an antiviral response following the introduction of dsRNA that are longer than 30 bp, the introduction of 21-23 bp siRNAs to induce RNAi without eliciting the antiviral response is considered a better strategy for gene knockdown (Dewitte-Orr *et al.*, 2009).

Transcript levels for *GDF9* were significantly reduced (P<0.05) following *GDF9* siRNA injection in GV oocytes followed by IVM co-culture of gene knockdown oocytes with compact oocytectomised cumulus cells (0.7±0.2 arb. units, n=6) in comparison to buffer control injected oocytes (6.7±0.2 arb. units, n=6). Off-target effects were assessed by analysing levels of *BMP15* following the *GDF9* knockdown and levels of *BMP15* following *GDF9* knockdown (1.4±0.3 arb. units, n=6) were not significantly different (P>0.05) to the control values (1.7±0.3 arb. units, n=6), suggesting that there were low/no off target affects incurred by the knockdown of this oocyte-specific gene. The function of *GDF9* was then evaluated following gene knockdown, by morphological evaluations of oocytes and cumulus cells and by meiotic progression. The latter was significantly reduced (P<0.05) when *GDF9* siRNA was injected into the oocytes (13.1% of viable oocytes injected with *GDF9* siRNA progressed to MII) in comparison to the buffer-injected control oocytes (26.0% of viable oocytes injected with control buffer progressed to MII). Meiotic maturation of sheep oocytes is known to be induced by paracrine factors released by gonadotrophin stimulated oocyte cumulus cell complexes (Buccione *et al.*, 1990b). The meiotic progression results combined with molecular analysis presented in this thesis confirmed that *GDF9* plays a regulatory role during cumulus expansion. The culture system was

proven to be suitable for studying the role of oocyte genes in meiosis and cumulus maturation.

The function of oocyte-derived *GDF9* on cumulus cells was assessed by morphological evaluations of cumulus expansion and mucification and also by direct assessment of the effect of oocyte gene knockdowns on the function (expression) of specific cumulus cell genes that have been shown in mouse studies to be controlled by oocyte-derived factors. These genes were *HAS2* (Elvin *et al.*, 1999), *GREMLIN1* (Pangas *et al.*, 2004), *AMH* (Kitahara *et al.*, 2012) and *LDH1* (Moore *et al.*, 2007), as well as members of the EGF family, *AREG* (Cotterill *et al.*, 2012), *EREG* (Zimin *et al.*, 2009) and *BTC* (Cotterill *et al.*, 2012); all induced by LH in mural granulosa to bind to the EGFR and promote COC maturation (Salmon *et al.*, 2004; Hussein *et al.*, 2005; Hsieh *et al.*, 2007; Sugiura *et al.*, 2009). Cumulus expansion was significantly reduced ($P<0.05$) in cumulus shells following gene knockdown in comparison with the controls (12.6% and 32.9% respectively for fully expanded cumulus shells). In addition, cumulus cell mRNA expression levels of *HAS2* were significantly reduced ($P<0.05$) in the cumulus cells following *GDF9* knockdown (1.3 ± 0.7 arb. units, n=3) in comparison with the controls (3.7 ± 0.4 arb. units, n=3), while there was a trend for reduction of *GREMLIN1* and *AMH* mRNA levels following the knockdown (0.3 ± 0.2 arb. units, n=5; 0.2 ± 0.1 arb. units, n=5) respectively in comparison with controls (0.7 ± 0.3 arb. units, n=5; 0.6 ± 0.3 arb. units, n=5) that were not significant ($P>0.05$). The transcript levels of the regulin genes were then evaluated. Transcript levels of these genes are induced by LH in mural granulosa cells and bind to the EGFR and have been shown to induce COC maturation (Park *et al.*, 2004; Hsieh *et al.*, 2007). These ligands are necessary for IVM as shown by their ability to induce oocyte maturation in COC cultures but not in cultures of denuded oocytes (Park *et al.*, 2004). In addition, mutant mice for *Egfr* and *Areg* as well as double mutant animals are unable to promote COC maturation, further demonstrating that the EGFR network is vital in COC maturation *in vivo* (Hsieh *et al.,* 2007). Furthermore, removal of oocytes from COCs resulted in the reduction of *Egfr* in cumulus cells with the levels restored after treatment with recombinant *Gdf9* or mixture of recombinant *Gdf9* with *Bmp15* (Su *et al.*, 2010). Recent work by Cotterill *et al.*, (2012) has demonstrated the presence of *AREG*, *EREG* and *BTC* in ovine mural granulosa cells and cumulus cells. In particular, *AREG* appeared to be most important for LH signalling events in sheep COCs but it was absent from oocytes (Cotterill *et al.*, 2012). In this thesis, transcript levels of *AREG*, *EREG* and *BTC* were similar between cumulus shells

co-cultured with *GDF9* siRNA-injected oocytes (0.5±0.4 arb. units, n=3; 0.7±0.3 arb. units, n=3; 0.2±0.3 arb. units, n=3) respectively, compared to cumulus shells co-cultured with buffer-injected control oocytes (0.7±0.6 arb. units, n=3; 0.7±0.3 arb. units, n=3; 0.3±0.4 arb. units, n=3) and were not statistically different (P>0.05). An explanation for these observations is that induction of AREG expression occurs very rapidly and peaks after LH exposure (Cotterill *et al.*, 2012). Therefore, the levels of *AREG* could have been dropped back down again during the 24 h exposure window of IVM in this study.

The results in this thesis confirm and extend the results obtained from the knockdown of *GDF9* in ovine oocytes by the means of dsRNA (Cotterill, 2008). Specifically, knockdown of *GDF9* by injecting dsRNA into ovine oocytes using the culture system detailed here significantly altered the degree of unexpanded and fully expanded cumulus shells when compared to the buffer-injected control group and oocyte *GDF9* knockdown was also associated with significantly reduced levels of *HAS2* and *GREMLIN1* (Cotterill, 2008).

The Gdf9 protein has been shown to bind to the Tgfβ type I receptor ALK5 which then recruits the secondary receptor BmprII (Moore *et al.*, 2003; Mazerbourg *et al.*, 2004). Binding of Gdf9 to the receptors present on the cumulus cells will recruit Smads2/3 and the co-Smad 4 (Mazerbourg *et al.*, 2004). Future follow up studies after *GDF9* knockdown should involve the assessment of receptor proteins and intracellular SMADs that are involved downstream of GDF9 signalling as well as to study the association of *GDF9* with the RNAi pathway.

Overall, these morphological evaluations of oocyte meiotic maturation and cumulus cell expansion along with transcript analysis of candidate genes in oocytes and cumulus cells have proven that the siRNA microinjection approach and IVM culture system detailed can be used for the creation of targeted gene specific knockdown of novel genes such as *GTSF1* during IVM of ovine oocytes. The system reported in Chapter 4 therefore formed the basis for the study of *GTSF1* function in ovine oocytes in Chapters 5 and 6.

8.3 Studies of the targeted knockdown of oocyte *GTSF1* using siRNA

Investigation of the molecular basis of oocyte-secreted factors and their function in signalling pathways are valuable means of advancing understanding of the mechanisms that control oocyte growth and maturation in different species. Recent studies have highlighted potential association of oocyte secreted factors with miRNAs. Small RNAs have important regulatory roles in many different cellular processes including cell proliferation, differentiation and apoptosis and may play important roles during development as shown by their tissue specific expression pattern and evolutionary conservation (Lewis *et al.*, 2003). The Dicer enzyme required to process miRNA precursors or dsRNA into RNAi molecules for miRNA and siRNA pathways respectively has resulted in significant differences in the expression of follicle development-related genes including *Gdf9*, *Bmp15*, *Amh*, *Inhba* and *Cyp17α1*, following its knockdown (Lei *et al.*, 2010). Similarly, *Ago2* deletion was associated with abnormal spindles and improper chromosome clustering in mouse growing follicles (Kaneda *et al.*, 2009). These studies illustrate that the genes involved in RNAi can affect oocyte development through global regulation of miRNA stability that affects gene expression in developing oocytes.

Cellular localisation of GTSF1 in bovine round spermatids and mature sperm indicates that the GTSF1 protein functions during post-meiotic spermatogenesis in addition to its already established role during the early primary spermatocyte development (Lu *et al*., 2012). The chromatoid bodies in the male germline and their equivalent P-bodies in oocyte are cytoplasmic aggregates that contain RNA and RNA-binding proteins. They are highly evolutionary conserved and have established roles in differentiation of germ cells and early embryo development (Kotaja *et al.*, 2006; Kotaja and Sassone-Corsi, 2007). Dicer and components of miRISC like the Argonaute family and several miRNA species are found in the chromatoid body and P-body and have functional roles in RNA storage and processing. The specific pattern of expression of *GTSF1* in the germline along with the gene's conserved domain with 2 tandem copies of CHHC Zn-finger that may be responsible for RNA-binding both suggest that *GTSF1* might be associated with the above processes. In addition, knockout of *Gtsf1* in male mice has been shown to increase transcription of the retrotransposons *Line1* and *Iap* as well as demethylation of their promoter region leading to their activation (Yoshimura *et al.*, 2009). The expression of these retrotransposons in the male gonad is regulated by a transcriptional silencing mechanism that requires *Piwi* family members *Mili* and *Miwi2* and this

mechanism itself is responsible for regulating the expression of retrotransposons in the germline so that they are not overexpressed and become deleterious for the offsprings (Aravin *et al.*, 2007b). In general, piRNA have been shown to be necessary for mammal spermatogenesis and maintenance of germline (Khurana and Theurkauf, 2010). Except from the association in gametogenesis; Piwi also associates with Dicer and therefore might act through the miRNA mechanism (Bernstein *et al.*, 2001; Yin and Lin, 2007). Even though *Gtsf1* knockout female mice have normal ovarian function, the similar expression patterns in male and female germ cells may imply that *GTSF1* functions in the maintenance of the oogonia population during ovarian development and oocyte meiotic progression during oogenesis of monovular species such as the sheep.

To examine the function of *GTSF1* during IVM of fully grown, secondary ovine oocytes, the ovine sequence of the gene acquired in Chapter 3 was used to design siRNA specific primers for *GTSF1*. Four siRNA species were tested and oocyte-specific *GTSF1* knockdowns were created using the microinjection and IVM system detailed in Chapter 4. The effects of *GTSF1* knockdown were examined on oocyte meiotic progression and cumulus mucification and expansion and candidate oocyte and cumulus genes and structural analysis of oocyte spindles by α-Tubulin immunostaining.

The data generated showed that a significant reduction ($P<0.05$) in *GTSF1* expression was induced following *GTSF1* siRNA injection (10.7±3.2 arb. units, n=4) in comparison with buffer injected controls (111.2±58.6 arb. units, n=4) without compromising oocyte survival and oocyte meiotic progression. Analysis of the 2 other oocyte-specific factors *GDF9* and *BMP15* expression showed that both *GDF9* was reduced following *GTSF1* knockdown (0.2±0.1 arb. units, n=4) and *BMP15* mRNA levels were reduced to (617.6±365.0 arb. units, n=4) in comparison with controls (0.38±0.1 arb. units, n=4; 1189.8±433.6 arb. units, n=4) respectively but these reductions were not significant ($P>0.05$). At the time the analysis took place, there was limited knowledge about *GTSF1*. More suitable candidates to confirm no off-target effects would include genes belonging to the same family as *GTSF1* (UPF0224), for examples the U11/U12 small nuclear ribonucleoprotein 48 kDa protein identified in *H. sapiens* and *M.* musculus (Ota *et al.*, 2004).

Knockdown of *GTSF1* did not significantly affect ($P>0.05$) oocyte meiotic progression and cumulus expansion. The knockdown experiments of Chapter 6 resulted in higher

survival and maturation rates in comparison with experiments in Chapter 5, but no significant differences (P>0.05) were observed between *GTSF1* injected oocytes and the control oocytes in either of the 2 experimental series. In particular, maturation rates of viable oocytes following the knockdown (33.3%) in Chapter 5 were not significantly different (P>0.05) to viable buffer-injected oocytes (19.6%) or viable N.C. siRNA-injected control oocytes (26.7%), while maturation rates of viable oocytes following the knockdown (54.5%) in Experiment 2 were no significantly different (P>0.05) to viable N.C. siRNA-injected control oocytes (47.1%). Similarly, cumulus shells co-cultured with injected oocytes for the different treatments were able to initiate expansion in both studies, but there were no significant differences between *GTSF1* siRNA-injected and control oocytes for the 2 experiments (P<0.05).

Preliminary studies of *GTSF1* in relation to meiotic spindle formation were undertaken. Although the numbers of were very low and extreme care must be taken in interpretation, the preliminary indications were that spindle formation might be affected by gene knockdown. Follow-up experimentation is needed to confirm these pilot results. Alternatively, interrogation of genes associated with spindle formation by real-time PCR could be used to confirm these effects.

The function of *GTSF1* was further investigated by gene expression analysis of potential target genes associated with the knockdown, based on its estimated function. The oocyte targets selected included *NOBOX* which is situated upstream of *GTSF1* (Krotz *et al.*, 2009), *CDC20* (Reis *et al.*, 2007), *TNRC6A* (Nishi *et al.*, 2013), *LSM14A* (Li *et al.*, 2012) and *INCENP* (Earnshaw and Cooke, 1991), while the list of candidate genes examined in the cumulus cells was the same as used for the validation experiments of Chapter 4. The oocyte expressed genes were selected because of their involvement with meiotic maturation (*CDC20*, *INCENP*), the RNAi pathway (*TNRC6A*), RNA processing and spindle formation (*LSM14A*). Following the targeted knockdown of *GTSF1,* the selected gene transcripts of both the oocyte and the cumulus cells were found not to be significantly different between knockdown oocytes and controls (P>0.05). The lack of significant effects in any of the genes analysed could be attributed to the low number of MII oocytes available following the knockdown and the cultures. Although *GTSF1* knockdown did not appear to affect the capacity of GV oocytes to complete meiotic progression over 24 h of IVM, it could still have functional importance for oocyte developmental competence. The limited number of oocytes and

the variability of the data meant that alternative ways to study the function of the gene should be considered. Additional *GTSF1* knockdown oocytes were therefore generated in Chapter 6 to facilitate more comprehensive microarray screening of the impact of *GTSF1* knockdown on maturation.

8.4 Transcriptome analysis of the impact of *GTSF1* knockdown in GV oocytes on MII oocytes derived by IVM

In an attempt to identify the genes and pathways downstream of *GTSF1* during oocyte maturation, the Affymetrix GeneChip bovine arrays were used to compare gene expression following *GTSF1* knockdown in MII oocytes in comparison with N.C. siRNA-injected oocyte. The IVM microinjected oocytes with transcript levels for *GTSF1* reduced by over 50% which were generated in Chapter 6, were divided in 3 groups based on the reduction of *GTSF1* transcript levels (0.5 ± 0.1 arb. units, n=5; 0.9 ± 0.1 arb. units, n=5; 1.1 ± 0.1, n=4) respectively, following *GTSF1* siRNA injection in comparison with N.C. siRNA-injected control oocytes (2.9 ± 0.4 arb. units, n=5; 2.5 ± 0.2 arb. units n=5; 2.8 ± 0.8 arb. units, n=4) and were sent for hybridisation onto the bovine arrays along with their respective controls. Primary bioinformatic analysis and normalisation, identified a total of 231 differentially expressed genes between the knockdowns and the controls (51 down-regulated and 180 up-regulated). Gene ontology analysis of the genes from the high-level knockdown group, revealed that knockdown of *GTSF1* affected biological processes such as oocyte development, actin cytoskeleton organisation and spindle assembly. In addition, the knockdown had a negative effect on cellular components associated with microtubule cytoskeleton as well as mitochondrial components and membrane transporters, while molecular functions such as ATP dependent helicase activity, calcium ion and cell adhesion binding, cytochrome c oxidase activity and ion trans-membrane transporter activity were also affected. Candidate genes including *AURKA*, *CDK2*, *COX17*, *PCBP1*, *FKBP4*, *ZNF706*, *TECR*, *TIMP1* appeared to be down-regulated following *GTSF1* knockdown, whereas *MYL9*, *MYL12A* and *CKAP2* appeared to be up-regulated following *GTSF1* knockdown. The impact of *GTSF1* knockdown on the gene transcripts obtained from the primary bioinformatic analysis was tested by real-time PCR of the original individual samples that were used for microarray experiments. These analyses confirmed a significant reduction ($P<0.05$) of only 2 genes following *GTSF1* knockdown. In particular, transcript levels of *TIMP1* were significantly reduced ($P<0.05$) following *GTSF1* knockdown (0.5 ± 0.1 arb. units, n=4) in comparison with the controls (5.0 ± 1.5 arb.

units, n=4) in addition to *MYL9* transcript levels that were significantly reduced (P<0.05) in the GTSF1 knockdown oocytes (0.2±0.1 arb. units, n=4) in comparison with the controls (0.5±0.1 arb. units, n=4). Transcript analysis of *AURKA*, *FKBP4* and *CDK2* were reduced following *GTSF1* knockdown (0.3±0.1 arb. units, n=4; 0.4±0.1 arb. units, n=4; 0.3±0.1 arb. units, n=4) respectively in comparison with controls (1.1±0.4 arb. units, n=4; 5.2±2.9 arb. units, n=4; 2.9±1.3 arb. units, n=4), but these reduction were not significant (P>0.05).

The variability of the data from the primary bioinformatic analysis and the failure to verify the majority of the targets by real-time PCR meant that there could have been a number of incorrect hybridisations between the bovine arrays and the ovine samples. A secondary bioinformatic analysis using a completely different approach than the primary bioinformatic analysis was thereafter performed to align the bovine probe sequences to the sheep genome sequences in order to provide more robust data for analysis. Gene ontology analysis following secondary bioinformatic analysis showed that *GTSF1* knockdown did affect a few transcripts associated with microtubule cytoskeleton in agreement with the primary bioinformatic analysis, however most of the down-regulated transcripts were associated with translation, ribosomal function and RNA-binding, all in-tune with the inferred function of *GTSF1* based on the background information and the previous results of this thesis. Several candidate genes were selected from the secondary bioinformatic analysis to be confirmed by real-time PCR, including the down-regulated genes, *TCOF1*, *PARP12*, *RPS8*, *SREK1IP1*, *CACNA1D*, *TARDBP*, *DHX35* as well as the up-regulated genes *PELO* and *IGFBP7*. The impact of *GTSF1* knockdown on the candidate gene transcripts obtained from the secondary bioinformatic analysis was therefore tested by real-time PCR conducted on the original individual samples used for microarray experiments. The levels of *TCOF1* were significantly reduced (P<05) following *GTSF1* knockdown (2.0±1.0 arb. units, n=4) in comparison with controls (7.8±1.7 arb. units, n=4), while transcript levels of *RPS8* and *CACNA1D* were significantly reduced (P<0.01) following the knockdown (2.7±0.9 arb. units, n=4; 5.1±1.4 arb. units, n=4) respectively, in comparison with controls (12.9±2.2 arb. units, n=4; 19.3±1.5 arb. units, n=4). The levels of *SREK1IP1* had the most significant reduction (P<0.005) in their transcript levels following the knockdown (3.0±0.7 arb. units, n=4) in comparison with controls (16.4±0.7 arb. units, n=4). Transcript levels of the other 3 down-regulated genes (*PARP12*, *TARDBP*, *DHX35*) as determined by the secondary bioinformatic analysis had decreased levels of expression

following the knockdown that were not significantly different to the controls (P>0.05), while the 2 up-regulated genes (*PELO*, *IGFBP7*) as determined by the secondary bioinformatic analysis showed increased levels of expression following the knockdown that were not significantly different to the controls (P>0.05). Even though, not all the targets originating from the secondary bioinformatic analysis were shown to have significantly altered transcript levels, confirmation of the reduced or increased transcript levels in down-regulated and up-regulated transcripts following the knockdown respectively, provided confidence that the alignment of the bovine probes to the ovine genome improved the validity of the microarray data. Unfortunately the limited number of oocytes in this study did not allow statistical confirmation of these genes. Generation of more knockdown samples in future experiments would allow repeat arrays to be analysed that would provide more robust and statistically verified targets for analysis by real-time PCR.

None-the-less, the variety of functions of the genes with significant reductions in their expression levels following the knockdown, suggests that *GTSF1* directly or indirectly affects several different biological processed linked with development. Even though meiotic progression of ovine oocytes during IVM was not affected by *GTSF1* knockdown based on the morphological evaluations of the MII oocytes, the microarray analysis in Chapter 6 showed that *GTSF1* knockdown did appear to have a molecular impact on oocyte maturation in this species. Functional annotation of the confirmed candidate genes affected by *GTSF1* knockdown indicated that these genes are involved in many important processes including RNA processing, translation and developmental competence. The *TCOF1* gene could be involved in protein synthesis of proteins necessary for the development of the oocyte and/or the early embryo because of its involvement with the production of rRNA and its implication in the transport of molecules between nucleus and cytoplasm (Hayano *et al.*, 2003). The *RPS8* gene that showed a significant reduction in its expression levels following the knockdown could be an rRNAs affected by the actions of *TCOF1*. The *RPS8* gene is involved in post-transcriptional modification because the ribosomal subunit that it encodes is involved in the activation of translationally inactive mRNA (Brown and Schreiber, 1996; Tomek *et al.*, 2002). It is possible therefore that *GTSF1* in this way affects translation of molecules important for maturation and for latter stages of development including fertilisation and early embryo development. This is further enhanced by the significant reduction in the transcript levels of *SREK1IP1* involved in post-transcriptional

modification, while down-regulation of a gene associated with the calcium channel, *CACNA1D*, could be associated with fertilisation because of the role that calcium plays in the cortical reaction. Another gene that showed significant reduction in its transcript levels was *MYL9*, associated with the cell-cycle, cytoskeleton and signal transduction, which could also be involved in calcium ion binding (Park *et al.*, 2011). Other cell cycle genes were also affected, like the *TIMP1*. Furthermore, the *AURKA* and *CDK2* genes that showed a trend in the reduction of their transcript levels in the knockdown have known roles in microtubule formation and oocyte maturation (Solc *et al.*, 2012).

The evidence presented in this thesis suggests that *GTSF1* is associated with cytoplasmic maturation and molecular maturation during the GV to MII stage transition. The molecular machinery that the oocytes acquire during their growth and maturation are vital for fertility and subsequent embryonic genome activation and development to the blastocyst stage. Thus the molecular maturation of a mature oocyte represents its inherent future developmental competence or quality (Sirard *et al.*, 2006). Follow-up studies of the results generated here for the role of *GTSF1* should involve evaluation of the effect of the gene on fertilisation potential and subsequent early embryo development. Based on the literature and the results presented in this thesis it is hypothesised that *GTSF1* might play an important role in fertilisation and the maternal to zygotic transition.

8.5 Localisation of GTSF1 protein during ovine oogenesis

During maturation of the oocyte, mRNA transcription as well as post-transcriptional modification of mRNA and storage is crucial for translation of important proteins for maturation, fertilisation and early embryo development and it is necessary for these proteins to be stored until the stage that need to be employed (Sirard, 2001). These developmental stages are regulated by translation of maternal mRNAs that must be stored in the oocyte and activated at the specific time of development (Colegrove-Otero *et al.*, 2005). The P-bodies in the oocyte are foci supposed to mediate this function along with miRNA induced mRNA silencing. The Mvh protein is localised in P-bodies and along with the mouse Piwi family members Mili and Miwi2 have been shown to be vital for piRNA processing (Tanaka *et al.*, 2000; Kuramochi-Miyagawa *et al.*, 2004; Carmell *et al.*, 2007). Based on the background information for *GTSF1* (Yoshimura *et al.*, 2009) and the results of the microarray analysis in this thesis, the association of *GTSF1* with the P-bodies was examined by assessing the localisation of GTSF1 and

MVH protein across oogenesis during oocyte progression from the GV to the MII stage *in vitro*. Immunofluorescence staining showed that GTSF1 is expressed during ovine gametogenesis in both the oocytes and spermatocytes. The results of Chapter 7 also showed that GTSF1 co-localises with MVH protein indicating that GTSF1 associates with the P-body in the secondary GV oocyte in sheep. This data further supports the belief that GTSF1 is involved in mRNA post-transcriptional regulation. It is also possible that the gene could be involved in retrotransposon repression similar to the findings of the mouse study following the *GTSF1* knockout in male mice (Yoshimura *et al.*, 2009). The findings reported here in the sheep are in agreement with recent studies conducted in the bovine, in which the GTSF1 protein was shown to be localised to the chromatoid body in male and the P-body in female gametogenesis (Lu *et al*., 2012). Furthermore, the potential 3´ UTR PRE domain that has been identified in the sequence of *GTSF1* has been found to be vital for the translational activation of several genes including *MOS*, *FGFR1*, *AURKA*, *B4* and *G10* (Lu *et al*., 2012). Several mechanisms have been shown to be involved in the activation of translationally inactive mRNA including phosphorylation of factors that initiate translation including the eukaryotic initiating factor (eIF)-4F, the 40S ribosomal subunit and the dephosphorylation of poly(A)-polymerase (Thach, 1992; Colgan *et al.*, 1996; Gavin and Schorderetslatkine, 1997; Tomek *et al.*, 2002). This model suggests that polyadenylation of the cytoplasmic mRNA stimulates the release of repressor molecules at the 5´ end resulting in the initiation of translation (Ferreira *et al.*, 2009). This finding supports the evidence presented in this thesis and in particular the reduction of the expression levels of *RPS8* following *GTSF1* knockdown as indicated by microarray analysis and verified by real-time PCR, with *RPS8* encoding a ribosomal protein that is a component of the 40S subunit.

8.6 Future studies

On the basis of the published results and the data presented here, it is possible to propose that *GTSF1* regulated oocyte meiotic maturation and acquisition of developmental competence in sheep (Figure 8.1). During the GV to MII transition, *GTSF1*, expressed by the oocytes, associates with P-bodies in the cytoplasm of the oocyte (Chapter 7). It is hypothesized that *GTSF1* is involved in RNA storage and processing; affecting genes associated with post-transcriptional modifications and subsequent translational activation such as *TCOF1, SREK1IP1*, *RPS8* and *CACNA1D* (Chapter 6). It is also hypothesized that the miRNA pathway might be involved in these

processes. The actions of these key genes seem to have an important effect on the dynamics of the cytoskeletal filaments and the molecular maturation as shown by the expression levels of certain genes such as *MYL9, TCOF1* and *TIMP1* following the knockdown (Chapter 6). In order to test this hypothesis, it will be necessary to conduct RNA immunoprecipitation experiments with GTSF1 antibody in order to isolate the protein as well as the RNAs bound to it. The purified RNA-protein complexes can be separated by RNA extraction and the identity of the RNAs can be determined by cDNA sequencing or verification RT-PCR (Keene *et al.*, 2006).

The initial *GTSF1* characterisation studies showed a high expression of the gene during the early stages of follicle development followed by a lack of expression during the secondary to antral stage. It is possible therefore that the gene also has an effect on the early stages of development regulating gene expression necessary for the activation of oocyte and/or follicle growth. *Gtsf1* has been shown to be down-regulated in *Nobox* deficient mouse ovaries supporting the idea that *GTSF1* plays an important role of the gene in activation of growth, since *NOBOX* in mammalian species is related to primordial follicle activation (Rajkovic *et al.*, 2004). Future research is necessary to characterise the actions of *GTSF1* during early oocyte growth and follicle development in monovular species and these should include targeted knockdown of *GTSF1* in primordial follicles using viral infection of primary oocytes in combination with microinjection to induce *GTSF1* knockdown and examination of the function of the gene during the early stages of development. In addition, generation of a cohort of *GTSF1* knockdown oocytes following injection at the secondary oocyte GV stage and IVM to the MII stage is necessary for a new series of microarrays using the Affymetrix GeneChip Ovine arrays. Finally, fertilisation and *in vitro* embryo development of *GTSF1* knockdown MII oocytes is necessary to confirm the effect of the gene on oocyte developmental competence.

A major problem throughout this thesis has been the limited number of oocytes available for analysis due to the low survival number following the microinjections. The knowledge gained over the years, suggests that generation of future targeted knockdowns should be performed manually using an SAS air syringe instead of the femtojet outflow system as a vehicle for delivering the siRNA into the oocytes. It is believed that this modification in the culture system will significantly improve oocyte survival after siRNA injection.
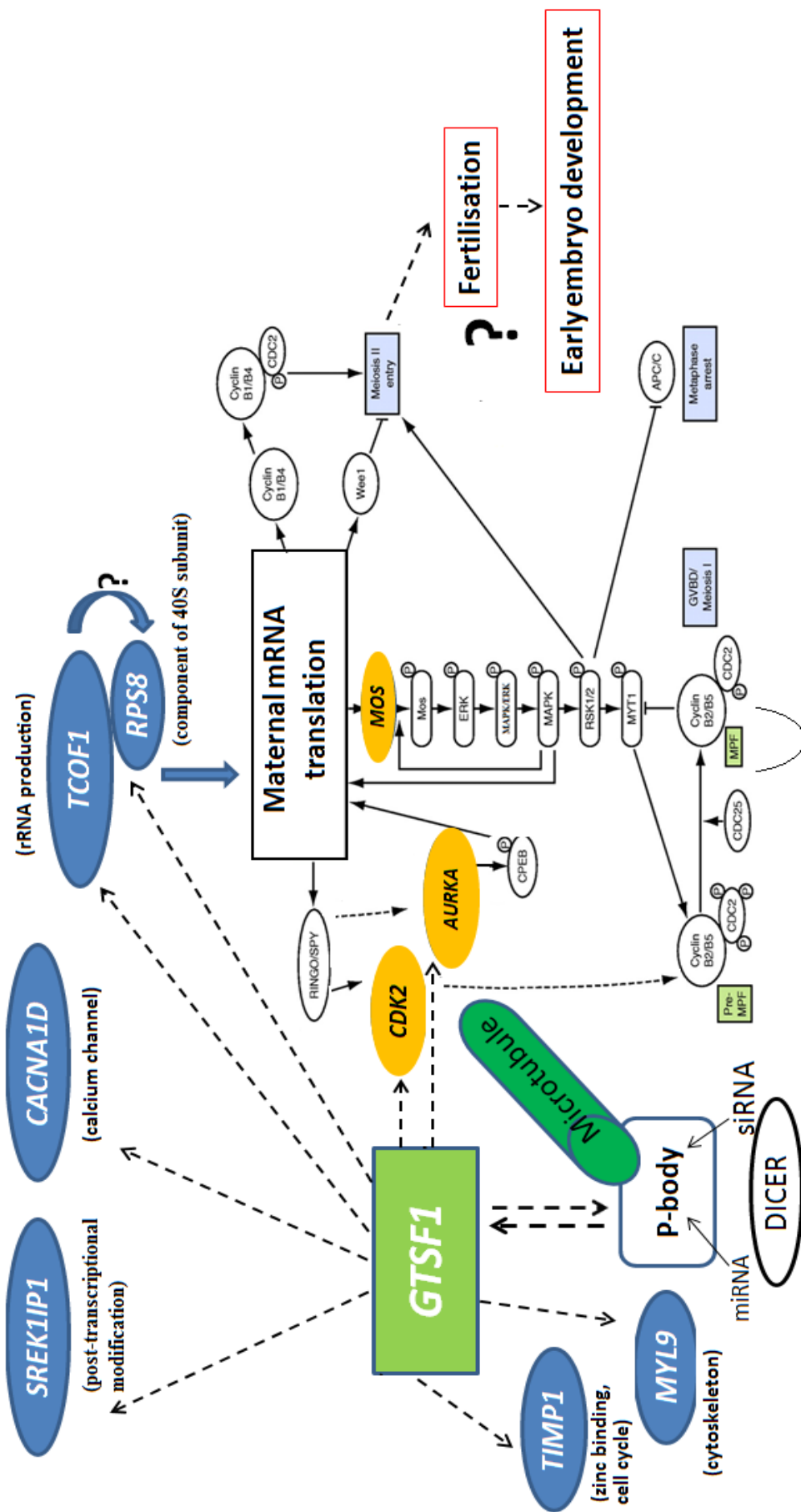
Figure 8.1: Proposed mode of action of *GTSF1* during ovine oocyte maturation. *GTSF1* associates with P-bodies and as a result it affects the post-transcriptional modification and translational activation of inactive mRNA that is necessary for subsequent development of the oocytes to the MII stage. Straight lines (——) signify literature based evidence (Brook *et al.*, 2009). Dotted lines (·······) signify hypothesised mode of action during oocyte maturation (Brook *et al.*, 2009). Broken lines signify (------) hypothesised associations of *GTSF1* during oocyte maturation. Image adapted from: Brook *et al.*, (2009).

250

8.7 Conclusion

Overall this thesis has shown that *GTSF1* may play a functional role during oocyte development in the sheep and specifically cytoplasmic and nuclear maturation of oocytes. Characterisation of *GTSF1* mRNA and protein expression and cellular localisation will inform future investigations of the role of *GTSF1* in oocyte and follicle development. Validation of the microinjection system for the creation of a gene specific knockdown following siRNA injection will allow investigation of other novel genes that might be important during gametogenesis.

References

Abrieu, A., Doree, M. and Fisher, D. (2001). The interplay between cyclin-B-Cdc2 kinase (MPF) and MAP kinase during maturation of oocytes. J Cell Sci **114**(Pt 2): 257-267.

Acevedo, N. and Smith G. D. (2005). Oocyte-specific gene signaling and its regulation of mammalian reproductive potential. Front Biosci **10**: 2335-2345.

Adams, G. P., Matteri, R. L. and Ginther, O. J. (1992). Effect of progesterone on ovarian follicles, emergence of follicular waves and circulating follicle-stimulating hormone in heifers. J Reprod Fertil **96**(2): 627-640.

Adams, M. D., Celniker, S. E., Holt, R. A., Evans, C. A., Gocayne, J. D., Amanatides, P. G., ... Venter, J. C. (2000). The genome sequence of Drosophila melanogaster. Science **287**(5461): 2185-2195.

Adhikari, D., Zheng, W., Shen, Y., Gorre, N., Hamalainen, T., Cooney, A. J., ... Liu, K. (2010). Tsc/mTORC1 signaling in oocytes governs the quiescence and activation of primordial follicles. Hum Mol Genet **19**(3): 397-410.

Aerts, J. M. and Bols, P. E. (2010). Ovarian follicular dynamics: a review with emphasis on the bovine species. Part I: Folliculogenesis and pre-antral follicle development. Reprod Domest Anim **45**(1): 171-179.

Ahtiainen, P., Rulli, S., Pakarainen, T., Zhang, F. P., Poutanen, M., Huhtaniemi, I. (2007). Phenotypic characterisation of mice with exaggerated and missing LH/hCG action. Mol Cell Endocrinol **260-262**: 255-263.

Aimone, J. B. and Gage, F. H. (2004). Unbiased characterization of high-density oligonucleotide microarrays using probe-level statistics. Journal of Neuroscience Methods **135**(1-2): 27-33.

Alak, B. M., Smith, G. D., Woodruff, T. K., Stouffer, R. L., Wolf, D. P. (1996). Enhancement of primate oocyte maturation and fertilization in vitro by inhibin A and activin A. Fertil Steril **66**(4): 646-653.

Albarracin, J. L., Morato, R., Izquierdo, D., Mogas, T. (2005). Effects of roscovitine on the nuclear and cytoskeletal components of calf oocytes and their subsequent development. Theriogenology **64**(8): 1740-1755.

Albertini, D. F. (1992). Cytoplasmic microtubular dynamics and chromatin organization during mammalian oogenesis and oocyte maturation. Mutat Res **296**(1-2): 57-68.

Altschul, S. F., Gish, W., Miller, W., Myers, E. W., Lipman, D. J. (1990). Basic local alignment search tool. J Mol Biol **215**(3): 403-410.

Alvord, W. G., Roayaei, J. A., Quinones, O. A., Schneider, K. T. (2007). A microarray analysis for differential gene expression in the soybean genome using Bioconductor and R. Briefings in Bioinformatics **8**(6): 415-431.

Amanai, M., Shoji, S., Yoshida, N., Brahmajosyula, M., Perry, A. C. (2006). Injection of mammalian metaphase II oocytes with short interfering RNAs to dissect meiotic and early mitotic events. Biol Reprod **75**(6): 891-898.

Amaravadi, R., Glerum, D. M. and Tzagoloff, A. (1997). Isolation of a cDNA encoding the human homolog of COX17, a yeast gene essential for mitochondrial copper recruitment. Human Genetics **99**(3): 329-333.

Ambros, V., Amsterdam, A., Gold, R. S., Hosokawa, K., Yoshida, Y., Sasson, R., Jung, Y., Kotsuji, F. (2004). The functions of animal microRNAs. Nature **431**(7006): 350-355.

Amsterdam, A., Gold, R. S., Hosokawa, K., Yoshida, Y., Sasson, R., Jung, Y., Kotsuji, F. (1999). Crosstalk Among Multiple Signaling Pathways Controlling Ovarian Cell Death. Trends Endocrinol Metab **10**(7): 255-262.

Anantharaman, V., Koonin, E. V., Aravind, L. (2002). Comparative genomics and evolution of proteins involved in RNA metabolism. Nucleic Acids Res **30**(7): 1427-1464.

Anderiesz, C., Ferraretti, A., Magli, C., Fiorentino, A., Fortini, D., Gianaroli, L., ... Trounson, A. O. (2000). Effect of recombinant human gonadotrophins on human, bovine and murine oocyte meiosis, fertilization and embryonic development in vitro. Hum Reprod **15**(5): 1140-1148.

Anderson, P. and Kedersha, N. (2006). RNA granules. J Cell Biol **172**(6): 803-808.

Anderson, R. A., Sciorio, R., Kinnell, H., Bayne, R. A. L., Thong, K. J., de Sousa, P. A., Pickering, S. (2009). Cumulus gene expression as a predictor of human oocyte fertilisation, embryo development and competence to establish a pregnancy. Reproduction **138**(4): 629-637.

Andreeva, A. and Tidow, H. (2008). A novel CHHC Zn-finger domain found in spliceosomal proteins and tRNA modifying enzymes. Bioinformatics **24**(20): 2277-2280.

Appasani, K. (2004). RNA interference: from biology to drugs and therapeutics. RNA Biol **1**(2): 118-121.

Aravin, A. A. and Bourc'his, D. (2008). Small RNA guides for de novo DNA methylation in mammalian germ cells. Genes Dev **22**(8): 970-975.

Aravin, A. A., Hannon, G. J. and Brennecke, J. (2007a). The Piwi-piRNA pathway provides an adaptive defense in the transposon arms race. Science **318**(5851): 761-764.

Aravin, A. A., Sachidanandam, R., Girard, A., Fejes-Toth, K., Hannon, G. J. (2007b). Developmentally regulated piRNA clusters implicate MILI in transposon control. Science **316**(5825): 744-747.

Armstrong, D. T., Weiss, T. J., Selstam, G., Seamark, R. F. (1981). Hormonal and cellular interactions in follicular steroid biosynthesis by the sheep ovary. J Reprod Fertil Suppl **30**: 143-154.

Assou, S., Anahory, T., Pantesco, V., Le Carrour, T., Pellestor, F., Klein, B., ... Hamamah, S. (2006). The human cumulus-oocyte complex gene-expression profile. Human Reproduction **21**(7): 1705-1719.

Bachvarova, R. F. (1992). A maternal tail of poly(A): the long and the short of it. Cell **69**(6): 895-897.

Bacich, D. J., Rohan, R. M., Norman, R. J., Rodgers, R. J. (1994). Characterization and relative abundance of alternatively spliced luteinizing hormone receptor messenger ribonucleic acid in the ovine ovary. Endocrinology **135**(2): 735-744.

Backstrom, C. T., McNeilly, A. S., Leask, R. M., Baird, D. T. (1982). Pulsatile secretion of LH, FSH, prolactin, oestradiol and progesterone during the human menstrual cycle. Clin Endocrinol (Oxf) **17**(1): 29-42.

Bae, C. D., Sung, Y. S., Jeon, S. M., Suh, Y., Yang, H. K., Kim, Y. I., ... Park, J. (2003). Up-regulation of cytoskeletal-associated protein 2 in primary human gastric adenocarcinomas. Journal of Cancer Research and Clinical Oncology **129**(11): 621-630.

Baird, D. T. (1978). Pulsatile secretion of LH and ovarian estradiol during the follicular phase of the sheep estrous cycle. Biol Reprod **18**(3): 359-364.

Baird, D. T., Burger, P. E., Heavon-Jones, G. D., Scaramuzzi, R. J. (1974). The site of secretion of androstenedione in non-pregnant women. J Endocrinol **63**(1): 201-212.

Baird, D. T. and McNeilly, A. S. (1981). Gonadotrophic control of follicular development and function during the oestrous cycle of the ewe. J Reprod Fertil Suppl **30**: 119-133.

Baker, J., Hardy, M. P., Zhou, J., Bondy, C., Lupu, F., Bellve, A. R., Efstratiadis, A. (1996). Effects of an Igf1 gene null mutation on mouse reproduction. Mol Endocrinol **10**(7): 903-918.

Balagopal, V. and Parker, R. (2009). Polysomes, P bodies and stress granules: states and fates of eukaryotic mRNAs. Curr Opin Cell Biol **21**(3): 403-408.

Barber, R. D., Harmer, D. W., Coleman, R. A., Clark, B. J. (2005). GAPDH as a housekeeping gene: analysis of GAPDH mRNA expression in a panel of 72 human tissues. Physiol Genomics **21**(3): 389-395.

Barnard, D. C. and Patton, J. G. (2000). Identification and characterization of a novel serine-arginine-rich splicing regulatory protein. Molecular and Cellular Biology **20**(9): 3049-3057.

Barrios, F., Filipponi, D., Campolo, F., Gori, M., Bramucci, F., Pellegrini, M., ... Dolci, S. (2012). SOHLH1 and SOHLH2 control Kit expression during postnatal male germ cell development. J Cell Sci **125**(Pt 6): 1455-1464.

Baugh, L. R., Hill, A. A., Claggett, J. M., Hill-Harfe, K., Wen, J. C., Slonim, D. K., ... Hunter, C. P. (2005). The homeodomain protein PAL-1 specifies a lineage-specific regulatory network in the C. elegans embryo. Development **132**(8): 1843-1854.

Bennett, R. A., Osathanondh, R. and Yeh, J. (1996). Immunohistochemical localization of transforming growth factor-alpha, epidermal growth factor (EGF), and EGF receptor in the human fetal ovary. J Clin Endocrinol Metab **81**(8): 3073-3076.

Berleth, T., Burri, M., Thoma, G., Bopp, D., Richstein, S., Frigerio, G., ... Nusslein-Volhard, C. (1988). The role of localization of bicoid RNA in organizing the anterior pattern of the Drosophila embryo. EMBO J **7**(6): 1749-1756.

Bernard, D. J., Chapman, S. C. and Woodruff, T. K. (2001). Mechanisms of inhibin signal transduction. Recent Prog Horm Res **56**: 417-450.

Bernstein, E., Caudy, A. A., Hammond, S. M., Hannon, G. J. (2001). Role for a bidentate ribonuclease in the initiation step of RNA interference. Nature **409**(6818): 363-366.

Bernstein, E., Kim, S. Y., Carmell, M. A., Murchison, E. P., Alcorn, H., ... Hannon, G. J. (2003). Dicer is essential for mouse development. Nat Genet **35**(3): 215-217.

Berthet, C., Aleem, E., Coppola, V., Tessarollo, L., Kaldis, P. (2003). Cdk2 knockout mice are viable. Current Biology **13**(20): 1775-1785.

Bertrand, E., Pictet, R. and Grange, T. (1994). Can hammerhead ribozymes be efficient tools to inactivate gene-function. Nucleic Acids Research **22**(3): 293-300.

Biase, F., Everts, RE., Oliveira, R., Santos-Biase, WK., Fonseca, Merighe GK., Smith, LC., ... Meirelles, FV. (2012). Messenger RNAs in metaphase II oocytes correlate with successful embryo development to the blastocyst stage. Zygote **10:**1-11

Biggins, S. and Walczak, C. E. (2003). Captivating capture: how microtubules attach to kinetochores. Curr Biol **13**(11): R449-460.

Bilodeau-Goeseels, S. (2008). Review: The regulation of meiotic maturation in bovine oocytes. Canadian Journal of Animal Science **88**(3): 343-349.

Bobola, N., Jansen, R. P., Shin, T. H., Nasmyth, K. (1996). Asymmetric accumulation of Ash1p in postanaphase nuclei depends on a myosin and restricts yeast mating-type switching to mother cells. Cell **84**(5): 699-709.

Bock, G., Gebhart, M., Scharinger, A., Jangsangthong, W., Busquet, P., Poggiani, C., ... Koschak, A. (2011). Functional Properties of a Newly Identified C-terminal Splice Variant of Ca(v)1.3 L-type Ca2+ Channels. Journal of Biological Chemistry **286**(49): 42736-42748.

Boland, M., Hazen, JL., Nazor, KL., Rodriguez, AR., Martin, G., Kupriyanov, S., Baldwin, KK. (2012). Generation of mice derived from induced pluripotent stem cells. J Vis Exp. **29**(69): e4003.

Bolstad, B. M., Collin, F., Simpson, K. M., Irizarry, R. A., Speed, T. P. (2004). Experimental design and low-level analysis of microarray data. DNA Arrays in Neurobiology, Vol 60. M. F. Miles. **60:** 25-+.

Braude, P., Bolton, V. and Moore, S. (1988). Human gene expression first occurs between the four- and eight-cell stages of preimplantation development. Nature **332**(6163): 459-461.

Braw-Tal, R. and Roth, Z. (2005). Gene expression for LH receptor, 17 alpha-hydroxylase and StAR in the theca interna of preantral and early antral follicles in the bovine ovary. Reproduction **129**(4): 453-461.

Brevini, T. A. L., Cillo, F., Antonini, S., Gandolfi, F. (2007). Cytoplasmic remodelling and the acquisition of developmental competence in pig oocytes. Animal Reproduction Science **98**(1-2): 23-38.

Brevini, T. A. L., Lonergan, P., Cillo, F., Francisci, C., Favetta, L. A., Fair, T., Gandolfi, F. (2002). Evolution of mRNA polyadenylation between oocyte maturation and first embryonic cleavage in cattle and its relation with developmental competence. Mol Reprod Dev **63**(4): 510-517.

Brook, M., Smith, J. W. S. and Gray, N. K. (2009). The DAZL and PABP families: RNA-binding proteins with interrelated roles in translational control in oocytes. Reproduction **137**(4): 595-617.

Brown, E. J. and Schreiber, S. L. (1996). A signaling pathway to translational control. Cell **86**(4): 517-520.

Brown, J. B. (1978). Pituitary control of ovarian function--concepts derived from gonadotrophin therapy. Aust N Z J Obstet Gynaecol **18**(1): 46-54.

Brown, R. S. (2005). Zinc finger proteins: getting a grip on RNA. Curr Opin Struct Biol **15**(1): 94-98.

Brum, D. S.*,* Leivas, F. G., Silva, C. A. M., Rubin, M. I. B., Rauber, L. P., Fialho, S. S., ... Bernardi, M. L. (2005). The effects of the number of oocytes and the volume of maturation medium in bovine in vitro embryo production. Animal Reproduction **2**(1): 70-73.

Brummelkamp, T. R.*,* Bernards, R. and Agami, R. (2002). A system for stable expression of short interfering RNAs in mammalian cells. Science **296**(5567): 550-553.

Brunet, S. and Maro, B. (2005). Cytoskeleton and cell cycle control during meiotic maturation of the mouse oocyte: integrating time and space. Reproduction **130**(6): 801-811.

Brunet, S.*,* Polanski, Z., Verlhac, M. H., Kubiak, J. Z., Maro, B. (1998). Bipolar meiotic spindle formation without chromatin. Curr Biol **8**(22): 1231-1234.

Brunet, S. and Verlhac, M. H. (2011). Positioning to get out of meiosis: the asymmetry of division. Hum Reprod Update **17**(1): 68-75.

Brusselmans, K.*,* De Schrijver, E., Verhoeven, G., Swinnen, J. V. (2005). RNA interference-mediated silencing of the acetyl-CoA-carboxylase-alpha gene induces growth inhibition and apoptosis of prostate cancer cells. Cancer Res **65**(15): 6719-6725.

Buccione, R.*,* Schroeder, A. C. and Eppig, J. J. (1990a). Interactions between somatic cells and germ cells throughout mammalian oogenesis. Biol Reprod **43**(4): 543-547.

Buccione, R.*,* Vanderhyden, B. C., Caron, P. J., Eppig, J. J. (1990b). FSH-induced expansion of the mouse cumulus oophorus in vitro is dependent upon a specific factor(s) secreted by the oocyte. Dev Biol **138**(1): 16-25.

Bukovsky, A., Svetlikova, M. and Caudle, M. R. (2005). Oogenesis in cultures derived from adult human ovaries. Reprod Biol Endocrinol. **3:** 17

Buratti, E. and Baralle, F. E. (2010). The multiple roles of TDP-43 in pre-mRNA processing and gene expression regulation. Rna Biology **7**(4): 420-429.

Burd, C. G. and Dreyfuss, G. (1994). Conserved structures and diversity of functions of RNA-binding proteins. Science **265**(5172): 615-621.

Burnicka-Turek, O.*,* Kata, A., Buyandelger, B., Ebermann, L., Kramann, N., Burfeind, P., ... Adham, I. M. (2010). Pelota interacts with HAX1, EIF3G and SRPX and the resulting protein complexes are associated with the actin cytoskeleton. Bmc Cell Biology **11**.

Bustin, S. A. (2010). Why the need for qPCR publication guidelines?--The case for MIQE. Methods **50**(4): 217-226.

Bustin, S. A.*,* Beaulieu, J. F., Huggett, J., Jaggi, R., Kibenge, F. S., Olsvik, P. A., ... Toegel, S. (2010). MIQE precis: Practical implementation of minimum standard guidelines for fluorescence-based quantitative real-time PCR experiments. BMC Mol Biol **11**: 74.

Cahan, P.*,* Rovegno, F., Mooney, D., Newman, J. C. St Laurent, G. III., McCaffrey, T. A. (2007). Meta-analysis of microarray results: challenges, opportunities, and recommendations for standardization. Gene **401**(1-2): 12-18.

Calder, M. D.*,* Caveney, A. N., Smith, L. C., Watson, A. J. (2003). Responsiveness of bovine cumulus-oocyte-complexes (COC) to porcine and recombinant human FSH, and the effect of COC quality on gonadotropin receptor and Cx43 marker gene mRNAs during maturation in vitro. Reproductive biology and endocrinology : RB&E **1**: 14-14.

Caliskan, M.*,* Chong, J. X., Uricchio, L., Anderson, R., Chen, P., Sougnez, C., ... Ober, C. (2011). Exome sequencing reveals a novel mutation for autosomal recessive non-syndromic mental retardation in the TECR gene on chromosome 19p13. Human Molecular Genetics **20**(7): 1285-1289.

Campbell, B. K.*,* Scaramuzzi, R. J. and Webb, R. (1996). Induction and maintenance of oestradiol and immunoreactive inhibin production with FSH by ovine granulosa cells cultured in serum-free media. J Reprod Fertil **106**(1): 7-16.

Campbell, B. K.*,* Souza, C., Gong, J., Webb, R., Kendall, N., Marsters, P., ... Baird, D. T. (2003). Domestic ruminants as models for the elucidation of the mechanisms controlling ovarian follicle development in humans. Reprod Suppl **61**: 429-443.

Canalis, E.*,* Economides, A. N., Gazzerro, E. (2003). Bone morphogenetic proteins, their antagonists, and the skeleton. Endocr Rev **24**(2): 218-235.

Canseco, R. S.*,* Sparks, A. E., Pearson, R. E., Gwazdauskas, F. C. (1992). Embryo density and medium volume effects on early murine embryo development. J Assist Reprod Genet **9**(5): 454-457.

Caplen, N. J., Parrish, S., Imani, F., Fire, A., Morgan, R. A. (2001). Specific inhibition of gene expression by small double-stranded RNAs in invertebrate and vertebrate systems. Proc Natl Acad Sci U S A **98**(17): 9742-9747.

Carabatsos, M. J., Elvin, J., Matzuk, M. M., Albertini, D. F. (1998). Characterization of oocyte and follicle development in growth differentiation factor-9-deficient mice. Dev Biol **204**(2): 373-384.

Carmell, M. A., Girard, A., van de Kant, H. J., Bourc'his, D., Bestor, T. H., de Rooij, D. G., Hannon, G. J. (2007). MIWI2 is essential for spermatogenesis and repression of transposons in the mouse male germline. Dev Cell **12**(4): 503-514.

Carmell, M. A. and Hannon, G. J. (2004). RNase III enzymes and the initiation of gene silencing. Nat Struct Mol Biol **11**(3): 214-218.

Cattanach, B. M., Iddon, C. A., Charlton, H. M., Chiappa, S. A., Fink, G. (1977). Gonadotrophin-releasing hormone deficiency in a mutant mouse with hypogonadism. Nature **269**(5626): 338-340.

Cecconi, S., D'Aurizio, R. and Colonna, R. (1996). Role of antral follicle development and cumulus cells on in vitro fertilization of mouse oocytes. J Reprod Fertil **107**(2): 207-214.

Cecconi, S., Mauro, A., Capacchietti, G., Berardinelli, P., Bernabo, N., Di Vincenzo, A. R., ... Barboni, B. (2008). Meiotic maturation of incompetent prepubertal sheep oocytes is induced by paracrine factor(s) released by gonadotropin-stimulated oocyte-cumulus cell complexes and involves mitogen-activated protein kinase activation. Endocrinology **149**(1): 100-107.

Cecconi, S. and Rossi, G. (2001). Mouse antral oocytes regulate preantral granulosa cell ability to stimulate oocyte growth in vitro. Dev Biol **233**(1): 186-191.

Chaigne, A., Verlhac, M. H. and Terret, M. E. (2012). Spindle positioning in mammalian oocytes. Exp Cell Res **318**(12): 1442-1447.

Chambers, E. L. (2003). Regualtion of follicle growth initiation and maintenance in the mammalian ovary. PhD thesis. University of Leeds.

Chambers, E. L., Gosden, R. G., Yap, C., Picton, H. M. (2010). In situ identification of follicles in ovarian cortex as a tool for quantifying follicle density, viability and developmental potential in strategies to preserve female fertility. Hum Reprod **25**(10): 2559-2568.

Chambraud, B., Sardin, E., Giustiniani, J., Dounane, O., Schumacher, M., Goedert, M., Baulieu, E. E. (2010). A role for FKBP52 in Tau protein function. Proc Natl Acad Sci U S A **107**(6): 2658-2663.

Channing, C. P., Schaerf, F. W., Anderson, L. D., Tsafriri, A. (1980). Ovarian follicular and luteal physiology. International review of physiology **22**: 117-201.

Charlesworth, A., Cox, L. L., MacNicol, A. M. (2004). Cytoplasmic polyadenylation element (CPE)- and CPE-binding protein (CPEB)-independent mechanisms regulate early class maternal mRNA translational activation in Xenopus oocytes. Journal of Biological Chemistry **279**(17): 17650-17659.

Chauhan, M. S., Palta, P., Das, S. K., Katiyar, P. K., Madan, M. L. (1997). Replacement of serum and hormone additives with follicular fluid in the IVM medium: Effects on maturation, fertilization and subsequent development of buffalo oocytes in vitro. Theriogenology **48**(3): 461-469.

Chen, J. J., Hsueh, H. M., Delongchamp, R. R., Lin, C. J., Tsai, C. A. (2007). Reproducibility of microarray data: a further analysis of microarray quality control (MAQC) data. Bmc Bioinformatics **8**: 412.

Cheng, A., Xiong, W., Ferrell, J. E., Solomon, M. J. (2005). Identification and comparative analysis of multiple mammalian Speedy/Ringo proteins. Cell Cycle **4**(1): 155-165.

Chian, R. C., Niwa, K. and Sirard, M. A. (1994). Effects of cumulus cells on male pronuclear formation and subsequent early development of bovine oocytes in vitro. Theriogenology **41**(7): 1499-1508.

Cho, Y. S., Iguchi, N., Yang, J., Handel, M. A., Hecht, N. B. (2005). Meiotic messenger RNA and noncoding RNA targets of the RNA-binding protein Translin (TSN) in mouse testis. Biol Reprod **73**(4): 840-847.

Choi, J. K., Yu, U., Kim, S., Yoo, O. J. (2003). Combining multiple microarray studies and modeling interstudy variation. <u>Bioinformatics</u> **19**: i84-i90.

Choi, T. S., Fukasawa, K., Zhou, R. P., Tessarollo, L., Borror, K., Resau, J., VandeWoude, G. F. (1996). The Mos/mitogen-activated protein kinase (MAPK) pathway regulates the size and degradation of the first polar body in maturing mouse oocytes. <u>Proc Natl Acad Sci U S A</u> **93**(14): 7032-7035.

Choi, Y., Yuan, D. and Rajkovic, A. (2008a). Germ cell-specific transcriptional regulator sohlh2 is essential for early mouse folliculogenesis and oocyte-specific gene expression. <u>Biol Reprod</u> **79**(6): 1176-1182.

Choi, Y., Ballow, D. J., Xin, Y., Rajkovic, A. (2008b). Lim homeobox gene, lhx8, is essential for mouse oocyte differentiation and survival. <u>Biol Reprod</u> **79**(3): 442-449.

Choi, Y. and Rajkovic, A. (2006). Genetics of early mammalian folliculogenesis. <u>Cell Mol Life Sci</u> **63**(5): 579-590.

Chu, M. X., Guo, X. H., Feng, C. J., Li, Y., Huang, D. W., Feng, T., ... Li, K. (2012a). Polymorphism of 5' regulatory region of ovine FSHR gene and its association with litter size in Small Tail Han sheep. <u>Mol Biol Rep</u> **39**(4): 3721-3725.

Chu, T., Dufort, I. and Sirard, M. A. (2012b). Effect of ovarian stimulation on oocyte gene expression in cattle. <u>Theriogenology</u> **77**(9): 1928-1938.

Chuma, S. and Nakatsuji, N. (2001). Autonomous transition into meiosis of mouse fetal germ cells in vitro and its inhibition by gp130-mediated signaling. <u>Dev Biol</u> **229**(2): 468-479.

Churchill, G. A. (2002). Fundamentals of experimental design for cDNA microarrays. <u>Nature Genetics</u> **32**: 490-495.

Cillo, F., Brevini, T. A., Antonini, S., Paffoni, A., Ragni, G., Gandolfi, F. (2007). Association between human oocyte developmental competence and expression levels of some cumulus genes. <u>Reproduction</u> **134**(5): 645-650.

Clemens, J. C., Worby, C. A., Simonson-Leff, N., Muda, M., Maehama, T., Hemmings, B. A., Dixon, J. E. (2000). Use of double-stranded RNA interference in Drosophila cell lines to dissect signal transduction pathways. <u>Proc Natl Acad Sci U S A</u> **97**(12): 6499-6503.

Cline, M. S., Smoot, M., Cerami, E., Kuchinsky, A., Landys, N., Workman, C., ... Bader, G. D. (2007). Integration of biological networks and gene expression data using Cytoscape. <u>Nature Protocols</u> **2**(10): 2366-2382.

Colegrove-Otero, L. J., Minshall, N. and Standart, N. (2005). RNA-binding proteins in early development. <u>Crit Rev Biochem Mol Biol</u> **40**(1): 21-73.

Colgan, D. F., Murthy, K. G. K., Prives, C., Manley, J. L. (1996). Cell-cycle related regulation poly(A) polymerase by phosphorylation. <u>Nature</u> **384**(6606): 282-285.

Colledge, W. H., Carlton, M. B., Udy, G. B., Evans, M. J. (1994). Disruption of c-mos causes parthenogenetic development of unfertilized mouse eggs. <u>Nature</u> **370**(6484): 65-68.

Conneely, O. M., Lydon, J. P., De Mayo, F., O'Malley, B. W. (2000). Reproductive functions of the progesterone receptor. <u>J Soc Gynecol Investig</u> **7**(1 Suppl): S25-32.

Conner, S. J., Lefievre, L., Hughes, D. C., Barratt, C. L. R. (2005). Cracking the egg: increased complexity in the zona pellucida. <u>Human Reproduction</u> **20**(5): 1148-1152.

Consortium., C. e. S. (1998). Genome sequence of the nematode C. elegans: a platform for investigating biology. <u>Science</u> **282**(5396): 2012-2018.

Conti, M. (2000). Phosphodiesterases and cyclic nucleotide signaling in endocrine cells. <u>Mol Endocrinol</u> **14**(9): 1317-1327.

Conti, M., Hsieh, M., Park, J. Y., Su, Y. Q. (2006). Role of the epidermal growth factor network in ovarian follicles. <u>Mol Endocrinol</u> **20**(4): 715-723.

Cooke, B. A. (1999). Signal transduction involving cyclic AMP-dependent and cyclic AMP-independent mechanisms in the control of steroidogenesis. <u>Mol Cell Endocrinol</u> **151**(1-2): 25-35.

Corcoran, D., Fair, T., Park, S., Rizos, D., Patel, O. V., Smith, G. W., ... Lonergan, P. (2006). Suppressed expression of genes involved in transcription and translation in in vitro compared with in vivo cultured bovine embryos. <u>Reproduction</u> **131**(4): 651-660.

Cotterill, M. (2008). Gene function during the development of ovine oocytes and ovarian follicles. PhD thesis. University of Leeds.

Cotterill, M., Catt, S. L., Picton, H. M. (2012). Characterisation of the cellular and molecular responses of ovine oocytes and their supporting somatic cells to pre-ovulatory levels of LH and FSH during in vitro maturation. <u>Reproduction</u> **144**(2): 195-207.

Cotterill, M., Harris, S. E., Collado Fernandez, E., Lu, J., Huntriss, JD., Campbell, B. K., Picton, H. M. (2013). The activity and copy number of mitochondrial DNA in ovine oocytes throughout oogenesis in vivo and during oocyte maturation in vitro. <u>Mol Hum Reprod.</u>

Cox, W. G. and Singer, V. L. (2004). Fluorescent DNA hybridization probe preparation using amine modification and reactive dye coupling. <u>Biotechniques</u> **36**(1): 114-122.

Crosby, I. M., Gandolfi, F. and Moor, R. M. (1988). Control of protein synthesis during early cleavage of sheep embryos. <u>J Reprod Fertil</u> **82**(2): 769-775.

Cui, X. S., Li, X. Y., Jeong, Y. J., Jun, J. H., Kim, N. H. (2006). Gene expression of Cox5a, 5b, or 6b1 and their roles in preimplantation mouse embryos. <u>Biol Reprod</u> **74**(3): 601-610.

Dalrymple, B. P., Kirkness, E. F., Nefedov, M., McWilliam, S., Ratnakumar, A., Barris, W., ... Cockett, N. E. (2007). Using comparative genomics to reorder the human genome sequence into a virtual sheep genome. <u>Genome Biol</u> **8**(7).

Danfour, M. A. (2001). Influence of the environment on mammalian oocyte development. PhD thesis. University of Leeds.

Davies, B. and Fried, M. (1993). The structure of the human intron-containing S8-ribosomal protein gene and determination of its chromosomal location at 1P32-P34.1. <u>Genomics</u> **15**(1): 68-75.

de Kretser, D. M., Hedger, M. P., Loveland, K. L., Phillips, D. J. (2002). Inhibins, activins and follistatin in reproduction. <u>Hum Reprod Update</u> **8**(6): 529-541.

De La Fuente, R., O'Brien, M. J. and Eppig, J. J. (1999). Epidermal growth factor enhances preimplantation developmental competence of maturing mouse oocytes. <u>Hum Reprod</u> **14**(12): 3060-3068.

de Oliveira, A. T., Lopes, R. F. and Rodrigues, J. L. (2005). Gene expression and developmental competence of bovine embryos produced in vitro under varying embryo density conditions. <u>Theriogenology</u> **64**(7): 1559-1572.

Dekel, N. (1988). Regulation of oocyte maturation. The role of cAMP. <u>Ann N Y Acad Sci</u> **541**: 211-216.

Demeestere, I., Basso, O., Moffa, F., Peccatori, F., Poirot, C., Shalom-Paz, E. (2012). Fertility preservation in female cancer patients. <u>Obstet Gynaecol Int</u> **2012:** 695041

Deng, W. and Lin, H. (2002). Miwi, a murine homolog of piwi, encodes a cytoplasmic protein essential for spermatogenesis. <u>Dev Cell</u> **2**(6): 819-830.

Desai, A. and Mitchison, T. J. (1997). Microtubule polymerization dynamics. <u>Annu Rev Cell Dev Biol</u> **13**: 83-117.

DeWitte-Orr, S. J., Mehta, D. R., Collins, S. E., Suthar, M. S., Gale, M. Jr., Mossman, K. L. (2009). Long Double-Stranded RNA Induces an Antiviral Response Independent of IFN Regulatory Factor 3, IFN-beta Promoter Stimulator 1, and IFN. <u>Journal of Immunology</u> **183**(10): 6545-6553.

Di Giacomo, M., Barchi, M., Baudat, F., Edelmann, W., Keeney, S., Jasin, M. (2005). Distinct DNA-damage-dependent and -independent responses drive the loss of oocytes in recombination-defective mouse mutants. <u>Proc Natl Acad Sci U S A</u> **102**(3): 737–742.

Diaz, F. J., O'Brien, M. J., Wigglesworth, K., Eppig, J. J. (2006). The preantral granulosa cell to cumulus cell transition in the mouse ovary: development of competence to undergo expansion. <u>Dev Biol</u> **299**(1): 91-104.

Diez-Roux, G., Banfi, S., Sultan, M., Geffers, L., Anand, S., Rozado, D., ... Ballabio, A. (2011). A high-resolution anatomical atlas of the transcriptome in the mouse embryo. <u>PLoS Biol</u> **9**(1): e1000582.

Diezel, W., Kopperschlager, G. and Hofmann, E. (1972). An improved procedure for protein staining in polyacrylamide gels with a new type of Coomassie Brilliant Blue. <u>Anal Biochem</u> **48**(2): 617-620.

diZerega, G. S. and Hodgen, G. D. (1981). Folliculogenesis in the primate ovarian cycle. <u>Endocr Rev</u> **2**(1): 27-49.

Dong, J., Albertini, D. F., Nishimori, K., Kumar, T. R., Lu, N., Matzuk, M. M. (1996). Growth differentiation factor-9 is required during early ovarian folliculogenesis. Nature **383**(6600): 531-535.

Donnison, M. and Pfeffer, P. L. (2004). Isolation of genes associated with developmentally competent bovine oocytes and quantitation of their levels during development. Biol Reprod **71**(6): 1813-1821.

Dorji, Ohkubo, Y., Miyoshi, K., Yoshida, M. (2012). Gene Expression Differences in Oocytes Derived From Adult and Prepubertal Japanese Black Cattle during In Vitro Maturation. Reproduction in Domestic Animals **47**(3): 392-402.

Downs, S. M. (1995). The influence of glucose, cumulus cells, and metabolic coupling on ATP levels and meiotic control in the isolated mouse oocyte. Dev Biol **167**(2): 502-512.

Downs, S. M., Hudson, E. R. and Hardie, D. G. (2002). A potential role for AMP-activated protein kinase in meiotic induction in mouse oocytes. Developmental Biology **245**(1): 200-212.

Downs, S. M. and Hunzicker-Dunn, M. (1995). Differential regulation of oocyte maturation and cumulus expansion in the mouse oocyte-cumulus cell complex by site-selective analogs of cyclic adenosine monophosphate. Dev Biol **172**(1): 72-85.

Dragovic, R. A., Ritter, L. J., Schulz, S. J., Amato, F., Armstrong, D. T., Gilchrist, R. B. (2005). Role of oocyte-secreted growth differentiation factor 9 in the regulation of mouse cumulus expansion. Endocrinology **146**(6): 2798-2806.

Dragovic, R. A., Ritter, L. J., Schulz, S. J., Amato, F., Thompson, J. G., Armstrong, D. T., Gilchrist, R. B. (2007). Oocyte-secreted factor activation of SMAD 2/3 signaling enables initiation of mouse cumulus cell expansion. Biol Reprod **76**(5): 848-857.

Draper, B. W., Morcos, P. A. and Kimmel, C. B. (2001). Inhibition of zebrafish fgf8 pre-mRNA splicing with morpholino oligos: a quantifiable method for gene knockdown. Genesis **30**(3): 154-156.

Driever, W. and Nusslein-Volhard, C. (1988). A gradient of bicoid protein in Drosophila embryos. Cell **54**(1): 83-93.

Drummond, A. E. (2005). TGFbeta signalling in the development of ovarian function. Cell Tissue Res **322**(1): 107-115.

Duggavathi, R. and Murphy, B. D. (2009). Development. Ovulation signals. Science **324**(5929): 890-891.

Dunphy, W. G., Brizuela, L., Beach, D., Newport, J. (1988). The Xenopus cdc2 protein is a component of MPF, a cytoplasmic regulator of mitosis. Cell **54**(3): 423-431.

Durlinger, A. L., Gruijters, M. J., Kramer, P., Karels, B., Ingraham, H. A., Nachtigal, M. W., ... Themmen, A. P. (2002a). Anti-Mullerian hormone inhibits initiation of primordial follicle growth in the mouse ovary. Endocrinology **143**(3): 1076-1084.

Durlinger, A. L., Gruijters, M. J., Kramer, P., Karels, B., Kumar, T. R., Matzuk, M. M., ... Themmen, A. P. (2001). Anti-Mullerian hormone attenuates the effects of FSH on follicle development in the mouse ovary. Endocrinology **142**(11): 4891-4899.

Durlinger, A. L., Visser, J. A. and Themmen, A. P. (2002b). Regulation of ovarian function: the role of anti-Mullerian hormone. Reproduction **124**(5): 601-609.

Dworkin, M. B., Shrutkowski, A. and Dworkin-Rastl, E. (1985). Mobilization of specific maternal RNA species into polysomes after fertilization in Xenopus laevis. Proc Natl Acad Sci U S A **82**(22): 7636-7640.

Earnshaw, W. C. and Cooke, C. A. (1991). Analysis of the distribution of the INCENPs throughout mitosis reveals the existence of a pathway of structural changes in the chromosomes during metaphase and early events in cleavage furrow formation. J Cell Sci **98 (Pt 4)**: 443-461.

Eberwine, J., Spencer, C., Miyashiro, K., Mackler, S., Finnell, R. (1992). Complementary DNA synthesis in situ: methods and applications. Methods Enzymol **216**: 80-100.

Edwards, R. G. (1965). Maturation in vitro of mouse, sheep, cow, pig, rhesus monkey and human ovarian oocytes. Nature **208**(5008): 349-351.

Edwards, R. G., Steptoe, P. C., Abraham, G. E., Walters, E., Purdy, J. M., Fotherby, K. (1972). Steroid assays and preovulatory follicular development in human ovaries primed with gonadotrophins. Lancet **2**(7778): 611-615.

Eichenlaub-Ritter, U., Vogt, E., Yin, H., Gosden, R. (2004). Spindles, mitochondria and redox potential in ageing oocytes. Reprod Biomed Online **8**(1): 45-58.

Elbashir, S. M., Lendeckel, W. and Tuschl, T. (2001). "RNA interference is mediated by 21- and 22-nucleotide RNAs." Genes Dev **15**(2): 188-200.

Elsik, C. G., Tellam, R. L., Worley, K. C., Gibbs, R. A., Muzny, D. M., Weinstock, G. M., ... Zhao, F. Q. (2009). The genome sequence of taurine cattle: a window to ruminant biology and evolution. Science **324**(5926): 522-528.

Elvin, J. A., Clark, A. T., Wang, P., Wolfman, N. M., Matzuk, M. M. (1999). Paracrine actions of growth differentiation factor-9 in the mammalian ovary. Mol Endocrinol **13**(6): 1035-1048.

Elvin, J. A., Yan, C. and Matzuk, M. M. (2000). Growth differentiation factor-9 stimulates progesterone synthesis in granulosa cells via a prostaglandin E2/EP2 receptor pathway. Proc Natl Acad Sci U S A **97**(18): 10288-10293.

Eppig, J. J. (1991). Intercommunication between mammalian oocytes and companion somatic cells. Bioessays **13**(11): 569-574.

Eppig, J. J. (1996). Coordination of nuclear and cytoplasmic oocyte maturation in eutherian mammals. Reprod Fertil Dev **8**(4): 485-489.

Eppig, J. J. (2001). Oocyte control of ovarian follicular development and function in mammals. Reproduction **122**(6): 829-838.

Eppig, J. J., et al. (1996). Mammalian oocyte growth and development in vitro. Mol Reprod Dev **44**(2): 260-273.

Eppig, J. J. and Schroeder, A. C. (1989). Capacity of mouse oocytes from preantral follicles to undergo embryogenesis and development to live young after growth, maturation, and fertilization in vitro. Biol Reprod **41**(2): 268-276.

Eppig, J. J., Wigglesworth, K. and Pendola, F. L. (2002). The mammalian oocyte orchestrates the rate of ovarian follicular development. Proc Natl Acad Sci U S A **99**(5): 2890-2894.

Ercolani, L., Florence, B., Denaro, M., Alexander, M. (1988). Isolation and complete sequence of a functional human glyceraldehyde-3-phosphate dehydrogenase gene. J Biol Chem **263**(30): 15335-15341.

Erickson, G. F. (1978). Normal ovarian function. Clin Obstet Gynecol **21**(1): 31-52.

Fair, T., Hulshof, S. C., Hyttel, P., Greve, T., Boland, M. (1997). Oocyte ultrastructure in bovine primordial to early tertiary follicles. Anat Embryol (Berl) **195**(4): 327-336.

Fair, T., Hyttel, P. and Greve, T. (1995). Bovine oocyte diameter in relation to maturational competence and transcriptional activity. Mol Reprod Dev **42**(4): 437-442.

Fan, H. Y., Liu, Z., Shimada, M., Sterneck, E., Johnson, P. F., Hedrick, S. M., Richards, J. S. (2009). MAPK3/1 (ERK1/2) in ovarian granulosa cells are essential for female fertility. Science **324**(5929): 938-941.

Favetta, L. A., Madan, P., Mastromonaco, G. F., St John, E. J., King, A., Betts, D. H. (2007). The oxidative stress adaptor p66Shc is required for permanent embryo arrest in vitro. Bmc Developmental Biology **7**.

Femino, A. M., Fay, F. S., Fogarty, K., Singer, R. H. (1998). Visualization of single RNA transcripts in situ. Science **280**(5363): 585-590.

Ferreira, E. M., Vireque, A. A., Adona, P. R., Meirelles, F. V., Ferriani, R. A., Navarro, P. A. (2009). Cytoplasmic maturation of bovine oocytes: structural and biochemical modifications and acquisition of developmental competence. Theriogenology **71**(5): 836-848.

Ferry, L., Mermillod, P., Massip, A., Dessy, F. (1994). Bovine embryos cultured in serum-poor oviduct-conditioned medium need cooperation to reach the blastocyst stage. Theriogenology **42**(3): 445-453.

Feuerstein, P., Puard, V., Chevalier, C., Teusan, R., Cadoret, V., Guerif, F., ... Royere, D. (2012). Genomic Assessment of Human Cumulus Cell Marker Genes as Predictors of Oocyte Developmental Competence: Impact of Various Experimental Factors. PLoS One **7**(7).

Findlay, J. K., Drummond, A. E., Dyson, M. L., Baillie, A. J., Robertson, D. M., Ethier, J. F. (2002). Recruitment and development of the follicle; the roles of the transforming growth factor-beta superfamily. Mol Cell Endocrinol **191**(1): 35-43.

Finn, R. D.*,* Mistry, J., Schuster-Bockler, B., Griffiths-Jones, S., Hollich, V., Lassmann, T., ... Bateman, A. (2006). Pfam: clans, web tools and services. <u>Nucleic Acids Res</u> **34**(Database issue): D247-251.

Fire, A. (1999). RNA-triggered gene silencing. <u>Trends Genet</u> **15**(9): 358-363.

FitzHarris, G.*,* Marangos, P., Carroll, J. (2007). Changes in endoplasmic reticulum structure during mouse oocyte maturation are controlled by the cytoskeleton and cytoplasmic dynein. <u>Dev Biol</u> **305**(1): 133-144.

Flemr, M.*,* Ma, J., Schultz, R. M., Svoboda, P. (2010). P-body loss is concomitant with formation of a messenger RNA storage domain in mouse oocytes. <u>Biol Reprod</u> **82**(5): 1008-1017.

Fortune, J. E. (2003). The early stages of follicular development: activation of primordial follicles and growth of preantral follicles. <u>Anim Reprod Sci</u> **78**(3-4): 135-163.

Fraser, A. G.*,* Kamath, R. S., Zipperlen, P., Martinez-Campos, M., Sohrmann, M., Ahringer, J. (2000). Functional genomic analysis of C. elegans chromosome I by systematic RNA interference. <u>Nature</u> **408**(6810): 325-330.

Fraser, H. M.*,* Groome, N. P. and McNeilly, A. S. (1999). Follicle-stimulating hormone-inhibin B interactions during the follicular phase of the primate menstrual cycle revealed by gonadotropin-releasing hormone antagonist and antiestrogen treatment. <u>J Clin Endocrinol Metab</u> **84**(4): 1365-1369.

Frick, J. E.*,* Ruppert, E. E. and Wourms, J. P. (1996). Morphology of the ovotestis of Synaptula hydriformis (Holothuroidea, Apoda): An evolutionary model of oogenesis and the origin of egg polarity in echinoderms. <u>Invertebrate Biology</u> **115**(1): 46-66.

Fujita, T., Umeki, H., Shimura, H., Kugumiya, K., Shiga, K. (2006). Effect of group culture and embryo-culture conditioned medium on development of bovine embryos. <u>J Reprod Dev.</u> **52**(1): 137-142.

Fulka, J., Jr.*,* First, N. L. and Moor, R. M. (1998). Nuclear and cytoplasmic determinants involved in the regulation of mammalian oocyte maturation. <u>Mol Hum Reprod</u> **4**(1): 41-49.

Fulop, C.*,* Salustri, A. and Hascall, V. C. (1997). Coding sequence of a hyaluronan synthase homologue expressed during expansion of the mouse cumulus-oocyte complex. <u>Arch Biochem Biophys</u> **337**(2): 261-266.

Funabiki, H. and Murray, A. W. (2000). The Xenopus chromokinesin Xkid is essential for metaphase chromosome alignment and must be degraded to allow anaphase chromosome movement. <u>Cell</u> **102**(4): 411-424.

Gache, V.*,* Waridel, P., Winter, C., Juhem, A., Schroeder, M., Shevchenko, A., Popov, A. V. (2010). Xenopus meiotic microtubule-associated interactome. <u>PLoS One</u> **5**(2): e9248.

Gaffre, M.*,* Martoriati, A., Belhachemi, N., Chambon, J. P., Houliston, E., Jessus, C., Karaiskou, A., (2011). A critical balance between Cyclin B synthesis and Myt1 activity controls meiosis entry in Xenopus oocytes. <u>Development</u> **138**(17): 3735-3744.

Gal, A. B.*,* Carnwath, J. W., Dinnyes, A., Herrmann, D., Niemann, H., Wrenzycki, C. (2006). Comparison of real-time polymerase chain reaction and end-point polymerase chain reaction for the analysis of gene expression in preimplantation embryos. <u>Reprod Fertil Dev</u> **18**(3): 365-371.

Galli, C. and Moor, R. M. (1991). Somatic cells and the G2 to M-phase transition in sheep oocytes. <u>Reprod Nutr Dev</u> **31**(2): 127-134.

Galloway, S. M.*,* McNatty, K. P., Cambridge, L. M., Laitinen, M. P., Juengel, J. L., Jokiranta, T. S., ... Ritvos, O. (2000). Mutations in an oocyte-derived growth factor gene (BMP15) cause increased ovulation rate and infertility in a dosage-sensitive manner. <u>Nat Genet</u> **25**(3): 279-283.

Gandhi, A. P.*,* Lane, M., Gardner, D. K., Krisher, R. L. (2000). A single medium supports development of bovine embryos throughout maturation, fertilization and culture. <u>Hum Reprod</u> **15**(2): 395-401.

Gardner, D. K.*,* Lane, M., Spitzer, A., Batt, P. A. (1994). Enhanced rates of cleavage and development for sheep zygotes cultured to the blastocyst stage in vitro in the absence of serum and somatic cells: amino acids, vitamins, and culturing embryos in groups stimulate development. <u>Biol Reprod</u> **50**(2): 390-400.

Gasca, S., Pellestor, F., Assou, S., Loup, V., Anahory, T., Dechaud, H., ... Hamamah, S. (2007). Identifying new human oocyte marker genes: a microarray approach. Reprod Biomed Online **14**(2): 175-183.

Gautier, L., Cope, L., Bolstad, B. M., Irizarry, R. A. (2004). Affy - analysis of Affymetrix GeneChip data at the probe level. Bioinformatics **20**(3): 307-315.

Gavin, A. C. and SchorderetSlatkine, S. (1997). Ribosomal S6 kinase p90(rsk) and mRNA cap-binding protein eIF4E phosphorylations correlate with MAP kinase activation during meiotic reinitiation of mouse oocytes. Mol Reprod Dev **46**(3): 383-391.

Ge, L., Sui, H. S., Lan, G. C., Liu, N., Wang, J. Z., Tan, J. H. (2008). Coculture with cumulus cells improves maturation of mouse oocytes denuded of the cumulus oophorus: observations of nuclear and cytoplasmic events. Fertil Steril **90**(6): 2376-2388.

Gebauer, F., Xu, W. H., Cooper, G. M., Richter, J. D. (1994). Translationnal control by cytoplasmic polyadenylation of c-mos is necessary for oocyte maturation in the mouse. Embo Journal **13**(23): 5712-5720.

Gerace, L. (1995). Nuclear export signals and the fast track to the cytoplasm. Cell **82**(3): 341-344.

Gerhard, D. S., Wagner, L., Feingold, E. A., Shenmen, C. M., Grouse, L. H., Schuler, G., ... Malek, J. (2004). The status, quality, and expansion of the NIH full-length cDNA project: the Mammalian Gene Collection (MGC). Genome Res **14**(10B): 2121-2127.

Ghanem, N., Hoelker, M., Rings, F., Jennen, D., Tholen, E., Sirard, M. A., ... Tesfaye, D. (2007). Alterations in transcript abundance of bovine oocytes recovered at growth and dominance phases of the first follicular wave. Bmc Developmental Biology **7**.

Gilbert, I., Robert, C., Vigneault, C., Blondin, P., Sirard, M. A. (2012). Impact of the LH surge on granulosa cell transcript levels as markers of oocyte developmental competence in cattle. Reproduction **143**(6): 735-747.

Gilchrist, R. B., Lane, M. and Thompson, J. G. (2008). Oocyte-secreted factors: regulators of cumulus cell function and oocyte quality. Hum Reprod Update **14**(2): 159-177.

Gilchrist, R. B., Ritter, L. J. and Armstrong, D. T. (2004). Oocyte-somatic cell interactions during follicle development in mammals. Anim Reprod Sci **82-83**: 431-446.

Gilchrist, R. B., Ritter, L. J., Myllymaa, S., Kaivo-Oja, N., Dragovic, R. A., Hickey, T. E., Mottershead, D. G. (2006). Molecular basis of oocyte-paracrine signalling that promotes granulosa cell proliferation. J Cell Sci **119**(Pt 18): 3811-3821.

Glisovic, T., Bachorik, J. L., Yong, J., Dreyfuss, G. (2008). RNA-binding proteins and post-transcriptional gene regulation. FEBS Lett **582**(14): 1977-1986.

Glister, C., Richards, S. L. and Knight, P. G. (2005). Bone morphogenetic proteins (BMP) -4, -6, and -7 potently suppress basal and luteinizing hormone-induced androgen production by bovine theca interna cells in primary culture: could ovarian hyperandrogenic dysfunction be caused by a defect in thecal BMP signaling? Endocrinology **146**(4): 1883-1892.

Goldenberg, R. L., Powell, R. D., Rosen, S. W., Marshall, J. R., Ross, G. T. (1976). Ovarian morphology in women with anosmia and hypogonadotropic hypogonadism. Am J Obstet Gynecol **126**(1): 91-94.

Gonzalez-Robayna, I. J., Falender, A. E., Ochsner, S., Firestone, G. L., Richards, J. S. (2000). Follicle-Stimulating hormone (FSH) stimulates phosphorylation and activation of protein kinase B (PKB/Akt) and serum and glucocorticoid-lnduced kinase (Sgk): evidence for A kinase-independent signaling by FSH in granulosa cells. Mol Endocrinol **14**(8): 1283-1300.

Goryachev, A. B., MacGregor, P. F. and Edwards, A. M. (2001). Unfolding of microarray data. Journal of Computational Biology **8**(4): 443-461.

Gosden, R. G., Telfer, E., Faddy, M. J., Brook, D. J. (1989). Ovarian cyclicity and follicular recruitment in unilaterally ovariectomized mice. J Reprod Fertil **87**(1): 257-264.

Gougeon, A. (1989). Some aspects of the dynamics of ovarian follicular growth in the human. Acta Eur Fertil **20**(4): 185-192.

Gougeon, A. (1996). Regulation of ovarian follicular development in primates: facts and hypotheses. Endocr Rev **17**(2): 121-155.

Gougeon, A. (2005). The biological aspects of risks of infertility due to age: the female side. <u>Rev Epidemiol Sante Publique</u> **53 Spec No 2**: 2S37-45.

Graham, N. S., May, S. T., Daniel, Z. C. T. R., Emmerson, Z. F., Brameld, J. M., Parr, T. (2011). Use of the Affymetrix Human GeneChip array and genomic DNA hybridisation probe selection to study ovine transcriptomes. <u>Animal</u> **5**(6): 861-866.

Gregory, S. G., Barlow, K. F., McLay, K. E., Kaul, R., Swarbreck, D., Dunham, A., ... Prigmore, E. (2006). The DNA sequence and biological annotation of human chromosome 1. <u>Nature</u> **441**(7091): 315-321.

Grimm, D., Streetz, K. L., Jopling, C. L., Storm, T. A., Pandey, K., Davis, C. R., ... Kay, M. A. (2006). Fatality in mice due to oversaturation of cellular microRNA/short hairpin RNA pathways. <u>Nature</u> **441**(7092): 537-541.

Grondahl, C., Breinholt, J., Wahl, P., Murray, A., Hansen, T. H., Faerge, I., ... Hegele-Hartung, C. (2003). Physiology of meiosis-activating sterol: endogenous formation and mode of action. <u>Hum Reprod</u> **18**(1): 122-129.

Groome, N. P., Illingworth, P. J., O'Brien, M., Pai, R., Rodger, F. E., Mather, J. P., McNeilly, A. S. (1996). Measurement of dimeric inhibin B throughout the human menstrual cycle." <u>J Clin Endocrinol Metab</u> **81**(4): 1401-1405.

Gruter, P., Tabernero, C., von Kobbe, C., Schmitt, C., Saavedra, C., Bachi, A., ... Izaurralde, E. (1998). TAP, the human homolog of Mex67p, mediates CTE-dependent RNA export from the nucleus. <u>Mol Cell</u> **1**(5): 649-659.

Gudermann, T., Nurnberg, B. and Schultz, G. (1995). Receptors and G proteins as primary components of transmembrane signal transduction. Part 1. G-protein-coupled receptors: structure and function. <u>J Mol Med (Berl)</u> **73**(2): 51-63.

Gui, L. M. and Joyce, I. M. (2005). RNA interference evidence that growth differentiation factor-9 mediates oocyte regulation of cumulus expansion in mice. <u>Biol Reprod</u> **72**(1): 195-199.

Halpin, D. M., Charlton, H. M. and Faddy, M. J. (1986). Effects of gonadotrophin deficiency on follicular development in hypogonadal (hpg) mice. <u>J Reprod Fertil</u> **78**(1): 119-125.

Hanahan, D. (1983). Studies on transformation of Escherichia coli with plasmids. <u>J Mol Biol</u> **166**(4): 557-580.

Hannak, E., Kirkham, M., Hyman, A. A., Oegema, K. (2001). Aurora-A kinase is required for centrosome maturation in Caenorhabditis elegans. <u>Journal of Cell Biology</u> **155**(7): 1109-1115.

Hanrahan, J. P., Gregan, S. M., Mulsant, P., Mullen, M., Davis, G. H., Powell, R., Galloway, S. M. (2004). Mutations in the genes for oocyte-derived growth factors GDF9 and BMP15 are associated with both increased ovulation rate and sterility in Cambridge and Belclare sheep (Ovis aries). <u>Biol Reprod</u> **70**(4): 900-909.

Harhay, G. P., Sonstegard, T. S., Keele, J. W., Heaton, M. P., Clawson, M. L., Snelling, W. M., ... Smith, T. P. L. (2005). Characterization of 954 bovine full-CDS cDNA sequences. <u>Bmc Genomics</u> **6**.

Hartshorne, G. M., Sargent, I. L. and Barlow, D. H. (1994). Meiotic progression of mouse oocytes throughout follicle growth and ovulation in vitro. <u>Hum Reprod</u> **9**(2): 352-359.

Hashimoto, S., Saeki, K., Nagao, Y., Minami, N., Yamada, M., Utsumi, K. (1998). Effects of cumulus cell density during in vitro maturation of the developmental competence of bovine oocytes. <u>Theriogenology</u> **49**(8): 1451-1463.

Hawkins, S. M., Buchold, G. M. and Matzuk, M. M. (2011). Minireview: The roles of small RNA pathways in reproductive medicine. <u>Mol Endocrinol</u> **25**(8): 1257-1279.

Hay, B., Jan, L. Y. and Jan, Y. N. (1988). A protein component of Drosophila polar granules is encoded by vasa and has extensive sequence similarity to ATP-dependent helicases. <u>Cell</u> **55**(4): 577-587.

Hayano, T., Yanagida, M., Yamauchi, Y., Shinkawa, T., Isobe, T., Takahashi, N. (2003). Proteomic analysis of human Nop56p-associated pre-ribosomal ribonucleoprotein complexes - Possible link between Nop56p and the nucleolar protein treacle responsible for Treacher Collins syndrome. <u>Journal of Biological Chemistry</u> **278**(36): 34309-34319.

Heber, S. and Sick, B. (2006). Quality assessment of affymetrix GeneChip data. <u>Omics-a Journal of Integrative Biology</u> **10**(3): 358-368.

Heasman, J. (2002). Morpholino oligos: Making sense of antisense? <u>Developmental Biology</u> **243**(2): 209-214.

Hegele-Hartung, C.*,* Grutzner, M., Lessl, M., Grondahl, C., Ottesen, J., Brannstrom, M. (2001). Activation of meiotic maturation in rat oocytes after treatment with follicular fluid meiosis-activating sterol in vitro and ex vivo. <u>Biol Reprod</u> **64**(2): 418-424.

Heid, C. A.*,* Stevens, J., Livak, K. J., Williams, P. M. (1996). Real time quantitative PCR. <u>Genome Res</u> **6**(10): 986-994.

Heldin, C. H.*,* Miyazono, K. and ten Dijke, P. (1997). TGF-beta signalling from cell membrane to nucleus through SMAD proteins. <u>Nature</u> **390**(6659): 465-471.

Hewitt, S. C.*,* Harrell, J. C. and Korach, K. S. (2005). Lessons in estrogen biology from knockout and transgenic animals. <u>Annu Rev Physiol</u> **67**: 285-308.

Hilleren, P.*,* McCarthy, T., Rosbash, M., Parker, R., Jensen, T. H. (2001). Quality control of mRNA 3'-end processing is linked to the nuclear exosome. <u>Nature</u> **413**(6855): 538-542.

Hillier, S. G.*,* Yong, E. L., Illingworth, P. J., Baird, D. T., Schwall, R. H., Mason, A. J. (1991). Effect of recombinant inhibin on androgen synthesis in cultured human thecal cells. <u>Mol Cell Endocrinol</u> **75**(2): R1-6.

Hirshfield, A. N. (1991). Development of follicles in the mammalian ovary. <u>Int Rev Cytol</u> **124**: 43-101.

Hochberg, Y. and Benjamini, Y. (1990). More powerful procedures for multiple significance testing. <u>Statistics in Medicine</u> **9**(7): 811-818.

Holder, A. T.*,* Spencer, E. M. and Preece, M. A. (1981). Effect of bovine growth hormone and a partially pure preparation of somatomedin on various growth parameters in hypopituitary dwarf mice. <u>J Endocrinol</u> **89**(2): 275-282.

Holen, T.*,* Amarzguioui, M., Wiiger, M. T., Babaie, E., Prydz, H. (2002). Positional effects of short interfering RNAs targeting the human coagulation trigger Tissue Factor. <u>Nucleic Acids Res</u> **30**(8): 1757-1766.

Hong, F. and Breitling, R. (2008). A comparison of meta-analysis methods for detecting differentially expressed genes in microarray experiments. <u>Bioinformatics</u> **24**(3): 374-382.

Hoodbhoy, T. and Talbot, P. (1994). Mammalian cortical granules: contents, fate, and function. <u>Mol Reprod Dev</u> **39**(4): 439-448.

Hotten, G.*,* Neidhardt, H., Schneider, C., Pohl, J. (1995). Cloning of a new member of the TGF-beta family: a putative new activin beta C chain. <u>Biochem Biophys Res Commun</u> **206**(2): 608-613.

Hsieh, M.*,* Lee, D., Panigone, S., Horner, K., Chen, R., Theologis, A., ... Conti, M. (2007). Luteinizing hormone-dependent activation of the epidermal growth factor network is essential for ovulation. <u>Mol Cell Biol</u> **27**(5): 1914-1924.

Huang, D. W.*,* Sherman, B. T. and Lempicki, R. A. (2009). Bioinformatics enrichment tools: paths toward the comprehensive functional analysis of large gene lists. <u>Nucleic Acids Research</u> **37**(1): 1-13.

Huang, H. F.*,* He, R. H., Sun, C. C., Zhang, Y., Meng, Q. X., Ma, Y. Y. (2006). Function of aquaporins in female and male reproductive systems. <u>Hum Reprod Update</u> **12**(6): 785-795.

Huber, W. and Gentleman, R. (2004). Matchprobes: a Bioconductor package for the sequence-matching of microarray probe elements. <u>Bioinformatics</u> **20**(10): 1651-1652.

Hulshof, S. C.*,* Figueiredo, J. R., Beckers, J. F., Bevers, M. M., van der Donk, J. A., van den Hurk, R. (1995). Effects of fetal bovine serum, FSH and 17beta-estradiol on the culture of bovine preantral follicles. <u>Theriogenology</u> **44**(2): 217-226.

Hunt, P. A. and Hassold, T. J. (2002). Sex matters in meiosis. <u>Science</u> **296**(5576): 2181-2183.

Hunter, A. W.*,* Caplow, M., Coy, D. L., Hancock, W. O., Diez, S., Wordeman, L., Howard, J. (2003). The kinesin-related protein MCAK is a microtubule depolymerase that forms an ATP-hydrolyzing complex at microtubule ends. <u>Mol Cell</u> **11**(2): 445-457.

Hunter, M. G.*,* Brankin, V., Quinn, R. L., Ferguson, E. M., Edwards, S. A., Ashworth, C. J. (2005). Oocyte-somatic cell-endocrine interactions in pigs. <u>Domest Anim Endocrinol</u> **29**(2): 371-384.

Hunter, M. G., Robinson, R. S., Mann, G. E., Webb, R. (2004). Endocrine and paracrine control of follicular development and ovulation rate in farm species. Anim Reprod Sci **82-83**: 461-477.

Huntriss, J., Gosden, R., Hinkins, M., Oliver, B., Miller, D., Rutherford, A. J., Picton, H. M. (2002). Isolation, characterization and expression of the human Factor In the Germline alpha (FIGLA) gene in ovarian follicles and oocytes. Mol Hum Reprod **8**(12): 1087-1095.

Huntriss, J., Hinkins, M. and Picton, H. M. (2006). cDNA cloning and expression of the human NOBOX gene in oocytes and ovarian follicles. Mol Hum Reprod **12**(5): 283-289.

Huppi, K., Martin, S. E. and Caplen, N. J. (2005). Defining and assaying RNAi in mammalian cells. Mol Cell **17**(1): 1-10.

Hussein, T. S., Froiland, D. A., Amato, F., Thompson, J. G., Gilchrist, R. B. (2005). Oocytes prevent cumulus cell apoptosis by maintaining a morphogenic paracrine gradient of bone morphogenetic proteins. J Cell Sci **118**(Pt 22): 5257-5268.

Inoue, H., Nojima, H. and Okayama, H. (1990). High efficiency transformation of Escherichia coli with plasmids. Gene **96**(1): 23-28.

Inoue, S. (1981). Cell division and the mitotic spindle. J Cell Biol **91**(3 Pt 2): 131s-147s.

Ioannidis, J. P., Allison, D. B., Ball, C. A., Coulibaly, I., Cui, X., Culhane, A. C., ... van Noort, V. (2009). Repeatability of published microarray gene expression analyses. Nat Genet **41**(2): 149-155.

Ireland, J. L., Scheetz, D., Jimenez-Krassel, F., Themmen, A. P., Ward, F., Lonergan, P., ... Ireland, J. J. (2008). Antral follicle count reliably predicts number of morphologically healthy oocytes and follicles in ovaries of young adult cattle. Biol Reprod **79**(6): 1219-1225.

Irizarry, R. A., Hobbs, B., Collin, F., Beazer-Barclay, Y. D., Antonellis, K. J., Scherf, U., Speed, T. P. (2003). Exploration, normalization, and summaries of high density oligonucleotide array probe level data. Biostatistics **4**(2): 249-264.

Ishizaki, C., Watanabe, H., Bhuiyan, M. M., Fukui, Y. (2009). Developmental competence of porcine oocytes selected by brilliant cresyl blue and matured individually in a chemically defined culture medium. Theriogenology **72**(1): 72-80.

Isobe, N., Maeda, T. and Terada, T. (1998). Involvement of meiotic resumption in the disruption of gap junctions between cumulus cells attached to pig oocytes. J Reprod Fertil **113**(2): 167-172.

Itoh, T., Kacchi, M., Abe, H., Sendai, Y., Hoshi, H. (2002). Growth, antrum formation, and estradiol production of bovine preantral follicles cultured in a serum-free medium. Biol Reprod **67**(4): 1099-1105.

Jackson, R. J. and Standart, N. (1990). Do the poly(A) tail and 3' untranslated region control mRNA translation? Cell **62**(1): 15-24.

Jaroudi, K. A., Hollanders, J. M., Sieck, U. V., Roca, G. L., El-Nour, A. M., Coskun, S. (1997). Pregnancy after transfer of embryos which were generated from in-vitro matured oocytes. Hum Reprod **12**(4): 857-859.

Jeong, H. J., Kim, H. J., Lee, S. H., Kwack, K., Ahn, S. Y., Choi, Y. J., ... Cha, K. Y. (2006). Gene expression profiling of the pre-implantation mouse embryo by microarray analysis: comparison of the two-cell stage and two-cell block. Theriogenology **66**(4): 785-796.

Jeong, Y. J., Choi, H. W., Shin, H. S., Cui, X. S., Kim, N. H., Gerton, G. L., Jun, J. H. (2005). Optimization of real time RT-PCR methods for the analysis of gene expression in mouse eggs and preimplantation embryos. Mol Reprod Dev **71**(3): 284-289.

Jeppesen, J. V., Kristensen, S. G., Nielsen, M. E., Humaidan, P., Dal Canto, M., Fadini, R., ... Yding Andersen, C. (2012). LH-Receptor Gene Expression in Human Granulosa and Cumulus Cells from Antral and Preovulatory Follicles. J Clin Endocrinol Metab.

Jin, Z. and Xie, T. (2007). Dcr-1 maintains Drosophila ovarian stem cells. Curr Biol **17**(6): 539-544.

Johnson, J., Canning, J., Kaneko, T., Pru, J. K., Tilly, J. L. (2004). Germline stem cells and follicular renewal in the postnatal mammalian ovary. Nature **428**(6979): 145-150.

Johnson, J. M.*,* Castle, J., Garrett-Engele, P., Kan, Z., Loerch, P. M., Armour, C. D., ... Shoemaker, D. D. (2003). Genome-wide survey of human alternative pre-mRNA splicing with exon junction microarrays. <u>Science</u> **302**(5653): 2141-2144.

Jones, K. T. (2004). Turning it on and off: M-phase promoting factor during meiotic maturation and fertilization. <u>Mol Hum Reprod</u> **10**(1): 1-5.

Jones, K. T. (2007). Intracellular calcium in the fertilization and development of mammalian eggs. <u>Clinical and Experimental Pharmacology and Physiology</u> **34**(10): 1084-1089.

Jose de los Santos, M.*,* Garcia-Laez, V., Beltran-Torregrosa, D., Horcajadas, J. A., Antonio Martinez-Conejero, J., Esteban, F., ... Labarta, E. (2012). Hormonal and molecular characterization of follicular fluid, cumulus cells and oocytes from pre-ovulatory follicles in stimulated and unstimulated cycles. <u>Human Reproduction</u> **27**(6): 1596-1605.

Juengel, J. L.*,* Hudson, N. L., Heath, D. A., Smith, P., Reader, K. L., Lawrence, S. B., ... McNatty, K. P. (2002). Growth differentiation factor 9 and bone morphogenetic protein 15 are essential for ovarian follicular development in sheep. <u>Biol Reprod</u> **67**(6): 1777-1789.

Junk, S. M. and Yeap, D. (2012). Improved implantation and ongoing pregnancy rates after single-embryo transfer with an optimized protocol for in vitro oocyte maturation in women with polycystic ovaries and polycystic ovary syndrome. <u>Fertil Steril</u> **98**(4): 888-892.

Kaivo-Oja, N.*,* Bondestam, J., Kamarainen, M., Koskimies, J., Vitt, U., Cranfield, M., ... Ritvos, O. (2003). Growth differentiation factor-9 induces Smad2 activation and inhibin B production in cultured human granulosa-luteal cells. <u>J Clin Endocrinol Metab</u> **88**(2): 755-762.

Kamal, A. and L. S. Goldstein (2002). "Principles of cargo attachment to cytoplasmic motor proteins." <u>Curr Opin Cell Biol</u> **14**(1): 63-68.

Kaneda, M.*,* Tang, F., O'Carroll, D., Lao, K., Surani, M. A. (2009). Essential role for Argonaute2 protein in mouse oogenesis. <u>Epigenetics Chromatin</u> **2**(1): 9.

Kapuscinski, J. (1995). DAPI: a DNA-specific fluorescent probe. <u>Biotech Histochem</u> **70**(5): 220-233.

Karaiskou, A.*,* Lepretre, A. C., Pahlavan, G., Du Pasquier, D., Ozon, R., Jessus, C. (2004). Polo-like kinase confers MPF autoamplification competence to growing Xenopus oocytes. <u>Development</u> **131**(7): 1543-1552.

Karsenti, E. and Vernos, I. (2001). The mitotic spindle: a self-made machine. <u>Science</u> **294**(5542): 543-547.

Kasa-Vubu, J. Z.*,* Dahl, G. E., Evans, N. P., Thrun, L. A., Moenter, S. M., Padmanabhan, V., Karsch, F. J. (1992). Progesterone blocks the estradiol-induced gonadotropin discharge in the ewe by inhibiting the surge of gonadotropin-releasing hormone. <u>Endocrinology</u> **131**(1): 208-212.

Katoh, M. (2003). Identification and characterization of human TIPARP gene within the CCNL amplicon at human chromosome 3q25.31. <u>International Journal of Oncology</u> **23**(2): 541-547.

Kedersha, N.*,* Stoecklin, G., Ayodele, M., Yacono, P., Lykke-Andersen, J., Fritzler, M. J., ... Anderson, P. (2005). Stress granules and processing bodies are dynamically linked sites of mRNP remodeling. <u>J Cell Biol</u> **169**(6): 871-884.

Keene, J. D.*,* Komisarow, J. M. and Friedersdorf, M. B. (2006). RIP-Chip: the isolation and identification of mRNAs, microRNAs and protein components of ribonucleoprotein complexes from cell extracts." <u>Nature Protocols</u> **1**(1): 302-307.

Kelly, A. E.*,* Sampath, S. C., Maniar, T. A., Woo, E. M., Chait, B. T., Funabiki, H. (2007). Chromosomal enrichment and activation of the aurora B pathway are coupled to spatially regulate spindle assembly. <u>Dev Cell</u> **12**(1): 31-43.

Kennerdell, J. R. and Carthew, R. W. (1998). Use of dsRNA-mediated genetic interference to demonstrate that frizzled and frizzled 2 act in the wingless pathway. <u>Cell</u> **95**(7): 1017-1026.

Kerr, M. K. (2003). Linear models for microarray data analysis: Hidden similarities and differences. <u>Journal of Computational Biology</u> **10**(6): 891-901.

Keskintepe, L.*,* Burnley, C. A. and Brackett, B. G. (1995). Production of viable bovine blastocysts in defined in vitro conditions. <u>Biol Reprod</u> **52**(6): 1410-1417.

Khurana, J. S. and Theurkauf, W. (2010). piRNAs, transposon silencing, and Drosophila germline development. J Cell Biol **191**(5): 905-913.

Kim, E.*,* Yoon, S. J.., Kim, E. Y., Kim, Y.., Lee, H. S., Kim, K. H., Lee, K. A. (2011). Function of COP9 signalosome in regulation of mouse oocytes meiosis by regulating MPF activity and securing degradation. PLoS One **6**(10): e25870-e25870.

Kim, J. H. and Richter, J. D. (2007). RINGO/cdk1 and CPEB mediate poly(A) tail stabilization and translational regulation by ePAB. Genes Dev **21**(20): 2571-2579.

Kimura, N.*,* Hoshino, Y., Totsukawa, K., Sato, E. (2007). Cellular and molecular events during oocyte maturation in mammals: molecules of cumulus-oocyte complex matrix and signalling pathways regulating meiotic progression. Soc Reprod Fertil Suppl **63**: 327-342.

Kimura, N.*,* Konno, Y., Miyoshi, K., Matsumoto, H., Sato, E. (2002). Expression of hyaluronan synthases and CD44 messenger RNAs in porcine cumulus-oocyte complexes during in vitro maturation. Biol Reprod **66**(3): 707-717.

King, R. W.*,* Peters, J. M., Tugendreich, S., Rolfe, M., Hieter, P., Kirschner, M. W. (1995). A 20S complex containing CDC27 and CDC16 catalyzes the mitosis-specific conjugation of ubiquitin to cyclin B. Cell **81**(2): 279-288.

Kitahara, G.*,* Nambo, Y., El-Sheikh Ali, H., Kajisa, M., Tani, M., Nibe, K., Kamimura, S. (2012). Anti-Mullerian hormone profiles as a novel biomarker to diagnose granulosa-theca cell tumors in cattle. J Reprod Dev **58**(1): 98-104.

Kleinschmidt, J. A.*,* Fortkamp, E., Krohne, G., Zentgraf, H., Franke, W. W. (1985). Co-existence of two different types of soluble histone complexes in nuclei of Xenopus laevis oocytes. J Biol Chem **260**(2): 1166-1176.

Kline, D. (2000). Attributes and dynamics of the endoplasmic reticulum in mammalian eggs. Curr Top Dev Biol **50**: 125-154.

Kloc, M.*,* Bilinski, S. and Etkin, L. D. (2004). The Balbiani body and germ cell determinants: 150 years later. Curr Top Dev Biol **59**: 1-36.

Kloos, D. U.*,* Choi, C. and Wingender, E. (2002). The TGF-beta--Smad network: introducing bioinformatic tools. Trends Genet **18**(2): 96-103.

Klug, A. (1999). Zinc finger peptides for the regulation of gene expression. J Mol Biol **293**(2): 215-218.

Koller, B. H.*,* Hagemann, L, J., Doetschman, T., Hagaman, J. R., Huang, S., Williams, P. J., ... Smithies, O. (1989). Germ-line transmission of a planned alteration made in a hypoxanthine phophoribosyltransferase gene by homologous recombination in embryonic stem-cells. Proc Natl Acad Sci U S A **86**(22): 8927-8931.

Korneev, S. A.*,* Park, J. H. and O'Shea, M. (1999). Neuronal expression of neural nitric oxide synthase (nNOS) protein is suppressed by an antisense RNA transcribed from an NOS pseudogene. Journal of Neuroscience **19**(18): 7711-7720.

Kotaja, N.*,* Bhattacharyya, S. N., Jaskiewicz, L., Kimmins, S., Parvinen, M., Filipowicz, W., Sassone-Corsi, P. (2006). The chromatoid body of male germ cells: similarity with processing bodies and presence of Dicer and microRNA pathway components. Proc Natl Acad Sci U S A **103**(8): 2647-2652.

Kotaja, N. and Sassone-Corsi, P. (2007). The chromatoid body: a germ-cell-specific RNA-processing centre. Nat Rev Mol Cell Biol **8**(1): 85-90.

Krisher, R. L. and Bavister, B. D. (1998). Responses of oocytes and embryos to the culture environment. Theriogenology **49**(1): 103-114.

Krotz, S. P.*,* Ballow, D. J., Choi, Y., Rajkovic, A. (2009). Expression and localization of the novel and highly conserved gametocyte-specific factor 1 during oogenesis and spermatogenesis. Fertil Steril **91**(5 Suppl): 2020-2024.

Kumar, C. C.*,* Mohan, S. R., Zavodny, P. J., Narula, S. K., Leibowitz, P. J. (1989). Characterisation and differential expression of human vascular smooth-muscle myosin light chain-2 isoform in non-muscle cells. Biochemistry **28**(9): 4027-4035.

Kuo, P.-H.*,* Doudeva, L. G., Wang, Y. T., Shen, C. K. J., Yuan, H. S. (2009). Structural insights into TDP-43 in nucleic-acid binding and domain interactions. Nucleic Acids Research **37**(6): 1799-1808.

Kuramochi-Miyagawa, S.*,* Kimura, T., Ijiri, T. W., Isobe, T., Asada, N., Fujita, Y., ... Nakano, T. (2004). Mili, a mammalian member of piwi family gene, is essential for spermatogenesis. Development **131**(4): 839-849.

Kuramochi-Miyagawa, S.*,* Watanabe, T., Gotoh, K., Takamatsu, K., Chuma, S., Kojima-Kita, K, ... Nakano, T. (2010). MVH in piRNA processing and gene silencing of retrotransposons. Genes Dev **24**(9): 887-892.

Laemmli, U. K. (1970). Cleavage of structural proteins during the assembly of the head of bacteriophage T4. Nature **227**(5259): 680-685.

Laissue, P.*,* Christin-Maitre, S., Touraine, P., Kuttenn, F., Ritvos, O., Aittomaki, K., ... Veitia, R. A. (2006). Mutations and sequence variants in GDF9 and BMP15 in patients with premature ovarian failure. Eur J Endocrinol **154**(5): 739-744.

Lang, M. and Orgogozo, V. (2011). Identification of homologous gene sequences by PCR with degenerate primers. Methods Mol Biol **772**: 245-256.

Larsen, M. R.*,* Trelle, M. B., Thingholm, T. E., Jensen, O. N. (2006). Analysis of posttranslational modifications of proteins by tandem mass spectrometry. Biotechniques **40**(6): 790-798.

Larue, L.*,* Ohsugi, M., Hirchenhain, J., Kemler, R. (1994). E-cadherin null mutant embryos fail to form a trophectoderm epithelium. Proc Natl Acad Sci U S A **91**(17): 8263-8267.

Lasko, P. (2000). The drosophila melanogaster genome: translation factors and RNA binding proteins. J Cell Biol **150**(2): F51-56.

Lass, A. (2001). Assessment of ovarian reserve - is there a role for ovarian biopsy? Hum Reprod. **16**(6): 1055-1057.

Lau, A. (2005). RNA interference in practice. Comp Funct Genomics **6**(5-6): 320-322.

Lawson, K. A.*,* Dunn, N. R., Roelen, B. A., Zeinstra, L. M., Davis, A. M., Wright, C. V., ... Hogan, B. L. (1999). Bmp4 is required for the generation of primordial germ cells in the mouse embryo. Genes Dev **13**(4): 424-436.

Lechniak, D.*,* Pers-Kamczyc, E. and Pawlak, P. (2008). Timing of the first zygotic cleavage as a marker of developmental potential of mammalian embryos. Reproductive Biology **8**(1): 23-42.

Lee, C. K.*,* Weindruch, R. and Prolla, T. A. (2000). Gene-expression profile of the ageing brain in mice. Nature Genetics **25**(3): 294-297.

Lefebvre, C.*,* Terret, M. E., Djiane, A., Rassinier, P., Maro, B., Verlhac, M. H. (2002). Meiotic spindle stability depends on MAPK-interacting and spindle-stabilizing protein (MISS), a new MAPK substrate. J Cell Biol **157**(4): 603-613.

Lei, L.*,* Jin, S., Gonzalez, G., Behringer, R. R., Woodruff, T. K. (2010). The regulatory role of Dicer in folliculogenesis in mice. Mol Cell Endocrinol **315**(1-2): 63-73.

Leonardsen, L.*,* Wiersma, A., Baltsen, M., Byskov, A. G., Andersen, C. Y. (2000). Regulation of spontaneous and induced resumption of meiosis in mouse oocytes by different intracellular pathways. J Reprod Fertil **120**(2): 377-383.

Leoni, G. G.*,* Bebbere, D., Succu, S., Berlinguer, F., Mossa, F., Galioto, M., ... Naitana, S. (2007). Relations between relative mRNA abundance and developmental competence of ovine oocytes. Mol Reprod Dev **74**(2): 249-257.

Levsky, J. M. and Singer, R. H. (2003). Fluorescence in situ hybridization: past, present and future. J Cell Sci **116**(Pt 14): 2833-2838.

Lewis, B. P.*,* Shih, I. H., Jones-Rhoades, M. W., Bartel, D. P., Burge, C. B. (2003). Prediction of mammalian microRNA targets. Cell **115**(7): 787-798.

Li, C. J. and Fan, B. Q. (1997). Changes in the 3-dimensional distribution of mitochondria during meiotic divisions of mouse oocytes. Theriogenology **48**(1): 33-41.

Li, G. P.*,* Bunch, T. D., White, K. L., Rickords, L., Liu, Y., Sessions, B. R. (2006). Denuding and centrifugation of maturing bovine oocytes alters oocyte spindle integrity and the ability of cytoplasm to support parthenogenetic and nuclear transfer embryo development. Mol Reprod Dev **73**(4): 446-451.

Li, L.*,* Baibakov, B. and Dean, J. (2008). A subcortical maternal complex essential for preimplantation mouse embryogenesis. Dev Cell **15**(3): 416-425.

Li, Y., Chen, R., Zhou, Q., Xu, Z., Li, C., Wang, S., ... Shu, H. B. (2012). LSm14A is a processing body-associated sensor of viral nucleic acids that initiates cellular antiviral response in the early phase of viral infection. Proc Natl Acad Sci U S A **109**(29): 11770-11775.

Li, Y., Ray, D. and Ye, P. (2013). Identification of germ cell-specific genes in mammalian meiotic prophase. BMC Bioinformatics.

Liang, C. G., Su, Y. Q., Fan, H. Y., Schatten, H., Sun, Q. Y. (2007). Mechanisms regulating oocyte meiotic resumption: roles of mitogen-activated protein kinase. Mol Endocrinol **21**(9): 2037-2055.

Liang, L., Soyal, S. M. and Dean, J. (1997). FIGalpha, a germ cell specific transcription factor involved in the coordinate expression of the zona pellucida genes. Development **124**(24): 4939-4947.

Liao, W. X., Moore, R. K., Otsuka, F., Shimasaki, S. (2003). Effect of intracellular interactions on the processing and secretion of bone morphogenetic protein-15 (BMP-15) and growth and differentiation factor-9. Implication of the aberrant ovarian phenotype of BMP-15 mutant sheep. J Biol Chem **278**(6): 3713-3719.

Lin, C. I. and Yeh. N. H. (2009). Treacle recruits RNA polymerase I complex to the nucleolus that is independent of UBF. Biochem Biophys Res Commun **386**(2): 396-401.

Lin, H. and Spradling, A. C. (1997). A novel group of pumilio mutations affects the asymmetric division of germline stem cells in the Drosophila ovary. Development **124**(12): 2463-2476.

Ling, N., Ying, S. Y., Ueno, N., Shimasaki, S., Esch, F., Hotta, M., Guillemin, R. (1986). A homodimer of the beta-subunits of inhibin A stimulates the secretion of pituitary follicle stimulating hormone. Biochem Biophys Res Commun **138**(3): 1129-1137.

Liu, H., Dibling, B., Spike, B., Dirlam, A., Macleod, K. (2004). New roles for the RB tumor suppressor protein. Curr Opin Genet Dev **14**(1): 55-64.

Liu, H. C., Tang, Y., He, Z., Rosenwaks, Z. (2010). Dicer is a key player in oocyte maturation. J Assist Reprod Genet **27**(9-10): 571-580.

Liu, Z. H., Shintani, Y., Sakamoto, Y., Harada, K., Zhang, C. Y., Fujinaka, Y., ... Saito, S. (1996). Effects of LHRH, FSH and activin A on follistatin secretion from cultured rat anterior pituitary cells. Endocr J **43**(3): 321-327.

Lockhart, D. J., Dong, H. L., Byrne, M. C., Follettie, M. T., Gallo, M. V., Chee, M. S., ... Brown, E. L. (1996). Expression monitoring by hybridization to high-density oligonucleotide arrays. Nature Biotechnology **14**(13): 1675-1680.

Logan, K. A., Juengel, J. L. and McNatty, K. P. (2002). Onset of steroidogenic enzyme gene expression during ovarian follicular development in sheep. Biol Reprod **66**(4): 906-916.

Lonergan, P., Gutierrez-Adan, A., Rizos, D., Pintalo, B., De La Fuente, J., Boland, M. P. (2003). Relative messenger RNA abundance in bovine oocytes collected in vitro or in vivo before and 20 hr after the preovulatory luteinizing hormone surge. Mol Reprod Dev **66**(3): 297-305.

Loutradis, D., Kiapekou, E., Zapanti, E., Antsaklis, A. (2006). Oocyte maturation in assisted reproductive techniques. Ann N Y Acad Sci **1092**: 235-246.

Lu, J., Huntriss, J. D., Jin, P., Hemmings, K. E., Cotterill, M., Cambell, B. K., Picton, H. M. (2012). Characterisation of GTSF1 during bovine gametogenesis. [abstract]. In: The annual conference of Society of Reproduction and Fertility, 2012 July 9-11; Edinburgh, UK.

Lunde, B. M., Moore, C. and Varani, G. (2007). RNA-binding proteins: modular design for efficient function. Nat Rev Mol Cell Biol **8**(6): 479-490.

Lundgren, K., Walworth, N., Booher, R., Dembski, M., Kirschner, M., Beach, D. (1991). Mik1 and wee1 cooperate in the inhibitory tyrosine phosphorylation of cdc2. Cell **64**(6): 1111-1122.

Lundy, T., Smith, P., O'Connell, A., Hudson, N. L., McNatty, K. P. (1999). Populations of granulosa cells in small follicles of the sheep ovary. J Reprod Fertil **115**(2): 251-262.

Lussier, J. G., Matton, P. and Dufour, J. J. (1987). Growth rates of follicles in the ovary of the cow. J Reprod Fertil **81**(2): 301-307.

Ma, J., Flemr, M., Stein, P., Berninger, P., Malik, R., Zavolan, M., ... Schultz, R. M. (2010). MicroRNA activity is suppressed in mouse oocytes. Curr Biol **20**(3): 265-270.

Malmanche, N.*,* Maia, A. and Sunkel, C. E. (2006). The spindle assembly checkpoint: preventing chromosome mis-segregation during mitosis and meiosis. <u>FEBS Lett</u> **580**(12): 2888-2895.

Mamo, S.*,* Carter, F., Lonergan, P., Leal, C. L. V., Al Naib, A., McGettigan, P., ... Fair, T. (2011). Sequential analysis of global gene expression profiles in immature and in vitro matured bovine oocytes: potential molecular markers of oocyte maturation. <u>Bmc Genomics</u> **12**.

Mamo, S.*,* Gal, A. B., Bodo, S., Dinnyes, A. (2007). Quantitative evaluation and selection of reference genes in mouse oocytes and embryos cultured in vivo and in vitro. <u>BMC Dev Biol</u> **7**: 14.

Mamo, S.*,* Gal, A. B., Polgar, Z., Dinnyes, A. (2008). Expression profiles of the pluripotency marker gene POU5F1 and validation of reference genes in rabbit oocytes and preimplantation stage embryos. <u>BMC Mol Biol</u> **9**: 67.

Maney, T.*,* Hunter, A. W., Wagenbach, M., Wordeman, L. (1998). Mitotic centromere-associated kinesin is important for anaphase chromosome segregation. <u>J Cell Biol</u> **142**(3): 787-801.

Marion, G. B. and Gier, H. T. (1971). Ovarian and uterine embryogenesis and morphology of the non-pregnant female mammal. <u>J Anim Sci</u> **32 Suppl 1**: 24-47.

Marioni, J. C.*,* Mason, C. E., Mane, S. M., Stephens, M., Gilad, Y. (2008). RNA-seq: an assessment of technical reproducibility and comparison with gene expression arrays. <u>Genome Res</u> **18**(9): 1509-1517.

Markholt, S.*,* Grondahl, M. L., Ernst, E. H., Andersen, C. Y., Ernst, E., Lykke-Hartmann, K. (2012). Global gene analysis of oocytes from early stages in human folliculogenesis shows high expression of novel genes in reproduction. <u>Molecular Human Reproduction</u> **18**(2): 96-110.

Masui, Y. and Clarke, H. J. (1979). Oocyte maturation. <u>Int Rev Cytol</u> **57**: 185-282.

Mathews, L. S.*,* Norstedt, G. and Palmiter, R. D. (1986). Regulation of insulin-like growth factor I gene expression by growth hormone. <u>Proc Natl Acad Sci U S A</u> **83**(24): 9343-9347.

Matsudaira, P. (1987). Sequence from picomole quantities of proteins electroblotted onto polyvinylidene difluoride membranes. <u>J Biol Chem</u> **262**(21): 10035-10038.

Matsumoto, K.*,* Kwon, O. Y., Kim, H., Akao, Y. (2005). Expression of rck/p54, a DEAD-box RNA helicase, in gametogenesis and early embryogenesis of mice. <u>Developmental Dynamics</u> **233**(3): 1149-1156.

Matsumoto, K.*,* Tanaka, K. J., Aoki, K., Sameshima, M., Tsujimoto, M. (2003). Visualization of the reconstituted FRGY2-mRNA complexes by electron microscopy. <u>Biochem Biophys Res Commun</u> **306**(1): 53-58.

Mattioli, M. and Barboni, B. (2000). Signal transduction mechanism for LH in the cumulus-oocyte complex. <u>Mol Cell Endocrinol</u> **161**(1-2): 19-23.

Mattson, B. A. and Albertini, D. F. (1990). Oogenesis: chromatin and microtubule dynamics during meiotic prophase. <u>Mol Reprod Dev</u> **25**(4): 374-383.

Mayes, M. A.*,* Laforest, M. F., Guillemette, C., Gilchrist, R. B., Richard, F. J. (2007). Adenosine 5 '-monophosphate kinase-activated protein kinase (PRKA) activators delay meiotic resumption in porcine oocytes. <u>Biol Reprod</u> **76**(4): 589-597.

Mayes, M. A. and Sirard, M. A. (2002). Effect of type 3 and type 4 phosphodiesterase inhibitors on the maintenance of bovine oocytes in meiotic arrest. <u>Biol Reprod</u> **66**(1): 180-184.

Mazerbourg, S.*,* Klein, C., Roh, J., Kaivo-Oja, N., Mottershead, D. G., Korchynskyi, O., ... Hsueh, A. J. (2004). Growth differentiation factor-9 signaling is mediated by the type I receptor, activin receptor-like kinase 5. <u>Mol Endocrinol</u> **18**(3): 653-665.

McGee, E.*,* Spears, N., Minami, S., Hsu, S. Y., Chun, S. Y., Billig, H., Hsueh, A. J. (1997). Preantral ovarian follicles in serum-free culture: suppression of apoptosis after activation of the cyclic guanosine 3',5'-monophosphate pathway and stimulation of growth and differentiation by follicle-stimulating hormone. <u>Endocrinology</u> **138**(6): 2417-2424.

McGee, E. A. and Hsueh, A. J. (2000). Initial and cyclic recruitment of ovarian follicles. <u>Endocr Rev</u> **21**(2): 200-214.

McGrath, S. A., Esquela, A. F. and Lee, S. J. (1995). Oocyte-specific expression of growth/differentiation factor-9. Mol Endocrinol 9(1): 131-136.

McGulnness, B. E., Anger, M., Kouznetsova, A., Gil-Bernabe, A. M., Helmhart, W., Kudo, N. R., ... Nasmyth, K. (2009). Regulation of APC/C Activity in Oocytes by a Bub1-Dependent Spindle Assembly Checkpoint. Current Biology 19(5): 369-380.

McKenzie, L. J., Pangas, S. A., Carson, S. A., Kovanci, E., Cisneros, P., Buster, J. E., ... Matzuk, M. M. (2004). Human cumulus granulosa cell gene expression: a predictor of fertilization and embryo selection in women undergoing IVF. Hum Reprod 19(12): 2869-2874.

McLachlan, R. I., Dahl, K. D., Bremner, W. J., Schwall, R., Schmelzer, C. H., Mason, A. J., Steiner, R. A. (1989). Recombinant human activin-A stimulates basal FSH and GnRH-stimulated FSH and LH release in the adult male macaque, Macaca fascicularis. Endocrinology 125(5): 2787-2789.

McLaughlin, M., Patrizio, P., Kayisli, U., Luk, J., Thomson, T. C., Anderson, R. A., ... Johnson, J. (2011). mTOR kinase inhibition results in oocyte loss characterized by empty follicles in human ovarian cortical strips cultured in vitro. Fertil Steril 96(5): 1154-1159 e1151.

McLeod, B. J., Peters, A. R., Haresign, W., Lamming, G. E. (1985). Plasma LH and FSH responses and ovarian activity in prepubertal heifers treated with repeated injections of low doses of GnRH for 72 h. J Reprod Fertil 74(2): 589-596.

McNatty, K. P., Fidler, A. E., Juengel, J. L., Quirke, L. D., Smith, P. R., Heath, D. A., ... Tisdall, D. J. (2000). Growth and paracrine factors regulating follicular formation and cellular function. Mol Cell Endocrinol 163(1-2): 11-20.

McNatty, K. P., Galloway, S. M., Wilson, T., Smith, P., Hudson, N. L., O'Connell, A., ... Juengel, J. L. (2005). Physiological effects of major genes affecting ovulation rate in sheep. Genet Sel Evol 37 Suppl 1: S25-38.

McNatty, K. P., Moore, L. G., Hudson, N. L., Quirke, L. D., Lawrence, S. B., Reader, K., ... Juengel, J. L. (2004). "The oocyte and its role in regulating ovulation rate: a new paradigm in reproductive biology." Reproduction 128(4): 379-386.

McNatty, K. P., Reader, K., Smith, P., Heath, D. A., Juengel, J. L. (2007). Control of ovarian follicular development to the gonadotrophin-dependent phase: a 2006 perspective. Soc Reprod Fertil Suppl 64: 55-68.

Megosh, H. B., Cox, D. N., Campbell, C., Lin, H. (2006). The role of PIWI and the miRNA machinery in Drosophila germline determination. Curr Biol 16(19): 1884-1894.

Mehlmann, L. M. (2005). Stops and starts in mammalian oocytes: recent advances in understanding the regulation of meiotic arrest and oocyte maturation. Reproduction 130(6): 791-799.

Meric, F., Searfoss, A. M., Wormington, M., Wolffe, A. P. (1996). Masking and unmasking maternal mRNA - The role of polyadenylation, transcription, splicing, and nuclear history. Journal of Biological Chemistry 271(48): 30804-30810.

Michalek, J. L., Besold, A. N. and Michel, S. L. (2011). Cysteine and histidine shuffling: mixing and matching cysteine and histidine residues in zinc finger proteins to afford different folds and function. Dalton Trans 40(47): 12619-12632.

Mikkelsen, A. L., Smith, S. and Lindenberg, S. (2000). Impact of oestradiol and inhibin A concentrations on pregnancy rate in in-vitro oocyte maturation. Hum Reprod 15(8): 1685-1690.

Millevoi, S., Loulergue, C., Dettwiler, S., Karaa, S. Z., Keller, W., Antoniou, M., Vagner, S. (2006). An interaction between U2AF 65 and CF I(m) links the splicing and 3' end processing machineries. EMBO J 25(20): 4854-4864.

Miyazawa, K., Shinozaki, M., Hara, T., Furuya, T., Miyazono, K. (2002). Two major Smad pathways in TGF-beta superfamily signalling. Genes Cells 7(12): 1191-1204.

Moenter, S. M., Caraty, A. and Karsch, F. J. (1990). The estradiol-induced surge of gonadotropin-releasing hormone in the ewe. Endocrinology 127(3): 1375-1384.

Mondou, E., Dufort, I., Gohin, M., Fournier, E., Sirard, MA. (2012). Analysis of microRNAs and their precursors in bovine early embryonic development.

Moniruzzaman, M., Sakamaki, K., Akazawa, Y., Miyano, T. (2007). Oocyte growth and follicular development in KIT-deficient Fas-knockout mice. Reproduction **133**(1): 117-125.

Moon, Y. S., Tsang, B. K., Simpson, C., Armstrong, D. T. (1978). 17 beta-Estradiol biosynthesis in cultured granulosa and thecal cells of human ovarian follicles: stimulation by follicle-stimulating hormone. J Clin Endocrinol Metab **47**(2): 263-267.

Moor, R. M. and Crosby I. M. (1985). Temperature-induced abnormalities in sheep oocytes during maturation. J Reprod Fertil **75**(2): 467-473.

Moor, R. M., Smith, M. W. and Dawson, R. M. (1980). Measurement of intercellular coupling between oocytes and cumulus cells using intracellular markers. Exp Cell Res **126**(1): 15-29.

Moore, R. K., Otsuka, F. and Shimasaki, S. (2003). Molecular basis of bone morphogenetic protein-15 signaling in granulosa cells. J Biol Chem **278**(1): 304-310.

Mootz, D., Ho, D. M. and Hunter, C. P. (2004). The STAR/Maxi-KH domain protein GLD-1 mediates a developmental switch in the translational control of C. elegans PAL-1. Development **131**(14): 3263-3272.

Morcock, D. R., Sowder, R. C. 2nd, Casas-Finet, J. R. (2000). Role of the histidine residues of visna virus nucleocapsid protein in metal ion and DNA binding. FEBS Lett **476**(3): 190-193.

Moreno, S. and Nurse, P (1990). Substrates for p34cdc2: in vivo veritas? Cell **61**(4): 549-551.

Mortazavi, A., Williams, B. A., McCue, K., Schaeffer, L., Wold, B. (2008). Mapping and quantifying mammalian transcriptomes by RNA-Seq. Nat Methods **5**(7): 621-628.

Mourot, M., Dufort, I., Gravel, C., Algriany, O., Dielelan, S., Sirard, M. A. (2006). The influence of follicle size, FSH-enriched maturation medium, and early cleavage on bovine oocyte maternal mRNA levels. Mol Reprod Dev **73**(11): 1367-1379.

Murphy, L. J., Bell, G. I., Duckworth, M. L., Friesen, H. G. (1987). Identification, characterization, and regulation of a rat complementary deoxyribonucleic acid which encodes insulin-like growth factor-I. Endocrinology **121**(2): 684-691.

Murray, A. W. and Kirschner, M. W. (1989). Cyclin synthesis drives the early embryonic cell cycle. Nature **339**(6222): 275-280.

Muttukrishna, S. and Knight, P. G. (1991). Inverse effects of activin and inhibin on the synthesis and secretion of FSH and LH by ovine pituitary cells in vitro. J Mol Endocrinol **6**(2): 171-178.

Muttukrishna, S., Tannetta, D., Groome, N., Sargent, I. (2004). Activin and follistatin in female reproduction. Mol Cell Endocrinol **225**(1-2): 45-56.

Nakajima, M., Hutchinson, H. G., Fujinaga, M., Hayashida, W., Morishita, R., Zhang, L., ... Dzau, V. J. (1995). The angiotensin-II type-2 (at(2) receptor antagonizes the growth effects of the at(1) receptor -gain-of-function study using gene-transfer. Proc Natl Acad Sci U S A **92**(23): 10663-10667.

Nepom, J. T., Benacerraf, B and Germain, R. N. (1981). Analysis of IR gene-function using monoclonal-antibodies- independent regulation of GAT and GLPHE T-cell responses by I-A and I-E subregion products on a single accessory cell-population. Journal of Immunology **127**(1): 31-34.

Neumann, E., Schaefer-Ridder, M., Wang, Y., Hofschneider, P. H. (1982). Gene transfer into mouse lyoma cells by electroporation in high electric fields. EMBO J **1**(7): 841-845.

Newton, H. (1998). The cryopreservation of ovarian tissue as a strategy for preserving the fertility of cancer patients. Hum Reprod Update **4**(3): 237-247.

Newton, H., Picton, H. M. and Gosden, R. G. (1999). In vitro growth of oocyte-granulosa cell complexes isolated from cryopreserved ovine tissue. J Reprod Fertil **115**(1): 141-150.

Nganvongpanit, K., Muller, H., Rings, F., Hoelker, M., Jennen, D., Tholen, E., ... Tesfaye, D. (2006). Selective degradation of maternal and embryonic transcripts in in vitro produced bovine oocytes and embryos using sequence specific double-stranded RNA. Reproduction **131**(5): 861-874.

Nicholson, A. W. (1996). Structure, reactivity, and biology of double-stranded RNA. Prog Nucleic Acid Res Mol Biol **52**: 1-65.

Nishi, K., Nishi, A., Nagasawa, T., Ui-Tei, K. (2013). Human TNRC6A is an Argonaute-navigator protein for microRNA-mediated gene silencing in the nucleus. RNA **19**(1): 17-35.

Nishikura, K. (2006). Editor meets silencer: crosstalk between RNA editing and RNA interference. Nat Rev Mol Cell Biol **7**(12): 919-931.

Noma, N., Kawashima, I., Fan, H. Y., Fujita, Y., Kawai, T., Tomoda, Y., ... Shimada, M. (2010). LH-induced neuregulin 1 (NRG1) type III transcripts control granulosa cell differentiation and oocyte maturation. Mol Endocrinol **25**(1): 104-116.

Norris, R. P., Freudzon, M., Mehlmann, L. M., Cowan, A. E., Simon, A. M., Paul, D. L., ... Jaffe, L. A. (2008). Luteinizing hormone causes MAP kinase-dependent phosphorylation and closure of connexin 43 gap junctions in mouse ovarian follicles: one of two paths to meiotic resumption. Development **135**(19): 3229-3238.

Norris, R. P., Ratzan, W. J., Freudzon, M., Mehlmann, L. M., Krall, J., Movsesian, M. A., ... Jaffe, L. A. (2009). Cyclic GMP from the surrounding somatic cells regulates cyclic AMP and meiosis in the mouse oocyte. Development **136**(11): 1869-1878.

Notarianni, E. (2011). Reinterpretation of evidence advanced for neo-oogenesis in mammals, in terms of a finite oocyte reserve. J Ovarian Res **4**(1): 1.

Nurse, P. (1990). Universal control mechanism regulating onset of M-phase. Nature **344**(6266): 503-508.

Nyholt de Prada, J. K., Lee, Y. S., Latham, K. E., Chaffin, C. L., VandeVoort, C. A. (2009). Role for cumulus cell-produced EGF-like ligands during primate oocyte maturation in vitro. Am J Physiol Endocrinol Metab **296**(5): E1049-1058.

O'Brien, J. K., Dwarte, D., Ryan, J. P., Maxwell, W. M., Evans, G. (1996). Developmental capacity, energy metabolism and ultrastructure of mature oocytes from prepubertal and adult sheep. Reprod Fertil Dev **8**(7): 1029-1037.

O'Carroll, D., Mecklenbrauker, I., Das, P. P., Santana, A., Koenig, U., Enright, A. J., ... Tarakhovsky, A. (2007). A Slicer-independent role for Argonaute 2 in hematopoiesis and the microRNA pathway. Genes Dev **21**(16): 1999-2004.

O'Doherty, E. M., Wade, M. G., Hill, J. L., Boland, M. P. (1997). Effects of culturing bovine oocytes either singly or in groups on development to blastocysts. Theriogenology **48**(1): 161-169.

O'Shea, L. C., Mehta, J., Lonergan, P., Hensey, C., Fair, T. (2012). Developmental competence in oocytes and cumulus cells: candidate genes and networks. Systems Biology in Reproductive Medicine **58**(2): 88-101.

Oh, Y. M., Nagalla, S. R., Yamanaka, Y., Kim, H. S., Wilson, E., Rosenfeld, R. G. (1996). Synthesis and characterization of insulin-like growth factor-binding protein (IGFBP)-7 - Recombinant human mac25 protein specifically binds IGF-I and II. Journal of Biological Chemistry **271**(48): 30322-30325.

Odorisio, T., Rodriguez, T. A., Evans, E. P., Clarke, A. R., Burgoyne, P. S. (1998). The meiotic checkpoint monitoring synapsis eliminates spermatocytes via p53-independent apoptosis. Nature Genetics **18**(3): 257-261

Oktay, K., Briggs, D. and Gosden, R. G. (1997). Ontogeny of follicle-stimulating hormone receptor gene expression in isolated human ovarian follicles. J Clin Endocrinol Metab **82**(11): 3748-3751.

Oktem, O. and Oktay, K. (2007). Quantitative assessment of the impact of chemotherapy on ovarian follicle reserve and stromal function. Cancer **110**(10): 2222-2229.

Oktem, O. and Urman, B. (2010). Understanding follicle growth in vivo. Hum Reprod **25**(12): 2944-2954.

Okumura, E., Fukuhara, T., Yoshida, H., Hanada Si, S., Kozutsumi, R., Mori, M., ... Kishimoto, T. (2002). Akt inhibits Myt1 in the signalling pathway that leads to meiotic G2/M-phase transition. Nat Cell Biol **4**(2): 111-116.

Orisaka, M., Orisaka, S., Jiang, J. Y., Craig, J., Wang, Y., Kotsuji, F., Tsang, B. K. (2006). Growth differentiation factor 9 is antiapoptotic during follicular development from preantral to early antral stage. Mol Endocrinol **20**(10): 2456-2468.

Oropeza, A., Wrenzycki, C., Herrmann, D., Hadeler, K. G., Niemann, H. (2004). Improvement of the developmental capacity of oocytes from prepubertal cattle by intraovarian insulin-like growth factor-I application. Biol Reprod **70**(6): 1634-1643.

Ortavant, R., Bocquier, F., Pelletier, J., Ravault, J. P., Thimonier, J., Vollandnail, P. (1988). Seasonality of reproduction in sheep and its control by photoperiod. Aust J Biol Sci. **41**(1):69-85.

Otsuka, F., Moore, R. K. and Shimasaki, S. (2001). Biological function and cellular mechanism of bone morphogenetic protein-6 in the ovary. J Biol Chem **276**(35): 32889-32895.

Otsuka, F., Yao, Z., Lee, T., Yamamoto, S., Erickson, G. F., Shimasaki, S. (2000). "Bone morphogenetic protein-15. Identification of target cells and biological functions." J Biol Chem **275**(50): 39523-39528.

Ota, T., Suzuki, Y., Nishikawa, T., Otsuki, T., Sugiyama, T., Irie, R., ... Sugano, S. (2004). Complete sequencing and characterization of 21,243 full-length human cDNAs. Nature Genetics **36**(1): 40-45.

Otoi, T., Willingham, L., Shin, T., Kraemer, D. C., Westhusin, M. (2002). Effects of oocyte culture density on meiotic competence of canine oocytes. Reproduction **124**(6): 775-781

Ou, S. H. I., Wu, F., Harrich, D., Garcia-Martinez, L. F., Gaynor, R. G. (1995). Cloning and characterization of a novel cellular protein, TDP-43, that binds to human immunodeficiency virus type 1 TAR DNA sequence motifs. Journal of Virology **69**(6): 3584-3596.

Oubridge, C., Ito, N., Evans, P. R., Teo, C. H., Nagai, K. (1994). Crystal structure at 1.92 A resolution of the RNA-binding domain of the U1A spliceosomal protein complexed with an RNA hairpin. Nature **372**(6505): 432-438.

Padmanabhan, K. and Richter, J. D. (2006). Regulated Pumilio-2 binding controls RINGO/Spy mRNA translation and CPEB activation. Genes Dev **20**(2): 199-209.

Palermo, G., Joris, H., Devroey, P., Van Steirteghem, A. C. (1992). Pregnancies after intracytoplasmic injection of single spermatozoon into an oocyte. Lancet **340**(8810): 17-18.

Pan, H., O'Brien M, J., Wigglesworth, K., Eppig, J. J., Schultz, R. M. (2005). Transcript profiling during mouse oocyte development and the effect of gonadotropin priming and development in vitro. Dev Biol **286**(2): 493-506.

Pandey, A., Gupta, S. C. and Gupta, N. (2010). Effect of FSH and LH hormones on oocyte maturation of buffalo and gene expression analysis of their receptors and Cx43 in maturing oocytes. Zygote **18**(3): 231-234.

Pangas, S. A., Choi, Y., Ballow, D. J., Zhao, Y., Westphal, H., Matzuk, M. M., Rajkovic, A. (2006). Oogenesis requires germ cell-specific transcriptional regulators Sohlh1 and Lhx8. Proc Natl Acad Sci U S A **103**(21): 8090-8095.

Pangas, S. A., Jorgez, C. J. and Matzuk, M. M. (2004). "Growth differentiation factor 9 regulates expression of the bone morphogenetic protein antagonist gremlin." J Biol Chem **279**(31): 32281-32286.

Panigone, S., Hsieh, M., Fu, M., Persani, L., Conti, M. (2008). Luteinizing hormone signaling in preovulatory follicles involves early activation of the epidermal growth factor receptor pathway. Mol Endocrinol **22**(4): 924-936.

Pant, D., Reynolds, L. P., Luther, J. S., Borowicz, P. P., Stenbak, T. M., Bilski, J. J., ... Grazul-Bilska, A. T (2005). Expression of connexin 43 and gap junctional intercellular communication in the cumulus-oocyte complex in sheep. Reproduction **129**(2): 191-200.

Paradis, F., Vigneault, C., Robert, C., Sirard, M. A. (2005). RNA interference as a tool to study gene function in bovine oocytes. Mol Reprod Dev **70**(2): 111-121.

Park, I., Han, C., Jin, S., Lee, B., Choi, H., Kwon, J. T., ... Cho, C. (2011). Myosin regulatory light chains are required to maintain the stability of myosin II and cellular integrity. Biochemical Journal **434**: 171-180.

Park, J. Y., Su, Y. Q., Ariga, M., Law, E., Jin, S. L., Conti, M. (2004). EGF-like growth factors as mediators of LH action in the ovulatory follicle. Science **303**(5658): 682-684.

Parvinen, M. (2005). The chromatoid body in spermatogenesis. Int J Androl **28**(4): 189-201.

Patrizio, P., Fragouli, E., Bianchi, V., Borini, A., Wells, D. (2007). Molecular methods for selection of the ideal oocyte. Reprod Biomed Online **15**(3): 346-353.

Payne, A. H. and Hales, D. B. (2004). Overview of steroidogenic enzymes in the pathway from cholesterol to active steroid hormones. Endocr Rev **25**(6): 947-970.

Payne, C. and Schatten, G. (2003). Golgi dynamics during meiosis are distinct from mitosis and are coupled to endoplasmic reticulum dynamics until fertilization. <u>Dev Biol</u> **264**(1): 50-63.

Pepling, M. E. (2010). A novel maternal mRNA storage compartment in mouse oocytes. <u>Biol Reprod</u> **82**(5): 807-808.

Pepling, M. E. and Spradling, A. C. (1998). Female mouse germ cells form synchronously dividing cysts. <u>Development</u> **125**(17): 3323-3328.

Pepling, M. E. and Spradling, A. C. (2001). Mouse ovarian germ cell cysts undergo programmed breakdown to form primordial follicles. <u>Developmental Biology</u> **234**(2): 339-351.

Perrin, B. J. and Ervasti, J. M. (2010). The actin gene family: function follows isoform. <u>Cytoskeleton (Hoboken)</u> **67**(10): 630-634.

Perry, J. A. and Kornbluth, S. (2007). Cdc25 and Wee1: analogous opposites? <u>Cell Division</u> **2**.

Peters, H. (1969). The development of the mouse ovary from birth to maturity. <u>Acta Endocrinol (Copenh)</u> **62**(1): 98-116.

Petzelt, C. (1979). Biochemistry of the mitotic spindle. <u>Int Rev Cytol</u> **60**: 53-92.

Pfeffer, P. L.*,* Sisco, B., Donnison, M., Somers, J., Smith, C. (2007). Isolation of genes associated with developmental competency of bovine oocytes. <u>Theriogenology</u> **68**: S84-S90.

Picton, H.*,* Briggs, D. and Gosden, R. (1998). The molecular basis of oocyte growth and development. <u>Mol Cell Endocrinol</u> **145**(1-2): 27-37.

Picton, H. M. (2002). Oocyte maturation in vitro. <u>Curr Opin Obstet Gynecol</u> **14**(3): 295-302.

Picton, H. M.*,* Danfour, M. A., Harris, S. E., Chambers, E. L., Huntriss, J. (2003). Growth and maturation of oocytes in vitro. <u>Reprod Suppl</u> **61**: 445-462.

Picton, H. M. and Gosden, R. G. (2000). In vitro growth of human primordial follicles from frozen-banked ovarian tissue. <u>Mol Cell Endocrinol</u> **166**(1): 27-35.

Picton, H. M. and McNeilly, A. S. (1991). Effect of basal and pulsatile LH release on FSH-stimulated follicle growth in ewes chronically treated with gonadotrophin-releasing hormone agonist. <u>J Endocrinol</u> **128**(3): 449-456.

Picton, H. M.*,* Tsonis, C. G. and McNeilly, A. S. (1990). "FSH causes a time-dependent stimulation of preovulatory follicle growth in the absence of pulsatile LH secretion in ewes chronically treated with gonadotrophin-releasing hormone agonist." <u>J Endocrinol</u> **126**(2): 297-307.

Pincus, G. and Enzmann, E. V. (1935). The comparative behavior of mammalian eggs *in vivo* and *in* vitro: The activation of ovarian eggs. <u>J Exp Med</u> **62**(5): 665-675.

Pisarska, M. D.*,* Bae, J., Klein, C., Hsueh, A. J. (2004). Forkhead l2 is expressed in the ovary and represses the promoter activity of the steroidogenic acute regulatory gene. <u>Endocrinology</u> **145**(7): 3424-3433.

Plourde, D.*,* Vigneault, C., Laflamme, I., Blondin, P., Robert, C. (2012). Cellular and molecular characterization of the impact of laboratory setup on bovine in vitro embryo production. <u>Theriogenology</u> **77**(9): 1767-1778.

Poguegeile, K.*,* Geiser, J. R., Shu, M., Miller, C., Wool, I. G., Meisler, A. I., Pipas, J. M. (1991). Ribosomal-protein genes are overexpressed in colorectal-cancer. Isolation of a cDNA clone encoding the human S3-ribosomal protein. <u>Molecular and Cellular Biology</u> **11**(8): 3842-3849.

Qiu, S.*,* Adema, C. M. and Lane, T. (2005). A computational study of off-target effects of RNA interference. <u>Nucleic Acids Res</u> **33**(6): 1834-1847.

Quirk, S. M.*,* Cowan, R. G., Harman, R. M., Hu, C. L., Porter, D. A. (2004). Ovarian follicular growth and atresia: the relationship between cell proliferation and survival. <u>J Anim Sci</u> **82 E-Suppl**: E40-52.

Radonic, A.*,* Thulke, S., Mackay, I. M., Landt, O., Siegert, W., Nitsche, A. (2004). Guideline to reference gene selection for quantitative real-time PCR. <u>Biochem Biophys Res Commun</u> **313**(4): 856-862.

Ragoussis, J. and Elvidge, G. (2006). Affymetrix GeneChip (R) system: moving from research to the clinic. <u>Expert Review of Molecular Diagnostics</u> **6**(2): 145-152.

Rajkovic, A., Pangas, S. A., Ballow, D., Suzumori, N., Matzuk, M. M. (2004). NOBOX deficiency disrupts early folliculogenesis and oocyte-specific gene expression. <u>Science</u> **305**(5687): 1157-1159.

Ralph, J. H., Telfer, E. E. and Wilmut, I. (1995). Bovine cumulus cell expansion does not depend on the presence of an oocyte secreted factor. <u>Mol Reprod Dev</u> **42**(2): 248-253.

Rannikki, A. S., Zhang, F. P. and Huhtaniemi, I. T. (1995). Ontogeny of follicle-stimulating hormone receptor gene expression in the rat testis and ovary. <u>Mol Cell Endocrinol</u> **107**(2): 199-208.

Raz, E. (2004). Guidance of primordial germ cell migration. <u>Curr Opin Cell Biol</u> **16**(2): 169-173.

Reader, K. L., Heath, D. A., Lun, S., McIntosh, C. J., Western, A. H., Littlejohn, R. P., ... Juengel, J. L. (2011). Signalling pathways involved in the cooperative effects of ovine and murine GDF9+BMP15-stimulated thymidine uptake by rat granulosa cells. <u>Reproduction</u> **142**(1): 123-131.

Reichenstein, M., Reich, R., LeHoux, J. G., Hanukoglu, I. (2004). ACTH induces TIMP-1 expression and inhibits collagenase in adrenal cortex cells. <u>Mol Cell Endocrinol</u> **215**(1-2): 109-114.

Reichman-Fried, M., Minina, S. and Raz, E. (2004). Autonomous modes of behavior in primordial germ cell migration. <u>Dev Cell</u> **6**(4): 589-596.

Reis, A., Madgwick, S., Chang, H. Y., Nabti, I., Levasseur, M., Jones, K. T. (2007). Prometaphase APCcdh1 activity prevents non-disjunction in mammalian oocytes. <u>Nat Cell Biol</u> **9**(10): 1192-1198.

Reizel, Y., Elbaz, J. and Dekel, N. (2010). Sustained activity of the EGF receptor is an absolute requisite for LH-induced oocyte maturation and cumulus expansion. <u>Mol Endocrinol</u> **24**(2): 402-411.

Renart, J., Reiser, J. and Stark, G. R. (1979). Transfer of proteins from gels to diazobenzyloxymethyl-paper and detection with antisera: a method for studying antibody specificity and antigen structure. <u>Proc Natl Acad Sci U S A</u> **76**(7): 3116-3120.

Reynolds, A., Anderson, E. M., Vermeulen, A., Fedorov, Y., Robinson, K., Leake, D., ... Khvorova, A. (2006). Induction of the interferon response by siRNA is cell type- and duplex length-dependent. <u>RNA</u> **12**(6): 988-993.

Richards, J. S. (2001a). Perspective: the ovarian follicle--a perspective in 2001. <u>Endocrinology</u> **142**(6): 2184-2193.

Richards, J. S. (2001b). New signaling pathways for hormones and cyclic adenosine 3',5'-monophosphate action in endocrine cells. <u>Mol Endocrinol</u> **15**(2): 209-218.

Richards, J. S., Fitzpatrick, S. L., Clemens, J. W., Morris, J. K., Alliston, T., Sirois, J. (1995). Ovarian cell differentiation: a cascade of multiple hormones, cellular signals, and regulated genes. <u>Recent Prog Horm Res</u> **50**: 223-254.

Richards, J. S., Russell, D. L., Robker, R. L., Dajee, M., Alliston, T. N. (1998). Molecular mechanisms of ovulation and luteinization. <u>Mol Cell Endocrinol</u> **145**(1-2): 47-54.

Richardson, B. E. and Lehmann, R. (2010). Mechanisms guiding primordial germ cell migration: strategies from different organisms. <u>Nat Rev Mol Cell Biol</u> **11**(1): 37-49.

Rime, H., Haccard, O. and Ozon, R. (1992). Activation of p34cdc2 kinase by cyclin is negatively regulated by cyclic amp-dependent protein kinase in Xenopus oocytes. <u>Dev Biol</u> **151**(1): 105-110.

Ririe, K. M., Rasmussen, R. P. and Wittwer, C. T. (1997). Product differentiation by analysis of DNA melting curves during the polymerase chain reaction. <u>Anal Biochem</u> **245**(2): 154-160.

Ritchie, M. E., Diyagama, D., Neilson, J., van Laar, R., Dobrovic, A., Holloway, A., Smyth, G. K. (2006). Empirical array quality weights in the analysis of microarray data. <u>Bmc Bioinformatics</u> **7**.

Rivera-Pomar, R., Niessing, D., Schmidt-Ott, U., Gehring, W. J., Jackle, H. (1996). RNA binding and translational suppression by bicoid. <u>Nature</u> **379**(6567): 746-749.

Robert, C., Barnes, F. L., Hue, I., Sirard, M. A. (2000). Subtractive hybridization used to identify mRNA associated with the maturation of bovine oocytes. <u>Mol Reprod Dev</u> **57**(2): 167-175.

Roche, J. F. (1996). Control and regulation of folliculogenesis--a symposium in perspective. Rev Reprod **1**(1): 19-27.

Roignant, J. Y., Carre, C., Mugat, B., Szymczak, D., Lepesant, J. A., Antoniewski, C. (2003). Absence of transitive and systemic pathways allows cell-specific and isoform-specific RNAi in Drosophila. RNA **9**(3): 299-308.

Ross, A. F., Oleynikov, Y., Kislauskis, E. H., Taneja, K. L., Singer, R. H. (1997). Characterization of a beta-actin mRNA zipcode-binding protein. Mol Cell Biol **17**(4): 2158-2165.

Roy, A. and Matzuk, M. M. (2006). Deconstructing mammalian reproduction: using knockouts to define fertility pathways. Reproduction **131**(2): 207-219.

Ruan, B., Watanabe, S., Eppig, J. J., Kwoh, C., Dzidic, N., Pang, J., ... Schroepfer, G. J. Jr. (1998). Sterols affecting meiosis: novel chemical syntheses and the biological activity and spectral properties of the synthetic sterols. J Lipid Res **39**(10): 2005-2020.

Russe, I., Sinowatz, F., Richter, L., Lehmann, M., Schallenberger, E. (1992). The development of the yolk sac in ruminants (sheep and cattle). Anat Histol Embryol **21**(4): 324-347.

Russell, A. G., Charette, J. M., Spencer, D. F., Gray, M. W. (2006). An early evolutionary origin for the minor spliceosome. Nature **443**(7113): 863-866.

Saga, Y. (2008). Mouse germ cell development during embryogenesis. Current Opinion in Genetics & Development **18**(4): 337-341.

Sagata, N. (1996). Meiotic metaphase arrest in animal oocytes: its mechanisms and biological significance. Trends Cell Biol **6**(1): 22-28.

Sagata, N., Watanabe, N., Vande Woude, G. F., Ikawa, Y. (1989). The c-mos proto-oncogene product is a cytostatic factor responsible for meiotic arrest in vertebrate eggs. Nature **342**(6249): 512-518.

Salhab, M., Dhorne-Pollet, S., Auclair, S., Guyader-Joly, C., Brisard, D., Dalbies-Tran, R., ... Uzbekova, S. (2013). In vitro maturation of oocytes alters gene expression and signaling pathways in bovine cumulus cells. Mol Reprod Dev **80**(2): 166-182.

Salmon, N. A., Handyside, A. H. and Joyce, I. M. (2004). Oocyte regulation of anti-Mullerian hormone expression in granulosa cells during ovarian follicle development in mice. Dev Biol **266**(1): 201-208.

Salustri, A., Yanagishita, M. and Hascall, V. C. (1989). Synthesis and accumulation of hyaluronic acid and proteoglycans in the mouse cumulus cell-oocyte complex during follicle-stimulating hormone-induced mucification. J Biol Chem **264**(23): 13840-13847.

Samaj, J., Read, N. D., Volkmann, D., Menzel, D., Baluska, F. (2005). The endocytic network in plants. Trends Cell Biol **15**(8): 425-433.

Sanchez, F., Adriaenssens, T., Romero, S., Smitz, J. (2009). Quantification of oocyte-specific transcripts in follicle-enclosed oocytes during antral development and maturation in vitro. Mol Hum Reprod **15**(9): 539-550.

Sanchez, F. and Smitz, J. (2012). Molecular control of oogenesis. Biochimica Et Biophysica Acta-Molecular Basis of Disease **1822**(12): 1896-1912.

Sarnova, L., Malik, R., Sedlacek, R., Svoboda, P. (2010). Shortcomings of short hairpin RNA-based transgenic RNA interference in mouse oocytes. J Negat Results Biomed **9**: 8.

Saskova, A., Solc, P., Baran, V., Kubelka, M., Schultz, R. M., Motlik, J. (2008). Aurora kinase A controls meiosis I progression in mouse oocytes. Cell Cycle **7**(15): 2368-2376.

Sasseville, M., Gagnon, M. C., Guillemette, C., Sullivan, R., Gilchrist, R. B., Richard, F. J. (2009). Regulation of gap junctions in porcine cumulus-oocyte complexes: contributions of granulosa cell contact, gonadotropins, and lipid rafts. Mol Endocrinol **23**(5): 700-710.

Sathananthan, A. H., Ng, S. C., Chia, C. M., Law, H. Y., Edirisinghe, W. R., Ratnam, S. S. (1985). The origin and distribution of cortical granules in human oocytes with reference to Golgi, nucleolar, and microfilament activity. Ann N Y Acad Sci **442**: 251-264.

Sawyer, H. R., Smith, P., Heath, D. A., Juengel, J. L., Wakefield, S. J., McNatty, K. P. (2002). Formation of ovarian follicles during fetal development in sheep. Biol Reprod **66**(4): 1134-1150.

Schaar, B. T., Chan, G. K., Maddox, P., Salmon, E. D., Yen, T. J. (1997). CENP-E function at kinetochores is essential for chromosome alignment. J Cell Biol **139**(6): 1373-1382.

Schatten, H. and Sun, Q. Y. (2011). Centrosome dynamics during mammalian oocyte maturation with a focus on meiotic spindle formation. <u>Mol Reprod Dev</u> **78**(10-11): 757-768.

Schellander, K*.,* Hoelker, M. and Tesfaye, D. (2007). Selective degradation of transcripts in mammalian oocytes and embryos. <u>Theriogenology</u> **68 Suppl 1**: S107-115.

Schena, M*.,* Shalon, D., Davis, R. W., Brown, P. O. (1995). Quantitative monitoring of gene-expression paterns with a complementary DNA microarray. <u>Science</u> **270**(5235): 467-470.

Schneider, D. T*.,* Schuster, A. E., Fritsch, M. K., Hu, J., Olson, T., Lauer, S., ... Perlman, E. J. (2001). Multipoint imprinting analysis indicates a common precursor cell for gonadal and nongonadal pediatric germ cell tumors. <u>Cancer Res</u> **61**(19): 7268-7276.

Schoenfelder, M. and Einspanier, R. (2003). Expression of hyaluronan synthases and corresponding hyaluronan receptors is differentially regulated during oocyte maturation in cattle. <u>Biol Reprod</u> **69**(1): 269-277.

Schroeder, A. C. and Eppig, J. J. (1984). The developmental capacity of mouse oocytes that matured spontaneously in vitro is normal. <u>Dev Biol</u> **102**(2): 493-497.

Schroeder, A. C*.,* Schultz, R. M., Kopf, G. S., Taylor, F. R., Becker, R. B., Eppig, J. J. (1990). Fetuin inhibits zona pellucida hardening and conversion of ZP2 to ZP2f during spontaneous mouse oocyte maturation in vitro in the absence of serum. <u>Biol Reprod</u> **43**(5): 891-897.

Schultz, R. M. (1993). Regulation of zygotic gene activation in the mouse. <u>Bioessays</u> **15**(8): 531-538.

Schupbach, T. and Wieschaus, E. (1991). Female sterile mutations on the second chromosome of Drosophila melanogaster. II. Mutations blocking oogenesis or altering egg morphology. <u>Genetics</u> **129**(4): 1119-1136.

Scott, J. E*.,* Cummings, C., Brass, A., Chen, Y. (1991). Secondary and tertiary structures of hyaluronan in aqueous solution, investigated by rotary shadowing-electron microscopy and computer simulation. Hyaluronan is a very efficient network-forming polymer. <u>Biochem J</u> **274 (Pt 3)**: 699-705.

Shabankareh, H. K., Sarsaifi, K. and Mehrannia, T. (2011). In vitro maturation of ovine oocytes using different maturation media: effect of human menopausal serum. <u>Assisted Reproduction and Genetics</u> **28**(6): 231-237

Shalom-Paz, E*.,* Almog, B., Shehata, F., Huang, J., Holzer, H., Chian, R. C., ... Tan, S. L. (2010). Fertility preservation for breast-cancer patients using IVM followed by oocyte or embryo vitrification. <u>Reprod Biomed Online</u> **21**(4): 566-571.

Shalon, D*.,* Smith, S. J. and Brown, P. O. (1996). A DNA microarray system for analyzing complex DNA samples using two-color fluorescent probe hybridization. <u>Genome Res</u> **6**(7): 639-645.

Shamsadin, R*.,* Adham, I. M., von Beust, G., Engel, W. (2000). Molecular cloning, expression and chromosome location of the human pelota gene PELO. <u>Cytogenetics and Cell Genetics</u> **90**(1-2): 75-78.

Shapiro, A. L*.,* Vinuela, E. and Maizel, J. V., Jr. (1967). Molecular weight estimation of polypeptide chains by electrophoresis in SDS-polyacrylamide gels. <u>Biochem Biophys Res Commun</u> **28**(5): 815-820.

Sharif, B*.,* Na, J., Lykke-Hartmann, K., McLaughlin, S. H., Laue, E., Glover, D. M., Zernicka-Goetz, M. (2010). The chromosome passenger complex is required for fidelity of chromosome transmission and cytokinesis in meiosis of mouse oocytes. <u>J Cell Sci</u> **123**(Pt 24): 4292-4300.

Sheth, U. and Parker, R (2003). Decapping and decay of messenger RNA occur in cytoplasmic processing bodies. <u>Science</u> **300**(5620): 805-808.

Shi, H*.,* Djikeng, A., Tschudi, C., Ullu, E. (2004). Argonaute protein in the early divergent eukaryote Trypanosoma brucei: control of small interfering RNA accumulation and retroposon transcript abundance. <u>Mol Cell Biol</u> **24**(1): 420-427.

Shi, Y. Y*.,* Tang, W., Hao, S. F., Wang, C. C. (2005). Contributions of cysteine residues in Zn2 to zinc fingers and thiol-disulfide oxidoreductase activities of chaperone DnaJ. <u>Biochemistry</u> **44**(5): 1683-1689.

Shimasaki, S.*,* Moore, R. K., Otsuka, F., Erickson, G. F. (2004). The bone morphogenetic protein system in mammalian reproduction. <u>Endocr Rev</u> **25**(1): 72-101.

Shoubridge, E. A. and Wai, T. (2007). Mitochondrial DNA and the mammalian oocyte. <u>Mitochondrion in the Germline and Early Development</u> **77**: 87-111.

Sibley, C. R.*,* Seow, Y. and Wood, M. J. (2010). Novel RNA-based strategies for therapeutic gene silencing. <u>Mol Ther</u> **18**(3): 466-476.

Silva, J. R.*,* Figueiredo, J. R. and van den Hurk, R. (2009). Involvement of growth hormone (GH) and insulin-like growth factor (IGF) system in ovarian folliculogenesis. <u>Theriogenology</u> **71**(8): 1193-1208.

Simoni, M.*,* Gromoll, J. and Nieschlag, E. (1997). The follicle-stimulating hormone receptor: biochemistry, molecular biology, physiology, and pathophysiology. <u>Endocr Rev</u> **18**(6): 739-773.

Siomi, M. C. and Kuramochi-Miyagawa, S. (2009). RNA silencing in germlines-exquisite collaboration of Argonaute proteins with small RNAs for germline survival. <u>Current Opinion in Cell Biology</u> **21**(3): 426-434.

Sirard, M. A. (2001). Resumption of meiosis: mechanism involved in meiotic progression and its relation with developmental competence. <u>Theriogenology</u> **55**(6): 1241-1254.

Sirard, M. A.*,* Richard, F., Blondin, P., Robert, C. (2006). Contribution of the oocyte to embryo quality. <u>Theriogenology</u> **65**(1): 126-136.

Sites, C. K.*,* Patterson, K., Jamison, C. S., Degen, S. J., LaBarbera, A. R. (1994). Follicle-stimulating hormone (FSH) increases FSH receptor messenger ribonucleic acid while decreasing FSH binding in cultured porcine granulosa cells. <u>Endocrinology</u> **134**(1): 411-417.

Skinner, M. K.*,* Schmidt, M., Savenkova, M. I., Sadler-Riggleman, I., Nilsson, E. E. (2008). Regulation of granulosa and theca cell transcriptomes during ovarian antral follicle development. <u>Mol Reprod Dev</u> **75**(9): 1457-1472.

Slot, K. A.*,* Kastelijn, J., Bachelot, A., Kelly, P. A., Binart, N., Teerds, K. J. (2006). Reduced recruitment and survival of primordial and growing follicles in GH receptor-deficient mice. <u>Reproduction</u> **131**(3): 525-532.

Smith, R. C.*,* Bement, W. M., Dersch, M. A., Dworkin-Rastl, E., Dworkin, M. B., Capco, D. G. (1990). Nonspecific effects of oligodeoxynucleotide injection in Xenopus oocytes: a reevaluation of previous D7 mRNA ablation experiments. <u>Development</u> **110**(3): 769-779.

Smith, R. C.*,* Dworkin, M. B. and Dworkin-Rastl, E. (1988). Destruction of a translationally controlled mRNA in Xenopus oocytes delays progesterone-induced maturation. <u>Genes Dev</u> **2**(10): 1296-1306.

Smith, R. C.*,* Dworkin, M. B. and Dworkin-Rastl, E. (1991). The maternal gene product D7 is not required for early Xenopus development. <u>Mech Dev</u> **35**(3): 213-225.

Smith, R. C.*,* Dworkin, M. B. and Dworkin-Rastl, E. (1992). Synthesis and modification of D7 protein during Xenopus oocyte maturation. <u>Mol Reprod Dev</u> **32**(3): 293-301.

Smith, G. W. and Rosa, G. J. M. (2007). Interpretation of microarray data: Trudging out of the abyss towards elucidation of biological significance. <u>Journal of Animal Science</u> **85**: E20-E23.

Smyth, G. K. (2004). Linear models and empirical bayes methods for assessing differential expression in microarray experiments. <u>Statistical applications in genetics and molecular biology</u> **3**: Article3-Article3.

Sokka, T. A.*,* Hamalainen, T. M., Kaipia, A., Warren, D. W., Huhtaniemi, I. T. (1996). Development of luteinizing hormone action in the perinatal rat ovary. <u>Biol Reprod</u> **55**(3): 663-670.

Solc, P.*,* Baran, V., Mayer, A., Bohmova, T., Panenkova-Havlova, G., Saskova, A., ... Motlik, J. (2012). Aurora Kinase A Drives MTOC Biogenesis but Does Not Trigger Resumption of Meiosis in Mouse Oocytes Matured In Vivo. <u>Biol Reprod</u> **87**(4).

Song, H. W.*,* Cauffman, K., Chan, A. P., Zhou, Y., King, M. L., Etkin, L. D., Kloc, M. (2007). Hermes RNA-binding protein targets RNAs-encoding proteins involved in meiotic maturation, early cleavage, and germline development. <u>Differentiation</u> **75**(6): 519-528.

Soper, S. F., van der Heijden, G. W., Hardiman, T. C., Goodheart, M., Martin, S. L., de Boer, P., Bortvin, A. (2008). Mouse maelstrom, a component of nuage, is essential for spermatogenesis and transposon repression in meiosis. Dev Cell **15**(2): 285-297.

Souza, C. J., Campbell, B. K., McNeilly, A. S., Baird, D. T. (2002). Effect of bone morphogenetic protein 2 (BMP2) on oestradiol and inhibin A production by sheep granulosa cells, and localization of BMP receptors in the ovary by immunohistochemistry. Reproduction **123**(3): 363-369.

Starz-Gaiano, M. and Lehmann, R. (2001). Moving towards the next generation. Mech Dev **105**(1-2): 5-18.

Stein, P., Zeng, F., Pan, H., Schultz, R. M. (2005). Absence of non-specific effects of RNA interference triggered by long double-stranded RNA in mouse oocytes. Dev Biol **286**(2): 464-471.

Stojkovic, M., Machado, S. A., Stojkovic, P., Zakhartchenko, V., Hutzler, P., Goncalves, P. B., Wolf, E. (2001). Mitochondrial distribution and adenosine triphosphate content of bovine oocytes before and after in vitro maturation: correlation with morphological criteria and developmental capacity after in vitro fertilization and culture. Biol Reprod **64**(3): 904-909.

Strausberg, R. L., Feingold, E. A., Grouse, L. H., Derge, J. G., Klausner, R. D., Collins, F. S., ... Marra, M. A. (2002). Generation and initial analysis of more than 15,000 full-length human and mouse cDNA sequences. Proc Natl Acad Sci U S A **99**(26): 16899-16903.

Strong, M. J., Volkening, K., Hammond, R., Yang, W., Strong, W., Leystra-Lantz, C., Shoesmith, C. (2007). TDP43 is a human low molecular weight neurofilament (hNFL) mRNA-binding protein. Molecular and Cellular Neuroscience **35**(2): 320-327.

Su, Y. Q., Sugiura, K. and Eppig, J. J. (2009). Mouse oocyte control of granulosa cell development and function: paracrine regulation of cumulus cell metabolism. Semin Reprod Med **27**(1): 32-42.

Su, Y. Q., Sugiura, K., Li, Q., Wigglesworth, K., Matzuk, M. M., Eppig, J. J. (2010). Mouse oocytes enable LH-induced maturation of the cumulus-oocyte complex via promoting EGF receptor-dependent signaling. Mol Endocrinol **24**(6): 1230-1239.

Su, Y. Q., Sugiura, K., Wigglesworth, K., O'Brien, M. J., Affourtit, J. P., Pangas, S. A., ... Eppig, J. J. (2008). Oocyte regulation of metabolic cooperativity between mouse cumulus cells and oocytes: BMP15 and GDF9 control cholesterol biosynthesis in cumulus cells. Development **135**(1): 111-121.

Su, Y. Q., Wu, X., O'Brien, M. J., Pendola, F. L., Denegre, J. N., Matzuk, M. M., Eppig, J. J. (2004). Synergistic roles of BMP15 and GDF9 in the development and function of the oocyte-cumulus cell complex in mice: genetic evidence for an oocyte-granulosa cell regulatory loop. Dev Biol **276**(1): 64-73.

Sugiura, K., Pendola, F. L. and Eppig, J. J. (2005). Oocyte control of metabolic cooperativity between oocytes and companion granulosa cells: energy metabolism. Dev Biol **279**(1): 20-30.

Sugiura, K., Su, Y. Q., Diaz, F. J., Pangas, S. A., Sharma, S., Wigglesworth, K., ... Eppig, J. J. (2007). Oocyte-derived BMP15 and FGFs cooperate to promote glycolysis in cumulus cells. Development **134**(14): 2593-2603.

Sugiura, K., Su, Y. Q. and Eppig, J. J. (2009). Targeted suppression of Has2 mRNA in mouse cumulus cell-oocyte complexes by adenovirus-mediated short-hairpin RNA expression. Mol Reprod Dev **76**(6): 537-547.

Sugiura, K., Su, Y. Q., Li, Q., Wigglesworth, K., Matzuk, M. M., Eppig, J. J. (2010). Estrogen promotes the development of mouse cumulus cells in coordination with oocyte-derived GDF9 and BMP15. Mol Endocrinol **24**(12): 2303-2314.

Suh, N., Baehner, L., Moltzahn, F., Melton, C., Shenoy, A., Chen, J., Blelloch, R. (2010). MicroRNA function is globally suppressed in mouse oocytes and early embryos. Curr Biol **20**(3): 271-277.

Sumbung, F. P., Williamson, P. and Carson, R. S. (1987). Response of prepubertal ewes primed with monensin or progesterone to administration of FSH. J Reprod Fertil **81**(2): 317-325.

Summerton, J. (1999). Morpholino antisense oligomers: the case for an RNase H-independent structural type. Biochim Biophys Acta **1489**(1): 141-158.

Sun, Q. Y. and Schatten, H. (2006). Regulation of dynamic events by microfilaments during oocyte maturation and fertilization. <u>Reproduction</u> **131**(2): 193-205.

Sun, X. F.*,* Zhang, W. H., Chen, X. J., Xiao, G. H., Mai, W. Y., Wang, W. H. (2004). Spindle dynamics in living mouse oocytes during meiotic maturation, ageing, cooling and overheating: a study by polarized light microscopy. <u>Zygote</u> **12**(3): 241-249.

Sutton-McDowall, M. L.*,* Gilchrist, R. B. and Thompson, J. G. (2010). The pivotal role of glucose metabolism in determining oocyte developmental competence. <u>Reproduction</u> **139**(4): 685-695.

Suzumori, N.*,* Yan, C., Matzuk, M. M., Rajkovic, A. (2002). Nobox is a homeobox-encoding gene preferentially expressed in primordial and growing oocytes. <u>Mech Dev</u> **111**(1-2): 137-141.

Svoboda, P.*,* Stein, P., Hayashi, H., Schultz, R. M. (2000). Selective reduction of dormant maternal mRNAs in mouse oocytes by RNA interference. <u>Development</u> **127**(19): 4147-4156.

Swetloff, A.*,* Conne, B., Huarte, J., Pitetti, JL., Nef, S., Vassalli, JD. (2009). Dcp1-bodies in mouse oocytes. <u>Mol Biol Cell.</u> **20**(23): 4951-4961.

Szollosi, D.*,* Calarco, P. and Donahue, R. P. (1972). Absence of centrioles in the first and second meiotic spindles of mouse oocytes. <u>J Cell Sci</u> **11**(2): 521-541.

Szollosi, D.*,* Desmedt, V., Crozet, N., Brender, C. (1988). In vitro maturation of sheep ovarian oocytes. <u>Reprod Nutr Dev</u> **28**(4B): 1047-1080.

Tabara, H.*,* Grishok, A. and Mello, C. C. (1998). RNAi in C. elegans: soaking in the genome sequence. <u>Science</u> **282**(5388): 430-431.

Tanaka, S. S.*,* Toyooka, Y., Akasu, R., Katoh-Fukui, Y., Nakahara, Y., Suzuki, R., ... Noce, T. (2000). The mouse homolog of Drosophila Vasa is required for the development of male germ cells. <u>Genes Dev</u> **14**(7): 841-853.

Tang, D.*,* Zhu, H., Wu, J., Chen, H., Zhang, Y., Zhao, X., ... Lin, X. (2012). Silencing myostatin gene by RNAi in sheep embryos. <u>J Biotechnol</u> **158**(3): 69-74.

Tang, F.*,* Kaneda, M., O'Carroll, D., Hajkova, P., Barton, S. C., Sun, Y. A., ... Surani, M. A. (2007). Maternal microRNAs are essential for mouse zygotic development. <u>Genes Dev</u> **21**(6): 644-648.

Tanghe, S.*,* Van Soom, A., Nauwynck, H., Coryn, M., de Kruif, A. (2002). Minireview: Functions of the cumulus oophorus during oocyte maturation, ovulation, and fertilization. <u>Mol Reprod Dev</u> **61**(3): 414-424.

Tesfaye, D.*,* Lonergan, P., Hoelker, M., Rings, F., Nganvongpanit, K., Havlicek, V., ... Schellander, K. (2007). Suppression of connexin 43 and E-cadherin transcripts in in vitro derived bovine embryos following culture in vitro or in vivo in the homologous bovine oviduct. <u>Mol Reprod Dev</u> **74**(8): 978-988.

Thach, R. E. (1992). Cap recap- The involvement of EIF-4F in regulating gene-expression. <u>Cell</u> **68**(2): 177-180.

Thatcher, T. H. and Gorovsky, M. A. (1994). Phylogenetic analysis of the core histones H2A, H2B, H3, and H4. <u>Nucleic Acids Res</u> **22**(2): 174-179.

Tilly, J. and Telfer, E. (2009). Purification of germline stem cells from adult mammalian ovaries: a step closer towards control of the female biological clock? <u>Mol Hum Reprod.</u> **15**(7): 393-398.

Tirone, E.*,* D'Alessandris, C., Hascall, V. C., Siracusa, G., Salustri, A. (1997). Hyaluronan synthesis by mouse cumulus cells is regulated by interactions between follicle-stimulating hormone (or epidermal growth factor) and a soluble oocyte factor (or transforming growth factor beta1). <u>J Biol Chem</u> **272**(8): 4787-4794.

Tiscornia, G.*,* Tergaonkar, V., Galimi, F., Verma, I. M. (2004). CRE recombinase-inducible RNA interference mediated by lentiviral vectors. <u>Proc Natl Acad Sci U S A</u> **101**(19): 7347-7351.

Tisdall, D. J.*,* Watanabe, K., Hudson, N. L., Smith, P., McNatty, K. P. (1995). FSH receptor gene expression during ovarian follicle development in sheep. <u>J Mol Endocrinol</u> **15**(3): 273-281.

Tomek, W.*,* Torner, H. and Kanitz, W. (2002). Comparative analysis of protein synthesis, transcription and cytoplasmic polyadenylation of mRNA during maturation of bovine oocytes in vitro. <u>Reprod Domest Anim</u> **37**(2): 86-91.

Tommerup, N. and Leffers, H. (1996a). Assignment of the human genes encoding 14,3-3 Eta (YWHAH) to 22q12, 14-3-3 zeta (YWHAZ) to 2p25.1-p25.2, and 14-3-3 beta (YWHAB) to 20q13.1 by in situ hybridization. Genomics **33**(1): 149-150.

Tommerup, N. and Leffers, H. (1996b). Assignment of human KH-box-containing genes by in situ hybridization: HNRNPK maps to 9q21.32-q21.33, PCBP1 to 2p12-p13, and PCBP2 to 12q13.12-q13.13, distal to FRA12A. Genomics **32**(2): 297-298.

Towbin, H., Staehelin, T. and Gordon, J. (1979). Electrophoretic transfer of proteins from polyacrylamide gels to nitrocellulose sheets: procedure and some applications. 1979. Biotechnology **24**: 145-149.

Toyooka, Y., Tsunekawa, N., Takahashi, Y., Matsui, Y., Satoh, M., Noce, T. (2000). Expression and intracellular localization of mouse Vasa-homologue protein during germ cell development. Mechanisms of Development **93**(1-2): 139-149.

Trounson, A., Anderiesz, C. and Jones, G. (2001). Maturation of human oocytes in vitro and their developmental competence. Reproduction **121**(1): 51-75.

Trounson, A., Wood, C. and Kausche, A. (1994). In vitro maturation and the fertilization and developmental competence of oocytes recovered from untreated polycystic ovarian patients. Fertil Steril **62**(2): 353-362.

Tsafriri, A., Cao, X., Ashkenazi, H., Motola, S., Popliker, M., Pomerantz, S. H. (2005). Resumption of oocyte meiosis in mammals: on models, meiosis activating sterols, steroids and EGF-like factors. Mol Cell Endocrinol **234**(1-2): 37-45.

Tsurumi, C., Hoffmann, S., Geley, S., Graeser, R., Polanski, Z. (2004). The spindle assembly checkpoint is not essential for CSF arrest of mouse oocytes. J Cell Biol **167**(6): 1037-1050.

Turunen, J. J., Will, C. L., Grote, M., Luhrmann, R., Frilander, M. J. (2008). The U11-48K protein contacts the 5' splice site of U12-type introns and the U11-59K protein. Mol Cell Biol **28**(10): 3548-3560.

Udagawa, Y., Hanai, J., Tada, K., Grieder, N. C., Momoeda, M., Taketani, Y., ... Miyazono, K. (2000). Schnurri interacts with Mad in a Dpp-dependent manner. Genes Cells **5**(5): 359-369.

Unhavaithaya, Y., Hao, Y., Beyret, E., Yin, H., Kuramochi-Miyagawa, S., Nakano, T., Lin, H. (2009). MILI, a PIWI-interacting RNA-binding protein, is required for germ line stem cell self-renewal and appears to positively regulate translation. J Biol Chem **284**(10): 6507-6519.

Usui, T., Suzuki, K., Kaji, Y., Amano, S., Miyata, K., Heldin, P., Yamashita, H. (1999). Hyaluronan synthase expression in bovine eyes. Invest Ophthalmol Vis Sci **40**(3): 563-567.

Uyar, A., Torrealday, S. and Seli, E. (2013). Cumulus and granulosa cell markers of oocyte and embryo quality. Fertil Steril.

Uzbekova, S., Arlot-Bonnemains, Y., Dupont, J., Dalbies-Tran, R., Papillier, P., Pennetier, S., ... Uzbekov, R. (2008). Spatio-temporal expression patterns of Aurora kinases A, B, and C and cytoplasmic polyadenylation-element-binding protein in bovine oocytes during meiotic maturation. Biol Reprod **78**(2): 218-233.

Vaccari, S., Weeks, J. L. 2nd, Hsieh, M., Menniti, F. S., Conti, M. (2009). Cyclic GMP signaling is involved in the luteinizing hormone-dependent meiotic maturation of mouse oocytes. Biol Reprod **81**(3): 595-604.

Valdimarsson, G., De Sousa, P. A. and Kidder, G. M. (1993). Coexpression of gap junction proteins in the cumulus-oocyte complex. Mol Reprod Dev **36**(1): 7-15.

Valente, L. and Nishikura, K. (2005). ADAR gene family and A-to-I RNA editing: diverse roles in posttranscriptional gene regulation. Prog Nucleic Acid Res Mol Biol **79**: 299-338.

Van Blerkom, J. (2004). Mitochondria in human oogenesis and preimplantation embryogenesis: engines of metabolism, ionic regulation and developmental competence. Reproduction **128**(3): 269-280.

Van Blerkom, J. (2008). Mitochondria as regulatory forces in oocytes, preimplantation embryos and stem cells. Reprod Biomed Online **16**(4): 553-569.

Van Blerkom, J. and Davis, P. (1995). Evolution of the sperm aster after microinjection of isolated human sperm centrosomes into meiotically mature human oocytes. Hum Reprod **10**(8): 2179-2182.

Van Blerkom, J., Davis, P. and Alexander, S. (2000). Differential mitochondrial distribution in human pronuclear embryos leads to disproportionate inheritance between blastomeres: relationship to microtubular organization, ATP content and competence. Hum Reprod **15**(12): 2621-2633.

Van Blerkom, J., Davis, P., Mathwig, V., Alexander, S. (2002). Domains of high-polarized and low-polarized mitochondria may occur in mouse and human oocytes and early embryos. Human Reproduction **17**(2): 393-406.

Van Doren, M., Broihier, H. T., Moore, L. A., Lehmann, R. (1998). HMG-CoA reductase guides migrating primordial germ cells. Nature **396**(6710): 466-469.

van Wagtendonk-de Leeuw, A. M., Mullaart, E., de Roos, A. P., Merton, J. S., den Daas, J. H., Kemp, B., de Ruigh, L. (2000). Effects of different reproduction techniques: AI MOET or IVP, on health and welfare of bovine offspring. Theriogenology **53**(2): 575-597.

Vanderhyden, B. C. (1993). Species differences in the regulation of cumulus expansion by an oocyte-secreted factor(s). J Reprod Fertil **98**(1): 219-227.

Vanderhyden, B. C. and Armstrong, D. T. (1989). Role of cumulus cells and serum on the in vitro maturation, fertilization, and subsequent development of rat oocytes. Biol Reprod **40**(4): 720-728.

Vanderhyden, B. C., Telfer, E. E. and Eppig, J. J. (1992). Mouse oocytes promote proliferation of granulosa cells from preantral and antral follicles in vitro. Biol Reprod **46**(6): 1196-1204.

Verlhac, M. H., Lefebvre, C., Guillaud, P., Rassinier, P., Maro, B. (2000). Asymmetric division in mouse oocytes: with or without Mos. Curr Biol **10**(20): 1303-1306.

Vernos, I., Raats, J., Hirano, T., Heasman, J., Karsenti, E., Wylie, C. (1995). Xklp1, a chromosomal Xenopus kinesin-like protein essential for spindle organization and chromosome positioning. Cell **81**(1): 117-127.

Virag, L. (2005). Structure and function of poly(ADP-ribose) polymerase-1: Role in oxidativestress-related pathologies. Current Vascular Pharmacology **3**(3): 209-214.

Visser, J. A. and Themmen, A. P. (2005). Anti-Mullerian hormone and folliculogenesis. Mol Cell Endocrinol **234**(1-2): 81-86.

Vitt, U. A., Hayashi, M., Klein, C., Hsueh, A. J. (2000). Growth differentiation factor-9 stimulates proliferation but suppresses the follicle-stimulating hormone-induced differentiation of cultured granulosa cells from small antral and preovulatory rat follicles. Biol Reprod **62**(2): 370-377.

Vitt, U. A., Mazerbourg, S., Klein, C., Hsueh, A. J. (2002). Bone morphogenetic protein receptor type II is a receptor for growth differentiation factor-9. Biol Reprod **67**(2): 473-480.

Viuff, D., Hyttel, P., Avery, B., Vajta, G., Greve, T., Callesen, H., Thomsen, P. D. (1998). Ribosomal ribonucleic acid is transcribed at the 4-cell stage in in vitro-produced bovine embryos. Biol Reprod **59**(3): 626-631.

Vogt, E., Kirsch-Volders, M., Parry, J., Eichenlaub-Ritter, U. (2008). Spindle formation, chromosome segregation and the spindle checkpoint in mammalian oocytes and susceptibility to meiotic error. Mutat Res **651**(1-2): 14-29.

Von Stetina, J. R. and Orr-Weaver, T. L. (2011). Developmental control of oocyte maturation and egg activation in metazoan models. Cold Spring Harb Perspect Biol **3**(10): a005553.

Voronina, E. and Wessel, G. M. (2003). The regulation of oocyte maturation. Curr Top Dev Biol **58**: 53-110.

Wandji, S. A., Srsen, V., Voss, A. K., Eppig, J. J., Fortune, J. E. (1996). Initiation in vitro of growth of bovine primordial follicles. Biol Reprod **55**(5): 942-948.

Wang, W. H. and Day, B. N. (2002). Development of porcine embryos produced by IVM/IVF in a medium with or without protein supplementation: effects of extracellular glutathione. Zygote **10**(2): 109-115

Wang, J., Mayernik, L. and Armant, D. R. (2002). Integrin signaling regulates blastocyst adhesion to fibronectin at implantation: Intracellular calcium transients and vesicle trafficking in primary trophoblast cells. Developmental Biology **245**(2): 270-279.

Wang, Q. and Sun, Q. Y. (2007). Evaluation of oocyte quality: morphological, cellular and molecular predictors. Reprod Fertil Dev **19**(1): 1-12.

Wang, Z., Gerstein, M. and Snyder, M. (2009). RNA-Seq: a revolutionary tool for transcriptomics. Nat Rev Genet **10**(1): 57-63.

Wassarman, P. M. and Kinloch, R. A. (1992). Gene expression during oogenesis in mice. Mutat Res **296**(1-2): 3-15.

Wassmann, K., Niault, T. and Maro, B. (2003). Metaphase I arrest upon activation of the Mad2-dependent spindle checkpoint in mouse oocytes. Current Biology **13**(18): 1596-1608.

Watanabe, T., Totoki, Y., Toyoda, A., Kaneda, M., Kuramochi-Miyagawa, S., Obata, Y., ... Sasaki, H. (2008). Endogenous siRNAs from naturally formed dsRNAs regulate transcripts in mouse oocytes. Nature **453**(7194): 539-543.

Wathlet, S., Adriaenssens, T., Segers, I., Verheyen, G., Janssens, R., Coucke, W., ... Smitz, J. (2012). New candidate genes to predict pregnancy outcome in single embryo transfer cycles when using cumulus cell gene expression. Fertil Steril **98**(2): 432-+.

Webb, R. and Campbell, B. K. (2007). Development of the dominant follicle: mechanisms of selection and maintenance of oocyte quality. Soc Reprod Fertil Suppl **64**: 141-163.

Weisenberg, R. C. (1972). Microtubule formation in vitro in solutions containing low calcium concentrations. Science **177**(4054): 1104-1105.

Welt, C. K. and Schneyer, A. L. (2001). Differential regulation of inhibin B and inhibin a by follicle-stimulating hormone and local growth factors in human granulosa cells from small antral follicles. J Clin Endocrinol Metab **86**(1): 330-336.

Whitaker, M. (2006). Calcium at fertilization and in early development. Physiological Reviews **86**(1): 25-88.

Wianny, F. and Zernicka-Goetz, M. (2000). Specific interference with gene function by double-stranded RNA in early mouse development. Nat Cell Biol **2**(2): 70-75.

Wilding, M., Dale, B., Marino, M., di Matteo, L., Alviggi, C., Pisaturo, M. L., ... De Placido, G. (2001). Mitochondrial aggregation patterns and activity in human oocytes and preimplantation embryos. Hum Reprod **16**(5): 909-917.

Wilkinson, M. L., Crary, S. M., Jackman, J. E., Grayhack, E. J., Phizicky, E. M. (2007). The 2'-O-methyltransferase responsible for modification of yeast tRNA at position 4. RNA **13**(3): 404-413.

Wilson, T., Wu, X. Y., Juengel, J. L., Ross, I. K., Lumsden, J. M., Lord, E. A., ... Montgomery, G. W. (2001). Highly prolific Booroola sheep have a mutation in the intracellular kinase domain of bone morphogenetic protein IB receptor (ALK-6) that is expressed in both oocytes and granulosa cells. Biol Reprod **64**(4): 1225-1235.

Winckler, J. (1974). Vital staining of lysosomes and other cell organelles of the rat with neutral red (author's transl). Prog Histochem Cytochem **6**(3): 1-91.

Womack, J. E. (2005). Advances in livestock genomics: Opening the barn door. Genome Res **15**(12): 1699-1705.

Wongsrikeao, P., Kaneshige, Y., Ooki, R., Taniguchi, M., Agung, B., Nii, M., Otoi, T. (2005). Effect of the removal of cumulus cells on the nuclear maturation, fertilization and development of porcine oocytes. Reprod Domest Anim **40**(2): 166-170.

Wood, K. W., Sakowicz, R., Goldstein, L. S., Cleveland, D. W. (1997). CENP-E is a plus end-directed kinetochore motor required for metaphase chromosome alignment. Cell **91**(3): 357-366.

Wu, J., Nayudu, P. L., Kiesel, P. S., Michelmann, H. W. (2000). Luteinizing hormone has a stage-limited effect on preantral follicle development in vitro. Biol Reprod **63**(1): 320-327.

Wu, X. (2009). Maternal depletion of NLRP5 blocks early embryogenesis in rhesus macaque monkeys (Macaca mulatta). Hum Reprod **24**(2): 415-424.

Wynn, P., Picton, H. M., Krapez, J. A., Rutherford, A. J., Balen, A. H., Gosden, R. G. (1998). Pretreatment with follicle stimulating hormone promotes the numbers of human oocytes reaching metaphase II by in-vitro maturation. Hum Reprod **13**(11): 3132-3138.

Xia, M., He, H., Wang, Y., Liu, M., Zhou, T., Lin, M., ... Sha, J. (2012). PCBP1 is required for maintenance of the transcriptionally silent state in fully grown mouse oocytes. Cell Cycle **11**(15): 2833-2842.

Xu, Y. W., Wang, B., Ding, C. H., Li, T., Gu, F., Zhou, C. (2011). Differentially expressed micoRNAs in human oocytes. Journal of Assisted Reproduction and Genetics **28**(6): 559-566.

Xu, Z., Williams, C. J., Kopf, G. S., Schultz, R. M. (2003). Maturation-associated increase in IP3 receptor type 1: role in conferring increased IP3 sensitivity and Ca2+ oscillatory behavior in mouse eggs. Dev Biol **254**(2): 163-171.

Yamada, Y., Davis, K. D. and Coffman, C. R. (2008). Programmed cell death of primordial germ cells in Drosophila is regulated by p53 and the Outsiders monocarboxylate transporter. Development **135**(2): 207-216.

Yan, C., Wang, P., DeMayo, J., DeMayo, F. J., Elvin, J. A., Carino, C., ... Matzuk, M. M. (2001). Synergistic roles of bone morphogenetic protein 15 and growth differentiation factor 9 in ovarian function. Mol Endocrinol **15**(6): 854-866.

Yang, M. Y. and Fortune, J. E. (2008). The capacity of primordial follicles in fetal bovine ovaries to initiate growth in vitro develops during mid-gestation and is associated with meiotic arrest of oocytes. Biol Reprod **78**(6): 1153-1161.

Yang, P. and Roy, S. K. (2006). A novel mechanism of FSH regulation of DNA synthesis in the granulosa cells of hamster preantral follicles: involvement of a protein kinase C-mediated MAP kinase 3/1 self-activation loop. Biol Reprod **75**(1): 149-157.

Yang, S. H., Medvedev, S., Reddi, P. P., Schultz, R. M., Hecht, N. B. (2005). Correlation between in vitro maturation and expression of LH receptor in cumulus cells of the oocytes collected from PCOS patients in HCG-primed IVM cycles. Hum Reprod **20**(8): 2097-2103.

Yao, L. J., Medvedev, S., Reddi, P. P., Schultz, R. M., Hecht, N. B. (2004). Aurora-A is a critical regulator of microtubule assembly and nuclear activity in mouse oocytes, fertilized eggs, and early embryos. Biol Reprod **70**(5): 1392-1399.

Yeo, C. X., Gilchrist, R. B. and Lane, M. (2009). Disruption of bidirectional oocyte-cumulus paracrine signaling during in vitro maturation reduces subsequent mouse oocyte developmental competence. Biol Reprod **80**(5): 1072-1080.

Yin, H. and Lin, H. (2007). An epigenetic activation role of Piwi and a Piwi-associated piRNA in Drosophila melanogaster. Nature **450**(7167): 304-308.

Yoshimura, T., Miyazaki, T., Toyoda, S., Miyazaki, S., Tashiro, F., Yamato, E., Miyazaki, J (2007). Gene expression pattern of Cue110: a member of the uncharacterized UPF0224 gene family preferentially expressed in germ cells. Gene Expr Patterns **8**(1): 27-35.

Yoshimura, T., Toyoda, S., Kuramochi-Miyagawa, S., Miyazaki, T., Miyazaki, S., Tashiro, F., ... Miyazaki, J. (2009). Gtsf1/Cue110, a gene encoding a protein with two copies of a CHHC Zn-finger motif, is involved in spermatogenesis and retrotransposon suppression in murine testes. Dev Biol **335**(1): 216-227.

Young, J. M. and McNeilly, A. S. (2010). Theca: the forgotten cell of the ovarian follicle. Reproduction **140**(4): 489-504.

Young, L. E., Fernandes, K., McEvoy, T. G., Butterwith, S. C., Gutierrez, C. G., Carolan, C., ... Sinclair, K. D. (2001). Epigenetic change in IGF2R is associated with fetal overgrowth after sheep embryo culture. Nat Genet **27**(2): 153-154.

Young, L. E., Sinclair, K. D. and Wilmut, I. (1998). Large offspring syndrome in cattle and sheep. Rev Reprod **3**(3): 155-163.

Yu, J., Deng, M., Medvedev, S., Yang, J., Hecht, N. B., Schultz, R. M. (2004). Transgenic RNAi-mediated reduction of MSY2 in mouse oocytes results in reduced fertility. Dev Biol **268**(1): 195-206.

Yuan, W., Lucy, M. C. and Smith, M. F. (1996). Messenger ribonucleic acid for insulin-like growth factors-I and -II, insulin-like growth factor-binding protein-2, gonadotropin receptors, and steroidogenic enzymes in porcine follicles. Biol Reprod **55**(5): 1045-1054.

Zaraza, J., Oropeza, A., Velazquez, M. A., Korsawe, K., Herrmann, D., Carnwath, J. W., Niemann, H. (2010). Developmental competence and mRNA expression of preimplantation in vitro-produced embryos from prepubertal and postpubertal cattle and their relationship with apoptosis after intraovarian administration of IGF-1. Theriogenology **74**(1): 75-89.

Zeleznik, A. J. (2004). The physiology of follicle selection. Reprod Biol Endocrinol **2**: 31.

Zhang, D. L.*,* Sun, X. J., Ling, L. J., Chen, R. S., Ma, D. L. (2002). Molecular cloning, characterization, chromosomal assignment, genomic organization and verification of SFRS12 (SRrp508), a novel member of human SR protein superfamily and a human homolog of rat SRrp86. Acta Genetica Sinica **29**(5): 377-383.

Zhang, L.*,* Jiang, S., Wozniak, P. J., Yang, X., Godke, R. A. (1995). Cumulus cell function during bovine oocyte maturation, fertilization, and embryo development in vitro. Mol Reprod Dev **40**(3): 338-344.

Zhao, X.*,* Batten, B., Singh, B., Arlinghaus, R. B. (1990). Requirement of the c-mos protein kinase for murine meiotic maturation. Oncogene **5**(11): 1727-1730.

Zhao, Y. and Chen, R. H. (2006). Mps1 phosphorylation by MAP kinase is required for kinetochore localization of spindle-checkpoint proteins. Curr Biol **16**(17): 1764-1769.

Zheng, P. and Dean, J. (2007). Oocyte-specific genes affect folliculogenesis, fertilization, and early development. Semin Reprod Med **25**(4): 243-251.

Zhuo, L. and Kimata, K. (2001). Cumulus oophorus extracellular matrix: its construction and regulation. Cell Struct Funct **26**(4): 189-196.

Zimin, A. V.*,* Delcher, A. L., Florea, L., Kelley, D. R., Schatz, M. C., Puiu, D., Salzberg, S. L. (2009). A whole-genome assembly of the domestic cow, Bos taurus. Genome Biol **10**(4): R42.

Appendix I – Suppliers Addresses

Abcam, 330 Cambridge Science Park, Cambridge, CB4 0FL, UK

Acrodisc, Pall Corporation, 5 Harbourgate Bussiness Park, Southampton road, Portsmouth, PO6 4BQ, UK

Affymetrix, Mercury Park, Wycombe Lane, Wooburn Green, High Wycombe, HP10 0HH, UK

Amersham Biosciences, Amersham place, Little Chalfont, Buckinghamshire, HP7 9NA, UK

Applied Biosystems, 850 Lincoln Centre Drive, Foster City, CA 94404, USA

Applied Imaging International, Square Scotswood Road, Newcastle upon Tyne, NE1 4EP, UK

Becton, Dickinson and Company (BD Plastipak^{TM}), Drogheda, Ireland

Bioline Ltd, 16 The Edge Bussiness Centre, Humber road, London, NW3 6EW

Bio-Rad Laboratories Ltd, Bio-Rad House, Maxted Road, Hemel Hampstead, Hertfordshire, HP2 7DX

Carl Zeiss Ltd, 509 Coldhams Lane, Cambridge, CB1 3JS, UK

Cook Medical, Brisbane Technology Park, 12 Electronics Street, Eight Mile Plains, Brisbane, QLD 4113, Australia

Eppendorf Ltd, Eppendorf House, Gateway 1000 Whittle Way, Arlington Business Park, Stevenage, SG1 2FP, UK

Fujifilm, St Martins Business Centre St Martins Way, Bedford MK42 0LF

Gilson Inc, 3000m Parmenter street, P.O. Box, 620027, Middleton, WI 53562-0027, USA

Humagen Fertility Diagnostics, 2400 Hunter's Way, Charlottesville, VA22911, USA

Invitrogen Ltd, 3 Fountain Drive, Inchinnan Bussiness Park, Paisley, PA4 9RF, UK

Keison International Ltd, 122 New London Road, Chelmsford, Essex, CM2 0RG, UK

Labinco B.V, Zinkstraat 64, 4823, Bredo, Netherlands

Leica Microsystems Ltd, Davy Avenue, Knowlhill, Milton Keynes, MK5 8LB, UK

Life Technologies Ltd,, 3 Fountain Drive, Inchinnan Business Park, Paisley, PA4 9RF, UK

Lotus Professional, Oughtibridge Mill, Oughtibridge, Sheffield S35 0DN, UK

Medichem International, Sevenoaks, Kent, TN15 0JL, UK

Melford Laboratories Ltd, Bildeston Road, Chelsworth, Ipswich, Suffolk, IP7 7LE, UK

Melter Toledo Ltd, 64 Boston Road, Beaumont Leys Leicester, LE4 1AW, UK

Millipore Ltd, Croxley green bussiness park, Watford, WD18 8YH, UK

MTG Medical Technology Verrtriebs GmbH, Opalstrasse 32 D, 84032, Altdorf, Germany

Millipore, 290 Concord Road, Billerica, MA 01821, USA

MSE/Sanyo, Worsley Bridge Road**,** Lower Sydenham**,** London, SE26 5AZ, UK

National diagnostics, Unit 4 Fleet Business Park**,** Itlings Lane**,** Hessle, North Humberside**,** HU13 9LX, UK

New Branswick-Eppendorf, Gateway 1000 Whittle Way, Arlington Bussiness Park, SG1 2FP, Stevenage, UK

Nonlinear Dynamics, Keel House, Garth Heads, Newcastle upon Tyne, Tyne and Wear, NE1 2JE, UK

Nunclon, Kamstrupvev 90, Postbox 280, DK-4000, Roskilde, Denmark

Olympus UK Ltd, (Microscopes), Great Western Industrial Park, Dean Way, Southhall, Middlesex, UB2 4SB, UK

Olympus UK Ltd (Cameras), 2-8 Honduras Street, London, EC1Y 0TX, UK

Philip Harris Ltd, Shenstone, Lichfield, WS14 OEE, UK

Promega UK Ltd, Delta House, Southampton Science Park, Southampton, Hampshire, SO16 7NS, UK

Research Instruments Ltd, Bickland Industrial Park, Falmouth, TR11 4TA, Cornwall, UK

Roche Diagnostics Limited, Charles Avenue, Burgess Hill, West Sussex, RH15 9RY, UK

Santa Cruz Biotechnology, Wembley, Middlesex, HA9 7YN, UK

Sigma-Aldrich Company Ltd, The Old Brickyard, New Road, Gillingham, Dorset, SP8 4XT

Science Products, Hofheimer Str 63, Hofheim, 65719, Germany

Scientific Laboratory Supplies (SLS), Head office, Orchard House, The Square, east riding of Yorkshire, HU13 0AE, UK

Simport, 2588 Bernard-Pilon, Beloeil, QC J3G 4S5, Canada

Sony, Pencoed Technology Park, Pencoed, South Wales, CF35 5HZ, UK

Starlab, Unit 4 Tanners Drive, Blakelands, Milton Keynes, MK14 5NA, UK

Takara Bio, 2 Avenue du Président John Fitzgerald Kennedy, 78100, Saint-Germain-en-Lave, France

Techno Plastic Products (TPP), Zollstrasse 7, CH-8219 Trasadingen, Switzerlans

Terumo UK Ltd, The Causeway, Egham, Surrey, TW20 9AW, UK

Thermo Fisher Scientific, Stafford House, Boundary Way, Hemel, Hempstead, HP2 7GE, UK

Thermo-Scientific, NanoDrop products, 3411 Silverside Rd, Bancroft Building, Wilmington, DE 19810, USA

Qiagen Ltd, Qiagen house, Fleming Way, Crawley, West Sussex, RH10 9NQ, UK

Vector Laboratories Ltd, 3 Accent Park, Bakewell Road, Orton Southgate, Peterborough, PE2 6XS, UK

VWR International, Hunter Boulevard, Magna Park, Lutterworth, Leistershire, LE17 4XN, UK

Appendix II – Stock solutions

A. TISSUE CULTURE STOCK SOLUTIONS

A1. Transferrin (5 mg/ml) suitable for cell culture (T0665, Sigma-Aldrich)
100 mg of holo-transferrin powder dissolved in 20ml of MEM containing 0.1% (w/v) fraction V cell culture grade BSA (85040C, Sigma-Aldrich) followed by filtration with a 0.2 cellulose acetate syringe filter. Aliquots of 20 μl stored at -20°C for 3 months.

A2. Sodium selenite (50 μg/ml) suitable for cell culture (S5261, Sigma-Aldrich)
1mg of sodium selenite dissolved in 20ml of MEM containing 0.1% (w/v) fraction V cell culture grade BSA followed by filtration with a 0.2 cellulose acetate syringe filter. Aliquots of 5 μl stored at -20°C for 3 months.

A3. Insulin (10 mg/ml) suitable for cell culture (I6634, Sigma-Aldrich)
10 mg of insulin dissolved in 20ml of MEM containing 0.1% (w/v) Fraction V cell culture grade BSA followed by filtration with a 0.2 cellulose acetate syringe filter. Aliquots of 5 μl stored at -20°C for 3 months.

A4. Long-R3 IGF1 stock (100μg/ml) suitable for cell culture (I1146, Sigma-Aldrich)
500 μg of long R3 IGF1 dissolved in 5 ml of MEM containing 0.1% (w/v) fraction V cell culture grade BSA followed by filtration with a 0.2 cellulose acetate syringe filter. Aliquots of 5 μl stored at -20°C for 3 months.

A5. Sodium Pyruvate (47 mM) suitable for cell culture (P5280, Sigma-Aldrich)
51.7 mg of sodium pyruvate dissolved in 10ml of embryo tested sterile H_2O followed by filtration with a 0.2 cellulose acetate syringe filter. Stored at 4°C for 1 week.

A6. Ovine LH (200 μg/ml) (L5269, Sigma-Aldrich)
9 mg of LH dissolved in 4.5 ml of 10% (w/v) BSA, fraction V cell culture grade and added to 40.5 ml of MEM followed by filtration with a 0.2 cellulose acetate syringe filter (bioactivity: 0.55 U/ml). Aliquots of 20 μl stored at -20°C for 3 months.

A7. Ovine FSH (200 μg/ml) (F8174, Sigma-Aldrich)
9 mg of FSH dissolved in 4.5 ml of 10% (w/v) BSA, fraction V cell culture grade and added to 40.5 ml of MEM followed by filtration with a 0.2 cellulose acetate syringe filter (bioactivity: 0.91 U/ml). Aliquots of 20 μl stored at -20°C for 3 months.

A8. Sodium bicarbonate stock (250 mM)
1.05 g of $NaHCO_3$ with 3 drops of phenol red and embryo tested sterile H_2O up to 50 ml, followed by filtration with a 0.2 cellulose acetate syringe filter. Stored at 4°C for 2 weeks.

A9. Hepes stock (250 mM)
3.254 g of Na Hepes added to 3 g of Hepes, 3 drops of phenol red and embryo tested sterile H_2O up to 100 ml, followed by filtration with a 0.2 cellulose acetate syringe filter. Stored at 4°C for 2 months.

A10. Penicillin/Streptomycin stock (10,000 Units penicillin and 10 mg/ml streptomycin) suitable for cell culture (P4333, Sigma-Aldrich)
600 mg of penicillin G (6 mg/ml) added to 500 mg of streptomycin sulphate (5 mg/ml) in embryo tested sterile H_2O up to 100 ml, followed by filtration with a 0.2 cellulose acetate syringe filter. Aliquots of 5 ml stored at -20°C for 3 months.

A11. α-MEM base stock suitable for cell culture (M4526, Sigma-Aldrich)
150 ml of α-MEM basis added to 1.5 ml Penicillin/Streptomycin stock and 0.15 g of fraction V cell culture grade BSA followed by filtration with a 0.2 cellulose acetate syringe filter. Stored at 4°C for 2 weeks.

B. MOLECULAR BIOLOGY STOCK SOLUTIONS

B1. 1X TBE
108 g of tris base added to 55 g of boric acid, 7.4 g of EDTA and Milli-Q H_20 up to 10 litres.
B2. Gel loading buffer
0.125 g of bromophenol blue added to 0.125 g of xylene cyanol FF, 15 ml of glycerol and 35 ml of sterile-distilled grade H_20.
B3. 100 bp ladder
12 μl of 100bp marker (Invitrogen) added to 20 μl of loading buffer, 0.4 μl of 5M NaCl and 67.6 μl of sterile-distilled H_20.

C. SDS-PAGE AND WESTERN BLOTTING STOCK SOLUTIONS

C1. Acrylamide-Bisacrylamide, 40% (w/v) acryl, 1.5% (w/v) bis
40 g of acrylamide added to 1.5 g of bis filled up to 100 ml in sterile-distilled H_20.
C2. Stacking gel buffer (0.5 M Tris)
12.1 g of Tris filled up to 200 ml in sterile-distilled H_20 with pH adjusted at 6.8.
C3. Lower gel buffer (1.5 M Tris)
36.3 g of Tris filled up to 200 ml in sterile-distilled H_20 with pH adjusted at 8.8.
C4. 20% (w/v) SDS
20 g of SDS filled up to 100 ml in sterile-distilled H_20.
C5. 1.5% (w/v) Ammonium persulfate (APS)
1.5 g of APS filled up to 100 ml in sterile-distilled H_20
C6. 0.5% (v/v) TEMED
1 ml of TEMED filled up to 200 ml in sterile-distilled H_20
C7. Western blotting sample buffer (2X SDS)
5 ml of Stacking Gel buffer added to 2 ml of 10% (w/v) SDS in sterile-distilled H_20, 1 ml of 0.1% (v/v) bromophenol blue in sterile-distilled H_20, 5 ml of 60% (v/v) glycerol in sterile-distilled H_20, 1 ml β-mercaptoethanol and 6 ml of sterile-distilled H_20.
C8. 10X running buffer
144 g of Glycine added to 30 g of Tris base, 25 ml of 20% (w/v) SDS in sterile-distilled H_20 filled up to 1 L in Milli-Q H_20 with pH adjusted to 8.3
C9. 10X Wash buffer
1% (v/v) PBS in Milli-Q H_20 with 1% (v/v) Tween-20 in Milli-Q H_20
C10. Blocking buffer
1.5 g of non-fat dry milk powder and 50 μl of Tween-20 in 50 ml of 1% (v/v) PBS in Milli-Q H_20
C11. 10X Transfer buffer
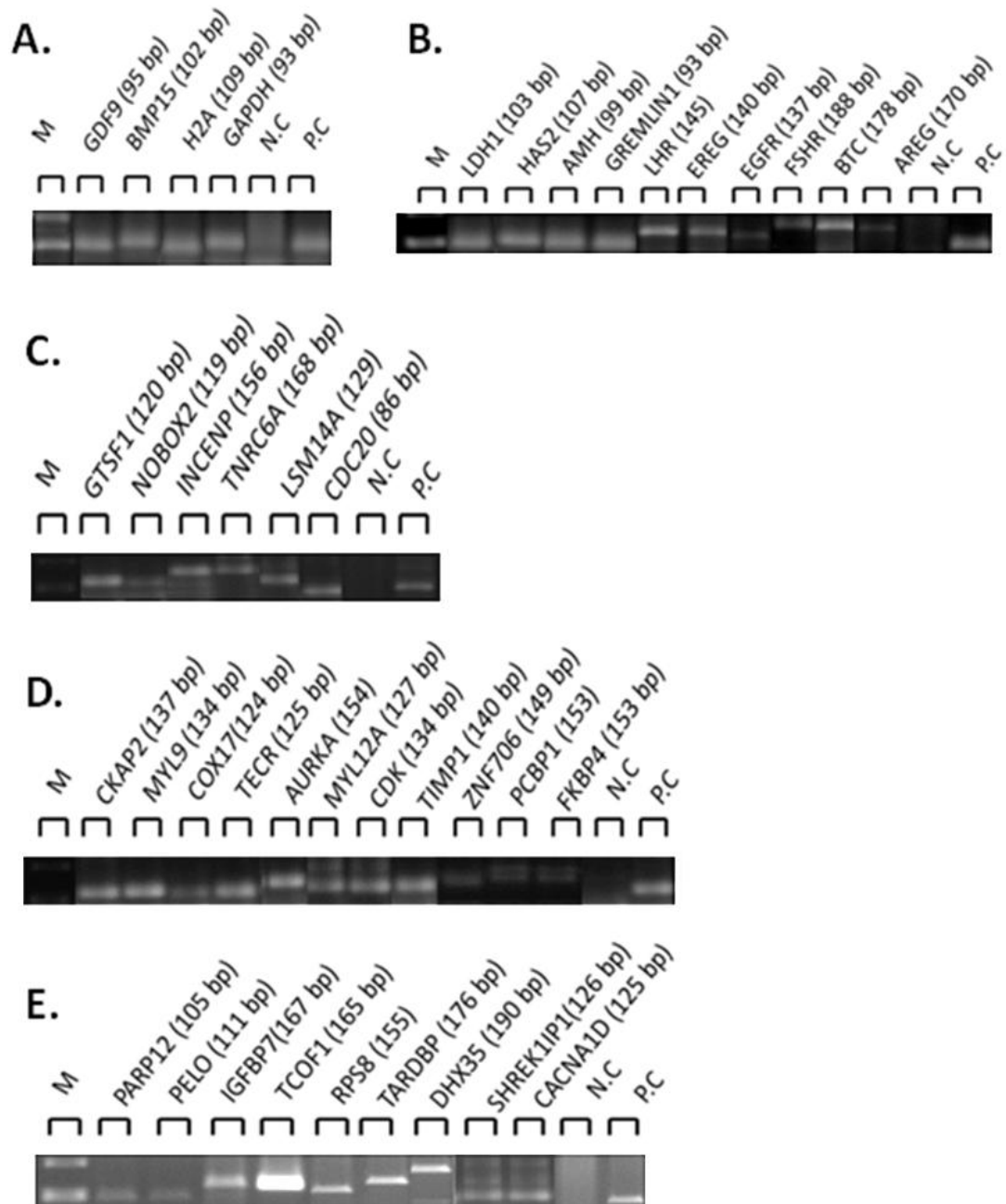144g of Glycine added to 30 g of Tris base and 20% (v/v) methanol filled up to 1 L in Milli-Q H_20

D. HISTOLOGY STOCK SOLUTIONS

D1. 20 X SSC
175.3 g of NaCl and 88.2 g of Sodium Citrate with a few drops of HCl in 1 L of sterile-distilled H_2O with pH adjusted at 7.0 and sterilised by autoclaving.

Appendix III

Verification of real-time PCR primers

Montage showing expression profiles obtained by RT-PCR to verify the validity of the real-time PCR primers used throughout the thesis. **A, C, D, E:** Expression profiles of the target genes in a previously verified cDNA library containing a cohort of 10 denuded GV oocytes. **B:** Expression profiles of the target genes in a previously verified cDNA library containing 2 oocytectomised cumulus cells. **N.C:** Contains sterile-distilled H_2O and no cDNA library. **P.C:** Expression profile of previously verified real-time *GAPDH* primers in a previously verified cDNA library.

Appendix IV

Primary bioinformatic analysis table of down-regulated and up-regulated genes from microarray group AB following *GTSF1* knockdown

Down-regulated genes
AB only (20 genes)
MGC140822, PCBP1, hnRNP-E1, FKBP52, FKBP4, MGC127596, CDK2, MGC127596, CDK2, MGC133632, ZNF706, GPSN2, MGC127748, TECR, AURKA, MGC134472, COX17, MGC128036, RBM17, TIMP1
Common to AB-ABC (4 genes)
CFDP2, MGC128687, BCNT, p97
Common to AB-BC-ABC (4 genes)
LOC616942, AHSG, AFFX-r2-Ec-bioC-5_at, AFFX-r2-Ec-bioC-5_at
Up-regulated genes
AB only (12 genes)
Bt.22353.1.S1_at, CKAP2, MGC148979, LOC787094, MGC139901, MRCL3, MRCL2, MYL12A, MYL9, Bt.22834.1.S1_at, DDX27, MGC139525
Common to AB-ABC (7 genes)
EZR, VIL2, Bt.77.1.S1_at, ANT1, SLC25A4, C21H15orf63, HYPK
Common to AB-BC-ABC (11 genes)
ARID2, OSBPL7, Bt.20481.1.S1_at, Bt.29800.1.A1_at, RPL26L1, Bt1237.1.S1_at, ARFIP1, MGC151527, MGC165765, UBFD1, MAPK6